A STUDY OF FERMENTATION HETEROGENEITY IN A PILOT SCALE AIRLIFT BIOREACTOR

A thesis submitted to the University of London
for the degree of
DOCTOR OF PHILOSOPHY
by
David James Pollard B.Sc. (Hons)

The Advanced Centre for Biochemical Engineering,
Department of Chemical and Biochemical Engineering,
University College London,
Torrington Place,
London.

March, 1995

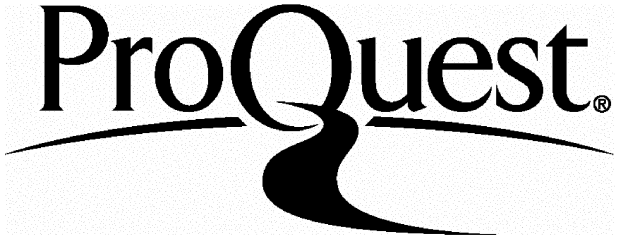

To my parents
and.....

..... *Sharon*

ABSTRACT

The extent of the heterogeneity in a large scale vessel can affect cell growth and product yields. Consequently, the examination of the impact of the engineering environment on the physiology of fermentation broths can lead to improved growth and production conditions which will be important for fermentation optimisation including scale up, design and operation of bioreactors.

Bioreactor heterogeneity has been studied in a multiconfigurable pilot scale airlift reactor (0.25 m^3) which can create different degrees of heterogeneity. Hydrodynamic and oxygen transfer performances of two air ring sparger configurations, ie. in the annulus or draft tube, in combination with a marine propeller fitted at the base of the reactor, were compared using Newtonian baker's yeast suspensions and batch cultures of non-Newtonian *Saccharopolyspora erythraea*. The cellular growth, morphology and productivity of the *S. erythraea* broths were also compared between the airlift reactor configurations and stirred tank.

The comparison of gas holdup, liquid velocity and mixing times between the two sparger configurations with baker's yeast suspension was influenced by the ratio of the cross sectional area of the downcomer to the riser and the bubble flow regime. The achievement of a critical liquid height above the draft tube for optimal liquid mixing demonstrated the importance of the top section to the liquid mixing performance of the vessel. The local DOT and k_La values were greater in the downcomer than in the riser. This was caused by the high gas content, long gas residence times and smaller bubble diameter in the downcomer compared to the riser. The gas holdup, liquid circulation and oxygen transfer with conventional airlift operation were improved by operating the marine propeller in conjunction with the annulus ring sparger to draw liquid down the draft tube. This led to a reduction in the extreme DOT heterogeneity and a increase of the OUR of the yeast suspension. Maximum OUR was obtained when the lowest DOT of the cycling DOT was at or above 10% (air saturation). The OUR improved if the cells experienced the same DOT changes at a greater frequency. This indicated that cells could respond to rapid DOT changes around the vessel and so the cell metabolism was not based on an average DOT of the vessel.

During the *S. erythraea* fermentations the enhancement of bubble coalescence with increasing apparent viscosity led to the reduction of the sectional gas holdups and local k_La values and the improvement of liquid mixing. The extent of the changes with increasing apparent viscosity were dependent on the broth morphology, reactor configurations and operating conditions. The relationships between broth rheology and the dry cell weight, morphology and liquid velocity were all influenced by the reactor configuration and operating conditions. DOT heterogeneity did not affect the growth of mycelial *S. erythraea* broths but the reduction of DOT heterogeneity improved the specific

erythromycin production rate and final specific erythromycin production which was proportional to the energy dissipation rate.

The study shows that an understanding of cell physiology and the effect of the engineering environment on their growth, productivity and morphology is essential for the enhancement of bioprocesses. The examination of reactor heterogeneity provides a better understanding of the effects of the translation of scale and as a result can lead to a more efficient process with improved productivity.

ACKNOWLEDGEMENTS

I would like to thank Drs. Andrew Ison, Parviz Ayazi Shamlou and Prof. Malcolm Lilly for sharing their extensive experience with me and providing support and encouragement throughout this study.

The successful operation of the pilot scale airlift reactor would not have been possible without the support of the technical staff (workshop, electrical and pilot plant) for which I am eternally grateful. I am especially indebted to Billy Doyle, Clive Orsborn, Chris Seaton and Stuart Pope for their invaluable support in the pilot plant, particularly when undertaking the laborious changes of reactor configuration.

I'm sincerely grateful for the technical expertise provided by Dr. Claire Turner, Dr. Mark Bulmer, David Hearle, Martin Smith and Emma Fischer as they sacrificed there own work to help mine. I' d also like to thank all my colleagues, past and present, for providing a friendly and humorous 'working' environment.

Thankyou to Sharon for her patience, understanding and nutritious support.

UCL is the Biotechnology and Biological Sciences Research Council's Interdisciplinary Research Centre for Biochemical Engineering and the council's support is gratefully acknowledged.

CONTENTS page

LIST OF FIGURES

Figure no.

SECTION 1.0 INTRODUCTION

SECTION 2.0 MATERIALS AND METHODS

SECTION 3.0 RESULTS

SECTION 3.4

LIST OF TABLES

1.0 INTRODUCTION

1.1 General concepts of airlift reactors

1.1.1 Introduction

The stirred tank has been the most frequently employed bioreactor for aerobic fermentations. However the limited gas throughput due to impeller flooding, the high degree of agitation and hence, high energy dissipation for mass transfer and mixing has led to investigations into alternative reactor design (Chisti, 1989). Of these various reactor types, bubble columns and airlift reactors have been of greatest potential (Schugerl *et al.*,1977). Airlift reactors are mechanically simple devices as the reactor contents is pneumatically agitated by a stream of air (Siegel *et al.*, 1988). Predominantly two types of reactor exist, 'internal' and 'external'. Both of which are characterised by fluid circulation in a cyclic pattern. Fluid motion is mainly due to the mean density difference between the upflow section, the riser, and the downflow section, the downcomer. The recirculation of the liquid through a downcomer allows high liquid circulation rates and efficient mixing which is combined with a controllable liquid flow in the absence of mechanical agitators, and at low shear rates. The airlift reactor also satisfies a high oxygen demand particularly for large airlift reactor configurations (50 - 100 m tall) (Zwietering *et al.*, 1992, Lin *et al.*, 1976). Early research into airlift design involved the large scale production of single cell protein. Although the interest in single cell protein has declined, airlift reactors have been used for industrial applications, such as biological waste treatment, cultivation of plant and animal cells and secondary metabolite production. Thus airlift reactors are increasingly becoming competitive with conventional stirred tank in a wide range of applications, particularly those involving large scale processes (Glennon *et al.*, 1988). However, the literature publications available on airlift reactors is still very limited. This lack of knowledge of various airlift and bubble columns is hindering the more extensive use of the reactors in industry (Chisti and Moo-Young, 1987) as a reliable design strategy is far from established.

1.1.2 Comparison between airlift reactor, bubble column and stirred tank

Although an airlift reactor can be considered as a type of bubble column as they are both pneumatically aerated, their hydrodynamic behaviour are different. The liquid flow in bubble columns can result in a random flow pattern of circulating cells where local liquid velocities can be high, whereas the liquid superficial gas velocity is very low or zero in batch operation (Onken and Weiland, 1983). In contrast airlift reactors have a hydrostatic pressure between the aerated and unaerated sections which causes liquid circulation around the loop of the vessel. This liquid flow will cause the bubbles in the upflow section to rise faster leading to a lowering of the gas holdup. As a result the airlift reactor has lower mean gas holdups than a bubble column. Airlift reactors also show a

greater uniform distribution of the gas phase across the column cross section with a maximum in local gas holdup near the column wall. This will become less marked with increased gas load and mean gas content compared to bubble columns (Onken and Weiland, 1983). The operation of an airlift reactor with gas input at one position at the base of the riser can lead to changing conditions, such as nutrients and dissolved oxygen around the vessel. These heterogeneous environmental conditions will act on each organism in the same way as the suspended cells periodically pass through the individual zones of the reactor.

As the superficial gas velocity and gas holdup increases, the radial velocity of liquid becomes increasingly more uniform. Onken and Weiland (1983) have shown that gas-liquid flow has a small effect on coalescence, indicating the influence of physical properties of solutes on the behaviour of airlift reactors is rather low compared to reactors with a non-directed flow, as in bubble columns and stirred tanks. It is claimed that the liquid flow in an airlift reactor produces a homogeneous field of shear stress which is relatively constant throughout the reactor (Merchuk, 1990, Siegel *et al.*, 1988). This is due to the mean density difference in the riser and downcomer whereas in a stirred tank shear will be greatest near the stirrer (or gas sparger in a bubble column) since the momentum is directly transferred to the fluid at this point (Merchuk, 1990). This in turn results in the transfer of energy to slower moving more distant elements of the fluid. Thus a wide variation of shear forces exists, the maximum shear gradient in a stirred tank with a flat blade turbine has been reported to be approximately four times the mean shear gradient. These high shear forces have been observed to cause changes in morphology of some filamentous microorganisms (Smith, 1985, Smith *et al.*, 1990). Stirred vessels have a gas throughput which is limited by impeller flooding criterion, and to achieve sufficient oxygen mass transfer, the degree of agitation necessary may cause damage to microorganisms passing through the high shear zone of the impeller. Therefore, airlift reactors have been chosen for the growth of shear sensitive mammalian and plant cells. Apart from low shear forces, airlift reactors also have lower power inputs compared to the high mechanical energy input required to achieve mass transfer in stirred vessels. The simple design and construction of airlift reactors allows extended aseptic operation made possible by the elimination of stirrer shafts, seals and bearings.

1.1.3 Industrial applications of the airlift reactor

The industrial applications of airlift reactors include the production of single cell protein, the treatment of wastewater, cultivation of plant and animal culture. To use stirred tank fermenters for the production of single cell protein (SCP) from methanol would be uneconomical due to the removal of the exothermic heat generated during the fermentation and, the high rates of aeration and agitation required for the high oxygen demand of the process with hydrocarbon substrates (Chen, 1990). Airlift reactors were designed for SCP production with internal or external loops which required a lower

energy input and had a greater surface area for heat exchange than stirred tanks. ICI Ltd. operated both an external loop reactor (Taylor and Senior, 1978), and a 1500 m^3 (working volume) continuous process internal loop airlift fermenter (2000 m^3) for SCP production of 1000 t/y from the growth of *Ps. methylotrophus* on methanol (Smith, 1980). For the internal configuration air and gaseous ammonia were introduced at the base of the fermenter and forced into solution by the hydrostatic pressure of the liquid column. Methanol was injected at 1000 sites along the downcomer as it was difficult to rapidly and uniformly distribute the methanol substrate. Sieve plates were used at regular intervals within the riser to disperse large bubbles formed by coalescence. Also a conical top section was used to reduce the amount of bubble entrainment into the downcomer and enhance the density difference for liquid circulation. Heat from the surrounding exothermic reaction was removed via the cooling jacket around the downcomer and from cooling cools at the base of the riser. A complete flow cycle was achieved in 120 seconds with a riser height of 45 m (Smith, 1980).

Hoechst AG - Uhde used a 40 m^3 airlift reactor for SCP production in the region of 1000 t/y from the growth of *Methylomonas clara* on methanol (Faust *et al.*, 1977). The airlift reactor was chosen as a clearly defined distribution of all components was required so that limits of substrate concentration would remain between 0.01% and 1% and the carbon dioxide level would be not exceeded above 1 ppm. Problems of foam production and sedimentation associated with stirred tank operation were also found to be limited by the loop reactor. The Mitsubishi Gas Chemical Company Inc. produced 500 t / y of SCP from a 20 m^3 airlift reactor at a rate of 5 $kg.m^{-3}.h^{-1}$ (Kuraishi *et al.*, 1977). The airlift reactor was used instead of the stirred tank as similar specific oxygen inputs could be used for both reactors yet the power input into the airlift reactor was lower than for the stirred tank. In addition the airlift reactor was much easier to scale up (Blenke, 1985). Airlift reactors were designed at pilot scale to couple heat and mass transfer processes using low pressure air. Fermenter cooling was accomplished by evaporating water in the fermenter with air which gained in humidity. Heat transfer by direct contact of air with the fermenter liquid is more efficient than indirect heat exchange which requires a finite temperature differential across the heat exchange surfaces (Chen, 1990).

A deep shaft pressure cycle reactor was employed by ICI Ltd. for the purification of biological waste water. The shaft was sunk up to 200 m in to the earth and the vessel internal diameter was 8 m. The air was introduced into the downflowing liquid within the draft tube and liquid circulation was started and stabilised by sparging air at a second position, at a shallow depth in the upflow. Oxygen transfer rates were up to 60 - 90 $mmol.L^{-1}.h^{-1}$ with energy requirements of 3 kg O_2 kWh^{-1} (Hines *et al.*, 1975). Blenke (1985) reported that Hoechst AG employed a BIOHOCH reactor with a volume of 8000 m^3 for wastewater treatment. The reactor contained a number of parallel draft tubes each with its own circulation loop but all were enclosed within a tank of 20 m tall and 23 to 45

m wide. The system was found to be between 50 - 80% more efficient than traditional basin systems.

Airlift reactors have been used for mammalian and plant cell culture. Mammalian cells lack the rigid cell wall of bacteria and the greater size and doubling time contributes to the vulnerability of the cells. High agitation rates may be detrimental to plant cell growth however, low agitation rates increase the number and size of aggregations (Merchuk, 1990). Thus the homogeneity of the stress forces in airlift reactors is the main advantage for the large scale cultivation of mammalian cells. Katinger *et al.* (1979) were the first to use airlift technology for animal cell culture. They cultured human lymphoblastoid cells and Baby Hamster kidney cells in 2 m^3 reactors. Monoclonal antibodies have also been cultured in airlift reactors at Celltech Ltd. A 10, 100, 1000, litre cascade system was constructed for the scale up of antibody production with a high level of automation. Methods for growing hybridoma cells in airlift reactors were applicable for numerous cell lines such as mouse, rat, and human origin all producing monoclonal antibodies (Arathoon, W.R. and Birch, J.R, 1986). Serum free medium was successfully used in a 1 m^3 fermenter to produce 260 g of antibody harvested over 260 hours. A 4 to 5 fold increase in yield over roller bottles was observed.

The use of airlift reactors in industry for metabolite production from microorganisms is limited. This is partly due to the fact that companies are loathed to make the capital expense of replacing the stirred tank technology which has a high degree of familiarity with technology which is less well known. Buckland and Lilly (1993) reported that air agitated tanks may be best suited to large scale operation above 200 m^3 as heat transfer (cooling) considerations becomes limiting beyond this scale with stirred tanks. Despite the reservations of using air agitated tanks some pharmaceutical companies including Merck & Co. Inc. use aerated tanks for metabolite production (Buckland and Lilly, 1993). However, virtually no literature publications have been produced in this area presumably due to the industrial sensitivity. Carrington *et al.* (1992) described oxygen transfer and mixing characteristics during the fermentation of *S. rimosus* in a 20 m^3 bubble column fitted with an internal helical coil. However, no details on antibiotic production were given.

1.1.4 Unicellular and filamentous fermentations in airlift reactors

The use of airlift fermenters for the cultivation of microorganisms has been limited apart from the research to single cell protein. Most of the airlift investigations in the literature have involved model media for hydrodynamic studies using non biological solutions. The small amount of research with airlift reactors using microorganisms has been at laboratory and pilot scale.

1.1.4.1 Studies with unicellular fermentation broths

Studies using yeast and filamentous organisms were performed for either hydrodynamic studies or secondary metabolite production which were usually compared with stirred tank vessels. The Newtonian characteristics of yeast broths have meant that hydrodynamic behaviour was similar to that with model media (Onken and Weiland, 1983, Russell, 1989). However, Frohlich *et al.* (1991b) and Lubbert *et al.* (1988) found differences between the hydrodynamics of a tower loop reactor when using model media compared to the measurements made with yeast broths. The differences were due to the coalescing behaviour of the two fluids. This stressed the importance of studying a reactor performance with biological fermentation broths and not model media systems.

McNeil and Kristiansen (1990) studied the fermentation of *Saccharomyces cerevisiae* in airlift and stirred tank fermenters. The behaviour of the yeast was found to be similar in both fermenters including overall biomass and ethanol concentration. Fermentations of *Candida lipolytica* (Seipenbusch *et al.*, 1976) and *Candida intermedia* on n-parrafin in internal loop airlifts have been demonstrated. The continuous cultivation of the yeast *Candida utilis* in a concentric draft tube airlift was demonstrated for the production of single cell protein by Huang *et al.* (1976). The characterisation of multistage airlift reactors was carried out using *E. coli* fermentations (Adler and Schugerl, 1983).

1.1.4.2 Filamentous fermentations

1.1.4.2.1 The engineering difficulties involved with filamentous fermentation in bioreactors

The fermentation of filamentous cultures involves different engineering problems than the fermentations of unicellular microorganisms. Filamentous cultures can form two types of morphology in submerged culture, pelleted and mycelial forms, although there is no clear boundary between the two culture morphologies. The mycelial fermentations often lead to entangled clumps that produce highly viscous non-Newtonian fermentation broths whereas, the pelleted broth consists of compact forms of hyphae with rheological behaviour nearer to Newtonian fluids. To maintain sufficient oxygen supply to a viscous filamentous mycelial culture a high power input would be necessary.

The significant factor affecting viscosity of mycelial culture fluids, such as Actinomycetes, is hyphal morphology. Banks (1977) suggested pseudoplastic type rheology seen in polymer solutions, where long polymer molecules align with each other at high shear rates resulting in low viscosity, could be expected in mycelial cultures. Generally, Bingham plastic fluids have a similar relationship between viscosity and shear stress but require a limiting shear stress to effect flow. Deindorfer and West (1960) studied the rheology throughout a streptomycin producing fermentation of *Streptomyces griseus*. The fermentation began with Newtonian rheology and as the hyphae lengthened

Bingham plastic behaviour developed. Hyphal fragmentation and lysis was observed at the end of the fermentation which had Newtonian rheological characteristics. The entanglement of mycelia from a number of filamentous broths including *Penicillium sp.* (Metz *et al.*, 1979), *Streptomyces aureofaciens* (Tuffile and Pinho, 1970), *Streptomyces niveus* (Steel and Maxon, 1966), *Streptomyces fradiae* (Ghildyal *et al.*, 1987) and *Saccharopolyspora erythraea* (Gavrilescu *et al.*, 1992, Warren *et al.*, 1995) have shown to produce a shear thinning (pseudoplastic) behaviour.

The high viscosity of mycelial fermentations affects the rate of oxygen transfer to the liquid. In Newtonian broths the k_La depends on the degree of agitation whereas, in non-Newtonian systems k_La has also been shown to decrease with increasing apparent viscosity (Tuffile and Pinho, 1970, Wang and Fewkes, 1977, Carrington *et al.*, 1992). In *Streptomyces* cultures it is not only the solubility of oxygen but the transfer of oxygen to the cell surface which is the limiting step in aeration (Bushell, 1988). To maintain sufficient oxygen supply to a viscous filamentous mycelial culture a high degree of agitation and hence, power input is required to produce adequate mixing. As the cell concentration increases then the viscosity would increase, with a reduction of the rate of oxygen transfer. An increase in agitation could reduce the broth viscosity due to the shear thinning behaviour of the mycelial broth. For viscous broths this tends to result in a low viscosity region around the impellers of a stirred tank which is well mixed with respect to oxygen and heat transfer. The shear rate decreases from the impeller region of a stirred tank towards the wall of the vessel. As a result broth viscosity will increase with increasing distance from the agitator in a stirred reactor. This leads to poor mixing and mass transfer rates with increasing distance from the impeller blades. Thus the microorganisms leaving the impeller region may experience dissolved oxygen tensions below the critical value for maximum rate of product formation and growth which may effect the overall productivity performance of the vessel (Lilly, 1983). Thus stirred tank reactors for mycelial culture require high pumping power from the impeller, to circulate broth through the high shear region and thus, avoid producing stagnant zones of oxygen limitation near the vessel wall (Stanbury and Whitaker, 1984). Wang and Fewkes (1977) demonstrated with a *Streptomyces niveus* culture that the ratio of impeller rotational speed to impeller diameter affected the critical dissolved oxygen tension in an exponential manner. Steel and Maxon (1966) designed multiple rod mixing impellers to reduce the power requirement of mycelial cultures and solve the oxygen starvation problem.

Increased agitation can improve the oxygen transfer rates in a viscous broth leading to improved growth and productivity. Koenig *et al.* (1981b) observed an increase in penicillin production when the stirrer speed was increased from 700 rpm, with oxygen limitation to 900 rpm. However, high agitation at 1500 rpm produced similar productivity as with agitation at 700 rpm but higher growth rates than at 900 rpm. This gives some evidence, as did the work of Dion (1954), that the shear forces associated with high energy dissipation rates into a stirred tank can cause mechanical damage to

filamentous broths. The damage could occur from the change of pressure which occurs over the blade from the back of the impeller to the impeller tip and the shear stresses created from the turbine tip (Markl and Bronnenmeier, 1985). The microorganisms may be able to recover from the exposure to the high shear zone and the damage may not occur instantaneously but gradually due to the hydrodynamic stresses. Smith *et al.* (1990) observed a decrease of the penicillin production rate and effective hyphal length at high agitation speeds with a glucose fed batch fermentations of *P. chrysogenum* in a complex media. Smith *et al.* (1990) proposed a hyphal break up model which assumed that hyphal breakup depended on the frequency of mycelial circulation through the zone of high energy dissipation around the impeller. The volumetric production rates produced good agreement with the circulation frequency ($1/t_c$) and P/D^3 which was the measure of the power dissipation from an impeller. The morphological measurements were not sufficient to correlate the model with the morphology changes. Makagiansar *et al.* (1993) studied the morphology and penicillin production from *P. chrysogenum* P1 in batch culture from 5, 100 and 1000 dm^3 scale with tip speeds of 2.5 to 6.3 ms^{-1}. The main hyphal length and hyphal growth unit increased during the growth phase and then decreased to a constant value which was dependent on the energy dissipation. High agitation caused a reduction in the specific penicillin production rate and hyphal length. The branching frequency was increased and mycelial fragmentation occurred earlier in the fermentation with high agitation. Both the specific penicillin production rate and the main hyphal length agreed with the hyphal breakup model of Smith *et al.* (1990) although improved correlations were produced by using P/D^3t_c. Belmar-Beiny and Thomas (1991) observed that an increase of agitation from 490 to 1300 rpm in a 7 L stirred tank caused earlier hyphal fragmentation of *Streptomyces clavuligerus* broth but did not effect clavulanic acid production.

For scale up agitation power/unit volume decreases with increasing scale of operation and so lower power input per unit volume results in larger mixing times and hence lower oxygen transfer rates. Therefore, a tank of 100 m^3, the mixing time of 100 s would result in a vessel heterogeneity even with Newtonian broths. The greater liquid height/tank diameter ratio of large scale tanks than lab. scale tanks results in gas moving upwards with limited backmixing. Also, the large hydrostatic pressure at the bottom of the vessel affects the dissolved oxygen distribution (Manfredini and Cavallera, 1983). The dissolved oxygen concentration (DOC) profile is also determined by the ratio of the rates of gas transfer and vertical bulk mixing. If the time constant of the rate of oxygen transfer is shorter than the mixing time then vertical DOC gradient will be observed (Buckland and Lilly, 1993). Manfredini and Cavallera (1983) observed DOC gradients during chlortetracyline and tetracycline production by strains of *Streptomyces aureofacians* in a 112 m^3 stirred tank. Dissolved oxygen gradients varied from 45% (air saturation) near the liquid surface to 62% at the lower impeller at 90 h into the chlortetracycline fermentation. At 137 h of the 150 h fermentation the dissolved oxygen

changes varied between 22% to 36% near the base of the vessel. Radial dissolved oxygen gradients between 22% near the impeller to 3% air saturation nearer the vessel wall were observed by Oosterhuis and Kossen (1984) during the fermentation of *Gluconobacter oxydans* in a 19 m^3 reactor. Thus the DOT reading is dependent on the positioning of the probe in the vessel. This reactor heterogeneity can result in the microorganisms at large scale experiencing changing environments of substrate (especially with fed batch operation), oxygen, pH and nutrients which may effect growth and productivity (Sweere *et al.*, 1988a). Buckland and Lilly (1993) concluded that the impact of rapid fluctuations in nutrient concentrations, including DOT in large vessels, is still poorly understood. Compartment models have been used to model the mixing heterogeneity observed in large scale vessels. For example, Bajpai and Reuss (1982) used a two zone mixing model where the tank is considered to be two zones, a small micromixed zone and a macromixed zone, where the elements are separated. Similarly, Oosterhuis and Kossen (1984) proposed a five compartment model to successfully predict the dissolved oxygen concentration (DOC) gradients of a 19 m^3 reactor as described above. At large scale, cells experience the changing environment which depends on the residence time distribution of the cells in the different zones of the vessel. Consequently, the circulation time distribution (CTD) is important for scaling the fluctuations observed in a large scale fermenter for the scale down compartment model simulations (Mohan *et al.*, 1995). The CTD is the distribution of probabilities for the time intervals that fluid takes to return to a fixed reference position after circulating through a tank. Thus, the cells will experience a log normal distribution of circulation times so the cells would experience circulation times and hence, dissolved oxygen heterogeneity in a random manner.

The following examples describe some of the model simulation systems used to study the impact of cycling dissolved oxygen tension on growth and production of microorganisms and particular attention will be made to the effect on antibiotic production.

Single tank compartment models have been used where the dissolved oxygen tension (DOT) fluctuates with a fixed frequency in a square or sine wave fashion by either varying the inlet gas composition or the fermenter head pressure to alter the liquid phase dissolved oxygen concentration. Sweere *et al.* (1988a) studied the impact of DOT fluctuations on baker's yeast production and relatively fast fluctuations in DOT with a frequency of 1 or 2 min^{-1} (reciprocal value of the sum of the air sparged period and the nitrogen sparged period) resulted in a reduction of the biomass concentration and an increase in metabolites, ethanol, acetic acid and glycerol. Abel *et al.* (1994) observed similar effects on baker's yeast where the aeration frequency of 0.27 min^{-1} and DOT variation from 67% (air saturation) to 0% every 60 seconds reduced the final biomass concentration and growth rate on glucose by half, and the metabolite concentration (ethanol and acetaldehyde) increased when compared to the control fermentation. The

fluorescence intensity indicated that respiratory metabolism changed periodically into a respiratory / repressive one during the DOT variation.

Yegneswaran *et al.* (1991) used the Monte Carlo method to simulate DOT fluctuations which used a random circulation time from the CTD. A log normal distribution of the air supply was used to cycle the DOT by on-off cycling of the air supply which involved supply of air for 5 s, followed by no aeration which ranged from 8 to 44 s with a mean time of 20 s. This resulted in a suppression of the production of cephamycin C and its precursors from *Streptomyces clavuligerus* when compared to continuous air supply operation. The Monte Carlo method produced a 44% reduction of the yield of cephamycin C when compared to a constant cycling period with air turned on for 5 s and then off for 20 s.

The Monte Carlo method was also used by Namdev *et al.* (1993) to study the effect of fluctuating DOT on a recombinant *E. coli* fermentation. The period of each cycle was selected by the Monte Carlo algorithm from a log-normal distribution of liquid circulation times with a mean of 20 s and a standard deviation of 8.9 s which characterised the bulk circulation of a typical large fermenter. The air was turned on for 5 s during each cycle. The oxygen uptake rate, carbon release and the onset of the second batch culture growth phase were affected by the rapid changes of DOT compared to continuous aeration operation. Also, the cycling DOTs prevented the amplification of the plasmid which occurred during the stationary phase with continuous aeration.

Suphantharika (1992) used a single lab. scale tank (20 L) with time pulsing of the nitrogen and oxygen supply to study the effects of DOT gradients on difficidin and oxydifficidin production from *Bacillus subtilis*.. Both difficidin and oxydifficidin were unaffected by DOT cycling around the critical DOT (C_{crit}) for difficidin production of 20% (air saturation) with a variation of 10% DOT and period of 30 s. However, cycling the DOT below the C_{crit} with the same amplitude and frequency had no effect on the antibiotic production, but resulted in an increase in biomass production rates.

Vardar and Lilly (1982) used a cycling head pressure method which sinusoidally varied between 1 and 2 bar in a 7 L stirred tank to simulate the effect of fluctuating DOT on penicillin production from *P. chrysogenum*. Cycling DOT from 23 to 37%, around the C_{crit} for penicillin production of 30% air saturation with a period of 2 minutes, resulted in a 30% reduction of the q_{pen} and DOT cycling between 10 - 15% with the same frequency resulted in a 70% reduction, when compared to production with the constant DOT conditions of 30% air saturation.

Two compartment model systems have been used consisting of a well mixed compartment with high dissolved oxygen concentration which is sparged with air, or a combination of air and nitrogen to control the DOT and this simulates the well mixed region around the impeller of a large scale vessel. This tank is connected to the second compartment, with low DOT close to the saturation constant of the microbial kinetics for oxygen in the other parts of the vessel. This is sparged with nitrogen to simulate the

poorly oxygenated zones near the impeller. The mean liquid circulation time and hence, the CTD can be controlled by altering the volumes of the two tanks and the circulation rate between the tanks. Sweere *et al.* (1988b) used a two compartment system with continuous culture and showed that the metabolism of baker's yeast was not effected until the cells experienced DOT below 1% for 15 s before returning to 30% DOT (% air saturation) of a 30 s circulation time. A circulation time of 50 s resulted in the cells experiencing DOT below 1% for a duration 25 s before returning to 30% in the aerated tank. The biomass yield was reduced by 50% and ethanol formation occurred, when compared to the continuous culture with continuous aeration at 30% DOT.

Abel *et al.* (1994) used a two compartment plug flow model where the well mixed stirred tank with a volume of 2550 ml was connected to a plug flow reactor with a volume of 450 ml. The biomass yield of baker's yeast was reduced and ethanol production increased if the cells experienced DOTs below 1% for 60 s with DOTs above 50% air saturation in the well mixed tank. However, the biomass yield was not effected when the cells spent a 10 s duration at DOT of 2%.

Larsson and Enfors (1988) showed that the passage of the whole of a *Penicillium chrysogenum* culture through the anaerobic plug flow reactor of a two compartment model resulted in a irreversible inhibition of respiration. This was with circulation times of 5 and 10 minutes, an anaerobic volume of 6% and DOT above C_{crit} (35%) in the well mixed stirred tank. Circulation times of 1 and 2 minutes with an anaerobic zone of 1% of the stirred tank did not produce any irreversible effects on the respiratory capacity.

A few examples exist of the use of loop reactors for scale down studies. Katinger (1976) used a tubular loop reactor to scale down a CTD to simulate substrate and oxygen concentration gradients observed in large scale recycle fermenters. Liquid circulation times were around 80 s with mixing times in the region of 5 min. The impact of two types of periodicity, 15 to 20 min and 3 to 8 min, with DOTs of 35 to 60% and 2 to 10% saturation were studied on the continuous culture of *Candida tropicalis* on n-alkanes. The biomass yield on substrate increased and the respiratory quotient and oxygen demand decreased when the oxygen limitation was intensified by an increase in feed rate or decrease in aeration rate.

Kristiansen and McNeil (1987) used a loop reactor to study the effect of liquid circulation times used at production scale on the growth on *A. pullulans*. The broth was circulated by a peristaltic pump with aeration at one point into the configuration. The morphology and production of polysaccharide was found to be dependent on the circulation time and the scale of the configuration could be determined from their results. The same loop reactor was used to simulate DOT gradients and there effect on *S. cerevisiae* (McNeil and Kristiansen, 1990). The sparging of gas into one section of the vessel, the riser, resulted in DOT gradients in the riser and downcomer. The biomass concentration decreased and ethanol production increased as the circulation time was varied from 10 to 100 s. The metabolism of the yeast cells when experiencing circulation

times of 10 s was found to be similar to a 10 L stirred tank, although no information was provided on the circulation time and DOT in the stirred tank. The CTD was not measured with the reactor, so this situation was less representative of the situation at large scale as only the mean circulation time was used.

Brandes *et al.* (1993) used a 60 L airlift tower loop reactor to study the effect of heterogeneity in large reactors on the stability of a temperature induced plasmid in *E.coli.*

1.1.4.2.2 Erythromycin production

The most significant commercial product from mycelial fermentations is the production of antibiotics. Products such as penicillin, tetracycline, erythromycin, cephalosporins, cephalomycins and clavulanic acid are made at large scale from 50 to 200 m^3 (Buckland and Lilly 1993). The widespread use of penicillin since the 1950s has meant that a large amount of literature can be found regarding penicillin production and its process development. However, only a small number of literature examples exist concerning the production of antibiotics such as erythromycin and clavulinic acid. The lack of published papers is presumably due to the commercial sensitivity of the research.

Erythromycin is produced from the filamentous actinomycete *Saccharopolyspora erythraea.* This organism is similar to *Streptomyces sp.* except that the cell wall contains large amounts of mesodiaminopimelic acid and no mycolic acid. This led to reclassification of the filamentous, spore producing organism from *Streptomyces erythreus* to *S. erythraea* in 1987 (Holt, 1989). The wild type strain NRRL 2338 was first obtained from a soil sample obtained in the Philippines by the Lilly Research Laboratories, Indianapolis in 1952 (McGuire *et al.*, 1952). The therapeutic action of erythromycin is mainly bacteristatic action at low concentrations 0.01-0.5 $\mu g\ mL^{-1}$ by binding covalently to the 50 S sub unit of the intact prokaryotic ribosomes. Bactericidal action has been reported at high concentrations above 2.5 $\mu g\ mL^{-1}$ (against *S. aureus*). Erythromycin is a macrolide antibiotic which consists of a 14 membered macrocyclic lactone ring to which sugars are attached (Garrod *et al.*, 1981). All the types of erythromycin shown in figure 1.1 have a desosamine ring but vary from four R groups. Erythromycin A and B have cladinose sugar, whereas erythromycin C has a mycarose sugar. Erythromycin A is usually the main product with B, C, D, E and F as minor components. The precise route and influences on the biosynthetic pathway is still under investigation however, five primary metabolism components are known to be involved in erythromycin production, propianate, 2-methylmalonate and oxygen, glucose and S-adenosyl- L-methionine (Corcoran and Hahn, 1975). A proposed pathway to produce the macrolactone ring attached to two sugar residues (figure 1.2), involves the sequential condensation of 6 methylmalonates to a propionate primer, followed by ring closure and sugar attachment (Higashide, 1984). Erythromycin production has been observed to take place during the transition from logarithmic growth phase to stationary phase when a specific nutrient becomes growth rate limiting (Stark and Smith, 1961) or after the growth

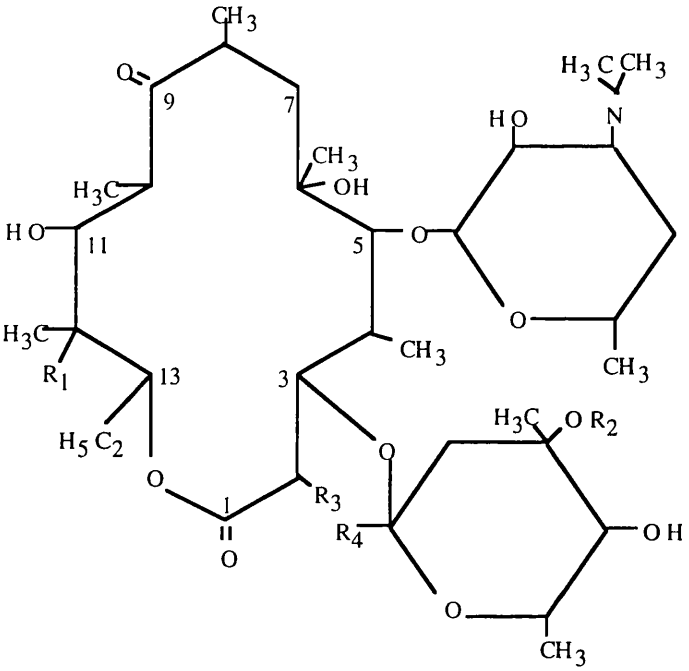

Erythromycin	R_1	R_2	R_3	R_4
A	OH	CH_3	CH_3	H
B	H	CH_3	CH_3	H
C	OH	H	CH_3	H
D	H	H	CH_3	H
E	OH	CH_3	CH_2 ----- O	
F	OH	CH_3	CH_2OH	H

Figure 1.1 Chemical structure of erythromycin (Corcoran and Hahn, 1975, Higashide, 1984)

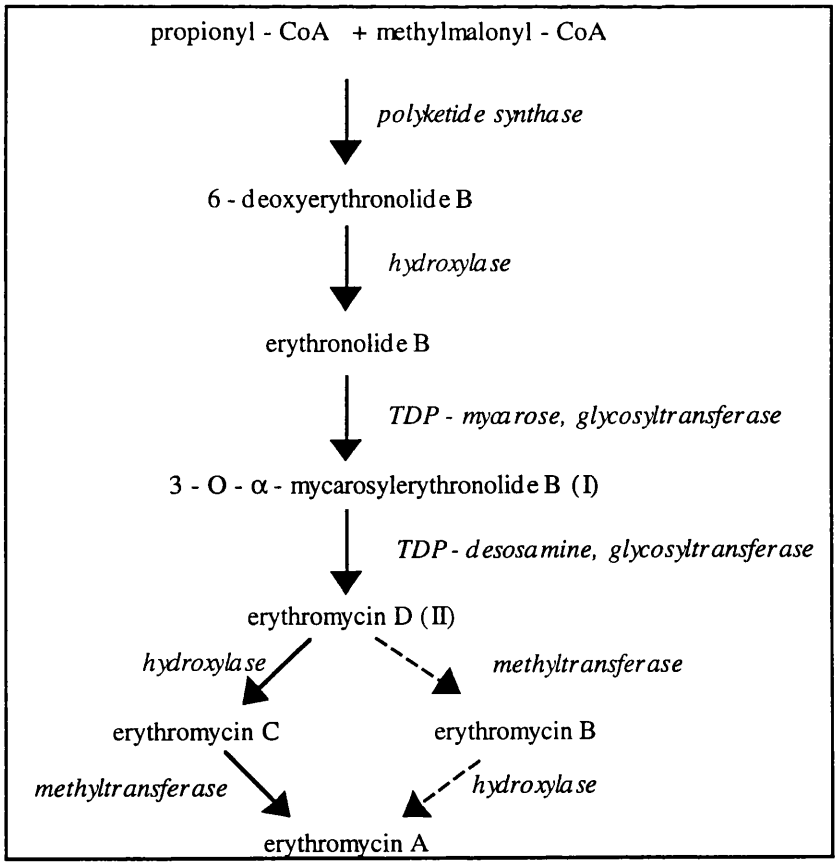

Figure 1.2 The biosynthetic pathway for erythromycin (Higashide, 1984, Divers, 1990)

phase (Queener and Day, 1986). The carbon and nitrogen source decrease during growth phase and some erythromycin production occurs. Stark and Smith, 1961 argued that once the nitrogen source is depleted, carbohydrate is then available for antibiotic production. Hence, the majority of erythromycin at a fast linear production rate occurs after the growth phase. Trilli *et al.* (1987) found evidence to suggest that erythromycin production was strongly linked to the growth phase from the close relationship between the specific growth rate and specific erythromycin production rate from a phosphate limited chemostat culture. Nitrogen limiting media have been found to produce greater yields of antibiotic than carbon limited due to the repressive effect of ammonium salts on erythromycin production (Flores and Sanchez, 1985, Potvin and Peringer, 1994). Glucose, fructose or sucrose are all useful carbon sources for erythromycin production (Corum *et al.*, 1954) although D-glucose may have a repressive effect at high concentration (100 gL^{-1}) (Wallace *et al.*, 1992, Escalante *et al.*, 1992). Glycine, glutamine, alanine, serine, valine, leucine, threonine, betaine and aspargine are appropriate nitrogen sources for growth and erythromycin production (Stark and Smith, 1961). Typical complex industrial media for erythromycin production include corn starch, soybean meal, corn steep, and soybean oil as used by Abbott Laboratories (Martin and Rosenbrook, 1967). The fed batch control of erythromycin with carbon source feeding is the usual industrial procedure for optimising erythromycin production (Warren, 1994). The mineral requirements for erythromycin production include magnesium and phosphate which are the most critical, followed by iron, zinc, cobalt, and calcium (Stark and Smith, 1961). Of the cited literature which use pH control, the optimum for erythromycin production is between pH 7-7.2 (Osman *et al.*, 1968, Warren, 1994) and the optimum temperature is between 30 - 35^{0}C (Kuznetsov, 1985). Only a few studies have been published on the impact of the engineering environment on erythromycin production which is necessary for process optimisation. Brinberg (1959) showed that erythromycin production was unaffected by the aeration rate when using a nutritionally weak medium containing 2% glucose and oxygen transfer rates of 18 $mgO_2.L^{-1}.min^{-1}$ were satisfactory. However, in a richer media erythromycin production only occurred with more vigorous aeration (29.6 $mgO_2.L^{-1}.min^{-1}$). It was suggested that it was due to an increase in cell mass or a specific action in supplying a greater amount of a specific intermediate.

Nash (1974) studied the effect of carbon dioxide on the growth and erythromycin production of *S. erythraea* in a 68 L stirred tank. Carbon dioxide was added to the incoming air at 0.1 vvm or 11% of the inlet air from 15 h into the 138 h fermentation. The exposure of the cells to increased partial pressure of carbon dioxide inhibited synthesis of erythromycin by 40% but had no effect on growth. The inhibition of erythromycin production was not due to a reduction in pH as it remained between 6.8 and 7.0 in both carbon dioxide sparged and unsparged systems.

Paca *et al.* (1978) found that erythromycin production was proportional to the power dissipation which was studied up to 4000 Wm^{-3} in a 300 L stirred tank. This may have been due to limiting effect of the DOT which was below 30% saturation during the production phase for the range of power inputs studied. Klein (1994) found that the specific erythromycin production rate (q_{ery}) was reduced by 3 fold when the DOT remained below 10% for the duration of 10 h during a 100 h *S. erythraea* fermentation in a 7 L stirred tank, when compared to the production at DOTs above 60%. However, the different DOTs regimes occurred from increased stirred speed, 250 to 500 rpm, which may also effect erythromycin production from the influence of agitation on morphology. Klein (1994) also provided evidence to suggest that erythromycin production was reduced and cell breakage (protein release) increased by a 2 fold increase of energy dissipation from 3000 to 14400 Wm^{-3} which correlated well with the breakup theory of Smith *et al.* (1990). Both Carrington *et al.* (1992) using a 20 m^3 bubble column and Roman and Gavrilescu (1994) with a 20 m^3 stirred tank showed that k_La decreased during the fermentation of *S. rimosus* and Carrington showed that k_La decreased exponentially with increasing broth viscosity.

1.1.4.2.3 Filamentous fermentations in airlift reactors

Airlift reactors have been used for the fermentation of filamentous fermentations due to the low power requirements and low shear characteristics when compared to stirred tanks. Malfait *et al.* (1981) produced an 18% dry cell weight enhancement in the yield of a filamentous mould *Monascus purpureus* in an external loop airlift (0.55 m^3) relative to that in a stirred tank. The yield improvement was achieved with a reduction in power input leading to a reduction in the cost of biomass. The airlift reactor was associated with a higher overall mass transfer coefficient than with the stirred tank and this was associated to the increased productivity. Malfait *et al.* (1981) claimed that shear damage to the cells in the stirred tank may contribute to its poor production. Schugerl (1990) compared the performance of airlift and stirred reactors for the production of secondary metabolites from mycelial cultures. The comparison was based on: a) physical properties such as oxygen transfer and volumetric mass transfer coefficient, b) cell mass productivity, c) productivity of primary and secondary metabolites and the efficiency of formation with regard to specific power input and substrate consumption.

The production of penicillin V by *Pencillium chrysogenum* in stirred tank and airlift tower loop reactors has been studied. *P. chrysogenum* can form highly viscous filamentous mycelia as well as pellet suspensions of low viscosity. Schugerl claimed that a high specific power input (4 - 5 kW m^{-3}) was needed to reduce the effective viscosity of the pseudoplastic medium and to supply the cells with sufficient oxygen. When pellets were formed, the viscosity could be reduced by a factor of 4 - 5 and maximum productivity occurred with a pellet diameter of 400 μm. As the pellet size can not be reduced in an airlift reactor, the inoculum must contain cells which are able to form pellets

with the optimum size and density after the growth phase. Schugerl produced the optimal size pellets in the airlift reactor by using a suitable media composition and inoculum prepared in the stirred tank. The media for the tower loop reactor was a 50% dilution of that used in stirred tanks. Schugerl found that operating airlift reactors with optimal pellet size and operating conditions made them more suitable for penicillin production than stirred tank reactors, since the latter cannot maintain optimal pellet size due to the variation of the energy dissipation rate. Therefore, without the adaptation of cell morphology to the reactor Schugerl claimed that it would not be possible to produce penicillin in airlift reactors. The penicillin production with regard to oxygen and substrate consumption and power input was greater in the airlift but, penicillin production (kg m^{-3} h^{-1}) was higher in the stirred tank, leading to a preference for the stirred reactor.

Cephalosporin C production by *Cephalosporin acremonium* in stirred tank and airlift reactor was also studied. Again the process had to be adapted for the airlift. The fermentation media was found by Schugerl to be highly viscous due to cell mass and peanut flour. Oxygen transfer was low and hence poor production occurred in the airlift reactors. Reducing the amount of peanut flour allowed sufficient oxygen supply. Volumetric productivities were higher in stirred tank than in airlift but specific productivity and yield coefficients were higher in airlift. The cost structure of production indicated that specific production was more important than volumetric production because of the high fraction of variable costs.

The third system that Schugerl (1990) studied was tetracycline production in airlift and stirred vessels by *Streptomyces aureofaciens.* Schugerl was unable to produce pellet formation in stirred reactors however, pellets of 200 μm diameter were formed in airlift reactors. Adjusting the medium dilution in the airlift reactor produced higher specific productivities and yield coefficients with pellet suspensions than mycelial cultures with stirred tank. This demonstrated that higher specific productivities and yield coefficients could only be obtained in the airlift reactor if pellet suspensions were used when compared to mycelial suspensions in the stirred tank. Schugerl (1990) concluded that it is necessary to reoptimise the process for new reactors. The three examples, indicated that optimal medium composition depends on reactor type and for penicillin and tetracycline production, reductions in inoculum size and quality were necessary. Koenig *et al.* (1981a) also found that much lower specific power inputs and higher penicillin yield coefficients with regard to biomass production, and lactose and oxygen consumption were achieved by operating a bench scale bubble column with a pelleted suspension of *P. chrysogenum* rather than a mycelial broth in a bench scale stirred tank.

The poor performance of an airlift reactor with viscous broths was observed by Suh *et al.* (1992) for xanthan gum production from *Xanthamonas campestris.* The high apparent viscosity in the airlift reactor (1.2 m^3) led to 40% lower oxygen transfer than in the well mixed bubble column (0.05 m^3) and the xanthan gum production rate was up to 2 fold lower than in the bubble column. The local non uniformity of the oxygen transfer

rate in the airlift reactor was shown to be the main cause of the low xanthan productivity. However, stagnant zones may also exist in stirred tanks as the xanthan production yield was greater in the stirred tank (1.5 m^3) fitted with Intermig impellers than in the airlift reactor, but 30% less than the bubble column.

Trager *et al.* (1989) compared the growth of *Aspergillus niger* and production of gluconic acid in a laboratory and pilot plant airlift (0.26 m^3 working volume) with stirred reactors. Fermentations in stirred and airlift reactors were completed simultaneously and the inoculum was mycelial type. Trager reported fine pellets in the airlift but mycelia in the stirred tank after 6 hours. The dissolved oxygen concentration was higher in the airlift than stirred tank at the end of the fermentation. Trager *et al.* (1989) reported that this may be due to small pellets in the airlift allowing higher mass transfer than the stirred tank where the suspension viscosity was higher. The gluconic acid production was similar in the laboratory airlift and stirred reactor at 85 - 90% w/w conversion of glucose to gluconic whereas, 98% was achieved with 0.26 m^3 airlift reactor.

Therefore various researchers have demonstrated that the airlift reactor can be used for the growth of mycelial cultures and production of secondary metabolites. In general, efficiencies of oxygen transfer and specific productivities with regard to power input, substrate and oxygen consumption are considerably higher than in stirred reactors. In stirred tanks the cell mass concentrations, volumetric productivities and specific power inputs are higher than in airlift reactors.

Metabolite production has also been investigated using immobilisation technology in airlift reactors with unicellular and mycelial microorganisms. Guo *et al.* (1990) studied the growth kinetics and amylase production of immobilised *Bacillus subtilis.* A lab. scale glass tubed reactor was used with 400 mL total volume and carrageenan gel entrapment techniques. The productivity of amylase by the immobilised cells was found to be significantly greater than that by free cells. The performance of immobilised *Arthrobacter simplex* for the dehydrogenation of hydrocortisone in a 4.3 L external loop airlift reactor compared favourably to that in a stirred tank (Kloosterman and Lilly, 1985). The physical stability of the calcium alginate beads was significantly greater in the airlift reactor. A continuous penicillin production system was developed by Keshavarz *et al.* (1990) which incorporated spores of *Penicillium chrysogenum* strain P2 immobilised on celite and was successfully scaled up to pilot plant scale (0.32 m^3). Penicillin and the ACV dimer were still synthesised after 500 h of operation. The production of thienamycin was produced from the successful immobilisation of *Streptomyces cattleya* cells to celite particles in a bubble column (Arcuri *et al.*, 1983). Continuous reactor operation at a high dilution rate was used during the growth phase for successful immobilisation. Citric acid was produced from glucose in continuous bench scale airlift cultivations by calcium alginate immobilised yeast cells of *Yarrowia lipolytica* (Rymowicz *et al.*, 1993). A bench scale concentric airlift reactor was found to produce greater enzyme stability when compared to a stirred tank with immobilised enzyme pellets of

penicillin acylase (Chang *et al.*, 1994). The lower shear stresses of the airlift reactor were suggested to be the reason for the reduction of enzyme fragment breakage.

1.2 Airlift configurations and design

1.2.1 Introduction

Airlift fermenters can be divided into two groups depending on the type of liquid recirculation employed (figure 1.3). External loop vessels have the riser and downcomer separated from each other by connecting horizontal sections near the top and bottom (figure 1.3f). These reactors usually have longer residence times for gas-liquid separation than the internal loop reactors (Choi, 1990). The internal loop reactors such as the concentric tube reactor contain the riser and downcomer in the same vessel. A cylindrical column contains an inner draft tube which separates the riser from the downcomer (figure 1.3c). Air is sparged at the base of the reactor which can travel up the draft tube and down the annulus, the downcomer or annulus can be sparged and hence the flow can be reversed. Split cylinder reactors have the draft tube divided into sections to increase communication between the riser and the downcomer (figure 1.3d) which increases oxygen transfer (Chisti and Moo-Young, 1987).

1.2.2 Airlift reactor geometry

An important section of the concentric and split reactors is the top section or gas separator which connects the riser to the downcomer. The region largely dictates the extent of gas disengagement and subsequently gas recirculation, downcomer gas holdup and the pressure difference between the riser and downcomer. Therefore, the design of the top section has a major influence on the liquid velocity of the airlift reactor. The top section also has an important function in the mixing of the liquid within the vessel. The mixing performance has been shown to increase with increasing liquid volume in the gas liquid separator up to a certain size, after which no further change in performance occurs (Chisti, 1989, Weiland, 1984, and Russell *et al.*, 1994). Siegel and Merchuk (1991) investigated the influence of gas-liquid separator configurations in airlift reactors. They were able to manipulate the disengagement properties and hence the fluid residence time and gas recirculation rate of an airlift reactor while keeping all other major design parameters constant. The top section had been designed so that movable baffles were controlled to change the reactor configuration from an external to an internal loop. They demonstrated external loop reactor characteristics by operating the reactor with an enlarged top section with a clear zone of horizontal two phase flow. High gas disengagement in the separator, low gas holdup in the downcomer, and relatively high liquid velocities were observed. In the concentric airlift, changing the liquid level had no significant effect on the riser or downcomer gas holdup. Thus liquid levels above the draft tube were not sufficient to cause additional turbulence in the top section which

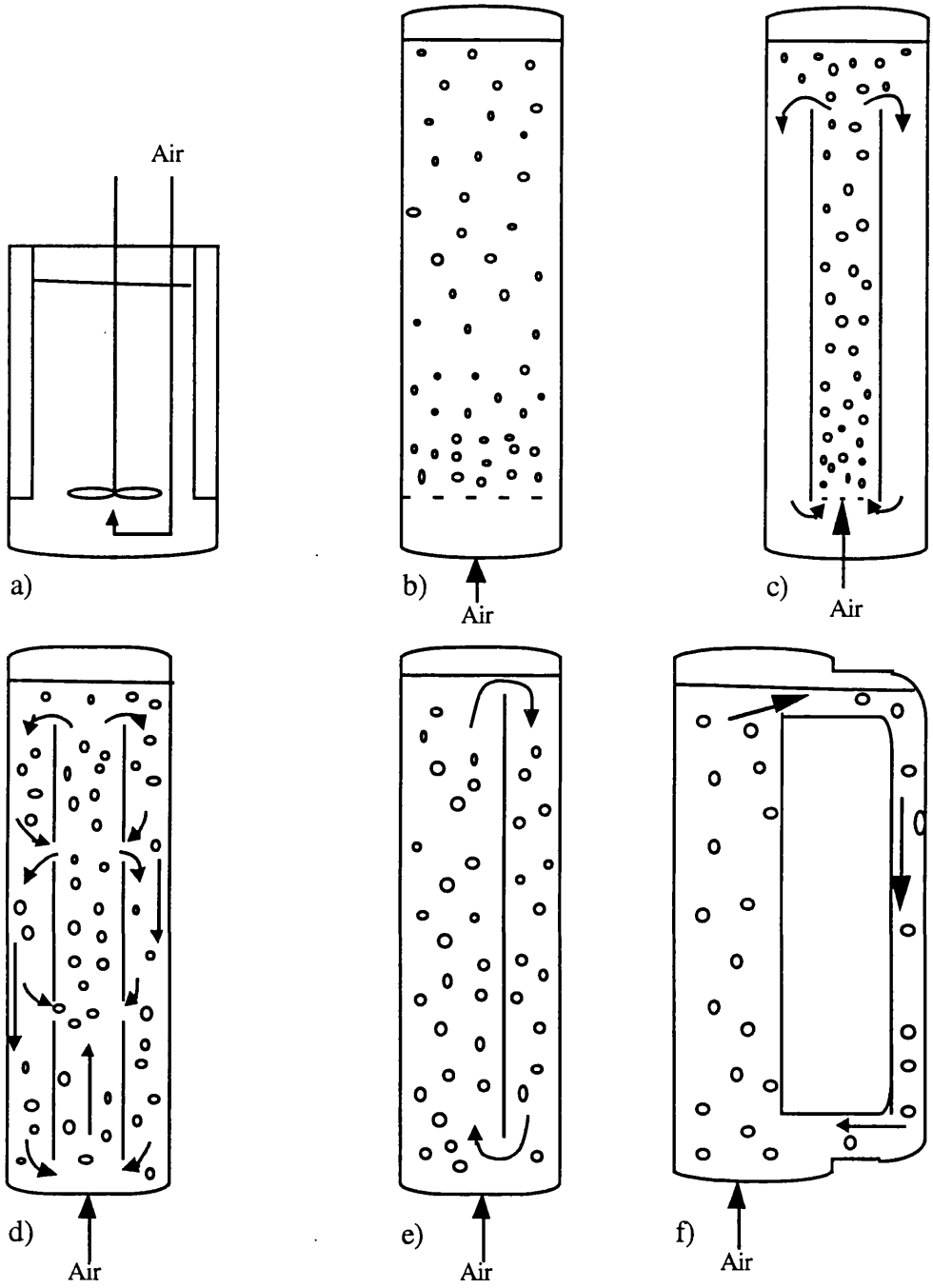

Figure 1.3 Types of bioreactor (idealised) : a) stirred tank, b) bubble column, c)concentric draft tube airlift, d) concentric split draft tube airlift, e) Split cylinder internal loop reactor, f) external loop.

would cause increased gas entrainment into the downcomer. Russell *et al.* (1994) reported that liquid velocity and sectional gas holdups were found to be independent of the top section height in a concentric airlift reactor. This led to the conclusion that the downcomer is essentially independent of the size of the top section. Other important parameters in the design of the concentric airlift reactor are the ratio of height to diameter (H/D) and ratio of the cross sectional area of the riser to that of the downcomer (A_D/A_R). The large ratios of H/D give airlift reactors there slim design and industrial reactors can

have ratios up to 10 (Choi, 1990). These high ratios allow high utilisation of oxygen, efficient mass transfer, mixing and circulation properties (Onken and Weiland, 1983).

1.2.3 Mechanical agitation in air sparged reactors

The power required for mixing and mass transfer in bubble columns and airlift reactors is supplied by the circulation of air from spargers, but some reactor designers have studied increased reactor performance by the addition of impellers. Possible increases in performance of a system will then be dictated by the type of impeller used and its positioning within the vessel. The characteristics of different impellers have been studied in stirred tanks. The introduction of power into a stirred tank can be made by a variety of impellers of which the most common are the disc turbine, pitch blade, and the marine propeller (figure 1.4). The disc turbine has four or six blades mounted on a disc. The disc limits the short circuiting of gas along the drive shaft. The disc stirrer is a radial flow impeller whereby the radial and tangential velocity components are nearly equal in magnitude at the impeller tip. The tangential component decreases more rapidly than the radial distance. The average velocity, which is taken as the radial and the tangential flow together, is maximum at a certain distance from the impeller tip (Sachs and Rushton, 1954). The pitched blade turbine produces axial flow with the radial flow proportional to the projected blade width (figure 1.4b).

The propeller produces an axial flow regime (figure 1.4c). Joshi *et al.* (1982) found that the position at which maximum velocity was realised depended on the pitch of the propeller blade. The cross sectional area of the flowing stream from the impeller did not depend on the impeller speed and is only a function of the vertical distance from the impeller plane. Hence, Joshi concluded that the extent of entrainment is not a function of the impeller speed, but at higher impeller speeds the discharge velocity only increases, increasing the discharge flow rates.

The traditional power curves, power number (Np) versus stirrer based Reynolds number for impellers in a single phase have been used to characterise an impeller with a power number. The turbine impeller has N_p values between 5.5 - 6.5 for a fully turbulent system (Re > 10,000) which are higher than for a pitched blade (1 - 3) and propeller (0.1 - 1) (Van't Riet and Tramper, 1991). Therefore, relatively more energy is supplied to the liquid and consumed energy is proportional to the pumping capacity of the stirrer. As mixing and mass transfer are a function of power consumption, the stirrer with the highest power number should be used for a stirred tank (Smith, 1985).

The discharge efficiency of impellers can be used to compare their performance. Rushton and Oldshue (1953) expressed pumping capacity as a function of the agitator diameter:

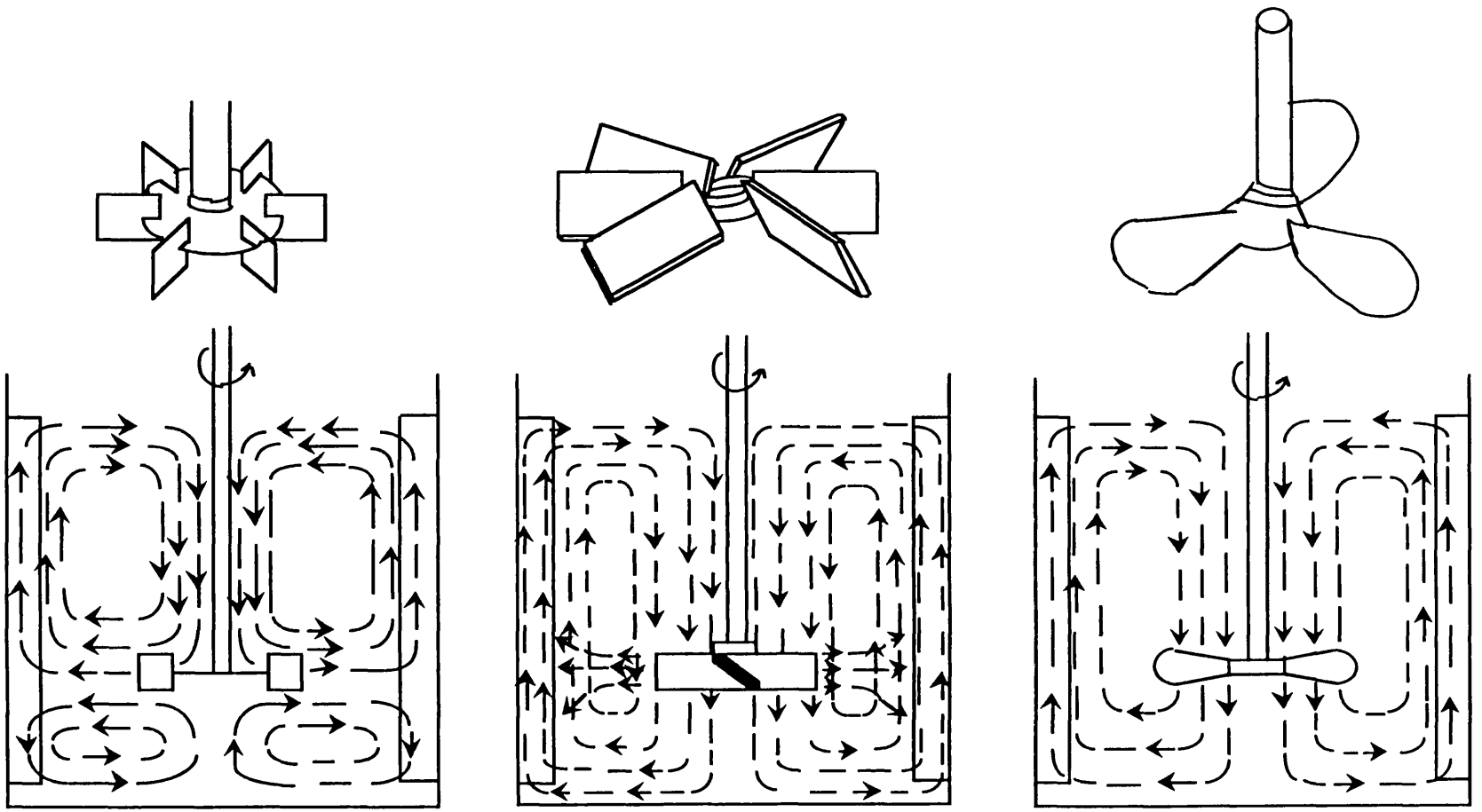

a) disc turbine-radial flow b) pitched turbine-axial and radial flow c) marine propeller-axial flow

Figure 1.4 Schematic diagram of three impellers and the flow regimes in baffled stirred tanks (unaerated) (Joshi *et al.*, 1982)

$$Q = N_Q N D^3 \qquad 1.1$$

where

N_Q = dimensionless discharge coefficient (–)

Q = pumping capacity: liquid volumetric flow rate ($m^3.s^{-1}$)

Various researchers have found different values of N_Q for different impellers, but they all show the general conclusion shown by Joshi *et al.* (1982) that N_Q for a turbine is higher than using a pitched blade or propeller. Also Nagata (1975) produced values for the dimensionless discharge coefficient for various impellers in one phase stirred tanks. He compared the ratio of power number versus discharge flow number. For a turbine the ratio was 2.7, pitched blade 2.3, and for the propeller was 1.5 for impellers using the same geometry. A large ratio value as with the turbine, demonstrates that the discharge efficiency is low and the impellers are described as shear type. For low ratio impellers, such as the propeller, discharge efficiency is high and hence are called circulation impellers.

The different types of impeller have been shown by Van't Riet and Tramper (1991) to have different types of outflow effects from each blade. The disc turbine has been shown to produce a trailing vortex pair behind each blade of the turbine. The maximum shear rates occur not far from the vortex axis and are about five times greater than those that control the average shear rate as derived by Smith (1985). At low gas flow rates bubbles are drawn over the blades to form a gas cavity behind the blades, in which the bubbles lose gas by breakaway from the elongated tail into the rapidly spinning liquid. As the flow rate increases the cavities increase in size. At high gas flowrates the agitator pumping action ceases to dominate the circulation pattern. The cavities formed behind the blades extend the whole distance from one blade to the other producing a flooded impeller and ineffective gas dispersion. In high viscosity liquids the same effect was observed except higher stirrer speeds were required for gas dispersion.

The flow field around a pitched blade impeller differs from that produced by a Rushton turbine in that the circulation around the blade in axial flow produces a single tip vortex. The single tip vortex results in a less efficient capture of gas so some bubbles will pass through the impeller plane. Thus with a pitched blade there remains a downflow of small bubbles entrained in a convected downflow nearer the turbine axis. At high gas rates clinging cavities are formed. The pitched blade agitator is often chosen over the Rushton turbine as the combination of strong developed roll vortices leaving the impeller tips, together with the large displaced liquid volumes, makes it useful for maintaining solid suspensions from settling.

The propeller produces a strongly spinning tip vortex which extends a considerable distance downstream which is similar to that found with pitched impellers at low gas flowrates (figure 1.5). At higher gas flow rates, vortex sheets are produced trailing from the whole length of the blade (Smith, 1985, Brauer, 1979). The propeller

was found by Cooper *et al.* (1944) to flood at lower nominal velocities of air, based on cross sectional area of the vessel, superficial gas velocity of 0.0058 ms^{-1} compared to 0.033 ms^{-1} for disc turbines. The propeller was found to be less efficient at breaking up streams of air bubbles.

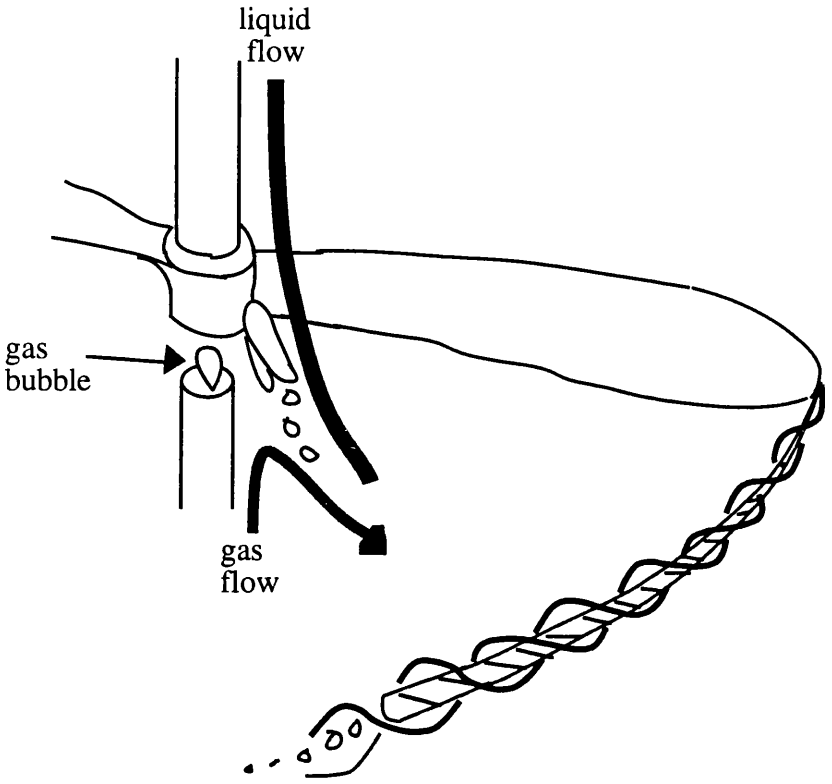

Figure 1.5 Bubble generation in vortex threads in the wake of a propeller stirrer (Brauer, 1979).

Therefore, by comparing the performance of the impellers it can be seen that the turbine is the most suitable for use in stirred tank fermenters. The turbine has a higher power number producing greater pumping power and mixing ability and hence greater shear rates throughout the vessel compared to the other impellers. The propeller has a lower power requirement, higher discharge coefficient, and axial flow which makes it suitable for a low shear circulation impeller.

The characterisation of impeller performance has enabled the study of combinations of impellers for the mixing of high viscosity broths in stirred tanks to be investigated. Anderson *et al.* (1982) used two different impellers driven on separate shafts. The top agitator was a positive pumping type, high flow, low shear 45^0 pitched blade agitator which was rotated slowly in a draft tube and moved the fluid around the vessel, while the other was a Rushton turbine rotated at high speed to disperse the gas. The Rushton turbine was the lower impeller as it is a good gas disperser and its power demand is not particularly increased with an increase in viscosity. The use of axial flow hydrofoil impellers has been investigated for retrofitting of stirred tanks for the mixing of viscous broths (Nienow, 1990). Improved mixing performance of a stirred tank was

observed using a A-315 Lightnin impeller than with a standard Rushton turbine for xanthan gum concentrations up to 25 kg m^{-3} (Galindo and Nienow, 1992).

The characterisation of the different types of impellers in stirred tanks has led to investigations into their use in improving airlift reactor performance. Blenke (1979) studied the performance of a propeller loop reactor. This was a tall bubble column with a H/D ratio of 5 - 10 containing a draft tube with a longitudinal driving marine propeller positioned in the middle of the tube facing downwards. Blenke concluded that the vessel was suitable for highly viscous fluids. The propeller loop reactor produced effective redispersion of coalesced gas bubbles, solid particles (cells) by the guided recirculation through the intense shear fields of the propeller.

The k_La of a conventional stirred tank was improved by using a stirred loop reactor by Keitel and Onken (1981). The stirred tank contained a concentric draft tube with the agitator between the ring sparger and the draft tube. Although the k_La was improved compared to that of the conventional stirred tank, lower gas holdups were obtained in the stirred loop reactor. A propeller instead of a Rushton turbine was found to produce smaller k_La values as gas dispersion was poorer. However, Keitel suggested the propeller may be favourable in conditions using low gas flow rates and low power consumption. Such reactor configurations have been studied for animal cell culture (Varecka and Bliem, 1990). The upward recirculation of liquid through a draft tube from the action of a propeller stirrer was found to improve the mixing and liquid circulation times with water compared to a conventional propeller only stirring in the range of low stirrer speeds upto 400 rpm in a 15 L reactor (Favre *et al.*, 1994).

Kawase and Moo-Young (1986a) studied the effect of a disc turbine on gas holdup and k_La in a bubble column with a draft tube. The 0.09 m diameter impeller was situated only 0.09 m below the liquid surface to promote localised bubble breakup. Over a range of impeller speeds it was shown that the impeller had little effect on gas holdup and k_La with water, but small improvements were observed with increasing propeller speed for CMC solutions. They concluded that the power input by mechanical agitation for water may be too small compared with that by the gas dispersion to increase the gas holdup or to improve the liquid circulation. For non-Newtonian fluids the agitator improved mass transfer and gas holdup by disrupting large spherical cap bubbles and increasing the gas-liquid surface area, rather than by enhancement of liquid circulation in the bubble column. Paca and Gregr (1976) added mechanical agitation (Rushton turbine) to each stage of a sieve tray bubble tower reactor to further improve oxygen transfer rates. This reactor could be more closely described as a multistage agitated tank tower. Other examples of impellers in tall aerated vessels is the use of a low shear marine impeller in a tall vessel which contained a fluidised bed around an internal draft tube. The propeller is situated at the bottom of a draft tube with the purpose of circulating cells and gas bubbles around the fluidised bed system (Reiter *et al.*, 1991). Imai *et al.* (1993) fitted a helical ribbon impeller to the outside of a rotating draft tube inside a 70 L working volume loop

reactor with annulus gas sparging. The helical ribbon aided the circulation of viscous broth, *A. oryzae,* up the outside of the draft tube and recirculation with the aid of a propeller inside the draft tube. Comparison details to other reactor configurations were not given in detail but, the mixing time with rotary draft tube operation was found to be shorter and amylase production greater than with tanks containing Rushton impellers.

Static methods have been used to improve vessel performance which comprise of perforated plates or static mixers to disperse large bubbles in the riser and improve oxygen transfer of the vessel. 19 perforated plates were installed at regular intervals in the 45 m tall riser of the ICI SCP high pressure concentric reactor (Smith, 1980). Kawase *et al.* (1993) improved the k_La values of an internal split tube airlift reactor containing carboxy methylcellulose solutions by installing four short draft tubes with their end sections covered by perforated plates. Potucek (1989) observed the increase of k_La from the installation of motion less mixers in the riser of a bench scale airlift reactor. The presence of 4 motionless mixers half way up the riser of an 80 L external loop reactor suppressed slug formation with a viscous *Cephalosporin acremonium* broth which improved the efficiency of gas dispersion and oxygen transfer (Zhou *et al.*, 1993). This produced a 13% increase of the maximal cephalosporin C volumetric productivity, and a 70% increase of volumetric productivity in relation to power input when compared to conventional reactor operation without static mixers. Merchuk *et al.* (1993) developed a helical flow promoter which was fitted to the outside of the upper section of the draft tube in a concentric airlift reactor. The flow promoter enhanced radial mixing in the downcomer and increased the mass transfer rate by 50%.

Therefore ancillary internals, such as impellers and baffles have been used to improve reactor performance. In general, the devices have slightly improved gas holdup and oxygen transfer. Chisti and Moo-Young (1987) suggested that they did not foresee any further use for or wide spread use of ancillary pieces in airlift reactors because stirred tank systems are so good there would be no need for extra complicated internals.

1.3 Airlift reactor dispersion characteristics

1.3.1 Introduction

Gas introduced into an airlift fermenter produces a density difference in gas holdup which provides the driving force for vertical circulation of the dispersion. The bubbles are sparged into the path of the circulating liquid and up into the riser. Therefore, the mean and variance of the distribution of bubbles entering the riser has a significant influence on the hydrodynamics and oxygen transfer in the fermenter (Ho *et al.*, 1977). Small bubbles are desirable as they will provide higher oxygen transfer rates than large fast rising bubbles due to larger specific gas - liquid interfacial area for mass transfer (Bhavaraju *et al.*, 1978). Small bubbles also have lower rise velocities and hence a longer residence time allowing greater oxygen transfer. However, small bubbles usually

come to equilibrium with respect to oxygen partial pressure quicker than larger bubbles and hence, become depleted of oxygen earlier than large ones (Bhavaraju *et al.*, 1978). Russell (1989) suggested that the lower rise velocity of the small bubbles will effect molecular diffusion between gas and liquid phases, reducing the liquid side film coefficient for mass transfer. This disadvantage is usually overlooked when compared to the advantages of small bubbles.

The bubble size distribution not only affects oxygen transfer but also liquid circulation and hence, the degree of gas recirculation in the downcomer. Bubbles must have rise velocities lower than the liquid velocity in the downcomer for entrainment to occur, otherwise the bubbles will disengage into the top section (Siegel *et al.*, 1988). Therefore, at low liquid velocities only small bubbles will be recirculated and they will not contain significant oxygen content once they reach the downcomer. Therefore, the bubble size is an important factor in influencing gas recirculation and hence, gas holdup and oxygen transport. The behaviour of the bubble size distribution also depends on other factors, which will be discussed in the following sections.

1.3.2 Dispersion characteristics

Under the highly turbulent conditions found in airlift reactors, the bubble size in dispersions is generally independent of the size at birth. Chisti and Moo-Young (1987) suggested that bubble size is controlled by the equilibrium between the dynamic pressure forces which work to break the bubble and the surface tension force which attempts to preserve its size and shape. Therefore, the local bubble size distribution in a given gas-liquid mixture is a result of a balance between the processes of dispersion and coalescence (Smith, 1985, Erickson and Desphande, 1981). Blenke (1985) explained that coalescence occurred due to the thinning of liquid lamella between neighbouring gas bubbles. This occurred rapidly in pure liquids so that even with the finest dispersion, uniform stable bubble sizes between 2 and 5 mm were observed above the sparger. In salt solutions of aqueous 1 N sodium sulphate solution the bubble sizes between 0.3 to 0.5 mm were formed and coalescence strongly impeded which led to larger gas - liquid interfacial area and a greater oxygen transfer rate. Thus Blenke (1985) concluded that coalescence behaviour must be considered when comparing experimental results obtained with different gas - liquid systems and when transferring results from model to large scale designs. Therefore, low rates of coalescence are desirable in order to maintain a reasonably small bubble size enabling greater oxygen transfer.

The rates of coalescence are mainly affected by the composition of the liquid phase and its properties. In pure liquids such as distilled water the rate of coalescence is high. Erickson and Deshpande, (1981) investigated the gas - liquid dispersion characteristics of a split cylinder airlift column with different solutions of low and high viscosity containing a surfactant. In distilled water they found that coalescence rates were large and bubble break up leading to a higher interfacial area depended on liquid

turbulence. The rapid coalescence resulted in low gas holdup in the lower part of the downcomer. On investigation of high viscosity liquids the coalescence rate was found to remain the same as with distilled water however, bubble breakup was reduced due to the reduction in turbulence of the high viscosity liquid. Therefore, as bubble breakup was reduced larger bubbles were found in the riser and hence an increased gas holdup in the upper section of the downcomer was observed.

Small concentrations of electrolytes, surfactants, and alcohols or oils have a profound effect on bubble size and gas holdup (Voigt and Schugerl, 1979, Bhavaraja *et al.*, 1978). Erickson and Delphande (1981) demonstrated that the addition of a surfactant, sodium lauryl sulphate, increased the gas holdup of distilled water in the split column airlift reactor by causing a decrease in coalescence. For highly viscous liquids, 1% carboxy methyl cellulose (CMC), Erickson and Delphande (1981) found that the addition of surfactant doubled the gas holdup in the lower section of the downcomer compared to the CMC solution without surfactant. Marrucci and Nicodemo (1967) also demonstrated a decrease in mean bubble diameter and an increase in gas holdup when they compared a coalescing pure water to a non-coalescing (electrolyte) solution. Kennard and Janekeh (1991) observed a smaller mean bubble size with addition of CMC, ethanol or starch solutions to water. Lee and Meyrick (1970) described the effect as being caused by solute concentration or temperature gradients which oppose the drainage and stretching of the liquid film between approaching bubbles and hence hinder coalescence. Voigt and Schugerl (1979) demonstrated that electrolytes reduce coalescence immediately following bubble formation while surface active substances reduce coalescence only after the bubble has been surrounded by surfactant. Robinson and Wilke (1973) measured the gas-liquid interfacial area in the presence of electrolyte and found that the interfacial area per unit volume increases with increasing concentration of the electrolyte.

Therefore, the bubble coalescence rate is influenced by the media composition, surface tension and liquid viscosity, all of which can change during a fermentation. The rate of coalescence is also influenced by the rate of gas flow into the fermenter (Deckwer, 1985). Therefore, at varying gas flow rates different flow regimes and hydrodynamic values will exist due to the rate of coalescence.

1.3.3 Bubble formation

Bubble formation is the remaining factor which affects bubble size and depends on the type of sparger used and the size of the sparger orifices. Three groups of sparger exist for airlift reactors: perforated plates and pipes, porous plates, and two phase injectors (dynamic spargers). Bubbles of a certain mean diameter will be produced by a certain sparger however, the local bubble diameter will depend on the coalescing properties of the medium, as previously mentioned. Therefore, in a non-coalescing media the choice of sparger will have a larger influence on bubble size than for coalescing

media (Russell, 1989). Bhavaraja *et al.* (1978) demonstrated that the mean bubble size was determined by turbulent forces at low viscosity (0.6 Pa.s) whereas, in high viscosity liquids bubble breakup did not occur and hence, bubble size was determined by the sparger design. The choice of sparger for a particular application depends on several factors. Orifice and perforated plates or pipe spargers cannot produce very small bubbles at normal gas flows but are cheap to install and operate (Chisti and Moo-Young, 1987). Porous plates are more expensive and have a high operation cost due to the large pressure changes. Chisti and Moo-Young (1987) claimed that porous plates are prone to blockages, nevertheless monoclonal antibody production was successfully cultivated from mammalian cells using porous plates with a pore size of 100 μm. Two phase injectors or dynamic gas spargers have a liquid jet supplying the kinetic energy to distribute the gas (Deckwer, 1985, Zlokarnik, 1985, Shah *et al.*, 1991). They are complex to design and require an external circulation mechanism. In a jet loop reactor the liquid is circulated through the gas sparger at liquid velocities greater than 20 ms^{-1} which produces high shear rates which are too large for mammalian or plant cell culture (Blenke, 1985).

As the bubble size formed from the sparger influences the hydrodynamic characteristics and liquid velocity of the riser then, the type of sparger would be expected to influence the overall liquid velocity. However, Onken and Weiland (1983) claimed that the type of gas distributor has only a small influence on liquid velocity as long as the gas phase is distributed uniformly across the cross section of the riser.

1.3.4 Flow regimes

The introduction of gas into the reactor at increasing flow rates can produce several different flow regimes. The riser superficial gas velocity (volumetric gas flowrate divided by the riser cross sectional area) determines the type of flow regime that will exist in the reactor. At low gas inputs (low superficial gas velocities) gas bubbles rise up the riser without interaction between them. This flow is characterised with uniformly sized bubbles and is called homogeneous or bubbly flow (Fig.1.6a). As the gas flow rate is increased the bubble density rises and greater bubble interaction occurs. This leads to increased coalescence and hence, a heterogeneous mixture containing different bubble sizes of a high turbulent nature (Fig.1.6b). This is a transitional region which leads to churn turbulent flow which contains a number of large bubbles which are less suitable for mass transfer (Deckwer, 1985). These large bubbles have no definite shape which fluctuates in the turbulent regime (Fig.1.6c). At higher gas flow rates spherical caps or bullet nosed bubbles may form which rise rapidly (Fig.1.6d). The frequency and size of spherical caps increases with gas flow rate and in reactors with small diameters, particularly with viscous fluids (Chisti and Moo-Young, 1988). If the cap size increases with increasing gas flow rate up to the diameter of the vessel then bubble slugs will develop called slug flow. Chisti and Moo-Young (1987) have shown that the flow

regime is not only determined by the superficial gas velocity but also by other parameters including sparger design, liquid properties and liquid velocity. For example, transition to slug flow will occur in small diameter tubes rather than in vessels of large size, and spherical cap bubbles form more readily in highly viscous fluids, such as mycelial cultures than in water systems.

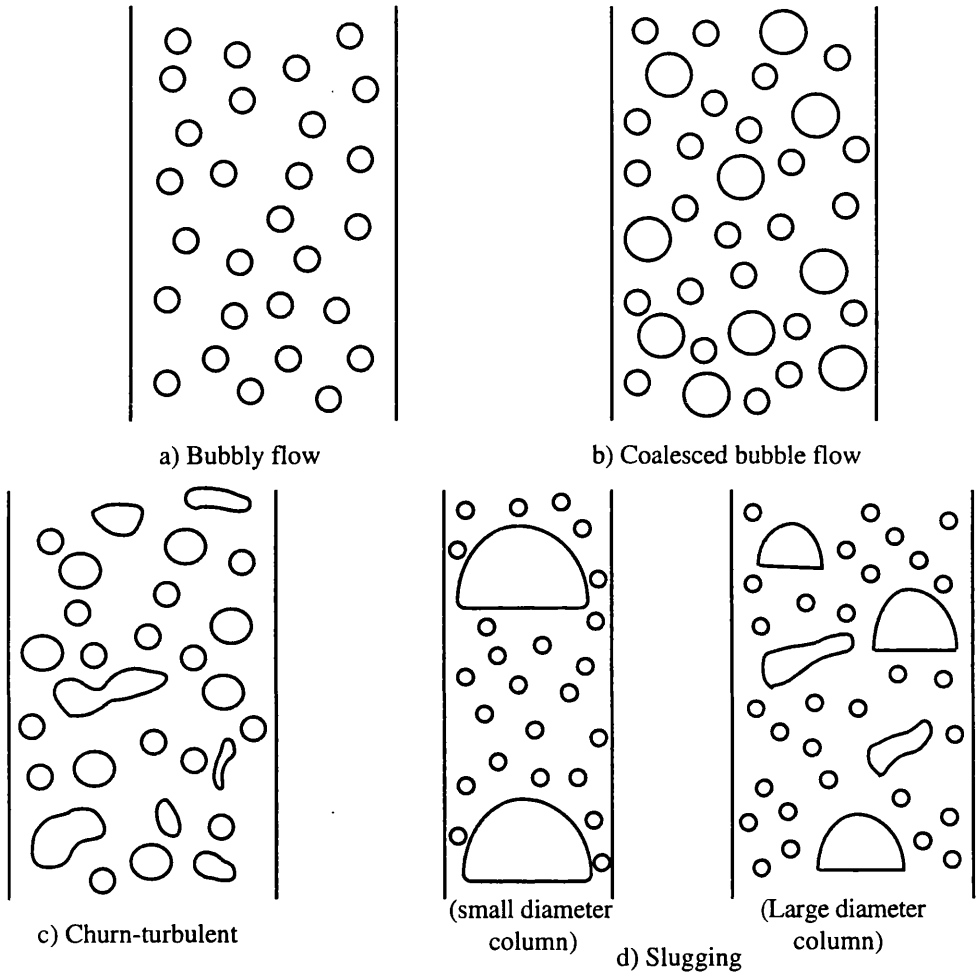

Figure 1.6 Reactor flow regimes (Chisti and Moo-Young, 1987).

1.4 Airlift reactor hydrodynamics

1.4.1 Introduction

The design, performance and evaluation of an airlift reactor depends on detailed knowledge of the hydrodynamic characteristics. The hydrodynamic and oxygen transfer performance can be controlled by manipulating the air flow rate introduced through the sparger. Therefore, an understanding of the relationship between gas flowrate and the other hydrodynamic parameters is essential. The relationship between hydrodynamic parameters such as gas holdup, liquid recirculation, liquid velocity and gas flow rate through the sparger is not simple. A complex inter-relationship between each of these hydrodynamic variables exists. The variables are also influenced by the reactor geometry and liquid properties which makes comparison between geometrically dissimilar reactors difficult. This inter-relationship between hydrodynamic variables will be discussed in the following sections.

1.4.2 Gas holdup

Gas holdup is the volumetric fraction of the gas in the total volume of the gas-liquid or solid dispersion. It determines the mean residence time of the gas phase in the reactor and influences the gas-liquid interfacial area. It also provides the driving force for liquid circulation via the difference in holdup between the riser and downcomer (Siegel *et al.*, 1988). The overall gas holdup refers to the reactor as a whole:

$$\varepsilon_o = \frac{V_g}{V_g + V_L} \qquad 1.2$$

where

V_g and V_L = gas and liquid volumes in the reactor

However, the distribution of gas in the airlift reactor is not uniform throughout the liquid in the reactor. Therefore, the overall holdup is an average value for the three sectional gas holdups, riser, downcomer, and top section. The gas holdup in each section increases as the gas flow rate increases. The gas holdup in the top section can be greater than in the riser and downcomer since the net liquid velocity in the top section is smaller than in other regions, so bubbles in the top section have a longer residence time. The entrainment of surface air due to intense turbulence takes place in the top section increasing gas holdup (Chen, 1990). Only some of the gas bubbles in the top section are entrained into the downcomer and so, gas holdup in the top section is higher than other regions and downcomer gas holdup is lower than the riser which causes liquid circulation (Choi and Lee, 1990). Thus, gas holdup values for the individual sections are more valuable and should be considered in order to be able to understand the overall hydrodynamic behaviour of a vessel (Siegel *et al.*, 1988, Merchuk, 1990).

The calculation of the individual gas holdup values can be made from separate equations for each section. The mean riser gas holdup (ε_R) can be defined from the gas residence time (t_R) :

$$t_R = \frac{\varepsilon_R A_R H_{DT}}{Q_{GR}} \qquad 1.3$$

where

Q_{GR} = mean volumetric flowrate of gas through the riser (m^3s^{-1})

ε_R = riser gas holdup (–)

t_R = mean gas residence time in the riser (s)

H_{DT} = draft tube height (m)

A_R = cross sectional area of the riser (m^2)

Russell (1989) used this equation in conjunction with the expression below from the drift-flux model of Zuber and Findley (1965) which can be used if a radially uniform gas holdup profile across the riser is assumed (Shah and Deckwer, 1983) :

$$U_{GR} = U_{LR} + U_{SR} \qquad 1.4$$

where

U_{SR} = mean relative velocity between the liquid and gas phases in the riser section (ms^{-1})

U_{LR} = mean linear liquid velocity (ms^{-1})

U_{GR} = mean linear of velocity of the gas phase of the riser (ms^{-1})

Therefore, Russell (1989) used the velocity of the gas phase in two phase upward flow and the residence time equation to produce an expression for the riser gas holdup:

$$\varepsilon_R = \frac{Q_{GR}}{(U_{LR} + U_{SR}) A_R} \qquad 1.5$$

The downcomer gas holdup value can be obtained in a similar manner (Russell, 1989). However, the slip velocity due to bubble buoyancy will be counter current to the liquid movement.

Thus the gas velocity U_{GD} is given by :

$$U_{GD} = U_{LD} - U_{SD} \qquad 1.6$$

where

U_{GD} = mean gas velocity through the downcomer

U_{SD} = mean slip velocity in the downcomer

So the mean downcomer gas holdup is given by:

$$\varepsilon_D = \frac{Q_{GD}}{A_D\,(U_{LD} - U_{SD})} \qquad 1.7$$

To produce a value for the top section gas holdup, Russell (1989) considered the top section hydrodynamics in two streams: the fraction of gas that will be separated from the gas-liquid dispersion and the fraction that will be recirculated through the downcomer. Thus, the top section gas holdup can be considered as the sum of these two fractional holdups.

The overall gas holdup has been experimentally determined by many researchers using two methods: manometrically or the volume expansion method. The volume expansion method involves the measurement of unaerated and aerated liquid heights to calculate the overall gas holdup via the following equation:

$$\varepsilon_o = \frac{(H_D - H_L)}{H_D} \qquad 1.8$$

where

H_D = liquid dispersion height (m)

H_L = unaerated liquid height (m)

The manometric technique is used to determine the individual riser and downcomer gas holdups. Manometers are connected to pressure taps located at two different axial positions either in the riser or in the downcomer of the reactor. Many researchers have used these methods and found them to be reliable (Bello *et al.*, 1981, Chisti *et al.*, 1988, Kawase and Moo-Young, 1986a, Siegel and Merchuk, 1991).

In general the gas holdup increases with an increase of superficial gas velocity (Choi and Lee, 1990). At a given gas velocity the gas holdup can be influenced by the bubble size distribution, the liquid velocity, the rate of gas recirculation and the liquid properties (Onken and Weiland, 1983). Many researchers have demonstrated that an initial rapid rise in gas holdup occurs with increasing superficial gas velocity followed by a more gradual increase (Russell *et al.*, 1994, Bello *et al.*, 1981, Siegel *et al.*, 1986, Chakravarty *et al.*, 1974). This diminishing dependence of gas holdup as the gas velocity is increased is due to the change in flow regime (Chisti, 1989). At high superficial gas velocities the flow regime becomes turbulent where large spherical cap bubbles are

formed. The formation of these large fast rising bubbles results in an increase of the mean bubble slip velocity and a reduction in the gas residence time in the riser. Hence, riser gas holdup is inversely proportional to the bubble rise velocity (Chisti, 1989, Russell *et al.*, 1994). Thus, the rate of increase of gas holdup with increasing gas velocity in churn turbulent regimes will be less than the rate of increase of gas holdup during the bubbly flow regime due to the counteracting effect of the increased bubble rise velocity.

An increase in superficial liquid velocity decreases the riser gas holdup at constant gas velocity conditions due to the reduction in gas residence time of the bubbles (Bello *et al.*, 1985). Onken and Weiland (1981) showed under constant superficial gas velocity conditions with water that an increase of the superficial liquid velocity increased the velocity of the rising bubbles and reduced the gas holdup by a factor of 2 to 4 compared to bubble column operation ie. with no liquid circulation in the loop.

The degree of gas entrainment into the downcomer is dependent on the geometry of the top section, the downcomer liquid velocity, the bubble size distribution and the liquid properties. In external loop reactors only a small fraction of the gas of the riser is entrained into the downcomer whereas a much larger fraction of the riser gas is entrained with concentric loop reactors. Bello *et al.* (1985) claimed that gas holdup in the downcomer of a concentric reactor can be in the order of 80 - 95% of the riser gas holdup. Frohlich *et al.* (1991b) observed that 85% of the riser gas holdup was entrained into the downcomer of a 4 m^3 tower loop reactor with a yeast broth. The entrainment of gas into the downcomer can only occur if the liquid velocity of the downcomer is greater than the bubble rise velocity of the bubble in stagnant liquid. Thus, a certain liquid velocity must be achieved before recirculation of gas can occur. The entrainment of a small amount of gas into the downcomer would lead to a large density difference between the riser and downcomer which would be beneficial for liquid circulation. Some concentric airlift reactors such as the concentric ICI SCP reactor (Smith, 1980) had conical top sections to minimise the entrainment of gas into the downcomer and maximise liquid circulation (Blenke, 1985). However, this regime prevents oxygen transfer taking place in the downcomer. Therefore, the gas residence time in the riser must be sufficiently long enough for oxygen transfer to take place in the riser of the vessel. Conversely, the entrainment of large bubbles would be advantageous to oxygen transfer in the downcomer as they would not become rapidly depleted of oxygen, unlike small bubbles. However, this may depend on the height of the reactor which will be further described in section 1.4.5. Radial gas holdup variation in the riser of airlift reactors have been reported (Lippert *et al.*, 1983). Local gas holdups were studied by Frohlich *et al.* (1991a) where the local gas holdup in the downcomer of a 4 m^3 tower loop reactor was smaller but increased more rapidly with superficial gas velocity than riser gas holdup in tap water and 1% ethanol solutions. The local gas holdup in the riser was nearly uniform along the reactor compared to the local gas holdup in the downcomer which was found to

vary along the reactor, highest at the top, smallest at the bottom. It was suggested that bubbles which obtain the critical size by coalescence, stagnate in the downcomer or move countercurrent to the liquid flow and therefore, have larger residence times than the downward moving bubbles. Axial variations of gas holdup in the riser and downcomer occur and higher gas holdups near the core than closer to the walls have been observed (Chisti, 1989).

Certain aspects of the geometric design of the airlift reactor have been found to influence gas holdup. An increase of the ratio of downcomer to riser cross sectional area (A_D/A_R) reduces the overall, riser and downcomer gas holdups, and increases liquid circulation (Bello *et al.*, 1985, Siegel *et al.*, 1988, Weiland, 1984). Weiland (1984) demonstrated that an increase of the A_D/A_R resulted in a reduction of the liquid velocity of the downcomer relative to the riser. As the downcomer liquid velocity dictates the amount of gas entrainment, then a reduction of the liquid velocity would reduce the downcomer gas holdup as the A_D/A_R increased. A reduction in downcomer gas holdup results in a greater proportion of gas disengagement from the top section which reduces the overall gas holdup. The reduction of downcomer gas holdup also increases the density difference between riser and downcomer and consequently improves liquid circulation. Chisti (1989) observed that the improved liquid circulation can reduce the gas residence time in the riser and decrease the riser gas holdup.

The presence of a draft tube has been found by many researchers to have no effect on gas holdup. The total gas holdup in an internal loop airlift reactor was exactly the same as in a corresponding bubble column when the superficial gas velocity based on the entire column cross section was used for comparison (Bello *et al.*, 1985, Chisti and Moo-Young, 1987). Chisti (1989) believed that the above results were due to an increase in liquid circulation in the airlift reactor which may have reduced the riser gas holdup because the bubble rise velocity had increased. The downcomer gas holdup may have increased because the liquid flowed against the bubble rise velocity.

Draft tube height has no effect on the overall gas holdup in a concentric airlift reactor (Russell *et al.*, 1994). However, the downcomer gas holdup at a given gas flowrate was observed to increase slightly with draft tube height. This is due to the increase in liquid circulation velocity with draft tube height. As the downcomer liquid velocity increases more gas will be drawn into the downcomer and recirculated. The downcomer gas flowrate will be increased and larger bubbles will be swept into the downcomer increasing the downcomer gas holdup. Russell *et al.* (1994) claimed that as the overall gas holdup remained constant and as the downcomer gas holdup increases with increasing draft tube height then the riser gas holdup must decrease. Thus, the large bubbles recirculated into the riser results in an increase in the mean bubble slip velocity in the riser and hence a decrease in riser gas holdup. Therefore, the changes in riser and downcomer gas holdups with increasing draft tube height will oppose each other, which results in a negligible change in the overall gas holdup.

The increase of clearance between the draft tube and vessel base was found by Ladwa *et al.* (1988) to increase the overall and downcomer gas holdup but decrease riser gas holdup. The reduction of riser gas holdup was claimed to be due to the increase of liquid velocity with bottom clearance. The influence of bottom clearance on gas holdup was maintained until the open area for liquid circulation was equal to the cross sectional area of the riser or downcomer depending on which was smallest. Similar effects were observed with water and 0.5% wt/vol. CMC solution by Merchuk *et al.* (1994).

The gas holdups and liquid velocity have been shown to be independent of the height of the ungassed and gassed liquid heights above the draft tube (Erickson and Deshpande, 1981, Russell *et al.* 1994, Chisti and Moo-Young, 1987). Russell *et al.* (1994) suggested this may be due to the two zone flow pattern where at a given gas flow rate the height of the zone of the circulating flow does not increase above a critical height. So the residence time of fluid in the top section will not change considerably as the top section is enlarged. Siegel and Merchuk (1991) also found that changing the degassed liquid level in a tower reactor in concentric configuration produced no significant influence on riser and downcomer gas holdup. However Bavarian *et al.* (1991) found different effects of liquid height depending on the gas distributor used. In a bubble column with a draft tube the gas holdup decreased with the static liquid height with a porous plate, whereas holdup increased with increasing liquid height with a perforated plate distributor.

The liquid properties of a fermentation broth such as viscosity and ion strength have been shown to influence gas holdup. Additives to water affect gas holdup because they alter bubble size which depends on bubble breakup and coalescence. The addition of salt to coalescing pure systems, such as water, will reduce coalescence and increase gas holdup (Marrucci and Nicodemo, 1967). The effect of additives on the coalescence properties of fluids was described in detail in section 1.3.2. Frohlich *et al.* (1991b) found that the riser gas holdup of a fermentation broth for baker's yeast in a 4 m^3 tower airlift reactor containing glucose (25% vol), potato protein liquor (10% vol) and antifoam by 0.025% vol was similar to a 1% ethanol solution, but 64% greater than tap water. This demonstrated the necessity of hydrodynamic studies to be undertaken with biological systems rather than with model media for accurate characterisation of the two phase flow.

Antifoam addition to a fermentation enhances bubble coalescence and thus the average bubble size should increase. Fields and Slater (1983) observed the above effects with antifoam addition to water and also observed that gas entrainment into the downcomer was reduced and overall gas holdup was lower than with water alone. Moo-Young *et al.* (1987) reported that influences of antifoam addition on gas holdup were only slight in viscous homogeneous liquids. However, Suh *et al.* (1992) showed that the addition of antifoam (0.012 vol%) decreased the maximum gas holdup of xanthan gum, at apparent viscosities of 0.003 - 0.005 Pa.s, with heterogeneous flow to low values

which were equivalent to those observed with xanthan gum solutions without antifoam at slug flow with apparent viscosity's above 0.1 Pa.s.

An increase in viscosity would lead to the formation of large bubbles in the riser which disengage from the vessel so, less gas flow occurs into the downcomer resulting in a reduction of overall gas holdup (Erickson and Deshpande, 1981). The reduced gas recirculation increases the density difference between the riser and downcomer, increasing the liquid velocity (Koide *et al.*, 1988, Fields *et al.*, 1984). However, increased viscosity of a broth could result in bubbles rising slowly due to increased viscous drag and as a result, enhancing the gas holdup (Heijnen and Van't Riet, 1984). Attempts have been made to simulate a viscous fermentation broth by using a polymer solution, such as CMC or xanthan gum, which allows the consistency of the medium to be varied. Kennard and Janekeh (1991) found that starch reduced bubble rise velocities which caused an increase in overall gas holdup and interfacial area. They found that the addition of 0.05% wt/v CMC and ethanol reduced bubble coalescence and as a result increased homogeneity of bubble flow, recirculation of smaller bubbles in the downcomer, and overall gas holdup. Philip *et al.* (1990) observed low gas holdup values for CMC solutions with any increase in riser superficial gas velocity. The average bubble size in the riser was lower for xanthan solutions than the CMC solutions and consequently the overall gas holdup in xanthan was higher than for CMC but only slightly lower than that of water. However, the CMC solutions were found to have small liquid velocities in the downcomer compared to water. Schumpe and Deckwer (1987) showed that for a range of superficial gas velocities from 0.03 to 0.15 ms^{-1} an increase in apparent viscosity from 0.001 to 0.003 Pa.s produced a small increase in gas holdup. For example, at the gas velocity of 0.03 ms^{-1}, the gas holdup increased from 0.145 to 0.16. However, from the increase of apparent viscosity from 0.003 to 0.1 Pa.s, large decrease of gas holdup occurred, such as from 0.16 to 0.06 at the gas velocity of 0.03 ms^{-1}. Therefore, although examples of increased gas holdup with simulated viscous solutions exist, in general a reduction in gas holdup has been observed with viscous systems of viscosities larger than 0.01 to 0.1 Pa.s (van't Riet and Tramper, 1991). Chisti (1989) disputed the use of these model non-Newtonian media and raised doubts to whether the results can be related to actual fermentations. Homogeneous polymer solutions follow the power law with consistency, K, and flow behaviour, n, being dependent on the concentration of dissolved polymer. In order to obtain low values of n, values of K are usually high, however in a mycelial culture n and K have been found to be both low. Only a small number of examples exist for the measurement of hydrodynamics during mycelial fermentations. Apparent viscosity has been used to observe viscosity by many workers. Chisti (1989) discussed the difficulties associated with this method. The rheological parameters K and n, are determined under laminar flow and conditions which may not be applicable to a bioreactor. Also, the shear rate of an airlift reactor is impossible to measure accurately which brings a large amount of

approximation into viscosity results. Moo-Young *et al.* (1987) demonstrated with *C. celluloyticum* fermentations that gas holdup increases with increasing gas flowrate and decreases with increasing shear thinning behaviour. This agrees with the results found with simulated liquids (Godbole *et al*, 1984, Kawase and Moo-Young, 1986a). The decrease of gas holdup with increasing viscosity has been measured from interval measurements as a function of gas velocity and apparent viscosity during the production of xanthan gum from *Xanthomonas campestris* in a 0.05 m^3 bubble column and 1.2 m^3 airlift reactor. Russell (1989) observed a decrease in downcomer gas holdup during a *Penicillium chrysogenum* fermentation in a concentric tube reactor with increasing broth consistency. Increasing broth viscosity causes the formation of large spherical cap bubbles with high rise velocities and the decrease of riser gas holdup. The fast rising bubbles reduce the mean bubble residence time in the riser and tend to disengage from the vessel reducing gas holdup (Clift *et al.*, 1978). Russell (1989) also observed that downcomer gas holdup values were larger than those observed in yeast fermentations under the same geometrical conditions. This was suggested to be due to the association of small bubbles with mycelial filaments, which didn't disengage from the liquid. Thus, the larger number of bubbles produces a large gas holdup which would not have been demonstrated by a polymer model solution. The gas holdup profiles for a reactor cannot be predicted separately from other hydrodynamic parameters as gas holdup and liquid circulation rates are interdependent parameters. Thus, the modelling of the two parameters will be described in section 1.4.3. An alternative approach is to develop correlations of gas holdup and liquid velocity from experimental measurements (Chisti, 1989). Researchers have shown a power law relationship between gas holdup and superficial gas velocity (Godbole *et al.*, 1984, Schumpe and Deckwer, 1987, Chisti and Moo-Young, 1987) as shown below :

$$\varepsilon_R = \alpha U_{sg}^{\beta} \qquad 1.9$$

where

ε_R = gas holdup of the riser (–)

U_{sg} = superficial gas velocity (ms^{-1}).

Many different correlations have been produced eg. U_{sg} expressed in terms of gas power input per unit volume of the column content or more specific equations for riser gas holdup as shown below (Koide *et al.*, 1984, Merchuk, 1990):

$$\varepsilon_R = a\,(U_{sg}^{\alpha})\left(\frac{A_D}{A_R}\right)^{\beta}(\mu)^{\gamma} \qquad 1.10$$

where

U_{sg} = superficial gas velocity based on the riser (ms^{-1})

μ = liquid viscosity (Pa.s)

A_R & A_D = the cross setional areas of the riser and downcomer (m^2)

A problem for these types of correlations is that too many of the important parameters tend to be lumped into coefficients and exponents of the correlation equations which can limit there application (Ayazi Shamlou *et al.*, 1994). The equations tend to be reactor specific and no general equation for gas holdup exists. Merchuk (1990) explained that no general correlation can be used to predict gas holdup in airlift reactors due to differences of reactor geometry and liquid properties. Chisti and Moo-Young (1987) warned that the correlations are based on the fresh gas input to the riser and the additional contribution of the recirculated gas also varies. This may explain the large differences between gas holdup and gas superficial correlations observed by various researchers using similar reactors.

1.4.3 Liquid circulation and velocity

The configuration of a concentric airlift reactor allows gas to be sparged into one section and the density difference between the bubbling liquids in the sparged section (riser) and the unsparged section (downcomer) induces directed circulation flow (Choi and Lee, 1990). A description of the liquid circulation with increasing gas flowrate in an airlift reactor was given by Chisti (1989). At low gas flow rates the bubbles are sparged into the riser which produce slow liquid circulation. As the gas velocity is increased, the liquid circulation increases and some bubbles become entrained by the liquid flow into the downcomer. The liquid flowing into the downcomer is usually incapable of sweeping larger bubbles into the downcomer as the large bubbles have high rise velocities which disengage in the top section. Thus, the mean bubble size found in the downcomer is smaller than the bubbles in the riser. The depth of penetration of a bubble into the downcomer depends on its size and tiniest bubbles penetrate the deepest. Larger bubbles are drawn into the downcomer only when the gas velocity is further increased and the penetration depth into the downcomer is increased. Increasing the gas velocity eventually results in the recirculation of most of the bubbles entering the downcomer. The liquid flow in the riser is observed to have some liquid downflow and circulation near the walls, but Chisti (1989) described it as smaller than that observed in bubble columns.

The magnitude of liquid circulation is one of the most important design and scale up parameters for airlift reactors (Merchuk, 1990). Liquid circulation influences the gas holdup for the riser and downcomer in the vessel, the prevailing flow regime, heat and mass transfer coefficients and the extent of mixing in the reactor (Chisti, 1989). The

velocity of the circulating liquid can be calculated in two ways, the superficial liquid velocity or the liquid linear velocity. The superficial liquid velocity is the volumetric liquid flow rate passing through the sparger, divided by the cross sectional area of the section through which it is flowing. However, this measurement does not take into account the actual cross sectional area available for flow, which is less than the actual cross sectional area of the riser due to the area occupied by the gas (Russell, 1989). The liquid linear velocity is the true velocity of the liquid. The two velocities in the riser can be related (Bello *et al.*, 1985) via:

$$U_{LR} = \frac{U_{sl}}{1-\varepsilon_R} \qquad 1.11$$

where

U_{LR} = riser liquid linear velocity (ms^{-1})

U_{sl} = riser superficial liquid velocity (ms^{-1})

ε_R = mean riser gas holdup (–)

The liquid velocity is not an independent variable but is determined by the hydrostatic pressure difference between the riser and downcomer gas holdups which provides the driving force for liquid circulation. Hence, the liquid circulation rate is essentially determined by a balance of the flow resistance with the circulation driving force (Wachi *et al.*, 1991). A contribution to liquid circulation is also made from the entrainment and transport of liquid in the wake of the ascending bubbles of the riser (Ayazi Shamlou *et al.*, 1994, Philip *et al.*, 1990).

Models have been created to predict the liquid velocities in airlift reactors. Two main methods have been used for the modelling of two phase flow: momentum and energy balances. One of the main models which has been incorporated in some part of many of the velocity models is the drift flux model of Zuber and Findlay (1965) which represents two phase flow. The general expressions are useful for the prediction of gas holdup which is applicable to non-uniform radial distributions of liquid velocity and gas fractions. The drift velocities are defined as the difference between the velocity of each phase and the volumetric flux density of the mixture, J (ms^{-1}):

$$J = U_{sg} + U_{sl} = \frac{(Q_{GR} + Q_{LR})}{A_R} \qquad 1.12$$

where

U_{sg} = superficial gas velocity (ms^{-1})

U_{sl} = superficial liquid velocity (ms^{-1})

Q_{GR} = volumetric gas flow rate (m^3s^{-1})

Q_{LR} = volumetric liquid flow rate (m^3s^{-1})

A_R = cross sectional area of the riser (m^2)

Zuber and Findlay (1965) derived a relationship between the weighted mean velocity of the gas phase and the weighted mean value of the flux of the gas phase. This was considered with the definition of the drift flux velocities which lead to a relationship for the linear gas velocity U_{GR} shown below:

$$U_{GR} = \frac{U_{sg}}{\varepsilon_R} = C_0 \,.\, J + \frac{(\varepsilon_R \quad U_{sg})}{\varepsilon_R} \qquad 1.13$$

where C_0 is the distribution parameter which is dependent on the radial distribution of the gas holdup and superficial liquid velocity (Merchuk, 1991). For most two phase flows including airlift reactors and bubble columns, the gas holdup at the centre of the circular pipe is greater than at the walls. Hence, Clark and Flemmer (1985) found values of C_0 of 1.07 while Zuber and Findlay (1965) recommended a maximum value of 1.6 and Govier and Aziz (1972) used a value of 1.15 for bubble swarms with bubble sizes ranging up to 20 mm. Zuber and Hench (1962) related the terminal rise velocity of a bubble (U_{BT}) to the drift velocity definition which lead to an expression:

$$\frac{U_{sg}}{\varepsilon_R} = \alpha.\, J + U_{BT} \qquad 1.14$$

where α is the pressure drop of the column. This expression was successfully used by Merchuk and Stein (1981a) to correlate gas holdup measurements in tower airlift reactors with high liquid velocities.

The energy balance method for modelling two phase flow in airlift reactors considers the steady state energy balance between the energy delivered by the sparged gas and the energy dissipated by the two phase flow around the column. Chakravarty *et al.* (1974) used the model to provide a link between superficial gas velocity, gas holdup and liquid velocity. The energy input was the potential energy of the gas bubbles once inside the reactor, thus neglecting the kinetic energy associated with gas injection. This was equal to the sum of the energy dissipation due to the downward movement of entrained bubbles in the downcomer, the energy converted into kinetic energy of the liquid, the energy losses due to the change of direction and magnitude of liquid velocity at the bottom of the reactor, and losses due to friction of the gas-liquid mixture on the walls. The rate of gas kinetic energy dissipation is generally assumed to be negligible compared to the power input from gas expansion as it is not more than 6% of the total energy input (Lehrer, 1968, Joshi and Sharma, 1979). The energy dissipated due to friction was solved by using two phase friction factors by Bello (1981) and Calvo (1989). Lee *et al.* (1987) described the rate of energy loss due to friction in the riser and downcomer as being equal to the energy loss in wakes behind the bubbles in the riser, energy loss due to drag of gas bubbles on liquid in the downcomer, and loss due to wall friction in the riser and downcomer. Lee *et al.* (1987) used the rate of pressure energy loss by the liquid and

gas phase and the rate of gain of potential energy of the liquid to evaluate energy loss by bubble wakes. Frictional losses in the walls were ignored. The energy lost in flow reversal was calculated using the single phase equations for friction loss coefficients from the change in direction of flow for a pipe. Accurate estimation of the coefficients has been shown to be difficult due to the variation of values from different workers. Similar models were used by Jones (1985), Freedman and Davidson (1969), Russell (1989). Chisti *et al.* (1988) extended a model used by Bello (1981) which also incorporated energy dissipation due to bubble wakes in the energy balance. The average liquid velocity (U_{LR}) for airlift reactors was given by the formula below:

$$U_{LR} = \left[\frac{2gH_D\ (\varepsilon_R - \varepsilon_D)}{\frac{K_T}{(1-\varepsilon_R)} + K_B \left(\frac{A_R}{A_D}\right)^2 \frac{1}{(1-\varepsilon_D)^2}} \right]^{0.5} \qquad 1.15$$

where

K_T = friction coefficient at the top of the loop

K_B = friction coefficient at the at the bottom of the loop

H_D = height of the unaeratd liquid column (m)

A_R & A_D = cross sectional area of the riser and downcomer respectively

The effect of gas velocity on the liquid velocity was not exerted directly in this model but indirectly from the effect of gas holdup. However, Chisti *et al.* (1988) demonstrated that most of the published data on riser liquid velocity was satisfactorily correlated using this correlation by choosing the appropriate value for the friction coefficient. Chisti (1989) ignored the friction coefficient for the top section with concentric airlift reactors as the top section was assumed to be an open channel rather than the constricted flow path of external loop reactors. For concentric reactors the friction coefficient for flow around the bottom of the vessel, K_B was considered to be the most important for concentric reactors which could be estimated using the equation below:

$$K_B = 11.402 \left(\frac{A_D}{A_B}\right)^{0.789} \qquad 1.16$$

where A_B was the minimal cross section at the bottom of the airlift reactor. Merchuk (1991) claimed that the method of K_B estimation must be improved for scale up and design purposes. The model was then completed by using an iterative process by assuming a value of the liquid velocity with the input parameters and continuing the calculation procedure until the model value of liquid velocity agreed with the assumed value. The model was further extended to incorporate pseudoplastic fluids (Chisti, 1989) which Merchuk (1991) considered to be an important improvement. Clark and Jones

(1987) incorporated the radial distribution of the gas holdup through the drift flux model by fitting values of the distribution parameter C_o. Ayazi Shamlou *et al.* (1994) used an energy balance for the expression of the primary bulk liquid flow (U_{bl}) which was produced from the holdup differentials in the column and the velocity of the liquid wake behind the bubble. The most significant contributions to energy dissipation in an airlift reactor were considered to be the liquid wake behind the bubbles (E_w), the bulk liquid flow through the riser (E_B) and losses due to flow reversal at the base of the riser (E_F). Other frictional losses including flow reversal at the top of the riser and energy losses associated with bubble breakup were ignored due to their relatively small size (Garcia *et al.*, 1991). The complete energy balance is shown below:

$$\left(\frac{\pi}{4}\right) T^2 U_{sg} \rho_L g H_L = \left(\frac{\pi}{4}\right) T^2 H_L U_{BT} \rho_L g \varepsilon_R (1-\varepsilon_R) + 0.512 n^2 \pi \rho_L H_L T [U_0^c]^3$$

energy input of the gas = energy dissipation from the bubble wake + energy dissipation from the liquid motion

$$+ \frac{1}{2} K_B \rho_L U_{sl}^3 \qquad 1.17$$

+ energy dissipation from flow reversal at the base of the vessel

The energy dissipation from the bubble wake incorporated the rate of loss of pressure energy of the liquid, rate of gain of potential energy of the liquid and the rate of pressure loss of the gas. The energy loss E_F from the flow direction at the base of the vessel was used from Chisti *et al.* (1988) and the K_B was calculated using equation 1.16. The energy dissipation from the bulk liquid flow E_B was developed from Rietema and Ottengraf (1970) and Kawase and Moo-Young (1986b) which enabled an equation for power law fluids to be used with the centre line liquid velocity U^c_o. The mean primary liquid velocity in the column U_{bl} was considered to be equal to 0.755 U_{co} (Verlaan *et al.*, 1986) and this led to the expression below for the primary bulk liquid flow (U_{bl}):

$$U_{bl} = 0.6 \left\{ \frac{Tg [U_{sg} - (1-\varepsilon_R) \varepsilon_R U_{BT}]}{4\left(0.512\, n^2 + \frac{K_B}{2\pi H_L T}\right)} \right\}^{\frac{1}{3}} \qquad 1.18$$

where

T = diameter of the riser section of the reactor (m)

H_L = unaerated liquid height in the column (m)

U_{BT} = terminal rise velocity of an isolated bubble (ms^{-1})

n = flow behaviour index of the broth (–)

This model was used in an iterative process for the prediction of riser gas holdup and riser superficial liquid velocity. An assumed gas holdup value was used with the bulk

liquid velocity to calculate a value of the total superficial liquid velocity from the equation below:

$$U_{sl} = U_{bl}\,[1 - \varepsilon_R\,(1 + k)] + U_{sg}\,(1 + k) \qquad 1.19$$

where k was the ratio of the liquid-wake volume to bubble volume as estimated using the equation below (Darton and Harrison, 1975):

$$k = \left(\frac{\varepsilon_w}{\varepsilon_R}\right) = 1.4\left(\frac{U_{bl}}{U_{sg}}\right)^{0.33} - 1 \qquad 1.20$$

where ε_w was the gas holdup of the bubble wake. The liquid bubble wake was assumed to have a similar liquid velocity as the bubble. The parameters were then added to the expression below which was derived from the drift flux theory.

$$\varepsilon_R = \frac{U_{sg}}{(C_o + 1)\,(U_{sl} + U_{sg}) + U_{BT}} \qquad 1.21$$

where

ε_R = riser gas holdup (–)

C_o = distribution parameter (–)

U_{sg} = superficial gas velocity (ms^{-1})

U_{sl} = superficial liquid velocity (ms^{-1})

U_{BT} = terminal velocity of an isolated bubble (ms^{-1})

Calculated gas holdup values would then be compared with the assumed value and the procedure repeated until both gas holdup values were equal. This expression was found to produce good agreement with a range of airlift reactors, including pseudoplastic fluids from the incorporation of the power law, K_B and C_o parameter. For low viscosity fluids such as water, K_B values were around 5 (Chisti *et al.*, 1988) and larger values (30) were required for viscous fluids (Ayazi Shamlou *et al.*, 1994).

The modelling of liquid circulation velocity by means of a steady state momentum balance has been demonstrated by a number of researchers including Blenke (1979), Hsu and Dudukovic (1980), Kubota *et al.* (1978), Freedman and Davidson (1969), Bello (1981) Verlaan *et al.* (1986), Merchuk and Stein (1981a) and Koide *et al.* (1984). The momentum balance is based on an overall momentum balance of the circulation loop, with empirical gas holdup and two phase pressure drop correlations. The models consider a steady state situation where the driving force, the hydrostatic pressure, is balanced with the total pressure drop in the circulation path due to friction from valves, bends, and flow area changes:

$$\Delta P_D = \Delta P_F = \sum_i \Delta P_i = \Delta P_1 + \Delta P_2 + \Delta P_3 \qquad 1.22$$

where ΔP_D (pressure drop driving force for liquid circulation) equals the ΔP_F, (pressure drop due to flow around the loop), which is the sum of the individual pressure losses, (ΔP_i), in the riser,(ΔP_1), top section,(ΔP_2), and the downcomer, (ΔP_3), (Onken and Weiland,1983).

The driving force for liquid circulation is the difference between the hydrostatic pressure in the downcomer and the riser (Merchuk and Stein, 1981a).

$$\Delta P_D = (1-\varepsilon_D)\rho_L g H_{DT} - (1-\varepsilon_R)\rho_L g H_{DT} \qquad 1.23$$

where

ρ_L= density of the liquid (kg m^{-2})

ε_D & ε_R = gas holdup for the downcomer and riser respectively

H_{DT} = height of the draft tube (m)

Many workers including Merchuk and Stein (1981a) and Bello (1981) assumed that the pressure drop due to acceleration of the liquid is negligible, thus leaving the sum of the pressure loss due to friction in flow through the riser, downcomer, and flow reversal in the top and base section of the column to be determined:

$$\Delta P_F = \Delta P_{FR} + \Delta P_{FD} + \Delta P_T + \Delta P_B \qquad 1.24$$

where

ΔP_{FR} = pressure loss due to friction in flow through the riser (Pa)

ΔP_{FD} = pressure loss due to friction in flow through the downcomer (Pa)

ΔP_T = pressure loss due to flow reversal at the top of the column (Pa)

ΔP_B = pressure loss due to flow reversal at the base of the column (Pa)

Russell (1989) claimed that in a concentric tube airlift reactor where gas holdup is significant in both riser and downcomer, the frictional losses in two phase flow will be greater than in single - phase flow, due to losses at the interface between the two phases. Some researchers ignored inter phase friction and only used single phase factors, (Verlaan *et al.*, 1986, Kubota *et al.*, 1978) while other researchers ignored frictional losses altogether (Freedman and Davidson,1969). Researchers have used empirical correlations for the estimation of two phase frictional factors (Merchuk and Stein, 1981a,

Hsu and Dudkonvich, 1980). Bello (1981) used the homogeneous flow model of Collier (1972) which derived an expression for pressure loss occurring when only liquid is flowing and used 'two phase frictional multiplier' to account for the gaseous phase. The frictional pressure losses are given below:

$$\Delta P_{FR} = \frac{2f_R U_{LR}^2 \rho_L H_{DT}}{D_R} \phi_{FR}^2 \qquad 1.25$$

$$\text{and } \Delta P_{FD} = \frac{2f_D U_{LD}^2 \rho_L H_{DT}}{D_D} \phi_{FD}^2 \qquad 1.26$$

where

f_R, f_D = friction factor based on total flow assumed liquid for riser and downcomer respectively.

ϕ_{FR}^2, ϕ_{FD}^2 = two phase frictional multiplier for riser and downcomer and downcomer respectively.

D_R = diameter of riser

D_D = diameter of downcomer (shell diameter)

The friction factors are functions of the Re numbers (Russell, 1989) and can be calculated using equations developed for smooth pipes. The two phase friction multiplier can only be evaluated empirically and different researchers employed empirical correlations for there estimation. Hsu and Dudokovich (1980), Verlaan *et al.* (1986) Chisti *et al.* (1988) and Bello (1981) used single phase equations for pipe flow to calculate pressure loss during change in direction of flow:

$$\Delta P_B = \tfrac{1}{2} K_B U_{LD}^2 \rho_L \qquad 1.27$$

$$\Delta P_T = \tfrac{1}{2} K_T U_{LR}^2 \rho_L \qquad 1.28$$

where

K_B = frictional loss coefficient for bottom section

K_T = frictional loss coefficient for top section

U_{LD} & U_{LR} = liquid linear velocity of the downcomer and riser

where K_B and K_T were estimated as discussed for the energy balance models.

The momentum model can now be derived by substituting equations into the balance equation:

$$\rho_L\, gH_{DT}(\varepsilon_R-\varepsilon_D) = \frac{2f_R\, U_{LR}^2\, \rho_L H_{DT}\, \phi_{FR}^2}{D_R} + \frac{2f_D\, U_{LD}^2\, \rho_L\, H_{DT}\, \phi_{FD}^2}{D}$$

$$+ \tfrac{1}{2}K_B U_{LD}^2 \rho_L + \tfrac{1}{2}K_T\, U_{LR}^2\, \rho_L \qquad 1.29$$

Russell (1989) related the volume flow of liquid to the liquid linear velocity, which allowed the downcomer liquid linear velocity to be substituted in the balance equation and the riser linear liquid velocity was derived as:

$$U_{LR} = \left[\frac{2gH_{DT}(\varepsilon_R - \varepsilon_D)}{4H_{DT}\left[\frac{f_R\phi_{FR}^2}{D_R} + \frac{f_R\phi_{FD}^2 z^2}{D_D} \right] + K_T + K_B Z^2} \right]^{0.5} \qquad 1.30$$

$$\text{where } Z = \frac{(1-\varepsilon_R)A_R}{(1-\varepsilon_D)A_D}$$

The calculation of the liquid velocity involves the fluid circulating along a well defined path, upflow in the riser and downflow in the downcomer. A mean circulation velocity (U_{LC}) is defined (Blenke, 1979) as:

$$U_{LC} = \frac{X_c}{t_c} \qquad 1.31$$

where

X_c = circulaton path length (m)

t_c = average time for one complete recirculation (s)

Tracer response techniques have been used to obtain the mean circulation times. A dampening or decaying sinusoidal type of response may be detected at some location downstream of the tracer injection point. The time difference between adjacent peaks being equal to the circulation time (Choi and Lee, 1990, Weiland, 1984). Therefore, the circulation time can be read from the peaks and converted to circulation velocity from a knowledge of the circulation path length. The liquid circulation velocity is itself controlled by the gas holdups in the riser and the downcomer and in turn affects the holdups by either enhancing or reducing the velocity of bubble rise (Chisti, 1989).

The liquid velocity increases with increasing superficial gas velocity which is a general relationship found in both concentric and external loop reactors (Merchuk and Stein, 1981a, Gopal and Sharma, 1982, Kloosterman and Lilly, 1985, and Verlaan *et al*, 1986). At large gas velocities, generally above 0.05 ms^{-1}, the rate of increase of the liquid velocity with increasing gas velocity is reduced (Weiland, 1984). This is due to the change in flow regime at high gas velocities (Siegel *et al.*, 1988, Chisti, 1989). The presence of large bubbles leads to enhanced turbulent dissipation of energy in the riser.

Therefore, the proportion of energy input by gas dispersion available for liquid motion will diminish (Merchuk and Stein, 1981a).

Weiland (1984) found that the liquid velocity increased with increasing downcomer cross sectional area to riser cross sectional area ie. the A_D/A_R ratio in a concentric airlift reactor. An increase in A_D/A_R results in a reduced liquid velocity in the downcomer relative to that in the riser. Therefore, fewer bubbles recirculate into the downcomer producing a lower downcomer gas holdup. Hence a larger density difference for liquid circulation is obtained, but fewer bubbles in the downcomer results in limited oxygen transfer in this region. A similar effect was observed by Bello *et al.* (1985) with both internal and external loop reactors.

Increasing the draft tube height caused an increase in hydrostatic pressure and hence increased liquid velocity (Russell *et al.*, 1994, Weiland, 1984). Russell *et al.* (1994) also investigated the effect of top section geometry and found that a constant circulation time was achieved with a changing liquid level in the top section. It was suggested that the liquid circulation path remained at a constant size as the liquid height increased in the top section. The gas sparger has been found to have little influence on liquid circulation rate (Merchuk, 1986, and Onken and Weiland, 1983) as long as the entire cross section of the riser is uniformly sparged.

Liquid velocity is effected by the properties of the circulating liquid. The effect of broth viscosity on liquid velocity has mostly been investigated by researchers using non-Newtonian simulating fluids. In general, an increase in broth viscosity will increase the frictional resistance to flow around the airlift loop and will impede liquid circulation and hence, reduce liquid velocity (Weiland, 1984, Onken and Weiland, 1983, and Koide *et al.*, 1988, Glennon *et al.*, 1988). However, researchers using low viscosity pseudoplastic media (CMC and xanthan gum solutions) have measured increases in liquid velocity with increasing viscosity, due to a reduction in viscous drag and increased density difference. Wachi *et al.* (1991) demonstrated with CMC solutions, (0.1% w/v, consistency (K) of 0.011 $Pa.s^n$ and flow behaviour (n) of 0.93), that the large bubbles in the riser disengaged from the vessel which reduced the downcomer gas holdup when compared to water. This increased the density difference for liquid circulation. Fields *et al.* (1984) demonstrated that the addition of a 0.1% xanthan gum solution to a concentric airlift reactor improved the liquid circulation performance of the reactor when compared to water. This was claimed to be due to a reduction of viscous drag. However, at higher concentrations of xanthan gum, 0.3 to 0.5% wt/v, the liquid circulation time increased with increasing xanthan concentration due to viscous drag around the vessel.

The inhibition of coalescence from the presence of salts and other constituents such as ethanol and glycerol in fermentation broths when added to water result in lower liquid velocities. The small bubbles recirculate into the downcomer increasing the downcomer gas holdup and reducing the driving force for liquid circulation (Weiland, 1984, Wachi *et al.*, 1991).

1.4.4 Liquid mixing

The mixing efficiency is an important characteristic of gas-liquid bioreactors as it will determine the bulk fluid and gas phase homogeneity, which will in turn affect the driving force for heat and oxygen mass transfer. Biological parameters such as growth rate, shear damage, pH and gas transfers will be controlled by the mixing performance. Different mixing behaviour has been observed around the loop of an airlift reactor. Fields and Slater (1983) observed that mixing consisted of the combined effects of local mixing in the riser, downcomer and top and bottom flow reversal sections. Axial dispersion occurs in the riser and downcomer due to differences between the gas-liquid phase velocities (Chisti, 1989). Turbulent mixing occurs in the top (gas disengagement) section and a certain amount of liquid backmixing will occur caused by recirculation, adding a final contribution towards the overall mixing pattern (Fields and Slater, 1983). Therefore, Blenke (1985) described two fundamental mixing effects: the longitudinal mixing which occurred in each circulation due to the velocity profile, turbulence, dead spaces and molecular diffusion and backmixing due to the recycling of the circulation flow. The axial dispersion model has been used to simulate the longitudinal mixing which occurs when the tracer is injected into an tower loop reactor and becomes homogeneously distributed (Merchuk, 1991). The dispersion model is based on the analogy between mixing in actual flow (plug flow) and diffusion-like eddy movement superimposed on the plug flow. Taylor's (1954) one dimensional diffusion model has been extensively used to model axial dispersion in single phase flows and was shown by Blenke (1979) to describe the dispersion due to single circulation in an unaerated jet-loop reactor. The empirical description of mixing assumes a single loop circulation is equivalent to flow through a pipe with uniform liquid velocity, U_{LC}, and axial dispersion coefficient, D_L, so that the tracer concentration, C at a point x in the loop at time t is given by:

$$\frac{\delta C}{\delta t} = D_L \frac{\delta^2 C}{\delta x^2} - U_{LC} \frac{\delta C}{\delta x} \qquad 1.32$$

By assuming 'open' boundary conditions Frohlich *et al.* (1991a) expressed a solution to the dispersion model for airlift reactors using the dimensionless Bodenstein number :

$$\Sigma(t) = \frac{1}{2}\left(\frac{Bo_L}{\pi\theta}\right)^{0.5} \exp\left[\frac{Bo_L\,(n-\theta)^2}{4\,\theta}\right] \qquad 1.33$$

where the Bodenstein number is calculated from:

$$Bo_L = \frac{U_{LC}\,H_L}{D_L} \qquad 1.34$$

where U_{LC} is the mean liquid velocity , H is the height of the column and D_L is the liquid phase dispersion coefficient (ms^{-2}). The Bodenstein number is the ratio of convective to

diffusive transport rates which decreases with enhanced backmixing (Fields and Slater, 1983). The equation (1.33) can also be expressed in terms of the Peclet number (Pe)

$$Pe = \frac{U_{LC}\, D}{D_L} \qquad 1.35$$

where D is the height of the liquid (unaerated)

Blenke (1979) demonstrated that the model can be applied to a loop reactor if the summation of dispersion traces for n complete circulations around the loop is described by:

$$E(t) = \sum_{n=0}^{\infty} \frac{1}{2}\left(\frac{Bo_L}{\pi\theta}\right)^{0.5} \exp\left[-\frac{Bo_L\,(n-\theta)^2}{4\,\theta}\right] \qquad 1.36$$

Therefore the overall liquid phase axial dispersion coefficient (D_L) can be obtained by fitting the equation to the experimental response of the reactor to a pulse of tracer with Bo or Pe number as the fitting parameter. Variations of this type of equation in terms of the open boundary conditions for airlift reactors have been made by Van der Laan (1958), Murakami *et al.* (1982) and Warnecke *et al.* (1985). Most significantly was the model proposed by Merchuk and Yunger (1990) that considered that both the riser and downcomer were plug flow sections and the gas separator (top section) represented a well mixed stage.

Of the few mixing studies that exist in the literature the overall dispersion coefficient of the vessel has been used to characterise the mixing performance. The zones of an airlift reactor are hydrodynamically different, hence the dispersion coefficients would also be expected to be different. Verlaan *et al.* (1986) used the Peclet number from the dispersion model to describe the mixing performance in the individual sections. The dimensionless Peclet number is similar to the Bodenstein number and can be defined from the axial dispersion model in a similar manner. The Peclet number for the whole reactor was found to increase with gas flow rate. The same trend was found for the individual zones. In Newtonian fluids the zones were found to be in an order of $Pe_{downcomer} > Pe_{riser} > Pe_{top\text{-}section}$. Chisti (1989) described the fully backmixed state of continuous flow reactors as Pe < 0.1 and plug flow behaviour was described as Pe >20. In Newtonian fluids $Pe_{overall}$ in airlift vessels (external and internal loop) was 30 - 80. Verlaan *et al.* (1989) showed that the Bodenstein number for the riser of a pilot plant external loop reactor with a 50 mM potassium chloride solution was between 30 - 40 and 40 - 50 in the downcomer, with values of 10 in the gas-disengagement section. This indicated that the liquid flow behaved like plug flow with superimposed dispersion and that plug flow could not be assumed in the top section. Frohlich *et al.* (1991a) studied the mixing performance of a pilot plant ($4m^3$) concentric loop airlift reactor and used the Bodenstein number (Bo) to describe the mixing performance. They found that the Bo

diminished with increasing gas velocity in tap water and ethanol solution, thus indicating improved mixing performance. In tap water the presence of antifoam produced a slight increase in Bo with superficial gas velocity and hence a decrease in the dispersion coefficient. Therefore, increasing gas velocity produces a reduction in Bo and enlarges the axial dispersion coefficient. Fields and Slater (1983) also studied the increase in Bo with water from the addition of antifoam and the decrease in Bo with ethanol addition. They attributed these changes to reflect the respective increase and decrease in liquid velocity. Gas disengagement from the water surface in the top section was enhanced by the addition of antifoam and hindered for smaller bubbles from the addition of ethanol. Thus the effect of additives may be partially attributed to changes in turbulence in the head section.

When a tracer is injected into a loop reactor it will circulate around the vessel and be mixed into the liquid phase, and the tracer concentration will reduce to a uniform value throughout the vessel (Onken and Weiland, 1983, Van't Riet and Tramper, 1991). The time that this process involves is described as the mixing time and can be used to characterise the mixing process. It is a measure of the homogeneity of components of the broth, such as microbes, dissolved oxygen and substrate concentrations. However, the mixing time is largely dependent on the measuring method applied and should therefore be considered as a relative measure of mixing performance and not an absolute one (Guy *et al.*, 1986a). Mixing time is defined as the time between the beginning of a mixing operation and the moment when the fluid reaches a required degree of homogeneity (Onken and Weiland, 1983, Siegel *et al.*, 1988). The degree of homogeneity is defined as the relative deviation of the tracer concentration of the pulse, C, at some time after injection from the equilibrium concentration after complete mixing, C_θ.

$$\text{Homogeneity} = \frac{C_\theta - C}{C_\theta} \qquad 1.37$$

Normally the mixing time is measured for 90, 95 or 99% homogeneity. Various tracer methods have been used, the most popular is pH. An acid or base pulse is injected into the reactor and detected by one or more pH electrodes. Other methods include flow followers which contain radio transmitters, radioactive tracers, and electrolyte tracers (Van't Riet and Tramper, 1991).

Most of the mixing studies with airlift reactors have produced data of mixing times to describe overall mixing performance of the reactor. Mixing time has been demonstrated to depend on the superficial gas velocity, volume of the vessel, column diameter ratio, and liquid properties (Weiland, 1984). Pandit and Joshi (1983) found that determination of the mixing time allowed an understanding of the liquid phase flow pattern, effect of surface active agents, change in bubble diameter and gas holdup. Mixing time was found to decrease steeply with an increase in gas superficial velocity whereas at higher gas velocities (generally above 0.06 ms^{-1}), the mixing time decreased at

a slower rate. This has been noted by many workers and Margaritis and Sheppard (1981) related this to the change in flow regime, from bubbly to churn turbulent regime, as described in section 1.4.2.

Russell (1989) found that the ratio of the mixing to circulation time of the pilot scale airlift reactor with baker's yeast broth remained constant with increasing gas velocity from 0.015 to 0.2 ms^{-1}. This indicated that the mixing time process was predominated by the bulk circulation of the liquid rather than axial dispersion due to ascending bubbles. This was also proposed by Weiland (1984).

The liquid mixing time has been shown to decrease with increasing liquid height above the draft tube, to a height above which no further improvement is observed (Chisti, 1989, Russell *et al.*, 1994, Sukan and Vardar-Sukan, 1987, and Weiland, 1984). This indicated the existence of two distinct zones in the top section. Chisti (1989) used dyes to demonstrate the existence of the two zone flow model. When the top section height was above a certain critical height the two zone model existed, whereby the bulk of the recirculating liquid flowed through the lower region, bypassing the upper region. As the liquid level above the draft tube reduced, the circulating flow moved through the entire top section. The decline in mixing time with increasing top section height defined the region of the top section where no upper section exists. As the top section increased up to the critical height the residence time of circulating liquid in the turbulent top section increased, and the rate of pulse dispersion was enhanced. This showed the importance of the top section hydrodynamics to the overall mixing performance of the reactor. Popovic and Robinson (1993) showed similar effects in a pilot scale external loop reactor with CMC solutions as the mixing time improved with increasing dispersion height in the riser.

Decreasing the ratio of downcomer to riser cross sectional area was found by Weiland (1984) to improve mixing in an airlift reactor. This was due to a larger difference in the liquid velocities of the two sections and increased mixing in the top section. Mixing time has been shown to increase with an increase in draft tube height (Onken and Weiland, 1983, Sukan and Vardar-Sukan, 1987 and Russell *et al.*, 1994). Onken and Weiland (1983) explained that the increase in draft tube height increases the length of the circulation path. This extends the distance that the tracer pulse has to travel between the end sections of the vessel where the bulk of the dispersion is suggested to take place and hence, prolongs the mixing time.

Liquid properties influence the mixing time as studied by Pandit and Joshi (1983). Mixing time increased in the presence of electrolytes, such as sodium sulphate and sodium chloride. The average bubble size was found to be small and so an increase in gas holdup and a decrease in the terminal rise velocity was expected. This resulted in a increase in liquid circulation and hence an increase in mixing time. The mixing time increases as the viscosity or the shear thinning properties of the liquid increase (Guy *et al.*, 1986b). However, Russell (1989) observed that the mixing time decreased from the

increase of apparent viscosity during a *P. chrysogenum* fermentation in a pilot scale airlift reactor. This was accounted for by the improved liquid circulation and increased turbulence due to the formation of large bubbles, as the viscosity of the broth increased. Glennon *et al.* (1988) observed a reduction of the Bo from the addition of xanthan gum (flow behaviour of 0.54) to a 300 L external loop airlift reactor when compared to water. This improved mixing performance was not associated with improved liquid circulation as liquid circulation was prolonged due to viscous drag. Glennon *et al.* (1988) suggested the improved mixing must have been due to improved axial dispersion coefficient leading to higher levels of dispersion in a single circulation. Fields *et al.* (1984) observed similar reductions of the Bo with xanthan gum concentrations from 0.1 to 0.5% w/v as a function of superficial gas velocity in a concentric pilot scale reactor. This was contributed to the disengagement of bubble slugs and the formation of slug flow in the downcomer from the coalescence of the small bubbles.

Van't Riet and Tramper (1991) provided data for the comparison of the mixing performance between stirred tanks, bubble columns and airlift reactors of the same dimensions. The tip speed of the stirred tank was keep constant at 5 ms^{-1} whereas, the superficial gas velocity of the bubble column and airlift was compared from 0.001 to 0.1 ms^{-1}. At the low gas velocities (0.001 ms^{-1}), the stirred tank had the best mixing performance with mixing times of 18 s compared to 33 s and 131 s for the bubble column and airlift reactor respectively, at 0.01 m^3 working volume. At high gas velocities (0.1 ms^{-1}) the airlift was preferable when the height/diameter ratio was 10. However, in the region between the highest and lowest gas velocities the difference between vessels was less distinct. At high gas velocities (0.05-0.1 ms^{-1}), the bubble column had lower mixing times than the stirred tank of the same dimensions at all of the working volumes studied. The mixing times for the bubble column and stirred tank were 7 s and 18 s respectively for a working volume of 0.001 m^3, and at 1227 m^3 the mixing times were 97 s for the bubble column and 230 s for the stirred tank. This provided evidence that the circulatory flow of bubbles in a bubble column produced greater mixing performance than the agitator of a stirred tank.

1.5 Oxygen transfer

1.5.1 Introduction

The solubility of oxygen in water is about 10 mg dm^{-3} under saturation conditions so a microbial culture must be supplied with sufficient oxygen to satisfy the oxygen demand (Stanbury and Whitaker, 1984). The oxygen demand is usually maintained by aeration and agitation however, the productivity of a fermentation process can be limited by oxygen availability, and is therefore an important factor in determining fermenter efficiency. In aerated stirred tanks the more viscous and non-Newtonian a broth becomes the higher the power input required to obtain a given oxygen transfer and degree of

mixing. High impeller speeds are required, but possible shear damage may occur (section 1.1). Thus, a gentler and more uniform mixing of airlift reactors or bubble columns could provide satisfactory mixing and efficient oxygen transfer for viscous broths (Merchuk, 1990).

Three steps were described by Bartholomew *et al.* (1950) to represent the transfer of oxygen to the cell during a fermentation, the transfer of oxygen from gas bubble into solution, transfer of the dissolved oxygen through the fermentation medium to the microbial cell and the uptake of the dissolved oxygen by the cell. Bartholomew *et al.* (1950) found the limiting step in the transfer of oxygen from air to the cell in a *Streptomyces griseus* fermentation was the transfer of oxygen to the solution which was improved by increasing agitation. Moo-Young and Blanch (1981) depicted eight diffusional resistances to oxygen transfer in the three steps between oxygen transfer to the cell as shown in figure 1.7. These diffusional resistances involve resistance in a gas film inside and around the bubble and biomass particle. Most of the resistances can be ignored and it is only the liquid film resistance at the gas-liquid interface which is virtually always the rate limiting step (Chisti, 1989). This reduces the problem of oxygen transfer to the problem of gas-liquid interfacial mass transfer and the oxygen transfer rate is dependent on the liquid side mass transfer coefficient, k_L.

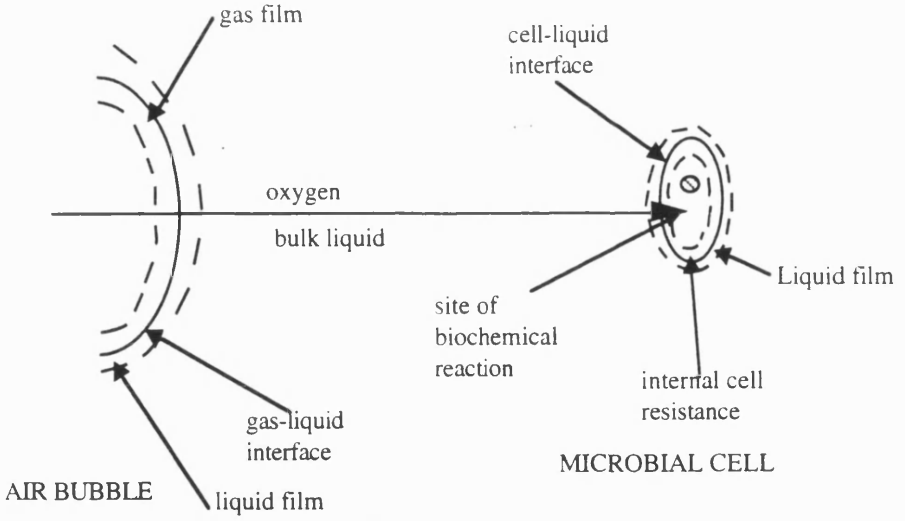

Figure 1.7 Oxygen transport from the bubble through the liquid to the cell. (Chisti, 1989).

The molar oxygen transfer rate per unit liquid volume, N_A, at a certain position within a fermenter can be defined from a knowledge of the k_La and the local driving force for oxygen transfer (C^*-C_L) :

$$N_A = k_L a\,(C^* - C_L) \qquad 1.38$$

where

$k_L a$ = volumetric oxygen mass transfer coefficient (s^{-1})

a = gas liquid interfacial area per unit volume (m^{-1})

C^* = saturation dissolved oxygen concentration ($mol.m^{-3}$)

C_L = dissolved oxygen concentration ($mol.m^{-3}$)

Therefore, during the evaluation of the oxygen mass transfer performance of a bioreactor, a knowledge of $k_L a$ is essential. The influence of reactor geometry, operating variables and liquid properties on $k_L a$ must be determined.

1.5.2 Volumetric mass transfer coefficient, $k_L a$ and oxygen transfer

The coefficient, $k_L a$, is usually experimentally measured as a single value, as the measurement of the separate parameters, liquid mass transfer coefficient, k_L, and the gas liquid interfacial area per unit volume, a, is extremely difficult (Chisti, 1989).

Researchers have used different methods for the calculation of the overall $k_L a$ of a vessel. The rate of oxygen transfer can be determined from the rate of oxidation of sodium sulphite to sodium sulphate which simulates the oxygen consumption of microorganisms (Blenke, 1985). These measurements can be restricted to the studied system due to the sensitivity of gas dispersion characteristics especially interfacial area, and gas holdup to variations of density, viscosity, ionic strength, and surface tension brought about by the presence of reactive solutes (Merchuk, 1991). The gassing out method has been used whereby oxygen is removed from the vessel by gassing out with nitrogen. The deoxygenated liquid is then aerated and the increase in oxygen concentration is monitored by dissolved oxygen probes. Another method used by Russell (1989) and Russell *et al.* (1995) was the gas balance method steady state approach developed by Sobotka *et al.* (1982) which involved measuring the oxygen content of the inlet and outlet gas streams during a fermentation to gain an estimate of the rate of oxygen transfer. The $k_L a$ was then determined from the measurement of the dissolved oxygen concentration. Merchuk (1990) warned that many researchers calculate overall $k_L a$, but as $k_L a$ varies throughout a reactor then local changes in $k_L a$ will be overlooked. Deckwer (1985) described the mass transfer coefficient, k_L as being dependent on the nature of the bubble surface. Small bubbles display a low k_L as they behave as rigid spheres, whereas large bubbles display higher k_L values due to there mobile surface. The specific interfacial area for mass transfer, a, is known to be related to the mean bubble size, d_B and the overall gas holdup (ε) (Chisti, 1989) by:

$$a = \frac{6\,\varepsilon}{d_B\,(1-\varepsilon)} \qquad 1.39$$

Thus large bubbles with large d_B values will reduce a_L and hence reduce oxygen transfer. Also large bubbles tend to reduce the gas holdup as they have high bubble rise velocities. Heijnen and van't Riet (1984) have shown that k_La is enhanced as the mean bubble diameter is reduced. Therefore Russell (1989) suggested that the beneficial effects of a small mean bubble diameter on the interfacial area predominate over the negative effect on k_L with respect to the rate of oxygen transfer. Chisti (1989) claimed that direct measurements of a_L is difficult and the k_L calculated from k_La investigations has led to contradicting results. Therefore, Chisti and Moo-Young (1988) used the ratio k_L/d_B to help to describe an understanding of the mass transfer phenomena. The k_L/d_B can be equated to:

$$\frac{k_L}{d_B} = \frac{k_L a\,(1-\varepsilon)}{6\,\varepsilon} \qquad 1.40$$

which was developed from the gas-liquid interfacial area equation (eq.1.39) and the equation for gas residence time (eq.1.3). Chisti and Moo-Young (1988) measured the overall volume mass transfer coefficient (k_La) and the gas holdup (ε) which altered the k_L/d_B to be measured thus, allowing k_L to be studied without difficult experimental work.

1.5.3 The influence of operating parameters, reactor geometry and fluid properties on k_La

Many researchers have shown that k_La increases with superficial gas velocity due to the corresponding rise in gas holdup (Chisti and Moo-Young, 1988, Bello *et al.*, 1985, Potucek, 1989, and Smith and Skidmore, 1990). Correlations have been made between overall k_La and superficial gas velocity in that k_La has been found to be approximately proportional to gas velocity. As k_La is also influenced by gas holdup then the local changes of gas holdup in an airlift reactor produce changes in k_La values around the airlift loop (Luttmann *et al.*, 1985). Thus k_La in the downcomer would be expected to increase in the downcomer as recirculation is enhanced with increasing gas velocity. The mean gas holdup in the riser is usually larger than in the downcomer, therefore higher k_La values would be expected in the riser (Bello *et al.*, 1985). Russell *et al.* (1995) measured local k_La values as a function of superficial gas velocity in a pilot scale airlift reactor with baker's yeast suspension. Downcomer k_La values were found to be higher than riser k_La which was made as one measurement near the sparger. The time constant for oxygen transfer ($1/k_La$) was slower than liquid circulation indicating that the measured local dissolved oxygen concentrations were not a representation of the equilibrium concentration from the balance between rates of oxygen transfer and oxygen depletion. Thus Russell et *al.* (1995) interpreted the local k_La measurements not as local oxygen transfer conditions, but as indicators of the rate of mass transfer the liquid flow had encountered prior to reaching the point of measurement. Hence, the local k_La

measurements were interpreted by considering the oxygen transfer changes that must have occurred between the probe positions. Therefore, the results indicated that the rate of oxygen transfer was higher in the riser and top section than in the downcomer and was lowest near the base of the fermenter.

An increase of the cross sectional area ratio, A_D/A_R decreases the overall k_La of an airlift reactor in Newtonian and non-Newtonian fluids (Bello *et al.*, 1985, Weiland, 1984 and Popovic and Robinson, 1989). Bello *et al.* (1985) claimed this was due to the variation of the liquid velocity and the relative amount of mass transfer in the downcomer (ie. the effect of downcomer volume). The increase of A_D/A_R produces an increase of the overall liquid velocity of the reactor due to the reduction of gas entrainment into the downcomer (section 1.4.2). The increased liquid velocity would reduce the gas holdup and subsequently reduce k_La. The effect of downcomer volume on the mass transfer rate was due to the negligible mass transfer in the downcomer. As A_D/A_R increases, the downcomer volume is enlarged and the effective volume for mass transfer, which Bello *et al.* (1985) considered to be the riser, decreases producing a corresponding reduction of the overall k_La.

The volumetric mass transfer coefficient has been shown to be dependent on the gas velocity, sparger design and physical properties of the liquid (Moo-Young *et al.*, 1987, and Chisti and Moo-Young 1987). Bovonsombut *et al.* (1987) found that the k_La from a bench top concentric airlift reactor was 50% higher with a porous plate sparger than with a perforated ring sparger in water. This increased up to 2 - 3 times greater when salts were added to the water, although the gas holdup profiles as a function of gas velocity were similar from the two sparger configurations. Bavarian *et al.* (1991) demonstrated with a porous plate gas distributor that k_La decreased with an increase of static liquid height at low superficial gas velocities. At high gas velocities, k_La was independent of static liquid height. For reactors with a perforated plate no effect of static liquid height on k_La was observed. The porous plate at low gas velocities produced small dispersed bubbles and hence higher k_La values than with the perforated plate, but at high gas velocities large spherical capped bubbles formed producing low k_La values. Russell *et al.* (1995) observed that local measurements of k_La in the riser and downcomer of a pilot scale airlift reactor with baker's yeast suspension were independent of the height of the liquid above the top section and increased with draft height. It was suggested that the increase of riser k_La with draft tube height was due to the increase of the gas residence time in the riser. This allowed a longer time for oxygen transfer to occur with the maximum gas content of the vessel before disengagement of a proportion of the gas from the top section occurred. Barker and Worgan (1981) observed that k_La increased with vessel size between working volumes of 0.0725 m^3 to 0.1 m^3 with similar aspect ratios between 9 and 4.7 : 1.

As k_La is influenced by the bubble size as described previously, then k_La would be expected to be influenced by the fluid properties of the broth. k_La in a coalescence

inhibiting alcohol solution was much greater than that of water (Weiland, 1984). The antifoam content of a fermentation broth will reduce k_La (Schugerl *et al.*, 1978). Kawase and Moo-Young (1990) observed that the liquid phase mass transfer coefficient of water decreased by 50% with the addition of 100 ppm of antifoam C.

An increase of broth viscosity has been shown to reduce k_La due to the enhanced coalescence which increases the bubble size, reducing the interfacial area and gas holdup (Bhavaraju *et al.*, 1978, Anderson *et al.*, 1982, Erickson *et al.*, 1983). Russell (1989) observed a reduction of lower riser k_La from 0.12 s^{-1} at 20 h into a *P.chrysogenum* batch culture pilot scale airlift fermentation to 0.005 s^{-1} at 190 h which corresponded to the increase of apparent viscosity from 0.015 to 0.07 Pa.s. Declining gas holdup and k_La with increasing apparent viscosity was observed by Moo-Young *et al.* (1987) from the interval measurements, as a function of superficial gas velocity, during the cultivation of *Chaetornium cellulolyticum* and *Neurospora sitophila* mycelial cultures for SCP production in 1 - 1.3 m^3 concentric airlift reactors. The k_La with *C. cellulolyticum* was found to be 65% lower than in water although the relationship with superficial gas velocity was similar to that of water. Similar reductions of k_La were observed by Barker and Worgan (1981) from interval measurements of k_La as a function consistency index during the cultivation of *A.orzyae* in a 0.0725 m^3 concentric airlift reactor. Carrington *et al.* (1992) found that k_La reduced exponentially with increasing broth viscosity where measurements were made from the fermentation of *S. rimosus* in a 20 m^3 bubble column fitted with an internal helical coil. Measurements made at intervals during the fermentation of *Xanthomonas campestris* in a 1.2 m^3 concentric airlift reactor revealed that the overall k_La decreased rapidly with an increase of xanthan gum concentration (Suh *et al.*, 1992). Similar reductions of k_La have been observed by researchers with pilot scale airlift reactors using increasing concentrations of pseudoplastic simulant fluids, such as carboxymethyl cellulose (CMC) (Halard *et al.* 1989, Kawase and Moo-Young, 1986a), non-Newtonian cellulose fibres (Chisti and Moo-Young, 1988), and xanthan gum (Schumpe and Deckwer, 1987) when compared to water.

1.5.4 Dissolved oxygen heterogeneity

The different sections of the airlift reactor have different flow characteristics and produce different concentration driving forces thus, oxygen transfer will vary in these sections (Onken and Weiland, 1983, Choi, 1990). Lindert *et al.* (1992) showed that the reactor height was an important geometric factor as it affects the saturation concentration and the driving force for mass transfer from the influence of pressure. Therefore the local oxygen transfer rate depends not only on the volume oxygen transfer coefficient but also on the local oxygen concentration in liquid and gas phases. However, the oxygen concentration profile along the liquid path is difficult to predict. The local oxygen transfer cannot be readily estimated and must be determined experimentally (Choi, 1990). Choi (1990) suggested that this justifies the use of scale down approach in airlift design.

Merchuk (1990) claimed that airlift reactors are well suited to processes with changing oxygen requirements because aeration efficiency and performance are relatively insensitive to changes in the operation conditions. Performance (lb oxygen hp^{-1} h^{-1}) decreases in mechanically stirred systems as the oxygen transfer rate increases, but it is quite constant in airlift reactors (Orazem and Erickson, 1979). From the few published studies of oxygen transfer during the cultivation of microorganisms in airlift reactors, it is evident that the introduction of gas at one position in the vessel (riser) leads to variation of the magnitude of gas holdup, and oxygen transfer rates around a reactor loop producing zones of high and low DOTs around the vessel. Of the few examples that exist, the characterisation of this DOT heterogeneity has been limited due to the small number of DOT probes that have been used, indicating that the heterogeneity may be greater than that observed from the measurements. The positions of the zones of DOT seem to be dependent on the geometry of the reactor configuration. For reactors with little gas entrainment into the downcomer, the DOT in the riser has been observed up to 4 times greater than in the downcomer during the cultivation of bacterial cells, *E. coli* and baker's yeast in pilot scale reactors (Adler and Schugerl, 1983, Trager *et al.*, 1992, Onken and Weiland, 1983, Merchuk and Stein, 1981a). These observations have mainly been observed in reactors with A_D/A_R values below 0.2 with vessel heights between 2.75 and 10 m tall. Onken and Weiland (1983) measured the DOT intervals along the riser of an external loop reactor with an A_D/A_R of 0.1 and height of 8.8 m during the fermentation of *Candida utilis*. At a biomass concentration of 5 gL^{-1} DCW the DOT (% saturation at 1 bar) did not increase above 1% until a height of 1 m above the sparger. The DOT then increased to a maximum value of 85% at a height in the reactor of 6 m above the sparger. The reactor was operated with limited gas entrainment hence, the DOT decreased from the top section and down the downcomer although no values were given. The reduction of DOT at the top of the reactor indicated that the gas was likely to be depleted of oxygen and hence, the reactor was sufficiently tall enough for complete oxygen transfer from the bubbles to occur in the riser. This would imply that the entrainment of gas in tall reactors (7 m) would have no benefit to oxygen transfer as the gas bubbles would likely to be depleted of oxygen as they reach the downcomer. Entrainment would also reduce the density difference for liquid circulation and the oxygen partial pressure of the fresh gas in the riser. Thus Onken and Weiland (1983) concluded that the entrainment of gas was only beneficial at small scale reactors. Therefore, the low value of A_D/A_R and reactor operation with limited gas entrainment enhances the overall liquid circulation rate and mixing, and the individual liquid velocity of the downcomer compared to the riser (Weiland, 1984). This results in a small residence time of the cells in the downcomer, limiting the effect of a low DOT environment on the metabolism of the cells. Popovic and Robinson (1993) recommended that the A_D/A_R should be between 0.1 and 0.25 for an external loop reactor in order to achieve acceptable values of liquid phase mixing and oxygen transfer coefficient in viscous non-Newtonian broths. This design regime was

used for the ICI SCP concentric airlift reactor where the A_D/A_R was 0.16 and the height of the riser was 45 m (Smith, 1980) which produced a long gas residence time in the riser for oxygen transfer (Kubota *et al.*, 1978). Sieve plates were used in the riser to disperse large bubbles formed by coalescence and improve oxygen transfer.

For reactors with a high proportion of gas entrainment in the region of 80% of the riser gas holdup, higher DOTs have been observed in the downcomer than in the riser during the growth of baker's yeast in batch culture (Lubbert *et al.*, 1988, McNeil and Kristensen, 1990, Russell, 1989, Russell *et al.*, 1995). Lubbert *et al.* (1988) observed that the gas circulation time was slower than the liquid circulation time hence, it was suggested that as the bubble rise velocity in the riser must have been faster than the liquid velocity, then the gas residence time in the downcomer must be large, aiding oxygen transfer in the downcomer. Frochlich *et al.* (1991a) provided further evidence for this hypothesis as the riser gas residence time was 11% faster than the gas residence time in the downcomer using a reactor of identical geometry with water.

Although airlift reactors have been used successfully for the cultivation of filamentous fermentations at pilot plant scale (Barker and Worgan, 1981, Blakebrough *et al.*, 1978a, Malfait *et al.*, 1981, Schugerl, 1990) oxygen transfer problems have been associated with some viscous fermentations in airlift reactors, and the cyclic change of the DOT around the reactor circulation loop has been found to reduce the productivity performance of the reactor when compared to stirred tank (Suh *et al.*, 1992, Schugerl, 1990, Schumpe and Deckwer, 1987). During viscous fermentations for cephalosporin C (Bayer *et al.*, 1989, Zhou *et al.*, 1993) and xanthan gum production (Suh *et al.*, 1992) the cyclic DOT changes including DOTs below 1% saturation in pilot scale concentric airlift reactors were shown to reduce the productivity performance of the reactor compared to production with reduced DOT heterogeneity in stirred tanks and bubble columns. Bhavaraju *et al.* (1978) found that it was difficult to achieve the required interfacial area for a viscous liquid from the operation gas only operated reactors. Merchuk and Stein (1981b) showed that cycling dissolved oxygen concentration (DOC) still existed in an airlift reactor with a height of 12 m compared to a height of 4 m but the DOCs around the taller vessel were 3 fold greater than with the shorter vessel due to the larger hydrostatic pressure. Similar increases in DOC have been observed by Ho *et al.* (1977) with increasing vessel height. Thus, at production scale a similar magnitude of DOT cycling may exist but the hydrostatic pressure increases the DOT around the vessel to higher values which are likely to have less of an impact on growth or productivity of the process. Onken *et al.* (1984) demonstrated that the oxygen transfer rate during the cultivation of *C. utilis* in a 0.02 m^3 concentric airlift reactor was 3 fold greater at the pressure of 7 bar compared to 1.5 bar. Barker and Worgan (1981) showed that the k_La increased with vessel size at a constant aspect ratio also, Russell (1989) showed that k_La increased with draft tube height. This evidence suggests that the oxygen transfer in production scale vessels may well be greater than at pilot scale leading to improved

productivity of viscous fermentations and successful application of airlift reactors at large scale. Buckland and Lilly (1993) suggested that the low oxygen transfer and heterogeneity problems associated with small scale aerated vessels would result in development and scale up for production scale aerated reactors taking place in stirred tanks. They recommended that airlift reactors are better suited for large scale operation above 200 m^3 where heat transfer (cooling) problems limit the use of stirred tanks.

1.5.5 Modelling of oxygen transfer

Most of the published models on mass transfer in airlift reactors have involved fitting simple fluid dynamic models to experimental values of concentration measured in steady or unsteady state conditions (Merchuk, 1991). The models assume either plug flow or complete mixing of the two phases. Complete mixing has been assumed to be justified when the mixing process (mixing time) is faster than the oxygen mass transfer time ($1/k_La$) (Merchuk, 1991, Deckwer, 1985, Russell, 1989, Chisti, 1989). In this situation the values of k_La from fitting experimental data to a model would be considered to be viable for scale up studies (Merchuk, 1991). However, when a biological demand exists in a reactor a changing dissolved oxygen concentration (DOC) around the vessel will exist and so local k_La values would vary (Russell, 1989). The variation of vessel hydrodynamics especially the gas density difference between the riser and downcomer and the bubble distribution within the reactor results in differences of the local DOC in the reactor. The local DOC in the riser would be greater than in the downcomer when the reactor is operated with limited gas entrainment in the downcomer. Due to the difficulties in local DOC measurement the mean concentration is used for the reactor as calculated from the inlet and outlet gas streams which assumes the complete well mixed theory (Merchuk, 1991). As the experimental measurements have shown that the rate of mass transfer in an airlift bioreactor is influenced by the physico-chemical properties of the two phase mixture, the superficial gas velocity, the gas holdup and the liquid circulation velocity then, several attempts have been made to describe k_La in terms of fluid dynamic characteristics and power dissipation (Kawase *et al.*, 1993, Henstock and Hanratty, 1979 and Banerjee *et al.*, 1970). However, the models do not provide a universal correlation as the different geometric configurations would result in different flow characteristics for the same power dissipation (Merchuk, 1991). Structured models have been developed which consider different areas within a reactor to have distinctive mass transfer characteristics. A small element (stage) or vessel volume of the reactor is considered to be perfectly mixed and the stages are extended to cover the whole of the vessel volume (Luttman *et al.*, 1985, Merchuk *et al.*, 1980, Merchuk and Stein., 1981b, Moresi, 1981, Lindert *et al.*, 1992, Zwietering *et al.*, 1992, Ho *et al.* 1977, Pigache *et al.*, 1992). Russell (1989) considered the models difficult to implement as they require localised k_La values and the inputed data in some published reports were obtained from existing correlations. The models tend to be sophisticated and require extensive experimental data

and sophisticated computer techniques to identify the appropriate model input parameters. The models also assume that the no gas entrainment occurs into the downcomer which is different from reality in some reactors as shown by Russell (1994), Lubbert (1988) and Frochlich *et al.* (1991a,b,c). Luttman *et al.* (1985) showed that a constant value of k_La could not be used to explain the DOC profiles of the reactor observed during baker's yeast cultivation. They suggested that this was due to a change of the interfacial area caused by bubble coalescence near the sparger. Schumpe and Deckwer (1980) also considered the distribution of bubble size and its effect on the overall mass transfer rate when considering the determinate factors of the interfacial areas within a reactor. Thus, the dependence of k_La on the fluid dynamics indicates that it is desirable to have model analysis which involves different k_La for each region of a reactor (Merchuk, 1991). Russell *et al.* (1995) estimated local k_La values around a vessel to vary as much as 5 fold around a pilot scale concentric airlift reactor with a 10 gL^{-1} dry cell weight suspension of baker's yeast. Ayazi Shamlou *et al.* (1994) successfully modelled the localised k_La values from Russell *et al.* (1995) as a function of superficial gas velocity by considering the change of the bubble distributions around the vessel. Higbie's penetration theory (1935) which related the mass transfer coefficient k_L to the liquid phase diffusivitiy and the exposure time was combined with the gas holdup and liquid circulation rate model (Ayazi Shamlou *et al.*, 1994) which produced an expression for predicting k_La. The model produced a good agreement of the experimental local k_La measurements of the riser when a mean bubble diameter of 7 mm was used for gas velocities below 0.06 ms^{-1} and a diameter of 5 mm for higher gas velocities. Downcomer k_La values were modelled by using a bubble diameter of 4 mm. The model demonstrated that the influence of the bubble size distribution on k_La dominated above the combined effect of gas holdup and liquid circulation and so, the change in bubble distribution around the reactor was of major influence on the oxygen transfer performance of the separate regions of the reactor.

1.6 Purpose of the study

The airlift reactor has gained increasing attention due to its advantages of simple construction, appealing mass / heat transfer characteristics, low power input and low shear forces. However, the application of airlifts in industry has been fairly limited to the production of single cell protein from n-alcanes using yeast and biological waste treatment. This is due to the lack of knowledge of basic reactor design. Correlations for gas holdup, liquid circulation and mass transfer exist but are empirically based and only suitable for a certain vessel scale and geometry. The majority of design recommendations have been reactor geometry specific and so a reliable strategy for design and scale up is far from being established (Chisti and Moo-Young, 1987). Most of the laboratory and pilot scale studies have involved water and non-biological systems which have been criticised by researchers for not providing identical behaviour to fermentation broths. Only a few examples of biological research can be found especially for non-Newtonian filamentous fermentations. These examples usually concentrate on either the overall reactor behaviour or on the culture production rate compared to stirred tank. Only a few studies have considered the hydrodynamic and oxygen transfer performance of the reactor inconjunction with the effect of engineering environment on the physiology of fermentation broths. This is especially important with airlift reactors as the cells circulate from aerated to unaerated sections of the reactor with the natural liquid circulation. Cell growth and productivity have been shown to be affected by changing environments such as nutrients, substrate, dissolved oxygen, especially at large scale with liquid circulation and mixing times some 10 times greater than those at lab. scale. Hence, the study of the influence of the engineering environment of airlift configurations in terms of geometry, operating conditions, hydrodynamics and oxygen transfer on the physiology of fermentation broths would be important for the design, operation and scale up of bioreactors. Also, the study of reactor heterogeneity would enable a greater understanding of the impact of reactor heterogeneity observed in large scale vessels.

This study will compare the hydrodynamic and oxygen transfer performance of different configurations of a pilot scale airlift reactor in terms of the individual sections of the reactor with Newtonian baker's yeast broths and non-Newtonian *Saccharopolyspora erythraea* broths. The impact of the engineering environment from the reactor configurations on the metabolism of the two broths will be studied. In addition the impact on cellular growth, morphology and productivity will be studied with the filamentous *S. erythraea* broths and compared with stirred tank.

2.0 MATERIALS AND METHODS

2.1 Variable volume airlift reactor

2.1.1 Reactor configuration

The airlift reactor manufactured by Chemap AG (Volketswil, Switzerland) was designed to be a multi-configurable fermenter. The working volume, draft tube height, top section design and air sparger could all be varied allowing different reactor configurations. The vessel consisted of three cylindrical sections although a conical top section could replace the third cylindrical section. The individual sections could be clamped together to form hermetic seams allowing different vessel heights to be studied. The conical top section provided an outer settling zone from the central degassing region, which was required during continuous culture of immobilised *Penicillium chrysogenum* (Keshavarz *et al.*, 1990). Batch fermentations were investigated for this study and so the conical top was not utilised.

For the majority of this study the tallest reactor configuration (4.11 m tall) with the three cylindrical sections was used, with a draft tube height of 2.77 m ,as shown in figure 2.1. Each individual cylindrical section was jacketed and contained a single rectangular sight glass mounted on the side of the vessel. Each section contained a number of 0.025 m diameter side ports for insertion of probes and a number of 0.01 m side ports for acid and alkali addition which could be capped when not in use. The bottom section (125 L total volume) was a fixed section which, contained the manual sample valve situated 0.53 m above the base of the vessel and, a pneumatically operated harvest valve fitted to the vessel base, both valves were steam sterilisable. The head plate of the reactor formed the same hermetic seam as the other vessel sections and contained five 0.019 m diameter ports, pressure gauge and the exit gas tubing incorporated through a mechanical foam breaker (Fundafom,Chemap AG). The system contained four discs of 0.18 m diameter which were situated 0.13 m below the top plate. The discs were rotated by a 2.2 kW motor and the centrifugal action of the discs prevented foam from entering the exit gas system. A conductance probe could be suspended from the head plate and would activate either the Fundafom or a dose of antifoam from the stainless steel antifoam reservoir. However, the Fundafom system was not used during this study.

The vessel internal diameter was 0.317 m and the draft tube external diameter was 0.217 m hence, the cross sectional area of the annulus of the vessel was 0.0419 m^2. The inside diameter of the draft tube was 0.211 m which gave a cross sectional area of 0.035 m^2. Thus, when the annulus of the vessel was sparged with air and became the riser, the ratio of downcomer to riser cross sectional area, (A_D/A_R) was 0.83. Hence, when the riser was the draft tube the A_D/A_R was 1.197. The dimensions of the three vessel sections used in this work are shown in table 2.1. As the vessel volume could be varied then the draft tube height must also be altered in order to allow for the change in vessel height. This was achieved by using draft tubes of different lengths. Six different

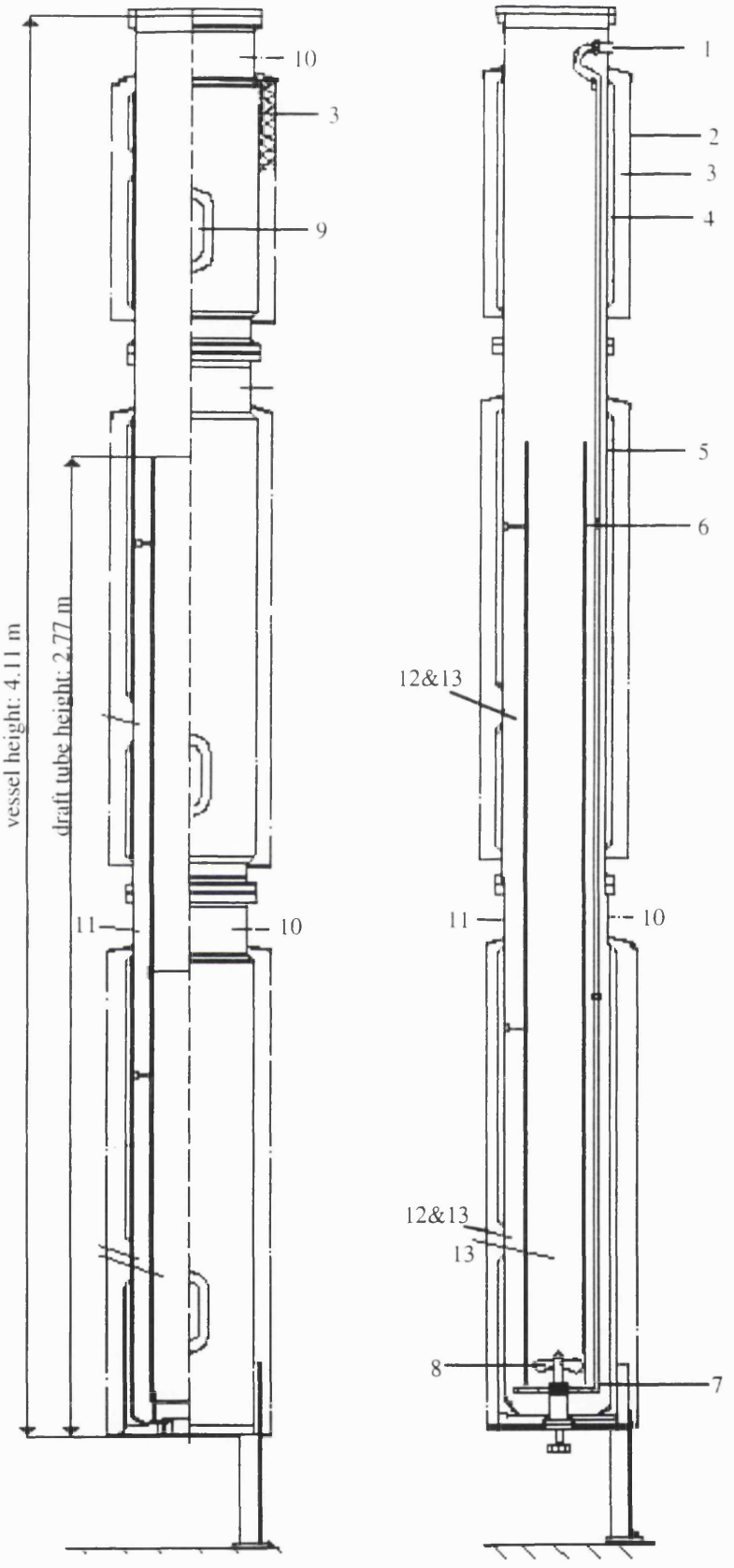

Figure 2.1 The tallest configuration of the pilot scale airlift reactor (Key : (1) air inlet, (2) vessel outside casing, (3) insulation cladding, (4) temperature circulation jacket, (5) inside vessel wall, (6) draft tube, (7) air ring sparger (draft tube or annulus), (8) marine propeller, (9) sight glass, (10) addition port, (11) pH probe, (12) pressure probe, (13) dissolved oxygen tension probe.

Table 2.1 Vessel section details

Vessel section	Section height (m)	Section volume (m^3)	Jacket volume (m^3)
Section 1 (base)	1.545	0.125	0.02
Section 2	1.59	0.125	0.014
Section 3	0.97	0.077	0.0075

lengths were provided which could be clipped together in a number of combinations to produce a variety of different heights. A rubber seal was incorporated between the draft tube lengths and held in place by the tube clips. This prevented leakage between the draft tube and annulus of the vessel. Each draft tube section had a number of horizontal struts with plastic cushions. The cushions sat against the vessel wall, holding the tubes firmly in the centre of the vessel. The six draft tube lengths were 1.11, 1.6, 0.61, 0.53, 0.45 and 0.24 m. The bottom draft tube was 1.11 m tall and had legs fitted to its base of 0.06 m in length producing a total draft tube height (H_{DT}) of 1.17 m from the vessel base. The legs of the tube produced the annular gap for liquid circulation at the base of vessel. This draft tube also contained a hole, 0.53 m from the vessel base, for the insertion of a dissolved oxygen tension probe from the outside of the vessel into the inside of the tube.

The reactor had three different sparger configurations as shown in figure 2.2. The perforated plate with a diameter of 0.13 m, had 120 orifices of 1 mm in diameter arranged in four concentric circles. This sparger was situated in the centre of the vessel base (figure 2.2.1) and vessel performance with this sparger using the draft tube as the riser was characterised by Russell (1989). In a conventional airlift reactor, liquid circulation would be controlled by the gas velocity however, the reactor could also operate with a marine propeller at the base of the vessel (figure 2.2.2.). The propeller may allow independent control of the liquid circulation in the vessel other than aeration. The three bladed propeller had a diameter of 0.16 m, a blade pitch of 120^0 and the distance from the vessel base to the propeller blades was 0.13 m. It was driven from beneath the vessel by belt drive from a variable speed reversible rotation motor (2.2 kW) and had a speed range of 0 to 1000 rpm. The impeller drive shaft was mechanically sealed and lubricated by static sterile steam condensate under 1 bar pressure above the vessel working pressure. The pressure was supplied by either steam or sterile compressed air. This system ran from the top of the vessel through the foam breaker and down to the propeller drive shaft. To use the propeller a different sparger to the central perforated plate must be used hence, two ring spargers (draft tube or annulus) with different diameters were studied. Both spargers had the same number of orifices, with 16 pairs of equally spaced orifices on the top of the sparger and 4 orifices underneath with a diameter of 2 mm. The orifices for each pair were spaced opposite each other and perpendicular to the axis of the ring sparger tube. The two ring spargers had different

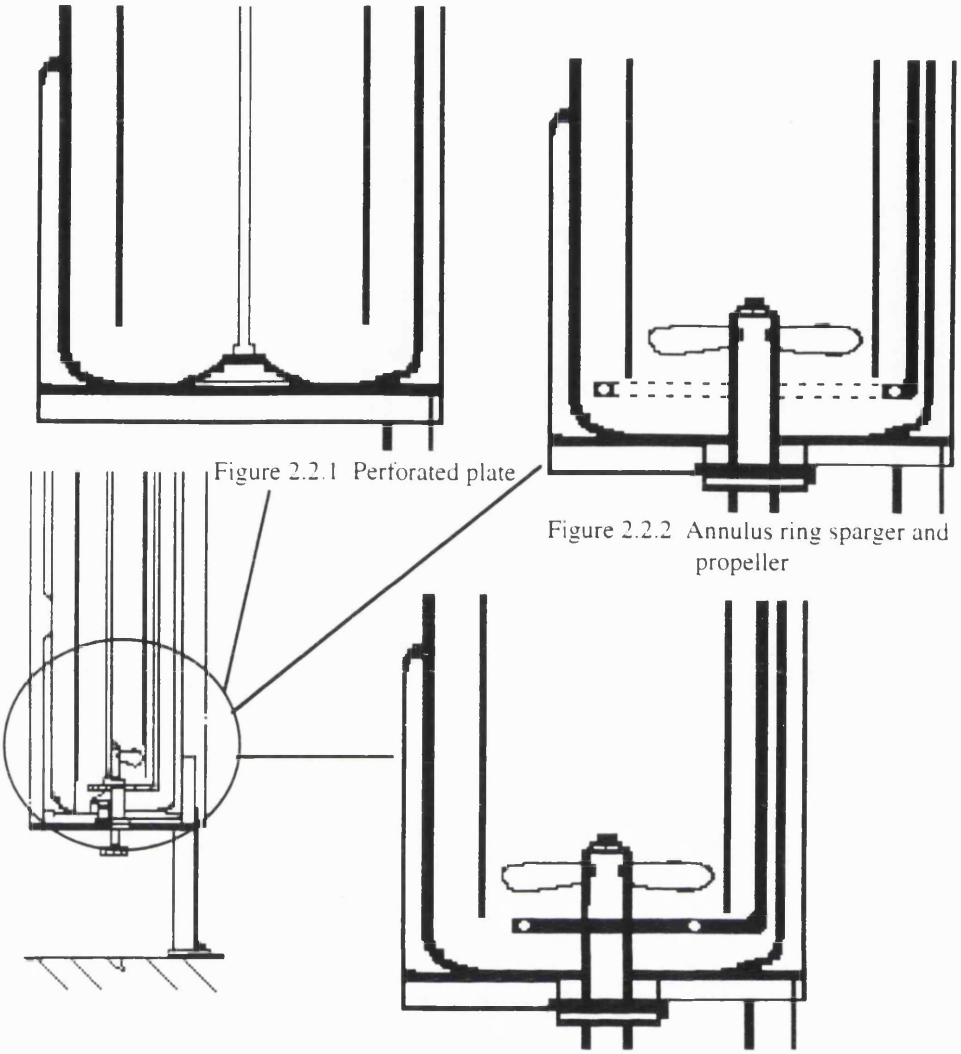

Figure 2.2.1 Perforated plate

Figure 2.2.2 Annulus ring sparger and propeller

Figure 2.2.3 Draft tube ring sparger and propeller

Figure 2.2 Schematic diagram of the sparger configurations of the airlift reactor.

diameters and so the spacing between pairs of orifices was also different. The draft tube ring sparger had the same diameter as the propeller of 0.16 m and was used to sparge air into draft tube (figure 2.2.3). This sparger was positioned 0.07 m beneath the propeller at the base of the draft tube and the spacing between the pairs of orifices was 0.03 m. The air line curved under the draft tube and was held on the inside of the vessel wall entering at the side of the top section of the vessel. For conventional airlift operation when the propeller was left static, air was sparged into the draft tube which became the riser, and liquid recirculated down the annulus of the vessel which was the downcomer. For combined aeration and propeller operation the propeller was rotated to push liquid up the riser in the direction of the aerated liquid flow. The annulus ring sparger (figure 2.2.2) had a diameter of 0.26 m and the spacing between the pairs of orifices was 0.051 m. The sparger was used to aerate the annulus of the vessel which became the riser and the draft tube was the downcomer. For combined aeration and propeller operation the

propeller was rotated to draw liquid down the draft tube in the direction of liquid flow with the intention of enhancing the liquid recirculation at the base of the vessel.

2.1.2 Instrumentation and control

The fermentation was monitored by a number of probes. pH was monitored by Ingold probe no.764-50 and mounted at the height of 1.48 m into the annulus of the vessel. Three dissolved oxygen tension probes were used, two of which were 0.07 m long, and the third was 0.15 m long. These were mounted at the heights of 0.53 m and 2.11 m in the annulus of the reactor and the probes protruded 0.02 m into the vessel. The third probe was inserted at a height of 0.53 m and protruded 0.1 m into the vessel through the hole in the draft tube. A fourth mobile dissolved oxygen tension probe was used to monitor dissolved oxygen tensions around the vessel with the non-sterile baker's yeast suspensions. A slim probe was required, connected to a long adjustable support, so that dissolved oxygen tensions could be measured at different heights within the vessel. This probe was constructed by the biochemical engineering department workshops and was based on the Ingold design. The probe contained the inner Ingold silver electrode and membrane system but also, extra O-ring and resin systems were introduced around the electrical cable exit of the probe to keep the unit waterproof. The membrane could be removed and electrolyte replaced as with a conventional Ingold dissolved oxygen probe. The probe was then connected to a stainless steel rod by an adjustable collar which allowed the radial position of the probe to be varied. The stainless rod was in three sections with a total length of 4.5 m. The sections were screwed together as the probe was lowered further into the vessel and the electrical cable of the probe clipped to the rod sections. The rod was graduated so that the actual probe position in the vessel was known. The probe was lowered into the vessel through the sight glass on the vessel top plate and was only used during non-sterile conditions. The probe could be lowered down the draft tube or annulus of the vessel and was held at the desired vessel height by a clamp system on the top plate. The probe used an existing dissolved oxygen amplifier and so, only one of the 0.07 m long dissolved oxygen probes was used when the mobile probe was required.

Temperature of the broth was measured by a resistance probe (Chemap AG) positioned into the annulus of the vessel at a height of 1.48 m above the vessel base. Two pressure transducer probes were used to measure the gas holdup in the annulus of the vessel and were placed at heights of 0.53 and 2.11 m from the vessel base. The probes were inserted inside stainless steel sleeves in order to fit the vessel ports of 0.025 m in diameter. Air flow rate was measured by a HI-TEC thermal mass flow sensor (Bronkhorst High Tech BV, The Netherlands). This flow sensor was calibrated to give a volumetric flow rate of gas at atmospheric pressure. Chemap standard amplifiers were used to process probe signals. Two 8-loop control units (Turnbull Control Systems Ltd, Worthing, U.K.) were used to monitor and control the parameters described, such as gas

flow rate and impeller speed. The data from the control units was monitored by a real time data acquisition system (Acquisitions Systems Ltd, Fleet, Hampshire). The pH was controlled by opening/closing a pneumatic valve from the reservoir of the acid or alkali. The steam or water for temperature control were controlled by pneumatic proportional valves. Also, the speed of the impeller was controlled by a frequency converter unit (Danfoss Ltd.) coupled to the impeller motor.

2.1.3 Ancillary equipment and piping systems

A schematic diagram of the air inlet and outlet lines plus the addition systems can be seen in figure 2.3. Compressed air from the existing pilot plant supply passed through a series of coarse filters with an oil separator and then, through a proportional pneumatic valve controlled as mentioned previously by a TCS controller unit (section 2.1.2). Air then passed through the inlet sterilisable cartridge filter unit (0.22 μm in size, Dominic Hunter Filters Ltd, Birtley) and for normal working operation valves 13.01, 13.02 and 13.03 would be open. Valve 13.08 allowed air to the head space and was usually closed except under sterilisation conditions. Air left the vessel via valves 14.03, 14.02, and 14.10 with the outlet filter cartridge between valves 14.02 and 14.10. Valve 14.10 was a proportional valve which could control the vessel positive pressure. The vessel was never operated at pressure other than atmospheric, and so the valve was only controlled during the sterilisation procedure. An air line was connected to the exit gas valve 14.10 to direct exit gas via a pump to a mass spectrometer (VG Gas Analysis Systems Ltd) for exit gas analysis.

Acid and alkali were stored in two 20 litre stainless steel reservoirs mounted to the base support structure of the airlift reactor with stainless steel tubing connections to the vessel side ports. The reservoirs could be pressurised with either steam or sterile air. The head pressure of the tanks were kept at 1 bar and the pneumatic valves 17.07 and 18.07 were automatically controlled for addition to the vessel. A third 10 L addition vessel existed for antifoam addition but was not used. The piping system for temperature control of the airlift can be seen in figure 2.4. Liquid was circulated via a centrifugal pump (Perfecta 3-125-2, Rutschi Pumpen, Geneva, Switzerland) through the jackets surrounding the vessel. Water flowed anticlockwise ($4m^3h^{-1}$) from valve 12.02 upwards through the vessel jacket and recirculated via valves 12.05, 12.04, and 12.06. Temperature was automatically controlled by valves 12.01 for steam or 12.02 for water.

2.1.4 Sterilisation procedure

To heat the vessel to 121^0C the vessel jacket was solely heated with steam thus, valves 12.01, 12.03 (figure 2.4) were opened, while valves 12.02, 12.06, 12.04, and 12.05 were closed. This resulted in steam injection in a clockwise direction from the vessel top section jacket down to the bottom section and condensate left the system through the thermostatic steam trap when valve 12.07 was open. The fermentation

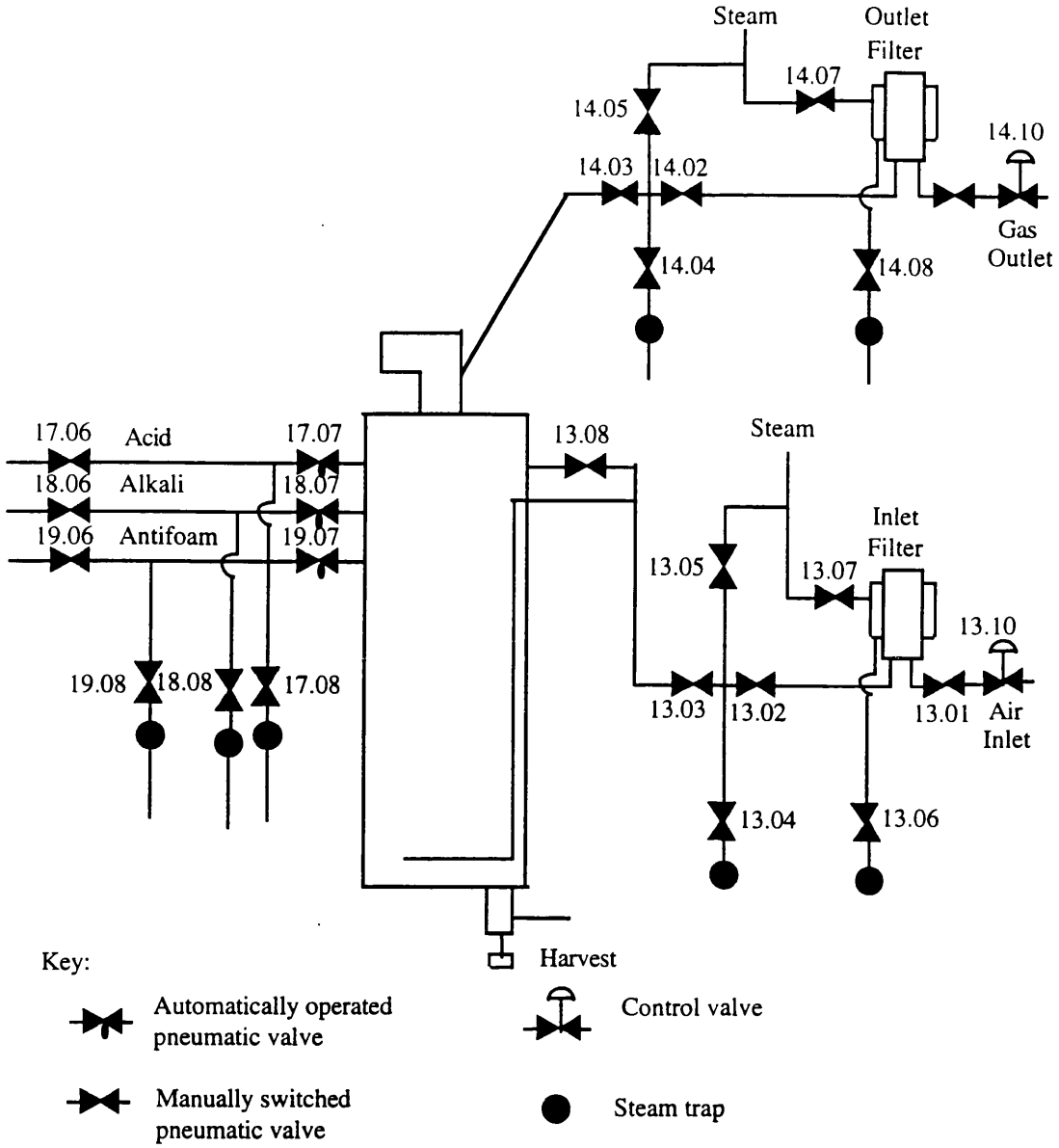

Figure 2.3 Schematic diagram of the air inlet / outlet systems of the airlift reactor including addition lines.

medium was mixed in a 250 L stirred tank and pumped to the top of the airlift via a monopump. While the vessel was filling, the mechanical seal system was filled with condensate as described in section 2.1.1. Also, the acid and alkali reservoirs and addition lines were steam sterilised. Valves 17.07, 18.07, and 19.07 on the addition lines were closed while valves 19.08, 18.08, 17.08, 19.06, 18.06, and 17.06 before the steam traps were opened (figure 2.3). The reservoirs were sterilised for 30 minutes at 1.2 bar and then valves 19.08, 18.08 and 17.08 were then closed. The tanks and lines up to valves 17.07, 18.07 and 19.07 were pressurised with air to prevent the formation of a vacuum. Once the vessel had been filled with medium steam was applied to the jacket. Air was sparged into the vessel to provide liquid circulation for heat exchange. Ports on the top plate were left open to allow sparged air to escape, as the exit filter was sterilised as the vessel heated to 100^0C. Valves on the exit gas line, numbers 14.03 and 14.01 (figure

2.3), were closed while the steam valves 14.05 and 14.07 were opened. Valve 14.07 let steam into the jacket of the filter housing. Spirax steam traps were used to remove condensate from the air lines via valves 14.04 and 14.08. The exit gas line was sterilised for 30 minutes at 1.2 bar. When the vessel reached 50^{0}C air from the sparger was switched off and liquid circulation was performed via the marine propeller at 400 rpm. The inlet air line was then sterilised by closing valves 13.03 and 13.01. Steam then entered via valves 13.05 to the filter and via 13.07 to the filter jacket. The condensate was removed through steam traps via valves 13.04 and 13.06 and the line was sterilised for 30 minutes at 1.2 bar. When the vessel temperature approached 100^{0}C the top plate ports were sealed for sterilisation.

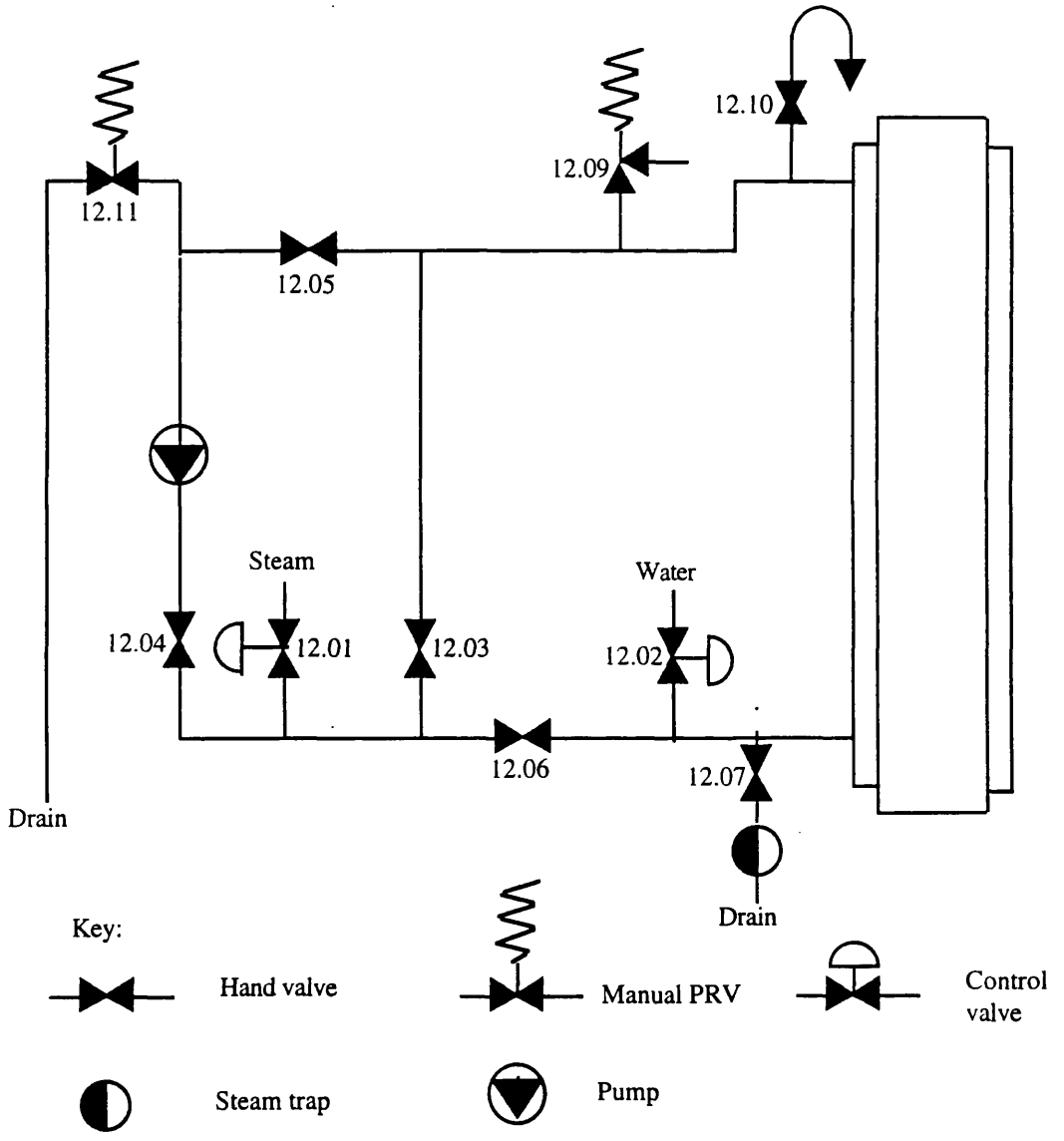

Figure 2.4 Temperature control system.

The vessel pressure was held at 121^{0}C, 1.0 bar for 40 minutes. Steam traps around the top plate were used to allow the sterilisation of the inlet and exit gas piping connected to the top plate. These areas were not sterilised when the air lines were separately sterilised. Therefore, valves 14.02 and 13.02 were closed and 14.03, 14.04 on the exit line and

valves 13.03, 13.04 on the inlet air line were opened (figure 2.3). Valve 13.08 was also opened to stop the vessel contents drawing out through the air inlet line steam trap via valve 13.04. The addition lines between the automatic valves and the top plate were also sterilised with the vessel by closing valves 17.06 and 18.06 and opening 17.07, 18.07, 18.08 and 17.08. When the sterilisation period was completed all valves to the steam traps were closed followed by closure of the steam inlet valves. The vessel was cooled rapidly by allowing water to flow in the anticlockwise direction by closing valve 12.07 to the steam trap leaving the vessel jacket, and valves 12.06 and 12.04 (figure 2.4). Valves 12.05 and 12.11 were fully opened to allow the maximum release of coolant water to drain. As the pressure of the vessel reached atmospheric, the exit gas line was opened (valves 14.03, 14.02, 14.10: figure 2.3) to stop a vacuum forming in the vessel. When the vessel reached working temperature the air was introduced into the vessel and the temperature circulation system was switched from crash cool format to liquid circulation using the centrifugal pump described in section 2.1.3.

2.2 Stirred tank fermenter

A 42 L stirred tank fermenter (LH Fermentation Ltd, Reading, U.K.) was used as a seed vessel for the airlift reactor. The vessel was jacketed and contained three Rushton turbine impellers with diameters of 0.1 m. Sterilisation of the vessel contents was performed by passing steam at 1.2 bar through the jacket for 30 minutes. The medium temperature was monitored by a resistance probe and adjusted by the flow of cooling water through the jacket via a solenoid valve, and by the introduction of heat by a heating element directly inside the vessel. pH and dissolved oxygen tension were measured by Ingold probes inserted into the 0.025 m ports on the side of the vessel. pH was regulated by the addition of 4 M ammonia or 4 M sulphuric acid via peristaltic pumps from addition reservoirs. Control of temperature, dissolved oxygen tension, pH, stirrer speed and air sparge rate was by TCS controller as described for the airlift reactor (section 2.1.2).

2.3 Fermentation of *Saccharomyces cerevisiae*

2.3.1 Fermentation media

The medium used was (gL^{-1}):

Glucose	10
Yeast extract	10
Ammonium sulphate	5
Potassium dihydrogen phosphate	2.5
Polypropylene glycol	0.25 mL L^{-1}

Yeast extract was 'Yeatex' supplied by CPC Ltd, Bovril Foods Ltd (Burton-on-Trent, U.K.). All other materials were standard grade and supplied by Fisons Scientific Equipment (Loughborough, U.K.). Softened tap water was used but not sterilised.

2.3.2 Fermentations conditions

The objective of the fermentation was to produce a microbial oxygen demand similar to an industrial fermentation. The fermentation used block baker's yeast (Distillers Company Ltd, Surrey) as an inoculum under non sterile conditions. This simplified the fermentation in that aseptic conditions and inoculum development were not needed. A large inoculum of either 5 or 10 gL^{-1} dry cell weight (DCW) of packed yeast was used in the airlift reactor so that the growth of contaminating organisms was greatly reduced. The medium was prepared in a 250 L stirred mixing vessel and pumped into the reactor using a monopump. Blocks of yeast were broken up into a stirred vessel and then pumped into the reactor. The total volume of the liquid was adjusted with water and then air was sparged into the vessel. The exit gas analysis showed that the yeast began to metabolise soon after the air was switched on. pH was maintained at pH 7 and vessel temperature was controlled at 26^0C. During the six hour fermentation the air flow rate was varied to perform hydrodynamic and oxygen transfer measurements as described in section 2.6. The short duration of the fermentation meant that evaporative losses were insignificant. A 25 mL sample was removed before and after the fermentation to confirm that the dry cell weight remained relatively constant throughout the fermentation. A sample of the yeast was filtered through pre-dried and weighed 0.45 μm filters (Millipore Ltd) and dried at 80^0C for 30 hours or until constant weight was achieved. The dry weight was found to increase by less than 1 gL^{-1}.

2.4 *Saccharopolyspora erythraea* fermentations

The strain of *Saccharopolyspora erythraea* was a wild type strain, NRRL B2338, donated by Dr. J. Cortes, Cambridge University.

2.4.1 Culture maintenance and spore production

Spores were produced from the mycelial growth on tap water agar medium after incubation for 11 days at 29^0C. The composition of the medium was as follows:

	gL^{-1}		gL^{-1}
Glucose	5	Tryptone	5
Sucrose	10	Yeast Extract	2.5
EDTA	0.036		

Medium was sterilised for 20 minutes at 121^0C, 1.0 bar and the glucose and sucrose were sterilised separately and added aseptically to the medium. pH of the medium was adjusted to pH 7 with sodium hydroxide before sterilisation. All chemicals were Analar

grade (Fisons Scientific Equipment, Loughborough, U.K.) and tryptone and yeast extract were from Unipath Ltd. (Basingstoke, U.K).

Spore suspensions were prepared from stock spore cultures using 20% glycerol solution and glass beads to scour the surface of the agar. Spore harvests were pooled and the spore concentration measured by plate counts. Spore suspensions were diluted to 10^{-8} and each dilution was plated onto Petri dishes containing nutrient broth. Plates were incubated at 29^{0}C for 72 hours and colonies were then counted.

2.4.2 Inoculum development

2.4.2.1 Shake flask culture

2 L Erlenmeyer baffled flasks were used with 500 mL of medium for spore germination. Each flask was inoculated with spore suspension to give a concentration of 10^6 spores mL^{-1}. The flasks were incubated for 48 hours at 29^{0}C at 150 rpm in an orbital shaker. Four flasks were inoculated to provide an 8% inoculum for the 25 L seed fermentation in the 42 L fermenter.

Composition of the media for liquid culture was adapted from Yamamoto *et al.* (1986) as follows:

	gL^{-1}
Bactopeptone	4.0
Yeast extract	6.0
Glycine	2.0
Magnesium sulphate,($MgSO_4.7H_2O$)	0.5
Potassium dihydrogen phosphate	0.68
Glucose-shake flasks & seed fermentation	10.0
- Large scale fermentation	30.0
Polypropylene glycol-large scale	1 mL L^{-1}

The glucose and potassium dihydrogen phosphate were sterilised separately and aseptically added to the medium. pH of the media was adjusted to 7.0 with sodium hydroxide before sterilisation. Sterilisation was for 20 minutes at 121^{0}C, 1.0 bar. Yeast extract was 'Yeatex' supplied by CPC Ltd, Bovril Foods Ltd., (Burton-on-Trent, U.K.). Bactopeptone was obtained from Unipath Ltd. (Basingstoke, U.K). All other chemicals were Analar grade (Fisons Scientific Equipment, Loughborough, U.K.)

2.4.2.2 Stirred tank seed fermentation

The 42 L fermenter was used to provide a 10% (25 L) inoculum for the large scale fermentation in the airlift fermenter. The liquid medium was sterilised in situ for 30 minutes at 121^{0}C, 1bar. The pH was controlled at pH 7.0 using 4 M ammonia solution and the temperature was controlled at 29^{0}C. The stirrer speed was maintained at 450 rpm and the airflow rate at 0.5 vvm. Glucose and potassium dihydrogen phosphate were aseptically added to the fermenter via a flask with side arm and inoculation needle for

entry into a top plate port. This flask was also used for inoculation of the vessel from the shake flask cultures. Fermentations which ran for 12 hours were used for inoculation into the airlift reactor to produce pelleted fermentations and 19 hour fermentations were used as inoculum to produce mycelial fermentations in the airlift reactor.

2.4.2.3 Large scale fermentation

The 25 L seed fermentation was used to inoculate the airlift reactor, via sterile flexible silicone tubing, to produce a final working volume of 250 L. The mobile stirred tank was moved to the base of the vessel and the tubing connected via sterile inoculation needles to the bottom of the 42 L tank and to the top plate of the airlift reactor. Air was supplied to the 42 L fermenter and a head pressure was created to transfer the culture to the airlift reactor. The 30% glucose and potassium solutions were sterilised separately and pumped from a 20 L sterile aspirator by a peristaltic pump (Watson-Marlow, Falmouth, U.K.) through sterile silicone tubing and inoculation needles into the top plate of the airlift reactor. The pH of the broth in the airlift reactor was controlled at pH 7.0 using 4 M ammonia solution and 4 M sulphuric acid. The temperature was controlled at 29^0C. The airflow rate usually commenced at 0.4 vvm for 9 hours which was then increased to 1.2 vvm. However, this procedure was varied in some fermentations as the airflow rate was continuously increased in small increments from 0.32 vvm to 1.2 vvm. The airlift reactor had no condenser fitted to the exit gas line and so, the liquid level may decrease due to surface evaporation. During the beginning of the fermentation it was found that the injection of acid / alkali for pH control was sufficient to maintain a constant volume. However, after 30 hours it was necessary to continuously add water to the vessel to composite for the water loss due to evaporation. The rate of evaporation was estimated by measuring the humidity of the inlet and outlet air streams using a sling psychrometer and calculating the amount of water absorbed by the air stream per unit time. Sterile water was introduced to the vessel by a peristaltic pump (Watson and Marlow, Falmouth, U.K.). Fermentation samples were regularly removed from the vessel every four hours for analysis via the manually operated sample valve (section 2.1.1).

2.5 Xanthan gum - non-Newtonian fermentation broth simulant studies

A small number of hydrodynamic studies were performed with the pseudoplastic fluid of xanthan gum (Rhodigel 200: Rhone - Poulenc, Usine de Melle, France). The solutions of xanthan gum (0.1 to 0.625% w/v) were prepared in a mixing tank by gradually adding xanthan powder to water until a homogenous solution was produced after approximately 4 h. The solutions were then pumped via a monopump to the airlift reactor for the hydrodynamic studies which were completed within 5 h.

2.6 Hydrodynamic measurements

2.6.1 Liquid velocity

A tracer response technique was used to measure the velocity of the liquid circulating around the reactor, as utilised by many other researchers including Chisti (1989) and Fields and Slater (1983). An alkali pulse was injected into the vessel and detected further along the liquid flow path by the pH probe. As the pulse passed the probe on each circulation around the reactor, a peak was indicated on the signal from the pH amplifier. This produced a sinusoidal type of response, on a chart recorder, where the amplitude of the peaks progressively decayed due to the gradual dispersion of the alkali pulse. The time taken for a single circulation of alkali pulse was equivalent to the time period between successive peaks or troughs of the response profile (figure 2.5).

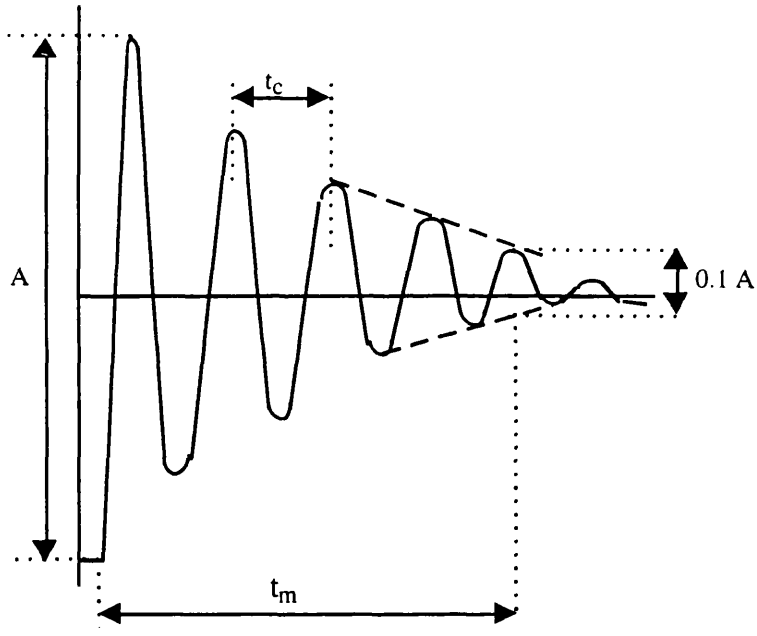

Figure 2.5 A typical tracer response profile from an addition of an alkali pulse detected by a pH probe (idealised). The t_c refers to the liquid circulation time, and t_m the mixing time to 90% homogeneity of the pulse amplitude A.

The pulse (4 M sodium hydroxide with yeast suspensions or 4 M ammonia solution with *S. erythraea* fermentations) could be injected into the reactor at two different positions, at the top of the vessel above the annulus, or in the middle of the vessel directly into the annulus. The pH probe was located in the annulus of the vessel at a height of 1.48 m from the base of the vessel. The volume of pulse injection was kept constant by controlling the over pressure of the alkali reservoir at 1 bar and by manually activating the pneumatic alkali addition valve for a time period of 2 s. No difference in liquid circulation time was observed from the different injection positions. A mean liquid circulation time was calculated from each response profile by averaging the circulation time values measured from all pairs of peaks and troughs in the profile. Liquid velocity

was then calculated from the mean liquid circulation time and distance for a single circulation around the vessel. The distance of a single circulation was the mean path length for liquid flow around the vessel loop incorporating the upflow in the riser, downflow in the downcomer and recirculation at the top and bottom of the vessel (figure 2.6). The vertical displacement of liquid beyond the ends of the draft tube was ignored. The length, l was given by equation 2.1 shown below, where D = internal diameter of the column (m) and D_R = diameter of the riser.

$$l = \frac{D - D_R}{4} + \frac{D_R}{4} = \frac{D}{4} \qquad 2.1$$

The liquid velocities in each section of the vessel were different due to the different cross-sectional areas of the riser and downcomer and as the volumetric flow around the loop remained constant. Appendix 3 showed that for the reactor with air sparging from the draft tube sparger the liquid velocities in the riser (U_{LR}) and downcomer (U_{LD}) were equivalent to :

$$U_{LR} = \frac{2.2\ H_{DT}}{t_c} \qquad U_{LD} = \frac{1.8\ H_{DT}}{t_c} \qquad 2.2$$

where H_{DT} was the height of the draft tube from the vessel base. For the annulus sparger, the riser was the annulus of the vessel and hence, the liquid velocities were calculated from:

$$U_{LR} = \frac{1.8\ H_{DT}}{t_c} \qquad U_{LD} = \frac{2.2\ H_{DT}}{t_c} \qquad 2.3$$

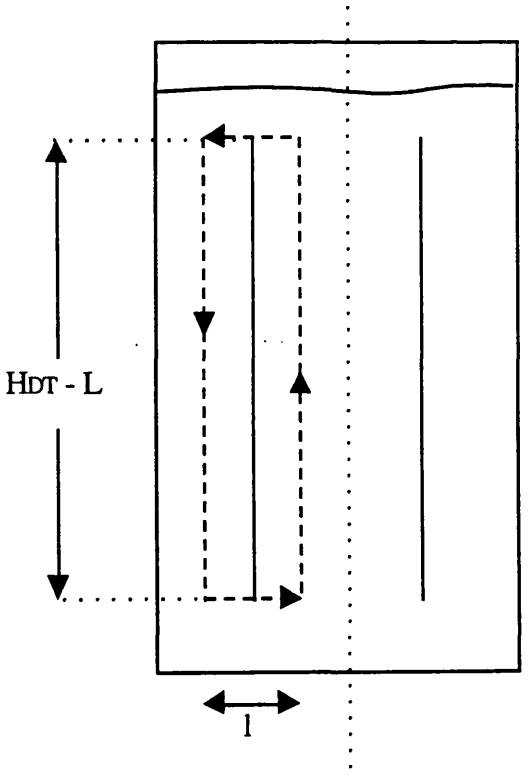

Figure 2.6 Path length of liquid flow around the draft tube, (where L refers to the clearance between bottom of the draft tube and vessel base, 0.06 m)

2.6.2 Liquid mixing

The liquid mixing time has been used to characterise the mixing performance of a reactor by many researchers (Fields and Slater, 1983, Chisti, 1989, Weiland, 1984, Siegel *et al.*, 1988, Russell *et al.*, 1994). Mixing time is defined as the time between the beginning of a mixing operation and the moment when the fluid reaches a required degree of homogeneity (Onken and Weiland, 1983, Siegel *et al.*, 1988). The mixing time was measured from the tracer response profile produced by an alkali pulse (section 2.6.1). As the pulse circulated around the reactor it mixed into the liquid phase and the tracer concentration was reduced to a uniform value throughout the vessel (Onken and Weiland, 1983, van't Riet and Tramper, 1991). This study used the time for the oscillatory response to decay to a tenth of the value of the initial peak as shown in figure 2.5. However, this method did not take into account the time taken for the pulse to circulate from the injection point to the pH probe. This resulted in a method where the rate of pulse dispersion was independent of the injection position. Guy *et al.* (1986a) concluded that the use of mixing time to describe the mixing performance of a vessel was only a relative method and not an absolute one. This was due to the mixing time being dependent on the degree of homogeneity specified, the measuring method and the flow conditions. This made comparison between different researchers characterisations rather difficult. However, although this was a relative method it did allow comparison of the mixing performance between the different configurations of the airlift reactor.

2.6.3 Gas holdup

The overall or mean gas holdup and gas holdup of the annulus of the vessel were measured with this airlift reactor. The overall gas holdup was measured using the volume expansion method. The holdup of the dispersed particles was the difference between the volume of the dispersion and volume of the liquid. In the airlift reactor the volumes were measured by the liquid level heights with and without air sparging. The height difference between the two phases was used to calculate the gas holdup by the equation :

$$\varepsilon_{overall} = \frac{H_D - H_L}{H_D} \qquad 2.4$$

where

H_D = height of gas–dispersion (m) = H_L + h

H_L = unaerated liquid height (m)

h = height of dispersion above draft tube (m)

The dispersion height was measured by a graduated rod suspended from the top plate as shown in figure 2.7. The height of the liquid was measured against the rod by visualisation through a sight glass in the top plate aided by a viewing lamp. The rod was

graduated in 0.05 m divisions so the best accuracy that could be achieved was within 0.02 m. At high air flow rates the liquid surface became turbulent such that a mean liquid dispersion height was measured.

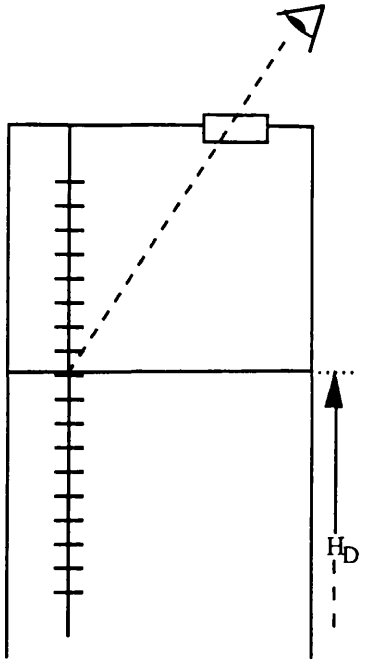

Figure 2.7 Estimation of the gassed liquid height, H_D

The gas holdup for the annulus of the vessel was measured by the hydrostatic pressure difference between two positions along the annulus and compared to the difference with that obtained without gas flow. An estimate was then made of the gas holdup by assuming that the gas holdup between the two probe positions was representative of the entire section. Thus, the riser gas holdup could be measured when using the annulus sparger and downcomer gas holdup measured when using the draft tube sparger. The equation for the estimation of downcomer gas holdup is shown below:

$$\varepsilon_D = 1 - \frac{\Delta P}{\rho_L \, g \Delta h} \qquad 2.5$$

where

ΔP = measured hydrostatic pressure difference in aerated system (Pa).

Δh = distance between pressure measurement points (m)

This equation assumes that acceleration effects have a negligible influence on the pressure drop as shown by Merchuk and Stein (1981a) and Chisti (1989). The hydrostatic pressure was measured by two pressure transducers supplied by Chemap AG (Volketswil, Switzerland). The transducers were positioned at heights of 0.53 m and 2.11 m which was below the top of the draft tube for the tallest configuration used for this study. The probes fitted flush with the vessel inside wall when inserted in the side ports. The probes were connected to amplifiers which gave readings to the nearest 0.001

bar. Therefore, with both sparger configurations only one of the sectional gas holdups, riser or downcomer could be measured with the overall gas holdup. So the other sectional gas holdup was estimated using a rearrangement of the equation shown below:

$$\varepsilon_{overall} = \frac{H_{DT} A_R \varepsilon_R + H_{DT} A_D \varepsilon_D + (H_D - H_{DT})(A_R + A_D).\ \varepsilon_{TS}}{H_D (A_R + A_D)} \qquad 2.6$$

where

H_{DT} = height of draft tube above the vessel base (m)

H_D = height of gas – liquid dispersion (m)

ε_R = riser gas holdup (–)

ε_D = downcomer gas holdup (–)

ε_{TS} = top section gas holdup (–)

A_R = riser cross sectional area (m^2)

A_D = downcomer cross sectional area (m^2)

This equation was based on the total volume of the dispersion being the sum of the gas volume in the riser, downcomer and top section and the total liquid volume as derived in appendix 2.0. The equation required an estimate of the top section gas holdup. Orazem *et al.* (1979) observed that top section gas holdup was between 1 and 2 times greater than the riser gas holdup, for a concentric airlift reactor. So it was assumed for this study that the gas holdup of the top section equalled that of the riser, as did Russell (1989). So equation 2.6 was rearranged for either riser or downcomer gas holdups depending on which sparger configuration was used, as shown in appendix 2.0.

2.7 Oxygen transfer measurements

2.7.1 Measurement of airlift oxygen transfer performance

The rate of oxygen transfer was estimated by a gas balance (steady state) method used by Sobotka *et al.* (1982). This method was adapted for the airlift reactor by Russell (1989) and Russell *et al.* (1995) where measurements were made under fermentation conditions. The inlet and exit gas compositions were monitored to obtain an estimate of the rate of oxygen transfer. Then the volumetric oxygen mass transfer coefficient was estimated from a knowledge of the dissolved oxygen concentration. The gas phase oxygen balance allowed the rate of oxygen transfer to the liquid phase to be calculated by:

$$N_A = \frac{1}{V_L}\left[\frac{P_{IN}.Q_{GO}}{RT_{IN}}\, y_{IN} - \frac{P_{EX}.Q_{GEX}}{RT_{EX}}\, y_{EX}\right] \qquad 2.7$$

where

N_A = specific rate of oxygen transfer to the liquid phase (moles m^{-3} liquid s^{-1})

V_L = total liquid volume (m^3)

y_{IN}, y_{EX} = oxygen mole fraction of inlet and exit air streams respectively (mole fraction)

P_{IN}, P_{EX} = pressure at inlet and exit positions (Pa)

T_{IN}, T_{EX} = temperature of inlet and exit air streams (K)

Q_{GO} = volumetric flowrate of gas entering the vessel ($m^3 s^{-1}$)

Q_{GEX} = volumetric flowrate of gas leaving the vessel ($m^3 s^{-1}$)

However, it was assumed that isothermal conditions existed and that the change in gas composition due to mass transfer and evaporation was small so the equation was simplified to:

$$N_A = \frac{P_{IN}\, Q_{GO}}{R\, T.\, V_L}(y_{IN} - y_{EX}) \qquad 2.8$$

where

$$P_{IN} = P_H + \rho_L\, g\, H_L \qquad 2.9$$

Therefore, the volumetric oxygen mass transfer coefficient (k_La) was estimated if the dissolved oxygen concentration (C_L) and the dissolved oxygen saturation concentration (C^*) were known:

$$k_La = \frac{N}{C^*(x) - C_L(x)} \qquad 2.10$$

C^* and C_L were position dependent due to the variation of hydrostatic pressure and gas composition in the vessel which lead to k_La varying with position. Russell *et al.* (1995) assumed that the rate of oxygen transfer (N_A) was constant throughout the vessel at steady state, which was equivalent to the microbial oxygen consumption rate and was not position dependent. The consequences of this will be discussed in section 4.1.3.
The saturation concentration at a given position $C^*(x)$ was determined by:

$$C^*(x) = \frac{y_{O2}(x).\ P(x)}{H} \cdot \frac{1000.\rho_w}{M_w}.\eta \qquad 2.11$$

where

$y_{O2}(x)$ = oxygen composition of gas phase at given position (mole fraction).

$P(x)$ = hydrostatic pressure at given position (Pa)

H = Henry's law constant for water (Pa.mole fraction^{-1})

ρ_w = density of water (kgm^{-3})

M_w = molecular weight of water (g mole^{-1})

η = factor to account for reduced solubility of oxygen in medium compared with that in water

The factor relating to oxygen solubility in the medium to that in water at the same temperature and pressure was calculated by a method derived by Schumpe *et al.* (1982). This was based on the concentration of each component of the medium and empirical constants as shown in appendix 5.0. The value of $y_{O2}(x)$ was estimated for each probe position from assuming that the gas phase composition in the riser was similar to the inlet air and the concentration in the downcomer was similar to the exit gas stream. Then, k_La values were estimated from the dissolved oxygen concentrations measured from the DOT probes and the oxygen saturation concentrations calculated for the probe positions. A sample calculation is shown in appendix 6.0.

2.7.2 Gas analysis

A mass spectrometer was used to measure the composition of the inlet and exit gases. The mass spectrometer determined the mole fraction of oxygen, nitrogen and carbon dioxide in each stream every two minutes. For each airflow rate ten measurements were recorded and the mean value calculated. The oxygen concentrations were normalised with nitrogen in the air stream. This is due to air absorbing water vapour as it passes through the vessel, and the subsequent increase of the vapour partial pressure will affect the concentrations of other components of the gas phase. The normalised difference between the inlet and exit oxygen mole fraction was calculated by:

$$(y_{IN} - y_{EX}) = O_{2IN} - O_{2EX} \cdot \frac{N_{2IN}}{N_{2EX}} \qquad 2.12$$

where

O_{2IN}, O_{2EX} = mean oxygen mole fraction for inlet and outlet streams respectively, as measured by mass spectrometer (mole fraction)

N_{2IN}, N_{2EX} = mean nitrogen mole fraction for inlet and outlet streams respectively, as measured by mass spectrometer (mole fraction)

This equation was then used in the calculation of the overall volumetric oxygen transfer rate in the fermenter.

2.7.3 Dissolved oxygen concentration measurement

The dissolved oxygen probes allowed the calculation of the dissolved oxygen tension (% air saturation) at the three probe positions and around the majority of the vessel with the mobile DOT probe. The probes were calibrated outside the vessel before each fermentation. The probe was placed in water which had either been previously sparged with nitrogen for calibration to zero % DOT or sparged with air to calibrate to 100% (air saturation) DOT. The dissolved oxygen concentration at each probe position and at any stage in the fermentation could be calculated from:

$$C_L = \frac{\%\,DOT}{100} \times C_0^* \qquad 2.13$$

where

C_0^* = saturation dissolved oxygen concentration in water, at calibration conditions (mole m^{-3})

DOT = dissolved oxygen tension reading from amplifier (% air saturation)

2.8 Total energy dissipation rate

For conventional airlift operation the reactor had a single source of power input from aeration. However, for combined aeration and propeller operation the reactor had two sources of power input. So, the effect of combined aeration and propeller operation on the hydrodynamic and oxygen transfer performance of the conventionally aerated vessel must be considered with respect to the total energy dissipation rate, P_{VT} (Wm^{-3}). Hence, the energy dissipation rate for combined aeration and propeller operation was the sum of the individual contributions from aeration (P_{VA}) and propeller operation (P_{VP}):

$$P_{VT} = P_{VA} + P_{VP} \qquad 2.14$$

For conventional operation the power input was assumed to occur from the kinetic energy and isothermal expansion of the gas as it rose up the riser. Chisti (1989) claimed that kinetic energy contribution was about 1.5% of the total aeration power input. Hence, the kinetic energy contribution was ignored by most researchers as isothermal gas expansion

was the predominant source. Therefore, Chisti (1989) derived the equation below to estimate the work done from the isothermal expansion of sparged gas, which was a function of the superficial gas velocity of the riser.

$$P_{VA} = \frac{P_g}{V_L} = \frac{\rho_L \, g \, U_{sg}}{1 + \frac{A_D}{A_R}} \qquad 2.15$$

where

V_L = liquid volume (m^3)

P_g = power input due to aeration (W)

U_{sg} = superficial gas velocity (ms^{-1})

A_R = cross sectional area of the riser (m^2)

A_D = cross sectional area of the downcomer (m^2)

ρ_L = liquid density ($kg.m^{-3}$)

For the marine propeller attempts were made to estimate the power consumption of the motor by measuring electrical current at a range of propeller speeds. However, large fluctuations in the current at each propeller speed produced inaccurate results. Also, the theoretical estimation of energy dissipation with mechanically agitated systems was recommended by other researchers (Buckland, 1993) rather than electrical current measurement. Hence, the energy dissipation rate from the marine propeller (P_{VP}) was theoretically estimated using the Reynolds number calculated for each propeller speed using the equation below:

$$Re = \frac{\rho \, N \, D_p^2}{\mu} \qquad 2.16$$

where

N = rotational speed of the propeller (rps)

D_p= propeller diameter (m)

μ = liquid viscosity (Pa.s)

ρ_L= liquid density ($kg.m^{-3}$)

The propeller power number was then found from the plot of power number as a function of Reynolds number for a three bladed marine propeller in a unaerated unbaffled stirred tank (Perry and Green, 1984). The power number was then used to calculate energy dissipation rate for a certain propeller speed from the equation below:

$$P_{VP} = \frac{P}{V_L} = \frac{P_0 \rho_L N^3 D_p^5}{V_L} \qquad 2.17$$

where

P_0 = propeller power number (–)

N = rotational speed of the propeller (rps)

D_p = diameter of the propeller (m)

ρ_L = liquid density ($kg.m^{-3}$)

V_L = working volume of the airlift reactor (m^3)

This method resulted in an estimate of energy dissipation rate from the propeller as the Reynolds numbers were from a stirred tank configuration which was dissimilar to the propeller arrangement in the airlift reactor. Also, the Re assumed turbulent flow from the propeller in the reactor. However, this seemed the only suitable method as the concealed arrangement of the propeller drive shaft at the base of the reactor made direct torque measurements impossible. Therefore, the total energy dissipation rate for aeration and propeller operation consisted of the individual contribution from conventional aeration plus propeller operation. A sample calculation is shown in appendix 7.1.

Total energy dissipation for the lab. scale stirred tank (25 L working volume) was assumed to the be the total power drawn by the three impellers where one was assumed to be under aeration and the top two were considered to be ungassed. The gassed power was calculated using the correlation from Michel and Miller (1962). An example of the calculation is shown in appendix 7.2.

2.9 Physical and chemical measurements of *S.erythraea* fermentation broths

2.9.1 Dry cell weight measurement

The dry cell weight of each fermentation sample was estimated by filtering a 2 mL sample through a pre-dried and weighed 0.2 μm filter (Millipore,Watford). The filter was dried at 85^{0}C until constant weight was observed after 40 h. Before the dried filter was weighed it was stored in a desiccater to cool and prevent moisture saturation. Four filters were used for each sample producing a mean estimated dry cell weight.

2.9.2 Density measurement

The density of each fermentation sample was measured, as an estimate was needed for the calculation of gas holdup in the annulus of the vessel. The density was determined using a 10 mL density bottle. The bottle was weighed when empty and then reweighed when full to enable estimation of the liquid density.

2.9.3 Fermentation broth rheology

2.9.3.1 Rheological measurement

Many types of rheometer have been used to study the rheology of fermentation broths. These include capillary viscometers (Bjorkman, 1987, Blakebrough *et al.*, 1978b), concentric cylinders (Ghildyal *et al.*, 1987, Wittler *et al.*, 1983), cup and bob viscometers (Banks, 1977), cone and plate viscometers (Charles, 1978) and impeller viscometers (Kemblowski and Kristiansen, 1986, Roels *et al.*, 1974, Bongenaar *et al.*, 1973). However, it has been reported that problems can be encountered when studying fermentation broth rheology with all of these rheometers. Standard rotational viscometers such as the concentric cylinders and cup and bob systems are versatile and widely used. Yet, there are associated problems with these systems which include the tendency to cause gravity settling of suspended particles, and phase separation such as the formation of less dense layers next to the rotating surface. Also large particles such as pellets can be the same size as the measuring gap of the instrument which causes destruction of the particles in the shear field (Kemblowski and Kristiansen, 1986, Banks, 1977). These problems were overcome by Roels *et al.* (1974) and Bongenaar *et al.* (1973) by using an impeller viscometer shaped like a Rushton turbine where the flow regime was similar to a standard fermenter. Kemblowski and Kristiansen (1986) successfully used a six vane impeller rheometer to analyse the rheology of *Aureobasidium pullulans* and claimed the method was more successful than other conventional methods. However, the impeller viscometers were constrained by the narrow shear range required for analysis under laminar flow conditions. Also, the complex flow pattern established by the impeller viscometer does not allow straightforward calculation of shear rate. Warren (1994) studied the rheology of three *Actinomycete* sp. *A. roseorufa*, *S. rimosus* and *S. erythraea* and found no obvious benefit using impeller systems instead of conventional rotational viscometers.

For this study a concentric cylinder was chosen against an impeller viscometer due to the difficulty in requiring laminar flow conditions. This transpired with low viscosity broths which occurred in the earlier stages of the *S. erythraea* fermentations. Also, Allen and Robinson (1990) found good agreement between the rheological measurements of *Streptomyces levoris* broths from pipeline, helical and rotating cylinder rheometers and suggested that slip effects were not significant problems in these rheometers. Hence, the rheometer used for this study was a Rheomat 115 rotational viscometer (Contraves AG, Zurich, Switzerland) with a plug in 7/7 module operating system and a concentric cylinder (MS-0/115) measuring unit with quick release coupling. Measurements were made at room temperature as Metz *et al.* (1979) reported that viscosity for mycelial suspensions was only slightly dependent on temperature and that it was not necessary to maintain a constant sample temperature during rheological analysis. Rheological measurements were made immediately after each sample was withdrawn

from the fermenter. The cup was filled with 20 mL of broth, the cylinder bob put in place and rotated for 10 seconds at the highest speed (step 15) to degas the broth (Metz *et al.*, 1979). Torque readings were then recorded as the speed was reduced to step 1. To minimise settling, readings were taken in a short time (5 seconds) of reaching each impeller speed setting. Measurement readings for each speed step were translated into shear stress using the table supplied by Contraves. The shear rate step range was from 24.3 to 3680 s^{-1}. The values of shear stress and shear rate were then used to determine the power law constants for determining the rheological behaviour of the sample. The power law relationship is:

$$\tau = K \gamma^n \qquad 2.18$$

where

τ = shear stress (Pa)

γ = shear rate (s^{-1})

K = consistancy index ($Pa.s^n$)

n = flow behaviour index (–)

Values of n and K were found from the slope and y axis intercept respectively, of a log - log plot of the shear stress versus shear rate. For continuity of rheological studies, the use of a single rheometer for all measurements throughout the work was desired. However, the mechanical breakdown of the Contraves rheomat 115 resulted in the use of a Bohlin cup and bob rheometer to analyse the samples from one *S. erythraea* fermentation. The bob dimensions were 0.045 m x 0.025 m with an annular gap of 0.001 m. The shear rate range was from 0.02 to 1000 s^{-1}.

2.9.3.2 Apparent viscosity

Investigators have used the concept of an average shear rate for air agitated vessels to calculate the apparent viscosity from the equation below:

$$\mu_a = \frac{\tau}{\gamma_a} = K(\gamma_a)^{n-1} \qquad 2.19$$

where

μ_a = apparent viscosity (Pa.s)

τ = shear stress (Pa)

γ_a = shear rate (s^{-1})

K = consistency index ($Pa.s^n$)

n = flow behaviour (–)

where the average shear rate (was proportional to the superficial gas velocity, U_{sg} :

$$\gamma_a = C\, U_{sg} \qquad 2.20$$

However, large variations existed in the value of C from 5000 (Nishikawa *et al.* (1977) from heat transfer coefficient measurements), 2800 (Schumpe and Deckwer, 1987) to 1500 (Henzler, 1980) which were all for bubble columns. Hence, Chisti (1989) questioned the applicability of these correlations especially as the shear rate could vary by three fold depending on which value of C was chosen. Allen and Robinson (1991) also explained that it was uncertain whether the value of C was independent of column diameter, sparger type, or rheological properties. Also, it was unclear whether the average shear rate estimated from stationary point positions within the bubble column were relevant to other areas of the vessel. Therefore, the use of these correlations from bubble column systems was difficult to use for the 'average' shear rate of an airlift reactor, especially when the bubble column has no net liquid flow and as an airlift reactor has distinct liquid flow direction. In the airlift reactor the shear rate in simple terms would be a function of the relative velocity between both the bubbles and liquid, and between the liquid and the column wall. The liquid circulation in simple terms is mostly a result of the density difference between gas holdup in the riser and downcomer and the gas holdup is determined by the superficial gas velocity. Also, the flow direction change in the vessel provides resistance to liquid flow. Thus a relationship between shear rate and liquid circulation velocity exists. Shi *et al.* (1990) used this analogy to obtain a correlation of average shear rate from the superficial gas velocity for an external loop reactor. The variable parameter of this correlation was only the superficial gas velocity and so, it was not applicable to this study as it could not be used to distinguish the average shear rate between the operating conditions of conventional aeration and, combined aeration and propeller operation. Therefore, the Blasius correlation for estimating shear stress at a vessel wall (Russell, 1989, Wood and Thompson, 1986, Boysan *et al.*, 1988) was used in this study for estimating the maximum shear stress of the reactor. The Blasius correlation for wall shear stress is a function of the liquid linear velocity as shown below:

$$\tau_w = \tfrac{1}{2}\, \rho_L U_m^2\, 0.079\, Re^{-0.26} \qquad 2.21$$

where

τ_w = shear stress at the wall (Pa)

U_m = mean liquid linear velocity (ms^{-1})

Re = Reynolds number

ρ_L = liquid density ($kg.m^3$)

Hence, the experimental measurements of liquid linear velocity in the riser and downcomer were used to calculate shear stress for the different airlift reactor configurations used in this study. Although this led to an estimate of the maximum shear stress and not an 'average' value, it did enable a comparison between the shear stress and apparent viscosity to be made between the aerated and, combined aerated and propeller operated airlift reactor configurations. As the Blasius correlation was only applicable to Newtonian broths, Russell (1989) used the correlation of Wilkinson (1960) for non-Newtonian broths shown below:

$$\tau_w = \tfrac{1}{2}\,\rho_L U_m^2\, a\,(Re')^{-b} \qquad 2.22$$

where

Re' = generalised Reynolds number

a,b = function of generalised flow behaviour (n')

where values for a and b were given by Wilkinson (1960) and tabulated in appendix 8.0. The generalised Re was given by :

$$Re' = \frac{D^{n'}\, U_m^{2-n'}\, \rho_L}{K'\, 8^{n'-1}} \qquad 2.23$$

where

D = diameter of the flow channel (m)

K'= generalised consistency index ($Pa.s^n$)

n' = generalised flow behaviour (–)

and the n' was equal to n (flow behaviour) for a power law fluid and the value of K' obtained from the equation below:

$$K' = K\left[\frac{3n+1}{4n}\right]^n \qquad 2.24$$

Therefore, for each measurement interval using the non-Newtonian broths, the liquid linear velocity of the riser and downcomer, rheological flow characteristics (n & K) and the broth density were used to calculate the generalised Re and then, the wall shear stress of the riser and downcomer. In all cases the Re were less than 10^5 which met the Blasius correlation criterion. The calculated shear stresses of the riser and downcomer were then used to calculate the corresponding apparent viscosity from the equation below:

$$\mu_a = \frac{\tau_\omega}{\left(\frac{\tau_\omega}{K}\right)^{\frac{1}{n}}} \qquad 2.25$$

A comparison of the apparent viscosity between reactor configurations using the value of the wall shear stress from the riser was complicated by the liquid linear velocity, as it was

influenced by the different cross sectional area ratios of the reactor configurations. Hence, apparent viscosity was estimated from the mean wall shear stress of the vessel obtained from the average of the values from the riser and downcomer so a more meaningful comparison could be made between the reactor configurations. An example of apparent viscosity calculation is demonstrated in appendix 8.0.

Apparent viscosity estimation for the stirred tank used the estimation of apparent shear rate from the method of Metzner and Otto (1957) :

$$\gamma_a = k_s N \qquad 2.26$$

where

N = rotational speed of the impeller (s^{-1})

k_s = average shear rate constant (–)

where Metzner *et al.* (1961) obtained at value of k_s for multiple rotating Rushton turbines of 11.4 for a pseudoplastic fluid ($0.14 > n < 0.7$) which was used in this study. Hence, the apparent viscosity was calculated from the equation below:

$$\mu_a = \frac{\tau}{\gamma_a} = K \frac{\gamma^n}{\gamma} = K (k_s N)^{n-1} \qquad 2.27$$

2.9.4 Morphology characterisation

Characterisation of the morphology of a filamentous organism during a fermentation is an important tool when studying the effect of the engineering environment on an organism. The morphological measurements were made using the semiautomatic image analysis described by Packer and Thomas (1990). A television camera was mounted on a Polyvar microscope (Reichert-Jung, Wien, Austria) and the video signal of the field of view was processed by a Magiscan 2A image analyser (Joyce Loebl Ltd, Gateshead, U.K). The image was digitised and analysed for the desired measurements. For each measurable organism the longest measurable path was found and considered to be the main hyphal length. The next longest length was hyphal branch. The total hyphal length and the number of tips were measured to calculate the hyphal growth unit. The clump area was also calculated. The final results were all processed by statistical analysis. For this study with *Saccharopolyspora sp.* morphological characterisation was completed from dry slides which were prepared immediately after sample removal from the fermenter. The fermentation sample was diluted so that only single organisms were present on the slide. This was between 10 to 400 times depending on the density of the sample. 40 µL of the diluted sample was spread over a slide and air dried. The slide was then heat fixed and stained with methylene blue stain (0.3 g methylene blue to 100 mL 35% ethanol solution) and air dried. The magnification was 10 x 40 and single pixels as well as objects with a circularity factor between 0.35 and 10^3 excluded. At least 200

organisms were analysed in each sample and mean values of the morphological parameters were obtained.

2.9.5 Glucose analysis

The glucose concentration of the fermentation sample supernatants was measured using HPLC (table 2.2). A 20 μL injection loop was used with an autosampler system. A standard curve was made using glucose (Sigma Ltd,) with a calibration range of 0.05 to 40 gL^{-1}.

Table 2.2 HPLC conditions for glucose analysis

Column:	Aminex HPX-87H, 300 mm.
Pre- column:	Biorad cation H^+ guard column
Mobile phase:	0.004 M H_2SO_4 (HPLC grade, Fisons)
Flow rate:	0.65 $mL.min^{-1}$
Detector wavelength	210 nm, (RI detection)

2.9.6 Determination of erythromycin concentration

Fermentation samples were centrifuged and supernatants stored at -20^{0}C until analysis. The thawed samples were then analysed for erythromycin using high pressure liquid chromatography, HPLC. The method was adapted from Tsuji and Goetz (1978) using a Partisil ODS, 10 μm, 250 mm column. However, with this method the lowest concentration of erythromycin dihydrate (Aldrich Chemical Co. Ltd Gillingham, U.K) that could be detected was 500 μgmL^{-1}. No erythromycin was detected in the fermentation samples and chemical extraction of erythromycin was attempted with a variety of solvents but was unsuccessful. As the erythromycin titres were undetectable by the HPLC method then a zone of inhibition bioassay was used to measure erythromycin concentration of the fermentation samples. *Arthrobacter citreus* was used as the test organism and was grown in a shake flask with nutrient broth for 24 hours at 30^{0}C. 300 mL of nutrient agar (Unipath Ltd, Basingstoke, U.K) was cooled to 45^{0}C after sterilisation and 5 mL of *A. citreus* broth added to the agar. The agar was mixed with the broth and 20 mL of agar was poured into each petri dish. Once the agar had solidified, four holes per plate were punched into the agar with a 3 mm cork borer (no.1). 40 μL of fermentation broth or erythromycin standard was added to the wells. All samples were analysed in triplicate and the calibration curve was made in a range of 5 - 100 μgmL^{-1} using erythromycin dihydrate (Aldrich Chemical Co. Ltd, U.K). Fermentation samples were also diluted between 1: 4 if necessary. The assay dishes were incubated at 30^{0}C. After 24 hours the plates were left at room temperature for 48 hours for the zones of inhibition to fully develop to clear distinct zones. The zones were measured and standard curves constructed using the equation below (2.28) where the logarithm of the antibiotic concentration is proportional to the squared distance between the reservoir and the zone border line.

$$\ln C' = \ln C_o - \frac{(d - x)^2}{4. D. T} \qquad 2.28$$

where

C' = antibiotic concentration (mgL^{-1})

$(d - x)$ = distance between reserviour and zone border (m)

D = diffusion coefficient (–)

T = absolute temperature (K)

3.0 RESULTS

3.1 Comparison of the hydrodynamic and oxygen transfer performance between the two sparger configurations of the conventionally aerated airlift reactor with the Newtonian baker's yeast suspension

The airflow rate is the primary means of controlling the hydrodynamics and oxygen transfer performance of a conventionally aerated airlift reactor. Therefore, an understanding of the relationship between airflow rate and the hydrodynamic and oxygen transfer parameters is important for reactor operation. To compare the hydrodynamic parameters between the sparger configurations, the superficial gas velocities based on the corresponding riser diameters must be used (appendix 1.1). For the following work the reactor was configured with a draft tube height of 2.77 m and a working volume of 0.25 m^3, which gave an unaerated liquid height (H_L) of 3.24 m (section 2.1.1). The 10 gL^{-1} dry cell weight (DCW) yeast suspension was used in this study.

3.1.1 The effect of superficial gas velocity on gas holdup

Superficial gas velocity increases up to 0.054 ms^{-1} produced an initial rapid rise in both overall and downcomer gas holdup for the reactor with the draft tube sparger (figure 3.1). This was followed by a reduced rate of increase at gas velocities above 0.054 ms^{-1}. The difference between the two holdups enlarged with increasing gas velocity. Also, the theoretically estimated average riser gas holdup (section 2.6.3) was above the overall and downcomer holdups at all gas velocities. This was as expected as the overall gas holdup was an average of the sectional gas holdups in the vessel (appendix 2.0).

For the annulus sparger configuration both riser and overall holdups showed an initial rapid rise with gas velocity increases up to 0.054 ms^{-1} followed by a reduced rate of increase with higher gas velocities (figure 3.2). The estimated average downcomer gas holdup profile was found to be lower than the other holdup profiles. The difference between the riser, overall and downcomer gas holdups enlarged with increasing superficial gas velocity but was smaller than with the draft tube sparger (figure 3.1). The differences between the holdup profiles from the two sparger configurations is confirmed in figure 3.3 whereby the overall gas holdup profiles were similar with both sparger configurations and gas velocities up to 0.054 ms^{-1}. At gas velocities above 0.054 ms^{-1} the overall gas holdup with the draft tube sparger increased to higher values than observed with the annulus sparger. At the highest achievable gas velocity (0.136 ms^{-1}) the overall gas holdup with the draft tube sparger was 0.147 compared to a value of 0.12 for the annulus sparger. Also, the difference between riser and downcomer gas holdup with the draft tube sparger was larger than with the annulus sparger configuration at all gas velocities.

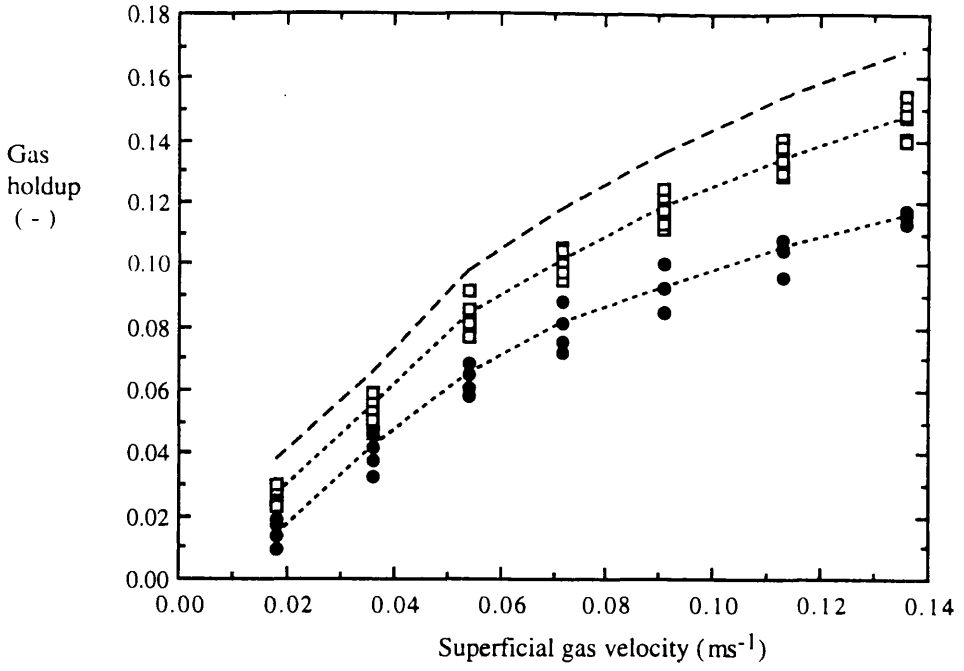

Figure 3.1 The effect of superficial gas velocity on the overall, downcomer, and riser gas holdup for the draft tube air sparged reactor with yeast broth, (10 gL^{-1} DCW). Gas holdup: overall (- -□- -), downcomer (- -●- -), and riser (calculated) (- - - - -)

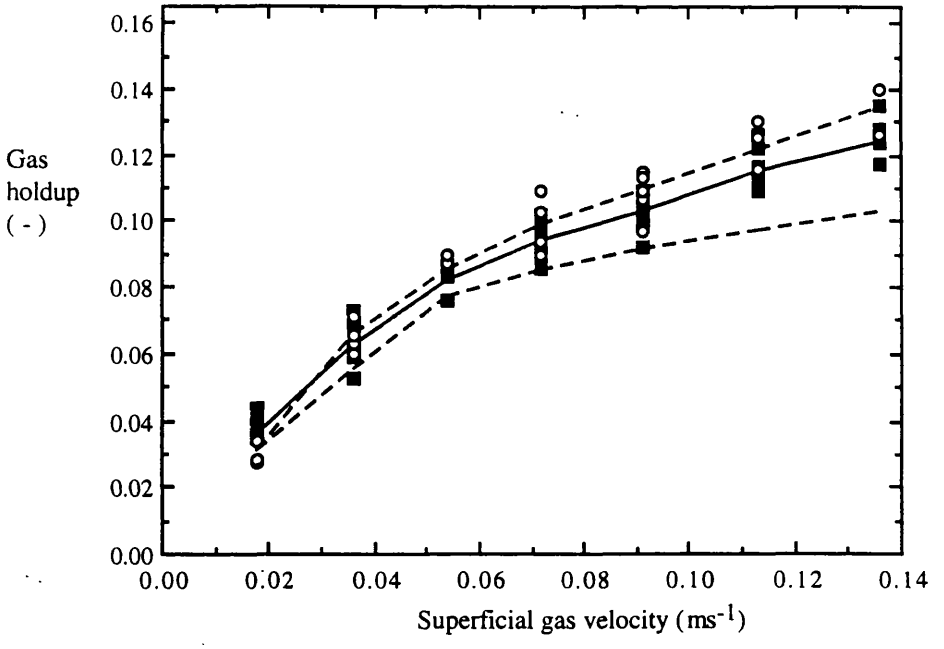

Figure 3.2 The effect of superficial gas velocity on the overall, riser and dowcomer gas holdup for the annulus sparged reactor, with yeast broth, (10 gL^{-1} DCW). Gas holdup: overall (—■—), riser (- -o- -), and downcomer (calculated) (- - - - -)

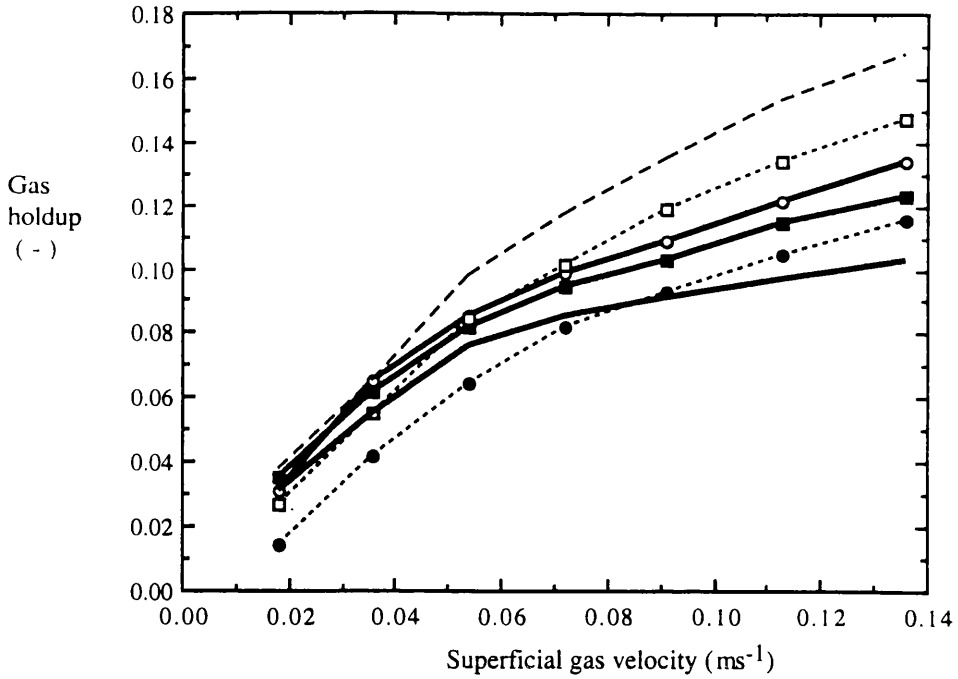

Figure 3.3 Comparison of the effect of superficial gas velocity on the overall, riser and downcomer gas holdups,(mean values) between the two sparger configurations with baker's yeast broth (10 gL^{-1} DCW). Annulus sparger gas holdup: overall (-■-), riser (-○-) ,downcomer (——),draft tube sparger gas holdup: overall (- □ ·),riser (- - · - -), and downcomer (- - ● - -).

3.1.2 The effect of superficial gas velocity on liquid circulation and mixing times

The liquid circulation times from both sparger configurations decreased gradually with increasing superficial gas velocity (figure 3.4). The rate of reduction was greater for superficial gas velocity increases up to 0.06 ms^{-1}. The relationship between the liquid circulation time and gas velocity was similar for both sparger configurations but the circulation times for the draft tube sparged reactor were shorter at all gas velocities.

The relationship of mixing time to superficial gas velocity (figure 3.4) was similar to that observed for the circulation time with a gradual decrease in mixing time with increasing gas velocity. The rate of decrease reduced with increasing gas velocity. For most gas velocities the values with the draft tube sparger were shorter than those with the annulus sparger. Thus the draft tube sparged reactor had greater mixing efficiency than with the annulus sparger. The values plotted in figure 3.4 were for pulse injection into the middle of the annulus of the vessel and detection at the same position in the vessel. No significant statistical difference could be found between the liquid mixing and circulation times from either a vessel top plate or side injection position using both sparger configurations. There was however, a difference in the amplitude of the injected pulse from the two injection sites. For the draft tube sparged reactor the amplitude of the pulse from top plate injection decreased more significantly with increasing gas velocity

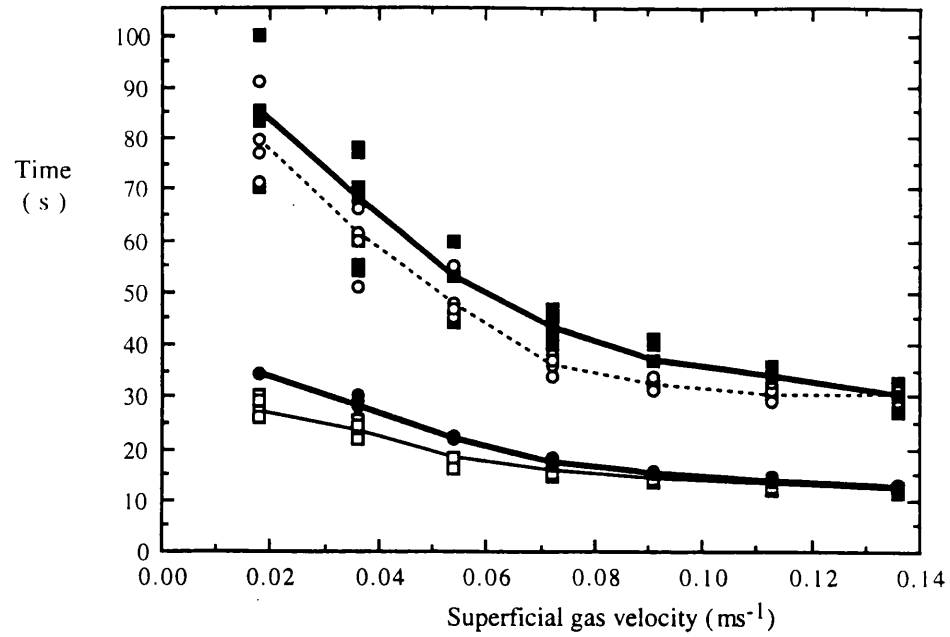

Figure 3.4 The effect of superficial gas velocity on the liquid circulation and mixing times for both sparger configurations with baker's yeast broth (10 gL^{-1} DCW, 0.25 m^3 working volume, H_{DT} of 2.77 m) Liquid circulation time: draft tube sparger (-□-), annulus sparger (—●—), Mixing time: draft tube sparger (-○-), annulus sparger (—■—).

than a pulse from middle injection. This was probably due to the middle injected pulse completing a full circulation of the vessel before detection. Whereas with top injection the pulse passed from the liquid surface through the top section and part of the downcomer before detection. As an attempt to clarify the mixing process the ratio of mixing to circulation time as a function of superficial gas velocity was calculated (figure 3.5). This was for the ungassed liquid height of 0.47 m above the draft tube which was equal to the working volume of 0.25 m^3. The ratio of mixing to circulation time was in the region of 2.5 for all gas velocities. Therefore, about 2.5 circulations of the vessel were required to disperse an injected alkali pulse to 90% homogeneity which was independent of gas velocity.

The relationship between superficial gas velocity and the liquid velocity of the individual sections of the reactor is shown in figure 3.6. The liquid velocities were calculated from the mean liquid circulation times and reactor path length theory (section 2.6.1). The liquid velocity profiles from both sparger configurations showed a similar relationship with superficial gas velocity, with a gradual increase of liquid velocity with increasing gas velocity and the rate of increase was greater for gas velocity increases up to 0.054 ms^{-1}. This trend was similar to the relationship between gas holdup and gas velocity (figure 3.3) and indicated the inter-relationship between gas holdup and liquid velocity. In addition there was an increase in the difference between riser and downcomer liquid velocities as the gas velocity was increased with both sparger systems.

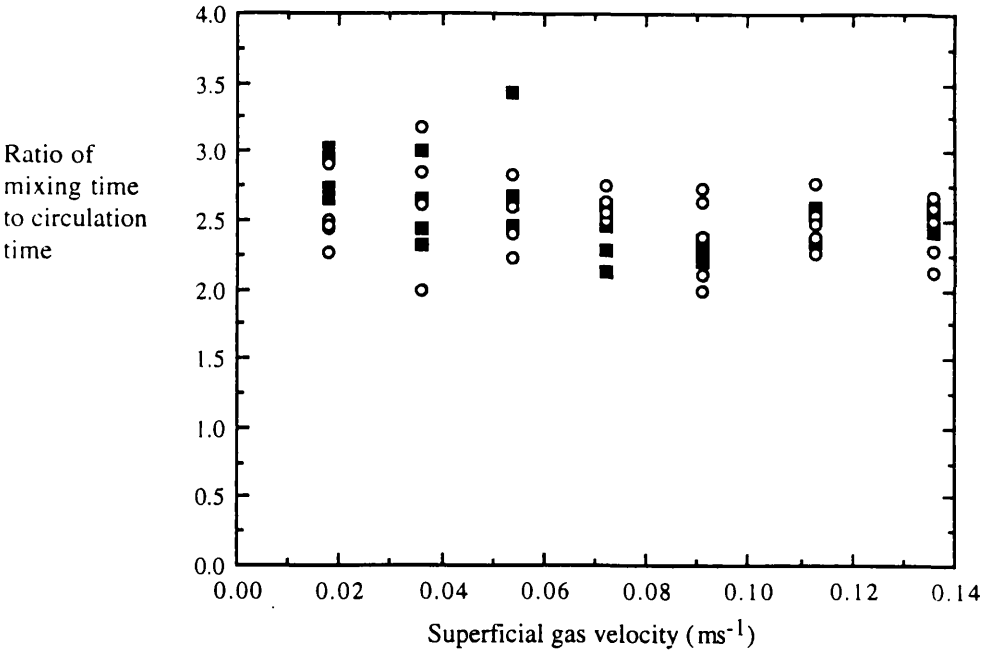

Figure 3.5 The effect of superficial gas velocity on the ratio of mixing to liquid circulation time at the ungassed height of 0.47 m above the draft tube, (H_{DT} of 2.77 m, working volume of 0.25 m^3) for the draft tube (■) and annulus (o) sparger configurations and with the baker's yeast suspension (10 gL^{-1} DCW)

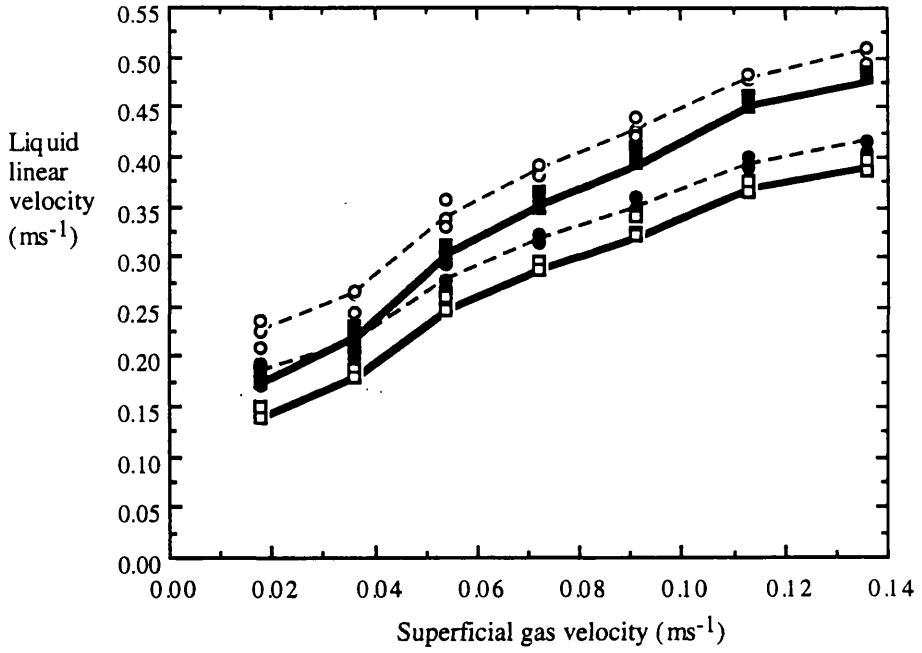

Figure 3.6 Comparison of the riser and downcomer liquid velocities between the two sparger configurations as a function of superficial gas velocity, with the baker's yeast broth (10 gL^{-1} DCW, H_{DT} of 2.77 m, working volume of 0.25 m^3) Draft tube sparger liquid velocities ; riser (- -o- -), downcomer (- -●- -), Annulus sparger liquid velocities: riser (—□—), downcomer (—■—).

This was similar to the increase in the difference between riser and downcomer gas holdup with increasing gas velocity (figure 3.3), and was expected as liquid circulation was primarily due to the density difference between the riser and downcomer. For the draft tube sparger the riser liquid velocity (U_{LR}) was between 20 - 25% greater than in the downcomer (U_{LD}). This was anticipated as the ratio of the downcomer to riser cross sectional area (A_D/A_R) was 0.83 and so the liquid from the riser flowed into the downcomer with a larger cross sectional area. For the annulus sparger configuration the riser liquid velocity was 20 - 25% less than the downcomer liquid velocity due to the smaller cross sectional area of the downcomer (A_D/A_R of 1.13). Despite the different cross sectional area ratios with the sparger configurations the downcomer liquid velocities for both sparger configurations were similar at gas velocities below 0.054 ms^{-1}. Also the U_{LD} with the annulus sparger was similar to the U_{LR} with the draft tube sparger and hence, the U_{LR} with the annulus sparged vessel was similar to the U_{LD} with the draft tube sparger with increasing gas velocity.

3.1.3 Dissolved oxygen tension measurements

Dissolved oxygen tensions were measured from the three fixed probe positions in the upper annulus, lower annulus and lower draft tube position of the reactor (figure 2.1) as a function of superficial gas velocity (figure 3.7). The dissolved oxygen tension (DOT % air saturation) for the draft tube sparger configuration (figure 3.7a) was below 3% in the lower riser probe position for all gas velocities but, increased at the upper and lower downcomer positions with increasing gas velocity. The DOT values at the upper downcomer were higher than at the lower downcomer position to the extent that at the maximum achievable gas velocity (0.136 ms^{-1}) the DOT was 63% compared to 22% in the lower downcomer position. The DOT profiles for the annulus sparged reactor are shown in figure 3.7b, and for this configuration the annulus DOT probes measured the DOT in the riser and the third probe measured the DOT in the lower downcomer. DOT values remained below 5% from the upper and lower riser probe positions with all gas velocities studied which was similar to the values from the lower riser position with the draft tube sparger. The DOT from the lower downcomer probe position increased with gas velocity and the values were higher than either the DOTs from upper or lower downcomer probe positions with the draft tube ring sparger. For example, at the highest gas velocity (0.136 ms^{-1}) the DOT was 73% compared to 22% in the corresponding position with the draft tube sparger. Therefore, analysing the DOT profiles from the three fixed probe positions and comparing between the sparger configurations confirmed that DOTs were higher in the downcomer than in the riser when utilising the 10 gL^{-1} DCW yeast suspension. Also, different values of DOT were obtained in the downcomers of the two sparger configurations. Given that air was introduced into the riser sections of both sparger configurations the differences in DOT between the riser and downcomer

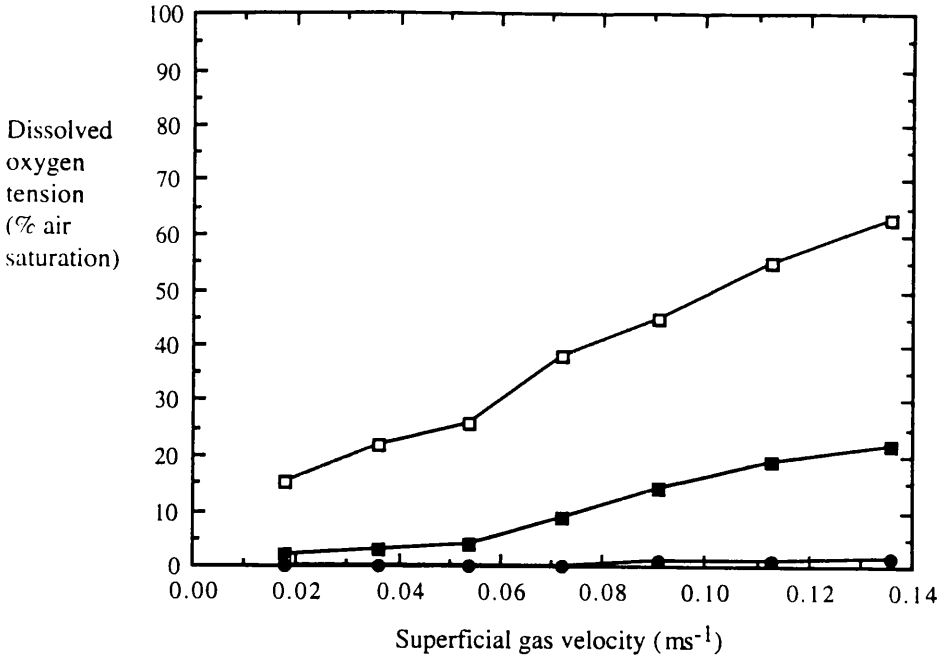

Figure 3.7a Draft tube air sparged reactor: Lower riser (●), upper downcomer (□) lower downcomer (■)

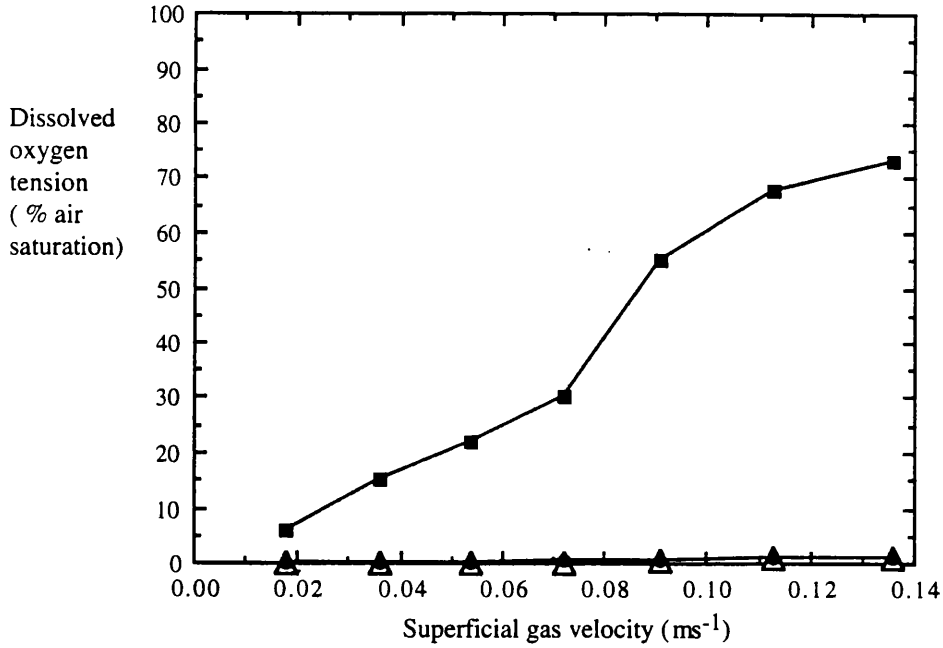

Figure 3.7b Annulus air sparged reactor: Lower riser (●), upper riser (△), lower downcomer (■)

Figure 3.7 The effect of superficial gas velocity on the dissolved oxygen tensions from the fixed probe positions with the draft tube sparger (figure 3.7a) and the annulus sparger configuration (figure 3.7b) using the baker's yeast broth (10 gL^{-1} DCW)

were great and initially unexpected. Repeated investigations with the DOT probe systems were performed by switching specific probes to different positions in the vessel but similar results were always obtained. DOT measurements under saturation conditions with tap water revealed that all three probes read 100% and the probes in the lower section of the vessel read above 100% due to the hydrostatic pressure when the probes were calibrated outside the vessel (section 2.7.3). The variation of DOT across the downcomer and riser i.e. the radial position of the probe was studied but no variation was observed. Thus, DOT measurement was not dependent on radial position of the probe.

To further characterise the DOTs around the vessel with the 10 gL^{-1} DCW yeast suspension a mobile DOT probe was used to measure the DOT in the riser, top section, and downcomer of the vessel which are in shown in figure 3.8. Figure 3.8.a shows the DOT profiles for four superficial gas velocities with increasing distance around the vessel with the draft tube sparger. The measuring distance was from the sparger positioned 0.06 m above the vessel base, up the riser into the top section and down the centre of the vessel to the base of the vessel below the draft tube (appendix 4.0). The superficial gas velocities varied from 0.036 ms^{-1} (80 $L.min^{-1}$, 0.32 vvm) to the highest achievable gas velocity which was restricted to 0.136 ms^{-1} (300 $L.min^{-1}$, 1.2 vvm) by the liquid dispersion height with the yeast broth used in this study. The DOTs in the riser and the top section remained below 1% and were independent of gas velocity as shown from the DOT profiles with the fixed probe positions (figure 3.7a). As the liquid recirculated into the downcomer the DOT increased to a maximum peak value at the same height in the upper downcomer for all gas velocities. The DOT then decreased further down the downcomer reaching values below 1% at the base of the vessel and on the subsequent recirculation back into the riser. As the gas velocity was increased the peak dissolved oxygen tensions increased in size and hence, a greater proportion of the downcomer had higher DOT values as the gas velocity was increased.

For the annulus sparger configuration (figure 3.8b) the DOTs in the riser were below 1% and independent of the gas velocity as observed with the draft tube sparger. In the top section where bubble disengagement from the liquid surface and bubble entrainment into the downcomer occurred there was only a small increase in DOT up to 10% with gas velocities above 0.072 ms^{-1}. The DOT then increased down the downcomer with maximum peak DOT values occurring near the base of the draft tube. From the bottom of the downcomer to the base of the vessel there was a reduction in the DOT to below 1%. For example, at the highest gas velocity (0.136 ms^{-1}) the DOT fell from 78% at the bottom of the downcomer to 0.1% at the base of the vessel. As the gas velocity was increased the DOT peaks increased in size and hence, a greater proportion of the downcomer had higher DOT values as the gas velocity was increased. This was similar to that observed with the draft tube sparger (figure 3.8a) however, with the annulus sparger the position of the highest DOT peak moved further down the downcomer towards the base of the vessel with increasing gas velocity. Therefore, the

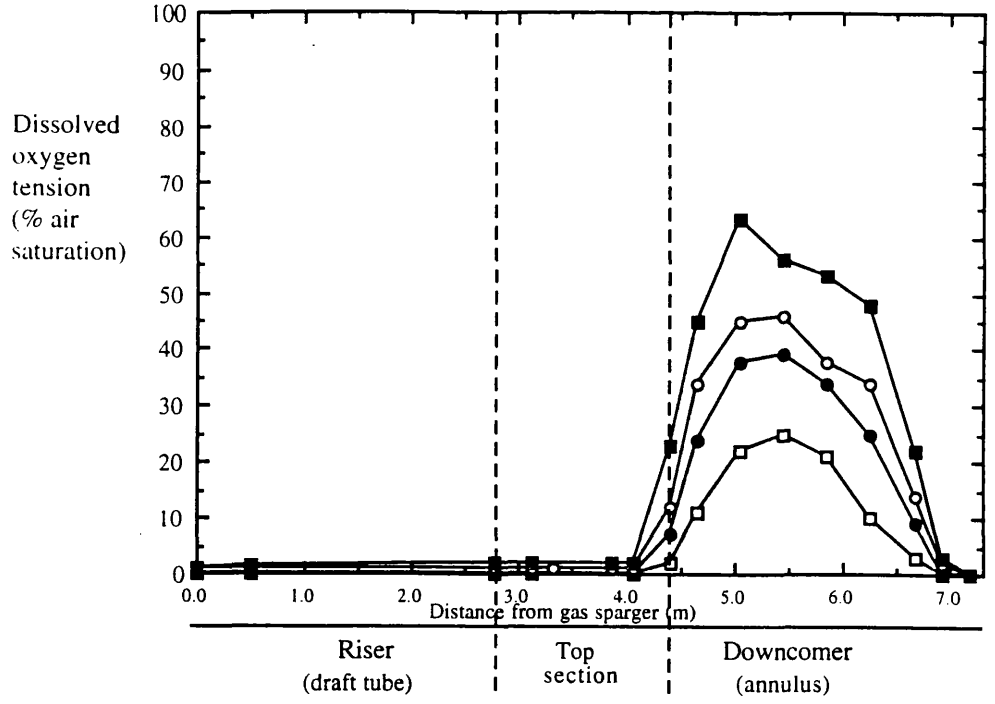

Figure 3.8 a Airlift reactor configured with the draft tube sparger

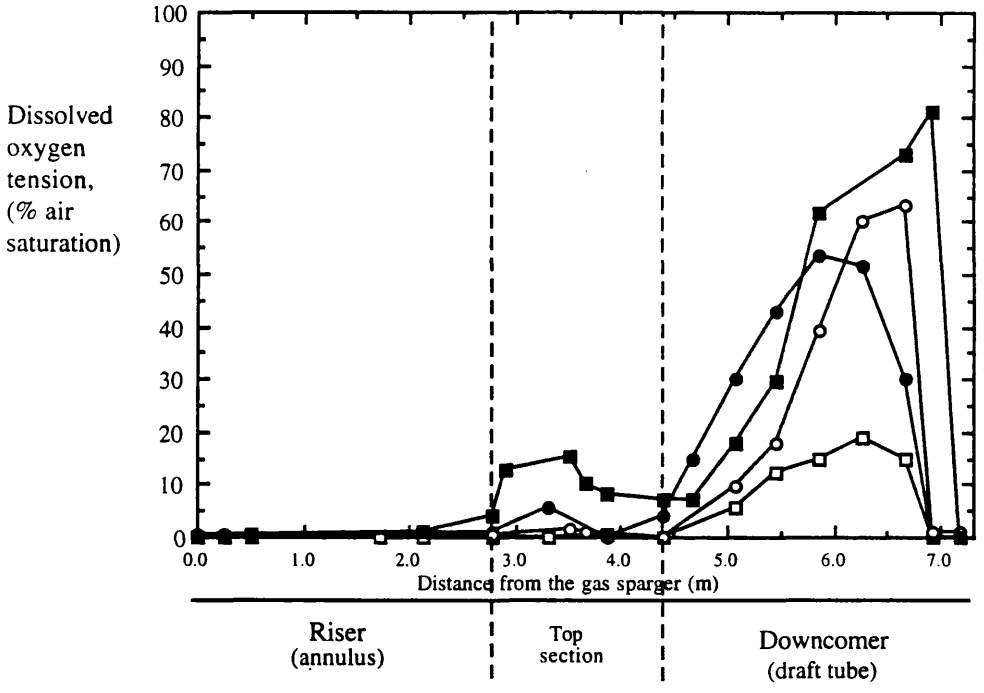

Figure 3.8b Airlift reactor configured with the annulus sparger

Figure 3.8 The dissolved oxygen tension (% air saturation) as a function of increasing distance from the draft tube sparger (figure a) and the annulus sparger (figure b) within the airlift reactor, using the baker's yeast suspension (10 gL^{-1} DCW) at superficial gas velocities, (ms^{-1}): 0036 (□), 0.072 (•), 0.091 (○), and 0.136 (■). The mobile dissolved oxygen tension probe was used.

use of the mobile dissolved oxygen tension probe demonstrated the existence of extreme DOT heterogeneity around the vessel with the 10 gL^{-1} DCW yeast suspension. Cells experienced DOTs below 1% for at least half there circulation around the vessel. If this was considered with the circulation time profile (figure 3.4) then at the lowest gas velocity (0.036 ms^{-1}) with the annulus sparger the cells experienced DOT values below 1% for at least 13 of there 24 second circulation around the vessel. This fell to a value of approximately 7 seconds for the 12 second circulation time at the high gas velocity of 0.136 ms^{-1}.

3.1.4 The effect of superficial gas velocity on the volumetric mass transfer coefficient (k_La)

The k_La values estimated using the DOTs from the fixed probe positions as a function of superficial gas velocity are shown in figure 3.9. At gas velocities below 0.054 ms^{-1} the k_La values from all probe positions were similar around the vessel with values below 0.02 s^{-1} from both sparger configurations. However, as the gas velocity increased above 0.054 ms^{-1} riser k_La increased up to 0.055 s^{-1} at the maximum gas velocity (0.136 ms^{-1}) for both sparger configurations. The k_La profile for the lower downcomer position with the draft tube sparger was slightly above the riser profile values at gas velocities above 0.091 ms^{-1}. Also the k_La values for the lower downcomer probe position with the annulus sparger and the upper downcomer with the draft tube sparger were similar with significant increases up to 0.2 s^{-1} with the gas velocity of 0.136 ms^{-1}. Therefore, it has been shown that as the gas velocity was increased a larger increase in k_La occurred in the downcomer probe positions compared to values in the riser for both sparger configurations. The downcomer k_La values which were up to 5 fold greater than in the riser even though the downcomer gas holdup was between 18 - 45% less than in the riser (at gas velocity of 0.136 ms^{-1}) for both sparger configurations (figure 3.3).

The k_La values were estimated for the whole of the vessel using the dissolved oxygen tensions measured with the mobile DOT probe, and for the annulus sparged reactor (figure 3.10). At the lowest gas velocity (0.036 ms^{-1}) similar values of 0.01 s^{-1} were observed around the vessel. As the gas velocity was increased above 0.036 ms^{-1} the k_La values increased in the riser and top section but with similar values along the riser path length at each gas velocity. The k_La values then increased down the downcomer reaching maximum peak values near the base of the downcomer. This was followed by a rapid reduction at the base of the vessel and subsequent recirculation into the riser. As the gas velocity was increased the k_La peak values also increased in size. The relationship of downcomer k_La values with gas velocity was similar to that observed with the downcomer DOTs (figure 3.8). The peak k_La values down the downcomer corresponded to the position of peak DOT. A similar relationship was found for the draft tube sparger configuration where maximum k_La peaks were measured in the upper downcomer corresponding to the position of high DOT (results not shown).

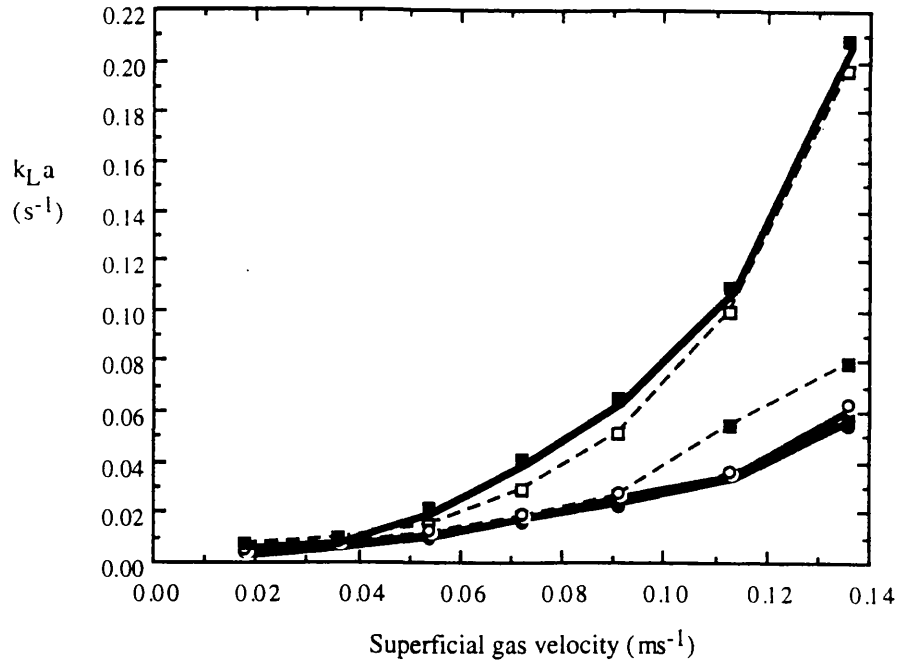

Figure 3.9 Comparison of the effect superficial gas velocity on $k_L a$ (from the fixed dissolved oxygen tension probe positions), between the two sparger configurations with the baker's yeast broth (10 gL^{-1} DCW). Draft tube sparger: lower riser (-●-), upper downcomer (-□-), lower downcomer (-■-) Annulus sparger: lower riser (—●—), upper riser (—○—), lower downcomer (—■—)

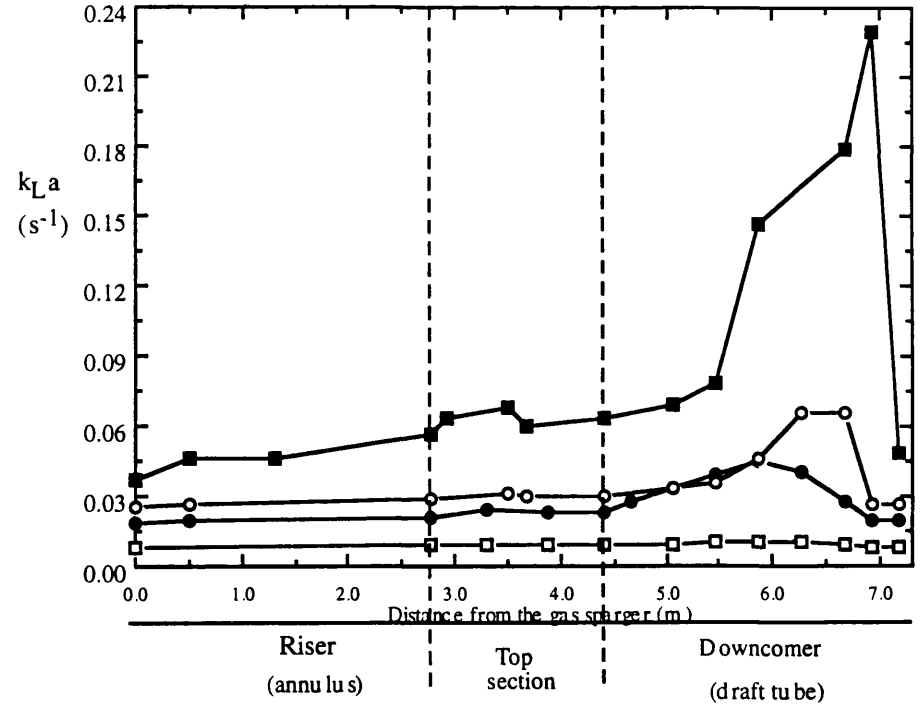

Figure 3.10 The effect of superficial gas velocity on the $k_L a$ values with increasing distance from the annulus sparger within the airlift reactor (H_{DT} of 2.77 m), using the bakers' yeast broth (10 gL^{-1} DCW) and superficial gas velocities of : (ms^{-1}) 0.036(□), 0.072 (●), 0.091 (○), 0.136 (■).

3.1.5 The effect of superficial gas velocity on the bubble flow regime

Visual observations of the change in bubble flow and estimates of bubble size with increasing gas velocity were attempted from the sight glass positions in the vessel (table 3.1). Sight glasses were situated in the lower third of all three vessel sections as shown in figure 2.1 and allowed the annulus of the vessel to be viewed. When fermentation broths were used only the liquid immediately behind the sight glass could be observed. However, the sight glasses were set back from the vessel wall so the liquid swirled around the sight glass and obscured the observation of the actual liquid flow. So the flow regime in the annulus of the vessel could only be observed with water by focusing through to the liquid flow in front of the draft tube and ignoring the swirling liquid directly behind the sight glass. Bubble sizes were estimated by observing the bubbles against a ruler fixed to the sight glass. A sight glass on the top plate allowed the liquid surface to be observed with water and fermentation broths.

Table 3.1 The effect of superficial gas velocity on the range of bubble diameters (mm) visually observed from the side vessel sight glasses of the conventionally operated airlift reactor with water

Reactor configuration and position of bubble visualisation	Superficial gas velocity (ms^{-1})		
	0.018	0.054 - 0.072	0.113 - 0.136
Riser (lower sight glass) of the annulus gas sparged reactor	0.5 - 5	3 - 8	5 - 15
Downcomer (lower sight glass) of the draft tube gas sparged reactor	1 - 3	1 - 7	1 - 8

For the annulus sparger configuration the annulus of the vessel was the riser and hence, the sight glasses showed the bubble flow from air sparged into the vessel (table 3.1). At low gas velocities (0.018 ms^{-1}) bubbles of approximately 3 - 5 mm in diameter were observed rising up the vessel with some smaller 0.5 - 2 mm diameter bubbles. Similar sized bubbles were observed at all side vessel sight glasses which indicated that coalescence of bubbles between the lower and middle sight glasses in the riser may not occur at low gas velocities. The bubbles rose in an upward direction with some side movement. From the side sight glass in the top section a large number of similar sized bubbles rose in an orderly manner before disengagement from the top section. The liquid surface observed from the top plate sight glass was found to be flat and non-turbulent. At higher gas velocities (0.054 - 0.072 ms^{-1}) the bubble flow in the annulus of the vessel became more turbulent with larger bubbles in the annulus of the vessel of 5 - 8 mm in diameter amongst smaller 3 - 5 mm diameter bubbles. The bubbles travelled passed the sight glass at a higher velocity than observed with the lower gas velocity. These bubbles rose up the riser colliding with the other smaller bubbles. The bubble collisions resulted in side ways movement and some swirly bubble motion as the bubbles rose. The

top section was more turbulent than at the low gas velocities. The larger bubbles could be seen rising faster than the other smaller bubbles causing turbulence as they burst on the liquid surface. At the high gas velocities (0.113 - 0.136 ms^{-1}) a mixed population of bubbles was observed in the riser (annulus) of the vessel. A population of large bubbles of 8 - 15 mm in diameter rose with higher rise velocities compared to the other smaller bubbles. These large bubbles were seen colliding with the other smaller bubbles (5 - 8 mm) as they rose up the riser and the flow of the large bubbles could be followed passed the lower and middle section sight glasses. The top section liquid surface was very turbulent due to the bursting of the large bubbles to the extent that the reactor had a rocking motion.

The draft tube sparger configuration allowed the bubble flow regime in the downcomer to be observed. At low gas velocities (0.018 ms^{-1}) small bubbles of 1 - 3 mm in diameter could be observed flowing down the downcomer (table 3.1). At the lower sight glass a smaller number of bubbles were observed than at the middle sight glass. Bubbles travelled at slower speeds through the lower section of the vessel compared to faster downward bubble velocities observed from the middle section sight glass. At the lower sight glass bubbles were observed moving further downwards passed the sight glass towards the base of the vessel. The bottom of the sight glass is about 0.2 m above the base of the draft tube so it seems reasonable to assume that these downward flowing bubbles were recirculated around the base of the vessel into the riser. At higher gas velocities (0.054 - 0.072 ms^{-1}) the bubble population increased with smaller, 0.5 - 2 mm diameter bubbles, and larger 4 - 7 mm diameter bubbles in the downcomer. Greater bubble collision occurred at the higher gas velocity and more bubbles passed the bottom sight glass. At the highest gas velocity (0.113 - 0.136 ms^{-1}) the size of the bubbles remained similar to lower gas velocities however, the number of bubbles increased. Bubbles travelled past both the middle and lower sight glass at similar velocities and with greater turbulent flow. The high speed at which the gas bubbles travelled past the lower sight glass provided further evidence that the majority of the gas in the downcomer was recirculated into the riser. Also, the large bubble population visually observed in the downcomer provided further evidence of the high gas content in the downcomer already shown by the high gas holdups and DOTs observed in this section of the vessel.

3.1.6 The effect of top section size on the vessel hydrodynamics and oxygen transfer

In the top section the amount of bubble disengagement from the liquid surface and bubble entrainment into the downcomer would have a dramatic effect on the hydrodynamic performance of the vessel. Thus, a study of the effect of top section size i.e. the liquid height above the draft tube on the hydrodynamic and oxygen transfer performance of the vessel would be important for the optimisation of reactor operation. The size of the top section can be described by either the height of unaerated liquid above the draft tube which was measured when no air sparging occurred, or the gassed height above the draft tube measured during aeration. The gassed height will mostly be referred to in this section as this was the actual sectional height the cells of the fermentation broth experienced. However, the gassed height was itself affected by the gas velocity and at a given gas velocity, both top section height measurements should show a similar effect on a measured parameter, when the size of the top section was changed by increasing the liquid volume.

3.1.6.1 The effect of top section size on overall gas holdup

The similar relationship between top section size and overall gas holdup for both ungassed and gassed liquid heights is shown for the draft tube sparger in figures 3.11. No significant change in overall gas holdup with increasing ungassed or gassed liquid heights was observed over the gas velocity range studied. The top section size was found to have a similar effect on overall gas holdup with the annulus sparger configuration, results not shown.

3.1.6.2 The effect of top section size on downcomer and riser gas holdup

The downcomer gas holdup measured when using the draft tube sparger configuration was unaffected by the change in gassed liquid height above the draft tube (figure 3.12). This implied that the downcomer gas holdup and the fraction of gas recirculated into the downcomer was independent of top section size. However, this did not take into account the flow rate of gas entering the downcomer and the difference between the gas and liquid flow rates. The riser gas holdup measured with the annulus sparged reactor was also found to be independent of top section size (figure 3.13).

3.1.6.3 The effect of top section size on liquid circulation and mixing

In general, the liquid circulation time was found to remain constant with increasing top section size over the gas velocity range studied and for both sparger configurations (figure 3.14 with the draft tube sparger). The liquid circulation was represented rather than the derived liquid velocity as it was difficult to predict an accurate path length for liquid circulation with the changing top section height.

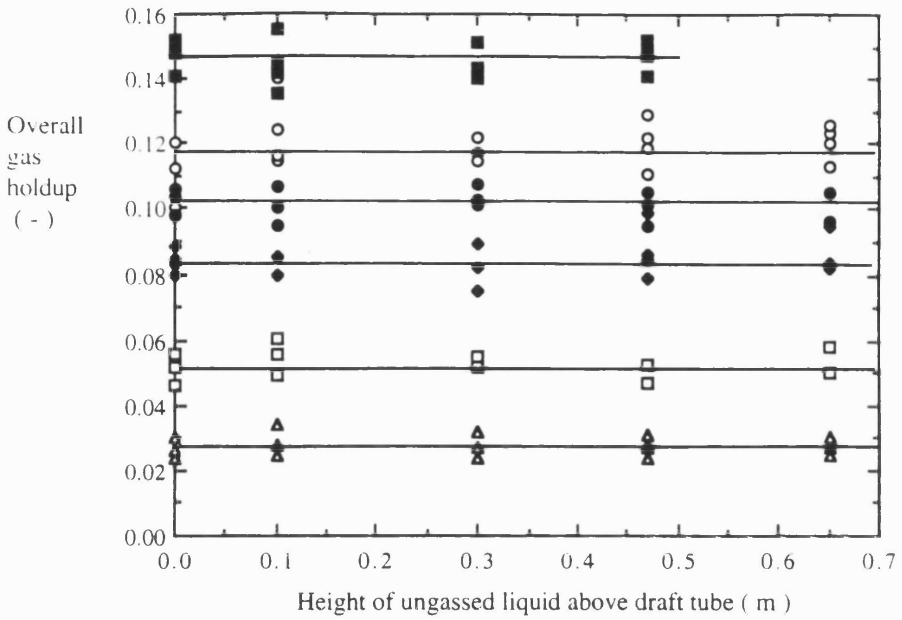

Figure 3.11a The effect of ungassed liquid height above the draft tube on the overall gas holdup with the draft tube gas sparged airlift reactor, (H_{DT} of 2.77 m) and baker's yeast broth using superficial gas velocities (ms^{-1}):,0.018 (▲), 0.036 (□), 0.054 (◆), 0.072 (●), 0.091 (○), 0.136 (■)

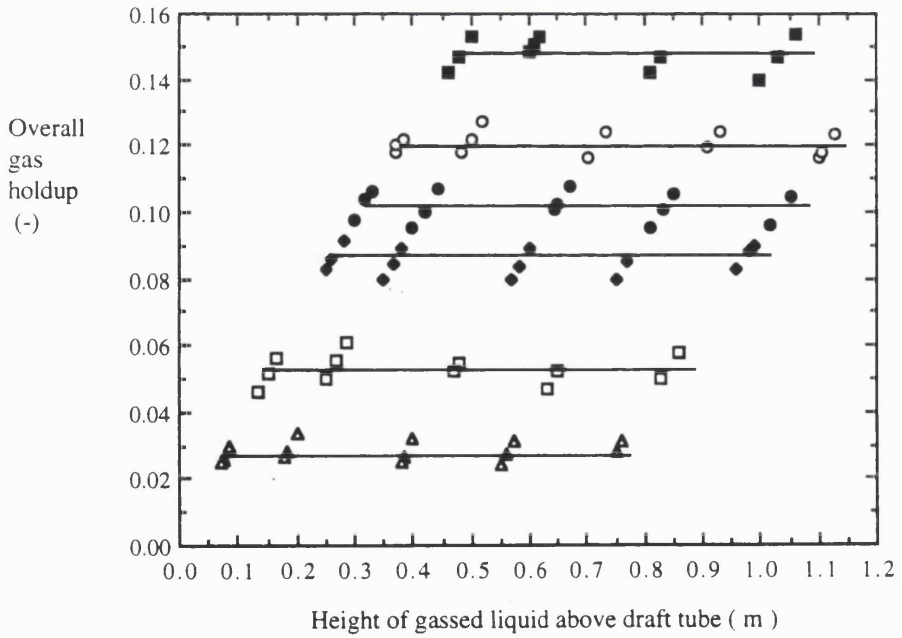

Figure 3.11b The effect of gassed liquid height above the draft tube on the overall gas holdup with the draft tube gas sparged airlift reactor, (H_{DT} of 2.77 m) and baker's yeast broth using superficial gas velocities (ms^{-1}):,0.018 (▲), 0.036 (□), 0.054 (◆), 0.072 (●), 0.091 (○), 0.136 (■)

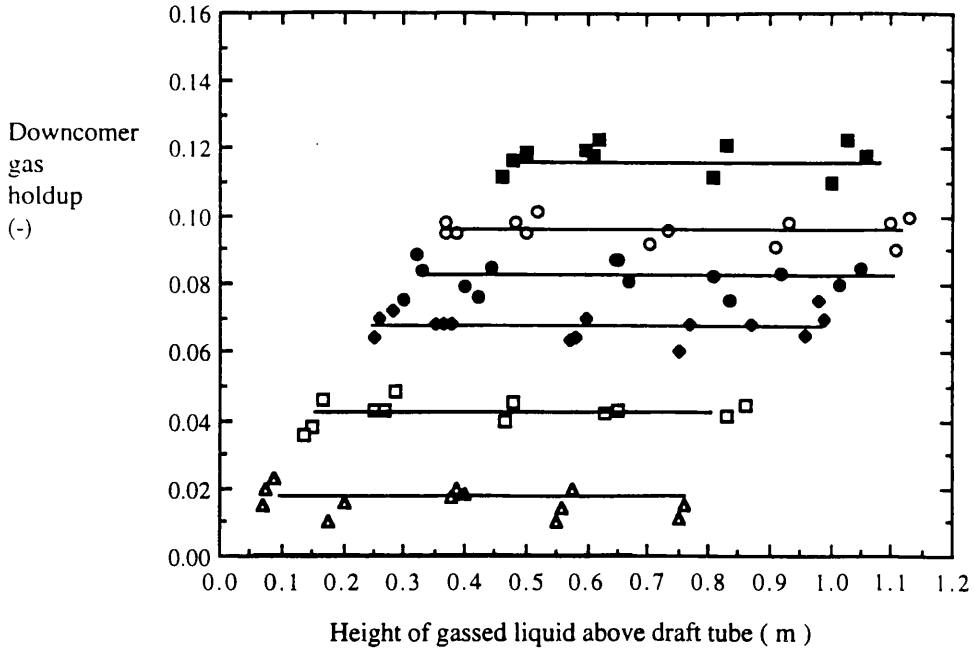

Figure 3.12 The effect of gassed liquid height above the draft tube on the downcomer gas holdup with the draft tube gas sparged airlift reactor, (H_{DT} of 2.77 m) and baker's yeast broth, using superficial gas velocities (ms^{-1}):,0.018 (▲), 0.036 (□), 0.054 (◆), 0.072 (●), 0.091 (○), 0.136 (■)

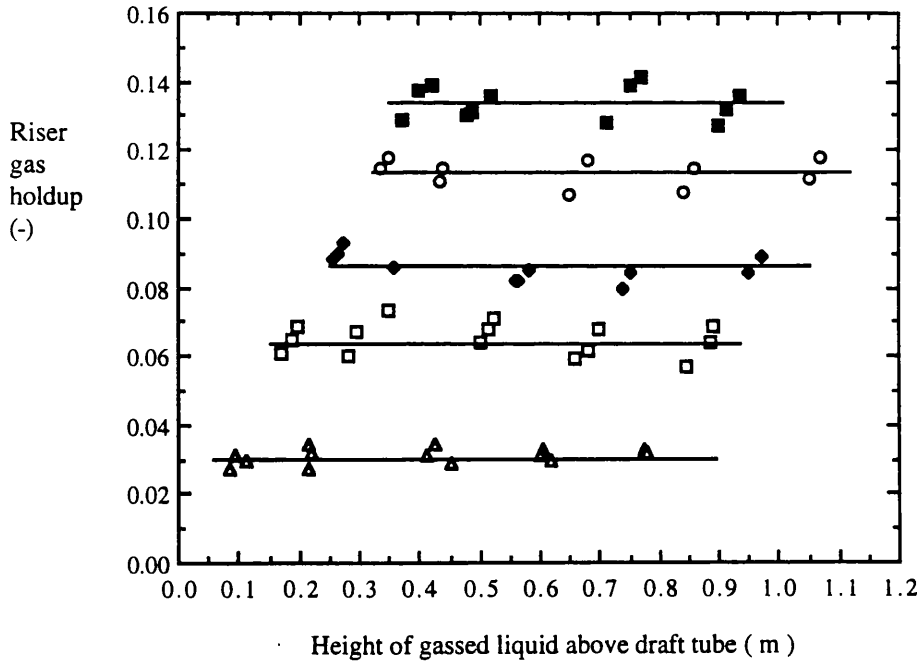

Figure 3.13 The effect of gassed liquid height above the draft tube on the riser gas holdup with the annulus gas sparged airlift reactor, (H_{DT} of 2.77 m) and baker's yeast broth, using superficial gas velocities (ms^{-1}):,0.018 (▲), 0.036 (□), 0.054 (◆), 0.072 (●), 0.091 (○), 0.136 (■)

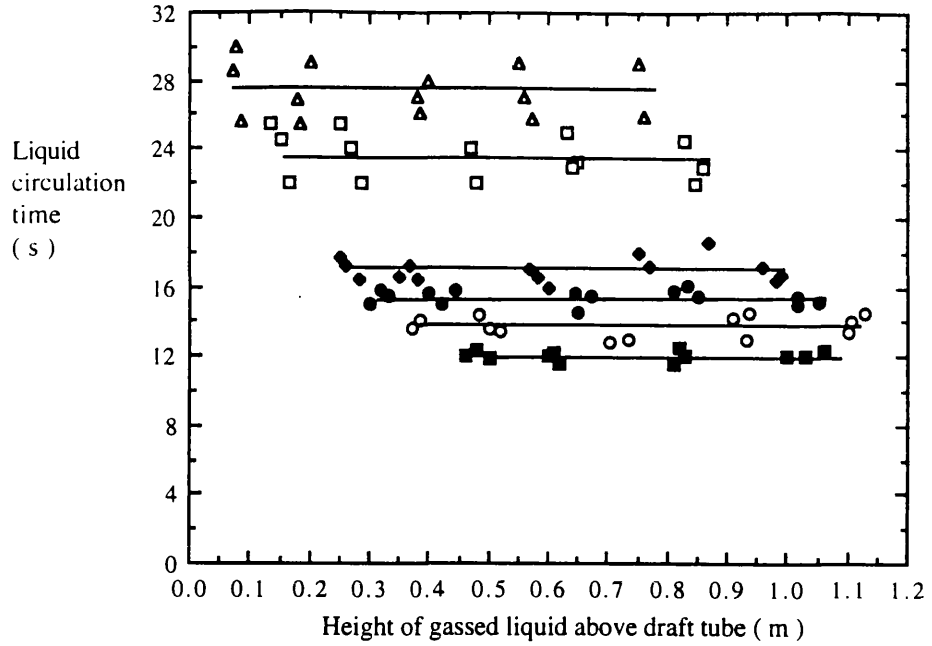

Figure 3.14 The effect of gassed liquid height above the draft tube on the liquid circulation time with the annulus gas sparged airlift reactor, (H_{DT} of 2.77 m) and baker's yeast broth, using superficial gas velocities (ms^{-1}):,0.018 (◠), 0.036 (□), 0.054 (◆), 0.072 (●), 0.091 (○), 0.136 (■)

The effect of top section size on the mixing performance of the vessel for the draft tube sparger configuration can be seen in figures 3.15 & 3.16. The effect of both ungassed and gassed liquid heights have been plotted to allow clearer analysis of the decrease of mixing time with increasing top section size. In figure 3.15 the largest reduction in mixing time with increasing ungassed liquid height occurred with gas velocities below 0.054 ms^{-1}. Hence, at the gas velocity of 0.018 ms^{-1} the mixing time reduced from 120 s at a ungassed height above the draft tube of 0.1 m to 75 s at a ungassed height of 0.5 m above the draft tube. At most gas velocities the mixing time decreased up to a certain liquid height above the draft tube (ungassed height of 0.47m) and then remained constant with further increases in top section height.

The gassed liquid height above the draft tube was found to have a similar relationship with mixing time to that of the ungassed liquid height (figure 3.16). At most of the gas velocities the mixing time reduced at a rapid rate with increasing gassed height, followed by a reduction in the rate of decrease above a certain gassed height. The gassed height at which no further reduction in mixing time occurred increased with gas velocity. At gas velocities below 0.054 ms^{-1} the gassed liquid height at which the mixing time became constant was around 0.5 m above the draft tube. At gas velocities above 0.054 ms^{-1} the mixing time became constant at gassed liquid heights between 0.7 and 0.9 m above the draft tube.

Therefore, as there was a reduction in mixing time then the mixing performance of the vessel increased with increasing top section size up to the critical liquid height. A similar relationship of mixing time with increasing gassed liquid height above draft tube was observed with the annulus sparger configuration, but this only applied to gas velocities up to 0.054 ms^{-1} (figure 3.17). At gas velocities above 0.054 ms^{-1} top section size had only a small effect on mixing time whereas, with the draft tube sparger it was only until the highest gas velocity, 0.136 ms^{-1} that the top section had no significant effect on mixing time.

3.1.6.4 The effect of top section size on k_La

Dissolved oxygen tensions of the whole of the vessel were measured using the mobile DOT probe at different gassed heights above the draft tube and at a range of gas velocities. The DOT profiles and the subsequent k_La values were found to be similar at all gassed liquid heights above the draft tube. This was illustrated in figure 3.18 with the k_La values measured from the lower riser probe position as a function of gassed liquid height above the draft tube with the annulus sparger. The k_La values remained relatively constant with increasing gassed height above the draft tube.

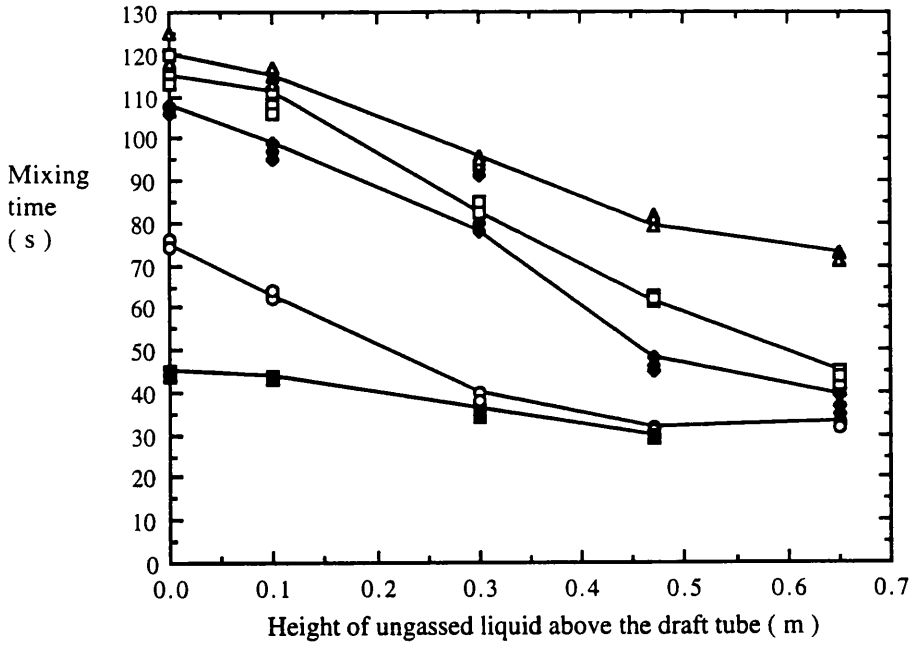

Figure 3.15 The effect of ungassed liquid height above the draft tube on the liquid mixing time with the draft tube gas sparged airlift reactor, (H_{DT} of 2.77 m) and baker's yeast broth, using superficial gas velocities (ms^{-1}):, 0.018 (▲), 0.036 (□), 0.054 (◆), 0.072 (●), 0.091 (○), 0.136 (■)

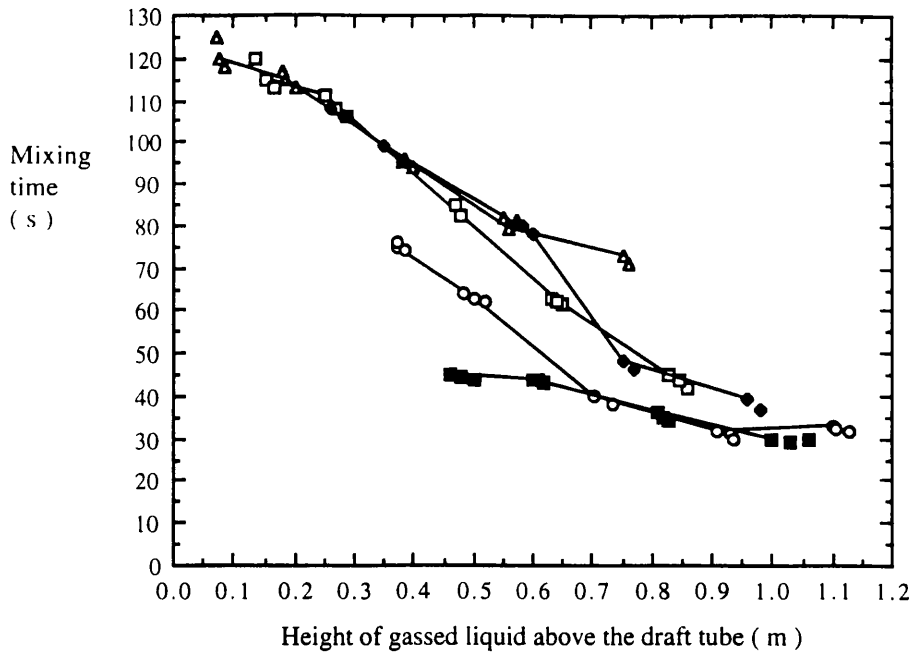

Figure 3.16 The effect of gassed liquid height above the draft tube on the liquid mixing time with the draft tube gas sparged airlift reactor, (H_{DT} of 2.77 m) and baker's yeast broth, using superficial gas velocities (ms^{-1}):,0.018 (▲), 0.036 (□), 0.054 (◆), 0.072 (●), 0.091 (○), 0.136 (■)

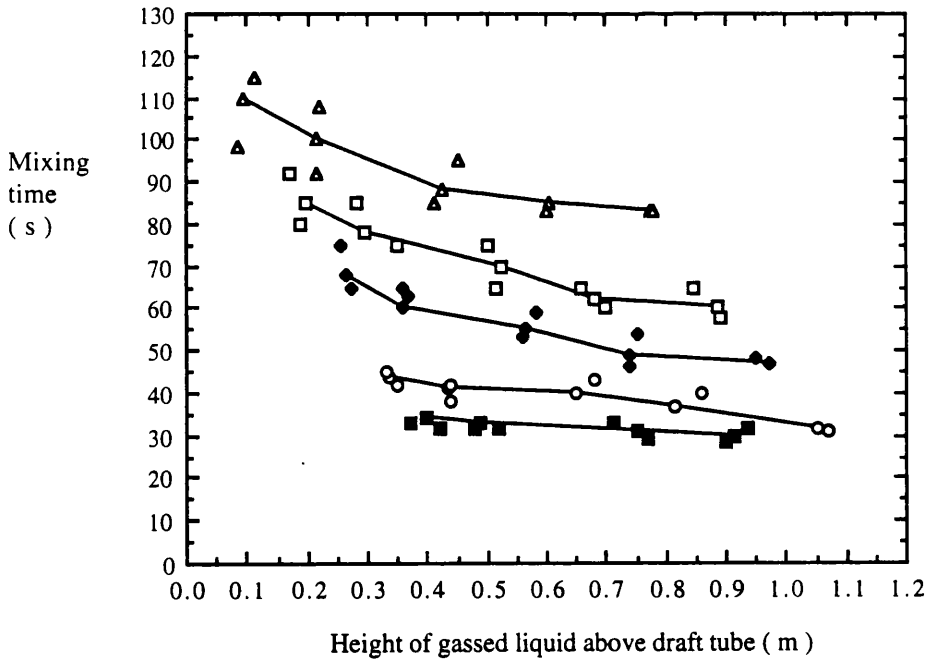

Figure 3.17 The effect of gassed liquid height above the draft tube on the liquid mixing time with the annulus gas sparged airlift reactor, (H_{DT} of 2.77 m) and baker's yeast broth, using superficial gas velocities (ms^{-1}):,0.018 (▲), 0.036 (□), 0.054 (◆), 0.072 (●), 0.091 (○), 0.136 (■)

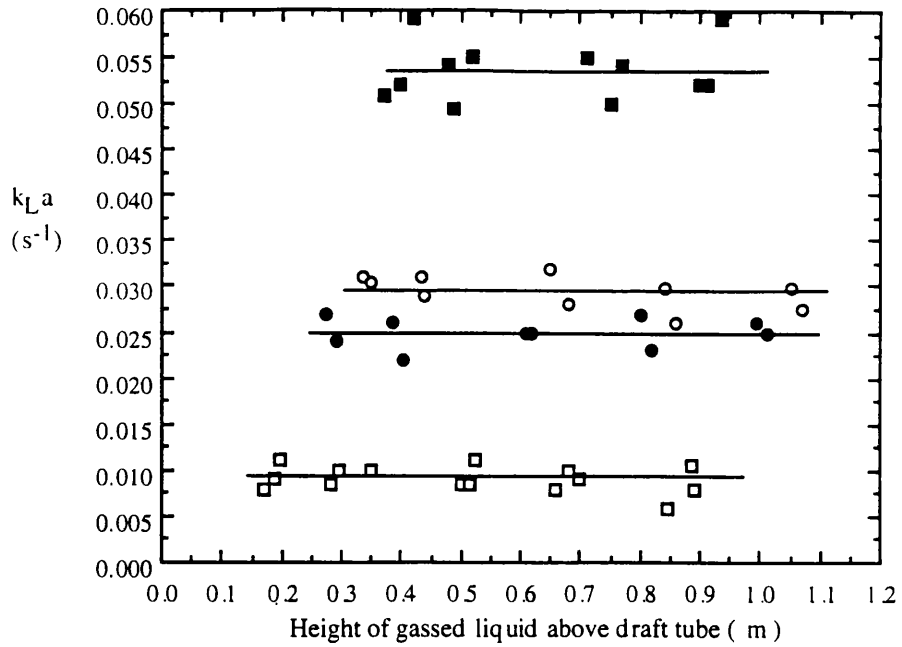

Figure 3.18 The effect of gassed liquid height above the draft tube on k_La from the lower riser position with the annulus gas sparged airlift reactor, (H_{DT} of 2.77 m) and baker's yeast broth, using superficial gas velocities(ms^{-1}): 0.036 (□), 0.072 (●), 0.091 (○), 0.136 (■).

3.2 Investigation of the use of the marine propeller with the draft tube air sparged airlift reactor

The marine propeller was rotated to draw liquid up the draft tube in the direction of the aerated liquid flow with the 10 gL^{-1} DCW yeast suspension. Gas holdup is controlled by the airflow rate in a conventional airlift reactor but, a change in airflow rate also effects the liquid circulation. However, the marine propeller may allow independent control of the liquid circulation in the aerated reactor.

3.2.1 The effect of propeller speed on the gas holdup of the aerated vessel

No significant change in overall or downcomer gas holdup occurred with propeller speeds up to 500 rpm for all gas velocities from 0.018 to 0.136 ms^{-1} although only three gas velocities are shown on figure 3.19. For gas velocities below 0.091 ms^{-1} propeller speeds above 500 rpm produced a gradual decrease of overall gas holdup, reaching values below 0.04 at the maximum propeller speed of 1050 rpm. For gas velocities above 0.072 ms^{-1} the gas holdup decreased gradually between 500 and 700 rpm which was followed by a rapid decrease in holdup with propeller speeds from 700 to 1050 rpm. For example, at the maximum gas velocity (0.136 ms^{-1}) the overall gas holdup reduced from 0.125 at 900 rpm to 0.07 at 1050 rpm. At propeller speeds between 500 and 700 rpm the liquid level in the top section began to fluctuate at all gas velocities. This was not shown on figure 3.19 as the mean holdup values were used. In general the

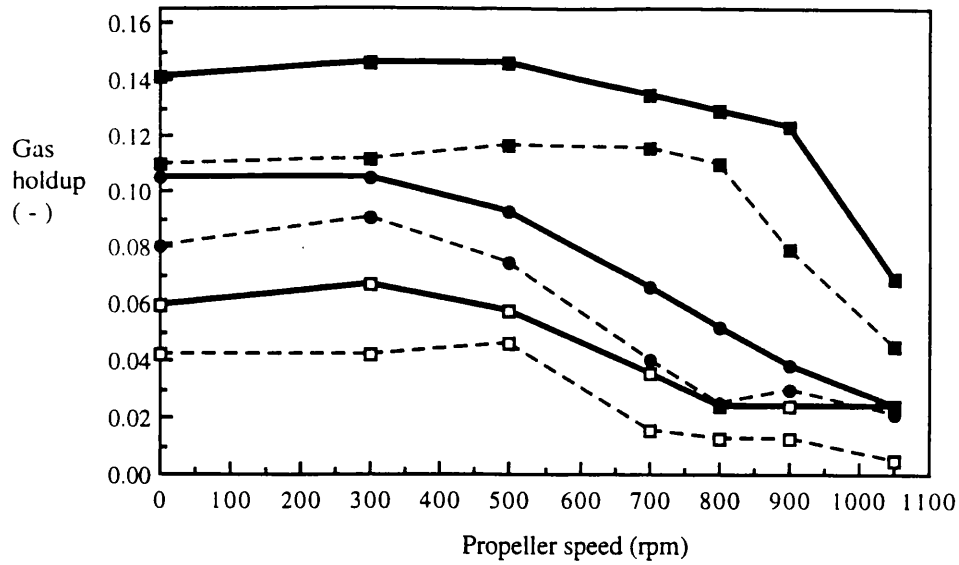

Figure 3.19 The effect of propeller speed on the overall and downcomer gas holdup of the draft tube gas sparged airlift reactor (H_{DT} of 2.77 m) with baker's yeast suspension (10 gL^{-1} DCW) at superficial gas velocities (ms^{-1}) : 0.036 (□), 0.072 (●), 0.136 (■). Overall gas holdup (⟵), downcomer gas holdup (⟵---)

liquid fluctuations began above propeller speeds of 500 rpm with an amplitude of 0.05 m and a frequency of 40 s. The fluctuations then increased in size and frequency with propeller speed. For gas velocities below 0.091 ms^{-1} maximum fluctuations occurred at 700 rpm which were 0.2 m in size with a mean frequency of 33 s. For gas velocities above 0.072 ms^{-1} the maximum fluctuations were observed before the rapid reduction in gas holdup occurred. Hence, maximum fluctuations were observed at 800 rpm with the gas velocity of 0.113 ms^{-1} and 900 rpm with the 0.136 ms^{-1}. The fluctuation frequency was around 30 s with a maximum length of 0.2 m. The amplitude of the liquid fluctuations reduced with further increases in propeller speed up to 1050 rpm where the liquid level was dominated by the lowest liquid level of the fluctuations at the previous propeller speed. For example, at the gas velocity of 0.072 ms^{-1} (160 $Lmin^{-1}$, 0.64 vvm) the maximum fluctuation of 0.2 m occurred at the propeller speed of 800 rpm which corresponded to the overall gas holdup cycling between 0.0795 and 0.024. As the propeller speed increased to 1050 rpm the amplitude of the fluctuations decreased in size although the lowest liquid height corresponding to the gas holdup of 0.024 remained constant. Thus at the maximum propeller speed (1050 rpm) the overall gas holdup was 0.024 where no liquid fluctuations occurred. No significant trend between the fluctuating frequency and gas velocity could be found although the fluctuation frequency increased from 40 to 30 s with the propeller speed increases at which fluctuations occurred. The downcomer gas holdup fluctuated in synchrony with the overall gas holdup. This could be visually observed through the side vessel sight glasses where entrainment of gas into the downcomer was observed when the amplitude of the fluctuating liquid was at its

highest. As the overall gas holdup reduced towards the lower liquid height of the fluctuation then, the amount of entrainment into the downcomer also decreased. At the lowest liquid level of the fluctuation no entrainment into the downcomer was observed.

3.2.2 The effect of propeller speed on the liquid circulation and mixing performance of the aerated vessel

Propeller operation produced a small decrease of the liquid circulation time from that of the conventionally aerated reactor (shown by values at 0 rpm in figure 3.20a) with most of the gas velocities.

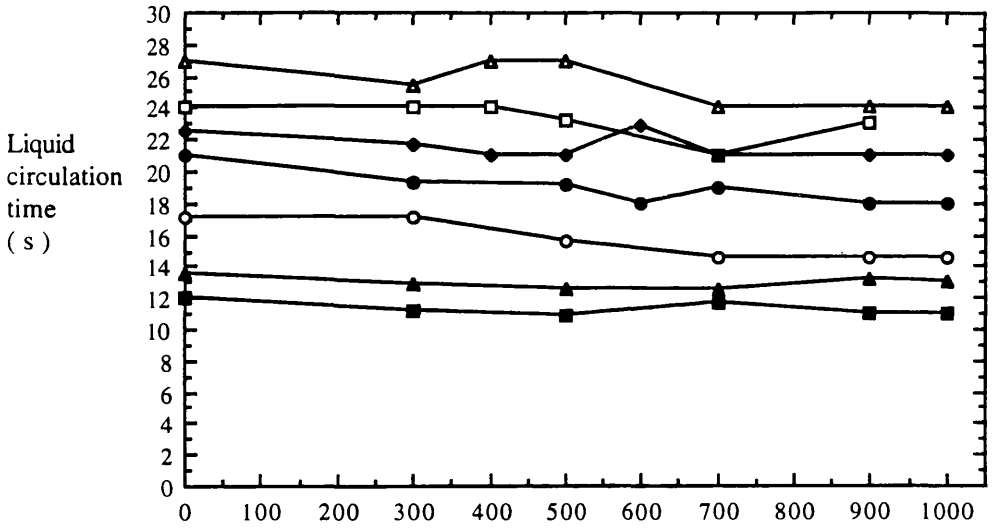

Figure 3.20a

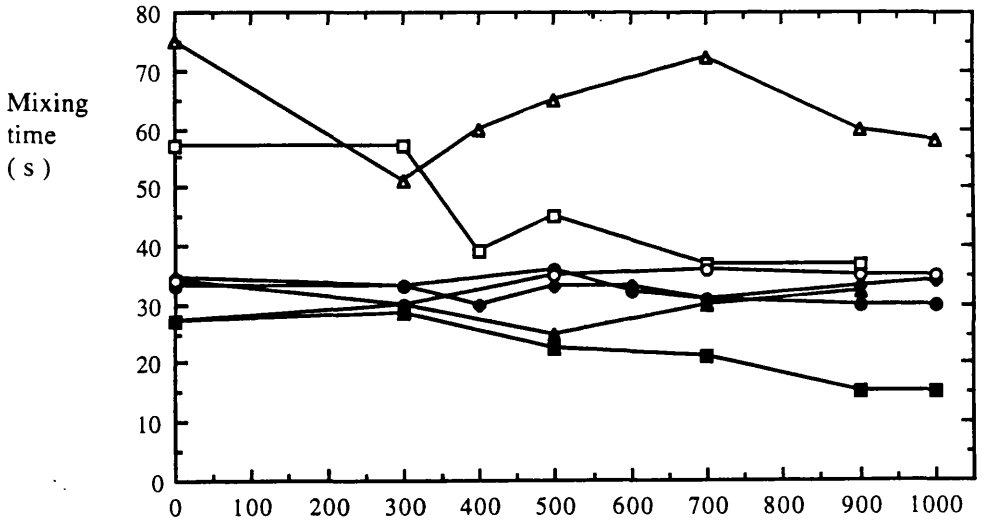

Figure 3.20b

Figure 3.20 The effect of propeller speed on the liquid circulation and mixing times of the draft tube gas sparged airlift reactor, (H_{DT} of 2.77 m) with baker's yeast broth, using superficial gas velocities (ms^{-1}):,0.018 (▲), 0.036(□), 0.054 (◆), 0.072 (●), 0.091 (o), 0.113 (▲), 0.136 (■)

The improved liquid circulation performance was insignificant compared to the improvement of circulation time with increased gas velocity. The mixing time also remained generally constant although some downward deflection occurred with the gas velocities below 0.054 ms^{-1} (figure 3.20b). However, the tracer response profiles were distorted when liquid fluctuations occurred with propeller operation so that, accurate measurement for the increase through the whole range of propeller speeds was difficult.

The insignificant impact of the propeller on the liquid circulation and mixing performance of the aerated vessel is confirmed in figure 3.21 which compared the propeller only performance (no aeration) to that of aeration and propeller operation at the lowest gas velocity of 0.018 ms^{-1}. The mixing and circulation performance with propeller only operation was considerably worse than with aeration. For example, at the propeller speed of 300 rpm the circulation and mixing times with propeller only operation were some 6 to 8 times longer than with aeration and propeller operation. Propeller speeds above 800 rpm were only able to produce similar liquid circulation's to the lowest gas velocity.

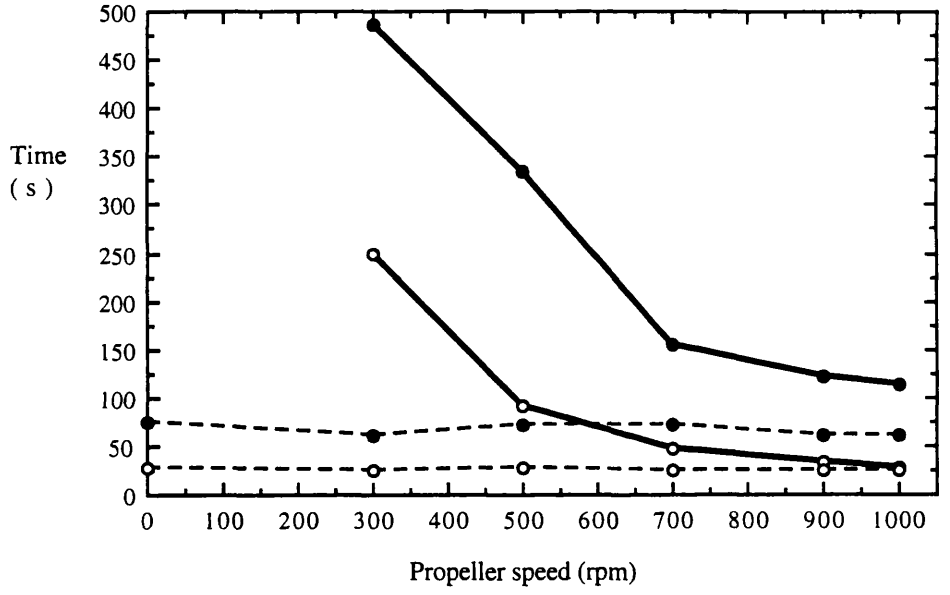

Figure 3.21 Comparison of the effect of propeller speed on the liquid circulation and mixing times between propeller operation with and without aeration from the draft tube gas sparged airlift reactor, (H_{DT} of 2.77 m) with baker's yeast broth, using the superficial gas velocity of 0.036 ms^{-1}. Propeller only operation(——), aeration and propeller operation (- - -). Liquid circulation time (o), mixing time (•)

3.2.3 The effect of propeller speed on the dissolved oxygen tension of the aerated vessel

For all gas velocities the dissolved oxygen tension in the lower riser position increased with propeller speed. The propeller speed at which the DOT increased above 5% was the speed at which liquid fluctuations were found to occur. However, this coincided with a reduction in downcomer DOTs with increasing propeller speed (figure

3.22). The k_La values also showed a corresponding change with propeller speed. The fluctuating liquid level at certain propeller speeds also caused the dissolved oxygen tensions to fluctuate in synchrony although this was not shown in figure 3.22 as the mean values were plotted. For example, at 800 rpm with the highest gas velocity the DOTs were below 1% in the riser when the overall gas holdup (liquid level) was at its highest during the gas holdup fluctuation. Also, the DOT was above 40% in the upper downcomer and above 15% in the lower downcomer. Then as the liquid fluctuation decreased in amplitude to the lowest liquid level the DOTs in the downcomer decreased to below 15% and, the riser DOT increased above 15%. Hence, as the propeller speeds were increased above 800 rpm the DOTs from the three fixed probe positions were similar to the values measured during the lowest liquid level of the fluctuating liquid at 800 rpm.

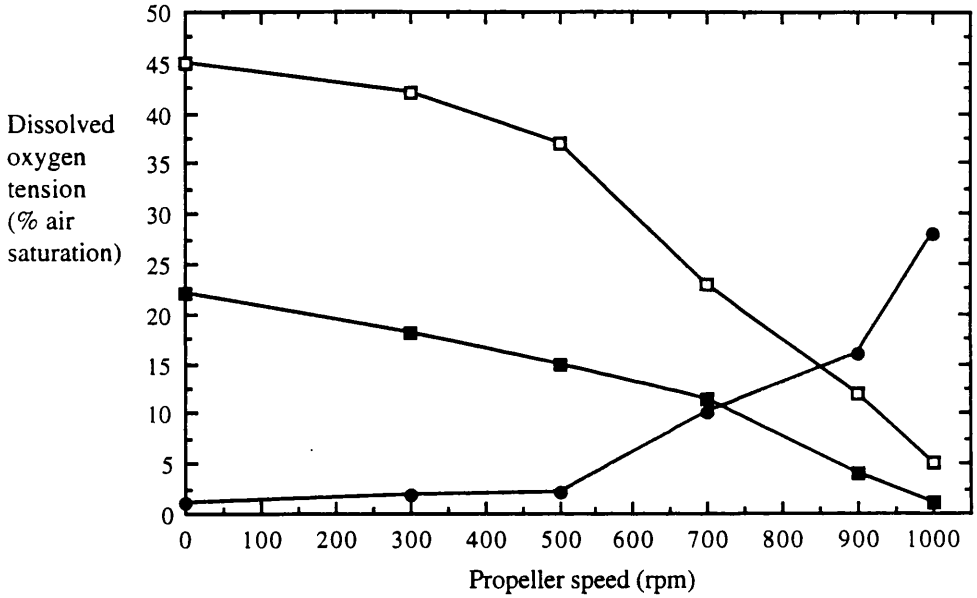

Figure 3.22 The effect of propeller speed on the dissolved oxygen tension (% air saturation) from the fixed probe positions of the draft tube gas sparged airlift reactor (H_{DT} of 2.77 m) with baker's yeast suspension (10 gL^{-1} DCW) at the superficial gas velocity of 0.136 ms^{-1}. Probe positions: lower riser (●), upper downcomer (□) lower downcomer (■)

The changes in DOT with propeller operation were also investigated using the mobile DOT probe (figure 3.23). The DOTs from propeller operation at 700 rpm with aeration at 0.136 ms^{-1} had increased above the aeration only values for most of the riser and top section yet, the DOTs in the downcomer were below the aeration values. Hence, at this propeller speed a greater proportion of the DOTs around the vessel were above 1% than at any other speed above or below 700 rpm. Thus, a small increase in oxygen uptake rate (OUR) was observed from the aeration value of 41 $mmol.L^{-1}.h^{-1}$ to 45 $mmol.L^{-1}.h^{-1}$. However, the OUR returned to 41 $mmol.L^{-1}.h^{-1}$ with the further increase in propeller

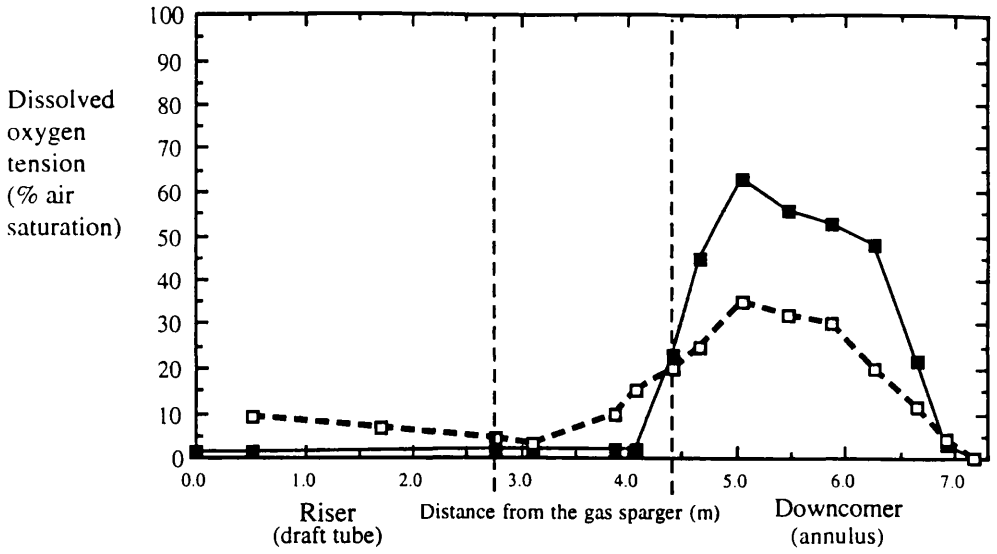

Figure 3.23 Comparison of the dissolved oxygen tension (% air saturation) with increasing distance from the sparger between, conventional aeration and combined propeller operation (700 rpm), with the draft tube gas sparged airlift reactor (H_{DT} of 2.77 m) and baker's yeast suspension (10 gL^{-1} DCW). The superficial gas velocity of 0.136 ms^{-1} was used with conventional aeration (■), and aeration and propeller operation (□)

speed due to the reduction of DOT to below 1% in the downcomer. At all other gas velocities below 0.136 ms^{-1} with the 10 gL^{-1} DCW broth no significant change in OUR occurred with propeller speed.

The gas holdup, liquid circulation and oxygen transfer performance of the aerated and propeller operated reactor was also found to be independent of top section size (unaerated liquid heights of 0.0 to 0.63 m above the draft tube). However, the results will not be described due to the inability of the propeller to significantly improve the hydrodynamic and oxygen transfer performance of the aerated vessel in this configuration.

3.3 Investigation of the use of the marine propeller with the annulus air sparged airlift reactor

The use of the marine propeller at the base of the vessel was investigated as an aid to liquid circulation with aeration from the annulus sparger using the baker's yeast suspension. Air was sparged into the annulus of the vessel which caused liquid to circulate down the draft tube. The marine propeller was rotated to draw liquid down the draft tube in the direction of liquid flow and aid recirculation at the base of the vessel (figure 2.2). In this configuration the marine propeller may allow independent control of the liquid circulation in the aerated reactor. The studies were carried out with the draft tube height (H_{DT}) of 2.77 m, working volume of 0.25 m^3 and with the 10 gL^{-1} dry cell weight (DCW) baker's yeast suspension unless specified.

3.3.1 The effect of propeller operation on the gas holdup of the aerated vessel

The overall and riser gas holdup increased with propeller speed for the range of gas velocities from 0.018 to 0.136 ms^{-1} although only three gas velocities are shown in figure 3.24. The values at 0 rpm of figure 3.24 referred to the aeration only operation which allowed a comparison to the combined aeration and propeller operation shown at increasing propeller speeds. For all gas velocities studied propeller speeds above 600 rpm produced the largest increase in gas holdup. The propeller had a greater influence on gas holdup at the low gas velocity of 0.036 ms^{-1} where propeller operation at 1000 rpm produced a two fold increase of overall gas holdup compared to conventional aeration. For propeller speeds below 600 rpm the difference between overall and riser gas holdup was similar to that for aeration only operation (0 rpm). As the propeller speed increased the overall gas holdup became larger than the riser gas holdup. The theoretically estimated downcomer gas holdup (equation A 2.3), using the overall and riser gas holdup values at high propeller speeds, was found to be greater than the overall and riser gas holdups. So at the gas velocity of 0.136 ms^{-1} and propeller speed at 1000 rpm, the estimated gas holdup for the downcomer was 20% larger than the overall gas holdup and 32% larger than the gas holdup in the riser. This indicated that high propeller speeds caused a change in the distribution of gas holdup in the vessel from the conventionally aerated reactor. The propeller speed at which the overall and downcomer gas holdups became greater than the riser gas holdup increased with superficial gas velocity.

3.3.2 The effect of propeller operation on the liquid circulation and mixing performance of the aerated vessel

Operation of the propeller during conventional aeration resulted in a decrease of the liquid circulation time at all gas velocities (figure 3.25). The circulation time at 1000 rpm with a gas velocity of 0.036 ms^{-1} (0.364 vvm) was 14 seconds which reduced from a value of 28 s for aeration only operation. However, at the gas velocity of 0.136

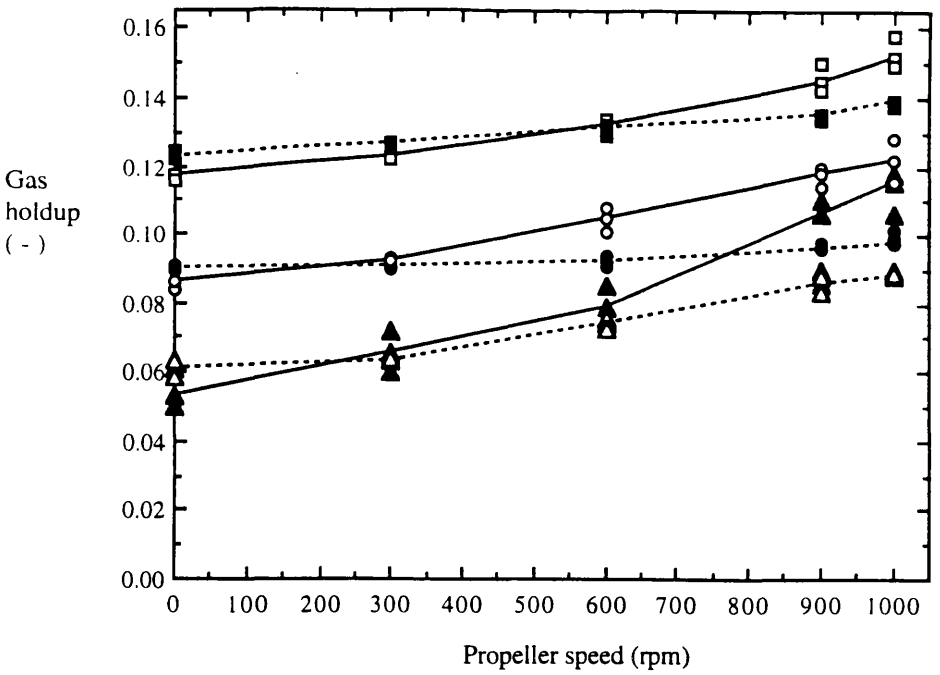

Figure 3.24 The effect of propeller speed on the riser and overall gas holdup of the annulus gas sparged reactor (H_{DT} of 2.77 m) with baker's yeast suspension (10 gL^{-1} DCW) at superficial gas velocities (ms^{-1}) : 0.036 (▲ ,△), 0.072 (● , ○), 0.136 (■ , □) Overall gas holdup (———), riser gas holdup (- - - -)

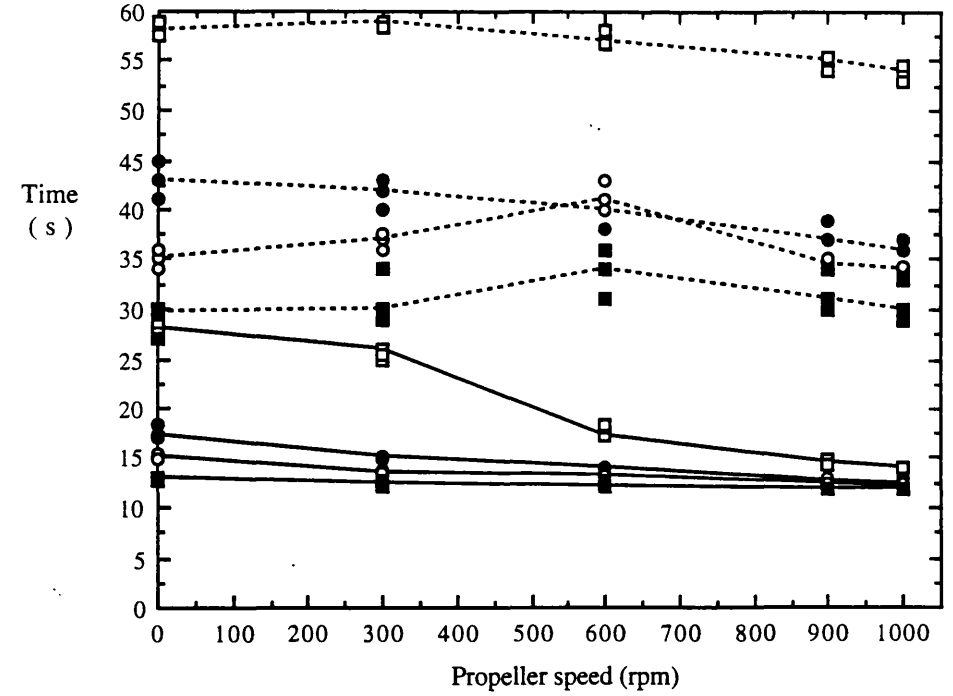

Figure 3.25 The effect of propeller speed on the liquid circulation and mixing times of the annulus gas sparged airlift reactor (H_{DT} of 2.77 m) with baker's yeast broth at superficial gas velocities (ms^{-1}) : 0.036 (□), 0.072 (●), 0.091 (○), 0.136 (■). Liquid circulation time (—) and mixing time (···)

ms^{-1} (1.432 vvm) the circulation time reduced from 13 seconds for aeration only operation to 11.9 seconds with propeller speed at 1000 rpm. This illustrated that the propeller had a greater influence on the liquid circulation time at low gas velocities. This was similar to the effect of the propeller on gas holdup (section 3.3.1) where the propeller had a greater effect at increasing overall gas holdup at gas velocities below 0.054 ms^{-1}. Although the propeller improved the circulation times, and hence the liquid velocity (appendix 9.3), of the aerated vessel a similar effect on the mixing time was not observed. The mixing time decreased from 58 s for aeration only operation to 53 s with propeller operation at 1000 rpm with the low gas velocity (0.036 ms^{-1}). At higher superficial gas velocities the influence of the propeller on the liquid mixing time was much less.

These observations are confirmed in figure 3.26 which shows the tracer response measurements from aeration and combined propeller operation with two gas velocities 0.036 and 0.072 ms^{-1}. The times between circulation peaks and, therefore, the liquid circulation times for aeration and propeller operation were shorter than for the aeration only operation. The amplitude of tracer response peaks decreased after pulse injection with both operating conditions and, aeration and propeller operation resulted in a greater number of discernible tracer response peaks after pulse injection compared to aeration only operation. For example, propeller operation at 900 rpm and aeration at 0.036 ms^{-1} produced seven tracer response peaks after pulse injection compared to three peaks for aeration only operation. However, it can be observed that it took a similar time to reach the same peak amplitude with both operating conditions. Hence, the mixing times from the propeller and aeration operation were similar to those measured with conventional aeration operation.

For propeller operation a trend of increasing mixing to circulation time ratio was observed with increasing propeller speed (figure 3.27). This was most significant with the low gas velocity (0.036 ms^{-1}) where an increase in ratio from 2.25 for aeration only, to 3.75 with propeller operation at 1000 rpm was observed. Whereas, with conventional aeration a constant ratio between 2.25 and 2.5 was obtained which was independent of the gas velocity (figure 3.5). Therefore, as the propeller speed was increased a greater number of circulations of the vessel were required to reduce the injected pulse to 90% homogeneity.

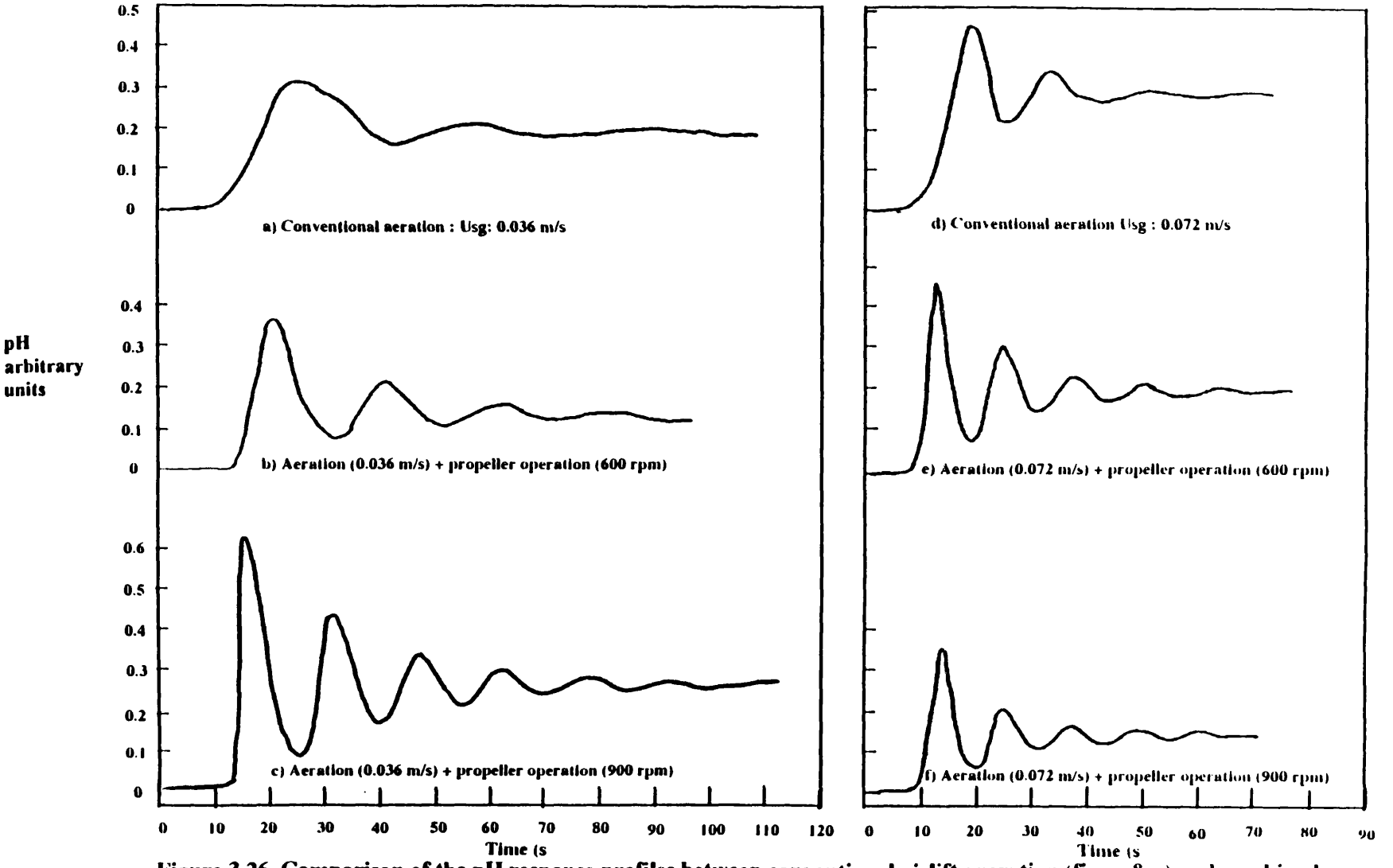

Figure 3.26 Comparison of the pH response profiles between conventional airlift operation (fig. a & c) and combined aeration and propeller operation. Superficial gas velocities (m/s): 0.036 (fig. a, b, c), 0.072 (fig. d, e, f) used with propeller speeds (rpm): 600 (fig. b, d), 900 (fig. c, e).

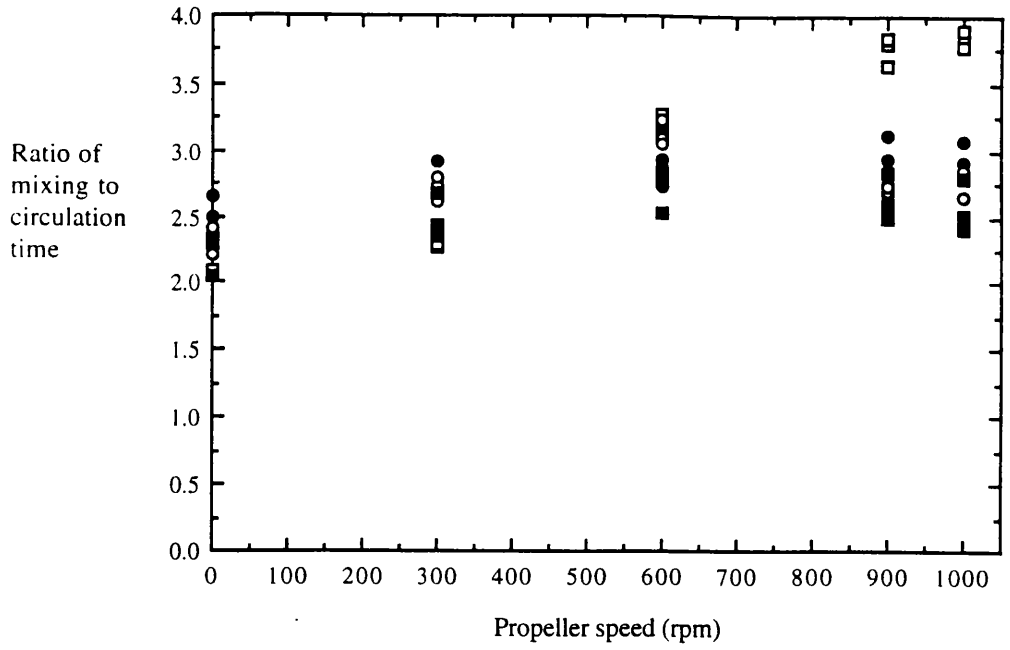

Figure 3.27 The effect of propeller speed on the ratio of mixing to liquid circulation time of the annulus gas sparged airlift reactor (H_{DT} of 2.77 m) with baker's yeast broth at superficial gas velocities (ms^{-1}) : 0.036 (□), 0.072 (•), 0.091 (o), 0.136 (■)

3.3.3 The effect of propeller operation on liquid circulation and mixing times in the absence of aeration

The liquid circulation and mixing performance of the vessel was studied when only the propeller was used (propeller only operation) with no air sparging into the vessel. Hence, the propeller was rotated to draw the liquid down the draft tube and circulate the liquid around the vessel base and up the annulus of the vessel. These studies were carried out with the 10 gL^{-1} DCW yeast broth. So, the comparison of these results with those from the combined aeration and propeller operation in section 3.3.2 provided further evidence of the influence of propeller operation on the liquid circulation and mixing times of the aerated vessel.

In figure 3.28a the bold curve shows the decrease of circulation time with increasing propeller speed with no aeration. There was a gradual fall in liquid circulation time from 30.5 seconds to 9.8 seconds with increases in propeller speed up to 1000 rpm. Figure 3.28a also shows the circulation time profiles for the aeration and combined propeller operation for the two gas velocities which were shown in figure 3.25. For propeller speeds below 600 rpm, the liquid circulation times for combined aeration and propeller operation were shorter than for the unaerated propeller only operation. As the propeller speed increased the liquid circulation from the non-aerated system became faster than with combined aeration and propeller operation. The propeller speed at which this occurred increased with superficial gas velocity. This demonstrated that although the circulation times of the aerated reactor were reduced by propeller operation , the liquid

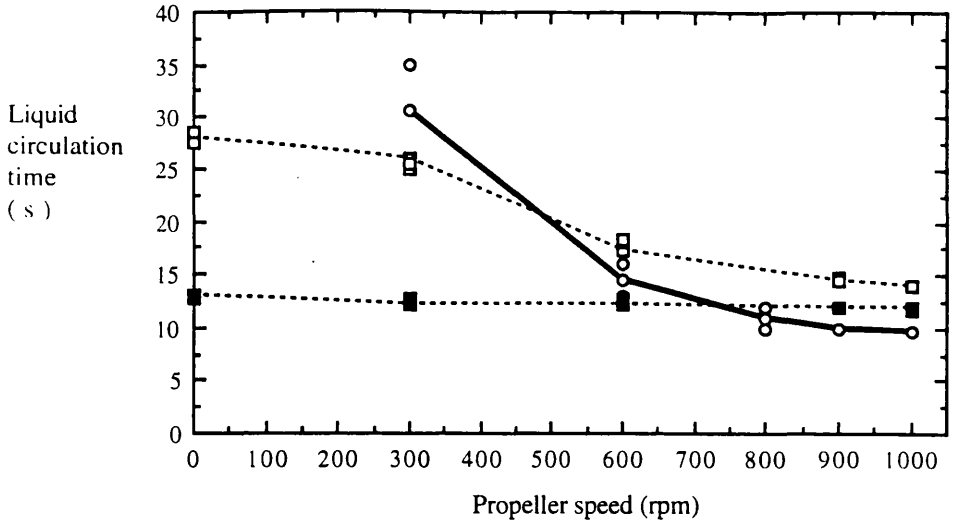

Figure 3.28a Comparison of the effect of propeller speed on the liquid circulation time, between propeller only operation and, combined propeller and aeration operation with the annulus gas sparged airlift reactor (H_{DT} of 2.77 m), using the baker's yeast broth and superficial gas velocities (ms^{-1}) : 0.036 (□), 0.136 (■) Propeller only operation (-o-), propeller and aeration (----)

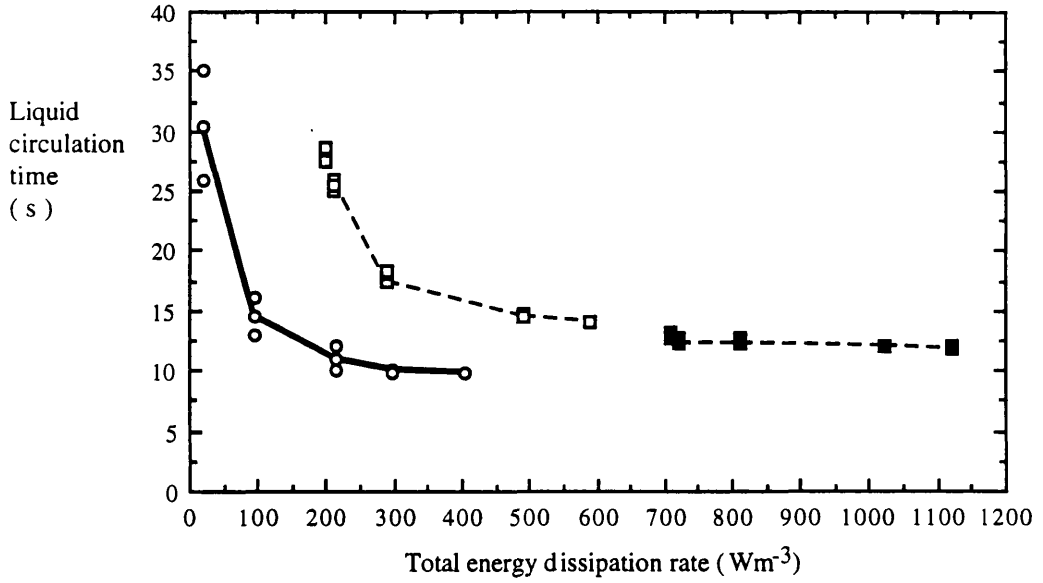

Figure 3.28b Comparison of the effect of the total energy dissipation rate on the liquid circulation time, between propeller only operation and, combined propeller and aeration operation with the annulus gas sparged airlift reactor (H_{DT} of 2.77 m), using the baker's yeast broth and superficial gas velocities (ms^{-1}) : 0.036 (□), 0.136 (■) Propeller only operation (-o-), propeller and aeration (----)

circulation was dominated by the effect from aeration rather than propeller speed at high gas velocities.

The comparison of the liquid circulation performance between propeller only and combined aeration and propeller operation must also be considered in respect to the total energy dissipation rate (section 2.8). The first data point of the total energy dissipation rate curves (figure 3.28b) for aeration and propeller operation referred to the energy dissipation rate from aeration only operation and then, subsequent points were for the total energy dissipation rate (P_{VT}) from aeration with increasing propeller speed. The liquid circulation times from both propeller only operation and combined propeller and aeration operation (gas velocity of 0.036 ms^{-1}) had a similar relationship with the total energy dissipation rate. The liquid circulation time reduced rapidly from small increases in P_{VT} followed by a reduced rate of decrease at higher P_{VT}. Similar circulation times of 30 s were produced with aeration only operation at the gas velocity of 0.036 ms^{-1} and from propeller only operation at 300 rpm. However, the energy dissipation rate with aeration at the low gas velocity (198 Wm^{-3}) was 11 fold greater than with propeller only operation (18 Wm^{-3}). For the gas velocity of 0.136 ms^{-1} the increase of P_{VT} from 710 Wm^{-3} for conventional aeration to 1120 Wm^{-3} at 1000 rpm only produced a reduction in circulation time from 13 to 11.9 s. Hence, despite the P_{VT} of 1120 Wm^{-3} with aeration and propeller operation the circulation time was still slower (11.9 s) compared to propeller only operation at 1000 rpm (9.8 s) with an P_{VT} of 404 Wm^{-3}. Therefore, the low power inputs with propeller only operation produced shorter liquid circulation times than with aeration and propeller operation. This provided further evidence that aeration reduced the influence of propeller operation on the liquid circulation time.

The mixing time for propeller only operation showed a gradual reduction with propeller speeds up to 1000 rpm compared to mixing times for combined aeration and propeller operation which remained constant for similar increases of propeller speed (figure 3.28c). For most propeller speeds the aerated and propeller operated reactor produced shorter mixing times and hence, greater mixing performance than propeller only operation. This confirmed that the mixing performance of the vessel from aeration and propeller operation was dominated by the gas velocity and not by propeller operation.

Increasing total energy dissipation rate (P_{VT}) from propeller only operation produced a similar relationship with mixing time as that observed with circulation time, with rapid decrease in mixing times with increasing P_{VT} up to 94 Wm^{-3} followed by a reduced rate of decrease with further increases of P_{VT} (figure 3.28d). The mixing times for propeller only operation above P_{VT} of 214 Wm^{-3} were similar to the mixing times observed with combined propeller and aeration operation (gas velocity of 0.036 ms^{-1}). For the gas velocity of 0.136 ms^{-1} the increase of P_{VT} from 710 - 1120 Wm^{-3} produced mixing time values around 30 seconds. These were considerably shorter than the 50 s achieved with propeller only operation at the 2 fold lower energy dissipation rate. Data from figure 3.28a and 3.28c showed that the mixing to circulation time ratios for the

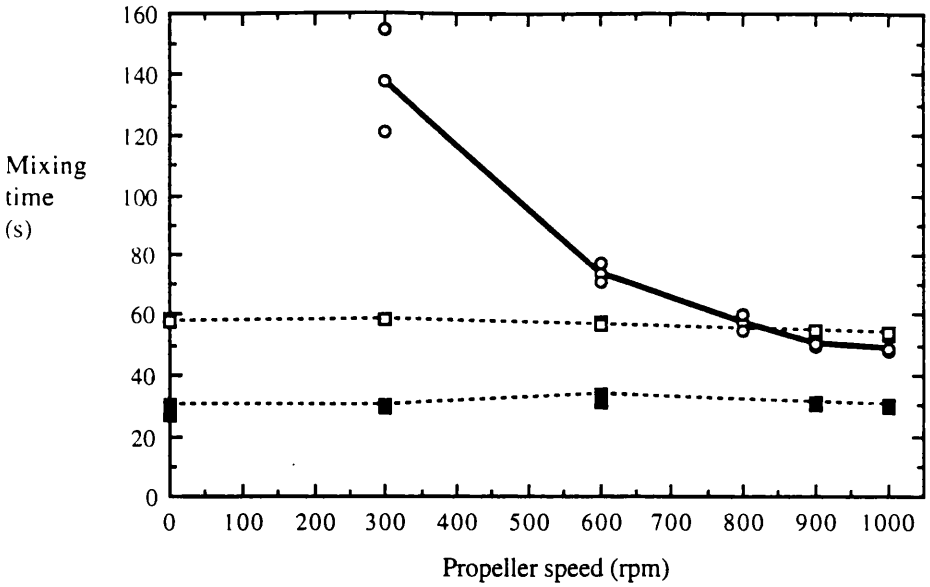

Figure 3.28c Comparison of the effect of propeller speed on the mixing time, between propeller only operation and, combined propeller and aeration operation with the annulus gas sparged airlift reactor (H_{DT} of 2.77 m), using the baker's yeast broth and superficial gas velocities (ms^{-1}) : 0.036 (□), 0.136 (■) Propeller only operation (-o-), propeller and aeration (- - - -)

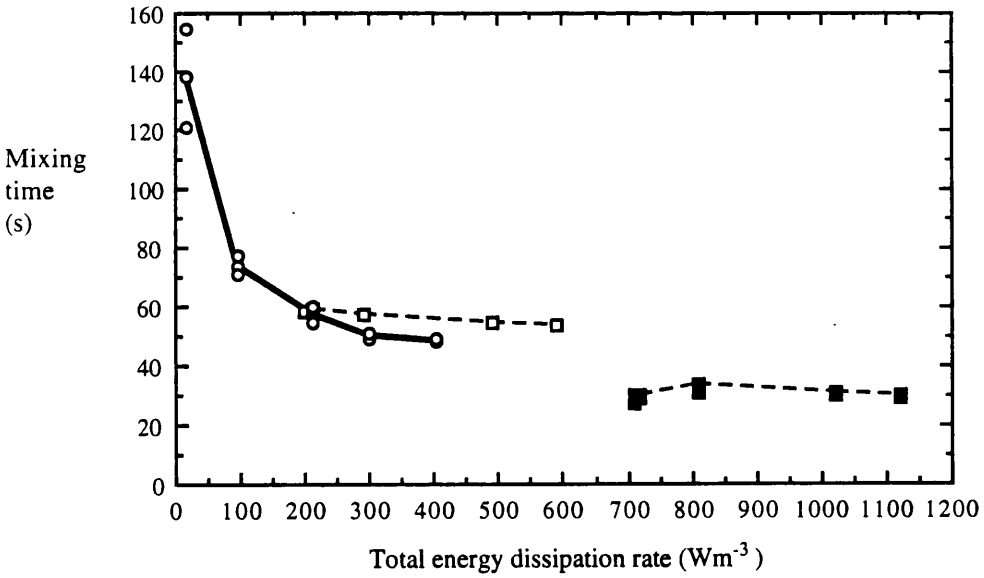

Figure 3.28d Comparison of the effect of total energy dissipation rate on the mixing time, between propeller only operation and, combined propeller and aeration operation with the annulus gas sparged airlift reactor (H_{DT} of 2.77 m), using the baker's yeast broth and superficial gas velocities (ms^{-1}) : 0.036 (□), 0.136 (■) Propeller only operation (-o-), propeller and aeration (- - - -)

propeller only operation was about 5. This value is observed for most stirred tank impellers and was double the value measured for the conventional airlift operation (section 3.1.2).

The mixing and circulation performance with propeller only operation was compared to the aeration operation with the same ungassed liquid height above the draft tube of 0.47 m from the working volume of 0.25 m^3. Yet the actual liquid gassed height for aerated systems was higher than the unaerated height with propeller only operation. The tallest possible liquid dispersion height at the gas velocity of 0.136 ms^{-1} and propeller operation at 1000 rpm was 3.82 m compared to 3.24 m for propeller only operation. Consequently, the liquid under the different operating conditions may have had different flow paths through the top section which could effect the liquid circulation and mixing time comparison. However, in section 3.1.6.3 it was shown that the circulation time was independent of top section size and so comparing aeration with propeller only operation would seem reasonable. Mixing times were found to decrease with increasing gassed liquid height above the draft tube with the aerated reactor. Therefore, the comparison of mixing time from propeller only operation to aeration may be slightly effected by the differences in liquid height.

3.3.4 The effect of propeller operation on the dissolved oxygen tensions of the aerated reactor

The improved hydrodynamic performance of the aerated vessel due to propeller operation resulted in a change in the dissolved oxygen tensions (DOTs, % air saturation) around the vessel with the baker's yeast suspension (10 gL^{-1} DCW). The mobile dissolved oxygen tension probe was used to measure the DOT around the vessel during propeller and aeration operation. However, the rotating propeller in the base of the draft tube made it impossible to measure DOT in the lower downcomer and base of the vessel. Figure 3.29 shows the DOTs measured with the mobile DOT probe using four gas velocities and subsequent propeller speeds. The DOT profiles from conventional aeration (figure 3.8b) are also plotted so a comparison to the propeller and aeration profiles could be made.

At the lowest gas velocity of 0.036 ms^{-1} (figure 3.29a) the DOTs in the riser and top section remained below 1% with increasing propeller speed. The DOTs in the downcomer increased above the aeration only profile with propeller operation. At 1000 rpm the DOT in the lower downcomer position was 65% (air saturation) compared to 15% with aeration only operation. Hence, the increases of DOT in the downcomer with propeller speed resulted in a greater proportion of the downcomer having higher DOTs as the propeller speed was increased.

The propeller had a similar effect on DOT at the 0.072 ms^{-1} gas velocity (figure 3.29b). For all propeller speeds the DOTs remained below 1% in the riser. In the middle of the downcomer the DOTs from propeller operation were similar to the aeration only

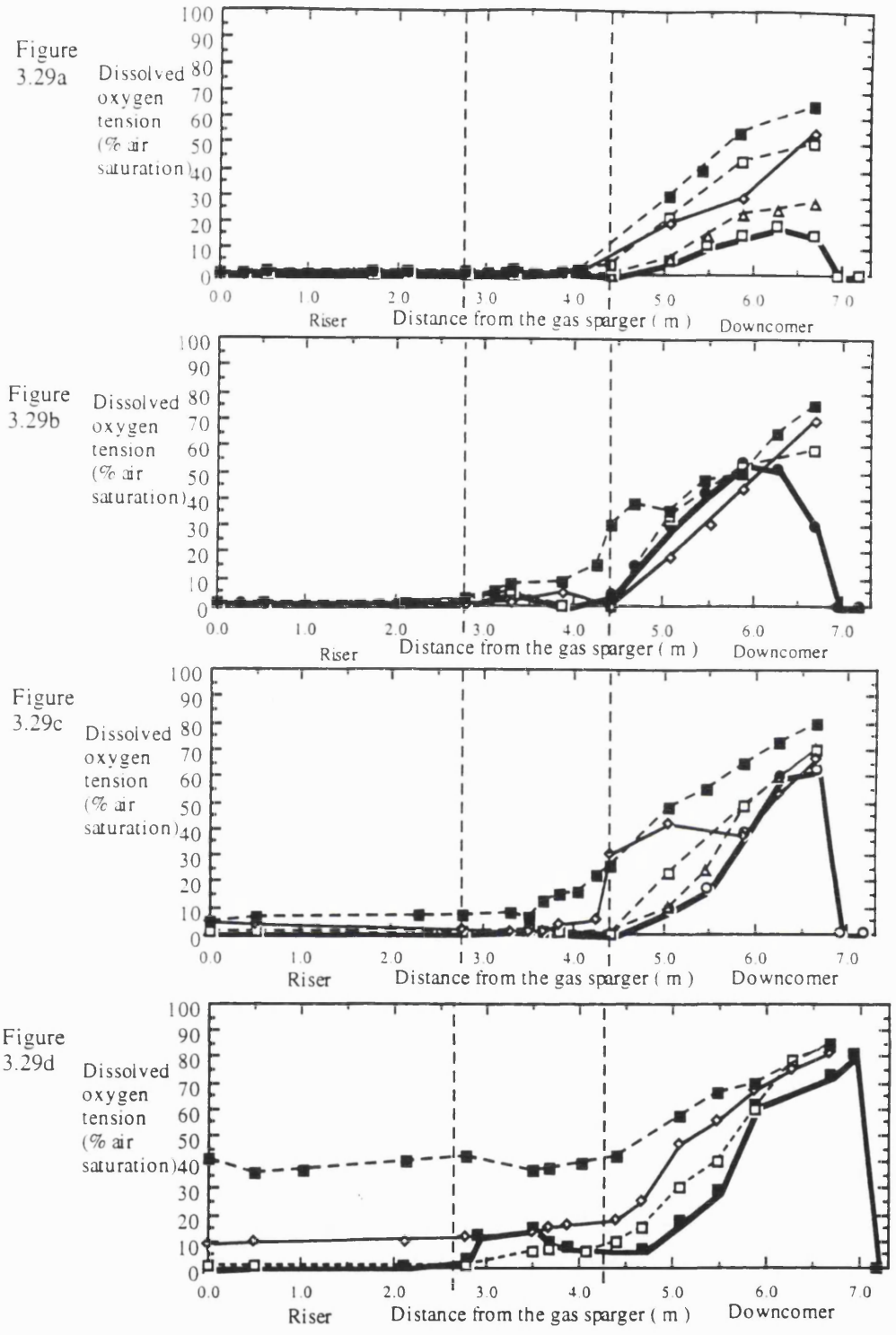

Figure 3.29 The effect of propeller speed on the dissolved oxygen tension (% air saturation) with increasing distance from the annulus gas sparger of the aerated airlift reactor (H_{DT} of 2.77 m). Using the 10 gL^{-1} DCW baker's yeast broth at superficial gas velocities (ms^{-1}) : Fig. a: 0.036 (-□-),Fig.b: 0.072 (-●-), Fig. c :0.091 (-○-), Fig. d: 0.136 (-■-), with propeller speeds (rpm): 300 (- △ -), 600 (- □ -), 900 (-◇-), 1000 (- ■ - ·)

profile however, in the lower downcomer DOTs were around 75% with propeller operation compared to 30% for aeration only operation.

At the gas velocity of 0.091ms^{-1} shown in figure 3.29c the DOTs in the riser were below 3% for all propeller speeds apart from 1000 rpm. At this speed DOTs of 6% were obtained along the riser. In the downcomer propeller speeds up to 600 rpm produced slightly higher DOTs above the aeration only profile. At 1000 rpm the DOTs in the part of the top section above the draft tube and in the downcomer were considerably higher than the aeration only values. In the upper downcomer propeller operation at 1000 rpm resulted in DOTs some five times larger than with aeration only operation. Whereas, in the lower downcomer the DOT from propeller operation was only 15% larger than with aeration only operation.

At the highest gas velocity of 0.136 ms^{-1} (figure 3.29d) the DOT in the riser, top section and downcomer increased with propeller speed. For propeller speeds below 700 rpm the DOTs in the riser were still below 1% and DOTs in the downcomer were slightly higher than aeration only values. At 900 rpm DOTs of 10% were found along the length of the riser and in the top section. This increased to a maximum value of 80% in the lower downcomer. At 1000 rpm the DOT was around 40% in the riser and top section, which increased to 81% in the lower downcomer. Therefore, at this high propeller speed the DOTs around the vessel were in excess of 30%. Hence, operating the propeller with maximum gas velocity and propeller speed produced a more homogenous DOT environment around the vessel. At this high gas velocity and propeller speed, the DOT was 81% near the base of the downcomer and 41% at the base of the riser, so it would seem reasonable to presume that the DOT of the liquid undergoing recirculation at the base of the reactor was not less than 40%.

3.3.5 The effect of the propeller on the volumetric mass transfer coefficient, k_La

As a consequence of the improved liquid circulation and gas holdup an increase in k_La values around the vessel was observed for all gas velocities. This is illustrated in figure 3.30 by the increase in k_La at the lower riser probe position as a function of propeller speed. It can be observed that the propeller had a greater influence on k_La at propeller speeds above 600 rpm at all gas velocities. Also, the propeller had a more pronounced effect on k_La at the low gas velocity (0.036 ms^{-1}) by increasing the k_La of conventional aeration by 3 fold with propeller operation at 1000 rpm compared to a 2 fold increase at the high gas velocity (0.136 ms^{-1}). The DOT values measured with the mobile DOT probe shown in figure 3.29 were used to estimate the k_La values around the vessel with propeller operation at two gas velocities (figures 3.31a & b). For the propeller at 300 rpm the k_La values were similar to the conventional aeration values around the vessel of 0.01 s^{-1} at the gas velocity of 0.036 ms^{-1} (figure 3.31a). As the propeller speed was increased to 1000 rpm k_La values around the vessel increased above

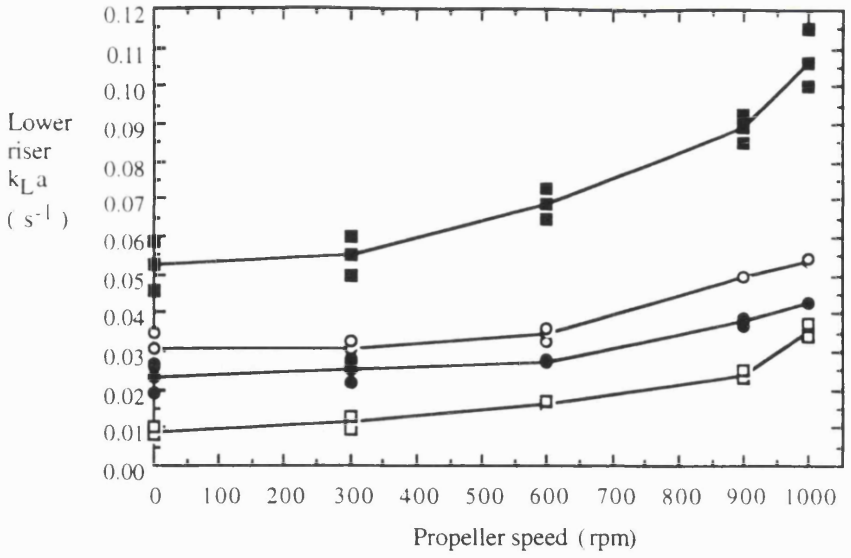

Figure 3.30 The effect of propeller speed on $k_L a$ from the lower riser position of the annulus gas sparged airlift reactor (H_{DT} of 2.77 m), using the baker's yeast broth (10 gL^{-1} DCW) and superficial gas velocities (ms^{-1}) : 0.036 (□), 0.072 (•), 0.091 (○), 0.136 (■)

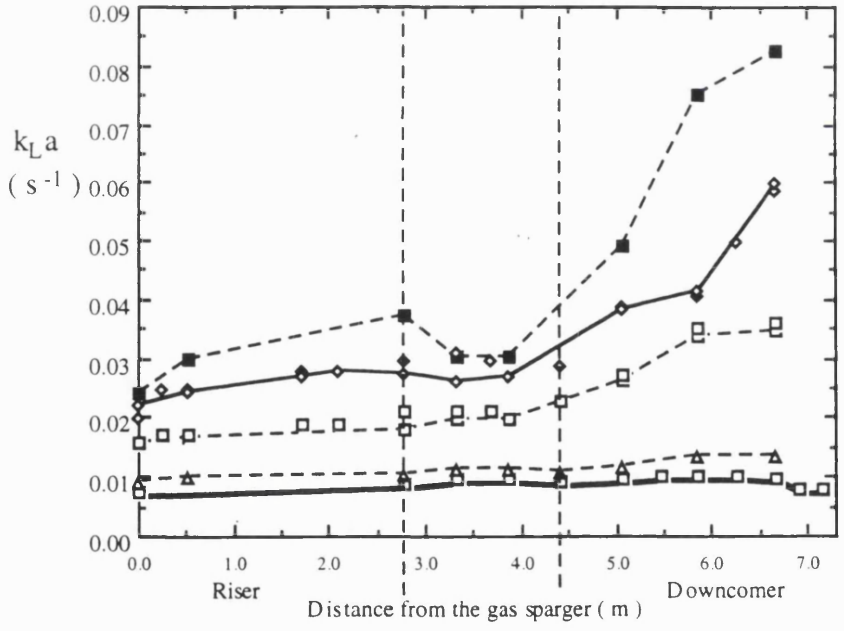

Figure 3.31a The effect of propeller speed on $k_L a$ with increasing distance from the annulus gas sparger of the aerated airlift reactor (H_{DT} of 2.77 m). Using the 10 gL^{-1} DCW baker's yeast broth at the superficial gas velocity: 0.036 ms^{-1} for aeration only operation (—□—), with propeller speeds (rpm): 300 (- △ -), 600 (- □ -), 900 (- ◇ -), 1000 (- ■ ·)

the conventional aerated values. At each propeller speed the k_La values remained constant along the riser, but in the downcomer k_La increased down the draft tube above the values for conventional aeration. At the propeller speed of 1000 rpm k_La values of 0.08 s^{-1} were reached in the lower downcomer compared to 0.01 s^{-1} for aeration only operation. The k_La profiles around the vessel with propeller speeds above 600 rpm had similar shapes to the DOT profiles shown in figure 3.29a.

Figure 3.31b shows the k_La values for the gas velocity of 0.136 ms^{-1} and propeller operation. At propeller speeds up to 600 rpm the k_La values in the riser of 0.06 s^{-1} were similar to the values for aeration only operation. In the downcomer the k_La values increased towards the base of the vessel to values of 0.35 s^{-1} in the lower downcomer compared to the aeration only value of 0.2 s^{-1}. The k_La profiles for the circulation loop around the vessel had a similar shape to the DOT profiles shown in figure 3.29d.

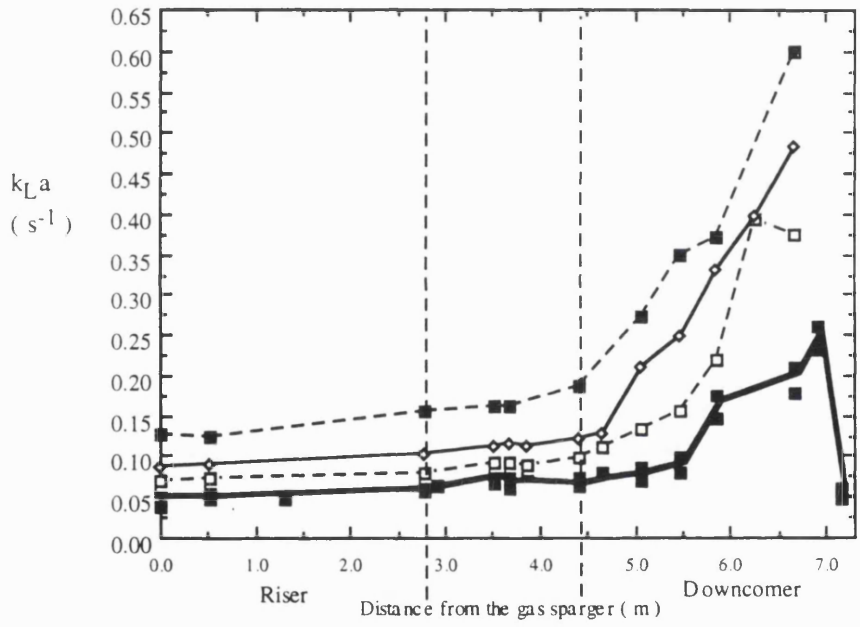

Figure 3.31b The effect of propeller speed on k_La with increasing distance from the annulus gas sparger of the aerated airlift reactor (H_{DT} of 2.77 m). Using the 10 gL^{-1} DCW baker's yeast broth at the superficial gas velocity: 0.136 ms^{-1} for aeration only operation (—□—), with propeller speeds (rpm): 300 (- △ -), 600 (- □ -), 900 (- ◇ -), 1000 (- ■ -)

At propeller speeds above 600 rpm the high DOTs in the lower downcomer of around 80% resulted in k_La values between 0.4 - 0.6 s^{-1}. These k_La values were extremely high when compared to conventional stirred tank values of 0.3 s^{-1} obtained in a 1 m^3 stirred tank during a fed batch *E. coli* fermentation of 20 gL^{-1} dry cell weight (Hobbs, 1994). As k_La was estimated using the equation shown below then, high DOT values resulted in the concentration driving force for oxygen transfer being very small.

$$k_L a = \frac{\text{oxygen transfer rate}}{C^*(x) - C_L(x)}$$

The dissolved oxygen concentrations were estimated values as described in section 2.7. Small differences in the driving force values would produce larger differences in $k_L a$ values. Therefore, errors in the estimation of the small driving forces would lead to large differences in $k_L a$ values. This demonstrates disadvantages of using this method in that high DOT values may lead to inaccuracies and erroneous $k_L a$ values. Hence, the $k_L a$ values estimated when the DOT was small resulted in a large driving force which produced more reliable results. However, the high $k_L a$ values above 0.3 s^{-1} only occurred in the lower downcomer position with the highest gas velocity of 0.136 ms^{-1}. The $k_L a$ values at all other gas velocities and propeller speeds were considered to be reliable.

3.3.6 The effect of the propeller operation on the oxygen uptake rate of the aerated baker's yeast suspension

The increase in gas holdup, $k_L a$ and change in DOT profile with propeller operation resulted in an increase in the oxygen uptake rate (OUR) of the baker's yeast broth (10 gL^{-1} DCW) in the aerated airlift reactor (figure 3.32). Propeller speeds above 300 rpm produced a more pronounced effect on the OUR of the broth for all gas velocities. The propeller had a greater influence on the OUR with gas velocities up to 0.054 ms^{-1}. At the gas velocity of 0.036 ms^{-1} a three fold increase in the OUR was observed from the aeration only value of 10 $mmol.L^{-1}.h^{-1}$ to a value of 30 $mmol.L^{-1}.h^{-1}$ at the propeller speed of 1000 rpm.

At the gas velocity of 0.136 ms^{-1} (1.432 vvm) an OUR of 44 $mmol.L^{-1}.h^{-1}$ was obtained with propeller operation at 600 rpm where the lowest (measurable) DOT around the vessel was 3% (figure 3.29d). When the propeller speed was increased to 900 rpm the lowest DOT increased to 10% and the OUR was 52 $mmol.L^{-1}.h^{-1}$. The same OUR was observed at 1000 rpm with DOTs above 30% (figure 3.29d). So 52 $mmol.L^{-1}.h^{-1}$ was the maximum OUR achievable with this reactor configuration and 10 gL^{-1} DCW yeast suspension which was obtained when the lowest (measurable) DOT around the vessel was up to 10%. The fact that the OUR did not increase between 900 and 1000 rpm was further evidence that the unmeasurable DOTs in the region of the propeller at the base of the vessel were around 10% at 900 rpm or 40% at 1000 rpm. Therefore, it has been shown that once the DOT around the whole of the vessel was up to 10% then no further increase in OUR was observed. At low gas velocities (0.036 ms^{-1}) the OUR increased from 10 $mmol.L^{-1}.h^{-1}$ to 30 $mmol.L^{-1}.h^{-1}$ at 1000 rpm and never reached a constant value. Hence, the lowest DOTs never increased to 10% air saturation in the riser

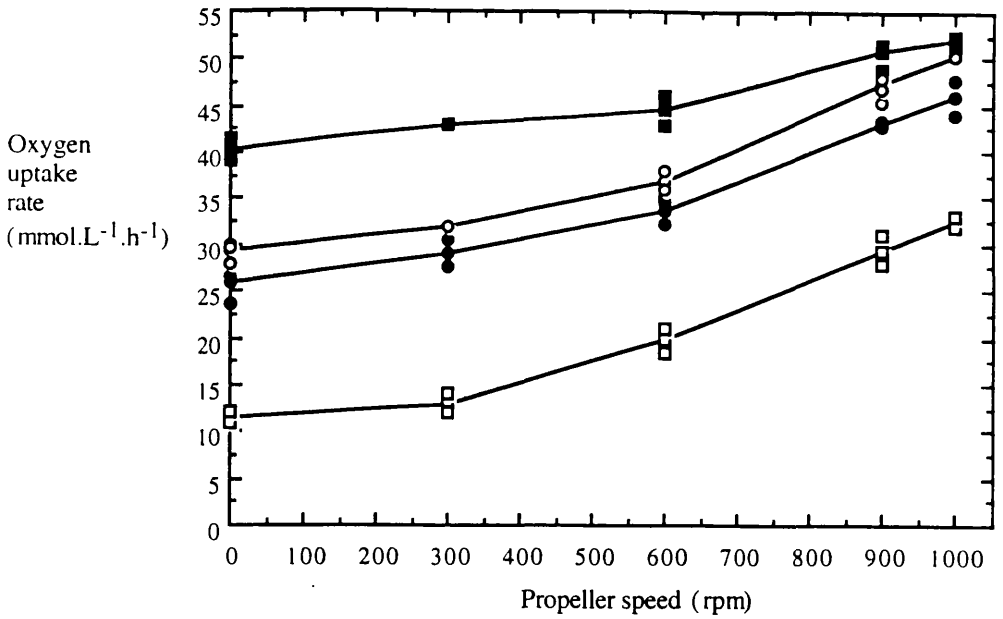

Figure 3.32 The effect of propeller speed on the oxygen uptake rate of the baker's yeast suspension (10 gL^{-1} DCW) in the annulus gas sparged airlift reactor (H_{DT} of 2.77 m), at superficial gas velocities (ms^{-1}) : 0.036 (□), 0.072 (●), 0.091(o), 0.136 (■)

at all propeller speeds. So, the oxygen transfer increases with propeller operation using gas velocities below 0.072 ms^{-1} were insufficient to increase the DOT in the riser above the near zero values. Hence, the presence of DOTs below 2% in the riser at all propeller speeds but increasing values in the downcomer resulted in the OUR increasing with propeller speed and never reaching a constant value. Therefore, the action of the propeller to reduce DOT heterogeneity and increase the OUR of the yeast broth above the aerated system demonstrated that the DOT heterogeneity of the conventionally aerated vessel had a detrimental effect on the OUR of the yeast broth.

3.3.7 The effect of propeller operation on the hydrodynamic and oxygen transfer performance of the aerated vessel with respect to total energy dissipation rate

The effect of total energy dissipation rate (P_{VT}) on the hydrodynamic and oxygen transfer performance between the conventionally aerated and combined aerated and propeller operated reactor was studied for two gas velocities (figure 3.33). The total energy dissipation rate (section 2.8) consisted of the energy dissipation rate from aeration and propeller operation at the corresponding speed. Hence, the first data point for all curves in figure 3.33 referred to the energy dissipation rate from conventional aeration (P_{VA}) and subsequent data were for total energy dissipation rate from combined aeration and propeller operation (P_{VT}) at increasing propeller speed.

For both gas velocities a small increase in P_{VT} (corresponding to propeller speed increases to 600 rpm) produced a more pronounced influence on the overall and riser gas holdup (figure 3.33a). For the low gas velocity (0.036 ms^{-1}) the highest P_{VT} 590 Wm^{-3}

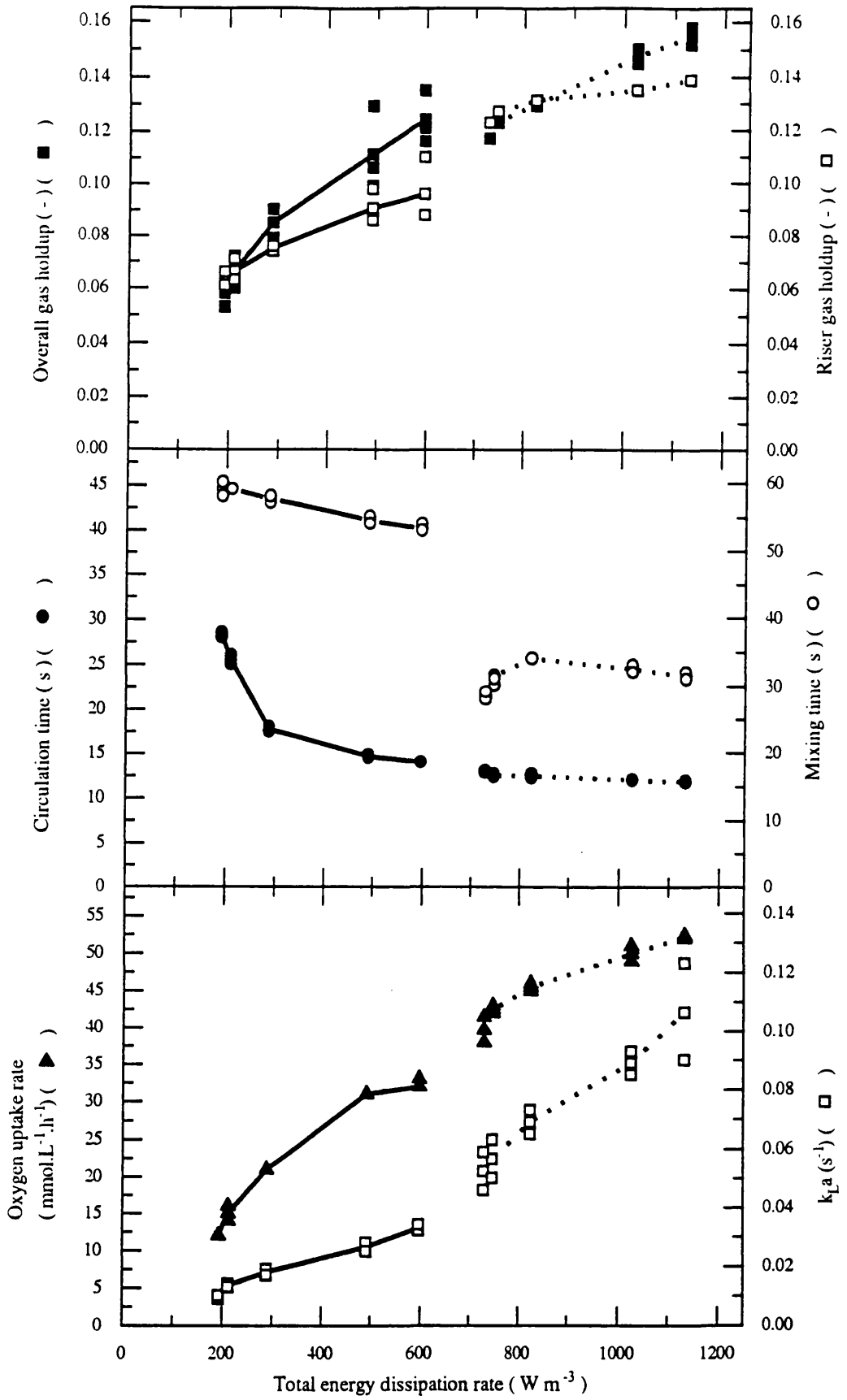

Figure 3.33 The effect of total energy dissipation rate on the hydrodynamic and oxygen transfer performance of the combined aerated and propeller operated airlift reactor (H_{DT} of 2.77 m, 10 gL^{-1} dry cell weight baker's yeast suspension) with superficial gas velocities(ms^{-1}) 0.036 (——), 0.136(- - -)

corresponding to aeration and propeller operation at 1000 rpm produced an increase of the overall gas holdup by 57% when compared to conventional aeration at the P_{VT} of 198 Wm^{-3}. This compared to a 30% increase in riser gas holdup over the same energy dissipation rate increase. The increase of gas holdup from P_{VT} increases with the gas velocity of 0.136 ms^{-1} (710 - 1120 Wm^{-3}) were not as significant as those observed at the gas velocity of 0.036 ms^{-1}.

An increase of P_{VT} from 198 - 290 Wm^{-3} produced a rapid reduction of the liquid circulation time from 28 - 17.4 seconds with the low gas velocity (figure 3.33b). For energy dissipation rates above 290 Wm^{-3} the circulation time decreased at a slower rate reaching a value of 14 seconds at the P_{VT} of 590 Wm^{-3}. At the gas velocity of 0.136 ms^{-1}, the P_{VT} increase from 710 - 1120 Wm^{-3} only produced a small reduction in circulation time from 13 to 11.9 seconds.

For the gas velocity of 0.036 ms^{-1} the mixing time decreased from 58 to 53 seconds with the P_{VT} increase from 198 to 590 Wm^{-3} (figure 3.33b). However, at the higher gas velocity of 0.136 ms^{-1} increases of P_{VT} from 710 to 810 Wm^{-3} produced no beneficial improvement of the mixing performance of the vessel. This demonstrated that the P_{VT} from aeration dominated the mixing performance of the airlift reactor as shown in section 3.3.2.

For the k_La (lower riser) P_{VT} from 198 to 590 Wm^{-3} produced a three fold increase in k_La from 0.008 to 0.03 s^{-1} with the low gas velocity. Whereas, a two fold increase in k_La from 0.055 to 0.11 s^{-1} occurred with the P_{VT} increase from 710 to 1120 Wm^{-3} with the high gas velocity (figure 3.33c). Also, the rate of increase of k_La with increasing energy dissipation rates with the 0.136 ms^{-1} gas velocity was greater than that observed with the low gas velocity of 0.036 ms^{-1}.

As observed for gas holdup the OUR increased at the fastest rate with increases of energy dissipation rate corresponding to propeller speeds up to 600 rpm for both gas velocities (figure 3.33c). For the low gas velocity (0.036 ms^{-1}) P_{VT} range from 198 to 590 Wm^{-3} produced a 300% increase in the OUR compared to the high gas velocity where the power input range of 710 to 1120 Wm^{-3} produced a 24% increase in OUR.

Finally it can be observed from figure 3.33 that with the low gas velocity and propeller speed at 1000 rpm the P_{VT} was 590 Wm^{-3} which was similar to the P_{VT} of the high gas velocity with no propeller operation of 710 Wm^{-3}. Hence, it was interesting to note that these similar energy dissipation rates resulted in similar values of gas holdup and liquid circulation time although the engineering environment and the operating conditions were quite different. However, these similar values of P_{VT} did not produce similar mixing performance. The mixing time with the 0.036 ms^{-1} gas velocity and 1000 rpm propeller operation was 52 seconds compared to 30 seconds for the 0.136 ms^{-1} gas velocity. This provided further evidence that the mixing performance of the vessel was dominated by aeration as shown in section 3.3.2.

3.3.8 Description of the flow regime with propeller and aeration operation

Water was used to visualise the effect of the propeller on the flow regime of aerated reactor using the individual side vessel sight glasses as described in section 3.1.5. As the marine propeller was used in conjunction with the annulus sparger then the side vessel sight glasses showed the bubble regime in the riser.

The propeller only operation (no aeration) with water was found to produce a vortex down from the surface of the liquid, as viewed from the top plate sight glass. This was due to the action of the propeller drawing the liquid down the draft tube. As the propeller speed was increased the vortex increased in length down the centre of the top section. At 1000 rpm the vortex reached a depth of 0.4 m from the liquid surface.

At low gas velocities (0.018 to 0.036 ms^{-1}) and propeller speeds below 600 rpm the bubbles passed the lower and middle sight glasses at a greater speed than with normal aeration. The bubbles moved in a direct upward movement compared to the more swirl like movement with aeration only operation as described in section 3.1.5. The bubble sizes observed in the lower and middle sight glasses were similar to those observed with normal aeration. Hence, a large population of spherical 2 mm diameter bubbles were observed amongst some larger 5 mm slug shaped bubbles. For this aeration and propeller operation no vortex occurred in the liquid surface as observed from the top plate sight glass. However, the liquid surface with propeller operation at 300 rpm was considerably more turbulent than that observed with aeration only operation. The turbulent liquid surface with the gas velocity of 0.036 ms^{-1} and propeller speed at 600 rpm, was similar to the liquid turbulence observed with aeration only operation with a gas velocity above 0.072 ms^{-1}. At propeller speeds above 600 rpm the bubbles moved past the sight glass at high speeds and the bubble population changed to a more varied population of sizes. Middle sized bubbles of 5 - 7 mm in diameter were most abundant but some large 7 - 9 mm diameter slug shaped bubbles and 0.5 - 2 mm diameter bubbles were observed passing the lower and middle sight glasses. These bubbles passed the lower sight glass in a swirling upward motion. The direction of the swirling was in the direction of propeller rotation from the lower downcomer. The swirling motion was less distinct at the middle sight glass where bubbles rose in a more upward direction. At the higher speeds (900 rpm) the liquid surface was more turbulent than at propeller speeds below 600 rpm.

At high gas velocities between 0.091- 0.136 ms^{-1} and propeller speeds below 600 rpm a large number of bubbles observed at the lower sight glass were between 5 - 8 mm in diameter, with some smaller 0.5 - 2 mm bubbles. This was similar to normal aeration operation. A small population of large slug shaped bubbles of 8 - 12 mm in diameter were also observed. However, these bubbles were smaller than the slug shaped bubbles of 10 - 20 mm in diameter observed during normal aeration. As the propeller speed was increased above 600 rpm the large slug shaped bubbles seemed to decrease in size and the

bubbles moved with the side ways swirly upward motion from the direction of propeller rotation. However, the bubbles travelled passed the sight glass at high speed which made it difficult to clarify the actual bubble size changes. This also made it impossible to determine whether more gas was present in the riser, due to the increase in gas holdup observed above 600 rpm. The liquid surface with the gas velocity of 0.136 ms^{-1} and propeller speed at 1000 rpm was more turbulent than with conventional aeration only operation.

3.3.9 The effect of top section size on the combined aerated and propeller operated vessel

The influence of propeller operation on the hydrodynamic and oxygen transfer performance of the aerated vessel was studied with two top section configurations using the ungassed liquid heights of 0.0 m and 0.47 m above the draft tube. Vessel performance at the unaerated liquid height of 0.47 m above the draft tube was previously described (section 3.3.1- 8) and will be compared to studies carried out using the lower ungassed liquid height.

For the smaller top section, the increase of overall and riser gas holdup with propeller speed was similar to that observed with the larger top section (figure 3.24). Similar rates of increase of overall and riser gas holdup with propeller speed were observed for both top section sizes. Also, similar liquid circulation times were produced at both top section configurations with propeller and aeration operation (figure 3.34).

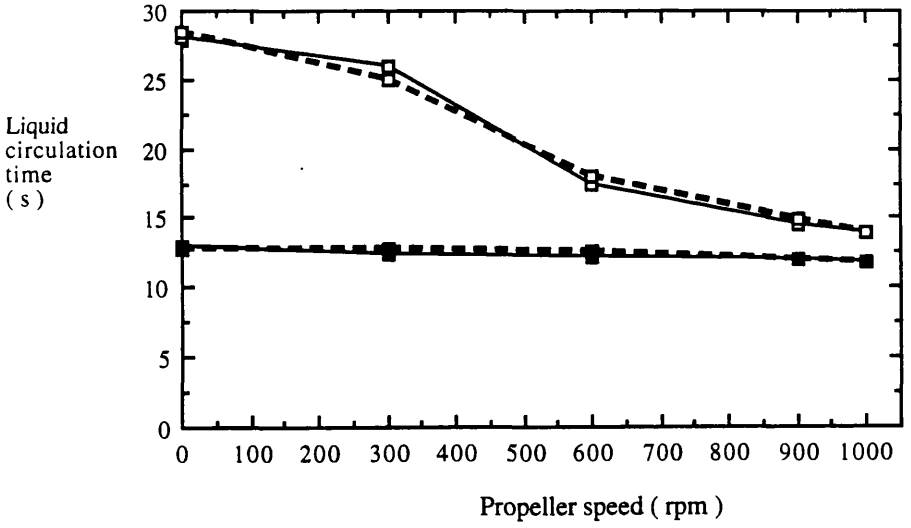

Figure 3.34 Comparison of the effect of propeller speed on the liquid circulation time between two top section sizes of the annulus gas sparged airlift reactor (H_{DT} of 2.77 m), using the baker's yeast broth at superficial gas velocities (ms^{-1}): 0.036 (□), 0.136 (■). and working volume of 0.213 m^3 : ungassed liquid height of 0.0 m above the draft tube (▪ ▪ ▪),and 0.25 m^3 :ungassed liquid height of 0.47 m above the draft tube (——).

The mixing times obtained with aeration only operation did not significantly change with propeller operation as observed at the larger top section (figure 3.35). However, the mixing times with the smaller top section were longer than with the taller top section. For example, at the gas velocity of 0.036 ms^{-1} and propeller operation the small top section produced mixing times in the region of 85 seconds, compared to 58 seconds with the larger top section. Therefore, the reactor had a better mixing performance when the larger top section was used. The decrease in mixing time with increasing ungassed liquid height above the draft tube was observed for conventional aeration (section 3.1.6.). This similar effect observed with combined aeration and propeller operation was further evidence that aeration dominated the mixing performance of the aeration and propeller operated vessel.

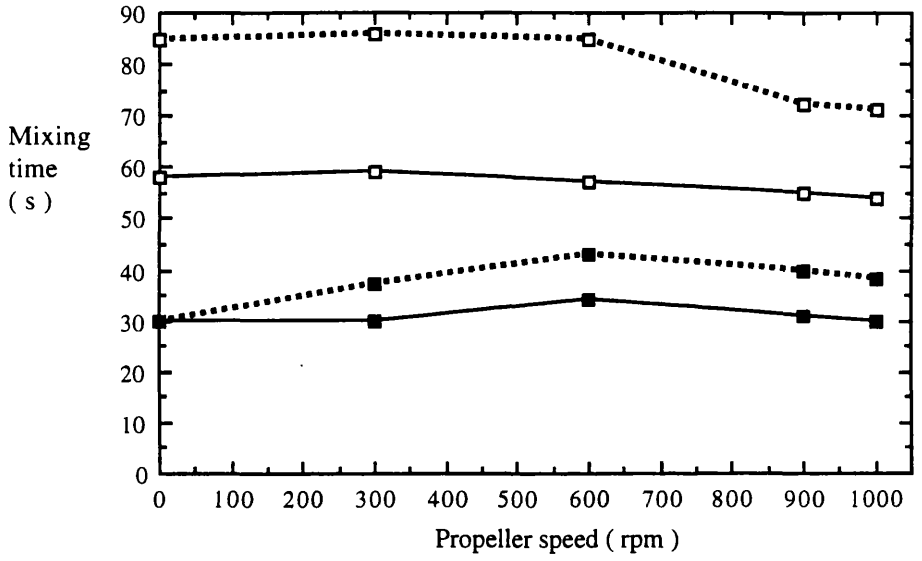

Figure 3.35 Comparison of the effect of propeller speed on the mixing time between two top section sizes of the annulus gas sparged airlift reactor (H_{DT} of 2.77 m), using the baker's yeast broth at superficial gas velocities (ms^{-1}): 0.036 (□), 0.136 (■). and working volume of 0.213 m^3 : ungassed liquid height of 0.0 m above the draft tube (▪▪▪),and working volume of 0.25 m^3 :ungassed liquid height of 0.47 m above the draft tube (——).

The mobile dissolved oxygen probe was used to compare the dissolved oxygen tensions (DOTs) around the vessel for the two top section configurations. Propeller operation at the smaller top section produced similar trends of DOT around the vessel as observed with the larger top section at all gas velocities. This is illustrated in figure 3.36 which compared the DOTs of the vessel for both top section sizes, with aeration only operation at the gas velocity of 0.136 ms^{-1}, and with aeration and propeller operation at 900 rpm. The aeration only DOT profiles were similar for the two configurations apart from the increase of DOT from 25 to 60% in the downcomer for the short top section

which occurred at a distance from the gas sparger of 5.79 m to 6.0 m whereas, the DOT increase occurred at a distance of 5.4 to 5.6 m away from the sparger with the larger top section. Comparison of the DOT profiles with aeration and propeller operation at 900 rpm showed that the DOT increased above the aeration only values with a similar trend around the vessel with both top sections. However, for the smaller top section (unaerated height of 0.0 m above the draft tube) propeller operation at 900 rpm resulted in DOTs of 25% (air saturation) in the riser and top section compared to DOTs of 10% with the larger top section. Nevertheless, the DOT of 80% was reached in the lower downcomer position for both top section configurations.

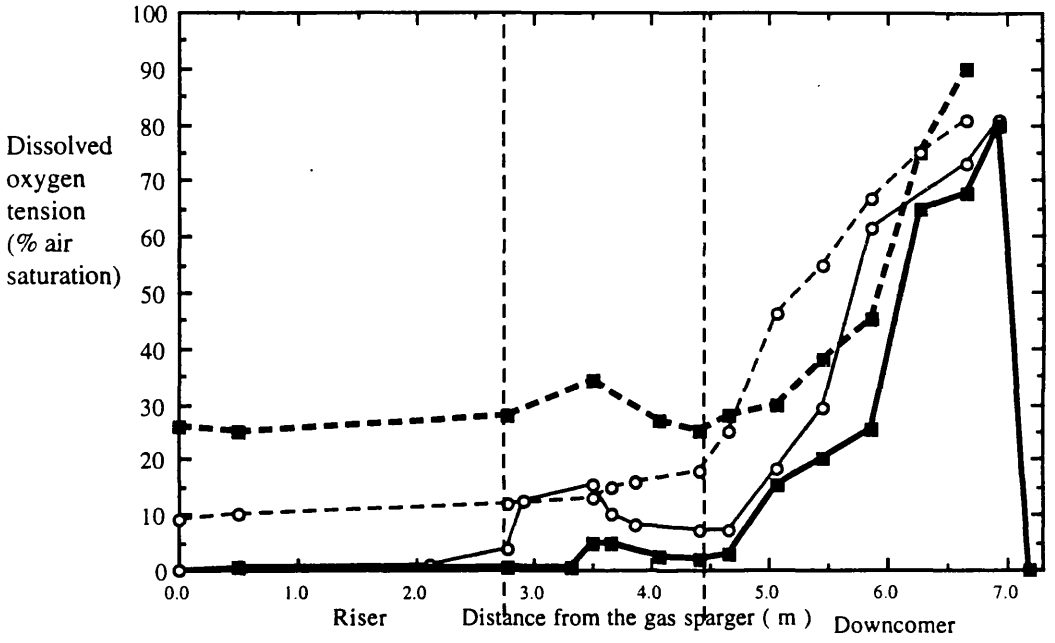

Figure 3.36 Comparison of the effect of the propeller on the dissolved oxygen tensions between two top section sizes of the annulus gas sparged airlift reactor (H_{DT} of 2.77 m), using the baker's yeast broth(10 gL^{-1} DCW) at the superficial gas velocity of 0.136 ms^{-1} with the ungassed liquid height of 0.0 m above the draft tube : aeration only operation (—■—), aeration and propeller operation at 900 rpm (- -■- -),and the ungassed liquid height of 0.47 m above the draft tube: aeration only (- -o- -),aeration and propeller at 900rpm (- -o- -).

In both top section sizes, the k_La values around the vessel increased with propeller speed and all gas velocities. The effect of the propeller on k_La values from the lower riser probe position is illustrated using two gas velocities in figure 3.37. No significant difference was observed in k_La values with the low gas velocity and propeller operation from the two top sections. However, with the gas velocity of 0.136 ms^{-1} propeller speeds up to 600 rpm produced k_La values with the small top section which were up to 30% greater than the values obtained with the large top section. At propeller speeds

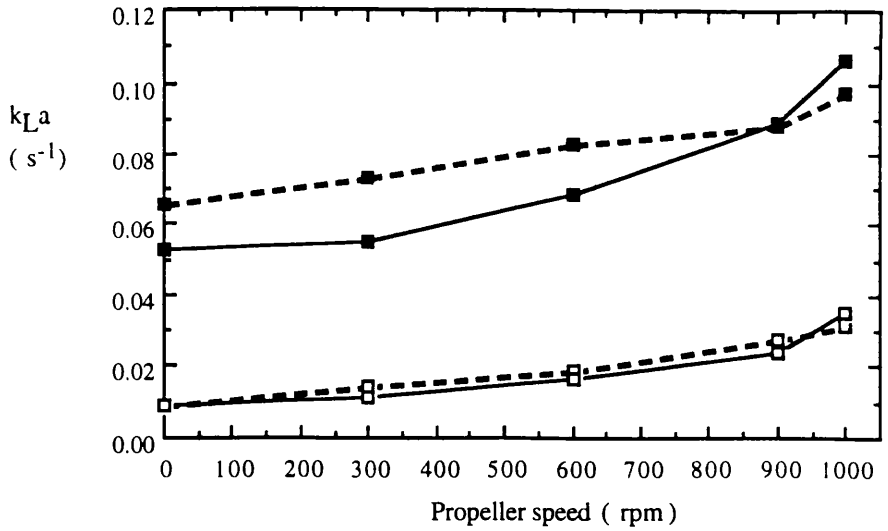

Figure 3.37 Comparison of the effect of propeller speed on the k_La (lower riser) between two top section sizes of the annulus gas sparged airlift reactor (H_{DT} of 2.77 m), using the baker's yeast broth at superficial gas velocities (ms^{-1}): 0.036 (□), 0.136 (■). and working volume of 0.213 m^3 : ungassed liquid height of 0.0 m above the draft tube (▪▪▪), and 0.25 m^3 :ungassed liquid height of 0.47 m above the draft tube (——).

above 800 rpm the k_La values for both top sections were reasonably similar with values of 0.09 to 0.1 s^{-1} at 1000 rpm.

Therefore, in general the effect of the propeller on the hydrodynamic and oxygen transfer performance of the aerated vessel was similar at both top section sizes, which resulted in similar OUR values for all operating conditons. This did not seem surprising as the total energy dissipation rate (Wm^{-3}) for aeration and propeller operation using the reactor with the small top section was not more than 10% greater than with the larger top section. Also, the similarities occurred despite the poorer mixing performance of the reactor with the shorter top section.

3.3.10 The effect of the propeller on the hydrodynamics and oxygen transfer of the aerated vessel with the 5 gL^{-1} dry cell weight baker's yeast suspension

The dissolved oxygen tension (DOT) in the riser could only be increased above 5% (air saturation) with high propeller speeds (above 800 rpm) and high gas velocities (above 0.072 ms^{-1}) with the 10 gL^{-1} DCW baker's yeast suspension. Therefore, the effect of the propeller was studied at a lower biomass concentration of 5 gL^{-1} DCW where the dissolved oxygen tensions (DOTs) around the vessel should be higher than with the 10 gL^{-1} DCW biomass concentration due to the lower oxygen demand. The likely presence of higher DOTs in the riser should enable the increase in DOT by the action of the propeller to be more readily observed. This may allow further elucidation of the mechanism by which the propeller increased the DOTs around the vessel. Using the 5 gL^{-1} DCW suspension also allowed the DOT profiles of the conventionally aerated reactor to be compared with the 10 gL^{-1} DCW biomass concentration. Hence, the investigations were performed with the working volume of 0.25 m^3 and with the draft tube height of 2.77 m.

At all operating conditions with aeration and propeller operation the gas holdups, liquid circulation and mixing times with the 5 gL^{-1} DCW broth were found to be similar to the 10 gL^{-1} DCW concentration at all operating conditions (results not shown). Also, the effect of the propeller on the DOTs and oxygen uptake rates (OUR) was found to be similar between the two biomass concentrations except that the actual values were different due to the biomass concentration.

3.3.10.1 The effect of the propeller on the dissolved oxygen tensions of the aerated vessel

The dissolved oxygen tension profiles for the vessel were measured with the mobile DOT probe at four superficial gas velocities for the 5 gL^{-1} DCW yeast suspension (figure 3.38). At the low gas velocity of 0.036 ms^{-1} (figure 3.38a) the DOTs remained below 2% in the riser and top section for both the aeration only and combined aeration and propeller operated systems, which was similar to the 10 gL^{-1} DCW yeast broth (figure 3.29a). The DOT in the downcomer for aeration only operation increased to a maximum peak value of 30% half way down draft tube compared to 15% with the 10 gL^{-1} DCW broth. Hence, the DOTs for the 5 gL^{-1} DCW broth were only greater than the 10 gL^{-1} DCW broth in the downcomer. Propeller speeds above 300 rpm significantly increased the DOTs in the downcomer above the aeration only values which was similar to the effect observed with the 10 gL^{-1} DCW broth except that the values were higher.

At the gas velocity of 0.072 ms^{-1}, the riser DOT remained below 1% with aeration only for both broth concentrations (figure 3.29b & 3.38b). In the downcomer the DOT increased to a peak value of 62% in the middle downcomer position which was greater than the 52% measured with the 10 gL^{-1} DCW broth. For propeller operation at 600 rpm

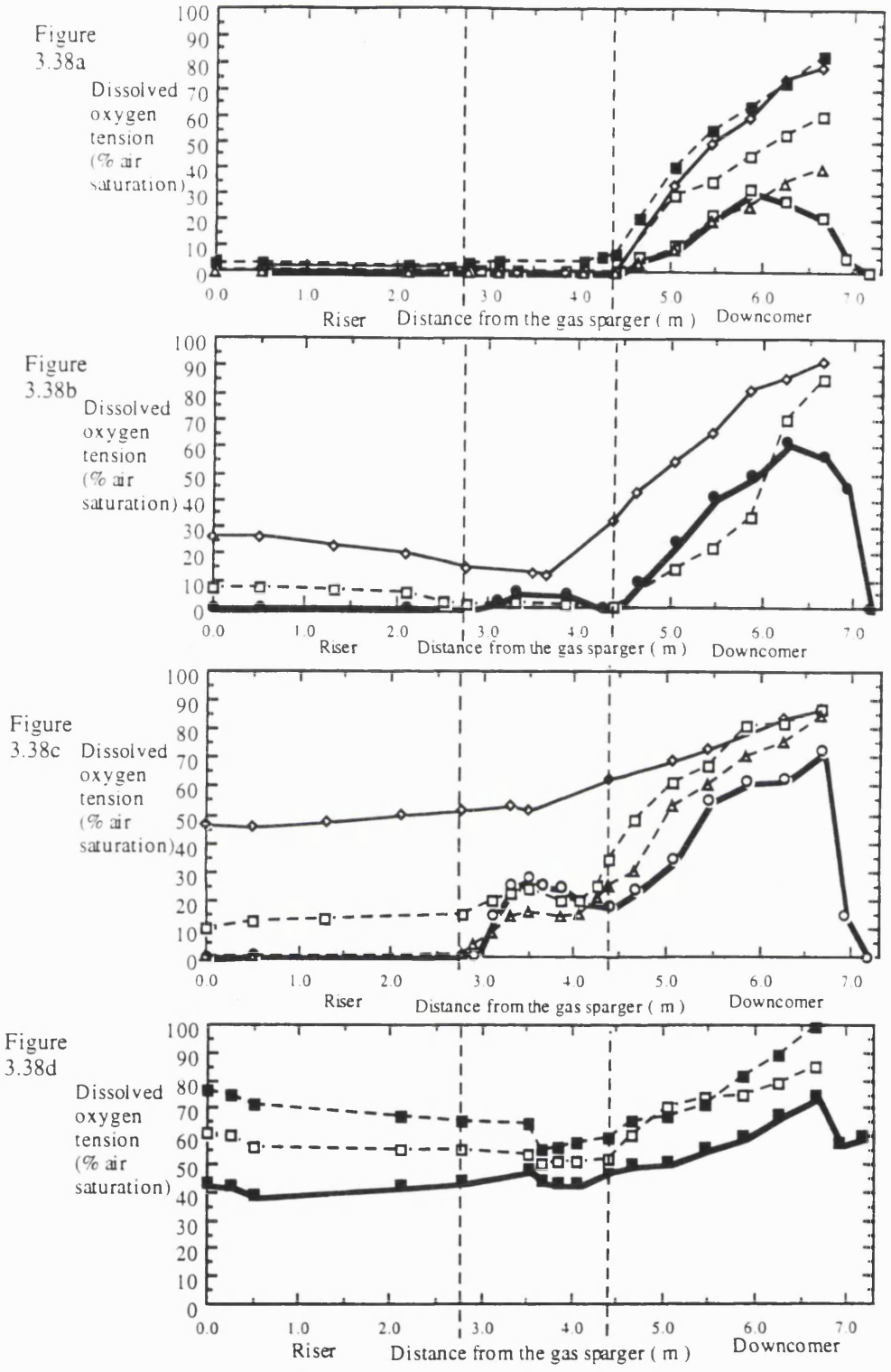

Figure 3.38 The effect of propeller speed on the dissolved oxygen tension (% air saturation) with increasing distance from the annulus gas sparger of the aerated airlift reactor (H_{DT} of 2.77 m). Using the 5 gL^{-1} DCW baker's yeast broth at superficial gas velocities (ms^{-1}) : Fig. a: 0.036 (—□—), Fig.b: 0.072 (—●—), Fig. c :0.091 (—○—), Fig. d: 0.136 (—■—), with propeller speeds (rpm): 300 (- △ -), 600 (- □ -), 900 (—◇—), 1000 (- ■ - ·)

the DOT in the riser was maintained above 5%, and at 900 rpm was above 10%. In the downcomer the propeller produced a similar effect on the DOT as with the 10 gL^{-1} broth except that the values were greater with the 5 gL^{-1} DCW broth. Therefore, with the 5 gL^{-1} DCW broth the DOT was increased above 5% around the vessel with a gas velocity of 0.072 ms^{-1} and propeller speed of 600 rpm compared to the higher gas velocity of 0.136 ms^{-1} and 900 rpm required with the 10 gL^{-1} DCW broth.

DOTs in the riser with aeration only operation using the 0.091 ms^{-1} gas velocity (figure 3.38c) still remained below 1% as with the 10 gL^{-1} DCW broth (figure 3.29c). However, the DOTs in the top section were above 5% and the DOT increased from 20% at the top of the downcomer to 73% in the lower downcomer. This was followed by the decrease of DOT to zero at the base of the vessel. Hence, these values were greater than those measured with the 10 gL^{-1} DCW broth. Propeller operation at 600 rpm was sufficient to increase the DOTs above 8% in the riser with values greater than 10% in the top section and, DOTs in the downcomer were significantly greater than the aeration only values. At 900 rpm the DOTs around the vessel were in excess of 40% whereas the DOTs were below 10% in the riser with the 10 gL^{-1} DCW broth.

At the maximum achievable gas velocity (0.136 ms^{-1}) the DOT was in excess of 35% around the vessel (figure 3.38d) which was similar to the DOT profile at the lower gas velocity (0.091 ms^{-1}) and propeller operation at 900 rpm. It is interesting to note that even at the high gas velocity the DOT still decreased at the base of the vessel from 75% in the lower downcomer to 57% at the base of the downcomer. Also, the lower downcomer DOTs values were similar to the 10 gL^{-1} DCW broth profile (figure 3.29d) although the values were lower at all other positions with DOT below 1% in the riser with the 10 gL^{-1} DCW suspension. Propeller operation resulted in an increase of DOT above the aeration only profile. This resulted in a difference of DOT of 71% at 1000 rpm in the lower riser compared to 56% with 600 rpm and 39% for aeration only operation. In the top part of the top section above the downcomer the differences between the DOTs with the different operating conditions were at there smallest with only a 10% difference in DOT.

These DOT profiles for aeration and propeller operation with the 5 gL^{-1} DCW broth were significantly different to the DOT heterogeneity observed with the 10 gL^{-1} broth concentration as shown in figure 3.39. The DOT profile with aeration only operation at 0.136 ms^{-1} for the 5 gL^{-1} broth was similar to the DOT profile achieved from aeration and propeller operation at 1000 rpm with the 10 gL^{-1} DCW broth. Also, the DOT profile for 1000 rpm with the 5 gL^{-1} broth had a similar shape to the DOT profile measured at the same operating conditions with the 10 gL^{-1} broth. However, the DOTs for the 5 gL^{-1} broth were some 30% greater in the riser and 10% larger in the downcomer when compared to the profile from the 10 gL^{-1} broth concentration.

Therefore, it has been shown that even with the 5 gL^{-1} DCW broth DOT values below 2% existed in the riser at gas velocities below 0.113 ms^{-1} and propeller speeds

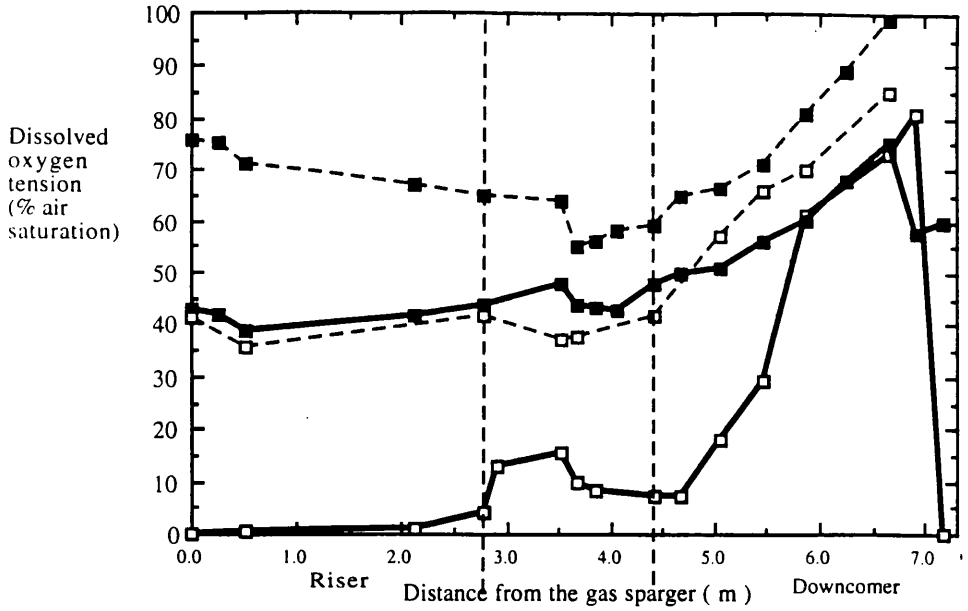

Figure 3.39 Comparison of the effect of propeller speed on the dissolved oxygen tension (% air saturation) with increasing distance from the annulus gas sparger of the aerated airlift reactor (H_{DT} of 2.77 m) between the 5 and 10 gL^{-1} DCW baker's yeast broth at the superficial gas velocity of 0.136 ms^{-1},: 5 gL^{-1} DCW (■),10 gL^{-1} DCW (□),aeration only operation (——),aeration and propeller operation (- - -)

below 600 rpm. However, the reactor with the 5 gL^{-1} broth had higher DOT values the downcomer than with the 10 gL^{-1} DCW broth with both operating regimes. Also, propeller operation increased the DOTs above 1% with the lower gas velocity of 0.072 ms^{-1} with the 5 gL^{-1} DCW broth compared to 0.091 ms^{-1} required with the 10 gL^{-1} DCW broth. It is also interesting to note that even with the 5 gL^{-1} DCW broth the propeller increased the DOT in the riser above the aerated only values but did not increase the DOT along the length of the riser. The DOT profiles at each gas velocity and propeller speed showed that the DOT remained relatively constant along the riser section of the vessel.

3.3.10.2 The effect of the propeller on the volumetric oxygen mass transfer coefficient, k_La

For most gas velocities the increasing propeller speed produced similar increases in k_La values with both biomass concentrations shown in figure 3.40 for lower riser k_La values. However, at the lowest gas velocity (0.036 ms^{-1}) k_La values with the 10 gL^{-1} broth were between 3 and 4 times greater than with the 5 gL^{-1} broth.

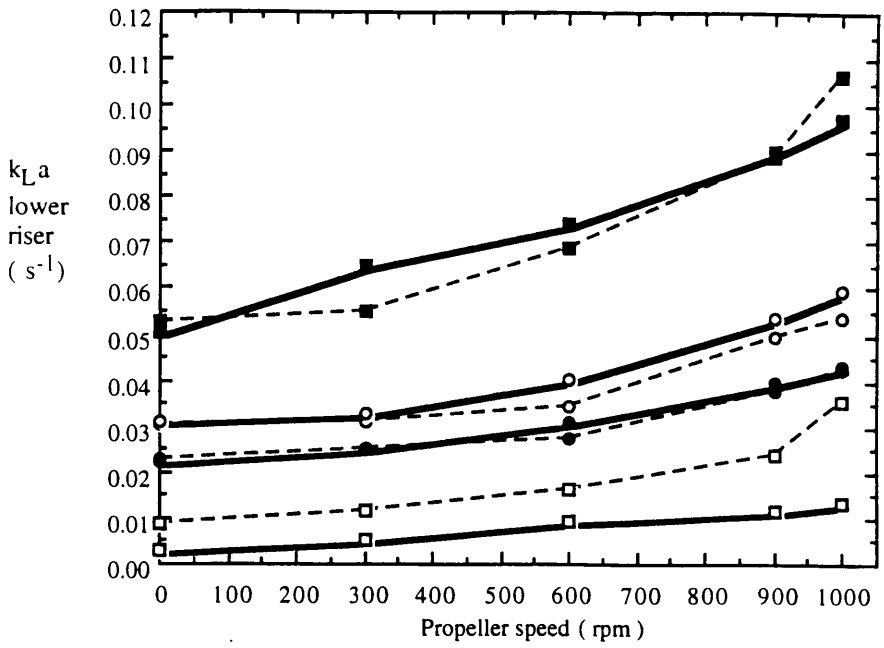

Figure 3.40 Comparison of the effect of propeller speed on k_La (lower riser) between the 5 and 10 gL^{-1} DCW baker's yeast broth with the annulus gas sparged airlift reactor (H_{DT} of 2.77 m) at superficial gas velocities (ms^{-1}) : 0.036 (□), 0.072 (●), 0.0.91 (○), 0.136 (■). 5 gL^{-1} DCW (——), 10 gL^{-1} DCW (- - -)

3.3.10.3 The effect of the propeller on the oxygen uptake rate of the yeast broth

The oxygen uptake rates (OUR) for the 5 gL^{-1} DCW broth were lower at all gas velocities than with the 10 gL^{-1} broth due to the lower biomass concentration (figure 3.41). Also, the propeller increased the OUR of the yeast broth at similar rates to those observed for the 10 gL^{-1} DCW broth. For example, figure 3.41 shows that at the gas velocity of 0.036 ms^{-1} the OUR increased with propeller speed at a similar rate with both biomass concentrations, except that the values for the 10 gL^{-1} DCW broth were double the values of the 5 gL^{-1} broth due to the difference of biomass concentration.

However, at the highest gas velocity of 0.136 ms^{-1} the OUR of the 5 gL^{-1} DCW broth did not increase with propeller speed but remained at a value of 23 $mmol.L^{-1}.h^{-1}$ (figure 3.41). This was different to the 10 gL^{-1} DCW broth with the same gas velocity where the OUR increased to a maximum value of 52 $mmol.L^{-1}.h^{-1}$ at 900 rpm and then, remained constant with the further increase of propeller speed to 1000 rpm (figure 3.41). Hence, it was explained for the 10 gL^{-1} DCW baker's yeast suspension (section 3.3.6) that the OUR did not reach a maximum value until the DOTs had risen up to 10% in the riser which was at 900 rpm with the gas velocity of 0.136 ms^{-1}. However, with the 5 gL^{-1} DCW broth the DOTs were in excess of 30% for conventional aeration at the gas velocity of 0.136 ms^{-1} and so, no improvement of the OUR was observed with propeller operation.

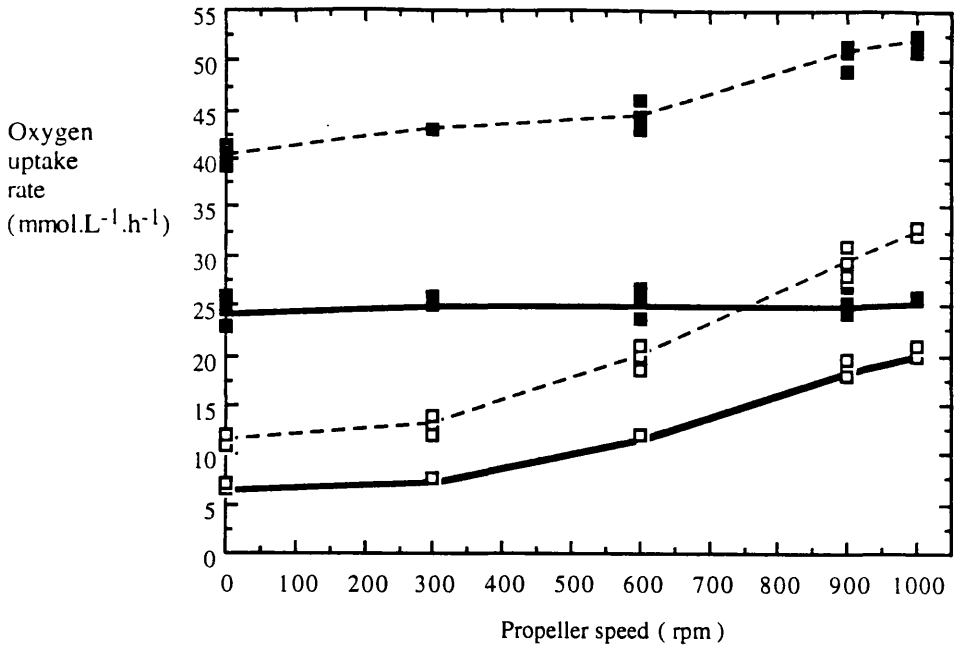

Figure 3.41 Comparison of the effect of propeller speed on the oxygen uptake rate between the 5 and 10 gL^{-1} DCW baker's yeast broth with the annulus gas sparged airlift reactor (H_{DT} of 2.77 m) at superficial gas velocities (ms^{-1}) : 0.036 (□), 0.136 (■). 5 gL^{-1} DCW (——); 10 gL^{-1} DCW (---)

At the other intermediate gas velocities between 0.036 and 0.136 ms^{-1} the OURs increased with propeller speeds until maximum values had been obtained when the DOTs were up to 10% in the riser. At the gas velocity of 0.091 ms^{-1} the OUR reached a maximum value of 24 $mmol.L^{-1}.h^{-1}$ at 600 rpm with the same value at 1000 rpm. Hence, from figure 3.38c it can be seen that the DOT around the vessel increased from 10% when the propeller speed reached 600 rpm up to 46% at 900 rpm.

Therefore, studying the effect of the propeller on the hydrodynamic and oxygen transfer performance of the aerated vessel with the 5 gL^{-1} DCW broth provided further evidence of the observations observed with the 10 gL^{-1} DCW biomass. It was shown that during aeration the propeller had a greater effect at increasing the DOT in the downcomer than in the riser at all gas velocities. A generalised trend was observed where propeller speeds up to 600 rpm increased the DOT in the downcomer followed by increases of DOT in the riser at propeller speeds above 600 rpm. However, this was a simplified observation as it was shown that the gas velocity and biomass concentration effected the increase of DOT with propeller operation. For instance the riser DOT with the gas velocity of 0.036 ms^{-1} remained below 2% with increases in propeller speed at both biomass concentrations. These 5 gL^{-1} DCW studies have also provided further evidence that the propeller increased the OUR until the DOTs around the vessel were up to 10% in the riser. Hence, this demonstrated that DOTs below 10% in the riser and top section (half the circulation of the vessel) were detrimental to the OUR of the yeast broth.

3.3.11 The effect of the propeller on the hydrodynamic and oxygen transfer performance of the aerated vessel using a short draft tube height

It has been shown that the propeller increased the oxygen transfer of the aerated vessel due to increased gas holdup and liquid circulation rates. However, the individual contribution of the two parameters to the improved oxygen transfer remained uncertain. So, the effect of the propeller was studied at a lower draft tube height (H_{DT} of 1.78 m) where the liquid circulation times would be different to those measured with the 2.77 m draft tube height. This would also enable the effect of the frequency that the cells experience the DOT heterogeneity on the OUR of the yeast broth to be studied. Ideally a draft tube height of half the original 2.77 m should have been studied however, the combinations of draft tube sections only allowed a height of 1.78 m to be used. In the lower draft tube system a working volume of 0.16 m^3 was used. This gave an equivalent sized top section as that used with the 0.25 m^3 working volume and 2.77 m draft tube height. The two draft tube heights were compared with identical superficial gas velocities and propeller speeds using the 10 gL^{-1} DCW baker's yeast suspension.

3.3.11.1 Comparison of the effect of propeller speed on the hydrodynamics of the aerated vessel using the two draft tube heights

The overall gas holdup profile as a function of superficial gas velocity and propeller speed for the reactor with the 1.78 m draft tube was found to be similar to the profiles of the taller draft tube system (results not shown). However, liquid circulation times from the shorter vessel were found to be shorter than those obtained with the taller draft tube system at all gas velocities. For example, with aeration operation at the gas

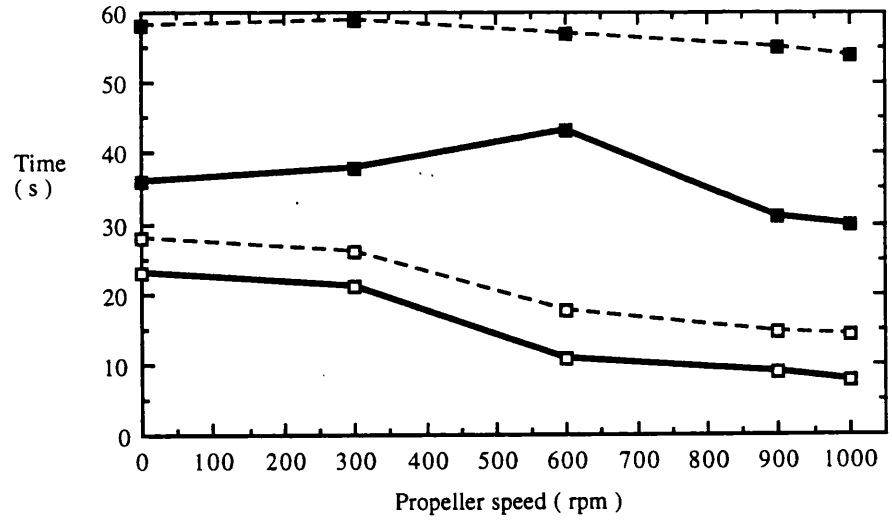

Figure 3.42 Comparison of the effect of propeller speed on the liquid circulation and mixing times between two draft tube heights of the annulus gas sparged airlift reactor with baker's yeast broth at the superficial gas velocity, 0.036 ms^{-1}. Liquid circulation time (□), mixing time (■), H_{DT} of 1.78 m (——), H_{DT} of 2.77 m (- - -)

velocity of 0.036 ms^{-1} (figure 3.42) the circulation time of the short reactor (23 s) was 18% faster than with the taller reactor (28 s). The mixing performance of the shorter vessel was also greater than with the taller vessel (figure 3.42). For example, at the gas velocity of 0.036 ms^{-1} the mixing time of the short reactor (17.5 s) was 71% lower than with the taller vessel (30 s). Hence, the ratio of mixing to circulation time for conventional aeration was found to be 1.5 for the short vessel compared to 2.5 for the taller vessel. Although the liquid circulation times were faster with the shorter vessel due to the shorter circulation path the actual riser liquid linear velocity was found to be between 20 to 25% slower than with the taller vessel for all gas velocities (results not shown). The propeller was found to reduce the circulation time from the aeration only values at a similar rate to that observed with the taller reactor (figure 3.42). Also, the propeller had no significant effect on the mixing time with the shorter vessel as shown by the insignificant change in mixing time with increasing propeller speed (figures 3.42).

During the study of the propeller at the two reactor heights the total energy dissipation rate (P_{VT}) must be considered due to the difference of the working volume of the two configurations. At all gas velocities the P_{VT} (Wm^{-3}) from combined aeration and propeller operation was found to be greater with the short reactor than with the taller reactor at each individual propeller speed. However, it was only significantly greater with values of P_{VT} corresponding to propeller speeds above 600 rpm (figure 3.43). Hence, the overall gas holdup profiles were similar for both reactor configurations despite the differences of P_{VT} (figure 3.43).

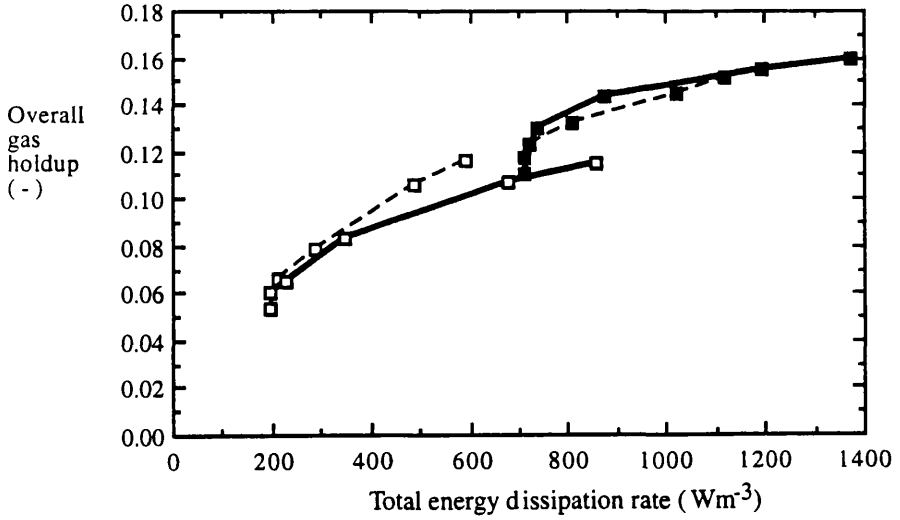

Figure 3.43 Comparison of the effect of total energy dissipation rate on overall gas holdup between two draft tube heights of the annulus gas sparged, propeller operated airlift reactor with baker's yeast broth at superficial gas velocities (ms^{-1}): 0.036 (□), 0.136 (■) , H_{DT} of 1.78 m (——), H_{DT} of 2.77 m (- - -)

For both reactor configurations the P_{VT} was the same for aeration only operation yet faster circulation times with the shorter reactor configuration were observed (figure 3.44). Also, although the P_{VT} for aeration and propeller with the short reactor was greater than with the taller reactor at each propeller speed the actual rate of reduction of the liquid circulation time with increasing P_{VT} was similar to the taller reactor (figure 3.44). It was also found (figure 3.44) that the liquid circulation times from aeration and propeller operation with the short reactor were slower than with propeller only operation as observed for the taller reactor (figure 3.28b).

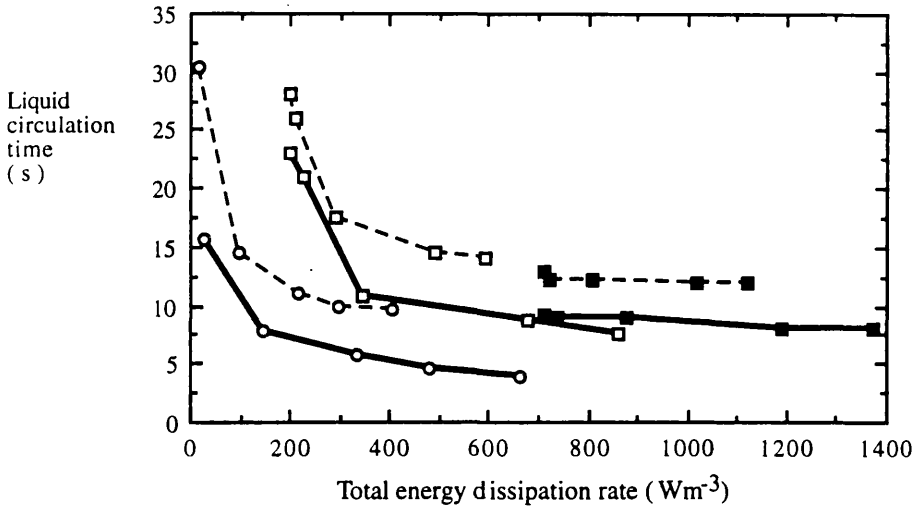

Figure 3.44 Comparison of the effect of total energy dissipation rate on liquid circulation time between two draft tube heights of the annulus gas sparged, propeller operated airlift reactor with baker's yeast broth at superficial gas velocities (ms^{-1}): 0.036 (□), 0.136 (■) , propeller only operation (○), H_{DT} of 1.78 m (——), H_{DT} of 2.77 m (- - -)

3.3.11.2 The effect of propeller speed on the dissolved oxygen tension profiles of the reactor with the shorter draft tube height

In general the propeller was found to have a similar effect on the DOT profiles of the aerated short reactor (figure 3.45) as observed with the tall reactor (figure 3.29) with the 10 gL^{-1} DCW yeast suspension. The aeration only DOT profiles for the riser, were also similar between the two reactor configurations with DOTs below 1% for all gas velocities. However, small differences were observed between the downcomer DOT profiles of the two reactor configurations for aeration only operation. At the gas velocity of 0.036 ms^{-1} for aeration only operation (figure 3.45a) the downcomer DOTs remained around 10% for the short reactor compared to reaching a peak value of 18% in the middle of the downcomer with the taller reactor (figure 3.29). Also at gas velocities above 0.054 ms^{-1} the DOTs in the upper downcomer with the short reactor were higher than with the taller reactor, although the peak values in the lower downcomer were very similar. For example, at the gas velocity of 0.091 ms^{-1} the DOT in the upper downcomer for aeration

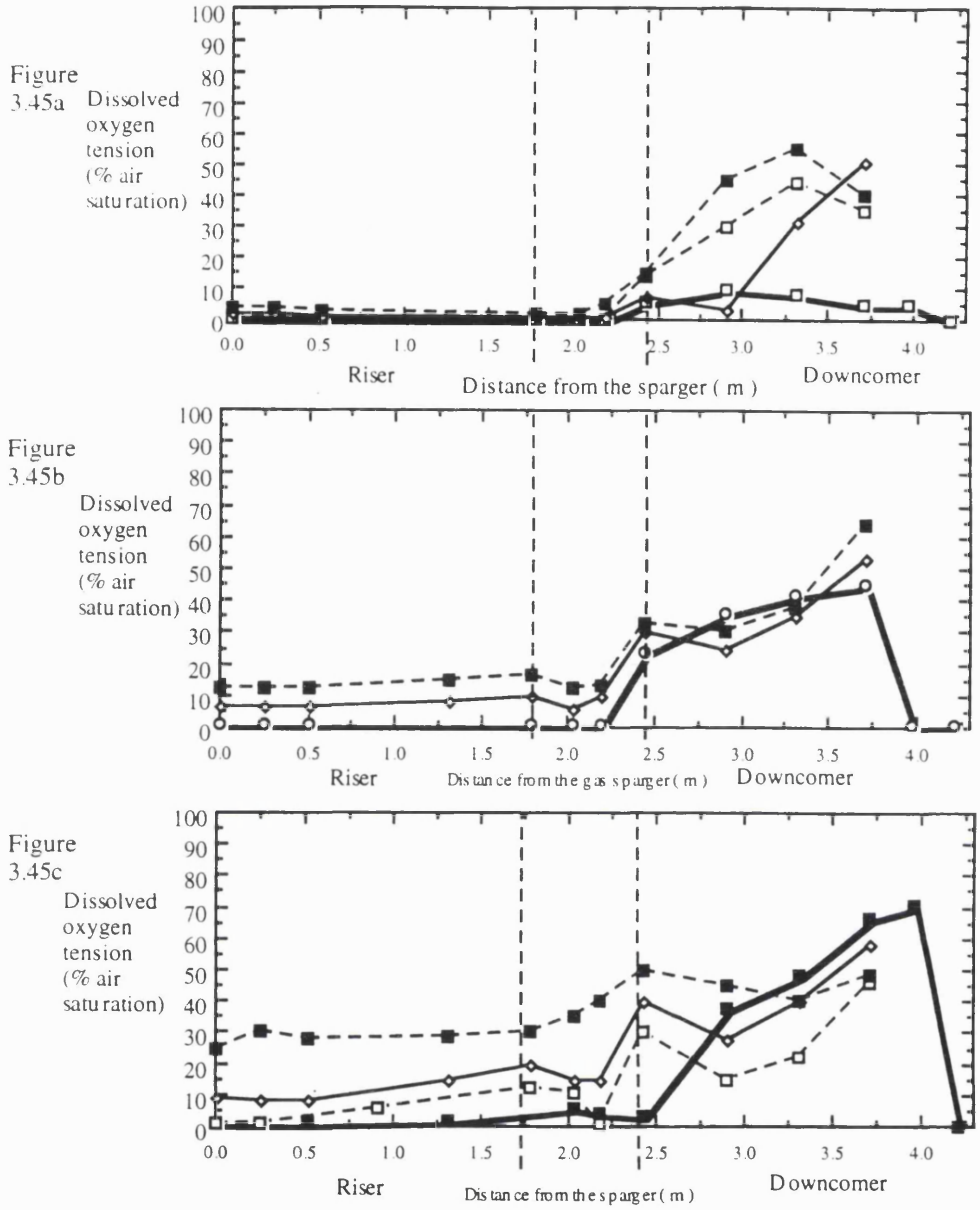

Figure 3.45 The effect of propeller speed on the dissolved oxygen tension (% air saturation) with increasing distance from the annulus gas sparger of the aerated airlift reactor (H_{DT} of 1.78 m). Using the 10 gL^{-1} DCW baker's yeast broth at superficial gas velocities (ms^{-1}) : fig. a: 0.036 (—□—), fig. b :0.091 (—○—), fig. c: 0.136 (—■—) with propeller speeds (rpm): 300 (-△-), 600 (-□-), 900 (—◇—), 1000 (-■-)

only was 35% (% air saturation) (figure 3.45b) compared to 10% with the taller reactor (figure 3.29c).

For propeller operation at gas velocities above 0.054 ms^{-1} the DOTs in the downcomer did not significantly rise above aeration only values (figures 3.45b & c) however, with the tall reactor the DOTs increased above the aeration values in the downcomer with increasing propeller speed (figure 3.29c&d). It could be speculated for the short reactor that the DOTs with propeller operation were in an upward trend in the

lower downcomer position and hence, the DOTs at the base of the vessel may have been greater than aeration only values. Therefore, only a few small differences in the DOT heterogeneity with aeration only and combined propeller operation existed between the two reactor configurations.

3.3.11.3 The effect of the propeller on k_La of the yeast broth using the reactor with the short draft tube configuration

The k_La values for the short reactor were found to be higher at all gas velocities and propeller speeds than those estimated for the taller draft configuration (figure 3.46). However, the rate of increase of k_La with increasing propeller speed was similar from both vessel heights. Similar observations were found from the comparison of the effect of total energy dissipation rate (P_{VT}) on the lower riser k_La values between the two reactor configurations (figure 3.47). The larger P_{VT} with the shorter reactor produced greater k_La values than the taller reactor especially at the gas velocity of 0.136 ms^{-1}. Also, for the short reactor the k_La values for all gas velocities were enhanced at a greater rate than with the tall vessel for increases of P_{VT} relating to propeller speeds up to 600 rpm (figure 3.47). For P_{VT} above 600 rpm the k_La increased at a similar rate for both reactor configurations.

3.3.11.4 The effect of the propeller on the oxygen uptake of the yeast broth with the short draft tube configured reactor

The OUR values for the yeast broth using the reactor with the 1.78 m draft tube were greater than with the 2.77 m draft tube configured reactor at all gas velocities and most propeller speeds. However, the rate of increase of the OUR with increasing propeller speed was similar with both draft tube heights. For example, at the low gas velocity (0.036 ms^{-1}) the propeller increased the OUR with the shorter vessel from 14 $mmol.L^{-1}.h^{-1}$ for aeration only operation to 45 $mmol.L^{-1}.h^{-1}$ with aeration and propeller operation at 1000 rpm whereas, for the taller vessel the OUR increased from 11 to 32 $mmol.L^{-1}.h^{-1}$ (figure 3.48). When this was considered with the DOT profiles shown in figures 3.45a and 3.29a then it was observed that both systems at 1000 rpm had similar DOT heterogeneity around the vessel yet, the 1.78 m draft tube had a higher OUR. The previous sections showed that the gas holdups of the two reactor configurations were similar but the liquid circulation and mixing times were shorter with the reactor with shorter draft tube. Thus, the greater liquid circulation and mixing performance of the shorter vessel compared to the taller reactor may account for the higher OUR and k_La values observed with the short draft tube reactor configuration.

At the gas velocity of 0.136 ms^{-1} the OUR reached the maximum value of 52 $mmol.L^{-1}.h^{-1}$ at 600 rpm with the short reactor and remained at this value with further increases in propeller speed. The DOT profiles from figure 3.45c showed that DOTs were above 10% for most of the vessel with these operating conditions and so, the OUR

was at the maximum value. Hence, a lower propeller speed of 600 rpm was used to produce the maximum OUR of 52 mmol.$L^{-1}.h^{-1}$ with the 1.78 m draft tube compared to 900 rpm required with the 2.77 m draft tube system (figure 3.29). These observations were also confirmed when the effect of total energy dissipation rate on the OUR was compared between the two reactor configurations at the two gas velocities (figure 3.49).

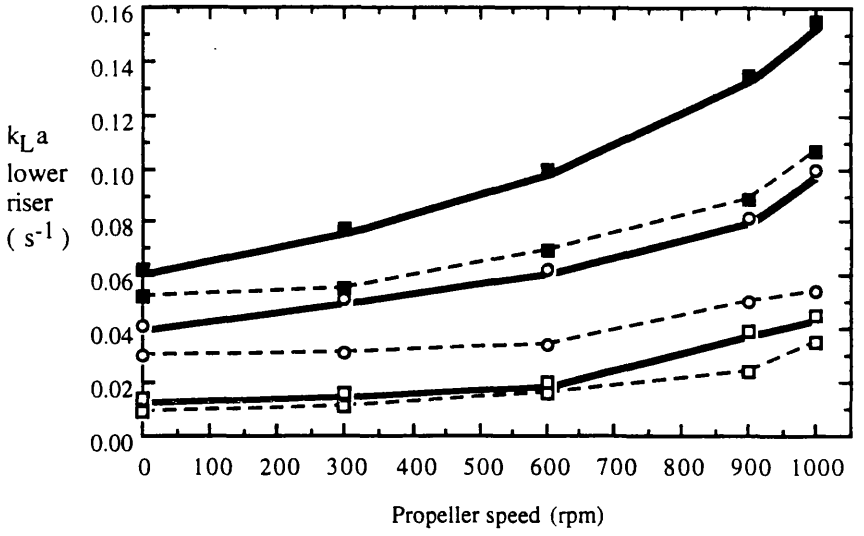

Figure 3.46 Comparison of the effect of propeller speed on k_La (lower riser) between two draft tube heights of the annulus gas sparged airlift reactor with baker's yeast broth (10 gL^{-1} DCW) at superficial gas velocities (ms^{-1}): 0.036 (□), 0.091 (○),0.136 (■), H_{DT} of 1.78 m (——), H_{DT} of 2.77 m (- - -)

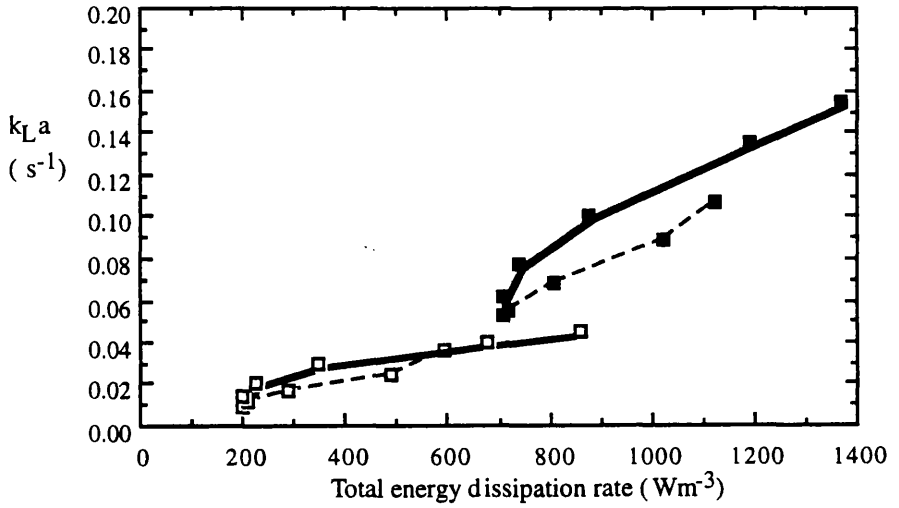

Figure 3.47 Comparison of the effect of total energy dissipation rate on k_La (lower riser) between two draft tube heights of the annulus gas sparged,propeller operated airlift reactor with baker's yeast broth at superficial gas velocities (ms^{-1}): 0.036 (□), 0.136 (■) , H_{DT} of 1.78 m (——), H_{DT} of 2.77 m (- - -)

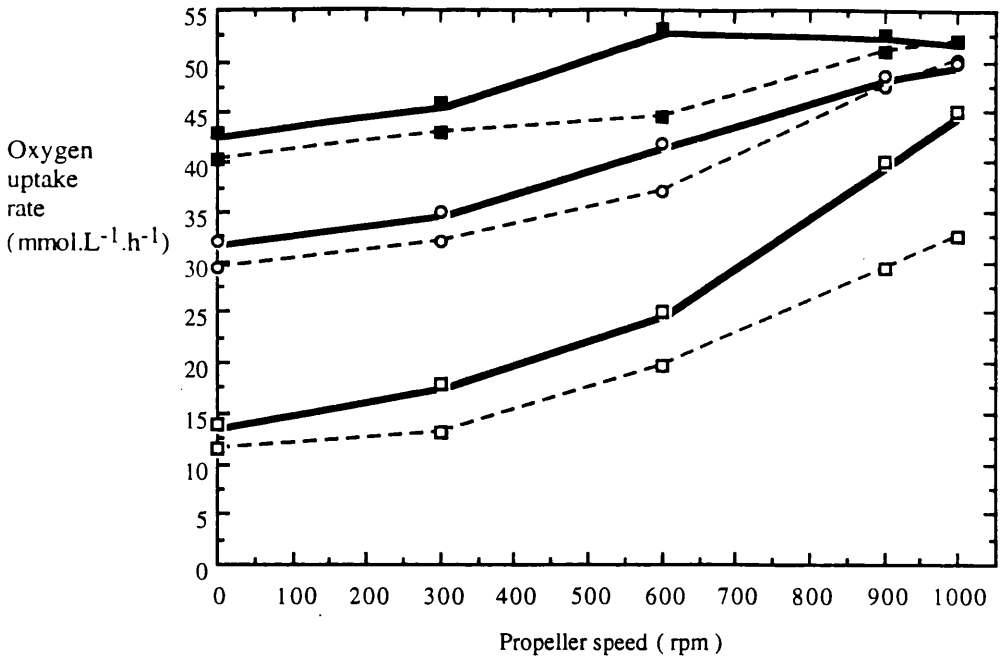

Figure 3.48 Comparison of the effect of propeller speed on the oxygn uptake rate between two draft tube heights of the annulus gas sparged airlift reactor with baker's yeast broth (10 gL^{-1} DCW) at superficial gas velocities (ms^{-1}): 0.036 (□),0.091 (o) ,0.136 (■), H_{DT} of 1.78 m (——), H_{DT} of 2.77 m (- - -)

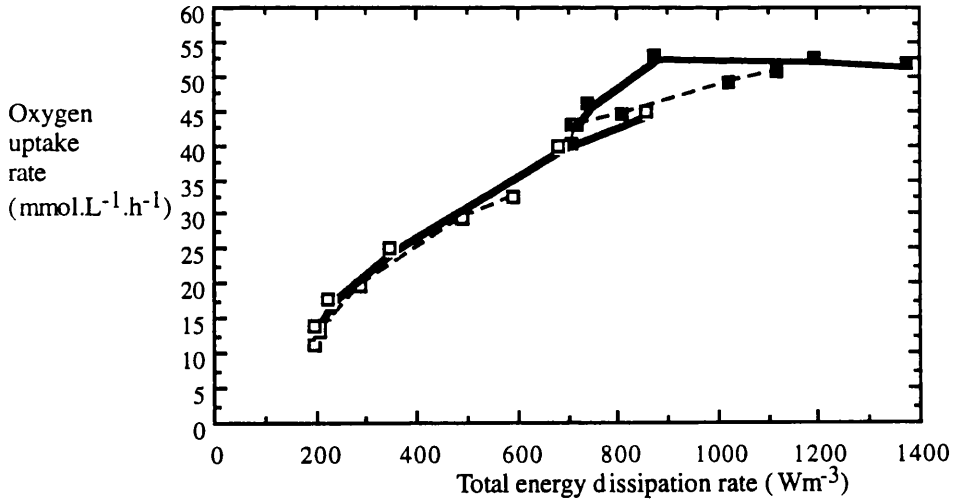

Figure 3.49 Comparison of the effect of total energy dissipation rate on the oxygen uptake rate between two draft tube heights of the annulus gas sparged,propeller operated airlift reactor with baker's yeast broth (10 gL^{-1} DCW) at superficial gas velocities (ms^{-1}): 0.036 (□), 0.136 (■) , H_{DT} of 1.78 m (——), H_{DT} of 2.77 m (- - -)

3.4 Impact of the engineering environment of the airlift reactor on the fermentation of *Saccharopolyspora erythraea*

The fermentation of *Saccharopolyspora erythraea* is complicated by the filamentous morphology and non-Newtonian pseudoplastic nature of the broth compared to the Newtonian baker's yeast suspensions. The fermentation was defined as the oxidation of glucose under aerobic conditions for the production of biomass and antibiotic. The effect of morphology on reactor performance was further studied by using pelleted and mycelial morphologies of *S. erythraea* broths. The morphology was manipulated for pelleted broths by inoculating the reactor when an OUR of 9 $mmol.L^{-1}.h^{-1}$ had been reached in the 25 L working volume seed vessel which was equivalent to 4.8 gL^{-1} DCW. For mycelial broths an inoculum of 25 L with a biomass concentration of 9.7 gL^{-1} DCW and OUR of 18 $mmol.L^{-1}.h^{-1}$ was used. Thus, for each *S. erythraea* fermentation the hydrodynamic and oxygen transfer characteristics were measured throughout the fermentation as completed with the yeast broths. In addition, the rheology, cellular morphology, glucose consumption and erythromycin production were monitored. Hydrodynamic measurements were also made as a function of superficial gas velocity at two intervals, 29 and 39 hours into the fermentations. At these times the gas velocity was varied between 0.068 to 0.2 ms^{-1} for up to 30 minutes while the gas holdup and tracer response measurements were made.

Comparisons were made between the pelleted and mycelial characterised broths with each conventionally aerated reactor configuration. This also led to comparisons between reactor configurations with similar morphologies. Hence, with a mycelial *S. erythraea* broth the effect of the engineering environment on cellular morphology, growth yields and productivity for the two aerated reactor configurations, draft tube or annulus air sparged are compared.

Also, the effect of the engineering environment from the combined aeration and propeller operation with the annulus sparger configuration was studied with a mycelial fermentation and compared to the conventionally operated reactor. Hence, the behaviour of mycelial fermentations under the influence of reduced DOT heterogeneity from propeller operation (as observed with the yeast broth, section 3.3) was compared to the effect of greater DOT heterogeneity from aeration only operation. The draft tube sparged configuration with propeller operation was not studied with the *S. erythraea* broths due to the limited beneficial effect of operating the propeller in this configuration as observed with the baker's yeast suspension (section 3.2). Finally the behaviour of the mycelial broths was also compared between the engineering environments of the airlift reactor and laboratory stirred tank. The majority of *S. erythraea* fermentations were duplicated in the pilot scale airlift reactor and the results were very similar. For simplicity most of the following figures show results from one set of fermentation data for each type of morphology and reactor configuration.

3.4.1.1 Study of the *S. erythraea* mycelial fermentation with the draft tube sparger configured reactor

During the first nine hours, the gas velocity was held at 0.045 ms^{-1} (airflow of 100 L min^{-1}, 0.33 vvm) and the dissolved oxygen tensions (DOTs, % of air saturation) as measured at the three probe positions fell with similar values (figure 50a). At nine hours the gas velocity was increased to 0.136 ms^{-1} (airflow of 300 L min^{-1}, 1.25 vvm) and was maintained at this value for the remainder of the fermentation. This allowed the changes in fermentation parameters to be studied under constant operating conditions. After 9 hours, the DOTs from the lower riser position and upper downcomer position reduced at similar rapid rates to the lowest DOT values during the fermentation at 19.4 h (figure 3.50a). Therefore, from 15 h into the fermentation, changing DOTs began to develop around the vessel as shown from the three fixed DOT probe positions. At 19.4 h extreme DOT heterogeneity had developed with DOTs below 1% in the riser and values between 20 and 70% in the downcomer. Between 19.4 and 43 h of the fermentation the DOT at the lower riser position remained below 1% although the DOT from the upper downcomer gradually increased, reaching 66% at 39 h. At 43 h, the DOT from the riser position rapidly increased to 82% at 57.3 h which coincided with a rapid increase at the upper downcomer position from 66% to 100% at 45 h. The lower downcomer DOT decreased during the growth phase but never fell below 50%. Hence, from 50 hours into the fermentation the DOTs cycled around the reactor between 65% to 100%.

The flow behaviour (n) decreased gradually at a constant rate from 0.9 at 2 h to 0.35 at 39 h into the fermentation and then gradually increased to 0.7 at 110 h (figure 3.50b). Similarly the consistency index (K) increased gradually during the first 20 hours from 0.05 $Pa.s^n$ at 2 h to 0.19 $Pa.s^n$ at 21 hours. However after 21 h, consistency changed rapidly from 0.33 $Pa.s^n$ at 29 h to the maximum value of 0.6 $Pa.s^n$ at 39 h. After 39 hours, K decreased rapidly from 0.6 $Pa.s^n$ at 39 hours to 0.3 $Pa.s^n$ at 60 hours and then decreased gradually to 0.1 $Pa.s^n$ at 110 hours. The apparent viscosity followed a similar relationship to fermentation time as consistency index, whereby a peak apparent viscosity occurred at 39 h into the fermentation.

The dry cell weight (DCW) increased rapidly from 0.95 gL^{-1} to 9 gL^{-1} at 18 hours, and then increased at a slower rate reaching a maximum mean value of 10.5 gL^{-1} at 28 h (Figure 3.50c). Between 28 and 120 h the DCW decreased slowly to 9.1 gL^{-1}. Hence, the maximum apparent viscosity (figure 3.50b) occurred some 8 h later than the maximum dry weight. The oxygen uptake rate (OUR) increased rapidly to a maximum value of 24 $mmol.L^{-1}.h^{-1}$ at 19 hours into the fermentation (figure 3.50f). This corresponded with the lower riser DOT reducing to below 1% (figure 3.50a). Between 19.3 and 27.7 h the OUR rapidly decreased to a value of 16 $mmol.L^{-1}.h^{-1}$ which was maintained until 43.25 h. During the growth phase, glucose consumption increased rapidly until it was depleted after 43.25 h (figure 3.50c). The completion of glucose

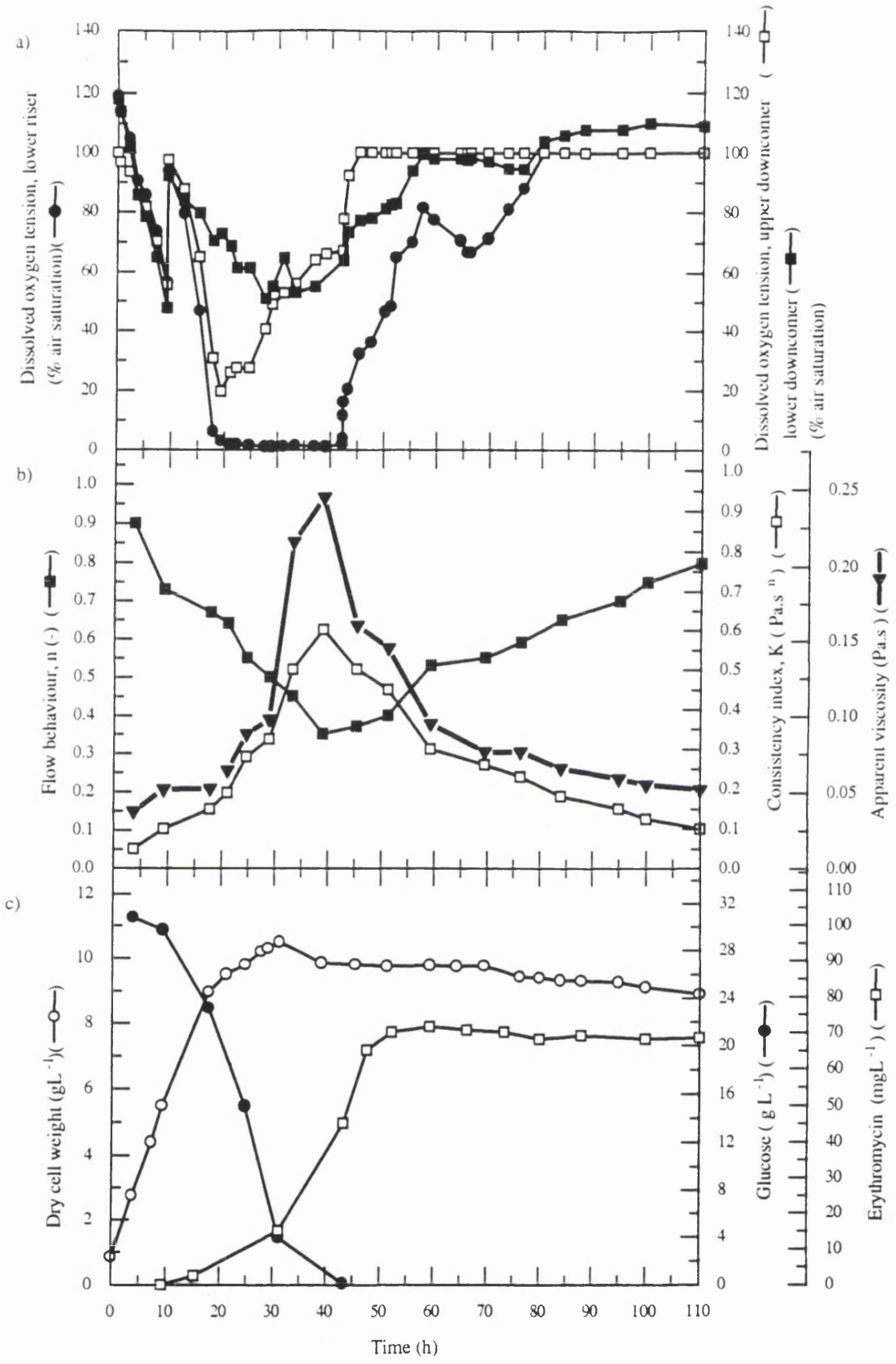

Figure 3.50(a, b & c) Mycelial *S. erythraea* fermentation in the draft tube air sparged airlift reactor. Changes in fermentation parameters: a) dissolved oxygen tension (% air saturation), b) rheological properties, flow behaviour, consistency index, and apparent viscosity, c) dry cell weight, glucose and erythromycin production

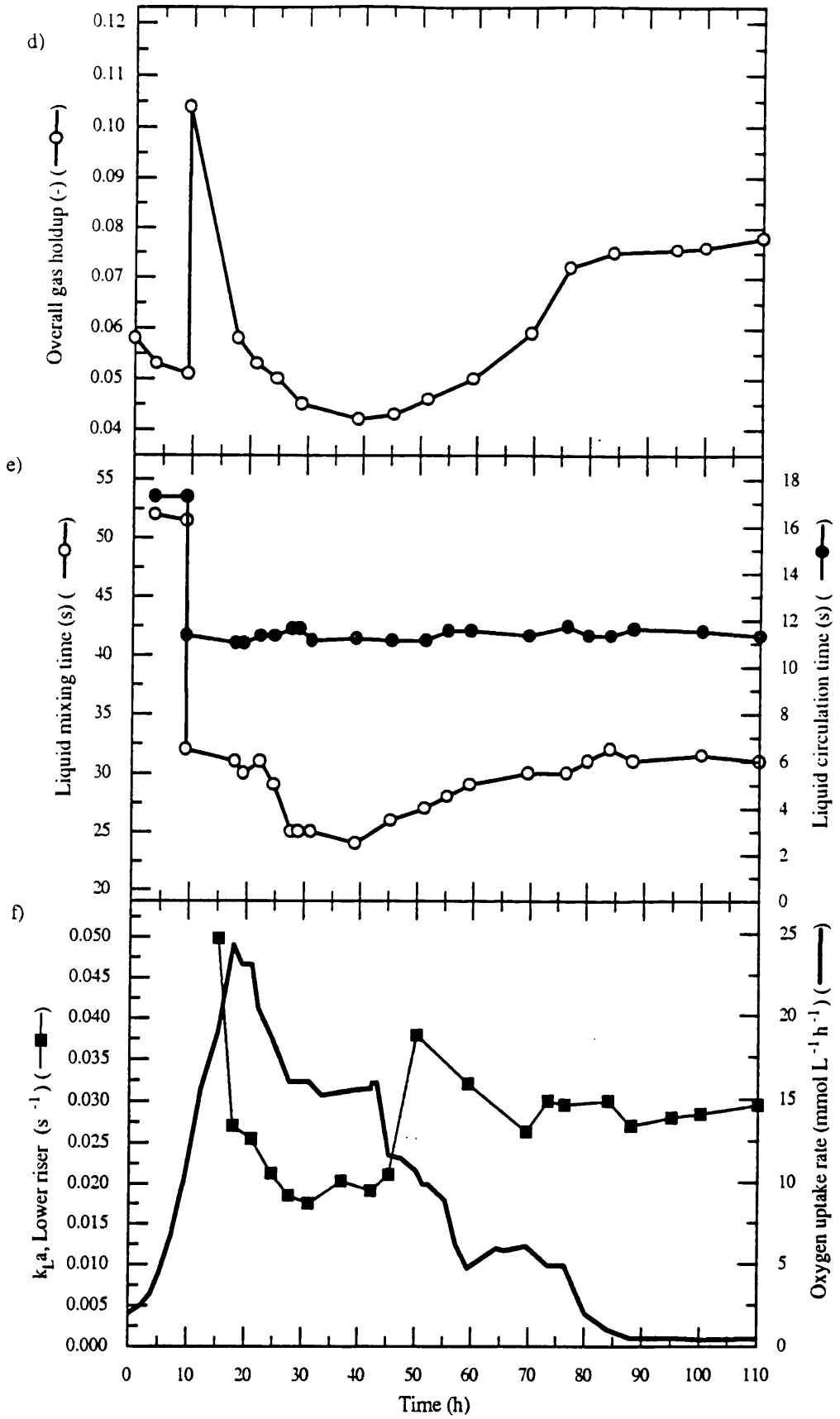

Figure 3.50(d, e & f) Mycelial *S. erythraea* fermentation in the draft tube air sparged reactor Changes of : d) overall gas holdup, e) liquid mixing and circulation time, f) lower riser k_La and oxygen uptake rate during the fermentation

consumption resulted in the rapid reduction of the OUR and the subsequent increase in DOT at the lower riser probe position (figure 3.50a). Erythromycin production began at a slow rate from 0.05 mg L^{-1} at 9 h to 15 mg L^{-1} at 31 h (figure 3.50c). Production progressed at a fast rate between 31 to 50 h into the fermentation when the dry cell weight had reached a maximum value and the OUR was in decline.

The overall gas holdup decreased slowly during the first 9 h of the fermentation (figure 3.50d) followed by an increase to 0.105 from the rise in gas velocity to 0.136 ms^{-1}. After 9 h, the gas holdup decreased rapidly to a value of 0.05 at 24.7 h and then decreased at a slower rate to the lowest value of 0.042 at 39 hours. The low values of gas holdup between 30 - 50 hours coincided to the region of highest apparent viscosity shown in figure 50b. From 39 to 69 h the holdup increased slowly to a value of 0.07 which was maintained for the remainder of the fermentation.

The liquid circulation and mixing times did not significantly change during the first nine hours of the fermentation (figure 3.50e). However, the increased gas velocity at nine hours caused the decrease in mixing and circulation times. For the remainder of the fermentation the circulation time was between 11 and 11.5 s meanwhile, the mixing time of 32 s at 9.3 h decreased slowly to 30 s at 19.4 hours and then changed rapidly to 25 s at 27.65 h. The lowest mixing time value of 24 s at 39 h coincided with the highest apparent viscosity shown in figure 3.50b hence, the change in mixing time was similar to the change in viscosity and gas holdup during the period between 9 - 60 h. After 40 h the mixing time gradually increased, returning to the original value of 32 s at 80.1 h. This improved mixing performance was also highlighted by the increase in turbulence of the liquid surface during the fermentation as visually observed from the top section sight glasses. Visual observations of the broth flowing through the downcomer via the side vessel sight glasses was made impossible by a thick viscous layer which formed on the inside of the sight glass. These problems were outlined in the yeast work (section 3.1.5) as the sight glasses were not flush mounted with the vessel inside wall. However, during the most viscous period of the fermentation, 36 to 57 hours into the fermentation, large slug bubbles approximately 50 mm in diameter were occasionally observed rising up the length of the downcomer past the three vessel section sight glasses. Rising bubbles were observed at approximately 1 minute intervals however, this may have occurred more frequently but could not be visually observed. Also, the flow of large upward flowing bubbles passed the sight glass briefly disrupting the broth layer allowing the downward flowing broth in the centre of the downcomer to be observed. Hence, the large downward flowing bubbles of 6 - 12 mm in diameter and a large proportion of small very spherical 2 mm diameter bubbles were observed.

Figure 3.50f shows the k_La values from 18 h into the fermentation for the lower riser probe position which decreased rapidly from 0.05 s^{-1} at 18 h to 0.018 s^{-1} at 29 h. This corresponded to the decrease in gas holdup and increase in viscosity while the lower riser DOT remained below 1%. The k_La values remained at the low values for a duration

of 12 h before increasing to 0.038 s^{-1} at 50 h which coincided with the increase in DOT (from below 1% to 60%) and gas holdup. Similar reductions were observed at the other probe positions however, the lower riser k_La was used as a comparison for all reactor configurations and morphologically different fermentations as it produced the lowest values of the three probe positions and the effect of other fermentation parameters could more easily be shown as the DOT remained constant below 1% with aeration only fermentation. Both the hyphal length and the hyphal growth unit increased during the growth phase but remained relatively constant for the remainder of the fermentation (figure 3.51). No significant change of the percentage of clumps was observed during the fermentation which remained above 80%. However, the branch length was found to increase up to 7 μm at 39 h which coincided with the maximum apparent viscosity and consistency index.

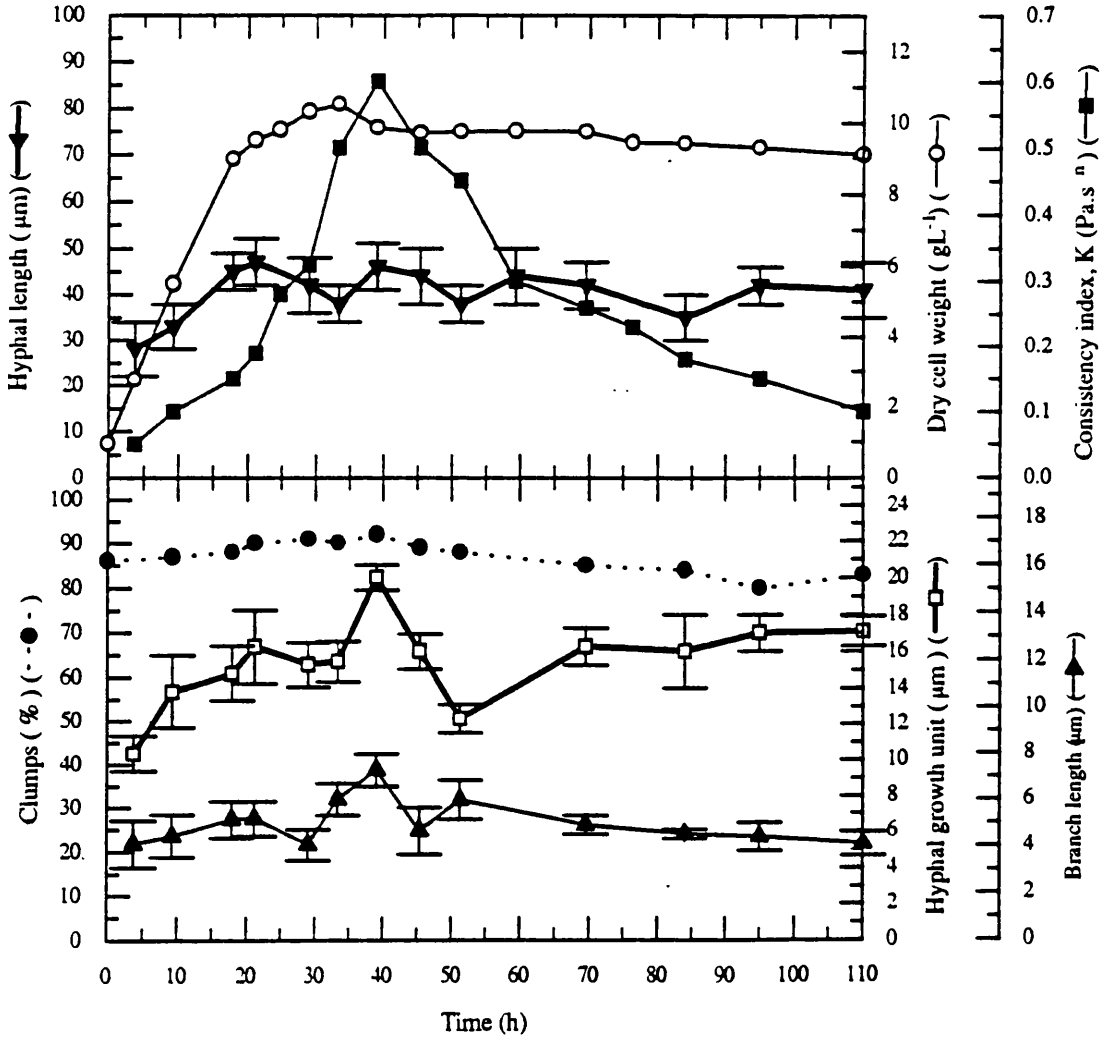

Figure 3.51 Comparison of the change in morphological characteristics (main hyphal length, hyphal growth unit, branch length and percentage clumps) to dry cell weight and consistency index during the mycelial *S. erythraea* fermentation in the draft tube sparged reactor

3.4.1.2 Study of the *S. erythraea* pelleted fermentation with the draft tube sparger configured reactor

The 50% smaller inoculum concentration used to produce a pelleted fermentation resulted in a slower reduction of DOT during the first 10 hours of the fermentation compared to the decrease of DOT with the mycelial fermentation. Thus the rise to the maximum gas velocity of 0.136 ms^{-1} to prevent DOT falling below 40% was delayed until 24 h. So during the first 15 h of the fermentation the DOT decreased with similar values around the vessel (figure 3.52a). Between 18 and 24 h the DOT fluctuated from the three probe positions due to the decrease in DOT which was then counteracted by the step wise increase in gas velocity. After 24 h once the maximum gas velocity was reached, large DOT heterogeneity developed around the vessel, with DOT below 1% (air saturation) in the lower riser and between 20 to 50 % in the downcomer (figure 3.52a). After a duration of 22 h the lower riser and upper downcomer DOT rapidly increased to values between 60 to 100 % for the remainder of the fermentation.

During the first 37 h of the fermentation, the flow behaviour (n) decreased to the lowest value of 0.47 and the consistency index (K) increased to the maximum value of 1.1 $Pa.s^n$ (figure 3.52b). These values were maintained for a further 12 h into the fermentation and hence, the apparent viscosity was maintained at the maximum value of 1.2 Pa.s during this period. From 47 to 82 h, n and K changed at a rapid rate to values of 0.8 and 0.115 $Pa.s^n$ respectively. These values then changed at a slower rate to final values at 110 h of 0.9 for n and 0.06 $Pa.s^n$ for K.

The dry cell weight (DCW) increased to a maximum value of 10.1 gL^{-1} at 37 h (figure 3.52c) then, decreased rapidly to 8 gL^{-1} and remained at this value for rest of the fermentation. The OUR reached the maximum value of 27 $mmol.L^{-1}.h^{-1}$ at 26 h (figure 3.52f) which corresponded to the decrease of DOT at the lower riser probe position to below 1% (figure 3.52a). The OUR then rapidly decreased to 17 $mmol.L^{-1}.h^{-1}$ at 32 h and was maintained at this value until 48 h followed by a rapid decrease reaching 1 $mmol.L^{-1}.h^{-1}$ at 83 h. The glucose concentration in the medium decreased slowly during the first 15 h of the fermentation and then, decreased rapidly at a constant rate, for a duration of 35 h with complete glucose consumption from the media occurring at 47.5 h (figure 3.52c). This coincided with the increase in DOT from the lower riser probe position (figure 3.52a) and the decrease in OUR. A small amount of erythromycin production occurred during the growth phase of the fermentation (figure 3.50c). But the majority of the production occurred when the dry cell weight had reached maximum value, glucose consumption was complete and the OUR was in decline.

The overall gas holdup increased during the first 23 h due to the step wise increases in gas velocity (figure 3.52d). However, from 27 to 36 h there was a rapid reduction in overall gas holdup from 0.085 to 0.066. After 38 h, the holdup remained at the low value of 0.067 for a duration of 24 h which coincided with the period of highest apparent viscosity. The holdup then increased to 0.085 at 74 h for the remainder of the

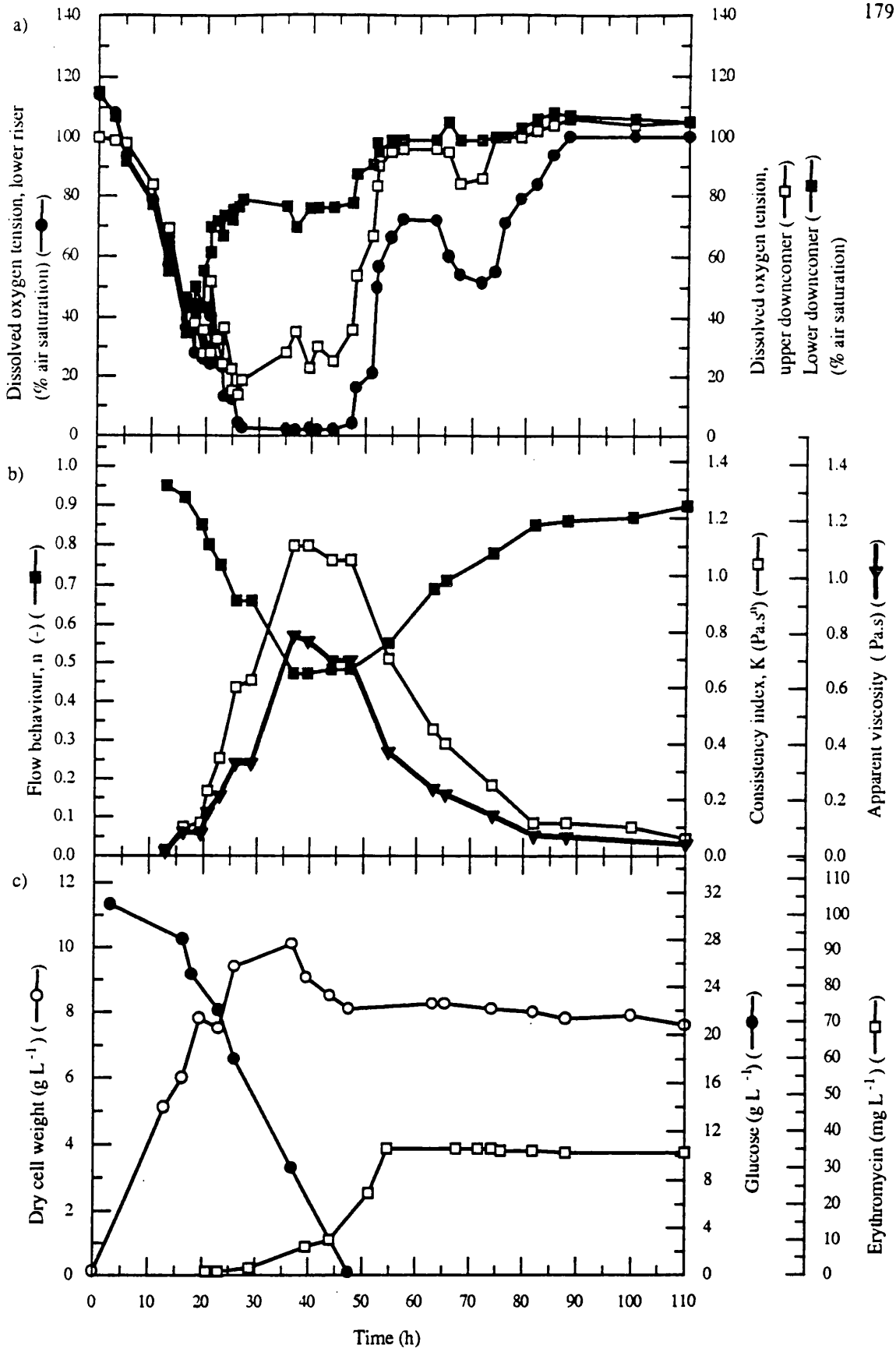

Figure 3.52 Pelleted *S. erythraea* fermentation in the draft tube sparged reactor. Changes of fermentation parameters: a) dissolved oxygen tension (% air saturation), b) rheological properties, flow behaviour, consistency index, and apparent viscosity, c) dry cell weight, glucose and erythromycin production

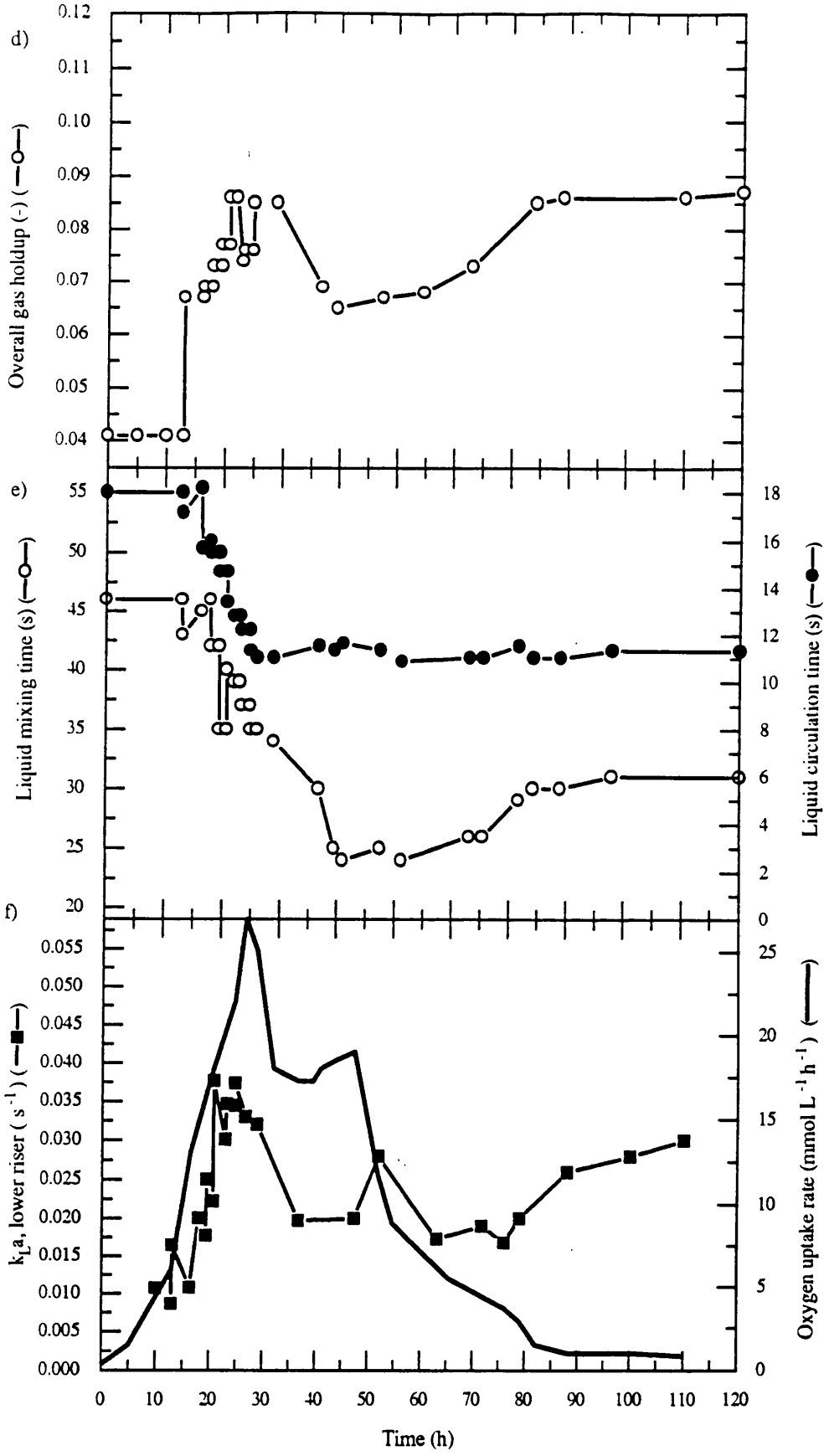

Figure 3.52 (d, e & f) Pelleted *S. erythraea* fermentation in the draft tube sparged reactor Change of a) overall gas holdup, b) liquid mixing and circulation time, c) lower riser k_La and oxygen uptake rate during the fermentation

fermentation. During the first 24 h the liquid circulation and mixing times decreased due to the step wise increase in gas velocity (figure 3.52e). After 24 h with the constant gas velocity of 0.136 ms^{-1} the circulation time remained constant at around 11.3 s for the remainder of the fermentation. However, the mixing time decreased rapidly from 35 s to a value of 24 s at 41 h. The mixing time remained around this value until 65 h when it increased to 30 s. Hence, the improvement in mixing time coincided with the decrease in gas holdup and increase in apparent viscosity.

The k_La from the lower riser probe position increased during the first 25 h to a value of 0.035 s^{-1} due to the step wise increase in gas velocity. After 24 h the k_La decreased rapidly to a value of 0.02 s^{-1} at 37 h. The k_La remained at this value for 10 hours then increased which coincided with the increase in gas holdup and riser DOT (figure 3.52a & d).

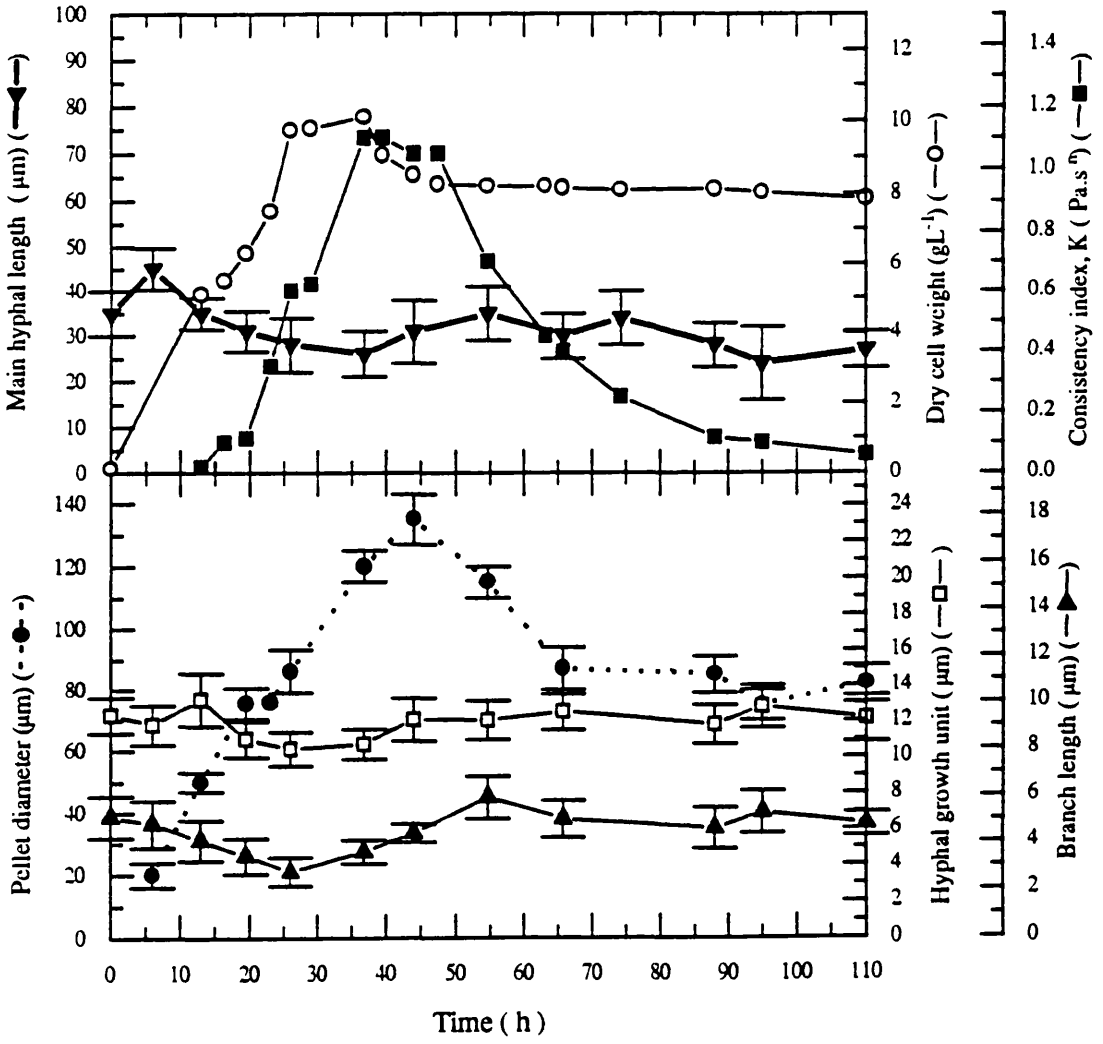

Figure 3.53 Comparison of the change in morphological characteristics (pellet diameter, main hyphal length, hyphal growth unit and branch length) to dry cell weight and consistency index during the pelleted *S. erythraea* fermentation in the draft tube sparged reactor

The mean pellet diameter was found to increase to maximum value of 135 μm at 43 h into the fermentation, which coincided with the region of highest apparent viscosity and not the maximum DCW which occurred some 10 h earlier (figure 3.53). Although, 90% of the proportion of the broth was pellets, the mycelial content was shown to remain at a similar length during the fermentation, and no significant change in branch length or hyphal growth unit occurred during the fermentation in relation to the change in rheology.

3.4.1.3 Study of the *S. erythraea* mycelial fermentation with the annulus sparger configured reactor

The riser of the reactor was now the annulus of the vessel and the DOT probes measured the DOT in the lower and upper riser positions and in the lower downcomer position. The gas velocity was kept at 0.045 ms^{-1} (air flow of 125 $Lmin^{-1}$, 0.4 vvm) during the first nine hours of the fermentation and the DOTs reduced with similar rates from the three probe positions reaching the DOT of 52% air saturation (figure 3.54a). At nine hours the gas velocity was increased to 0.136 ms^{-1} (airflow rate of 358 $Lmin^{-1}$, 1.43 vvm). After nine hours the DOT from the lower riser and upper riser rapidly reduced to below 1% at 12 h, (lower riser DOT profile was only shown in figure 54a as upper riser profile was similar) and remained below 1% for a duration of 36 h. At 48 h into the fermentation there was a rapid increase in riser DOT to 40% at 49.8 h and then a gradual increase to 90% at 70 h. At the lower downcomer position, the DOT after 12 h remained above 100% for the majority of the fermentation. However, from 30 to 49 h the DOT from the lower downcomer fluctuated from 100 to below 1% where the DOT changed rapidly within 1 minute between the high and low values but remained at each value for approximately 30 minutes. This occurred at the same time during each duplicate fermentation but was not observed during fermentations with the draft tube sparger configuration. It can be observed that the fluctuations occurred after the growth phase during the most viscous part of the fermentation (figure 3.54b) and hence, the DOT changes were assumed not to be a physiological response of the broth but to a physical mechanism affecting the probe. At the highly viscous part of the fermentation the probe membrane may have become covered with broth reducing the DOT to zero. The attached broth may rhythmically build around the probe and then, be removed by the liquid flow resulting in the DOT rise to 100%.

The flow behaviour (n) was found to decrease rapidly to a value of 0.5 at 20.5 h, which coincided with a rapid increase in consistency index (K) to 1.0 $Pa.s^n$ (figure 3.54b). Also, the apparent viscosity increased rapidly during the first 20 h but the rate of increase was not as great as that observed with the increase in K. After 20 h n and K changed at a slower rate where the lowest value of n (0.43) and maximum value of K (1.1 $Pa.s^n$) was obtained at 38 h. However, a large increase in apparent viscosity occurred during this period from 0.95 to 1.25 Pa.s at 38 h which then reduced back to

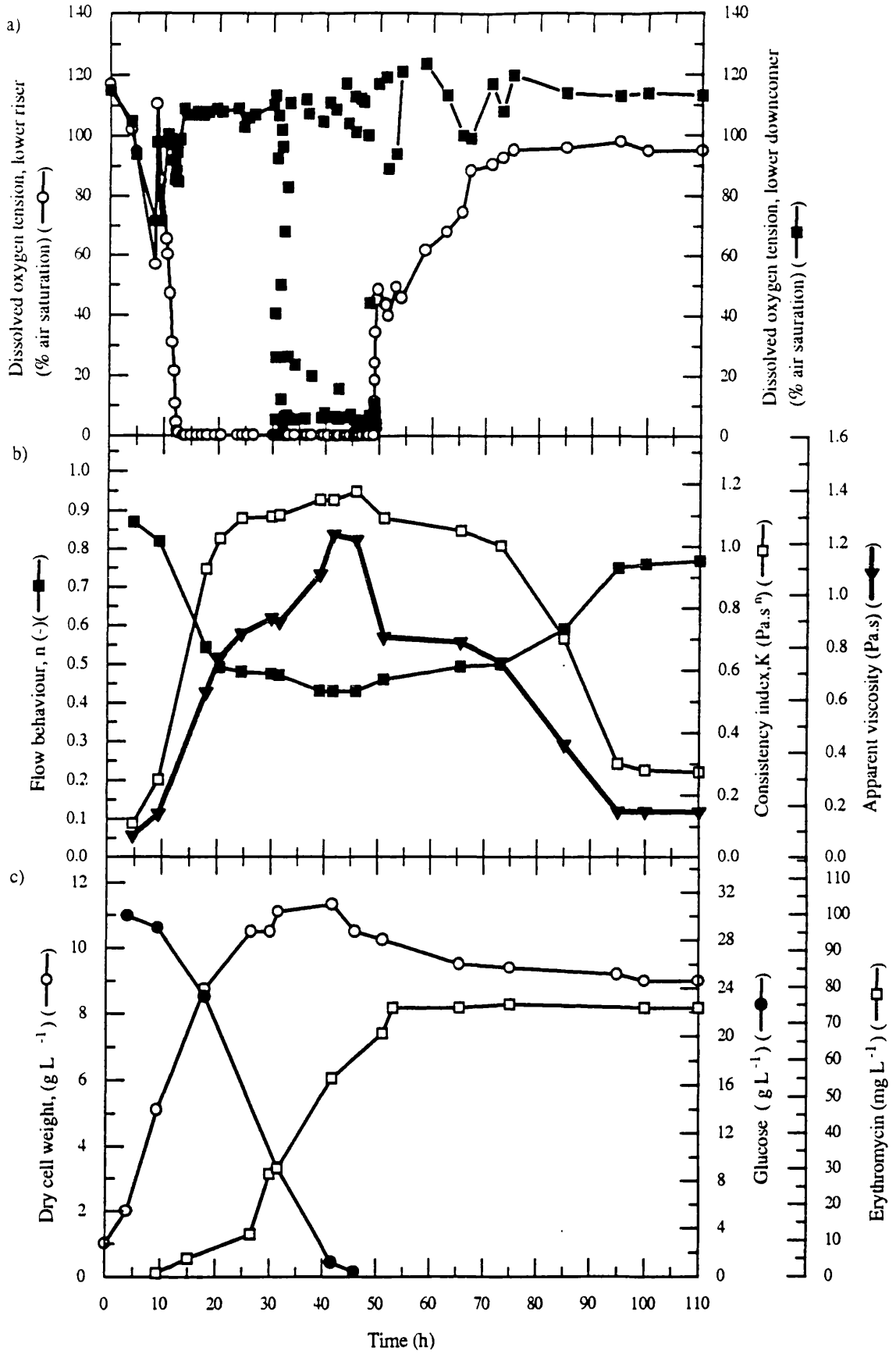

Figure 3.54 (a, b & c) Mycelial *S. erythraea* fermentation in the annulus sparged reactor. Changes of fermentation parameters, a) dissolved oxygen tension, b) rheological properties, flow behaviour, consistency index apparent viscosity c) dry cell weight, glucose and erythromycin production

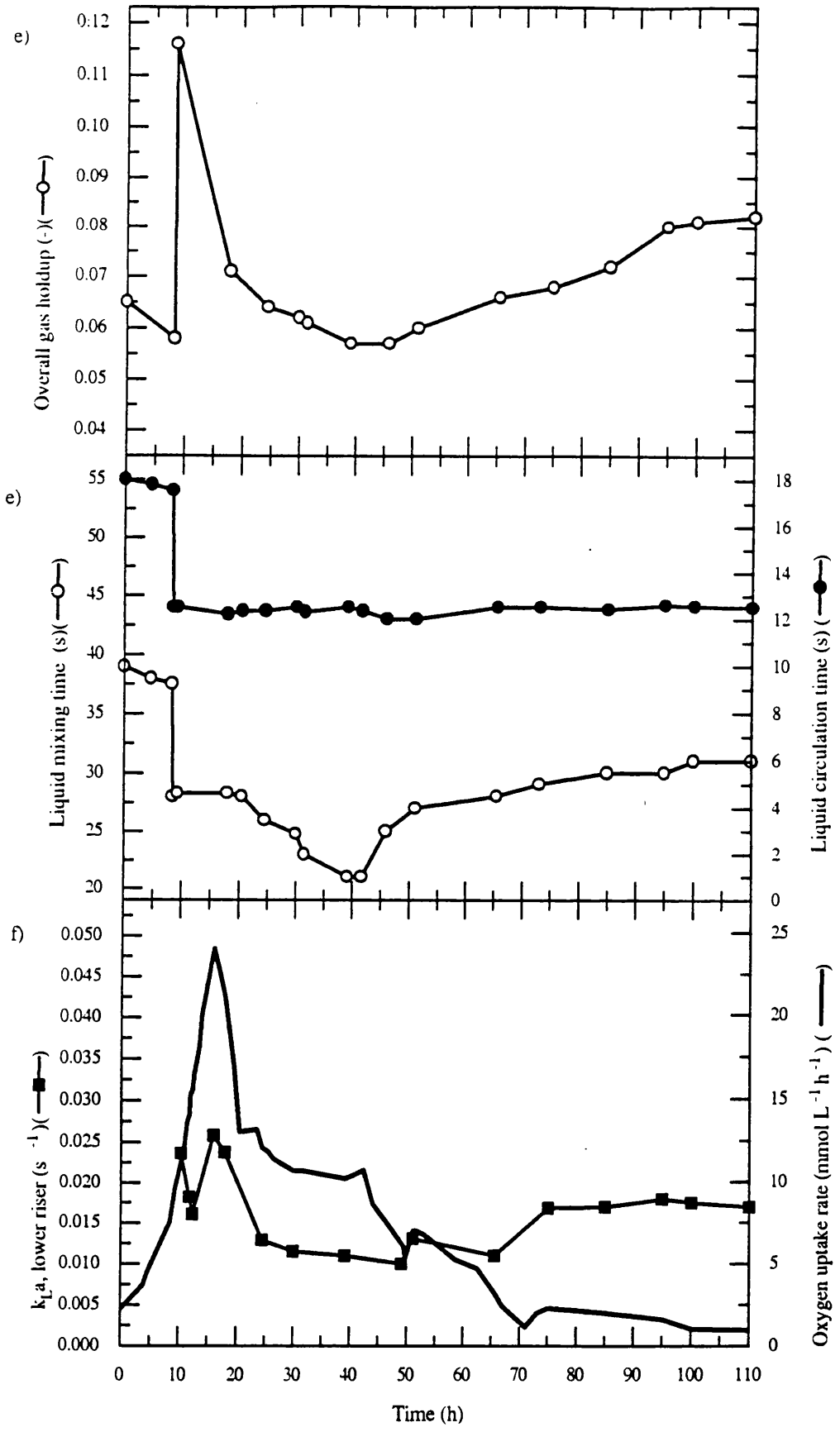

Figure 3.54 (d, e & f) Mycelial *S. erythraea* fermentation in the annulus sparged reactor. Changes of a) overall gas holdup, e) liquid mixing and circulation time, f) lower riser k_La and oxygen uptake rate during the fermentation

0.8 Pa.s at 50 h. Similar values of n, K and apparent viscosity were maintained until 73 h into the fermentation where n and K began to change rapidly reaching an n of 0.76 and K of 0.27 Pa.s^n at 85 h. The apparent viscosity reduced rapidly from 60 to 90 h to 0.2 Pa.s although, the rate of decrease was not as fast as the rate of change of K over the same period of the fermentation.

The dry cell weight (DCW) increased to a maximum value of 11.1 gL^{-1} at 30 h (figure 3.54c), which coincided with the increase in K and apparent viscosity (figure 3.54b). After 31 h the dry weight gradually decreased to a value of 9 gL^{-1} at 60 h. The oxygen uptake rate (OUR) increased to a maximum value of 24 $mmol.L^{-1}.h^{-1}$ at 17 h (figure 3.54f). Also, the lower riser DOT had reached below 1% (figure 3.54a) at an OUR of 18 $mmol.L^{-1}.h^{-1}$ before the maximum OUR was achieved. After 18 h the OUR decreased rapidly to a value of 12 $mmol.L^{-1}.h^{-1}$ at 20h which then remained at a value of 10 $mmol.L^{-1}.h^{-1}$ for a duration of 20 h. At 40 h into the fermentation the OUR decreased rapidly corresponding to the complete consumption of glucose (figure 3.54c) and the increase of DOT from both riser probe positions in the vessel (figure 3.54a).

Erythromycin production increased at a slow rate during the first 25 h (up to 10 mgL^{-1}) but the majority of production occurred from 26 to 50 h when the dry cell weight was maximum, glucose consumption near completion and the OUR was in decline (figure 3.54c).

The overall gas holdup reduced from 0.065 to 0.058 during the first 9 h, and increased to 0.116 (figure 3.54d) due to the gas velocity increase to 0.136 ms^{-1}. After nine hours the gas holdup decreased rapidly to 0.071 at 18 h, followed by a slower rate of decrease to a value of 0.057 at 39 h. After 50 h, the gas holdup gradually increased to 0.08 at the end of the fermentation. The duration of gas holdup values below 0.065 from 20.5 to 75 h, coincided with the region of highest apparent viscosity (above 0.8 Pa.s) of the fermentation shown in figure 3.54b.

At 9 h the liquid circulation time and the mixing time had been reduced by the increase in gas velocity and the circulation time remained constant at 12.5 s for the remainder of the fermentation (figure 3.54e). However, the mixing time decreased from 28 s at 20.5 h to 21 s at 40 h which coincided with an increase in apparent viscosity (figure 3.54b). After 42h, the mixing time increased rapidly to 26 s at 50 h and then gradually increased to 30 s at the end fermentation with the reduction in broth viscosity. The turbulent liquid surface presumably associated with the disengagement of large bubbles was observed from the top section sight glasses during the most viscous region of the fermentation (20 to 70 h). However, the build up of a mycelial layer in the sight glasses obstructed the characterisation of the bubble flow in the riser.

The k_La for the lower riser probe position decreased after 18 h into the fermentation, reaching the lowest value of 0.012 s^{-1} at 22 h (figure 3.54f). The k_La remained at the low values until 50 h when k_La increased slowly to 0.015 s^{-1} at 75h. During the period between the 13 and 45 h, the DOT in the riser remained below 1% yet

the k_La reduced corresponding with the decrease in gas holdup and increase in apparent viscosity.

Hyphal length, hyphal growth unit and branch length were shown to increase during the growth phase which coincided with the increase in consistency and dry cell weight (figure 3.55). The further small increase in K to the maximum value at 43 h did not correspond to a large change in morphology although, a small increase from 65 to 72 μm occurred with the hyphal growth unit. The decrease in viscosity and K corresponded to the decrease in hyphal and branch length from 75 h into the fermentation. No significant change of the percentage clumps occurred during the fermentation.

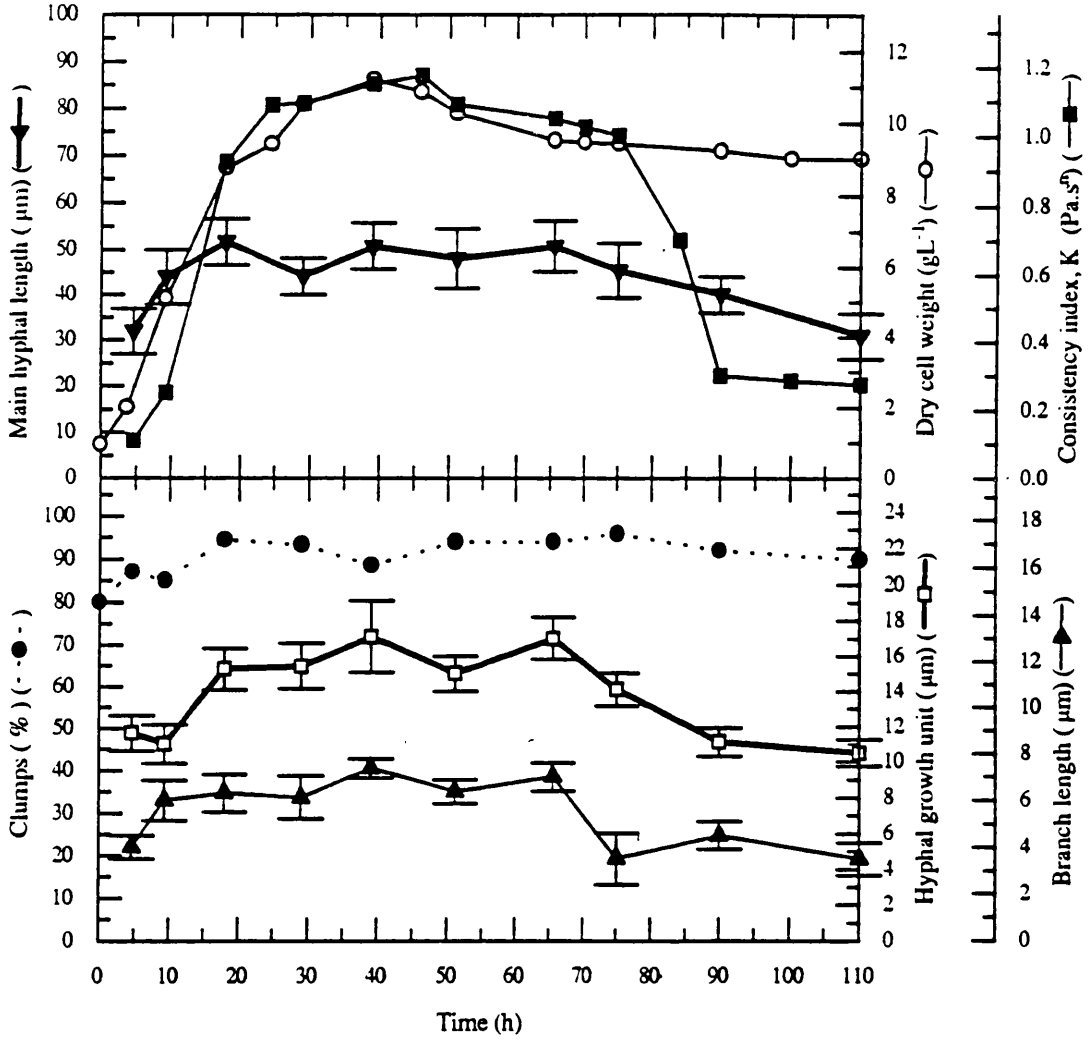

Figure 3.55 Comparison of the change in morphological characteristics (hyphal length, hyphal growth unit, branch length and percentage clumps) to dry cell weight and consistency index during the mycelial *S. erythraea* fermentation in the annulus sparged reactor

3.4.1.4 Study of the *S. erythraea* mycelial fermentation using the annulus sparger configured reactor with propeller operation

The propeller was operated to draw the liquid down the draft tube in the direction of the liquid flow from aeration. During the first 9 h the gas velocity was kept constant at 0.045 ms^{-1} (125 $Lmin^{-1}$) and the DOTs fell to 48% (air saturation) with similar values around the vessel (figure 3.56a). After nine hours the propeller was operated at 600 rpm and successive step wise increases in propeller speed (figure 3.56d) and gas velocity were performed to prevent the DOT in the riser from reaching values below 10%, although this was only successive up to 25 h into the fermentation. The step wise increases in operating conditions produced a succession of fluctuations of the DOT at each probe position during the first 24 h (figure 3.56a). The maximum gas velocity (0.136 ms^{-1}) was required at 11.6 h which was followed by increases of propeller speed to 900 rpm at 24 h. Although, the propeller was operated for short intervals at 1000 rpm with the yeast suspension (section 3.3), over heating of the propeller drive shaft made it impossible for continuous propeller operation at 1000 rpm. At the maximum achievable operating conditions (0.136 ms^{-1} and 900 rpm) the DOT was still only 23% (air saturation) in the lower riser at 25 h. However, after 25 h the DOT from the lower riser further decreased and remained below 10% for a duration of 2.1 h up to 37.5 h into the fermentation. The DOT then increased rapidly to 99% at 42.8 h. Propeller operation was then ceased (figure 3.56d), due to the operational difficulties from the over heating of the propeller drive shaft, and the remainder of the fermentation was completed with aeration only operation as the DOTs were no longer near values below 10%. The lower riser DOT then increased from the aeration only value of 75% to 115% at 75 h. The DOT at the lower downcomer remained around 100% after the first 12 h of the fermentation.

During the first 20 h into the fermentation, the flow behaviour (n) rapidly decreased from 0.9 to 0.5 and K increased up to 1.08 $Pa.s^n$ (figure 3.56b). A similar but slower rate of increase occurred with the apparent viscosity. From 20 to 50 h, small changes in n and K occurred and the apparent viscosity was shown to decrease between 30 to 43 hours due to the increase in liquid velocity (figure 3.56e). Once propeller operation ceased, the apparent viscosity returned to a high aeration only value of 1.4 Pa.s before decreasing towards the end of the fermentation.

The dry cell weight (DCW) increased to a maximum value of 11.75 gL^{-1} at 25 h (figure 3.56c) which coincided with the duration of highest apparent viscosity (figure 3.56b). The DCW remained at this value for a duration of 20 h until decreasing to 9.5 gL^{-1} at 75 h. The maximum oxygen uptake rate (OUR) of 23 $mmol.L^{-1}.h^{-1}$ was produced at 16 h (figure 3.56f) and during the following 21.5 h, the OUR remained relatively constant at this maximum value. At 37.5 h into the fermentation the OUR decreased rapidly to 10 $mmol.L^{-1}.h^{-1}$ at 38.1 h, which corresponded to the complete glucose consumption from the medium (figure 3.56c) and the increase in lower riser

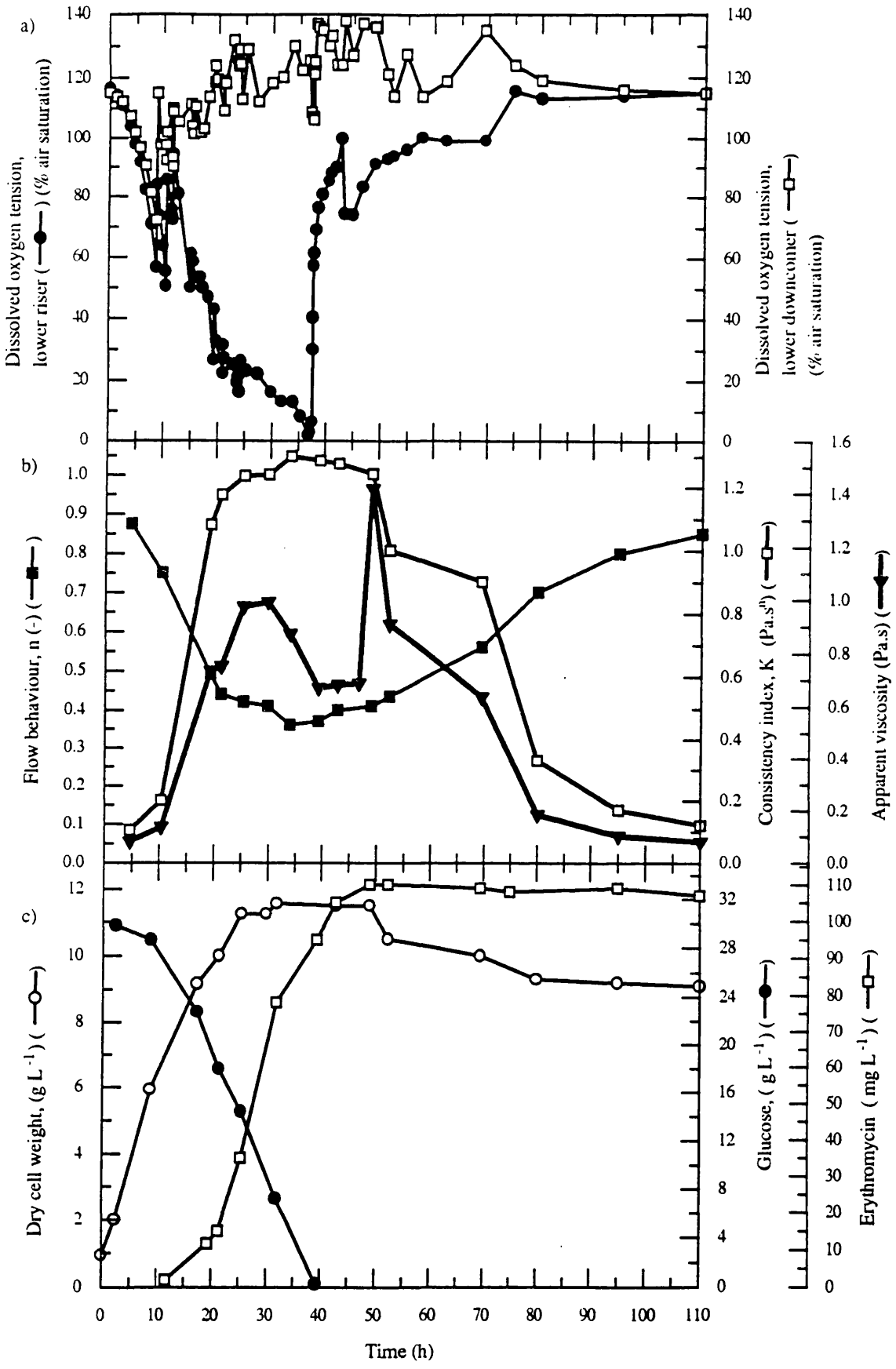

Figure 3.56 (a, b & c) Mycelial *S. erythraea* fermentation with the annulus sparged reactor and propeller operation. Changes of fermentation parameters: a) dissolved oxygen tension (% air saturation), b) rheological properties, flow behaviour, consistency index and apparent viscosity, c) dry cell weight, glucose and erythromycin production

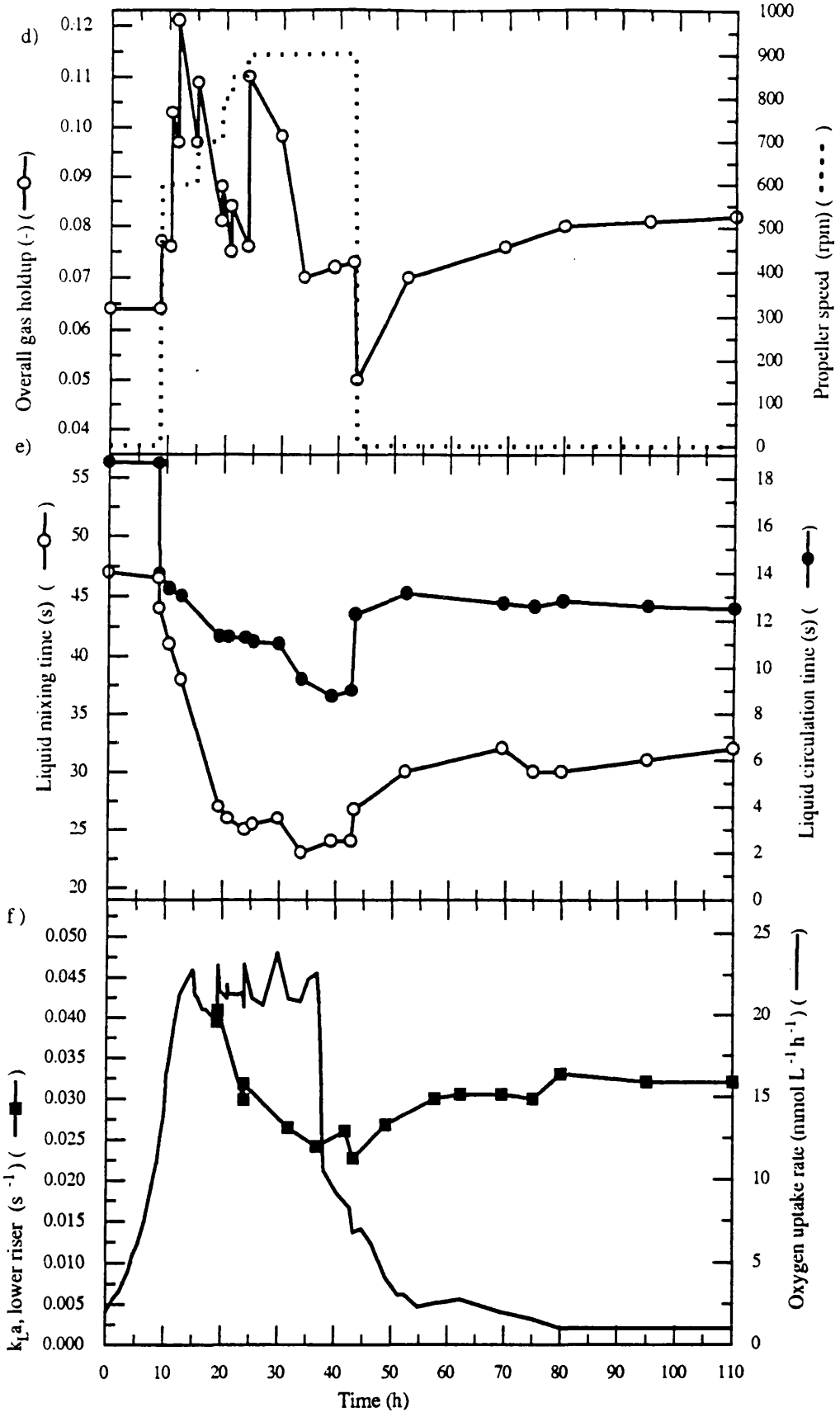

Figure 3.56 (d, e & f) Mycelial *S. erythraea* fermentation in the annulus sparged reactor with aeration and propeller operation. Changes of : d) overall gas holdup and propeller speed, e) liquid mixing and circulation times, f) lower riser k_La and oxygen uptake rate

DOT (figure 3.56a). After 39 hours the OUR decreased and reached 2 mmol.$L^{-1}.h^{-1}$ at 80 h and remained at this value for the rest of the fermentation.

Erythromycin production started after 10 h and increased rapidly (8 fold) as the rate of growth slowed. The rapid linear production phase of erythromycin production, up to 80 mg L^{-1}, occurred before the maximum DCW was obtained. After 30 h when the maximum DCW was achieved the erythromycin production proceeded at a reduced rate reaching a maximum value of 110 mgL^{-1} at 50 h.

Once the maximum achievable operating conditions were obtained, the overall gas holdup decreased rapidly from 0.11 at 24 h to the lowest value during the fermentation of 0.07 at 34 h (figure 3.56d). On removal of propeller operation, the gas holdup returned to the aerated value of 0.05 however, this soon increased to 0.07 during the following 10 h. The overall holdup then gradually increased to a final value of 0.08 at the end of the fermentation. Therefore, during the most viscous period of the fermentation from 17 to 43 h the gas holdup was obtained above 0.069.

During the first 22 h the liquid circulation and mixing time decreased with the stepwise increases in gas velocity and propeller speed (figure 3.56e). However, after 24 h the gas velocity and propeller speed were constant up to 43 h, and a decrease in circulation time was observed during this high viscosity period of the fermentation (figure 3.56b). This referred to a change in circulation time from 11.3 s at 24 h to 8.3 s at 40 h, which referred to an increase of riser liquid linear velocity from 0.44 to 0.6 ms^{-1}. At 43 h propeller operation was removed and the circulation time returned to a conventional aeration value of 12.5 s for the remainder of the fermentation. The mixing time also decreased from 25 to 23 s between the period of 24 to 43 h. After 43 h the mixing time gradually returned to the aeration only value of 30 s.

Lower riser k_La decreased from 0.04 s^{-1} to the lowest value of 0.025 s^{-1} at 40 h into the fermentation coinciding with the decrease in gas holdup. The k_La then gradually increased to 0.035 s^{-1} at the end of the fermentation.

The hyphal length and growth unit were found to increase during the growth phase with consistency index and dry cell weight (figure 3.57). Also, the decrease in K and apparent viscosity corresponded with the decrease in both the morphological parameters including percentage clumps from 70 h. No significant change in branch length was observed during the fermentation.

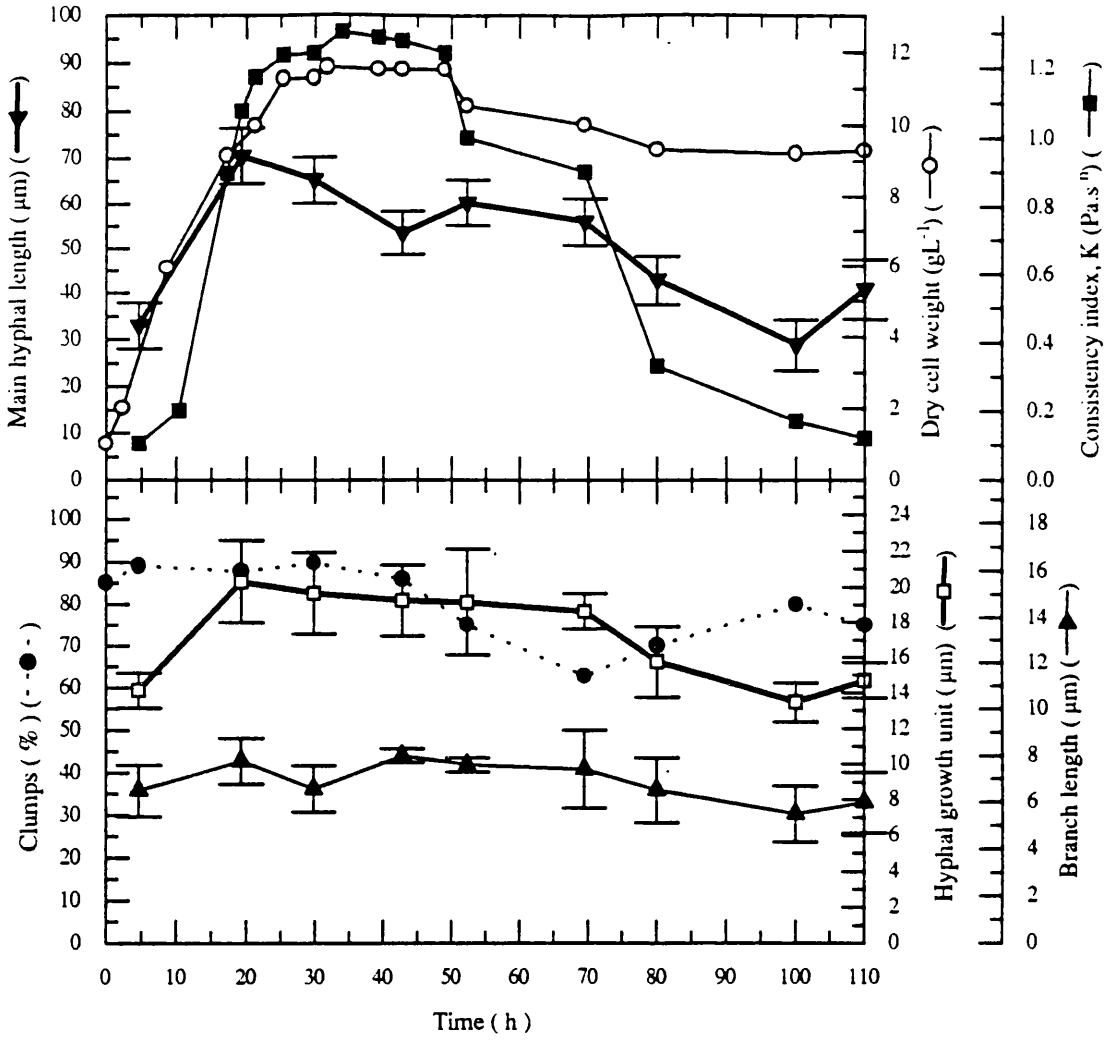

Figure 3.57 Comparison of morphological parameters (main hyphal length, hyphal growth unit, branch length and % clumps) to dry cell weight and consistency index during the mycelial *S. erythraea* fermentation in the annulus sparged reactor with propeller operation

3.4.1.5 Comparison between the characteristics of the mycelial and pelleted fermentations using the draft tube sparger configured reactor

The changes in fermentation parameters during the pelleted fermentation (figure 3.52) were very similar to those observed with the mycelial fermentation (figure 3.50) although, there was a time difference between them due to the smaller concentration of inoculum used for pelleted fermentation. Hence, the lower riser DOT for the pelleted broth fell below 1% (air saturation) at 26.75 h compared to 19 h with the mycelial fermentation as shown in figure 3.58. Nevertheless, the DOT remained below 1% for the same duration of 22 hours with both broths and the small reduction in DOT between 60 to 70 h into the fermentation was also observed with both broths (figure 3.58). The maximum DCW and OUR achieved for both broths were similar although the rates of increase were slower for the pelleted broth (figures 3.59 & 3.60), where maximum values were obtained 7 h later than with the mycelial fermentation. The rate of glucose consumption during the first 16 h of the pelleted fermentation was slower than with the mycelial broth although, the rate of consumption after 16 h was similar to the mycelial

broth (figure 3.60). Hence, the glucose consumption with the pelleted broth was completed some 7 hours later than with the mycelial broth. For both pelleted and mycelial broths, the maximum OUR coincided with the decrease of riser DOT below 1% (figures 3.50 & 3.52). Also, the decline of the OUR to values below 10 $mmol.L^{-1}.h^{-1}$ corresponded with complete glucose consumption from the medium and the increase in riser DOT.

Erythromycin production with the pelleted fermentation began some 10 h later than with the mycelial broth (figure 3.61) although production began with a slow phase for a duration of 20 h with both broths. As the maximum DCW was obtained during the fermentation, the erythromycin production changed to a fast rate of production which was similar for both broths although the final specific production with the pelleted fermentation was 4 mg g^{-1} compared to 7.5 mg g^{-1} for the mycelial fermentation (figure 3.61).

The comparison between the fermentations was hampered by the difference in rheometers, Bohlin cup and bob compared to Contraves concentric cylinder, due to the different shear rate ranges of the rheometers resulting in different consistency values between the fluids. However, both n and K profiles followed similar rates of change during the fermentations in relation to the dry cell weight profiles. The lowest n values for the mycelial fermentation was 0.35 compared to 0.45 for the pelleted broth (figures 3.50b & 3.52b). During the most viscous period for both fermentations between 20 - 60 h, the lower riser k_La and gas holdups for the pelleted fermentation were 17 and 58% greater, respectively than for the mycelial fermentation (figure 3.50 & 3.52). However, the mixing times reduced to similar values during the viscous period of both broths even though the gas holdups and viscosity were different between the broths. These differences in hydrodynamics will be further described in section 3.4.2.

Both fermentations showed that the region of highest viscosity was between 30 to 50 h which did not coincide with the increase in DCW (figures 3.50 & 3.52). A change in hyphal length or growth could not account for this observation although an increase branch length for the mycelial broth (figure 3.51) and an increase pellet diameter (figure 3.53) coincided with the most viscous period of the fermentation.

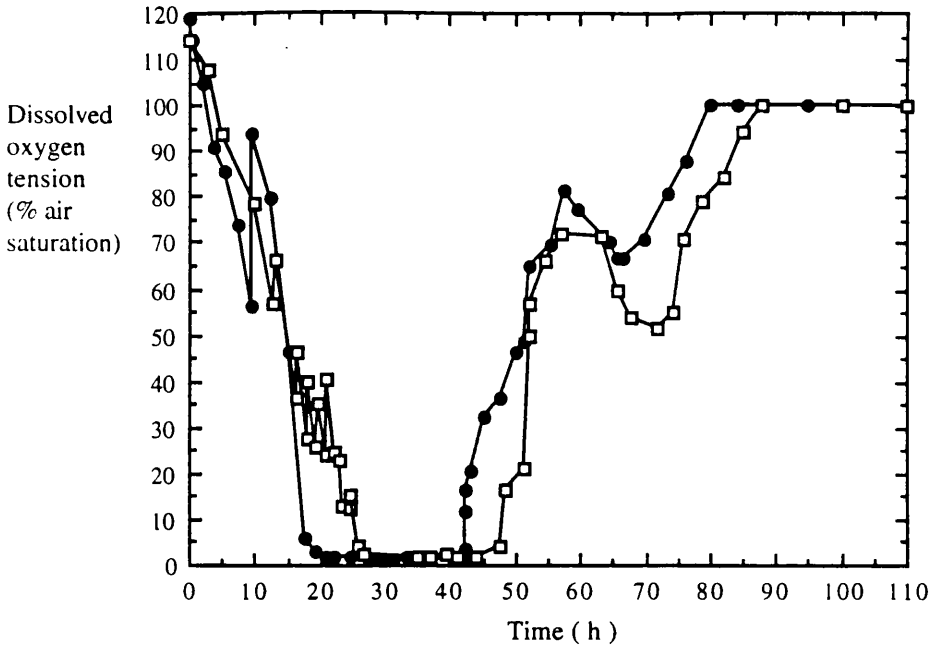

Figure 3.58 Comparison of the lower riser dissolved oxygen tension between the mycelial (•) and pelleted (□) *S. erythraea* fermentations using the draft tube sparged reactor

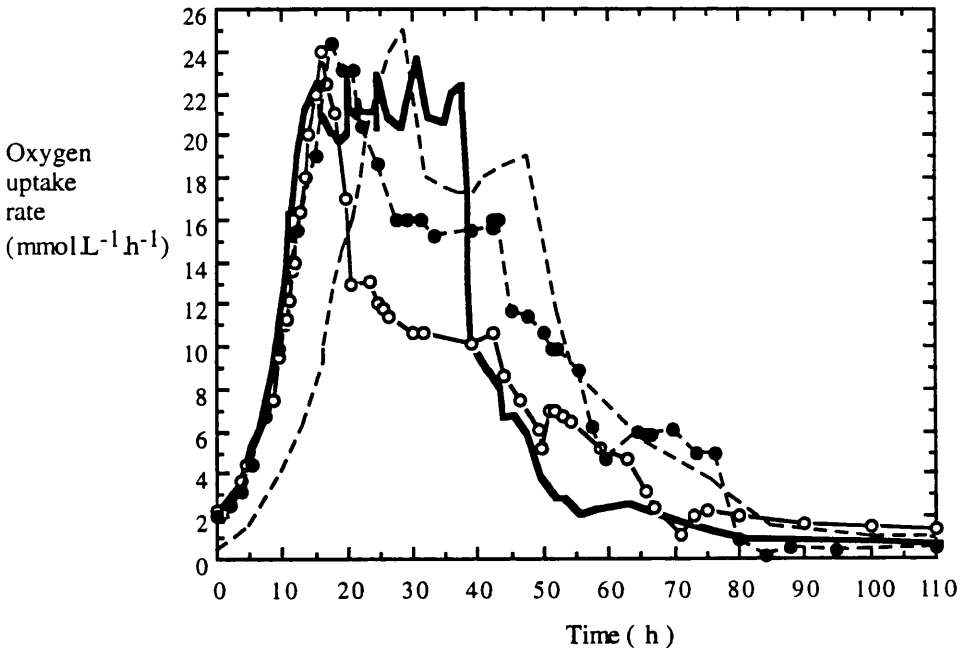

Figure 3.59 Comparison of the oxygen uptake rate profiles during the *S. erythraea* fermentations of mycelial; draft tube sparged (-•-), annulus gas sparged (—o—) pelleted; draft tube sparged (- - -),and mycelial; annulus sparged plus propeller operation (——)

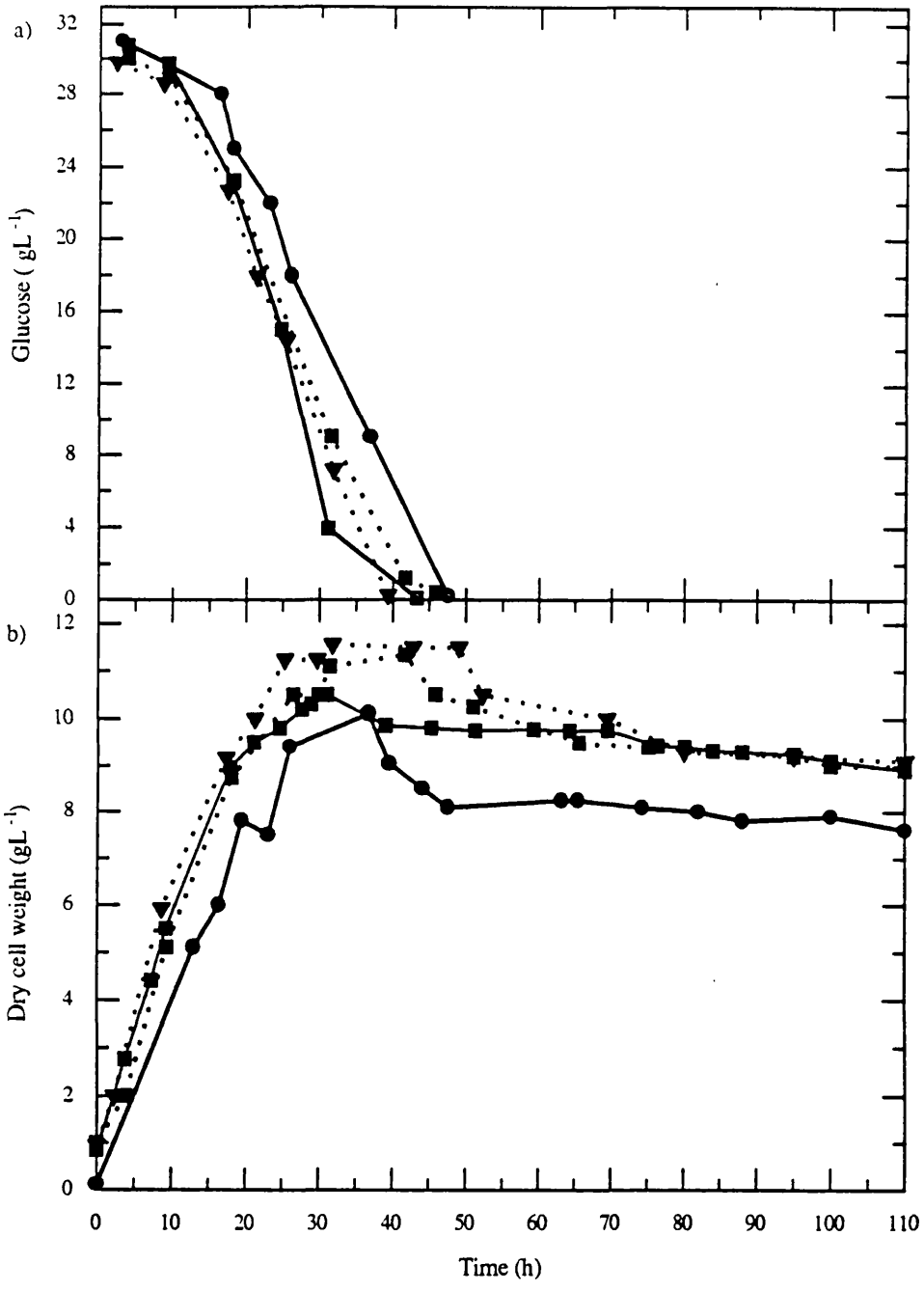

Figure 3.60 a & b Comparison of glucose consumption and dry cell weight between the *S. erythraea* fermentations of : pelleted (●), mycelial (■) in the draft tube sparged reactor (——), and annulus sparged reactor (·····), and mycelial with combined aeration and propeller operation (·-▼-·)

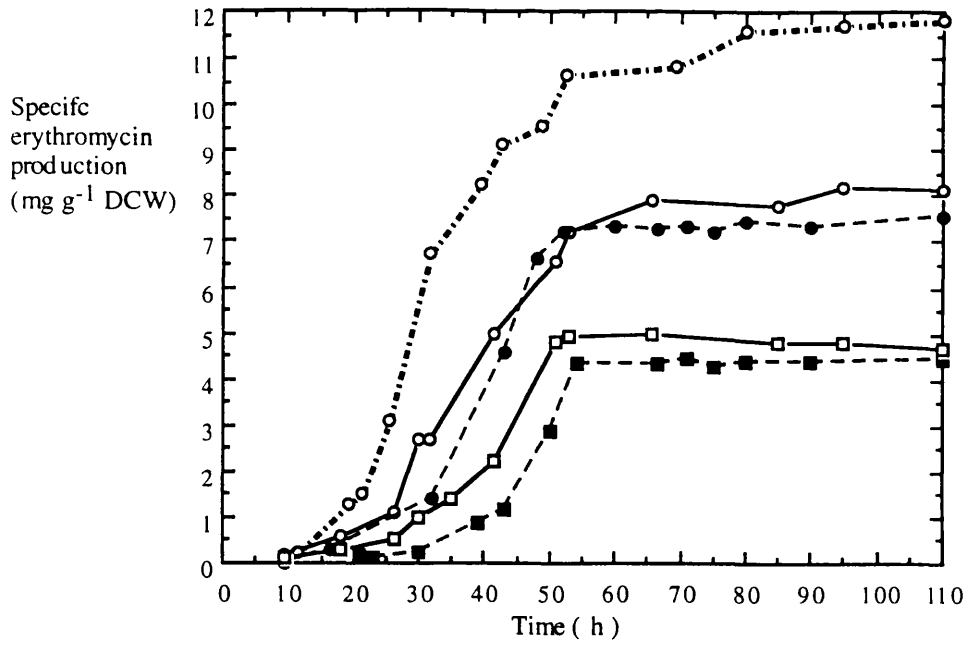

Figure 3.61 Comparison of specific erythromycin production from the *S. erythraea* fermentations; mycelial (circles)pelleted (squares) in the reactor configurations of : draft tube sparged (closed symbols- - - -), annulus sparged (open symbols———) annulus sparged and propeller operation (open symbols— • —)

3.4.1.6 Comparison of the fermentation characteristics from the mycelial fermentations in the two aerated reactor configurations

During the first 9 h, the DOTs reduced with similar values around the vessel for the mycelial fermentations in both reactor configurations (figures 3.62 & 3.63). However, the rate of reduction of riser DOT after the increase in gas velocity to 0.136 ms^{-1} was faster with the broth in the annulus sparger configured reactor than in the reactor with the draft tube sparger (figure 3.62). Whereby, the lower riser DOT was below 1% (air saturation) at 12 h into the fermentation with the annulus sparger configuration compared to 19 h in the draft tube sparger. The riser DOT with the annulus sparger also remained below 1% for a duration of 38 h compared to 25 h with the draft tube sparger configured reactor hence, the DOT from the broth with the annulus sparger rose some 8 h later than with the draft tube sparger. This rise in DOT followed similar profiles for both fermentations except that the DOT profile with the annulus sparger configuration did not have the secondary decrease in DOT observed at 60 h with the draft tube sparger configuration (figure 3.62). Apart from the first 9 h, the lower downcomer DOTs with the annulus sparger configuration were greater than with the draft tube sparger at all times during the fermentation (figure 3.63). Also, the fluctuations of DOT observed between 30 and 50 h with the lower downcomer probe position from the annulus sparger configuration were not observed with the draft tube sparger configuration.

Although a direct comparison of the rheology of the broths was difficult, due to the use of different rheometers, it seemed reasonable to compare flow behaviour (n)

values. The flow behaviour during the fermentation with the draft tube sparger configured reactor decreased up to 40 h into the fermentation with a peak value of 0.35 and then increased at a similar rate to 0.75 at the end of the fermentation (figure 3.50b). Whereas, with the annulus sparger the n values decreased rapidly during the first 20 hours to 0.5 and maintained for duration of 60 h with a small decrease to a minimum value at 40 h, of 0.44 (figure 3.54b). Hence, the flow behaviour profiles were considerably different between the reactor configurations, whereby values of n below 0.5 were maintained for a duration of 50 h (20 h - 70 h into the fermentation) with the annulus sparged reactor compared to 30 h (30 - 60 h into the fermentation) with the draft tube sparger configuration.

The dry cell weight (figure 3.60) and oxygen uptake rate (figure 3.59) profiles during the fermentations were similar from both reactor configurations. However, the OUR maintained during 19 to 43 h into the fermentation with the draft tube reactor configuration (16 $mmol.L^{-1}.h^{-1}$) was greater than with the annulus sparger configuration (12 $mmol.L^{-1}.h^{-1}$).

The glucose concentration in the medium was similar during the first 20 h of the fermentation for both broths (figure 3.60). Between 20 and 35 h the glucose consumption was faster from the broth in the draft tube configured reactor than with the annulus sparger configuration. However, the completion of glucose consumption occurred at similar times around 45 h for both fermentations.

The specific erythromycin production was similar for both fermentations with the slow production rate which occurred during the first 25 hours followed by a rapid increase of antibiotic production between 30 and 50h (figure 3.61). The final specific erythromycin production was slightly greater with the broth in annulus sparger configuration reaching 7.7 mgg^{-1} DCW at 60 h compared to 7 mgg^{-1} DCW at 50 h. Similar erythromycin production occurred between the two fermentations even though the difference of OURs occurred between 19 to 43 h (figure 3.59) and that the DOT in the lower riser of the annulus sparger reactor remained below 1% for 13 h longer (figure 3.62) than with the broth in the draft tube sparger configured reactor.

Overall gas holdup followed a similar shape profile during the fermentation in both reactor configurations (figures 3.50f & 3.54f). However, from 20 h into the fermentation, gas holdup reduced at a slower rate with the broth in the annulus configured reactor to the lowest value of 0.055 at 40 h compared to a faster rate of reduction in the draft tube sparger reactor reaching 0.043 at 40 h. This faster rate of holdup reduction between 20 and 40 h with the draft tube sparged reactor coincided with the larger change in flow behaviour (n) during this period compared to the small change associated with the annulus sparger. The mixing time profiles also followed a similar profile during the fermentation although the minimum time at 40 h was 21.5 s with the

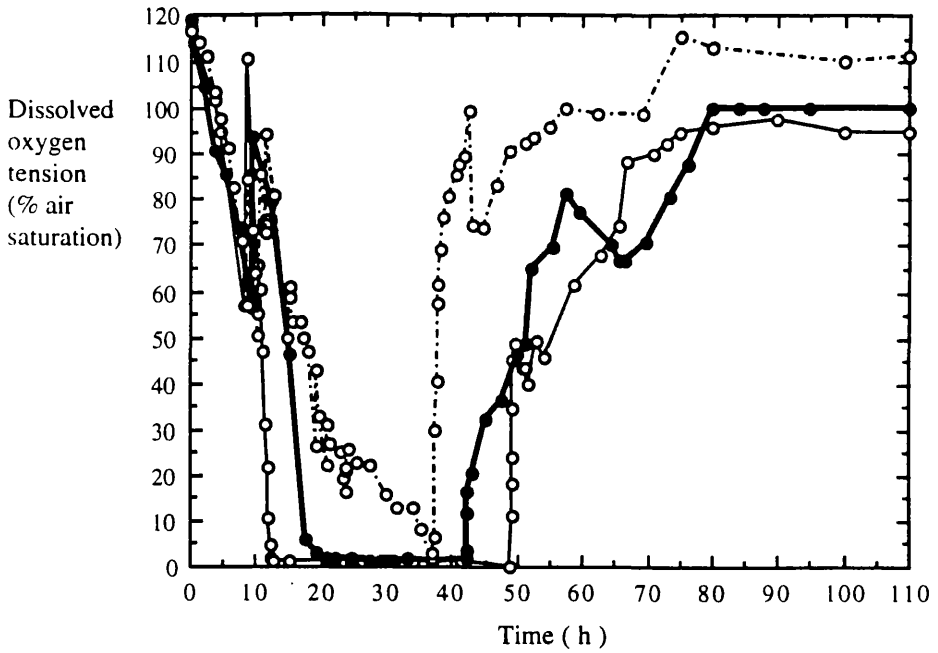

Figure 3.62 Comparison of the lower riser dissolved oxygen tensions (% air saturation) from the three mycelial *S. erythraea* fermentations; draft tube sparged (—●—) annulus sparged (—o—), and annulus sparged plus propeller operation (··o··)

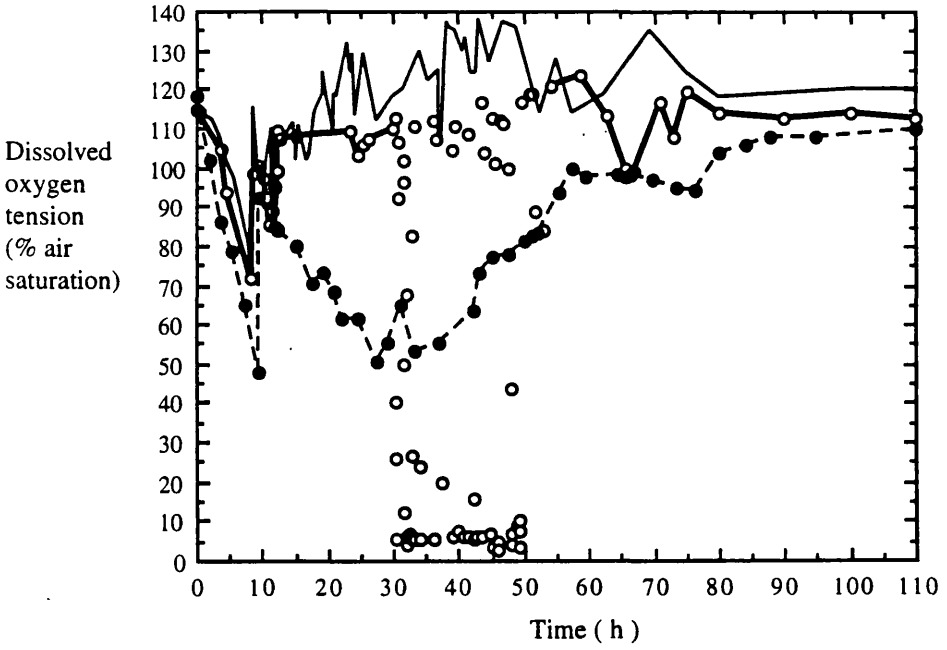

Figure 3.63 Comparison of the lower downcomer dissolved oxygen tensions during the mycelial *S. erythraea* fermentations in the reactor configurations of : draft tube sparged (··●··), annulus sparged (—o—), and annulus sparged plus propeller operation (——)

broth in the annulus sparger configuration rather than 24.8 with the draft tube sparger configuration (figures 3.50e & 3.54e). Also, the liquid circulation time after 9 h remained constant during the change in rheology of the fermentation for both broths however, circulation for the annulus sparger configuration was maintained at 12.5 s compared to 11.3 s for the reactor with draft tube sparger.

During the most viscous period of the fermentation 20 to 50 h of the fermentations the lower riser k_La from both fermentations (figures 3.50f & 3.54f) decreased during the increase in viscosity while the lower riser DOT remained below 1%. The change in k_La was also similar to the change in gas holdup for both broths.

For the mycelial fermentation in the annulus sparger configured reactor the increase in consistency index (K) was found to occur with the increase in DCW which may be associated with the increase in hyphal length, hyphal growth unit and branch length during this period (figure 3.55). However, for the mycelial fermentation in the draft tube sparger reactor the hyphal length and growth unit increased during the growth phase, but the consistency index did not reach a maximum value with the dry cell weight but increased to a maximum value some 8 h later (figure 3.51). This coincided with an increase in branch length with the draft tube sparged reactor which remained constant in the reactor during the same period with the annulus sparger configuration. The mean main hyphal length was consistently between 2- 10 μm shorter with the broth in draft tube sparger configuration than with the broth with the reactor configured with the annulus sparger (figure 3.64).

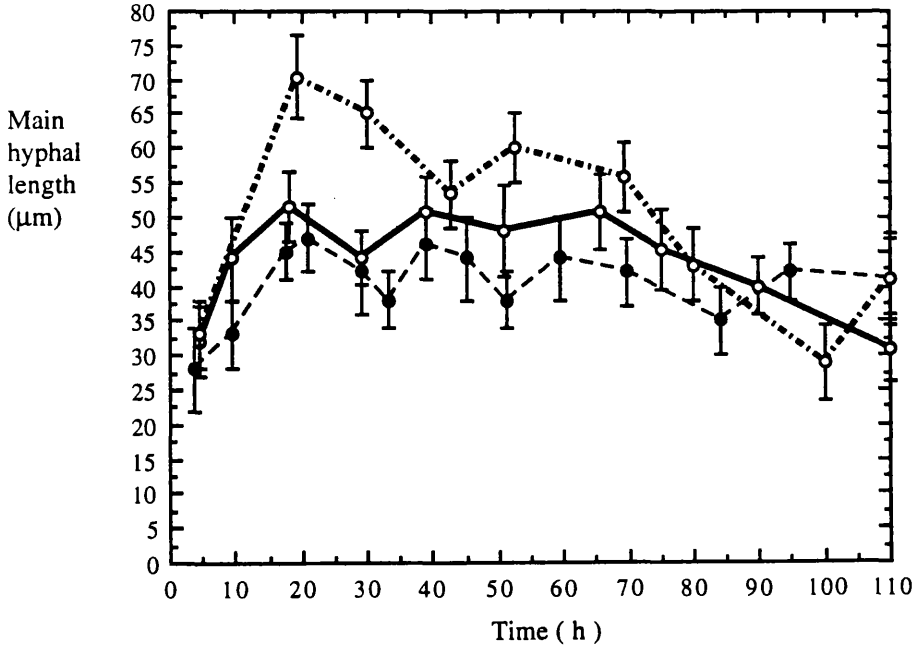

Figure 3.64 Comparison of main hyphal length from mycelial *S. erythraea* fermentations with the reactor configurations; draft tube air sparged (-•-), annulus air sparged (—o—) and annulus air sparged plus propeller operation (-·o·-)

3.4.1.7 Comparison of the mycelial fermentation to the pelleted fermentation with aeration from the annulus sparger

The pelleted fermentation produced almost identical DOT profiles, rheological properties, dry cell weights and oxygen uptake rates as the mycelial fermentation as similar inoculum concentrations were used for both broths (results not shown). The pelleted diameter was similar to the pellets produced with the draft tube sparger configuration. However, the erythromycin production was less than with the mycelial fermentation (annulus air sparged) but similar to the pelleted broth with the draft tube air sparging (figure 3.61). The circulation and mixing times were similar to the mycelial annulus air sparged broth although the gas holdup was greater with the pelleted broth which will be described in section 3.4.2.

3.4.1.8 Comparison of the mycelial fermentation characteristics between the conventional aerated annulus sparged reactor and the combined aerated and propeller operated reactor

Propeller operation was sufficient to prevent the riser DOT from reaching values below 5% saturation for most of the fermentation apart from a short duration between 35 and 37 h (figure 3.62). This was considerably different from the severe oxygen limitation in the lower riser from 13 to 48 h in conventionally aerated reactor (figure 3.62). Also, the DOT at the lower riser with propeller operation rose some 14 h earlier than with conventional aeration. The DOTs from the lower downcomer were similar from both conventional aeration and propeller operated fermentations (figure 3.63). Hence, propeller operation reduced the DOT heterogeneity that the cells experienced around the vessel compared to the heterogeneity observed with conventional aeration. Also, the DOT fluctuations observed at 30 to 50 h with the aerated fermentation were not observed during the fermentation with the propeller operation (figure 3.63)

Both fermentations showed a rapid increase in consistency and apparent viscosity and similar decrease in flow behaviour during the first 20 h (figures 3.54b & 3.56b). However, after 20 h higher consistency values above 1.2 $Pa.s^n$ occurred with the broth from propeller operation compared to values below 1.2 $Pa.s^n$ with aeration only operation. Nevertheless, propeller operation resulted in lower apparent viscosities (below 1.0 Pa.s) than aeration only operation (above 0.95 Pa.s). The apparent viscosity decreased from 0.95 Pa.s at 25 h to 0.7 Pa.s at 40 h due to the decrease of the liquid circulation time observed with propeller operation (figure 3.56b). Whereas, during the same period with aeration only operation (figure 3.54b), the apparent viscosity increased from 0.95 to 1.275 Pa.s due to a small increase in K from 1.05 $Pa.s^n$ to 1.2 $Pa.s^n$ and an increase in circulation time from 12.2 to 12.5 s. However, after propeller operation was removed at 43 h the apparent viscosity returned to an aeration only value of 1.4 Pa.s (figure 3.56b). Also the reduction in apparent viscosity and K was similar in both

reactors although it began at 50 h with the propeller operated broth compared, to 70 h with the broth with aeration only operation.

No significant difference between the DCW for both fermentations was observed (figure 3.60). Also the OUR (figure 3.59) and glucose consumption (figure 3.60) were similar for both fermentations during the first 20 h hence, the different DOT heterogeneity that the cells experienced in the two operating conditions seemed not to effect the growth rate. However, after 20 h the OUR was maintained at the maximum value of 25 $mmol.L^{-1}.h^{-1}$ until 38 h compared to the aerated only fermentation where the OUR was maintained at 16 $mmol.L^{-1}.h^{-1}$ until 48 h. Hence, the glucose concentration reduced at a faster rate after 20 h with propeller operation, where the glucose in the medium was below 0.05 gL^{-1} at 38 h compared to 48 h with aeration only operation. Hence, propeller operation resulted in a higher rate of metabolism, causing complete glucose consumption to occur some 10 h earlier than with conventional aeration operation (figure 3.60).

Erythromycin production began at 10 h into the fermentations under both operating conditions (figure 3.61). However, the rates of erythromycin production during the slow and fast production phases were greater with propeller operation than with aeration only operation. Also, the change from the slow to fast production phases with propeller operation occurred at 20 h into the fermentation which was before the maximum DCW was achieved (figure 3.56c). Whereas, with aeration only operation the change to the faster production phase occurred 5 hours later. Although, the final production value occurred at the same time of 50 h into the fermentation with both reactor configurations, the specific erythromycin production from propeller operation was 11 mgg^{-1} compared to 7 mgg^{-1} with aeration only operation.

The gas holdup during the fermentations under the two operating conditions was found to decrease with increasing viscosity once constant operating conditions were achieved (figures 3.54d & 3.56d). However, propeller operation enabled the gas holdup to remain above 0.07 compared to values near 0.055 during the viscous period of the fermentation with aeration only operation (20 - 70 h). The higher gas holdup with propeller operation resulted in greater oxygen transfer shown by the larger lower riser k_La values of 0.025 s^{-1} compared to 0.015 s^{-1} during the period of 20 - 40 h with aeration only operation. This accounted for the reduced DOT heterogeneity associated with propeller operation. Once the operating conditions were constant (after 24 h) with propeller operation then the liquid circulation time reduced with the increasing viscosity to a fast time of 8.25 s (figure 3.56e) whereas, the circulation time remained constant with the aeration only operation at 12.5 s during the change in viscosity (figure 3.54e). Also, the mixing times decreased with increasing viscosity once the operating conditions remained constant with propeller operation from 25 to 22 s however, a more significant reduction in mixing times was observed with aeration only operation from 27 to 21 s (figures 3.54e & 3.56e).

For both broths the consistency index (K) was found to increase with dry cell weight which was also associated with an increase in main hyphal length and growth unit (figures 3.55 & 3.57) . However, during the first 70 h of the fermentations, the main hyphal length for the broth under propeller operation was between 3 to 20 μm longer than with aeration only operation also, a larger growth unit was observed with propeller operation. Branch length and the percentage of clumps were similar for both broths although the percentage of clumps decreased to 68% during the fermentation with propeller operation at 70 h whereas, it remained constant at 90% with the aerated only broth. Also, both broths showed that the decrease in K and apparent viscosity was associated with an decrease in main hyphal length.

3.4.2 Comparison of the hydrodynamic measurements made at two intervals during each *S. erythraea* fermentation

Measurements of gas holdup, liquid velocity and mixing time were made as a function of gas velocity, by stopping normal operation for a short time interval, and then reverting back to normal operation. Measurements were taken during the stationary phase at 29 and 39 hours into each fermentation. This was during the most viscous period of the fermentation, which enabled hydrodynamic comparisons to be made between the two measurement intervals with respect to, the change in broth viscosity which occurred during this period, and with the Newtonian baker's yeast suspensions. The hydrodynamic changes between the two intervals could also be related to the erythromycin production which was taking place in the stationary phase. Measurements were carried out within 30 minutes to minimise any effect on oxygen uptake rate and antibiotic production. The superficial gas velocity range was between 0.068 and 0.191 ms^{-1}, where the lower value was restricted to prevent a reduction of the oxygen uptake rate and the upper value was determined by the availability of sufficient head space.

3.4.2.1 Comparison of the relationship between gas holdup and superficial gas velocity for the mycelial and pelleted fermentations in the draft tube sparged reactor

For the yeast broth (section 3.1) overall gas holdup increased rapidly with the increase in gas velocity upto 0.054 ms^{-1} (figure 3.65). This was followed by a reduction in the rate of increase of gas holdup with further gas velocity increases as described in section 3.1.1. The profile from the pelleted fermentation at 29 h, which had a 200 fold greater apparent viscosity than yeast (table 3.2), showed a similar gas holdup to gas velocity relationship as the yeast broth, although the values were reduced. At 39 h the apparent viscosity had doubled and lower values of holdup were observed than at 29 h. Also, the gas holdup increased gradually with gas velocity increases above 0.113 ms^{-1} and hence, at the gas velocity of 0.145 ms^{-1}, the overall holdup was 0.07 at 39 h compared to 0.09 at 29h. The difference between overall and downcomer gas holdups

Table 3.2 Rheological characteristics of the baker's yeast and *S. erythraea* broths used in the draft tube air sparged reactor at 29 and 39 h into the fermentations.

Broth type and morphology		Flow behaviour n (-)	Consistency index K (Pa.s^n)	Apparent viscosity, μ_a (Pa.s) at gas velocity of 0.136 ms^{-1}
Baker's yeast		1	0.02	0.003
Pelleted	29 h	0.66	0.625	0.33
	39 h	0.47	1.1	0.77
Mycelial *	29 h	0.5	0.525	0.098
	39 h	0.35	0.6	0.214

* mycelial broth rheology measured using a Bohlin cup & bob rheometer rather than the Contraves concentric bob used for all other broths.

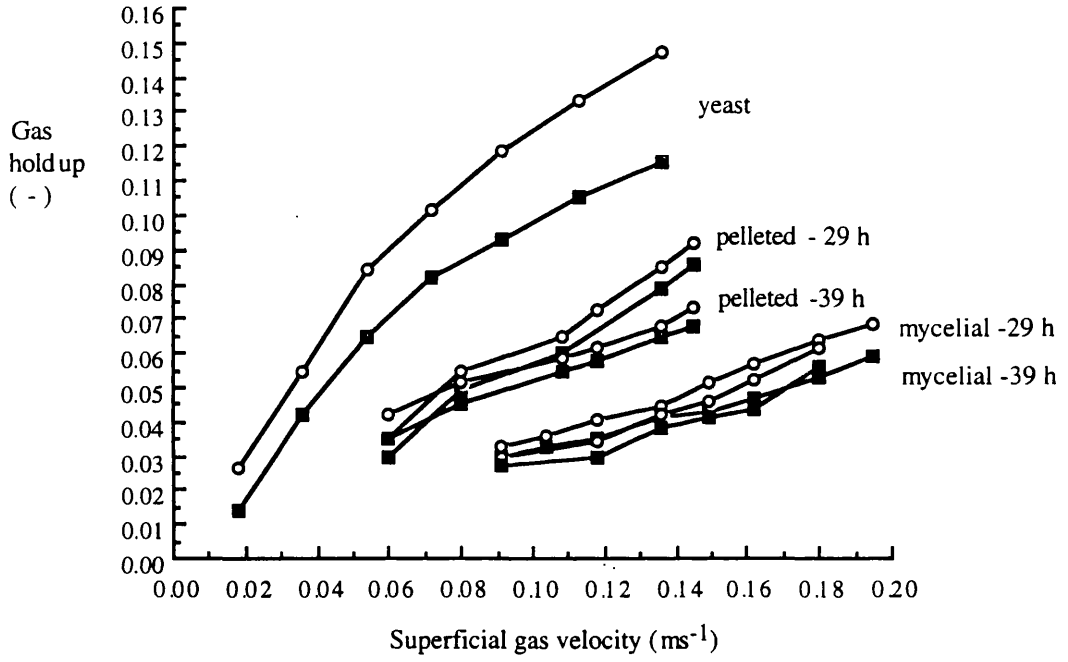

Figure 3.65 Comparison of the effect of superficial gas velocity on overall and downcomer gas holdup between the baker's yeast broth, and mycelial / pelleted broths of *S. erythaea*, with the draft tube sparged airlift reactor configuration. Overall gas holdup (—o—), downcomer gas holdup (—■—) measurements were made at 29 and 39 h into the *S. erythraea* fermentations.

with the pelleted broth was much smaller than at the same gas velocities with the yeast broth. The holdup values with the mycelial broths were further reduced from the other broths, yeast and pelleted and the flow behaviour (n) at 29 h was similar to that of the pelleted broth at 39 h but lower than the other broths at 39 h (table 3.2). A large increase in gas velocity was required to produce only a small increase in gas holdup with the mycelial broths (figure 3.65). Also, no significant difference in gas holdup was observed between the two measurement periods of 29 and 39 h and the overall and downcomer gas holdup remained within close proximity at all gas velocities as observed with the pelleted broth.

3.4.2.2 Comparison of gas holdup measurements between mycelial and pelleted fermentation in the annulus aerated and propeller operated reactor.

A gradual reduction in the rate of increase of gas holdup was observed with increasing gas velocity for the yeast suspension and the riser and overall gas holdups were within close proximity (figure 3.66). The pelleted broth gas holdups increased with gas velocity at a similar rate to the yeast broth yet the apparent viscosity was 600 fold greater than with the yeast suspension (table 3.3) hence, the holdup values were reduced. A similar rate of increase of holdup with gas velocity was observed with the mycelial broths although the values were further reduced from those of the pelleted broths and the apparent viscosity was greater, (0.91 against 0.76 Pa.s). For both pelleted and mycelial profiles the riser gas holdup was within closer proximity to the overall gas holdup than observed with the yeast broth at the same gas velocities.

For propeller operation (900 rpm) with the mycelial broths, the holdup followed a similar rate of increase with gas velocity as for the mycelial fermentation with aeration only operation. Except that the values for propeller operation fell between those measured with the pelleted and yeast broth. Nevertheless, the apparent viscosity at 29 h for propeller operation was similar to the mycelial broth from conventional aeration (table 3.3). Also, the overall gas holdup was greater than the riser gas holdup at all gas velocities which was a characteristic observed with propeller operation using the yeast broths as shown in figure 3.66. It can also be seen that propeller operation with the mycelial broths produced a similar improvement of gas holdup above the aeration only operation values as with the yeast broth.

Table 3.3 Rheological characteristics of the baker's yeast and *S. erythraea* broths used in the annulus air sparged reactor configurations at 29 and 39 h into the fermentations.

Broth type and morphology		Flow behaviour n (-)	Consistency index K (Pa.s^n)	Apparent viscosity, μ_a (Pa.s) at gas velocity of 0.136 ms^{-1}
Baker's yeast		1	0.02	0.003
Pelleted	29 h	0.5	0.95	0.76
	39 h	0.48	1.01	0.9
Mycelial	29 h	0.47	1.095	0.91
	39 h	0.43	1.15	1.1
Mycelial + propeller (900 rpm)	29 h	0.41	1.24	0.99
	39 h	0.37	1.29	0.67

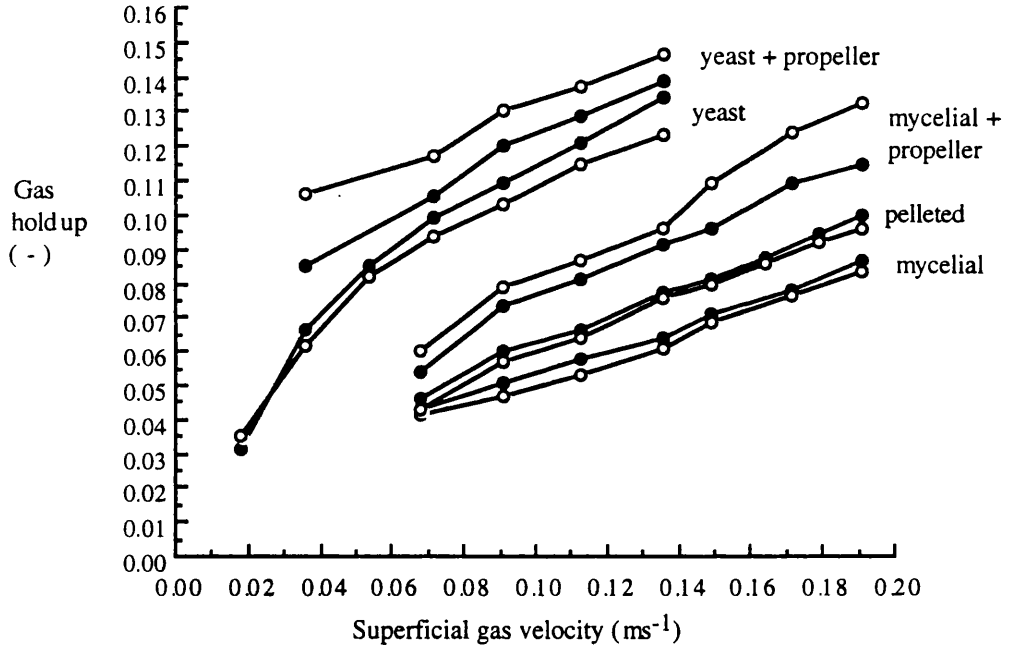

Figure 3.66 Comparison of the effect of superficial gas velocity on overall and riser gas holdup between the operating conditions of aeration only and,combined aeration and propeller operation (900 rpm), with the annulus sparged reactor. Measurements were taken at 29 h into the mycelial / pelleted *S. erythraea* fermentations and with the yeast suspension (10 gL^{-1} DCW). Overall gas holdup (o), riser gas holdup (•)

3.4.2.3 Comparison of the relationship of overall gas holdup and superficial gas velocity between different morphologies and reactor configurations

The differences between the yeast profiles of the two aerated configurations were described in section 3.1.1, where the increase in gas velocities above 0.054 ms^{-1} resulted in lower gas holdup with the annulus sparger configuration than with the draft tube sparger configured reactor (figure 3.67). However, the mycelial gas holdup profiles with the annulus sparger were higher at 29 h than the profiles measured with the draft tube sparger yet the flow behaviour were similar. Nevertheless, the rate of increase of gas holdup with gas velocity was similar between the two configurations. The profiles with the pelleted broths of the two aerated configurations were similar between the gas velocities of 0.095 and 0.136 ms^{-1} yet, the apparent viscosity with the broth from the annulus sparger was 2 fold greater than with the broth from the draft tube sparged reactor. However, at gas velocities above 0.136 ms^{-1}, the pelleted fermentation with the draft tube sparger had an upward trend compared to the gradual increase observed with the broth with the annulus sparger.

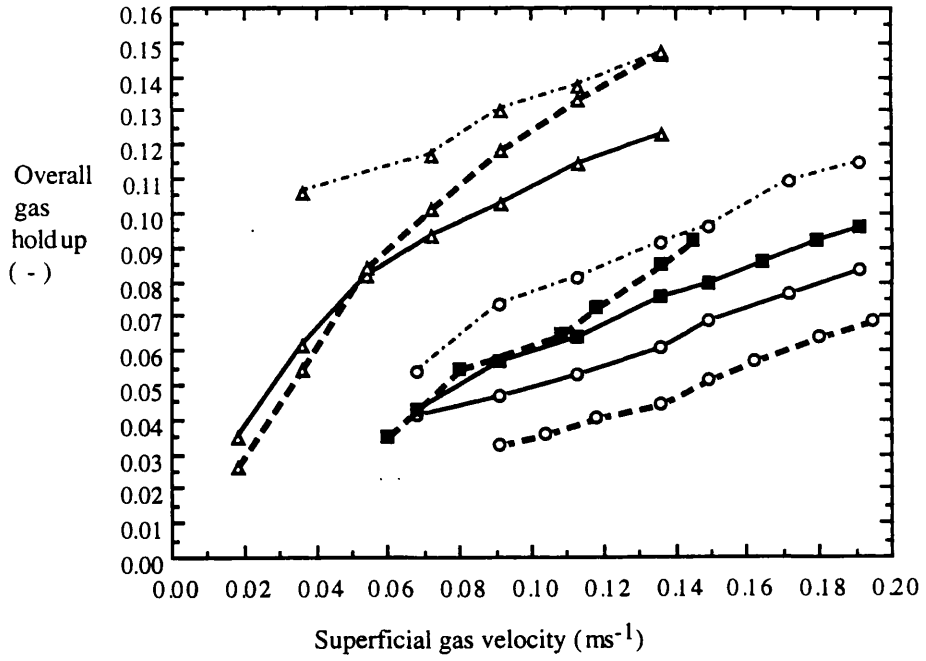

Figure 3.67 Comparison of the effect of superficial gas velocity on overall gas holdup between the two sparger configurations, annulus air sparged (——), draft tube air sparged (- - -) and the annulus sparged / propeller operated reactor (·-··). Measurements were made at 29 h into the mycelial (o) / pelleted (■) *S. erythraea* fermentations and baker's yeast broth (▲)

3.4.2.4 Comparison of the liquid circulation times and velocities between the different morphological broths and operating conditions

The effect of gas velocity on the liquid circulation time was similar for the aerated only mycelial broths with a constant rate of decrease with increasing gas velocity (figure 3.68). However, the circulation times with the annulus sparger were slower than those for the draft tube sparger at both time intervals. Figure 3.68 also shows that the aeration only circulation times for the mycelial broths were similar to the corresponding yeast broths even though the apparent viscosity was 1000 fold greater (table 3.2 & 3.3).

Although, faster liquid circulation occurred with the draft tube sparger configuration than with the annulus sparger configuration the difference was not as significant in relation to liquid velocities due to the difference in cross sectional areas of the riser and downcomer between the two sparger configurations (appendix 9.1). The effect of gas velocity on the liquid velocities of the pelleted fermentations were similar to the effect with the mycelial broths at both time intervals and both aeration configurations (appendix 9.2).

For aeration and propeller operation at 900 rpm the circulation times at 29 h were lower than with the aeration only operation (annulus sparger) although they decreased with a similar rate of reduction with the increasing gas velocity (figure 3.68). The improvement of the circulation times with propeller operation compared to conventional aeration with the mycelial broths at 29 h can be seen in figure 3.68 to be similar to the improvement of liquid circulation by propeller operation with the yeast suspension, despite the differences in rheological characteristics (table 3.2 & 3.3). However, the circulation times at 29 h with combined aeration (annulus sparger) and propeller operation were similar to those obtained at 29 h with aeration only operation from the draft tube sparger configuration. Nevertheless, at 39 h the circulation times were considerably faster with propeller operation than the other operating conditions and the rate of decrease was reduced above gas velocities of 0.136 ms^{-1}. The effect of propeller operation on liquid circulation was further confirmed in figure 3.69 whereby, the riser and downcomer liquid velocities at 39 h with the mycelial broths under propeller operation were significantly greater than under conventional aeration operation and the apparent viscosity was also 36% lower than with normal aeration (table 3.3).

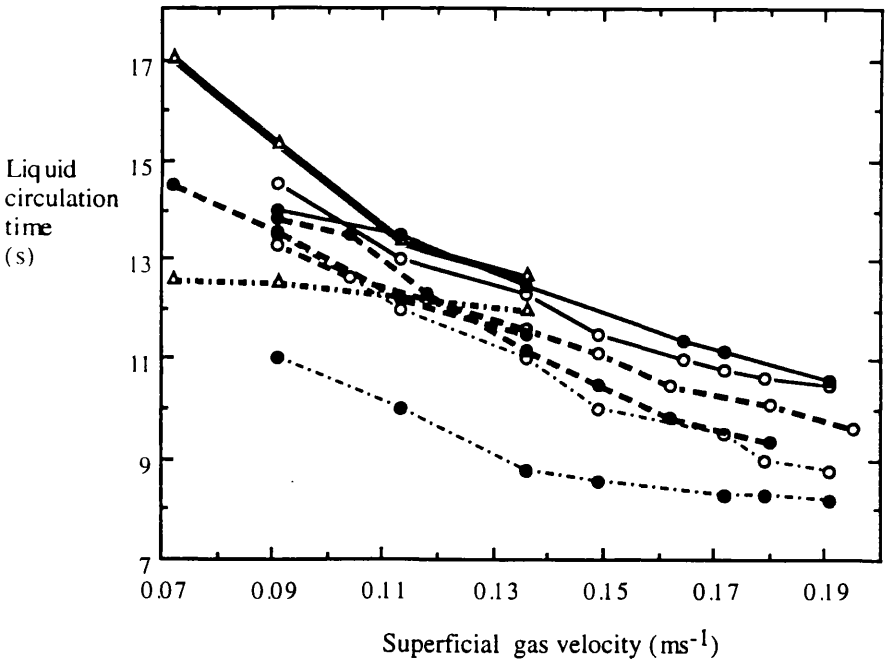

Figure 3.68 Comparison of the effect of superficial gas velocity on the liquid circulation times at 29 h (open symbols) and 39 h (closed symbols) into the fermentations of mycelial *S. erythraea* broths with aeration from the draft tube sparger (-o-), annulus sparger (—o—), and annulus sparged/ propeller operated (- -o- -) and also compared with the baker's yeast broths; draft tube sparged (—●—) annulus sparged (—▲—), and annulus / propeller operated (-▲-)

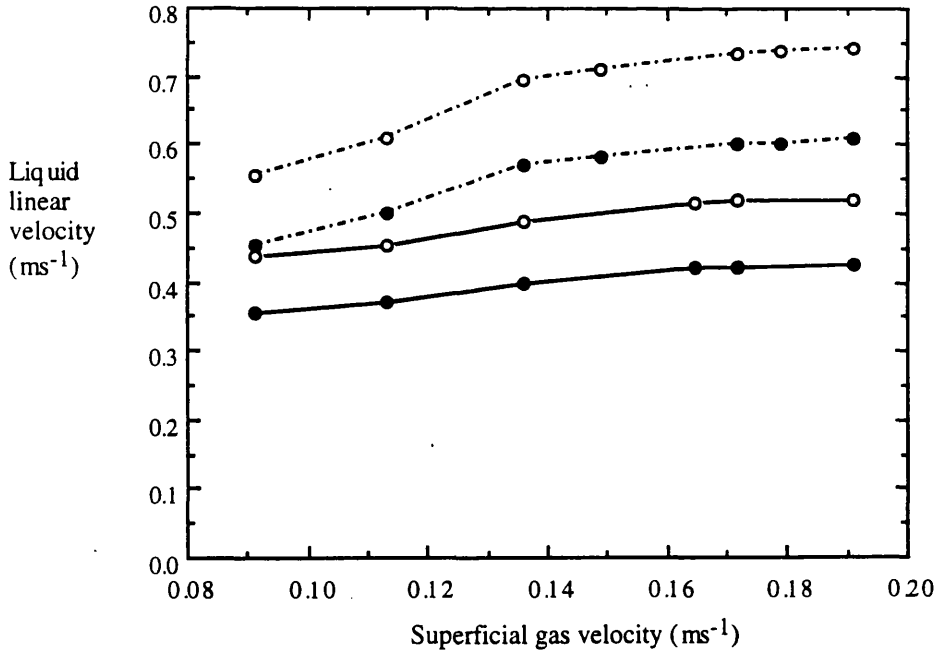

Figure 3.69 Comparison of the effect of superficial gas velocity on riser and downcomer liquid linear velocities at 39 h into mycelial *S. erythraea* fermentations with aeration from the annulus sparger (—), and aeration / propeller operation (– –). Liquid linear velocity : riser (●) and downcomer (o)

3.4.2.5 Comparison of the effect of gas velocity on the mixing time measured with the different broths and operating conditions

The mixing times for the mycelial broths at both time intervals and aeration only configurations showed a similar rate of decrease with the increasing gas velocity (figure 3.70). Also, the mixing times at 29 h for mycelial broths from both sparger configurations were similar and had similar flow behaviours (tables 3.2 & 3.3). At 39 h, the mixing times from air sparging with the annulus sparger were lower than with the draft tube sparger configuration hence, there was a greater change in mixing times between 29 and 39 hours with the broth in the annulus sparger configuration. However, there was a greater reduction in flow behaviour during the 10 h duration from 0.5 to 0.35 with the draft tube sparger broth compared to 0.47 to 0.43 with the annulus sparger broth. The mixing times from the pelleted broth with draft tube air sparging at 29 h were considerably slower than with the mycelial broths and the apparent viscosity of the pelleted broth (draft tube sparger) was 3 fold lower than with the mycelial broths (annulus sparger). At 39 h the mixing times and apparent viscosities were similar between the pelleted and mycelial broths.

For propeller operation with annulus air sparging the mixing times at 29 h were similar to normal aeration only values although they were slower at gas velocities above 0.15 ms^{-1} (figure 3.71). Mixing times at 39 h with propeller operation were only similar to mixing times with conventional aeration above the gas velocity of 0.14 ms^{-1}. To compare the mixing times of the mycelial broths with the yeast broth involved a comparison at the same gassed heights and under the same operating conditions as it was shown in section 3.1.6.3 that mixing time decreased with increasing top section height. Thus, the mixing times with the highly pseudoplastic *S. erythraea* broths were shown in figure 3.71 to be considerably shorter than the mixing times with the Newtonian yeast suspension.

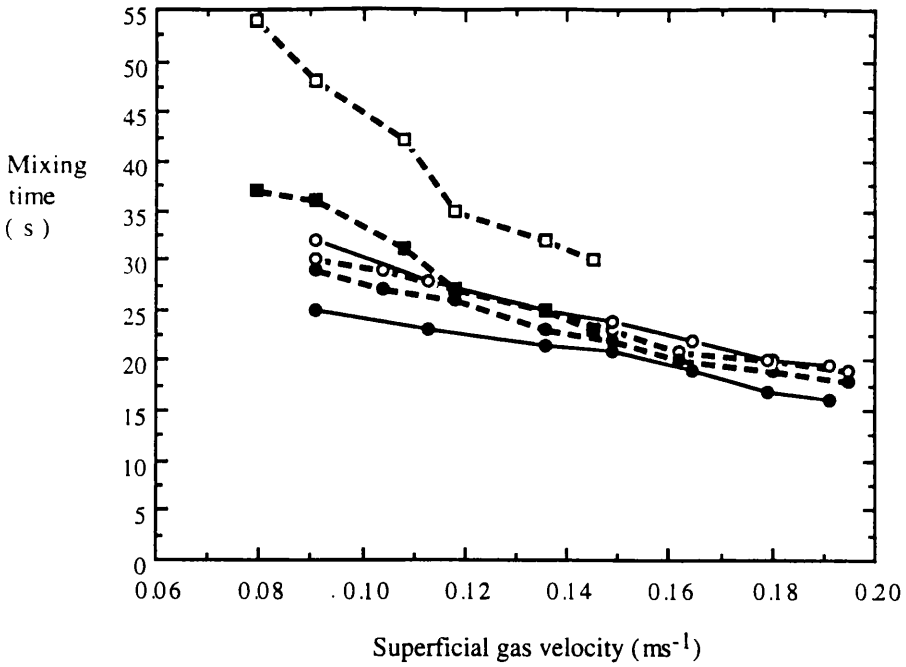

Figure 3.70 The effect of superficial gas velocity on the liquid mixing time measured at 29 & 39 h into the mycelial / pelleted *S. erythraea* fermentations with aeration from the draft tube sparger (• • • •), and annulus sparger (——). Symbols ; mycelial broths (circles), pelleted (squares), measuring interval : 29 h (open), 39 h (closed)

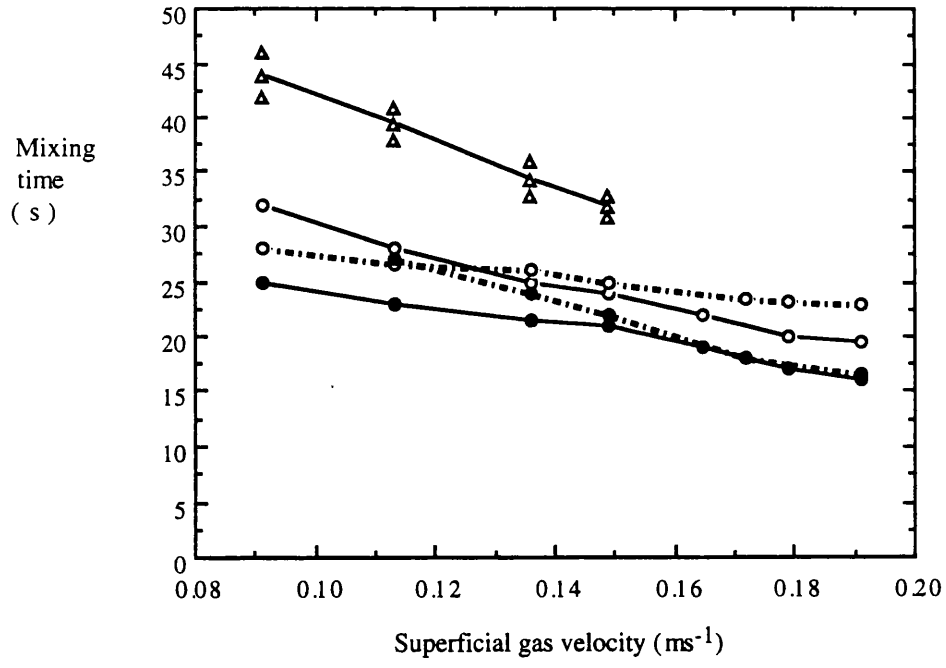

Figure 3.71 Comparison of the effect of superficial gas velocity on liquid mixing time between the mycelial *S. erythraea* broths, and baker's yeast suspensions with aeration from the annulus sparger (——), and with annulus aeration / propeller operation (• • • •). Symbols: measuring interval at 29 h (open), 39 h (closed) into the mycelial fermentations, mycelial broths (circles) and baker's yeast (triangles)

3.4.3 Hydrodynamic investigation of the draft tube air sparged reactor with xanthan gum

A characteristic of the aerated *S. erythraea* airlift reactor fermentations was that the liquid circulation rate remained constant with the changing apparent viscosity during the fermentation. This was further investigated by studying the effect of apparent viscosity on the liquid circulation and gas holdup at increasing concentrations of xanthan gum. Xanthan was recommended by Buckland (1993) as a preferred pseudoplastic broth simulant fluid. The concentration range (0.1 to 0.625% w/v) of xanthan gum was chosen to give a range of apparent viscosities (table 3.4) which were observed during the different *S. erythraea* fermentations.

Table 3.4 The concentration and rheology of xanthan gum solutions used for the hydrodynamic studies with and without antifoam addition

Xanthan gum concentration (% w/v)	Flow behaviour, n (-)	Consistency index, K ($Pa.s^n$)	Apparent viscosity (mean) (Pa.s)	Ap.viscosity (mean) with antifoam addition (0.1% v/v) (Pa.s)	Symbol
0.1	0.7	0.35	0.183	0.183	○
0.2	0.6	0.8	0.49	0.49	●
0.25	0.55	1.0	0.68	0.68	□
0.325	0.47	1.2	1.05	1.0	■
0.375	0.41	1.3	1.55	1.08	△
0.5	0.35	1.45	4.73	1.9	▲
0.625	0.3	1.7	19.88	13.7	⊠

(Apparent viscosity measured with a superficial gas velocity of 0.136 ms^{-1})

3.4.3.1 Effect of superficial gas velocity on gas holdup with increasing concentrations of xanthan gum

The relationship of overall gas holdup and superficial gas velocity was similar for the yeast and 0.1% w/v xanthan solution (figure 3.72). Also, for larger xanthan concentrations the gas holdups were similar to yeast with gas velocity increases up to 0.035 ms^{-1}. However, for gas velocity increases above 0.035 ms^{-1}, the rate of increase of gas holdup was reduced with increasing xanthan gum concentration. Hence, the relationship of gas holdup to gas velocity with increasing pseudoplastic viscosity (table 3.4) showed a similar relationship to the gas holdup interval measurements with the *S. erythraea* broths (figure 3.65). However, the gas holdup values from the interval measurements as a function of gas velocity for the *S. erythraea* broths (section 3.4.2)

were found to be much lower than the xanthan gum solutions of equivalent rheological characteristics. Therefore, the antifoam concentration used in the *S. erythraea* broths was added to the xanthan gum solutions and the gas holdup values were lower than with the xanthan solutions without antifoam although, the rates of increase with gas velocity were similar (figure 3.72). Hence, the gas holdup values from the *S. erythraea* broths were now found to be closer to the rheologically equivalent xanthan gum solution when it contained antifoam. This is confirmed in figure 3.74a where the overall gas holdup values from the *S. erythraea* broths at different apparent viscosities through the fermentations and at the gas velocity of 0.136 ms^{-1}, were found to be similar to the xanthan solutions containing antifoam, rather than the higher holdup values associated with the xanthan solutions without antifoam. All three fluids show a similar rapid decrease in gas holdup with apparent viscosity increases up to 1.0 Pa.s followed by a slower rate of decrease with the xanthan solutions above 1.2 Pa.s.

The difference between the overall and downcomer gas holdup for the 0.1% xanthan solution was found to be similar to the yeast suspension (figure 3.73). As the xanthan concentration (with and without antifoam) was increased to 0.625% w/v the difference between the overall and downcomer gas holdup decreased. Hence, the density difference between the riser and downcomer for xanthan gum solution of 0.625% w/v was similar to the combined xanthan and antifoam solution. Similar small density differences were observed with the *S. erythraea* broths (figure 3.65). Hence, a comparison of the gas holdup profiles as a function of gas velocity between fluids of equal rheological properties, 5% xanthan solution, 5% xanthan + antifoam solution and the mycelial broth at 39 h showed that they all had a similar difference between overall and downcomer gas holdup.

3.4.3.2 The effect of superficial gas velocity on the liquid circulation rates of the draft tube sparged reactor with increasing concentrations of xanthan gum

For xanthan gum solutions up to 0.25%, the liquid circulation rates were found to be similar to those with the yeast broth. However, further increases of the xanthan gum concentration resulted in a reduction in the liquid velocities in the reactor. This is demonstrated in figure 3.74b for the constant operating conditions of 0.136 ms^{-1}. The riser liquid velocity decreased with increases of apparent viscosity above 0.5 Pa.s (0.25% xanthan solution). However, the riser liquid velocity did not decrease until the apparent viscosity was above 1.2 Pa.s with the xanthan gum and antifoam solution. The liquid velocities from the *S. erythraea* broths at gas velocities of 0.136 ms^{-1} had similar values to the xanthan gum solutions with antifoam (figure 3.74b). Also, the relationship between gas velocity and riser liquid velocity was similar for both the *S. erythraea* broths and the xanthan gum solutions with and without antifoam, however the values for the xanthan gum solution without antifoam were reduced (figure 3.75). Therefore, the

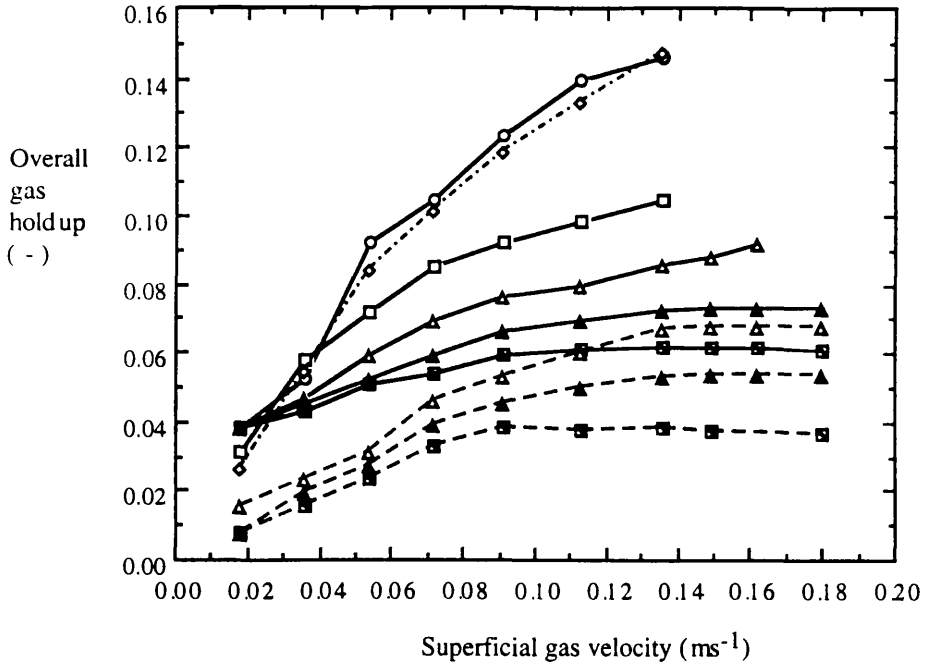

Figure 3.72 The effect of superficial gas velocity on overall gas holdup with xanthan gum solutions (—)(%w/v): 0.1 (○), 0.25 (□), 0.325 (△), 0.5 (▲), 0.625 (■) compared to xanthan gum solutions containing antifoam (- -) and to the yeast suspension (-◇-) with the draft tube air sparged airlift reactor

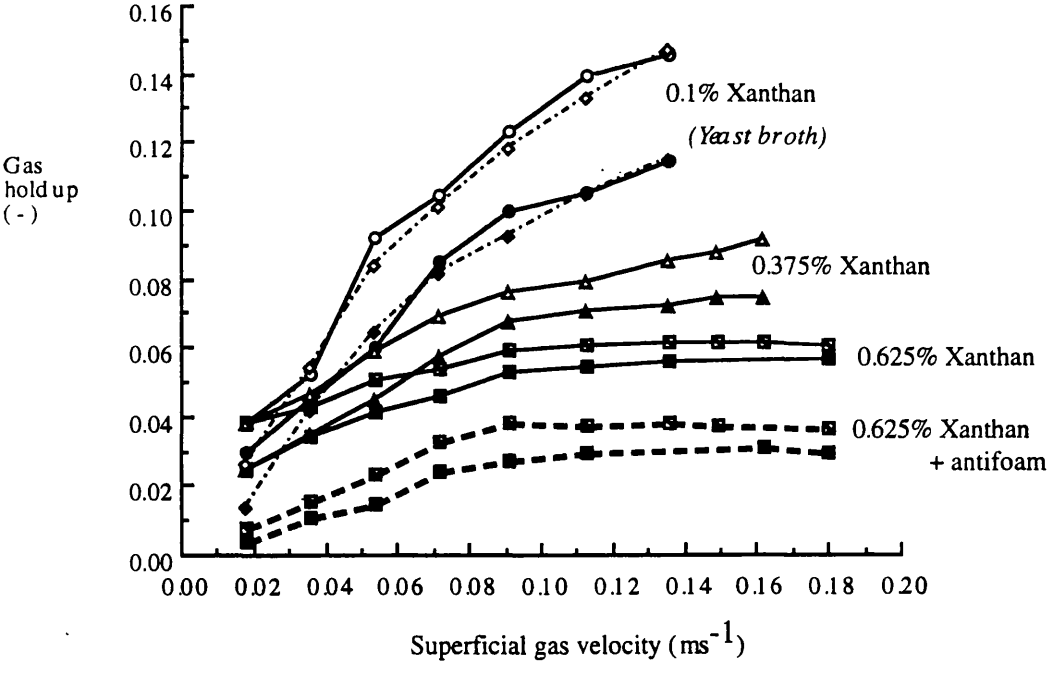

Figure 3.73 The effect of superficial gas velocity on the overall and downcomer gas holdups of xanthan gum solutions (%w/v) (——), with antifoam (▪▪▪▪) and baker's yeast (▪◇▪) in the draft tube air sparged reactor. Symbols: overall gas holdup (open), downcomer (closed)

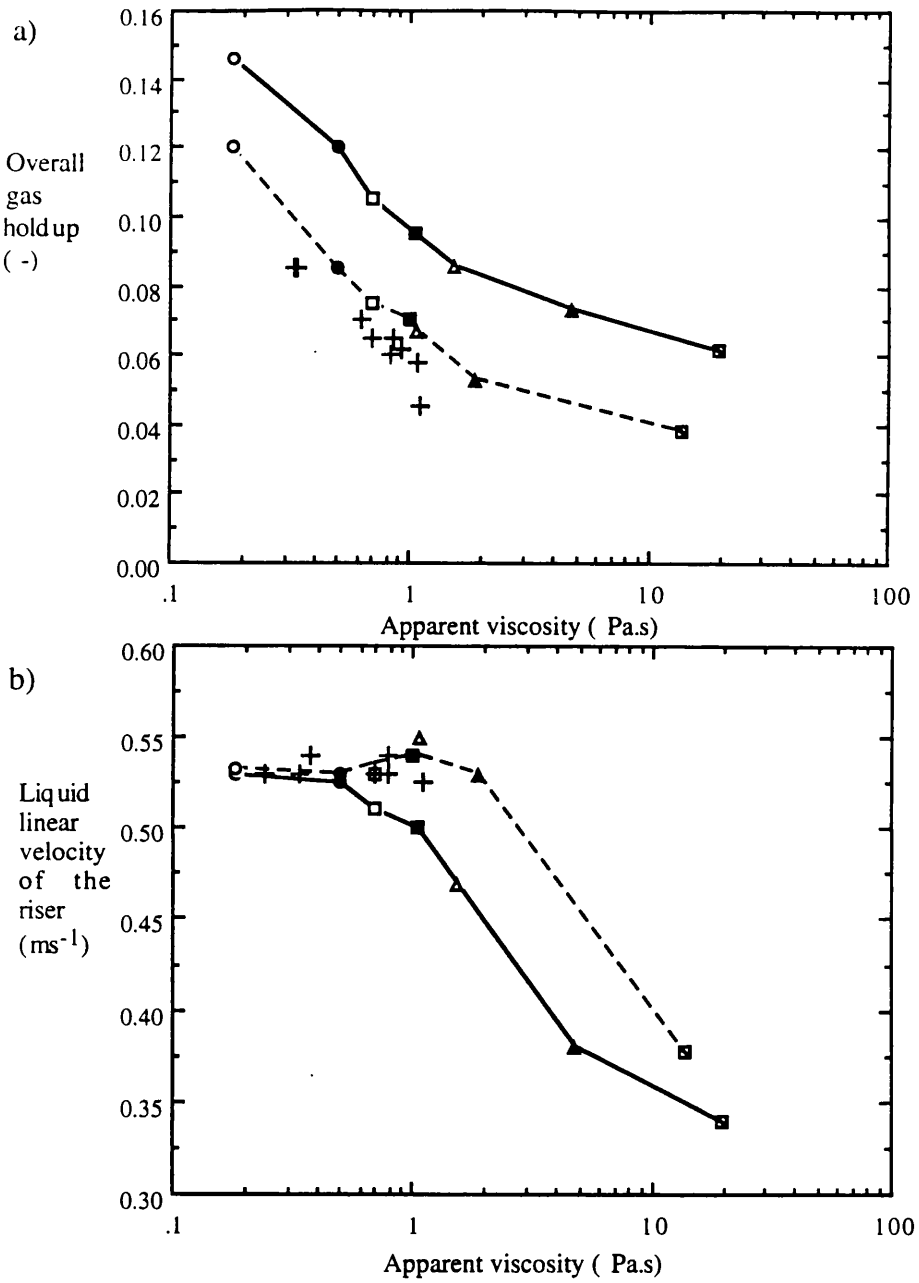

Figure 3.74 The effect of apparent viscosity on the overall gas holdup (a), riser liquid linear velocity (b) of xanthan gum solutions (——), with antifoam (- - -), and *S. erythraea* broths (+) using the draft tube sparged reactor at a constant gas velocity of 0.136 ms^{-1}. Xanthan concentrations as shown in table 3.4

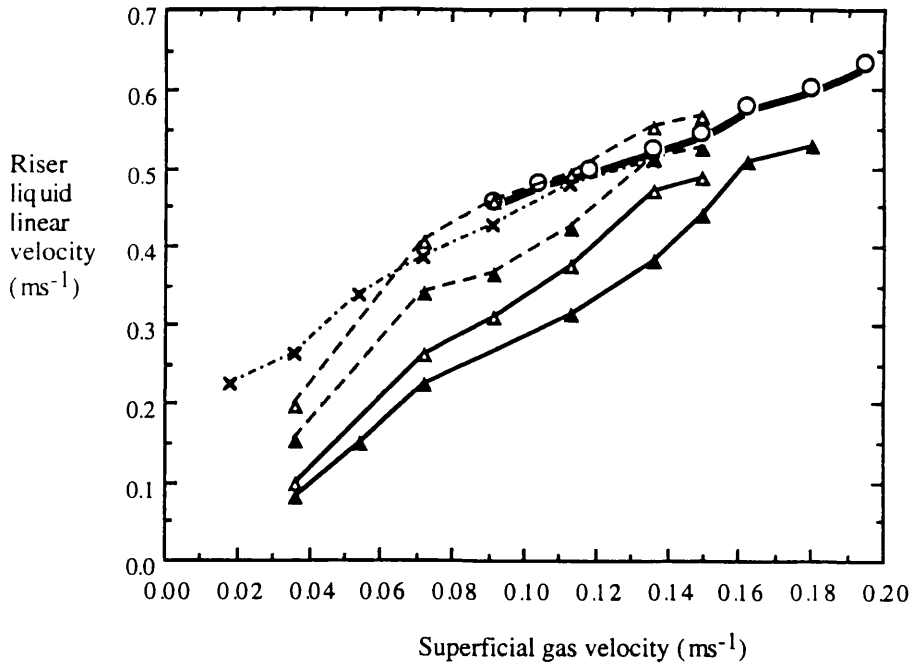

Figure 3.75 Comparison of the effect of superficial gas velocity on riser liquid linear velocity from the draft tube sparged reactor with xanthan gum solutions (—) of concentration (%w/v); 0.375 (▲), 0.5 (▲) and with antifoam (- - -), compared to baker's yeast (—✱—), and mycelial *S. erythraea* broth from an interval measurement at 29 h into the fermentation (—O—)

antifoam constituent of the medium for the *S. erythraea* broths reduced the impact of apparent viscosity on the liquid velocity until higher apparent viscosities were achieved than with viscous solutions without antifoam.

3.4.3.3 The effect of superficial gas velocity on the bubble flow regime

The bubble flow in the top section and downcomer was visually observed with xanthan gum solutions containing antifoam. The liquid motion in the top section was turbulent at all gas velocities whereas bubbly flow with a calm liquid surface was observed for gas velocities below 0.054 ms^{-1} with water (section 3.1.5). The turbulent motion became enhanced at lower gas velocities as the xanthan concentration was increased. As the superficial gas velocity was increased large slug shaped bubbles of 10 - 30 mm in diameter were observed rising through the top section. The slug shaped bubbles disengaged from the liquid surface enhancing the turbulent liquid surface. The superficial gas velocity at which slug formation occurred decreased as the xanthan gum concentration increased. Hence, slug formation occurred at the gas velocity of 0.091 ms^{-1} with the xanthan gum concentration of 0.25% w/v compared to 0.072 ms^{-1} with the xanthan concentration of 0.5%. Amongst the slug shaped bubbles in the top section were small bubbles ranging in diameter from 0.5 to 4 mm in diameter. In the downcomer the majority of bubbles at all gas velocities had diameters of 0.5 - 2 mm although some bubble diameters were up to 4 - 6 mm. Occasionally at the highest superficial gas

velocity (0.136 ms^{-1}) large bubble slugs (10 - 25 mm in diameter) were observed rising up against the wall of the downcomer at high speed, but this only occurred with xanthan concentrations equal to and greater than 0.5% w/v. A single slug shaped bubble could be followed rising from below the lower downcomer sight glass and rising passed each of the sight glasses to disengagement in the top section.

3.4.4 Study of an *S. erythraea* fermentation in a laboratory stirred tank reactor

The comparison of erythromycin production between the mycelial fermentations from conventional aeration and aeration + propeller operation (section 3.4.1) revealed that the specific erythromycin production and final volumetric titre could be improved if the DOT heterogeneity was reduced. Therefore, the effects of cycling DOTs on growth rates and erythromycin production from the heterogeneous environments of the airlift reactor were compared to the less heterogeneous environment of a 42 L stirred tank. The 25 L (working volume) stirred tank performance was not compared to the airlift reactor on an equal energy dissipation basis but at a dissipation rate necessary to prevent oxygen limitation as an attempt to maximise erythromycin production.

3.4.4.1 The mycelial laboratory scale stirred tank fermentation

The dissolved oxygen tension (DOT) decreased rapidly during the first 17 h into the fermentation (figure 3.76b). Then, the airflow rate and stirrer speed were step wise increased (figure 3.76a) to prevent the DOT in the vessel from falling below 10% (air saturation). However, at 23 h the DOT had reached 10% and maximum OUR of 28 $mmol.L^{-1}.h^{-1}$ was obtained. Under constant operating conditions from 23 h, the DOT further decreased to below 1% for a duration of 5 h at 32 h. Meanwhile, the OUR had remained above 20 $mmol.L^{-1}.h^{-1}$ before the rapid increase in DOT at 37 h, which coincided with glucose depletion from the medium and a rapid decrease in OUR. Once, the DOT had increased above 50% (40 h) then, the stirrer speed and airflow rate were reduced to minimise the effect of shear on morphology. Erythromycin production began some 10 h before the maximum DCW (11 gL^{-1}) was achieved (figure 3.76c). Then, at 30 h the erythromycin production increased at a rapid rate, reaching a near maximum value of 330 mgL^{-1} at 42 h, followed by a slow rate of production to 350 mgL^{-1} at 70 h.

Rapid rheological changes occurred during the first 20 h of the fermentation with the rapid reduction in flow behaviour (n) from 0.95 to 0.45 and the increase in consistency (K) from 0.07 to 1.05 $Pa.s^n$ (figure 3.77). The apparent viscosity also increased rapidly to 1.1 Pa.s but at a slower rate than the rate of increase of consistency. Between 20 to 65 h the rheology changed at a slower rate with the lowest n value of 0.33 and highest consistency of 1.4 $Pa.s^n$ achieved at 40 h. However, the apparent viscosity decreased to 0.05 Pa.s at 40 h and then increased, due to the step wise changes in stirrer speed. From 65 h the consistency and flow behaviour changed rapidly to values at the

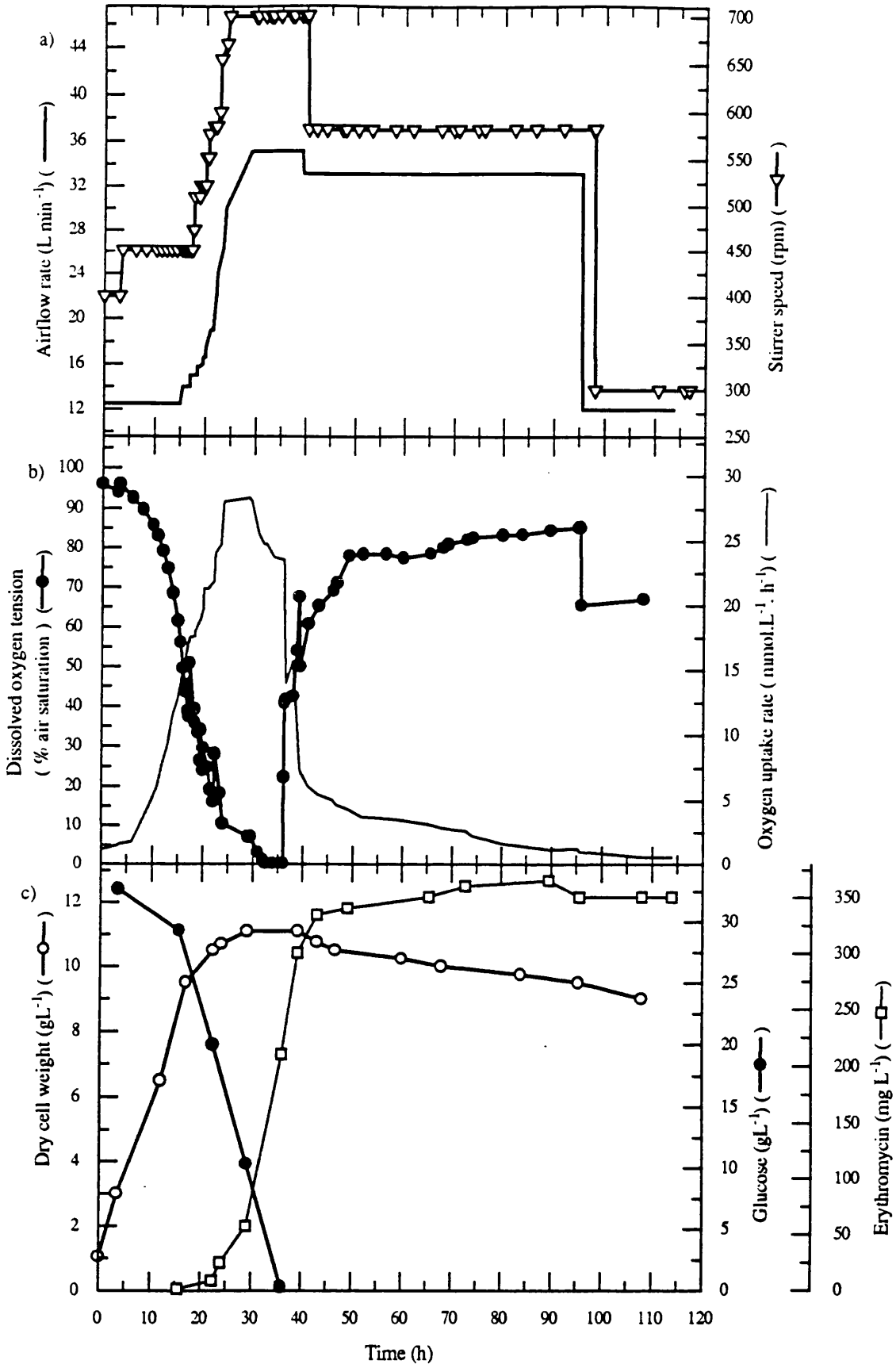

Figure 3.76 (a, b & c) Lab. scale mycelial fermentation of *S. erythraea*. Change of : a) operating conditions, b) dissolved oxygen tension (% air saturation), c) dry cell weight, glucose, and erythromycin production during the fermentation

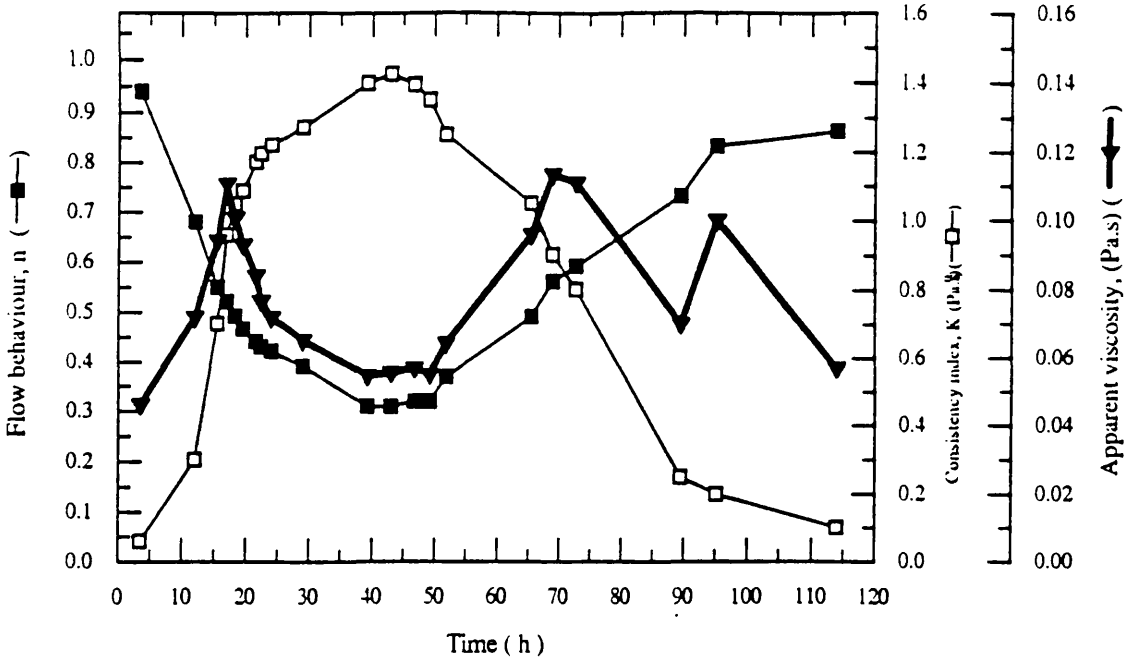

Figure 3.77 Rheological properties, flow behaviour, consistency index and apparent viscosity during the lab. scale stirred tank mycelial *S. erythraea* fermentation

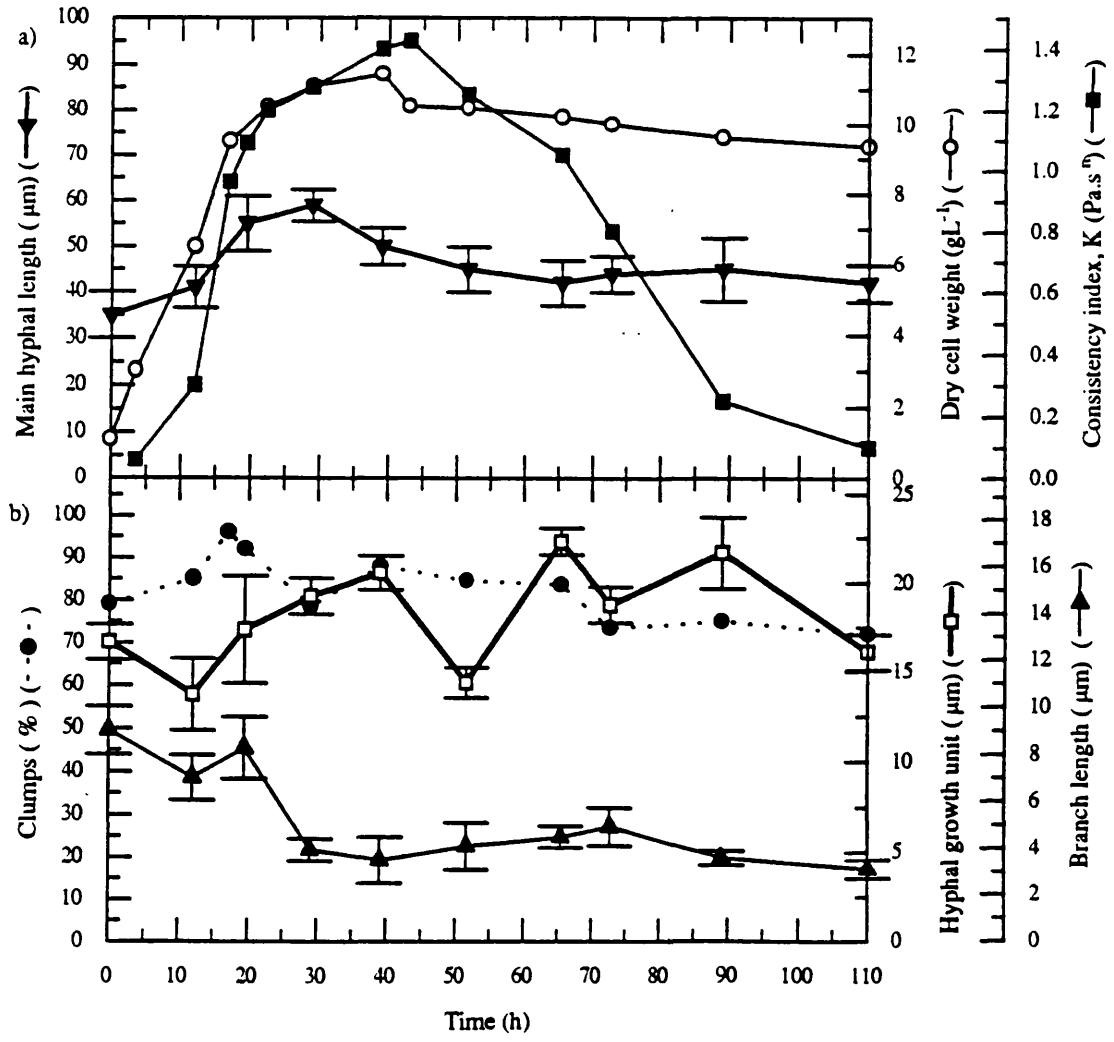

Figure 3.78 (a & b) Comparison of the rheological and morphological changes during the mycelial *S. erythraea* stirred tank fermentation. Change of a) dry cell weight, consistency index and main hyphal length, b) percentage clumps, hyphal growth unit and branch length.

end of the fermentation (110 h) which were similar to those observed at 3 h into the fermentation. The increase in consistency index corresponded with an increase in dry cell weight and main hyphal length (figure 3.78). However, the decrease in consistency index from 45 h could not be related to a change in dry weight or morphology. The hyphal length decreased gradually from 28 h and the branch length decreased rapidly at 20 h from 8 μm to 4 μm at 30 h which remained around this value for the rest of the fermentation.

3.4.4.2 Comparison of the stirred tank fermentation to the mycelial broth in the aerated + propeller operated reactor

The inoculum concentration for the stirred tank was of a similar biomass concentration to that used for the mycelial fermentations however, due to operational difficulties the inoculum volume was only 8% of the stirred tank working volume compared to 10% for the airlift reactor. Therefore, the increase in OUR to the maximum value of 28 $mmol.L^{-1}.h^{-1}$ with the stirred tank broth occurred five hours later than with the broth in the propeller operated reactor (figure 3.76b & 3.56f)). The maximum OUR of 28 $mmol.L^{-1}.h^{-1}$ for the stirred tank broth was greater than the propeller operated airlift broth of 22.5 $mmol.L^{-1}.h^{-1}$. However, the OUR was found to rapidly decrease at the same time for both broths at 38 h. Therefore, the OUR had been maintained above 20 $mmol.L^{-1}.h^{-1}$ for both broths compared to values of 12 and 16 $mmol.L^{-1}.h^{-1}$ observed with the conventional aerated mycelial fermentations (figures 3.50 & 3.54). Despite the small difference in OUR during the first 20 h, both stirred tank and propeller operation broths had similar DCW profiles. Glucose consumption with propeller operation from the airlift was complete some five hours later than with the stirred tank (figure 3.79). The DOT profile for the stirred tank and from the lower riser position for propeller operated airlift broths were similar up to 25 h. After 25 h the DOT profile of the stirred tank broth had DOTs below 10% for a duration of 12 h whereas the riser DOT for the propeller operated airlift broth remained below 10% DOT for only 2.1 h (figure 3.79).

The consistency index and flow behaviour profiles (figure 3.78) were similar to those from the broths in the annulus sparger airlift reactor configurations (figures 3.54 & 3.56) and hence, the DCW correlated well with consistency index. However, the apparent viscosity was some ten times smaller than with the airlift reactor configurations and decreased during the increase in consistency from 20 h into the stirred tank fermentation, due to the increase in stirrer speed. Whereas, the apparent viscosity during the airlift reactor fermentations increased gradually from 20 h, and at a similar rate to the consistency index as the operating conditions remained constant.

The main hyphal length during the stirred tank fermentations remained mostly between the lengths measured during the propeller operated airlift fermentation and the conventional aerated fermentation (annulus sparger) and the hyphal growth unit was found to follow a similar relationship (figure 3.80). Also, the main hyphal length

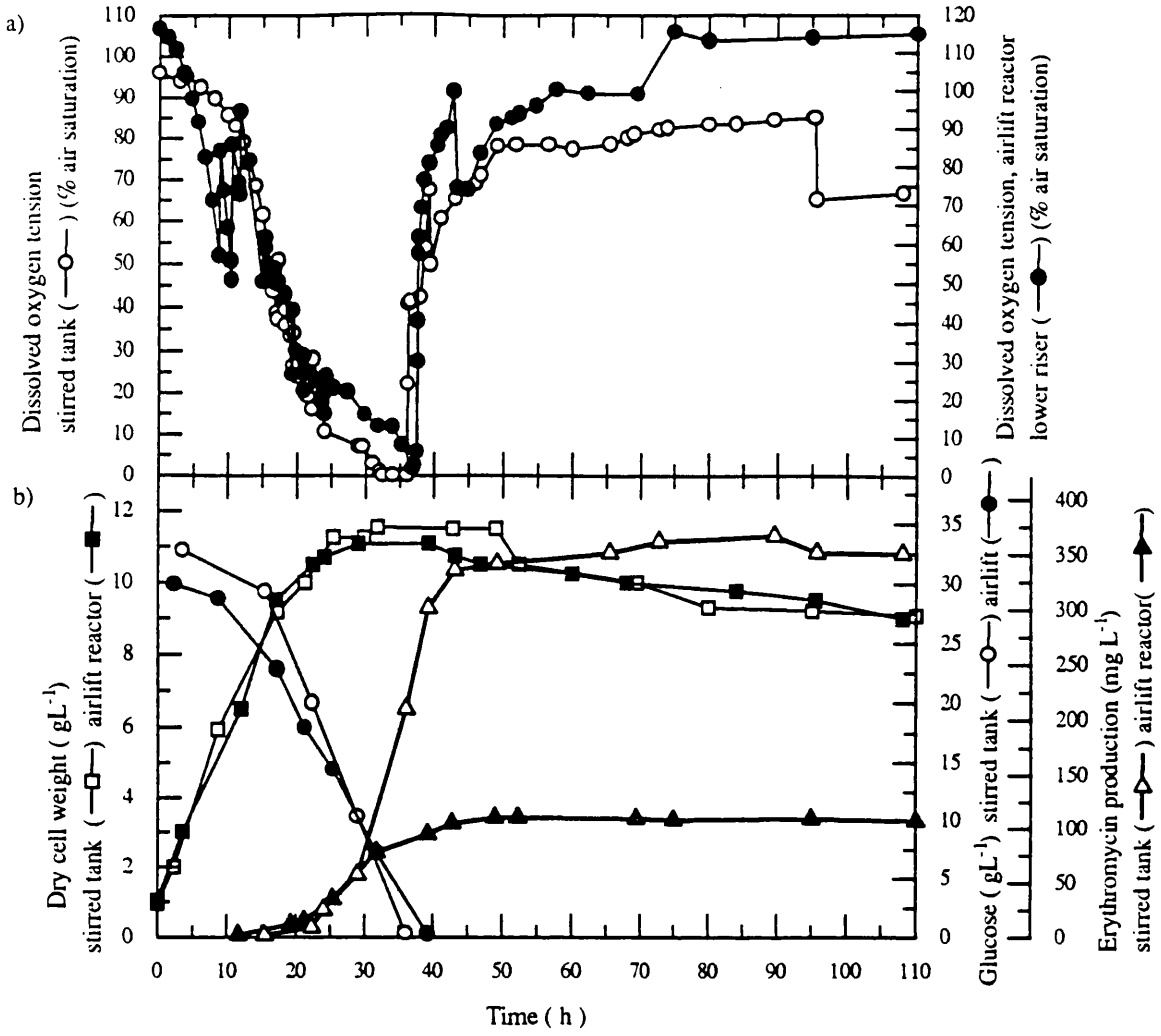

Figure 3.79 (a & b) Comparison of mycelial *S. erythraea* fermentation parameters between the lab. scale stirred tank (open symbols) and the annulus sparged airlift reactor with propeller operation (closed symbols). Change of fermentation parameters; a) dissolved oxygen tension (% air saturation) and b) glucose consumption, dry cell weight and erythromycin production

decreased gradually after 30 h in the stirred tank which was similar to that observed with the aerated propeller broth but different from the aerated only broth where hyphal length only decreased after 65 h. Also, the branch length was maintained around 4 μm from 30 h onwards in the stirred tank fermentation (figure 3.78) compared to values between 6-8 μm measured during the annulus sparged airlift reactor configurations (figures 3.55 & 3.57).

Despite the similarities between the stirred tank and airlift reactor fermentations already discussed the final specific erythromycin titre for the stirred tank broth was above 30 mgg^{-1} (figure 3.81). This was three fold greater than with the broth of the aeration and propeller operated airlift and some 4 fold greater than with the mycelial broths under aeration operation with the airlift reactor (figure 3.81). The production rate with the stirred tank reactor was similar to the broth from aeration and propeller airlift operation up to 28 h. However, after 28 h the erythromycin production rate increased rapidly to a final

production value at 38 h compared to the onset of a slower production phase from 28 h with the airlift reactor broths and hence, to final production titres some 10 later than with the stirred tank.

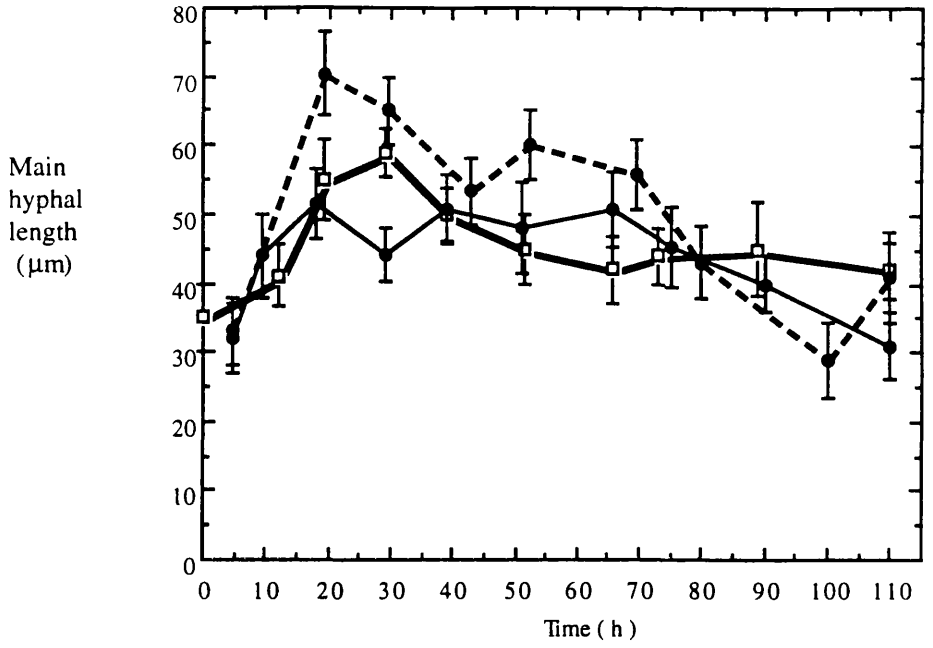

Figure 3.80 Comparison of the main hyphal length between the mycelial *S. erythraea* fermentations with the airlift reactor configurations of annulus air sparging (—●—), aeration / propeller operation (· ●· ·), and lab. scale stirred tank (—□—)

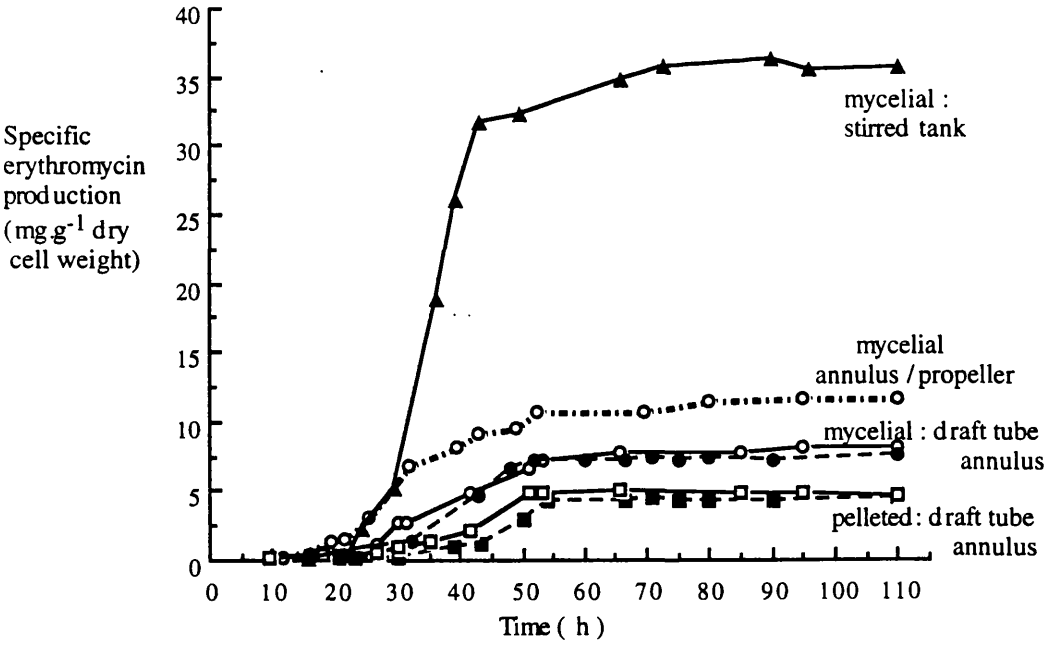

Figure 3.81 Comparison of specific erythromycin production between the mycelial / pelleted *S. erythraea* fermentations with the stirred tank (—▲—), aerated airlift reactor; draft air tube sparged (——), annulus sparged (· · ·), and aerated / propeller operated reactor (· · ·)

4.0 DISCUSSION

4.1 Comparison of the hydrodynamic and oxygen transfer performance between the two sparger configurations of the airlift reactor with the Newtonian baker's yeast broth

4.1.1 The effect of superficial gas velocity on gas holdup

For both sparger configurations a reduction in the rate of increase of gas holdup occurred with increasing gas velocities above 0.054 ms^{-1} (figure 3.3). This diminishing dependence of gas holdup on the gas velocity, as the gas velocity was increased, was due to a change in the flow regime and has been described by many researchers (Chisti and Moo-Young, 1988, Onken and Weiland, 1983 and Russell *et al.*, 1994). As the gas velocity was increased, the flow regime became more turbulent where large spherical cap bubbles formed as churn turbulent flow developed. Chisti and Moo-Young (1987) suggested that a transitional flow regime known as 'coalesced bubble flow' occurred between the homogenous bubbly flow and churn turbulent flow. In this study, the transitional flow regime started above the gas velocity of 0.054 ms^{-1} in which the gas holdup profiles began to flatten as the gas velocity was further increased. The formation of a greater proportion of large fast rising bubbles in the riser would increase the mean bubble slip velocity causing a reduction in the gas residence time. So, as the bubble rise velocity was inversely proportional to the riser gas holdup then, the formation of larger bubbles above the gas velocity of 0.054 ms^{-1} reduced the rate of increase of the riser gas holdup. The increase of the mean bubble rise velocity would begin to counteract the increase in riser gas holdup with increasing gas velocity.

The difference between the riser and downcomer gas holdup was found to increase with increasing gas velocity for both sparger configurations. This was due to the change in flow regime at the gas velocities above 0.054 ms^{-1} which caused a reduction in the rate of increase of the liquid linear velocity with increasing gas velocity. It will be discussed in the following sections that the liquid linear velocity of the downcomer (U_{LD}) dictated the extent of gas entrainment into the downcomer. So, as the gas velocity was increased the rate of increase of the U_{LD} would reduce and consequently, the rate of increase of the downcomer gas holdup would follow a similar relationship.

The differences between the gas holdup profiles of the two sparger configurations were partly explained by the effect of the different cross sectional areas of the individual sections of the reactor. The cross sectional area of the annulus of the vessel was 17% larger than the area of the draft tube hence, the ratio of cross sectional area of the downcomer to that of the riser, A_D/A_R for the reactor with the annulus sparger was 0.83 compared to 1.197 for the draft tube sparger. Siegel *et al.* (1988) explained that an increase in the A_D/A_R resulted in a reduction of the liquid linear velocity of the

downcomer relative to that in the riser. This would result in a decrease of bubble entrainment into the downcomer. The smaller gas holdup in the downcomer relative to the riser produced a greater density difference for liquid circulation and so the overall liquid velocity would increase. Also, the overall gas holdup decreased with increasing A_D/A_R due to the reduction in gas entrainment into the downcomer and increased disengagement from the top section (Siegel *et al.*, 1988, Chisti, 1989 and Weiland, 1984). Nevertheless, Weiland (1984) showed that an increase in A_D/A_R from 0.3 to 1.8 in a concentric reactor (1.7 m tall) only produced a 20% difference in overall gas holdup in water, using a gas velocity range of 0.001 to 0.03 ms^{-1}. Chisti (1989) found that as the liquid linear velocity of the riser, U_{LR} increased with A_D/A_R, a reduction in the riser gas holdup was observed due to a reduction of the gas residence time in the riser.

For the annulus sparger with the lower A_D/A_R of 0.83, the U_{LD} was 20% greater than the U_{LR} hence, a large proportion of the gas from the riser was entrained into the downcomer. This resulted in a small density difference between the riser and downcomer for liquid circulation. For the draft tube sparger with the higher A_D/A_R of 1.197, the U_{LD} was 20% smaller than the U_{LR} (figure 3.6) due to the larger cross sectional area of the downcomer. Hence, the lower U_{LD} relative to the U_{LR} resulted in a smaller proportion of the gas from the riser being entrained into the downcomer compared with the annulus sparger. Thus, the density difference for liquid circulation was greater with the draft tube sparger than with the annulus sparger. This was shown by the shorter liquid circulation time, with increasing gas velocity, for the draft tube sparged reactor compared to the annulus sparged configuration (figure 3.4). Therefore, with the annulus sparger, a larger proportion of the gas introduced into the riser remained in the reactor than with the draft tube sparger. This may increase the chance of bubbles being depleted of oxygen in the vessel with the annulus sparger which will be discussed in section 4.1.3. Thus, the overall gas holdup would be expected to be higher with the annulus sparger than with the draft tube sparger. In fact, the overall gas holdup with the annulus sparger was 10% greater than with the draft tube sparger at gas velocities up to 0.054 ms^{-1} (figure 3.33). Also, the increase in A_D/A_R would have expected to produce a lower riser gas holdup with the draft tube sparger than with the annulus sparger due to the higher U_{LR}. This was also observed below the gas velocity of 0.054 ms^{-1}. However, above the gas velocity of 0.054 ms^{-1} the overall and riser gas holdup with the draft tube sparger were in fact 17% larger than the values for the annulus sparger.

So, the differences between the gas holdup profiles from the two sparger configurations above the gas velocity of 0.054 ms^{-1} were not fully explained by the effect of the A_D/A_R. Most of the literature studies on the effect of the A_D/A_R on reactor hydrodynamics, and most significantly the work of Weiland (1984), were completed by using the same sparger location inside the draft tube and varying the draft tube diameter. However, in this study the effect of the increasing A_D/A_R was produced by changing the sparger location from the annulus to the draft tube of the vessel and so, the sparger

geometry did not remain constant as the A_D/A_R was increased. The large difference in gas holdup profiles between the two sparger configurations transpired at gas velocities above 0.054 ms^{-1} where the transition from bubbly to more turbulent flow occurred. This implied that during the change in flow regime a difference in the mean bubble size distribution between the risers of the two sparger configurations may have developed. The reactor configuration with the annulus sparger produced the lowest gas holdup during the change in bubble regime which implied that a greater proportion of large bubbles were formed that increased the mean bubble size distribution. To produce an increase in the mean bubble size during the change in bubble regime implied that greater rates of coalescence occurred in the riser of the annulus sparger than in the riser with the draft tube sparger. It is well known that the bubble size distribution is generally independent of the size of the bubbles from the sparger and is effected by the fermentation medium composition, surface tension and wall effects (Chisti, 1989). However, the medium composition was identical for the sparger configuration comparison therefore, the difference in bubble size must have been due to difference in the fluid dynamic effects and physico - chemical interactions at the gas - liquid interface brought about by the different geometry of the riser configurations. Although the size of the orifices for both spargers were the same, the different spacing between the orifices may have resulted in different bubble flow behaviour and coalescence properties as the bubbles flowed up the risers of the two spargers configurations. Thus, the annulus sparger with the 70% wider spacing between the pairs of orifices compared to the draft tube sparger would be expected to produce higher rates of coalescence, as the gas holdup was lower than with the draft tube sparger (above gas velocities of 0.054 ms^{-1}). This would seem surprising as the bubbles formed from the draft tube sparger would be closer together due to the smaller orifice spacing and hence, would be more likely to collide and coalesce. However, the difference in liquid velocities of the riser and downcomer between the sparger configurations may also be important in determining coalescence rates. Onken and Weiland (1983) found evidence to show that for a constant gas velocity an increase in the superficial liquid velocity would produce a decrease in the coalescence frequency and mean bubble diameter. The effect of the superficial liquid velocity on the bubble size distribution was measured at a height of 1.1 m above the gas sparger in a tubular loop airlift reactor of 8.5 m tall with a vessel diameter of 0.1 m and 0.1M sodium chloride solution. For each gas velocity in the range of 0.0049 to 0.022 ms^{-1}, the mean bubble diameter was found to decrease with an increase in superficial liquid velocity in a range of 0.001 to 0.3 ms^{-1}. For example, at the constant gas velocity of 0.022 ms^{-1} an increase in superficial liquid velocity from 0.04 to 0.26 ms^{-1} produced a decrease in the mean bubble diameter from 1.75 to 1 mm. Although the gas velocity range studied was low (0.0049 to 0.022 ms^{-1}) compared to the range of 0.018 to 0.136 ms^{-1} used for this study, it still provided evidence to show that a slower liquid velocity would produce higher rates of coalescence than with a faster liquid velocity under constant gas velocity conditions.

Similar observations were observed by Chisti (1989) where the relative magnitude of coalescence and size of spherical bubbles were lower in a tall split tube airlift reactor of 3.45 m compared to a shorter 2.23 m reactor over the same range of power inputs, with solutions of 1% cellulose fibres and sodium chloride. In the shorter reactor the diminishing dependence of gas holdup on the power input was observed above 5 x 10^{-2} Wm^{-3}. However, in the taller reactor the rate of gas holdup increase did not change for the same increase in power input. Hence, the distinction between bubble and coalesced bubble flow was reduced in the taller reactor. The increased liquid circulation velocity with reactor height imposed a strong vertical component on the gas bubbles in the taller reactor, thereby reducing interactions between bubbles which causes coalescence. Therefore, comparing the superficial liquid velocities in this study showed that the riser with the annulus sparger configuration had a 20 - 30% weaker vertical velocity component than in the riser with the draft tube sparger. Hence, this would provide a more conducive environment for high rates of coalescence in the riser with the annulus sparger, leading to lower gas holdup, when compared to the draft tube sparger. Onken and Weiland (1983) found that although an increase in liquid velocity produced lower rates of coalescence, the gas holdup actually decreased due the reduction of the gas residence time in the riser. In this study the higher overall gas holdup was produced with the draft tube sparger with the greater liquid velocity and lower coalescence rates compared to the annulus sparged reactor. This indicated that in this study the liquid velocity had a greater influence on gas holdup from the effects of coalescence and bubble diameter than on the gas residence time.

The location of the spargers may also effect the bubble distribution and flow within the riser which would ultimately effect coalescence rates. The annulus sparger was positioned in the centre of the annulus of the vessel with an equal distance between the vessel and draft tube wall hence, bubbles would be expected to rise up the centre of the annulus. The draft tube sparger had a diameter near to the that of the draft tube hence, bubbles would travel nearer the draft tube walls than in the centre of the vessel although bubbles may travel in the centre of the riser in the upper portions of the vessel. Ayazi Shamlou *et al.* (1994) modelled the riser gas holdup and liquid velocity profiles as a function of gas velocity for the draft tube sparger and perforated plate sparger used by Russell *et al.* (1994). The model was based on the simple interactions between the liquid, the gas bubbles and the liquid wake associated with the gas bubbles. The interactions were solved as an energy balance and the final equation for the prediction of gas holdup expressed the relationship between gas holdup, superficial gas velocity and liquid velocity which was based on the drift flux theory of Zuber and Findley (1965). The relationship incorporated a distribution parameter C_0 which is dependent on the radial distribution of the gas holdup and superficial liquid velocity (Merchuk, 1991). A C_0 of 0.7 was used in the model to describe the profile across the riser with the draft tube sparger. Hence, the liquid velocity and gas holdup would be higher nearer the draft tube than in the centre of

the riser as the sparger diameter was near to that of the draft tube. Ayazi Shamlou *et al.* (1994) successfully modelled the gas holdup and liquid circulation rates from the perforated plate sparger studied with the baker's yeast suspension by Russell (1989). This sparger was located in the centre of the vessel base and had a diameter of 0.13 m with 120 orifices of 0.001 m in diameter. Whereas, the draft ring sparger had a diameter of 0.16 m with 32 orifices of 0.002 m in diameter. The spacing between the orifices for the plate sparger was considerably smaller than the draft tube sparger. The gas holdup values with the perforated plate were found to be lower than with the draft tube sparger at all gas velocities (figure 4.1). At the high gas velocity of 0.136 ms^{-1} the riser gas holdup with the draft tube sparger was 50% higher than with the perforated plate and the U_{LR} with the draft tube sparger was 20% less than with the plate sparger. Therefore, from these results it can be concluded that for the perforated plate, the mean bubble size in the riser must have been larger than in the riser with the draft tube sparger. Hence, the rates of coalescence with the perforated plate must have been greater than with the draft tube sparger in order to have produced larger mean bubble diameters. This would account for the lower gas holdups and higher liquid velocities than with the draft tube sparger. To model the gas holdup profile and liquid velocities of the riser a C_0 value equal to unity was used for the perforated plate as the sparger was located below the centre of the draft tube (figure 4.1). Therefore, this provided evidence to indicate that spargers with liquid velocity and gas holdup distributions near unity for the reactor and yeast broth used in this study were more likely to produce higher rates of coalescence. As the annulus ring sparger was situated in the centre of the annulus of the vessel, then a C_0 value of unity would seem appropriate and this was shown to be successful for modelling the riser gas holdup and liquid velocity with this sparger (figure 4.1). Hence, the comparison between the draft tube ring sparger and the perforated plate described above provided evidence to suggest that a C_0 of near unity would account for the high rates of coalescence with the annulus sparger.

The recirculation of gas around the loop of the vessel may also have been an important factor which effected the fluid dynamics in the vessel. Frohlich *et al.* (1991b) studied gas recirculation around the loop of a 4 m^3 tower loop reactor from local measurements of the gas residence time. The percentage of gas recirculated (ratio of gas throughput of the downcomer compared to the riser) with a yeast broth was found to be as great as 85% in a high gas holdup system. The riser gas holdup was 0.21 compared to 0.18 for the downcomer gas holdup at a gas velocity of 0.175 ms^{-1}. This was compared to 26% for water which was a lower gas holdup system where riser gas holdup was 0.14 compared to 0.1 for the downcomer at the same gas velocity. For this study the comparison of gas holdup profiles of the riser to the downcomer implied that a larger proportion of the gas from the riser with the annulus sparger was entrained into the downcomer compared to that obtained with the draft tube sparger. Hence, with the annulus sparger a higher proportion of gas may be recirculated from the downcomer at

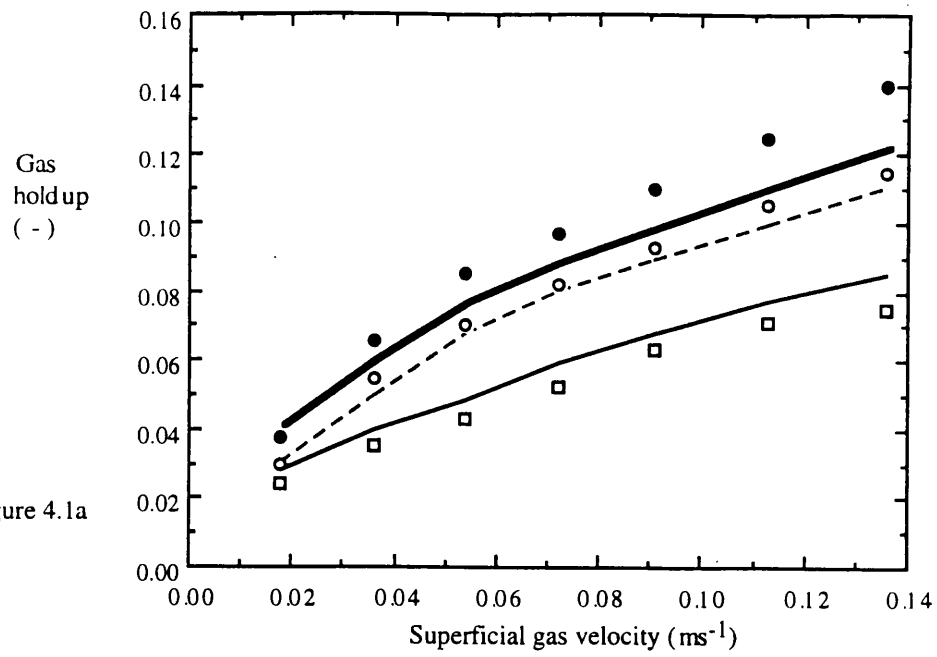

Figure 4.1a

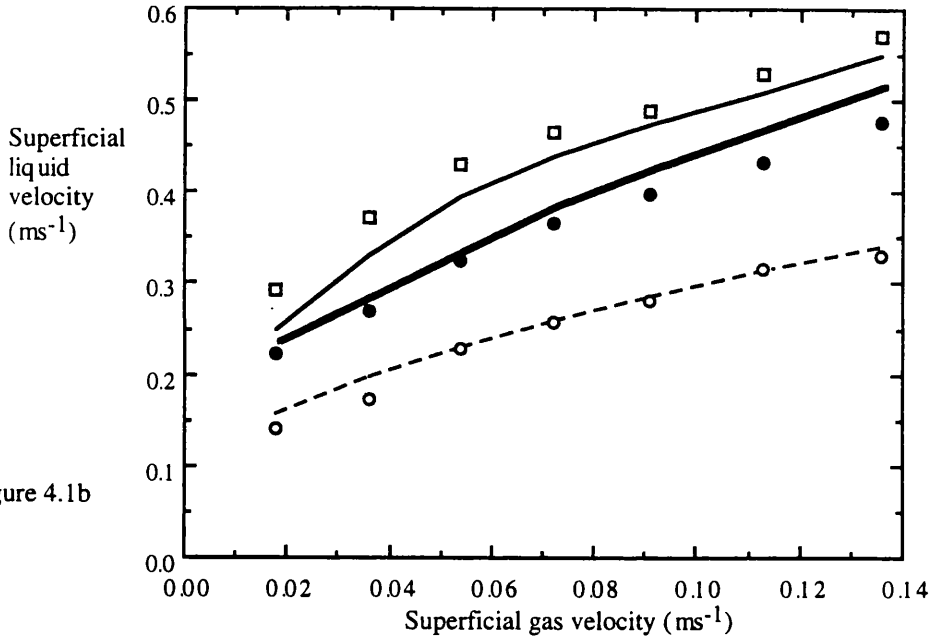

Figure 4.1b

Figure 4.1 Comparison between model predictions (Ayazi Shamlou *et al.*, 1994) and experimental measurements of riser gas holdup and superficial liquid velocity, as a function of superifical gas velocity for the airlift reactor (H_{DT} of 2.77 m) with the draft tube sparger(●), annulus ring sparger(o) and perforated plate(□)(Russell *et al.*, 1994) using the baker's yeast broth (10 gL^{-1} DCW). Model predictions : draft tube sparged reactor, C_0 of 0.7(——), annulus sparger, C_0 of 1 (- - -), and perforated plate sparger, C_0 of 1 (——)

the base of the vessel into the riser compared to when the draft tube sparger was used. Although this would be expected to result in a higher riser gas holdup than with the draft tube sparger, the recycled bubbles from the downcomer may coalesce with the new bubbles in the riser. Thus, large bubble diameters would be formed with high rise

velocities which would reduce gas holdup. This effect of coalesce from the recirculation of gas would certainly be expected to be greater at gas velocities above 0.054 ms^{-1} when the bubbles in the downcomer were at there largest.

The extra wall resistance's in the riser with the annulus sparger may cause greater energy dissipation than in the riser with the draft tube sparger. This may also effect the bubble behaviour and flow regime in the riser. The riser with the annulus sparger had a two fold greater surface area from the vessel inside wall and the outer wall of the draft tube compared to the riser with the draft tube sparger, where the liquid and bubbles only comprehended the inside wall of the draft tube. Hence, the extra wall resistance of the riser with the annulus sparger would result in greater energy dissipation and less energy for liquid circulation. This may make a small contribution to the poorer liquid circulation performance associated with the reactor with the annulus sparger than with the draft sparger. However, the wall frictional forces have been shown by Ayazi Shamlou *et al.* (1994) and Chisti (1989) to be negligible. Even though the frictional resistance's with the annulus sparger would have been greater than with the draft tube sparger, it is obvious that the size and effect of the frictional forces on bubble behaviour would have been minimal.

Therefore, it has been shown that the change in flow regime with superficial gas velocity successfully explained the effect of superficial gas velocity on the gas holdup. The effect of the ratio of downcomer to riser cross sectional area was shown to contribute to the differences in riser and downcomer gas holdup between the spargers at low gas velocities, but at gas velocities above 0.054 ms^{-1} the concept was less successful at explaining the gas holdup differences. It was proposed that this was due to different coalescence effects brought about by the different fluid dynamic conditions of the two risers which effected the physico - chemical interactions of the bubbles.

4.1.2 The effect of superficial gas velocity on the liquid circulation and mixing

The change in the flow regime from bubbly to more turbulent flow was observed to reduce the rate of decrease of the liquid circulation time with increasing gas velocity (figure 3.4). Consequently, a reduction in the rate of increase of liquid velocity with increasing gas velocities above 0.054 ms^{-1} was also observed (figure 3.6). These effects were contributed to the formation of larger bubbles as the gas velocity increased, resulting in greater turbulent dissipation of energy in the riser. This would reduce the amount of energy available from gas dispersion for liquid circulation (Merchuk and Stein, 1981a). The draft tube sparger configuration had a faster liquid circulation performance than the reactor with the annulus sparger (figure 3.4). This was due to the higher A_D/A_R ratio of the draft tube sparged reactor causing a greater density difference for liquid circulation than with the annulus sparger, as discussed in section 4.1.1. Liquid circulation might be expected to be limited with a small density difference between the riser and downcomer.

However, liquid circulation would also occur from the entrainment and transport of liquid in the wake of the ascending bubbles (Philip *et al.*, 1990, Ayazi Shamlou *et al.*, 1994). Hence, Ayazi Shamlou *et al.* (1994) successfully modelled the gas holdup and liquid circulation profiles as a function of gas velocity from the yeast broth with the draft tube sparger (figure 4.1) by considering the contribution of the bubble wake to the sectional gas holdups and liquid velocities. Hence, the primary bulk liquid flow velocity was calculated from the contribution of the holdup differentials in the column and the liquid wake velocity using an energy balance.

For both sparger configurations the rate of reduction of the mixing time with increasing gas velocity was found to decrease (figure 3.4). This was similar to the effect of superficial gas velocity on the liquid circulation time which suggested that a close correlation existed between the two parameters. Hence, the draft tube sparged vessel had the fastest liquid circulation and greater mixing performance than the annulus sparged reactor at the same gas velocities. Also, the constant ratio of mixing to circulation time of 2.5 for the range of gas velocities and with both sparger configurations, indicated that about 2.5 circulations of the vessel were required to disperse an alkali pulse to 90% homogeneity. Thus, the mixing performance of the vessel was primarily determined by the frequency at which the alkali pulse passed through the end section of the vessel. All of this evidence suggested, as did the observations of Russell (1989) and Weiland (1984), that the mixing performance of the vessel was controlled predominately by the bulk circulation of the liquid rather than the axial dispersion due to ascending bubbles.

4.1.3 The effect of superficial gas velocity on the dissolved oxygen tensions and k_La measurements

The dissolved oxygen tensions (DOTs) and k_La values in the downcomer for both sparger configurations were shown to be greater than the values in the riser, for all gas velocities with the 10 gL^{-1} DCW yeast suspension (figures 3.7, 3.8, & 3.9). This provided an indication that the oxygen transfer rate changed around the vessel. In the riser and top section for both spargers the DOTs remained below 1% (air saturation) and low k_La values were observed when compared to the downcomer. For the draft tube sparger the DOT increased rapidly from the top section to high values in the upper downcomer and then, decreased slowly to the lower downcomer position (figure 3.8a). High k_La and DOTs values were measured in this region of the vessel whereby, the OTR was certainly equal to / or exceeded the OUR for most of the downcomer. This was also observed in the downcomer with the annulus sparger where the DOT increased from the top section to peak values in the lower downcomer position (figure 3.8b), and corresponding increases in k_La values were observed (figure 3.10). For both sparger configurations the DOT decreased to values below 1% at the base of the downcomer and around the base of the vessel. Hence, the oxygen demand of the yeast broth may be affected by the low DOT. Similar observations were observed with gas velocities below

0.091 ms^{-1} with the 5 gL^{-1} DCW yeast where DOTs below 1% were measured in the riser (figure 3.38). However, at the maximum gas velocity (0.136 ms^{-1}) the DOT was in excess of 30% around the vessel and in which, the OTR was balanced by / or greater than the OUR. Therefore, it has been demonstrated that the OTR of the gas to the liquid changed throughout the reactor. However, this can only be concluded if the OUR of the yeast broth was considered to be constant around the vessel.

For both sparger configurations with the 10 gL^{-1} DCW yeast broth the OUR was dominated by the fundamental operating conditions of the reactor. The OUR for both sparger configurations increased proportionally from 5 $mmol.L^{-1}.h^{-1}$ at the gas velocity of 0.018 ms^{-1} to a value of 45 $mmol.L^{-1}.h^{-1}$ at the maximum gas velocity of 0.136 ms^{-1} (figure 4.2). A similar relationship between gas velocity and OUR was observed with the 5 gL^{-1} DCW yeast suspension (figure 4.2). The increase of the OUR with gas velocity indicated that the DOT heterogeneity, with values below 1% along the length of the riser, affected the OUR of the 10 gL^{-1} DCW yeast suspension at all gas velocities. This was further emphasised by the influence of the marine propeller on the

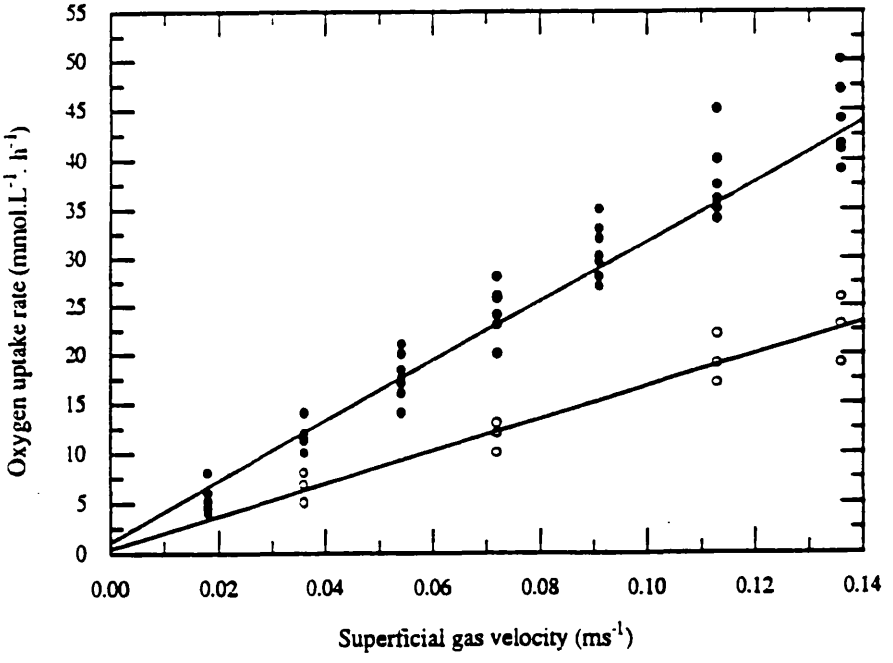

Figure 4.2 The effect of superficial gas velocity on the oxygen uptake rate of the yeast suspension (10 gL^{-1} dry cell weight) (•) with aeration from the draft tube and annulus sparged airlift reactor (H_{DT} of 2.77 m) and 5 gL^{-1} dry cell weight suspension with annulus gas sparging (○)

OUR of the yeast broth with conventional aeration from the annulus sparger. Although this will be discussed in detail in section 4.3, the OUR of both the 5 and 10 gL^{-1} DCW yeast broths were found to increase with increasing total energy dissipation rate (combined aeration and propeller operation) until the DOTs in the whole of the vessel increased approximately above 10% (air saturation). For the 10 gL^{-1} DCW yeast broth the DOTs in the riser did not increase above 10% until a gas velocity of 0.136 ms^{-1} and propeller speed of 900 rpm were used hence, the maximum obtainable OUR for this biomass concentration, and reactor configuration was 52 $mmol.L^{-1}.h^{-1}$. This maximum value was considerably greater than the 6 $mmol.L^{-1}.h^{-1}$ obtained with conventional aeration using the lowest gas velocity (0.018 ms^{-1}), and further highlighted the effect of the DOT heterogeneity at reducing the OUR of the yeast broth (10 gL^{-1} DCW). The aerobic degradation of glucose can proceed by two pathways under the conditions of aerobic ethanol formation. Glucose can be metabolised oxidatively yielding biomass and carbon dioxide. Also, it can be metabolised reductively yielding ethanol and carbon dioxide from the conversion of pyruvate into acetaldehyde by decarboxylation, and reduction into ethanol by hydrogenation. The ratio of these two glucose metabolisms depends on the respiratory capacity of the cells (Sonnleitner and Kappeli, 1986) and hence, the supply of oxygen. For aerobic conditions and sub critical glucose concentration glucose is metabolised oxidatively and the residual respiratory capacity is used for ethanol consumption. In the absence of oxygen glucose is metabolised reductively and no ethanol is consumed. As the dissolved oxygen tension is increased the respiratory capacity of the cell and part of the oxidatively metabolised glucose increases. Therefore, periodically changing gas composition and dissolved oxygen concentration results in an interchange between aerobic and anaerobic phases. Abel *et al.* (1994) studied the effect of gas composition and DOT on the metabolism of a yeast fermentation in batch culture where the aeration frequency (reciprocal value of the sum of the air sparged period and the nitrogen sparged period) was 0.27 min^{-1} and the DOT varied from 67% to a duration at 0% for 60 seconds. This environment reduced the final biomass concentration and growth rate on glucose by half and the metabolite concentration (ethanol and acetaldehyde) increased when compared to the control fermentation (unlimited dissolved oxygen tension). The fluorescence intensity indicated that the respiratory metabolism changed periodically into a respiratory / repressive one during the variation in DOT. The changes of DOT between 30 to 2% with an aeration frequency of 0.76 min^{-1} and duration at 2% DOT for 10 s had less of an effect than the previous example when compared to the control. In a third experiment the fluorescence intensity indicated that the cells did not experience a change from oxidative to the oxidoreductive metabolism with DOT changes from 55 to 5% with an aeration frequency of 0.56 min^{-1}. However, the cell growth rate on glucose, yield coefficient of the growth on glucose and final cell concentration were smaller than with the greater aeration frequency of 0.76 min^{-1}. This occurred with the lower aeration frequency of 0.56 min^{-1} and higher DOTs of 55

to 5%, compared to the higher frequency (0.76 min^{-1}) with DOTs between 30 to 2%. This demonstrated that the impact of DOT changes on cell metabolism decreased with increasing aeration frequency due to the slow response of cells to variations of their environment. Researchers using fed batch and continuous culture systems found that yeast cells were less sensitive to DOT variations in continuous culture than in batch culture (Abel *et al.* 1994). Sweere *et al.* (1988b) using a continuous culture two fermenter system found no significant effect on cell metabolism until the circulation time was greater than 30 s (15 s at DOT below 1% and 15 s at DOT of 30% saturation). The fed batch and continuous cultures were operated with carbon limitation and all the substrate was consumed as it entered the vessel. This resulted in the cells having a longer response time to changes of DOT than with the batch culture of this study, which had an excess glucose concentration in the media up to 10 gL^{-1}.

Therefore, the batch culture studies of Abel *et al.* (1994) would suggest that although the metabolism (OUR) of the yeast cells in this study was affected by the DOT changes around the reactor, the actual OUR may not have varied around the reactor as the cells could not follow the change in DOT from a rapid fluctuation around the vessel. This would result in an intermediate respiration capacity according to the average DOTs (Abel *et al.*, 1994). Therefore, it was assumed for this study that the OUR remained constant around the vessel. Hence, the OUR measured from the exit gas analysis was considered to be a true representation of the OUR of the broth. However, it must be considered that the DOT heterogeneity around the vessel may have caused small fluctuations of the OUR of the yeast cells as they circulated around the vessel. In this situation the OUR from exit gas analysis would be considered to be an average value of the OUR in the reactor. The local positional k_La values were calculated using the gas balance method (section 2.7) and hence, the OUR was used from the exit gas analysis. So, if small fluctuations in the OUR did occur around the vessel then, the use of the average OUR from exit gas analysis would lead to small inaccuracies in the calculation of the local k_La values. For example, if the OUR varied around the vessel then the low DOTs below 1% in the riser would cause a reduction in the OUR from the average value calculated from exit gas, and this would lead to an overestimate of k_La. However, in the downcomer with the DOTs above 10% the OUR would be expected to be greater than the average OUR which would lead to an underestimate of k_La. At the base of the vessel the low DOTs would reduce the OUR from the average value and hence, the k_La would also be an overestimate. It was calculated that if the OUR had fluctuated around the vessel up to as much as 10% from the average value (from exit gas analysis) then, the positional k_La values would only deviate by 10%.

So returning to the oxygen transfer, if it is assumed that the OUR remained constant around the vessel then, the change in k_La values around the vessel indicated that the OTR varied around the vessel, and the environment of the downcomer was more conducive to oxygen transfer than the riser with both sparger configurations. However,

it must be considered that although the estimation of positional k_La values was a steady state measurement the required equilibrium conditions between the gas and liquid phases were not met for each k_La measurement position. If the time constant for oxygen transfer ($1/k_La$) had been smaller than the liquid circulation time then Oosterhuis and Kossen (1984) considered that the vessel would be poorly mixed compared to oxygen transfer performance. In this situation the oxygen transfer rate at each position in the vessel was at a similar speed with the liquid circulation and so, the dissolved oxygen tension could be considered to be local values from the balance between the local oxygen transfer rate and oxygen uptake rate (Russell *et al.*, 1995). However, in this study and from Russell *et al.* (1995) the time constant for oxygen transfer ($1/k_La$) at each probe position was found to be longer than the liquid circulation time for most gas velocities apart from 0.136 ms^{-1} (figure 4.3). Thus, the oxygen transfer rate is considered to be poor when

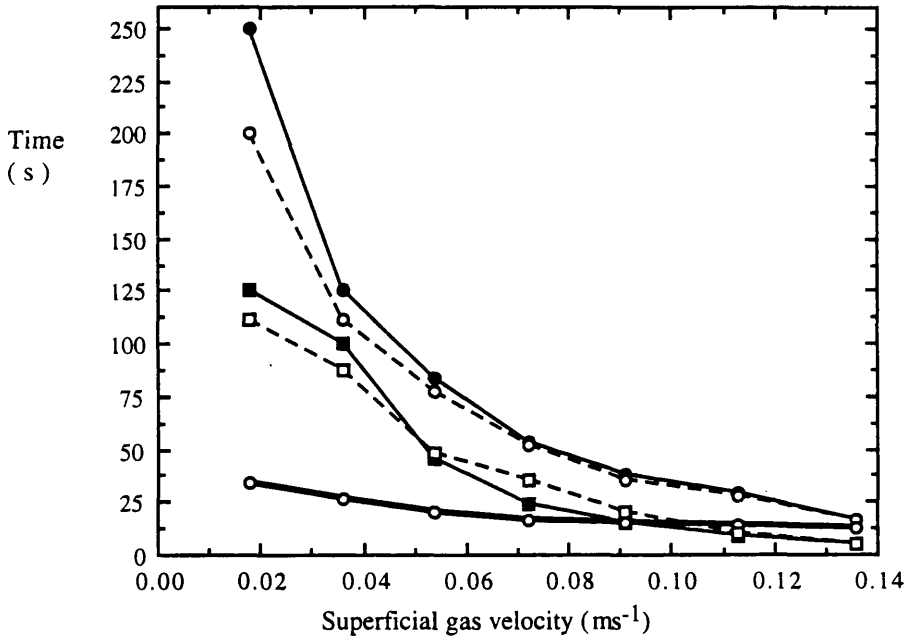

Figure 4.3 Comparison of the time constants for oxygen transfer $1 / k_La$ from the fixed probe positions to the liquid circulation time, as a function of superficial gas velocity with the conventionally aerated airlift reactor (H_{DT} of 2.77m) and 10 gL^{-1} DCW baker's yeast suspension. Draft tube sparged reactor : lower riser (-o-), upper downcomer (-□-), Annulus sparged reactor: lower riser (—●—) lower downcomer (—■—) and liquid circulation time (—o—)

compared to the circulation of the liquid (Oosterhuis and Kossen, 1984). Hence, in this situation the DOTs were not measurements of local oxygen transfer changes but instead reflected the amount of oxygen transfer to the liquid and, the amount of metabolic oxygen consumption which had occurred in the liquid prior to it reaching the probe position. Therefore, the k_La values could not be considered to be positional values as the DOT probe was measuring the oxygen transfer history of the liquid prior to reaching the probe.

Unfortunately it was impossible to quantify how far back from the probe the oxygen transfer of the liquid originated from, in relation to the distance within the reactor and the liquid circulation time. Russell *et al.* (1995) observed similar k_La profiles from the three fixed probe positions as in this study, and described the oxygen transfer changes around the vessel by considering the change in oxygen transfer that must have occurred between two k_La measurements at two fixed probe positions. This only provided a qualitative description of the oxygen transfer changes over the distances (1.6 to 2 m) between probe positions. The use of the mobile DOT probe in this study showed that DOTs especially in the downcomer, changed rapidly over small distances that were 0.2 m apart. Thus, it was difficult to interpret the change in oxygen transfer over this small distance. Although the k_La measurements cannot be considered as positional values within the reactor, the local k_La values for the riser were relatively constant along the whole length of the riser from the base of the vessel and so, it was reasonable to presume that these values were representative for this section of the vessel. Also, the difference in magnitude of the k_La values between the riser and downcomer clearly indicated that greater oxygen transfer occurred in the downcomer than in the riser, and that the position of the greatest region of oxygen transfer in the downcomer varied with the sparger configuration. Explanations for these observations will now be discussed.

The differences in the fluid dynamics between the riser and downcomer may contribute to the larger OTR in the downcomer. In figure 3.3 it was shown that the gas holdups varied in the reactor and gas holdup is an important factor for the oxygen transfer performance of the airlift reactor, as shown by equation 4.1 which was derived by Russell (1989) and Chisti (1989) below :

$$k_La \ \alpha \ \frac{\varepsilon}{1-\varepsilon} \qquad 4.1$$

The small difference between the riser and downcomer gas holdups, especially with the annulus ring sparger (figure 3.3), indicated that the downcomer had a high gas content. The density difference between the riser and downcomer with the draft tube sparger was greater than with the annulus sparger but the actual downcomer gas holdups values were quite similar between the sparger configurations, especially above the gas velocity of 0.054 ms^{-1}. So, the downcomers with both sparger configurations had a high gas content which was visibly observed (in water) with bubbles in the range of 1 - 7 mm in diameter descending through the sight glasses of the upper and lower downcomer sections with the draft tube sparger (table 3.1). It is well known that bubble size effects the OTR as k_La is strongly influenced by the specific interfacial area (a) which was defined by Winkler (1990) as:

$$a = \frac{6\,\varepsilon}{d_B\,(1-\varepsilon)} \qquad 4.2$$

where

ε = gas holdup (–)

d_B = Sauter mean bubble diameter (m)

Therefore, large bubbles in the riser of an airlift reactor were more likely to disengage from the top section resulting in entrainment of smaller bubbles into the downcomer. This was shown by Frohlich *et al.* (1991a) whereby the local bubble diameters in the riser with water and yeast broth, as measured by electrical conductivity, were found to be 5 to 35% greater than in the downcomer over the gas velocity range of 0.056 to 0.175 ms^{-1}. These measurements were from a 4 m^3 tower loop reactor with a height of 6.8 m, and similar effects were observed during the cultivation of yeast in a laboratory reactor 2.5 m tall (0.08 m^3 working volume) where the bubble diameter after 10 hours into the yeast fermentation was 13 mm in the riser, compared to 4 mm in the downcomer at a superficial gas velocity of 0.091 ms^{-1}. Therefore, the smaller bubbles in the downcomer relative to the riser may improve the oxygen transfer in the downcomer relative to the riser. This concept of changing bubble distributions in the airlift was addressed by Ayazi Shamlou *et al.* (1995) from the modelling of experimental k_La values measured from the fixed DOT probe positions in this study. The model was an extension of the gas holdup and liquid circulation rate model for the draft tube sparged reactor (Ayazi Shamlou *et al.*, 1994) referred to in section 4.1.1. Higbie's penetration theory was combined with the gas - liquid circulation rate model to obtain an expression which was capable of predicting the volumetric oxygen mass transfer coefficient. The relationship between the mass transfer coefficient k_L, liquid phase diffusivity and the exposure time was used from the equation below:

$$k_L = \frac{2}{\pi^{\frac{1}{2}}}\left(\frac{\zeta}{t}\right)^{\frac{1}{2}} \qquad 4.3$$

where t = exposure time or surface renewal time (s)

ζ = liquid phase diffusivity (m^2s^{-1})

The exposure time was determined theoretically in terms of the local fluid dynamics at the gas - liquid interface for bubble diameters greater than 2.5 mm depending on the diameter of the bubble and its rise velocity from the equation below, (Higbie, 1935, Azbel, 1981, Winkler, 1990):

$$t = \left(\frac{d_B}{u_r} \right) \qquad 4.4$$

where t = exposure time (s)

d_B = mean bubble diameter (m)

u_r = gas – liquid slip velocity (ms^{-1})

Where, the slip velocity, u_r was defined (Ayazi Shamlou *et al.*, 1994) as :

$$u_r = \frac{[U_{BT} + C_0 (U_{sg} + U_{sl})]}{(1 - \varepsilon)} \qquad 4.5$$

where:

U_{BT} = terminal bubble rise velocity

C_0 = velocity profile distribution parameter

U_{sg} = superficial gas velocity

U_{sl} = superficial liquid velocity

ε = gas holdup

The equations 4.3, 4.4, and 4.5 were combined to gave an expression for k_L:

$$k_L = \left(\frac{4\zeta}{\pi} \right)^{\frac{1}{2}} \left\{ \frac{U_{BT} + C_o (U_{sg} + U_{sl})}{(1 - \varepsilon) d_B} \right\}^{\frac{1}{2}} \qquad 4.6$$

where U_{BT} = terminal velocity of an isolated bubble (ms^{-1})

C_O = distribution parameter

U_{sg} = superficial gas velocity (ms^{-1})

U_{sl} = total superficial liquid velocity in the riser (ms^{-1})

where k_L could be considered to be reasonably independent of gas holdup as small holdups will produce a small change in the term (1- ε). However, the equation shows that k_L is influenced by the liquid linear velocity which in turn is influenced by the gas holdup. So gas holdup does influence k_L but indirectly. For this model the bubble diameters fell between 2.5 and 8 mm therefore, k_L was expected to decrease with increasing bubble diameter as indicated by equation 4.5. Equations 4.2 and 4.5 were combined to give an expression for the volumetric mass transfer coefficient k_La using the liquid phase diffusivity, the diameter d_B and the terminal velocity U_{BT} of the bubble were k_La was very sensitive to d_B:

$$k_L a = 12\left(\frac{\zeta}{\pi}\right)^{\frac{1}{2}}\left(\frac{U_{BT}+C_o(U_{sg}+U_{sl})}{d_B^3}\right)^{\frac{1}{2}}\left(\frac{\varepsilon}{(1-\varepsilon)^{\frac{3}{2}}}\right) \qquad 4.7$$

Very few studies have shown the effect of superficial gas velocity on the bubble population distribution. Yet, the work of Bukur and Patel (1989) indicated that the Sauter mean bubble diameter below a superficial gas velocity of 0.06 ms^{-1} was a function of the column and sparger geometry and decreased with increasing gas velocity. In the absence of experimental values in this study the observations of Bukur were used to explain the k_La profiles in this reactor. Thus, the experimental k_La profiles for the fixed probe positions with the draft tube sparger were successfully modelled when a bubble diameter of 7 mm was assumed in the riser for low gas velocities. For gas velocities above 0.06 ms^{-1} a 5 mm diameter was used. In the downcomer the Sauter mean bubble diameter was likely to be smaller due to large bubbles disengaging from the top section. Hence, k_La data for the downcomer was modelled by using a Sauter mean bubble diameter of 4 mm. Therefore, the model was able to demonstrate that the influence of d_B on k_La dominated over the combined effect of gas holdup and liquid circulation velocity. Hence, the change in bubble distribution was a major factor for the higher k_La values in the downcomer than in the riser of the airlift reactor.

The model also showed that the liquid circulation time, gas holdup and slip velocity were important parameters which influenced the oxygen transfer in the individual sections of the reactor. These interrelated parameters would effect the gas residence time in the individual sections of the reactor. The bubbles in the riser would travel faster than the liquid velocity but in the downcomer the mean rise velocity of the entrained bubbles would counteract against the downward liquid velocity. Therefore, the slip velocity (the velocity of a bubble relative to liquid phase) would be greater in the downcomer than in the riser due to the opposing velocity components. The slip velocity as defined by equation 4.5 (Ayazi Shamlou *et al.*, 1994) was shown to be a complex parameter. However, in its simplest form it can be described as the difference between the mean bubble velocity and the liquid velocity. Thus, describing the slip velocity in these simple terms it was estimated that for a constant gas velocity, the downcomer slip velocity was three times greater than in the riser for the reactor with the draft tube configuration, and up to five times greater than in the riser with the annulus sparger. A bubble rise velocity of 0.25 ms^{-1} was used for these simple estimations as the data from this study indicated that the mean bubble diameters were in the region of 2 to 6 mm, and Clift *et al.* (1978) showed that the terminal rise velocity of single bubbles was independent of bubble diameter in this range. The greater difference between the riser and downcomer slip velocities with the annulus sparger configuration compared to the draft tube sparger could be partially attributed to the effect of the A_D/A_R on liquid velocity. It was discussed in section 4.1.2 that the lower A_D/A_R with the annulus sparger resulted in a 20% larger downcomer liquid velocity (U_{LD}) than with the draft tube sparger and so, the slip velocity

in the downcomer with the annulus sparged reactor would be larger than with the draft tube sparger. However, the U_{LR} with the annulus sparger was 20% less than with the draft tube sparger hence, the riser slip velocity would be the lowest with the annulus sparger. So, it must be appreciated that this was a simplistic explanation as the differences in fluid dynamic conditions between the sparger configurations discussed in section 4.1.1 would also contribute to the difference in slip velocities in the individual sections of the reactor. Nevertheless, it has been demonstrated in simple terms that the slip velocity in the downcomer was greater than in the riser for both sparger configurations. Hence, as k_L was found to be primarily equal to the square route of the slip velocity (equation 4.6) then, k_L would be expected to be greater in the downcomer. This would lead to an enhancement of the oxygen transfer in this region of the vessel compared to the riser. The greater slip velocity of the downcomer compared to the riser also had consequences for the gas residence time. It was conceivable that the counteraction of the downward liquid velocity against the bubble rise velocity in the downcomer would result in a larger gas residence time than in the riser. This would allow more time for oxygen transfer to take place and hence, greater oxygen transfer in the downcomer than in the riser. Lubbert *et al.* (1988) studied the gas residence time distribution by helium pulse techniques in a 4 m^3 pilot scale airlift tower loop reactor. The reactor demonstrated a high gas content in the downcomer which was only a few percent less than the riser. The gas circulation time was found to be slower than the liquid circulation time. Therefore, it was suggested that as the bubble rise velocity in the riser must be faster than the liquid circulation, then the gas residence time in the downcomer must be large aiding oxygen transfer in that region of the vessel. This was confirmed by Frohlich *et al.* (1991a) in a reactor of identical geometry to that of Lubbert *et al.* (1988) which had a diameter of 0.692 m, height of 6.8 m, a A_D/A_R of 0.535 and a perforated ring sparger of 0.035 m in diameter with 4 mm orifices. The mean gas residence time in the riser with water was between 48% to 20% faster than in the downcomer over the gas velocity range of 0.054 to 0.175 ms^{-1}. The total gas circulation time around the reactor was between 18% - 25% slower than the liquid circulation time. The mean local bubble diameter of the riser with water as measured by electrical conductivity increased from 4.1 to 5.8 mm with the gas velocity range of 0.056 to 0.175 ms^{-1}, and was found to be 5 to 35% greater than in the downcomer. Similar observations were observed during a yeast fermentation (final biomass of 13 gL^{-1} DCW) in a laboratory airlift reactor which had a similar A_D/A_R value as the pilot plant reactor but a shorter height of 2.5 m and vessel diameter of 0.02 m (Frohlich *et al.* 1991c). The local bubble diameter in the downcomer was smaller (4 mm) than in the riser (10 -13 mm) at the gas velocity of 0.091 ms^{-1}. Frohlich *et al.* (1991a) also found that the riser gas holdup was 11% greater than the downcomer and the riser gas residence time was 11% shorter than the downcomer gas residence time. Hence, this explained the higher DOT of 70% half way down the downcomer of the 0.08 m^3 reactor compared to the DOT below

1% half way up the riser at 13 h into a 20 h yeast fermentation as shown by Lubbert *et al.* (1988). Lubbert *et al.* (1988) also reported that similar effects were observed in a variety of pilot scale airlift reactors ranging from 0.078 m^3 to 4 m^3 although the exact oxygen transfer details at the larger reactor scales were not given. Therefore, the reactor characteristics of a small density difference between riser and downcomer, greater bubble diameter in the riser, and high DOTs in the downcomer were similar to the observations found in this study. This provided evidence to suggest that the gas circulation time was slower than the liquid circulation time in this study. Similar DOT heterogeneity as shown in this study was observed by McNeil and Kristiansen (1990) during a batch *S. cerevisiae* fermentation in a 0.0055 m^3 external loop reactor. The DOT in the downcomer was 90% (air saturation) compared to 60% in the riser at biomass concentrations of 3 gL^{-1} DCW. However, at greater biomass concentrations above 3 gL^{-1} DCW the DOTs in the riser and downcomer had reached 1%. A comparison to the reactor in this study such as k_La was impossible as no operating or geometric parameters were given.

The detailed comparison between the DOT profiles of the downcomers from the two sparger configurations, measured by the mobile probe, emphasised the difference between the positioning of the region of greatest oxygen transfer. This would not have been possible from the insufficient data obtained from the three fixed DOT probe positions. It was shown that the greatest region of oxygen transfer occurred in the upper downcomer with the draft tube sparged reactor but in the lower downcomer position with the annulus sparger using the 10 gL^{-1} DCW yeast suspension (figure 3.8). Thus, riser DOTs remained below 1% for an approximate distance of 2.77 m from the sparger with both sparger configurations. The DOT with the annulus sparged reactor increased down the downcomer to maximum values at a distance of 6.25 m away from the sparger compared to 5.5 m with the draft tube sparger. This was presumably due to the 20% larger downcomer linear velocity with the annulus sparged reactor, which produced a 10% greater downcomer slip velocity than with the draft tube sparged reactor. The greater downcomer liquid velocity with the annulus sparged reactor would reduce the bubble residence time in the downcomer and hence, the bubbles would travel further down the downcomer before maximum oxygen transfer occurred. Similar dissolved oxygen tension heterogeneity was measured by Onken and Weiland (1981) along the circulation path of an external loop airlift reactor (8.8m tall), during the fermentation of *Candida utilis.* For a biomass concentration of 5 gL^{-1} DCW and superficial liquid velocity (riser) of 0.067 ms^{-1} the DOT (% saturation at 1 bar) did not increase above 1% until a height of 1m above the sparger. The DOT increased at a constant rate to a maximum value of 85% at a height in the reactor of 6 m, above this height the DOT decreased to 75% at a height of 8 m above the sparger. At the same biomass concentration and gas velocity but at a higher riser liquid velocity of 0.21 ms^{-1}, the DOT increased above 1% at 1 m above the sparger, but at a slower rate where the maximum value of 60% was reached at 8 m. Although, the exact details were not given the reactor

was operated with limited gas entrainment and the downcomer DOT decreased linearly with increasing distance from the top of the vessel. Hence, the position of greatest oxygen transfer moved further away from the sparger with increasing liquid velocity as shown in this study. Also, Onken and Weiland (1981) suggested that the decrease in DOT above the region of greatest oxygen transfer, 6 m above the sparger in the tall reactor, implied that the bubbles were probably depleted of oxygen. However, this does not comply with the work in this study as the measurements of inlet and exit gas compositions suggested that a variation in oxygen composition was small. So, it is unlikely that the bubbles were depleted of oxygen at the base of the downcomer. Therefore, a complete explanation of the large change in DOT at the base of the vessel has yet to be established.

The examples of DOT heterogeneity with maximum oxygen transfer occurring in the riser with tall vessels (8 m) (Onken and Weiland 1983, and Trager *et al.* 1992) compared to the maximum oxygen transfer in the downcomer of the shorter vessel in this study, suggested an influence of vessel height on the gas residence time of the bubbles and oxygen transfer. The tall vessels resulted in long gas residence times in the riser and so, most of the oxygen transfer occurred in the riser. Whereas, in the shorter vessels (2 m tall) the riser gas residence time was shorter resulting in the greatest oxygen transfer not occurring until the downcomer. However, the influence of the A_D/A_R on gas holdup and liquid velocity in relation to oxygen transfer must also be considered. Adler and Schugerl (1983) observed that the region of maximum oxygen transfer (DOTs of 70% : 3.8 gL^{-1} DCW) was in the riser during an *E. coli* fermentation using an external loop airlift reactor which had a similar height to the reactor in this study yet, the A_D/A_R was 0.11. Hence, although the external loop reactors used by Adler and Schugerl (1983), Onken and Weiland (1983) and Trager *et al.* (1992) had different vessel heights (2.75 to 8.8 m, 9.75 m respectively), the A_D/A_R were similar at 0.1 and the reactors were operated without gas entrainment. Whereas, in this study the A_D/A_R was either 0.83 or 1.13 and between 65 -75 % of the gas in the riser was entrained into the downcomer as observed with the reactors of Lubbert *et al.* (1988) discussed previously.

As the position of maximum oxygen transfer was in the riser with the tall vessels then, the entrainment of gas into the downcomer would have no benefit as the oxygen depleted bubbles would not contribute to the oxygen transfer performance of the vessel. Also, recirculated bubbles into the riser would diminish the oxygen partial pressure of the fresh gas. Hence, the tall external loop reactors 8 - 9 m tall (Onken and Weiland 1981) were operated with no gas entrainment, to increase the density difference between the riser and downcomer and enhance liquid circulation. Also, the low A_D/A_R of 0.11 would result in a short residence time of the cells in the oxygen depleted zone of the downcomer. Hence, Onken and Weiland (1983) suggested that gas entrainment would only be advantageous for short reactors. This was demonstrated in this study where gas

entrainment was essential to achieve the maximum oxygen transfer of a vessel with a draft tube height of 2.77 m and A_D/A_R of 0.83 or 1.13.

The local k_La measurements in this study were difficult to compare to the overall k_La measurements from the literature with mostly air / water systems. However, the overall k_La values (average of the position k_La measurements) with the yeast suspension and concentric reactor used in this study were found to be similar to the overall k_La values of other internal and external loop reactors of similar height (Lindert *et al.* 1992, Barker and Worgan 1981, Bello *et al.*, 1985). This indicated that despite the differences in gas entrainment and maximal oxygen transfer positioning brought about by the different A_D/A_R, reactors of similar height would have similar overall k_La values. However, it was shown in this study that the poor oxygen transfer performance in the riser with DOTs below 1% was detrimental to the OUR of the yeast broth (10 gL^{-1} DCW) but, there was evidence to suggest that this may improve on scale up. The increase in hydrostatic pressure with the vessel height would result in pressures higher than 1 atmosphere in production vessels, for instance the ICI deep shaft reactor of 65 m in length had an hydrostatic pressure of 6.5 bars, 7.5 bars absolute (Onken *et al.* 1984). Thus, the hydrostatic pressure at production scale would improve the oxygen saturation concentration and avoid DOTs below 10%. This was demonstrated by Trager *et al.* (1992) where the DOT heterogeneity at atmospheric pressure was from 100% in the riser decreasing to 50% in the downcomer during the fermentation of *A. niger* (2 gL^{-1} DCW) in an external loop reactor. However, at 1 bar above atmospheric the DOT heterogeneity was from 270% in the riser to 170% in the downcomer, hence the amplitude of the DOT cycling remained similar with increasing pressure while the individual DOT values increased. Similarly, Onken *et al.* (1984) demonstrated that the oxygen transfer rate increased proportionally to aeration rate at 1.5 and 7 bars during the fermentation of *C. utilis* in a 1.1 m tall, 0.02 m^3 concentric airlift reactor. The maximum oxygen transfer rate of 5 $gO_2\ L^{-1}.h^{-1}$ was obtained at 7 bars compared to 1.5 $gO_2\ L^{-1}.h^{-1}$ from working at 1.5 bars. This was due to the higher gas flow rates obtainable at 7 bar of 15 L min^{-1} compared to 3.5 L min^{-1} at 1.5 bar due to the lower specific volume of the air at higher pressures. The limited data of the k_La of tall vessels made it impossible to make direct k_La comparisons with the reactor height in this study but, evidence existed to suggest that k_La may also improve with scale up, as k_La has been shown to increase with vessel height (Barker and Worgan 1981, Onken and Weiland 1983, Russell *et al.* 1995). Also, k_La increases with a reduction of A_D/A_R and hence, this was presumably one of the reasons why the A_D/A_R of 0.1 was used in the taller reactors of 8 to 9 m (Onken and Weiland 1983, Trager *et al.* 1992) and with the 60 m tall ICI SCP pressure cycle concentric reactor.

To summarise this section a qualitative description of the oxygen transfer changes around the vessel with the 10 gL^{-1} DCW yeast broth could be made which incorporated the explanations that have been put forward in this discussion.

For both spargers the DOT along the length of the riser and top section was below 1% air saturation and hence, the driving force remained large. A small increase in k_La was observed towards the top of the vessel which was probably due to the reduction in hydrostatic pressure at the top of the riser, leading to gas expansion and an increase in local gas holdup. However, the k_La values were considerably lower than the values in the downcomer. These low k_La values were predicted by the model derived by Ayazi Shamlou *et al.* (1995) when a larger Sauter mean bubble diameter of 5 - 7 mm was used for the riser, which would result in small gas residence times. This would contribute towards the low OTR in the riser compared to the downcomer.

In the downcomer the changes in oxygen transfer differed between the sparger configurations. For the draft tube sparger there was a rapid increase in DOT and k_La between the top section and the upper downcomer, indicating an increase in OTR. The gas holdup may have contributed to this increase as the top section gas holdup may be similar to the riser holdup, as Merchuk (1991) found that the mean top section gas holdup was similar to the mean riser gas holdup. Also, the local gas holdup in the upper downcomer would be at its highest due to the low hydrostatic pressure. The mean bubble diameter may have been smaller than in the riser due to the entrainment of smaller bubbles. This was shown by Ayazi Shamlou *et al.* (1995) whereby a Sauter mean bubble diameter of 4 mm was required to model the k_La values in the downcomer, which indicated that the smaller bubble size would be of greater benefit to oxygen transfer than the larger bubbles in the riser. Also, the downcomer slip velocity which was approximately three times greater than in the riser, would lead to an enhancement of k_L and the long gas residence time relative to that in the riser would allow more time for oxygen transfer to occur. From the upper downcomer to the base of the downcomer the DOT decreased with k_La. Therefore, the OTR decreased down the downcomer due to the low gas holdup. This low rate of OTR occurred around the base of the reactor due to the low gas holdup and oxygen depletion and hence, would be expected to eventually reach zero. However, the OTR was maintained in the riser at the low level due to the introduction of gas from the sparger. So, for reasons that have been already discussed this OTR remained low along the riser and was considerably smaller compared to the OTR in the downcomer.

For the annulus sparger there was a large increase in OTR from the top section to the lower downcomer shown by the increase in DOT and k_La. Thus, the increase of OTR down the downcomer would be due to the smaller mean bubble diameter than in the riser, as explained above for the draft tube sparger. Also, the downcomer slip velocity, which was five times greater than in the riser and 10% greater than in the downcomer with the draft tube sparger, would result in a smaller gas residence time in the downcomer than with the draft tube sparger. So, the bubbles in the downcomer with the annulus sparger would travel further down the downcomer before the large increases in oxygen transfer occurred. It was likely that the large decrease in DOT and k_La at the base of the

downcomer was due to the formation of large bubbles by coalescence which produced smaller k_La values than in the upper downcomer.

Therefore, it has been shown that none of the single explanations satisfactorily describe the oxygen transfer changes around the vessel. However, by using them in conjunction with each other a general qualitative summary of the oxygen transfer changes around the vessel could be described although the explanation remained very complex. The importance of fluid dynamics in determining the oxygen transfer performance of the separate sections of the reactor has been demonstrated. It was hypothesised that the changing bubble distribution in the reactor dominated the oxygen transfer performance of the separate sections of the vessel over the effects of liquid circulation time and gas holdup. The gas holdup, slip velocity and liquid circulation rates were found to be important factors. It was predicted that the greater slip velocity of the downcomer relative to the riser would enhance oxygen transfer through the improvement of k_L. Also, the longer gas residence time in the downcomer relative to the riser would be beneficial to allow sufficient time for oxygen transfer to occur. This demonstrated the importance of experimental measurements of gas residence times in the separate sections of the reactor to be undertaken, which may allow a greater understanding of the oxygen transfer changes in the reactor in relation to the circulation time. The detailed comparison of the oxygen transfer between the riser and downcomer by using the mobile probe emphasised the necessity for gas entrainment with a reactor of this height and A_D/A_R (0.83 - 1.13) in order to achieve sufficient oxygen transfer. The importance of using a mobile DOT probe to study the oxygen transfer around the vessel compared to using a small number of fixed probe positions has also been shown.

4.1.4 The effect of top section configuration on the hydrodynamic and oxygen transfer performance of the conventionally aerated vessel

The fluid dynamics of the top section of an airlift reactor have been shown by many researchers (Chisti 1989, Weiland 1984, Russell *et al.*, 1994, Merchuk *et al.*, 1994) to have an important influence on the overall performance of the vessel. The top section would influence the gas disengagement from the vessel and the amount of entrained gas into the downcomer which would also affect liquid circulation. The investigation of the effect of gassed height above the draft tube on gas entrainment was especially important for this study as the downcomer section of the vessel was the region of highest oxygen transfer with both sparger configurations.

4.1.4.1 The effect of top section size on the sectional gas holdups and liquid circulation with the two sparger configurations

The overall, riser and downcomer gas holdups from the reactor configured with either the annulus or draft tube sparger were found to be independent of the gassed liquid height above the draft tube (figure 3.11). This was identical to the observations of

Russell *et al.* (1994) in which the same reactor was used as for this study, but with the perforated plate sparger.

The fact that the downcomer gas holdup (directly measured with the draft tube sparger) was independent of top section size (figure 3.12) implied that the height of the liquid above the draft tube did not effect the entrainment of gas into the downcomer. However, the flow rate of gas entering the downcomer, the liquid velocity and the bubble slip velocity must also be considered. The liquid circulation time was found to be independent of top section height (figure 3.14). This implied that the liquid circulation time did not change with the increase in path length due to the increasing top section height. Hence, it seemed reasonable to assume that the liquid velocity through the top section and into the downcomer was also constant with increasing liquid height above the draft tube. This suggested that the path length for liquid circulation did not change with the increase in liquid height above the draft tube and provided evidence of two distinct zones in the top section. The lower zone, where the bulk of the liquid recirculation took place into the downcomer and an upper zone which was bypassed by the flowing liquid. This will be discussed in greater detail in relation to the mixing time in section 4.1.4.2. As the downcomer gas holdup and the liquid velocity were found to be independent of top section liquid height then, the fraction of gas entrained into the downcomer may also have been independent of the top section size. Although the downcomer gas holdup was not directly measured with the annulus sparger, the fact that the overall gas holdup, riser gas holdup and liquid velocity remained independent of top section size, indicated that the entrainment of gas into the downcomer was also independent of top section size as with the draft tube sparger. This can be described by using the equation for downcomer gas holdup (ε_D) derived by Russell (1989):

$$\varepsilon_D = \frac{Q_{GD}}{A_D\,(U_{LD} - U_{SD})} \qquad 4.8$$

where

U_{LR} = downcomer liquid linear velocity

U_{SD} = slip velocity between liquid and gas phases in the downcomer

A_D = cross sectional area of the downcomer

Q_{GD} = mean volumetric flow rate of gas in the downcomer

In section 4.1.1 it was discussed that the downcomer liquid velocity would determine the degree of the gas entrainment into the downcomer. At a constant gas flow rate the bubble size would be expected to be the same in the downcomer regardless of the top section size, as it was concluded that the downcomer liquid velocity was independent of the top section size. Thus, the mean bubble slip diameter would also remain independent of top section size due to the constant bubble size and liquid velocity. Therefore, as the lower terms of the equation remained constant with increasing top section liquid volume, then the gas flow rate would also be expected to be constant. Russell *et al.* (1994) suggested

that the independence of the gas entrainment upon the liquid volume in the top section may result from the two zone flow pattern. The height of the lower zone, where bulk liquid circulation occurred, would not increase as the top section size increased and so the residence time of the liquid in the top section remained constant with top section height. This implied that the degree of bubble disengagement from the top section was not altered as the liquid volume of the reactor was increased. This was also confirmed by the constant overall gas holdup with the changing top section which showed that the total gas content in the reactor did not alter.

4.1.4.2 The effect of the top section height on the mixing performance of the vessel

The mixing time decreased with increasing gassed liquid height above the draft tube up to a certain gassed height with both spargers (figures 3.16 & 3.17). Above the critical height no further improvement in mixing performance was observed. This demonstrated the importance of the top section geometry on the mixing performance of the vessel. The ungassed liquid height (critical height) at which no further increase in mixing performance occurred remained constant with increasing gas velocity and was equivalent to 0.47 m above the draft tube for both sparger configurations. This corresponded to the working volume of 0.25 m^3. Weiland (1984) found a similar ungassed critical height value of 0.4 m above the draft tube in a 0.054 m^3 concentric draft tube reactor with a column diameter of 0.2 m and height of 1.7 m with water. For a gas velocity of 0.0105 ms^{-1} the mixing time at the height of the draft tube was 150 seconds which reduced to 50 seconds at the ungassed height of 0.4 m above the draft tube. Above the height of 0.4 m no significant change in mixing performance occurred. Weiland (1984) concluded that the ungassed height above the draft tube for optimum mixing performance should be twice the column diameter. However, this remained simplistic as it ignored the effect of the gassed heights with increasing gas velocity.

The critical gassed liquid height at which mixing time remained constant for this study was found to increase with gas velocity (figures 3.16 & 3.17). At gas velocities below 0.06 ms^{-1} the critical gassed height was between 0.4 to 0.55 m above the draft tube which increased up to 0.75 to 0.9 m with gas velocities above 0.06 ms^{-1}. Russell *et al.* (1994), using the same reactor as in this study but with the perforated plate sparger, found that the gassed critical height increased with gas velocity and both the ungassed and gassed critical heights were similar to those obtained with both the sparger configurations used in this study. This seemed surprising considering the difference in gas holdup, liquid velocity and mixing time profiles described in section 4.1.1. This emphasised the importance of the geometry of the reactor and in particular the cross sectional area and liquid height in the reactor in determining the mixing performance of the vessel.

The presence of the critical height, above which no further increase in mixing performance occurred, was further evidence for the existence of a two zone flow pattern

in the top section of the reactor as briefly discussed in section 4.1.4.1. This model was originally described by Chisti (1989) but also used by Russell *et al.* (1994) to describe the changes in mixing time with increasing top section height. Chisti (1989) used phenolphythalein dyes in an acidified liquid to visibly observe the changes in mixing and liquid flows patterns as the top section of an airlift reactor was increased. The reactor was a split tube internal loop reactor, 4.35 m tall with a perforated pipe sparger, column diameter of 0.243 m and A_D/A_R of 0.41. Between the draft tube and gassed liquid heights above the draft tube up to 0.5 m, the liquid flowed through the whole of the top section. As the liquid level was increased above the 0.5 m (measured up to 1 m) two zones were formed. Poor intermixing between the two zones was observed and the bulk liquid circulation predominated in the lower section. These observations resemble the effect of top section size obtained in this study. The rapid decrease in mixing time before the critical height was reached, indicated the existence of the lower zone where no upper zone was present. Russell *et al.* (1994) described the improved mixing up to the critical height as being due to the increased residence time of the liquid in the turbulent top section which enhanced the rate of pulse dispersion. The existence of the upper zone became apparent when the mixing time became constant with top section size as the high degree of mixing in the lower zone did not interfere with the upper zone. Further evidence for the two zone model was the decrease of the injected pulse amplitude with increasing top section height, which then remained constant when the critical height was reached.

Small differences did occur in the effect of the gassed liquid height on the mixing times between the two sparger configurations but only above the gas velocity of 0.054 ms^{-1}. For the draft tube sparger at all gas velocities the mixing time decreased rapidly to the critical height above which no further improvement in mixing performance occurred (figure 3.16). However, at gas velocities above 0.054 ms^{-1} for the annulus sparger (figure 3.17) the mixing time was found to decrease gradually with increasing gassed height above the draft tube. Hence, the actual position of the critical height was less distinct than with the draft tube sparger. Also, the mixing times for each gas velocity above 0.054 ms^{-1} but at the low gassed heights (below 0.4 m above the draft tube) were considerably shorter (40% reduction) than the mixing times at the same gas velocity with the draft tube sparger. These differences were difficult to explain however, they occurred at gas velocities above 0.054 ms^{-1} where the flow regime began to change with increasing gas velocity. Hence, the difference in fluid dynamics and bubble interactions associated with the two spargers in the transitional flow regime (section 4.11) may account for the difference in mixing time profiles.

Therefore, it has been shown that a two zone flow pattern was used to explain the effect of the top section configuration on the mixing time of the vessel. This also demonstrated the importance of the top section configuration in determining the overall mixing performance of the vessel.

4.1.4.3 The effect of the top section configuration on oxygen transfer performance of the vessel

The dissolved oxygen tensions from the mobile probe and k_La values remained constant with increasing top section height (figures 3.18) for both sparger configurations. This would seem reasonable considering it was previously concluded that the entrainment of gas was also independent of the top section height. This independence of oxygen transfer occurred even though the mixing performance increased with the top section size.

4.2 The effect of the marine propeller on the hydrodynamic and oxygen transfer performance of the aerated vessel with the draft tube sparger

The vessel performance with the draft tube sparger was compared to combined operation with the marine propeller. The propeller was operated to pump liquid up the draft tube in the direction of the liquid flow from aeration. This configuration did not produce any significant improvement in gas holdup, liquid circulation or liquid mixing of the aerated vessel and was detrimental to gas holdup with propeller speeds above 500 rpm (figure 3.19 & 3.20). This implied that the total gas content within the vessel was decreasing with propeller operation above 500 rpm. Hence, entrainment of gas into the downcomer was reduced as gas disengagement from the top section increased. Consequently, propeller operation above 500 rpm changed the bubble size distribution of aeration operation to a distribution involving a majority of large fast rising bubbles with small gas residence times in the riser and top section, resulting in little gas entrainment. The low gas holdup at propeller speeds above 700 rpm was probably due to the near flooding of the propeller with gas from the sparger. This would result in large coalesced fast rising bubbles leaving the trailing edge of the propeller which would reduce the riser and downcomer gas holdup. This seemed feasible as the propeller was the same diameter as the sparger and was only 0.07 m above the sparger. The build up of gas within the vicinity of the propeller also accounted for the increase of DOT in the lower riser position (figure 3.22). Also, the reduction in gas entrainment was marked by the decrease in downcomer DOT with increasing propeller speed (figure 3.22).

The liquid fluctuations and hence, changes in overall and downcomer gas holdup observed at 500 to 700 rpm probably marked the transition to a partially flooded propeller. The part of the liquid level fluctuation from the high overall gas holdup to low holdup values, was probably due to the build up of gas behind the propeller, with the formation of large bubbles leaving the trailing edge of the propeller. The large bubbles in the riser would decrease the overall gas holdup and entrainment into the downcomer, which would account for the decrease of downcomer DOT. Also, the build up of gas by the trapping action of the propeller would account for the increase of the DOT in the lower riser position. As the propeller speed range of 500 - 700 rpm was not large enough for near total propeller flooding then, the large build up of gas behind the propeller would eventually be released. This marked the return to a bubble distribution similar to aeration

only operation and resulted in the increase of the liquid level to the high gas holdup values. Hence, as the propeller speed increased above the speeds at which fluctuations occurred, the propeller was probably nearly totally flooded producing the characteristic low gas holdup from the release of large bubbles from the propeller.

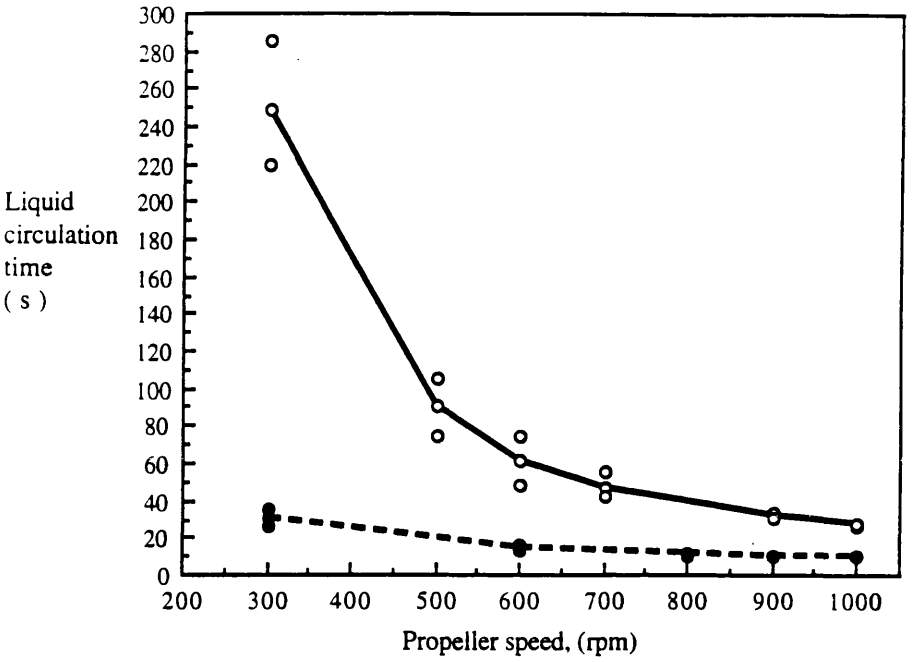

Figure 4.4 Comparison of the liquid circulation time as a function of propeller speed, between propeller only operation (without aeration) of the airlift reactor configured with the draft tube sparger (0) and the annulus sparger (•) with baker's yeast, H_{DT} of 2.77 m and working volume of 0.25 m^3.

Therefore, no significant benefits were observed by operating the marine propeller with the draft tube sparger in this configuration. This was partly due to the poor contribution of the propeller to the liquid circulation rates of the aerated vessel. When the draft tube sparger was present under the propeller, the liquid circulation times from propeller only operation (either direction and with no aeration) with increasing propeller speed were found to be considerably slower than with propeller only operation (in either direction) with the annulus sparger present (figure 4.4). Hence, the only difference between the configurations was the positioning of the spargers although no aeration was used. This indicated that the presence of the draft tube sparger under the propeller, with the same diameter, restricted the formation of the liquid circulation flow loops of the propeller (figure 1.4). Therefore, vessel performance with aeration and propeller operation with the draft tube sparger, may be improved if the propeller was situated underneath the sparger with a smaller diameter of sparger or propeller. Hence, the liquid circulation flow would not be blocked by the sparger and gas flooding would be limited. This could not be investigated in this study as it was not possible to change the length or positioning of the propeller drive shaft mounting and the location of the sparger within the

draft tube. Therefore, the greater contribution of the propeller to the liquid circulation with the annulus sparger, resulted in a more detailed investigation being concentrated on this configuration, than with the relatively functionless draft tube sparged propeller configuration.

4.3 The hydrodynamic and oxygen transfer performance of the annulus air sparged airlift reactor with propeller operation

The marine propeller was used in conjunction with the annulus sparger to aid entrainment of liquid into the top of the downcomer and recirculation at the base of the vessel into the riser. The improved vessel performance with propeller operation was compared with conventional aeration using the 5 and 10 gL^{-1} DCW yeast broth suspension.

4.3.1 The effect of the propeller on the gas holdup and liquid circulation of the aerated vessel

The propeller was found to increase the overall gas holdup, riser gas holdup and liquid circulation rates of the aerated vessel (figures 3.24 & 3.25). The propeller had the greatest effect of decreasing the liquid circulation time and increasing gas holdup of the aerated vessel at the low gas velocity of 0.036 ms^{-1}. The propeller was more effective at gas velocities below 0.054 ms^{-1} and had less of an influence at higher gas velocities due to the dominating effect of the gas velocity. This was probably due to extra energy dissipation from the formation of turbulence in the riser at gas velocities above 0.054 ms^{-1} which resulted in less energy available for liquid circulation. The reduction of the influence of the propeller at increasing both the gas holdup and liquid velocity with increasing gas velocity emphasised that the improved gas holdup was interrelated to the enhanced liquid velocity.

In relation to the total energy dissipation rate for the combined aeration propeller operation, small increases of energy dissipation relating to propeller operation up to 600 rpm produced the greatest change of the hydrodynamic and oxygen transfer parameters (figure 3.33). Overall and riser gas holdup increased at similar rates for propeller speeds up to 600 rpm but above 600 rpm, overall holdup increased at a faster rate reaching greater values than the riser gas holdup for all gas velocities (figure 3.24). The increase of overall gas holdup implied that there was an increase in the total gas content within the vessel and a decrease in the rate of gas disengagement from the top section compared to conventional aeration operation. It was discussed in section 4.1.1 that the overall gas holdup was an average value of the gas holdup of the riser, top section and downcomer. Therefore, it seemed reasonable to assume that as the overall and riser gas holdup were within close proximity up to propeller speeds of 600 rpm then, a similar increase in downcomer and top section gas holdup also occurred. A similar conclusion was found from estimating the downcomer gas holdup from the riser and overall holdup values

using equation A2.3, as the direct measurement of downcomer gas holdup was not possible with this reactor configuration.

The increase of downcomer gas holdup with propeller operation indicated that the action of the propeller to draw liquid down the draft tube increased the entrainment of gas into the downcomer. The entrainment of gas was enhanced in the annulus aerated reactor configuration by the 20% greater downcomer liquid velocity (U_{LD}) compared to the riser liquid velocity (U_{LR}) due to the A_D/A_R of 0.83. Also, it was discussed in section 4.1.1 that the magnitude of the U_{LD} determined the amount of gas entrainment into the downcomer. Thus, the increase of liquid velocity in the vessel by propeller operation would promote gas entrainment into the downcomer and decrease gas disengagement from the top section. The propeller may have produced some degree of bubble breakup (Brauer, 1979) which would also increase gas holdup. This may have begun above the propeller as turbulent and swirling liquid flow was observed in the top section with propeller operation. This swirling liquid flow was even observed in the riser at propeller speeds above 600 rpm (section 3.3.8). In the region of the propeller, bubble cavities would form behind the blades where smaller bubbles would leave the trailing edge (Brauer, 1979). Hence, the propeller would produce a different bubble distribution at the base of the downcomer compared to the aeration only operation.

The increase in riser gas holdup may have occurred by a number of ways. The enhancement of liquid recirculation by the action of the propeller would promote gas recirculation into the riser from the high gas content in the downcomer. Also, the mean bubble diameter of the recirculating gas would be smaller than in the riser due to the bubble breakup from the propeller, further enhancing riser gas holdup. The mean bubble diameter in the riser may also have been reduced compared to conventional aeration operation by the increase in liquid velocity from propeller operation. It was discussed in section 4.1.1 from the work of Onken and Weiland (1983) that for a constant gas velocity the bubble interactions and hence, bubble coalescence would reduce as the superficial liquid velocity increased, aiding gas holdup. However, the increase in U_{LR} by propeller operation would also decrease the gas residence in the riser which would produce some degree of counteraction against the increase of gas holdup. The counteracting effect of the decrease in gas residence time may account for the reduction in the rate of increase of the riser gas holdup at energy dissipation rates corresponding to propeller operation above 600 rpm (figure 3.33a).

The greater reduction in the rate of increase of riser gas holdup compared to overall gas holdup at propeller speeds above 600 rpm resulted in overall gas holdup values some 11- 32% greater than riser gas holdup, over the range of gas velocities studied. This implied that the gas holdup of the top section and downcomer was greater than the riser, assuming that the overall gas holdup was the average value of the vessel. Hence, the effect of the propeller at increasing turbulence and bubble break-up in the downcomer may have been greater at propeller speeds above 600 rpm. Also, the top

section gas holdup would be expected to increase with propeller speed due to the increase of gas entering the top section. Top section gas holdup may also have been greater than the riser and downcomer gas holdup. Equation 2.6 derived by Russell (1989) for estimating the sectional gas holdups from experimental values as discussed in section 4.1.1 assumed that the top section gas holdup was equal to the riser gas holdup. Thus, the equation can be derived to estimate the top section gas holdup using the holdup values obtained at high propeller speeds. The top section gas holdup estimated from the riser and overall experimental values resulted in a gas holdup which was 1.5 times greater than the riser gas holdup. This did not seem unreasonable as various researchers have experimentally observed values in this range with aeration configurations. Orazem *et al.* (1979) observed top section values in the range of 1 - 2 times greater than the riser gas holdup with a concentric loop reactor. Hence, the top section may have made a considerable contribution to the overall gas holdup of the vessel with propeller operation especially above speeds of 600 rpm. An increase in top section gas holdup may have expected to produce a similar increase in downcomer gas holdup due to the entrainment of gas. However, it may be possible that the propeller disrupted the flow path of bubbles that ultimately disengaged from the top section and so their residence time would be increased in the top section. The top section was very turbulent with propeller operation compared to aeration only operation. At gas velocities below 0.054 ms^{-1} the bubbly flow and calm liquid surface with the aeration was totally disrupted into a turbulent surface with the propeller operation (section 3.3.8). So the action of the propeller drawing liquid down the draft tube, disrupted the normal bulk flow path of the top section. Hence, the vertical flow of larger bubbles from the riser which under conventional conditions would normally disengage, may have been disrupted. The action of the propeller may have drawn disengaging bubbles further across into the centre of the top section before leaving the vessel. Hence, the bubble residence time in the top section would be increased improving the overall gas holdup. The turbulence in the top section and fast bulk circulation flow may have caused some degree of bubble breakup at high propeller speeds which would also increase gas holdup in the top section. The increased turbulence in the top section may have resulted in surface aeration contributing to the gas holdup in the top section although this was probably minimal.

It has been demonstrated that in general both the gas holdup and liquid circulation performance of the aerated vessel were increased by propeller operation. For conventional aeration, liquid circulation was controlled by the gas velocity which also affected gas holdup. Whereas, propeller operation allowed independent control of the liquid circulation with the aerated vessel, but the gas holdup was also influenced. Therefore, for a constant superficial gas velocity, propeller operation resulted in a greater gas holdup and liquid circulation performance than the aerated only vessel. However, this improved vessel performance by propeller operation could be matched by conventional aeration by increasing the gas velocity. For example, propeller operation at

1000 rpm with the gas velocity at 0.036 ms^{-1} produced a similar gas holdup and liquid circulation performance to that for aeration only operation at 0.072 ms^{-1}. The energy dissipation rate studies showed that the increase to the higher gas velocity with aeration only operation would have a more desirable smaller energy dissipation rate (348 Wm^{-3}) than from the propeller and aeration operation at the lower gas velocity (602 Wm^{-3}). Nevertheless, the improved vessel performance from propeller operation could not be matched by an increase in gas velocity from aeration only operation when the maximum allowable gas velocity of 0.136 ms^{-1} was used.

The propeller had no significant effect on the mixing time of the aerated vessel apart from a small (15%) reduction at the low gas velocity of 0.036 ms^{-1} with propeller speed at 1000 rpm. This implied that the mixing performance of the reactor was dominated by aeration which was further emphasised by the increase of the ratio of mixing to circulation time from 2.2 - 3.0 with increasing propeller speed (figure 3.27). As the liquid circulation time reduced with increasing propeller speed, a greater number of circulations of the vessel were required to reduce the injected pulse to 90% homogeneity. The effect of the propeller on the mixing and circulation performance of the aerated vessel was further emphasised by the comparison of the propeller only performance (without aeration) to that of the aerated vessel. The mixing performance of the vessel with propeller only operation was poor when compared to aeration only operation (figure 3.28c & d). Also, the liquid mixing to circulation time ratio for the propeller only system was found to be 5 compared to 2.5 for aeration operation. Although the propeller reduced the liquid circulation times of the aerated vessel, the actual circulation times for propeller only operation were 70 - 35% faster than compared to aeration only and combined aeration and propeller operated systems (figure 3.28a &b). Applying aeration to the propeller only operated reactor actually decreased the liquid circulation rates of the vessel (increased circulation time) although the mixing performance was improved. This implied that a difference in the velocity profiles across the cross sections of the riser and downcomer existed between the operating conditions. For propeller only operation the liquid circulation flow would be expected to be a streamlined, parabolic type velocity profile over the cross section of the riser. Fast peak velocities existed in the centre of the riser, the pipe axis, with slower movement towards the boundary layer and vessel wall. The pH probe which detected the circulating pulses penetrated 0.04 m into the riser, which would not be far from the highest region of velocity at the pipe axis of 0.05 m from the inner vessel wall. Hence, the liquid velocities calculated from the circulation times would be near to the maximum possible values and would be greater than the mean velocity of the bulk liquid flow. Limited radial mixing probably occurred in this situation however, the Re number of the liquid was found to be in the lower turbulent section (1-4 $x10^4$) where a limited amount of radial mixing would be expected. For aeration only operation which demonstrated greater mixing but poorer liquid circulation than with propeller only operation, the velocity profile was probably flatter across the cross section

of the riser, where greater radial mixing occurred. In this situation the pH would measure a liquid circulation time through the bulk of the liquid flow which would produce a mean liquid velocity closer to the actual value. Therefore, with combined propeller and aeration operation, the propeller would increase the liquid flow by streamlining the flow to produce a more parabolic shaped velocity profile across the riser compared to the flatter profile with aeration only operation. This would reduce the radial mixing, however a counteraction to this may have been the increased turbulent flow and bubble breakup caused by the propeller in the downcomer. This would result in no significant change of the mixing time of the vessel. Flattening of the velocity profile with aeration could be due to extra energy dissipation from turbulent mixing resulting in less energy for liquid circulation.

4.3.2 The effect of the propeller on the DOT and k_La values of the aerated vessel

At all gas velocities (0.036 - 0.136 ms^{-1}), the propeller was found to increase the DOTs and k_La values of the downcomer above the conventional aeration values (figure 3.29 & 3.31). A greater proportion of the downcomer had high DOTs as the propeller speed was increased. During propeller operation the k_La profiles showed a similar trend as with conventional airlift operation where values in the downcomer were between 2 and 5 fold greater than in the riser (figure 3.31). This increase of k_La and DOT was probably dominated by the increase of gas entrainment into the downcomer and associated bubble breakup with propeller operation. Also, the oxygen transfer in the downcomer would be enhanced by the greater slip velocity and gas residence time than in the riser as described for conventional aeration (section 4.1.3). In the riser, gas holdup increased with propeller speed but the subsequent improvement of oxygen transfer was insufficient to enhance the DOT above 1% air saturation, at gas velocities below 0.091 ms^{-1} with the 10 gL^{-1} DCW yeast broth. Hence, the OUR exceeded the OTR in this region of the vessel under those operating conditions. The DOTs were increased above 5% in the riser with the 10 gL^{-1} DCW broth by either a gas velocity of 0.091 ms^{-1} and propeller operation of 1000 rpm, or a gas velocity of 0.136 ms^{-1} and a propeller speed of 600 rpm (figure 3.29c & d). It was only at the gas velocity of 0.136 ms^{-1} and propeller speed of 1000 rpm that the DOT remained above 30% in the whole of the vessel with the 10 gL^{-1} DCW yeast broth. The increase of oxygen transfer in the riser with propeller operation could have originated from the increase of riser gas holdup but also, from the high recirculation rates of liquid and gas from the downcomer at the base of the vessel as discussed in section 4.3.1. At all gas velocities the downcomer DOT above the propeller increased to high values with increasing propeller speed (figure 3.29). Therefore, it could be speculated that with propeller operation with low gas velocities (0.036 ms^{-1}), the DOT increased through the propeller region of the reactor and then decreased to below 1% towards the base of the vessel. As the gas velocity and propeller speeds were increased, high DOTs

above 10% may have penetrated further around the base of the vessel. Thus, at the gas velocity of 0.136 ms^{-1} and propeller speed of 1000 rpm, the DOT was sufficiently high enough in the downcomer (85%) and the liquid circulation time sufficiently fast enough for the DOT to only decrease to 41%, after passing around the base of the vessel and into the riser. However, it remained uncertain as to whether the increased DOT around the base of the vessel was due to recirculated gas or high DOTs in the recirculating liquid. The DOT was also shown to remain mostly constant along the riser at all operating conditions. This implied that the oxygen transfer performance of the recirculated liquid from the downcomer dominated the oxygen transfer performance of the riser.

The effect of the propeller on the DOT profile of the aerated vessel, as with conventional airlift operation, was found to be independent of top section size. Gas holdup, liquid circulation and k_La were similar at the two ungassed liquid heights of 0.0 m and 0.47 m above the draft tube with aeration and propeller operation. However, the mixing time was found to be poorer at the lower liquid height which implied that the two zone mixing model described for conventional aeration existed with combined aeration and propeller operation.

As a consequence of propeller operation the OUR was found to increase with propeller speed (figure 3.32) and was dominated by the increased liquid circulation rates, gas holdups and improved DOT in the downcomer. For both biomass concentrations the largest increase of OUR (3 fold) occurred with propeller operation with the lowest gas velocity of 0.036 ms^{-1}, which corresponded to the largest improvement of gas holdup and liquid circulation time. Hence, as the propeller speed increased a greater proportion of the downcomer had higher DOTs yet, for gas velocities below 0.136 ms^{-1}, the DOT in the riser remained below 1% with the 10 gL^{-1} DCW broth as with conventional aeration. So with propeller operation the cells experienced greater DOT changes around the vessel, as higher DOTs were involved in the downcomer compared to conventional aeration. Nevertheless, the liquid circulation rates improved with propeller operation and so the OUR was enhanced as the cells experienced the DOT changes at a higher frequency than with conventional aeration. This is emphasised in table 4.1 by comparing nos. 1 & 2. For the 10 gL^{-1} DCW yeast suspension the maximum OUR was 52 $mmol.L^{-1}.h^{-1}$ as the OUR did not increase any further when the DOTs in the riser rose from 10% with the propeller speed of 900 rpm, to above 30% at 1000 rpm with the gas velocity of 0.136 ms^{-1} (see table 4.1: compare nos. 5, 6 & 7). The studies with the 5 gL^{-1} DCW yeast broth confirmed the previous observations in which the maximum OUR (24 $mmol.L^{-1}.h^{-1}$) was obtained when the DOTs reached 10% in the riser with the gas velocity of 0.072 ms^{-1} and 900 rpm (Table 4.1: compare nos. 8 & 9). Also, the DOT remained above 35% at all operating conditions with the 0.136 ms^{-1} gas velocity and so the OUR remained at the maximum value (Table 4.1: compare 12 & 13). The gas holdup, circulation and k_La values with the 5 gL^{-1} DCW broth were found to be similar to the values measured with the 10 gL^{-1} DCW yeast broth, indicating that the hydrodynamic performance of the vessel

Table 4.1 Comparison of the effect of cycling dissolved oxygen tension (DOT) on the oxygen uptake rate of the baker's yeast suspension, between the airlift reactor configurations of conventional aeration with annulus gas sparging and combined aeration and propeller operation.

Operating conditions	Gas velocity (ms^{-1}) propeller speed (rpm)	DOT riser & Top section (% saturation)	Circulation time in the riser and top section (s)	DOT downcomer (% air saturation	Circulation time in the downcomer (s)	Oxygen uptake rate (mmol. L^{-1}. h^{-1})
Draft tube height of **2.77 m**, working volume of 0.25 m^3 with the **10** gL^{-1} DCW yeast suspension						
1) Aeration only operation	0.036	< 1	15.5	0.1 - 19	12.5	11.4
2) Aeration + propeller operation	0.036 . 1000	< 1	7.65	11 - 65	6.35	32.4
3) Aeration only operation	0.091	< 1	8.3	0.1 - 63.2	6.7	29.4
4) Aeration + propeller operation	0.091 . 1000	6	6.7	26 - 80	5.5	49
5) Aeration only operation	0.136	< 1	7.1	7.2 - 81	5.9	42
6) Aeration + propeller operation	0.136 . 900	11	6.6	18 - 81	5.4	51
7) Aeration + propeller operation	0.136 . 1000	36	6.5	42 - 85	5.3	52
Draft tube height of **2.77** m, working volume 0.25 m^3 with the **5** gL^{-1} DCW yeast suspension						
8) Aeration only operation	0.072	< 1	10.2	0.1 - 57	8.3	10.5
9) Aeration + propeller operation	0.072 . 900	26 - 15	6.8	33 - 92	5.65	23
10) Aeration only operation	0.091	< 1	8.3	18 - 73	6.7	18.5
11) Aeration + propeller operation	0.091 . 600	10 - 15	7.1	34 - 87	5.9	24
12) Aeration only operation	0.136	43 - 44	7	48 - 75	5.5	23.5
13) Aeration + propeller operation	0.136 . 1000	76 - 65	6.8	59 - 99	5.3	23
Draft tube height of **1.78** m, working volume 0.16 m^3 with the **10** gL^{-1} DCW yeast suspension						
14) Aeration only operation	0.036	< 1	11.75	6 - 10	11.25	14
15) Aeration + propeller operation	0.036 . 1000	< 1	4.3	11 - 50	3.3	45
16) Aeration only operation	0.09	< 1	7.0	28 - 62	6	32
17) Aeration + propeller operation	0.09 . 1000	12 - 15	4.25	30 - 63	4.5	51

was independent of the biomass concentrations used in this study. Therefore, the use of the propeller with the 5 and 10 gL^{-1} DCW yeast broth showed that the OUR was not affected by DOT heterogeneity if the lowest DOT of the cycling DOTs was above 10%. Whereby, the cells experienced DOTs of 10% for half the circulation of the vessel, i.e. 6.5 s out of the 12 s circulation time, with DOTs from 10 to 80% for the remainder of the circulation. This was emphasised in table 4.1 by comparing nos. 5 & 6 to 10 & 11.

The comparison of propeller operation between the tall (2.77 m H_{DT}) and short reactor (1.78 m H_{DT}) emphasised the effect of the frequency of DOT cycling on the OUR of yeast cells (10 gL^{-1} DCW broth). Under all operating conditions the liquid circulation times from the short reactor were 20 - 30% faster than with the tall reactor (figure 3.42). Nevertheless, the improvement of liquid circulation with propeller operation at the shorter reactor height was of a similar magnitude to that with the tall vessel (figure 3.42 & 44). The gas holdup and DOT changes around the vessel were similar for conventional aeration and with propeller operation at both reactor heights (figures 3.43, 45 & 29) Thus, similar OURs were obtained at both reactor heights with propeller speeds above 800 rpm and using gas velocities above 0.072 ms^{-1} as the DOTs were above 10% in the vessel (figure 3.48). However, for propeller speeds below 800 rpm with all gas velocities, the OURs with the shorter vessel were found to be between 12 to 50% greater than with the taller vessel. Hence, the greater liquid circulation with the shorter reactor may account for the larger OURs of the yeast broth than obtained with the tall vessel for the same DOT profiles. For example, at the gas velocity of 0.036 ms^{-1} with conventional aeration, the liquid circulation time and OUR for the short vessel were both 22% greater than with the tall reactor (table 4.1: nos. 1-14). Similarly, at the same gas velocity but with propeller operation, the circulation time and OUR for the short reactor were 22 and 84% greater respectively than with the tall reactor (table 4.1: nos. 2&15). Therefore, the comparison of the tall to short reactor showed that the influence of DOT heterogeneity on the OUR of the yeast broth was reduced if the cells experienced similar DOT changes at a greater frequency. However, the maximum OUR, even with the faster circulation times of the short reactor configuration was not obtained until the DOTs in the riser and top section, which occurred for half the circulation of the vessel, had risen up to 10% with changing DOTs above 30% in the downcomer (table 4.1: nos. 17&4). This occurred at circulation times of 12 s with the tall reactor compared to 8 s circulation times with the short reactor. This suggested that the achievement of the maximum OUR was more dependent on the lowest DOT of the cycle rather than the frequency that the cells experienced the DOT changes, as shown within the circulation times obtained in this study. Abel *et al.* (1994) indicated that the yeast cells could not respond to rapid changes in DOT and the cells assumed a metabolism based on the average DOT of the cycle. However, in this study the OUR was improved if the cells experienced the DOT changes at a greater frequency. This suggested that the cells were responding to the rapid change

of DOT around the vessel and hence, cell metabolism was not based on an average DOT of the vessel.

The increase in oxygen transfer by propeller operation with the conventionally aerated reactor was shown to be caused by the interrelated effect of increased gas holdup and liquid circulation. However, the comparison of the influence of the propeller on k_La and DOT between the tall and short reactor configurations gave some evidence of the individual contribution of gas holdup and liquid circulation to the enhancement of oxygen transfer by propeller operation. The propeller produced similar increases of gas holdup at both reactor heights, but the k_La values of the short reactor with the faster liquid circulation rates were between 30 - 66% greater than the taller reactor (figure 3.46). This, implied that the action of the propeller at improving liquid circulation had a greater influence on enhancing oxygen transfer than the gas holdup improvement. Nevertheless, despite the greater k_La values of the short reactor the DOT heterogeneity was found to be similar between both reactor heights with identical operating conditions (figures 3.29 and 3.45). This was presumably due to the greater OUR of the broth at the shorter vessel height, brought about by the improved oxygen transfer. The conclusion that liquid circulation with propeller operation had a greater influence on oxygen transfer than gas holdup may have been influenced by the mixing performance of the shorter vessel, which was 60 - 70% greater than the tall vessel (figure 3.42). Russell *et al.* (1994) also found a reduction of mixing performance (increased mixing time) with increasing vessel height with the yeast broth and reactor used in this study. The lengthening of the circulation path with increasing draft tube height extended the distance that an injected pulse would have to travel between the end sections of the vessel, where the bulk of the dispersion was shown to occur (Russell *et al.*, 1994 and Weiland, 1984). The liquid circulation times of the short vessel were faster than with the tall vessel due to the reduced liquid circulation path. However, the riser and downcomer liquid linear velocity of the short vessel were around 20% less than with tall vessel. This was due to the reduction of the hydrostatic head difference as the draft tube height decreased which reduced liquid circulation. This agreed with Russell *et al.* (1994) using the same reactor configuration and yeast broth in this study but with the perforated plate sparger. They showed that the liquid linear velocity was approximately proportional to the square root of the reactor height.

Therefore, this study has shown that the propeller can be used to reduce the DOT heterogeneity observed with conventional aeration (5 & 10 gL^{-1} DCW broths) and consequently, improve the oxygen uptake rate of the cells. However, at gas velocities below 0.072 ms^{-1} a similar vessel performance from aeration and propeller operation could be produced by simply increasing the gas velocity alone, as discussed in section 4.3.1. For gas velocities above 0.072 ms^{-1} and propeller speeds of up to 600 rpm with both broth biomass concentrations, the increased vessel performance including increased OUR and reduced DOT heterogeneity could not be improved by further increases in gas

velocity alone. Hence, a less heterogeneous DOT environment with values above 35% and maximum OUR of 52 mmol.L^{-1}.h^{-1} could only be achieved with the maximum gas velocity and propeller speed for the 10 gL^{-1} DCW yeast broth. The total energy dissipation rate estimations (figure 3.33) showed that the energy dissipation rate with combined aeration and propeller operation were not considerably greater than with conventional aeration. This indicated that the use of the propeller to reduce DOT heterogeneity of an aerated airlift reactor vessel may be a viable prospect for scale up. However, it was discussed in section 4.1.3 that the extreme DOT heterogeneity of conventional aeration observed with the pilot scale reactor in this study may improve with scale up due to improved oxygen saturation conditions from the increased hydrostatic pressure and from improved k_La. So, the propeller operated airlift reactor may not be required to reduce DOT heterogeneity at production scale although the improved gas holdup and liquid circulation rates may be of some benefit with non-Newtonian fermentations. Nevertheless, the use of the propeller, to study the impact of different degrees of reactor heterogeneity, especially DOT, has demonstrated the use of the airlift reactor as a scale down tool to simulate the heterogeneity observed in large scale stirred tank production vessels. This will be discussed in greater detail in section 4.4.1.6.

4.3.3 Comparison of the propeller operated airlift reactor configurations to other airlift reactors with mechanical agitation.

Comparison of the propeller loop reactor performance used in this study to other loop reactors with mechanical agitation was limited due to the lack of literature examples. Although large scale propeller airlift loop reactors are known to exist in industry, up to 200 m^3 (Blenke, 1985), the lack of literature data rendered a direct comparison to the propeller operated reactor configurations in this study unworthy. Concentric airlift reactors with propeller agitation have been studied for microcarrier technology and for mammalian cell culture (Varecka and Bliem, 1990, and Favre *et al.*, 1994). However, comparison of the lab. scale systems to the pilot scale propeller operation with microbial fermentations in this study was also inappropriate, as the operating conditions for the low oxygen demand and low shear conditions for mammalian cell culture were much lower than the operating conditions (total energy dissipation rate) used in this study. Similar increases in gas holdup and k_La from propeller operation in this study were observed by Kawase and Moo-Young (1986a) with a CMC solution (n of 0.54, K of 1.22 Pa.s^n) using a concentric airlift reactor with mechanical agitation. The flat six bladed impeller of 0.09 m in diameter was rotated in the top section of the concentric airlift reactor with a vessel diameter of 0.12 m. The agitator disrupted the large spherical capped bubbles increasing the gas holdup of the CMC solution. However, no improvement in gas holdup was observed with water, whereas in this study, the annulus sparged and propeller operated configuration improved the gas holdup and k_La of the conventionally aerated reactor with both yeast and non-Newtonian broths and with a 30% lower total

energy dissipation rate than used with the configuration of Kawase and Moo-Young (1986a). Keital and Onken (1981) observed improved k_La and mixing especially with viscous broths by operating a stirred tank (0.155 m^3) with a draft tube. A Rushton turbine with a diameter of 0.15 m compared to the vessel diameter of 0.45 m was operated above the sparger which were situated 0.1 m and 0.15 m below the draft tube respectively. Propeller stirrers were investigated but vessel improvement was limited compared to the performance with the turbine due to the poorer dispersion ability. Hence, the poor performance of the draft tube sparged agitated vessel in this study could be improved by replacing the propeller with a Rushton turbine to disperse the gas leaving the sparger which was situated beneath the stirrer. This would also be beneficial to gas holdup improvement during viscous fermentations from the dispersion of large bubbles formed by coalescence. The draft tube sparged and propeller operated vessel performance may also be improved by adding baffles to the vessel to avoid the vortex flow. Marquart and Blenke (1980) studied fluid pumping in a circulating loop reactor with a marine propeller located inside the draft tube of a vessel with a height to diameter ratio of 10. Axial baffles were added to the upper and lower ends of the draft tube to enhance the volume flow from the propeller by avoiding circumferential rotary motion of the liquid. Marquart and Blenke (1980) reported that a draft tube diameter to vessel diameter ratio of 0.65 produced the optimum turbulent flow and propeller pumping from a propeller loop reactor and this ratio existed in the reactor in this study. Also, Marquart and Blenke (1980) improved the volume flow from the propeller by using flow profiles which were situated around the propeller and attached to the draft tube. For propeller rotation with a clearance gap between the propeller and the draft tube, the radial discharge from a marine propeller flowed back to the suction side of the propeller so that an inner circulation about the propeller was superimposed on the axial main circulation. The flow profiles inhibited the inner circulation and directed the radial discharge into the axial discharge. Thus, similar flow profiles could also have increased the propeller performance in this study. Similar improvements in vessel performance as shown in this study with the annulus sparged and propeller operated configuration were produced with non-mechanical additions to a conventionally aerated vessel, such as static mixers. Zhou *et al.* (1993) found a 2 fold increase in the specific cephalosporin C productivity with regard to energy dissipation when an external loop airlift reactor (2.75 m tall) was fitted with static mixers (0.6 m in length) positioned half way up the riser. The mixers produced a two fold increase in k_La compared to conventional aeration as the motionless mixers suppressed slug flow formation and improved gas dispersion. Similarly perforated plates were placed at regular intervals along the ICI deep shaft reactor (100 m tall) to reduce coalescence (Kubota *et al.*, 1978).

Siegel *et al.* (1986) increased the overall gas holdup of a 4 m tall split tube airlift reactor with water by gas sparging into the riser and at the top of the downcomer which was considered to be an advantage with aerobic fermentations. This was similar to the

increase of overall and downcomer gas holdup from annulus gas sparging and propeller operation used in this study. However, propeller operation increased the liquid velocity of the vessel whereas, the overall liquid velocity was reduced with the two sparger system. Also, large coalesced air pockets were generated in the downcomer with the two sparger system resulting in unstable flow when the difference between the liquid and gas velocities in the downcomer was less than 0.25 to 0.3 ms^{-1}.

4.4 The fermentation of *Saccharopolyspora erythraea*

In large scale production vessels (100 m^3) cells can experience changing environments including substrate, pH, nutrient concentrations and dissolved oxygen which can influence biomass yield and productivity. Therefore, a greater understanding of the impact of the engineering environment, especially reactor heterogeneity, on the physiology of *S. erythraea* will lead to improved growth and production conditions. This would be important for fermentation optimisation including scale up, design and operation of bioreactors. The effect of different degrees of reactor heterogeneity on the behaviour of *S. erythraea* broths will be discussed. This includes the effect of reactor heterogeneity, especially cycling dissolved oxygen tension on rheology, morphology, growth rate, cell metabolism, erythromycin production and reactor hydrodynamics. These results will also be discussed in relation to the homogenous environment of the laboratory stirred tank, the Newtonian baker's yeast suspension and compared with previously reported studies on reactor heterogeneity.

4.4.1 Dissolved oxygen heterogeneity and erythromycin production

S. erythraea cells from both the pelleted and mycelial broths were found to experience changing dissolved oxygen tensions (DOTs) around the airlift reactor, (cycling DOT) for all operating conditions. During the growth phase of the *S. erythraea* fermentations with conventional aeration, DOT heterogeneity increased to a cycling variation of below 1% in the riser to 100% in the downcomer position which began between 12 - 20 h into the fermentation (figures 3.50, 3.52, 3.54, & 3.56). Hence, these profiles were similar to those observed with the baker's yeast suspension at equivalent gas velocity and biomass concentration (figure 3.8). However, differences were observed between the downcomer DOT profiles of the yeast and mycelial *S. erythraea* broths with draft tube air sparging. The highest DOTs (around 100%) with the mycelial broth occurred in the lower downcomer position but in the upper downcomer with the yeast broth. This demonstrated hydrodynamic and possible bubble distribution differences between the broths which will be discussed in section 4.4.3. It must be considered that the DOT heterogeneity during the *S. erythraea* fermentations may have been greater than that observed by the measurements as only the three fixed probe positions (section 2.1.2) were used with the sterile fermentations whereas, with the non-sterile yeast broth the use of the mobile probe was possible. Therefore, differences in

DOT heterogeneity around the vessel may have existed between the two rheologically different broths, which could not be detected. It is well known that the accuracy of the DOT measurement must also be considered when studying cycling DOTs environments. For example, Trager *et al.* (1991) calculated a deviation of 50% from the actual oxygen concentration when a probe with a response time of 18 s was used to monitor cycling DOT of 60 s from a continuously fluctuating gas composition in a well mixed lab. scale stirred tank. Whereas, a 5% deviation occurred when a response time of 3 s was used. In the airlift reactor, though the DOT was continuously changing around the vessel it was not cycling at each individual probe position but, varying with the changing metabolism of the cells. Nevertheless, precautions were taken to ensure that the probe response times were around 9 - 10 seconds which in most circumstances was below the liquid circulation time of the vessel, and the recorded DOTs were assumed to be reasonable representative of the true DOT values. Aeration and propeller operation reduced the DOT heterogeneity during a mycelial fermentation compared to conventional aeration (figure 3.62). This enabled the effect of cycling DOTs on erythromycin production to be discussed in conjunction with the results from the homogenous DOT environment of the 25 L working volume lab. scale stirred tank fermentation.

4.4.1.1 The effect of dissolved oxygen tension on erythromycin production

Although erythromycin is a secondary metabolite, it was shown during all the *S. erythraea* fermentations performed in this study that erythromycin production began at a slow rate during the growth phase (9 - 13 h into the growth phase) when DOTs were above 50% (figure 3.50c). Production then progressed at a fast linear production rate in the stationary phase where the final titre was achieved when substrate utilisation was near completion (figure 3.50c). This occurred some 20 hours after the maximum dry cell weight was obtained. This batch culture profile was observed by other researchers Corum *et al.* (1954), Stark and Smith *et al.* (1961), Klein (1994) and by Trilli *et al.* (1987) where continuous culture studies showed that production of the erythromycin groups (A, B, C, D and E) were growth associated. Differences of the antibiotic production profiles in relation to the other fermentation parameters were apparent from the different degrees of reactor heterogeneity associated with the different reactor configurations.

The mycelia during the majority of the growth and production phase with conventional aeration (annulus sparger) experienced changing DOTs from below 1% (air saturation) throughout the length of the riser to 100% in the downcomer with a circulation time of 11 s (figure 3.54). Whereas, the cells experienced a reduced DOT heterogeneity from aeration and propeller operation of changing DOTs from 10 to 100% and circulation times of 11- 8.5 s (figure 3.56). The extreme DOT heterogeneity of conventional aeration resulted in a two fold reduction in specific erythromycin production rate (q_{ery}) (calculated

from the linear portion of the production phase) and final titre (table 4.2) compared to erythromycin production with the reduced DOT changes from aeration and propeller operation. The DOT changes with conventional aeration resulted in a delay of the onset of the fast linear production phase which began some 7 hours later than with combined aeration and propeller operation (figure 3.61). Also, the slow rate of erythromycin production which occurred before the fast linear phase, progressed at a slower rate and for a longer duration with conventional aeration than with propeller and aeration operation (figure 3.61). The DOT profile from the mycelial fermentation in the well mixed stirred tank was similar to the riser DOT profile from the aerated and propeller operated airlift reactor (figure 3.79) yet, the q_{ery} and final titre from the stirred tank were 4 and 3 fold greater respectively than with combined propeller and aeration operation (table 4.2). This suggested that the changing DOTs of the combined aerated and propeller operated reactor was detrimental to erythromycin production.

Table 4.2 Comparison of erythromycin production between the different morphology *S. erythraea* broths and reactor configurations

Reactor configuration & morphology	Apparent viscosity (Pa.s)	Total energy dissipation rate (Wm^{-3})	Final specific erythromycin production (mg g^{-1} DCW)	Specific erythromycin production rate (q_{ery}) ($mg.g^{-1}.h^{-1}$)	Erythromycin production with respect to energy dissipation ($mg.W^{-1}.h^{-1}$)
Draft tube sp.					
Pelleted	0.77	607	4. 2	0.28	3.74
Mycelial	0.214 *	607	7.0	0.33	5.18
Annulus sp.					
Pelleted	0.8	727	4.75	0.27	3.8
Mycelial	1.0	727	7.5	0.25	3.9
Annulus sp. +propeller					
Mycelial	0.7	1576	11.75	0.5	3.8
Lab. stirred tnk					
Mycelial	0.06	7120	35	2.07	3.3

* rheology measured with the Bohlin cup and bob rheometer rather than the Contraves concentric cylinder

4.4.1.2 Effect of dissolved oxygen tension heterogeneity on the oxygen uptake rate

Comparison of the dry cell weight and oxygen uptake rate of the growth phase from the mycelial broths with the airlift reactor configurations to the profile from the stirred tank, involving DOTs above 20% during the growth phase, revealed no significant difference (figure 3.60 & 3.79). Thus, the changing DOTs involving values below 1% air saturation for 25 h of the 35 h growth phase for conventional airlift operation, did not effect the respiration and growth rate of the mycelial broths. However, the DOT heterogeneity with conventional aeration operation resulted in a reduction of the OUR during the non growth phase from 23 to 12 - 16 $mmol.L^{-1}.h^{-1}$ (figure 3.59). Whereas, the OUR was maintained above 20 $mmol.L^{-1}.h^{-1}$ during the production phase with both the reduced DOT heterogeneity of propeller + operation and the stirred tank (figure 3.76b). This implied that with conventional aeration operation, the oxygen limitation (DOTs below 1%) of the DOT cycle during the production phase produced a reduction in the respiration rate of the broth. This also prolonged substrate utilisation with conventional aeration operation for a further 8 hours (figure 3.79) than with the reduced DOT changes from propeller operation, and resulted in the lower q_{ery} and final titre (table 4.2). The oxygen limiting values (DOT below 1%) in the riser of the aerated airlift were probably caused by the increase in broth viscosity causing a reduction in gas holdup and k_La which will be discussed in greater detail in section 4.4.2. The dry cell weight, morphology and rheology (n &K) were found to be similar between the broth from aeration / propeller operation and the stirred tank fermentation (section 3.4.4). This suggested that the changing DOTs with propeller operation (DOT cycling of 10 -100 - 10%) were the main cause of the reduced erythromycin production compared to production from the well mixed non cycling DOTs of the 25 L stirred tank. Wang and Fewkes (1977) showed that during the transfer of oxygen from gas to the mycelium of an *S. niveus* fermentation in a laboratory scale stirred tank, that not only the oxygen transfer from the gas was important but also the contribution from the resistance to oxygen transfer from the bulk liquid to the mycelium. Even though it is a tentative explanation it may be possible that the oxygen transfer with aeration and propeller operation was sufficient to produce similar growth rates to those of the stirred tank. However, the 10 fold larger apparent viscosity with airlift reactor operation (table 4.2) may have provided an extra resistance to oxygen transfer from the liquid to the mycelia which restricted erythromycin production. Higashide (1984) commented that the aerobic requirement for erythromycin synthesis during the production phase was considerably greater than the requirement during the growth phase, although no exact details were given. Also Bushell (1988) expressed the oxygen requirement of *Streptomyces* sp. to be between 2 - 4 $mmol.g^{-1}.h^{-1}$ compared to 0.26 $mmol.g^{-1}.h^{-1}$ for *E.coli* during the growth phase. Martin and McDaniel (1975) also expressed that polyene macrolide antibiotic production were strongly aerobic processes. Wang and Fewkes (1977) indicated that any change in

morphology may effect the response to DOT and so different morphologies could be associated with different erythromycin production in this study. However, morphological differences between aeration / propeller and the stirred tank broths in this study were not particularly significant (figures 3.57 & 3.80). Although with propeller operation the main hyphal length and branch length was 3 - 20 μm and 2 μm longer respectively than with the stirred tank broth. Makagiansar (1992) showed that q_{pen} increased with main hyphal length in batch culture, but above 100 μm in length the q_{pen} remained relatively independent of hyphal length. Also Belmar-Beiny and Thomas (1991) showed that clavulanic acid production from *Streptomyces clavuligerus* was independent of stirrer speed and hyphal fragmentation.

It must be considered that the erythromycin production rate and final titre for the broth in the stirred tank may have been greater than for the airlift reactor configurations due to the condition of the inoculum and media after sterilisation. The condition of the inoculum for the stirred tank may have been more conducive for antibiotic production than the inoculum for the airlift reactor, as Smith and Calam (1980) found that the condition of *P. chrysogenum* inoculum to be important for the final productivity of the production process. The inoculum transfer into the airlift reactor via over pressure from the stirred tank may have enforced a short period of oxygen limitation (1.5 L min^{-1} of broth) on the inoculum since, the transfer took 20 minutes. This may have effected the final antibiotic titre compared to the direct inoculation of the stirred tank from shake flasks. Morphological characteristics between the inoculum for the stirred tank and aeration / propeller operation were similar which suggested that the over pressure with inoculum transfer to the airlift had no significant detrimental effect on morphology. Also, the over pressure may not have affected the cells metabolism as Vardar and Lilly (1982) showed that an over pressure of one atmosphere during a penicillin V production did not effect production. Differences in medium sterilisation procedures may have affected the media, especially the protein composition which would ultimately effect erythromycin production. Therefore, the longer heating up and sterilisation time of 45 minutes for the airlift reactor could have had a greater detrimental effect on the media composition than the 30 minute sterilisation time used with the stirred tank.

4.4.1.3 Comparison of the influence of DOT on erythromycin production in this study to literature examples

The comparison of the effect of cycling DOT on erythromycin production in this study to the effect of DOT on the production of other antibiotics was limited due to the small number of studies in this area. Similar effects of changing DOT on the onset of cephalosporin production from *Cephalosporium acremonium* were observed in a 60 L airlift tower loop reactor by Bayer *et al.* (1989). When the DOT in the riser was controlled at 20%, antibiotic production began at 30 h into the fermentation. Whereas with conventional aeration, changing DOTs were present around the vessel (although not

quantified) and the DOT in the riser fell below 10% for the duration of 35 h at the end of the growth phase. This resulted in a delay in the onset of antibiotic production by 70 h. The oxygen limiting values (below 1% air saturation) involved in the DOT cycle with conventional aeration resulted in a two fold decrease in the volumetric antibiotic yield, compared to the fermentation with DOT control above 20%. Vardar and Lilly (1982) showed that cycling the DOT from 23 to 37% around the C_{crit} (critical dissolved oxygen concentration) for penicillin production of 30% with a period of 2 minutes produced a 30% reduction in the antibiotic production rate (and a 70% reduction when the DOT was cycled around 15 - 10%). The reduced production rate was equal to the rate observed with a constant DOT of 26%, which indicated that the cells maintained a metabolic rate according to the lower DOT rather than the imposed mean value, as the cells were unable to adjust to the rapid DOT changes. As with this study, Vardar and Lilly (1982) reported no effect on the growth or respiration rates by the cycling DOTs although the C_{crit} for growth (OUR) was found to be 7% (constant DOT) such that the, C_{crit} values for growth and penicillin production were separate parameters. Larsson and Enfors (1988) found that circulation times of 1 and 2 minutes with an anaerobic zone of 1% of the aerated stirred tank reactor volume of a two compartment fermentation system had no irreversible effect on the respiration rate of *P. chrysogenum*. However, irreversible inhibition occurred with circulation times of 5 and 10 minutes with anaerobic volume of 6% of the aerobic stirred tank volume. Also, Trager *et al.* (1992) showed that growth or gluconic acid production from *Aspergillus niger* were not affected from cycling DOTs from 50% in the riser to 10% in the downcomer of a 9.5 m tall (260 L working volume) external loop bioreactor. The comparison between the different degrees of reactor heterogeneity in this study showed that the OUR of *S. erythraea* during the growth phase was not affected by DOT changes involving limiting values (below 1% air saturation) from conventional aeration. Whereas, the comparison of aeration to aeration and propeller operation with the yeast suspension in this study (section 3.3.6) revealed that the OUR was affected by the similar DOT heterogeneity experienced by the *S. erythraea* cells. This was presumably due to the faster rate of metabolism and response of the baker's yeast to changing DOT when compared to *S. erythraea*. Further examples of the effect of cycling DOT on antibiotic product include observations reported by Yegneswaran *et al.* (1991) with the suppression of growth and cephamycin C productions during the cycling of DOT by two methods, Monte Carlo method: Log normal distribution consisted of an air supply of 5 s followed by no aeration for 8 seconds to 44 s and a Periodic cycling method with 5 s air supply and 20 s no air supply. Suphantharika (1992) showed that cycling DOT above C_{crit} (20% air saturation) for difficidin production with a DOT variation of 10% and period of 30 s had no effect on either difficidin or oxydifficidin production from *B. subtilis*. Cycling DOT below C_{crit} (10% variation and a period of 30 s) resulted in an increase in biomass production and specific production rates. Suphantharika *et al.* (1994)

reported that difficidin production was reduced by DOTs below 20% whereas the C_{crit} for growth was 5% and oxydifficidn was found to be produced independently of DOT.

Similar effects of DOT on the onset of the linear antibiotic production phase as observed in this study were found by Rollins *et al.* (1988) for cephamycin C production using controlled DOT operation. Controlling the DOT at 50% air saturation throughout the fermentation of *S. clavuligerus* brought the onset of antibiotic production forward by 9 hours and the specific antibiotic production rate and final titre were increased two fold compared to the uncontrolled fermentation. The uncontrolled fermentation had a duration of 10 h with DOTs below 1% during the growth phase even with operating conditions of 750 rpm and 16 $Lmin^{-1}$ airflow rate in a 10 L fermenter. A similar improvement was observed when the DOT was maintained at 100%, whereby a 5 fold increase of the specific antibiotic production rate was observed and a 2.5 increase in final titre, with antibiotic production occurring 15 h earlier than with no DOT control. The growth rates and biomass yield was unaffected by the DOT environment which was similar to the observations with *S. erythraea* in this study. Enzymic studies of the cephamycin production pathway under the different DO environments (Rollins *et al.*, 1990) revealed that an increase in DOT control up to 100% produced an increase in the specific activities by 2.3 and 1.3 fold of deacetoxycephalosporin C synthetase and isopenicillin N synthetase respectively with the improvement of cephamycin production. The actual activity of a multi subunit enzyme ACV synthetase which catalyses the first step in the biosynthetic pathway of the ß lactam ring antibiotic cephamycin C was not affected by DO conditions, but the stability of the enzyme during the growth phase was reduced by the oxygen limitation that occurred during the growth phase (Rollins *et al.*, 1991). Also, the last stage in the conversion of penicillin N to cephamycin was shown to be most sensitive to the oxygen state of the cultures and hence, limited antibiotic production occurred under low DOT environments. Therefore, the cycling and low DOTs (below 40%) may have a similar effect on the enzymes involved with erythromycin production. Multiple enzyme complexes are known to be involved in the assembly of the polyketide skeleton (Divers, 1990) although the effect of dissolved oxygen tension on the individual enzyme catalysed steps is not known. However, the dissolved oxygen concentration may directly effect the polyketide enzyme complex involved with the conversion of propionate and methyl malonate to erythromycin D, and oxygen is known to be directly involved in erythromycin A production from another route via glucose and S-adensoyl-L-methionine (Corcoran and Hahn, 1975). The onset of the production of the 16 membered macrolide antibiotic tylosin by *S. fradiae* (compared to erythromycin as a 14 membered macrolide) was also found to be affected by the DOT environment (Chen and Wilde, 1991). Tylosin production occurred 25 h earlier under saturation conditions than with the uncontrolled DOT fermentation involving DOTs below 25% during the growth phase. Substrate utilisation and tylosin yield were reduced by 3 fold when the DOT was switched from 100% to 25% during the growth phase. Feren and Squires (1969) also found that the

C_{crit} for capreomycin production (polyene macrolide) from *Cephalosporium* sp. was between 8 - 10% and the C_{crit} for respiration (OUR) was between 0 to 8%. However, the converse was true for cephalosporin C, where C_{crit} for production was 0 to 7%, whereas the OUR was effected by DOTs between 13 - 23 %. Martin and McDaniel (1975) found that the C_{crit} for Candicidin production (polyene antibiotic) from *S. griseus* was 20% air saturation.

4.4.1.4 Effect of energy dissipation on erythromycin production

The erythromycin production rate with regard to energy dissipation (mg W^{-1}. h^{-1}) was found to be similar between the mycelial fermentations in the aerated, aerated / propeller operated airlift reactor configurations and stirred tank vessel (table 4.2). Hence, the specific erythromycin production rate (q_{ery}) was directly proportional to the total energy dissipation rate used in this study (table 4.2). Similar results were observed by Paca *et al.* (1978) as the erythromycin titre (relative concentration) was directly proportional to power dissipation (Wm^{-3}) which was studied up to 4000 Wm^{-3} using a 0.3 m^3 stirred tank. During the growth phase DOTs were above 20%, but during the production phase the DOT ranged from below 1% at the energy dissipation rate of 1800 Wm^{-3}, up to 25% at 4000 Wm^{-3}. The exact C_{crit} for erythromycin production was not known, but it seemed reasonable to assume that the erythromycin production would be effected at DOTs below 40% as shown from the literature examples previously discussed (section 4.4.1.3). Thus, the linear relationship of erythromycin production and energy dissipation rate in this study and of Paca *et al.* (1978) involved DOTs which were limiting to erythromycin production. If the small 10 h duration of oxygen limitation was prevented in the lab. scale stirred tank by an increase in stirrer speed and hence, energy dissipation rate then a large increase in antibiotic production may occur which was not proportional to the energy dissipation rate. Klein (1994) showed that specific erythromycin production was reduced by 3 fold when the DOT remained below 10% for a duration of 10 h during a 100 h *S. erythraea* stirred tank fermentation compared to a fermentation with DOTs above 60%. However, these results may have been affected by morphological changes as the fermentation with limiting DOTs was operated at a stirrer speed of 250 rpm compared to 500 rpm for DOTs above 60%. Therefore, it is likely that if the energy dissipation rate was further increased to avoid oxygen limiting DOTs (above 35%) then, the erythromycin production may remain constant with increasing energy dissipation rate. This was demonstrated by Makagiansar (1992) as the q_{pen} was not affected until the energy dissipation rate in batch culture increased above 10,000 Wm^{-3} with the DOT remaining above 35% saturation. However, the main hyphal length decreased continually from 150 μm at the dissipation rate of 3800 Wm^{-3} to 58 μm at a dissipation rate of 33,600 Wm^{-3}. Klein (1994) provided some evidence to suggest that erythromycin production followed a similar regime where cell breakage (protein release) increased and erythromycin production decreased by a 2 fold increase of the energy

dissipation rate from 3000 to 14400 Wm^{-3}. Both these examples were found to correlate well with the break up theory of Smith *et al.* (1990) which suggested that hyphal breakup depended on the frequency of mycelial circulation through the zone of high energy dissipation of the impeller. Attempts at correlating hyphal length or q_{ery} to this hyphal breakup model were not made in this study due to the insufficient amount of experimental data at different energy dissipation rates and the lack of applicability of the model to conventional airlift reactor operation. Therefore, the q_{ery} may remain constant with energy dissipation up to a maximum value beyond which the q_{ery} decreases due to shearing effects on morphology. However, Belmar-Beiny and Thomas (1991) found that clavulanic acid production was independent of stirrer speed (energy dissipation rate up to the 15000 Wm^{-3}) despite the acceleration of initial hyphal fragmentation phase with increasing stirrer speed.

4.4.1.5 Reactor productivity performance with respect to energy dissipation

The proportionality of energy dissipation with erythromycin production rate within the operating (DOT) limits of this study implied that erythromycin production rate and final titre would probably be similar from an equal power dissipation comparison between the stirred tank and airlift reactor, although this was not carried in this study. Malfait *et al.* (1981) found that the biomass yield for *Monascus purpures* was 18% greater in a 55 L external loop airlift reactor than in a stirred tank. Here, the power requirements of the airlift reactor were 50% less and the k_La was 2.5 fold greater than with the stirred tank. The low shear capacity of an airlift reactor has also been shown to produce greater productivity by less mycelial damage than in a stirred tank (Wase *et al.*, 1985, Stasinopoulos and Seviour, 1992, Chang *et al.*, 1994). However, Schugerl (1990) compared the production of a variety of antibiotics between lab. scale stirred tanks and tower loop airlift reactors and volumetric productivity was higher in the stirred tank but specific productivity, especially in respect to the energy dissipation rate and yield coefficients were greater in the airlift reactor. For penicillin V production the benefits of airlift reactor technology were only observed when pelleted morphologies were used due to the lower apparent viscosity, resulting in greater oxygen transfer and lower energy dissipation requirement than for a mycelial broth. Similarly, the beneficial improvements of tetracycline production in the airlift reactor were only possible when a pelleted broth was compared to a mycelial broth in the stirred tank. Trager *et al.* (1989) also found that airlift and stirred tank reactors performed equally well for gluconic acid production from *Aspergillus niger* only if pelleted fermentations were performed in the airlift reactor. Therefore, in this study with pelleted broths of *S. erythraea,* the beneficial effects of greater gas holdup and k_La with the lower viscosity pelleted broths (draft tube sparged) compared to the higher viscosity mycelial broth (annulus sparged) (table 3.2 & 3.3: section 3.4.2) did not reduce the DOT heterogeneity, and specific erythromycin

production with the pelleted broth was 2 fold less than observed with the mycelial broth. This may have been due to dissolved oxygen gradients of the individual pellets leading to oxygen limitation. Wittler *et al.* (1986) used microprobes to measure the dissolved oxygen partial pressure gradients in the pellets for penicillin production and found that the optimum pellet diameter for penicillin production was 400 μm. The change in oxygen uptake rate during the fermentations for the pelleted broths (draft tube aerated) was similar to the mycelial profile indicating that respiration was not effected by the pelleted morphology. Nevertheless, the oxygen requirement may not have been sufficient for the pelleted broth to produce similar erythromycin production to that from mycelial broths.

The comparison of erythromycin production between conventional aeration and combined aeration / propeller operation emphasised the poor performance of the conventionally aerated airlift reactor with viscous broths. Similar poor reactor productivity with viscous broths was discussed by Suh *et al.* (1992) for xanthan gum production from *Xanthomonas campestris* in a pilot scale airlift reactor. Similar effects of DOT on xanthan gum production were observed as with the mycelial broths and conventional aeration in this study whereby, growth rates and respiration were unaffected by the cycling DOTs of the airlift reactor during the growth phase. However, in the non growth phase a reduction in the OUR was observed due to oxygen limitation (DOTs below 1%) from an increase in broth viscosity which also resulted in a decrease of specific xanthan production. Cycling the gas composition into a bubble column with no oxygen transfer for 20% of a 5 minute period produced similar specific xanthan production as the airlift reactor. This confirmed that the cyclic depletion of oxygen in the airlift reactor effected the respiration and xanthan production. Xanthan production was found to be directly proportional to the oxygen transfer rate in the airlift reactor under oxygen limiting conditions. Suh *et al.* (1992) showed from the comparison of the airlift reactor to a bubble column with reduced DOT heterogeneity, that oxygen limitation should be avoided for xanthan production. However, stagnant zones may also exist in stirred tank reactors which may account for the reduction in final xanthan titre by 30% compared to the bubble column. The poor performance of the conventional aeration configuration in this study with respect to erythromycin production resulted in a similar conclusion to that of Suh *et al.* (1992) that oxygen limiting values should be avoided in a cycling DOT environment. However, as expressed by Pons *et al.* (1990) operation of the reactor with over pressure may reduce the oxygen limitation. The poor performance of the pilot scale airlift reactor in respect to antibiotic production in this study may be improved at production scale due to the large hydrostatic pressure, producing a high driving force for oxygen transfer. This may avoid the oxygen limiting values below 40% (air saturation) which would effect erythromycin production. This will be further discussed in section 4.4.4.

4.4.1.6 Large scale heterogeneity and scale down

In stirred tanks the reduction in mixing efficiency and mass transfer capacity during scale up (Lilly, 1983) can result in cells at production scale experiencing fluctuating environments of substrate, oxygen, pH and nutrient concentrations which can effect biomass yields and productivity (Sweere *et al.*, 1988a). Hence, the inefficient bulk mixing and mass transfer in conjunction with the hydrostatic pressure can lead to oxygen concentrations gradients at production scale (Vardar and Lilly 1982). These can be vertical gradients as observed by Manfredini and Cavallera (1983) at 112 m^3 scale for tetracycline and chlortetracyline production by *Streptomyces aureofaciens.* Axial DOT variation at 90 h into a chlortetracycline fermentation increased from 45% near the liquid surface to 62% near the lower impellers, compared to 22% at the top to 36% near the base at 137 h of the 150 h fermentation. Radial as well as axial DO gradients were observed by Oosterhuis & Kossen (1984) in a 19 m^3 fermenter of *Gluconobacter oxydans* involving DOT changes from 15% near the impeller to 3% nearer the vessel wall. Carrington *et al.* (1992) observed DOT cycling at 80 h into an antibiotic fermentation (unnamed) when the apparent viscosity had reached 1350 cP, in a 20 m^3 bubble column with air sparging inside the helical cooling coil acting as a type of split draft tube. The DOT cycling involved DOT increasing from 17% near the sparger to 44 % in the top section with a corresponding decrease down the downcomer back to 17% in the sparger. At lower viscosities 420 and 880 cP the DOT around the vessel remained constant at 40% +/- 4%.

Therefore, it could be argued that the airlift reactor circulation path could either simulate the dissolved oxygen gradients of the radial zone or the vertical axis of the large scale stirred tank. The circulation loop with DOTs below 1% during the duration of the riser, and high DOTs in the downcomer could mimic the change from the well mixed oxygenated region in the vicinity of the stirrer to a stagnant oxygen limited zone experienced in production scale stirred tanks. However, the DOT heterogeneity from below 1% in the riser to 100% in part of the downcomer with conventional aeration in this study was severe DOT cycling compared, to the smaller changes of DOT (20 - 40%) observed from the literature examples of large production scale vessel heterogeneity previously described above. Nevertheless, the effect of different degrees of DOT heterogeneity on erythromycin production, previously discussed with the airlift reactor, could be used to simulate the effect of DOT gradients on erythromycin production in production scale stirred tanks. This could be at the scale of 100 m^3 as the liquid circulation times (transport time of the broth volume) of 10 - 20 s were measured at this scale by Geraats (1994) which were within the operating region of 30 - 10 s with the airlift reactor in this study. Successful scale down approaches using two compartment stirred tank systems were proposed by Oosterhuis & Kossen (1984), and Sweere *et al.* (1988b) which were discussed in section 4.1.3. Geraats (1994) successfully used a two compartment model to simulate the fluctuating environment of a 100 m^3 production vessel

and successfully solved the productivity loss during scale up of lipase production from *Ps. alcaligenes* by changing the circulation time and gas composition of the compartment system to study different degrees of heterogeneity. Single stirred tank systems have been used by Sweere *et al.* (1988a) to study physiological effects of cycling DOT on yeast metabolism by varying the gas composition, and a similar system was used by Suphantharika (1992) to study effect of cycling DOT on difficidin and oxydifficidin production by *B. subtilis*. Thus, the use of the propeller with conventional aeration of the airlift reactor in this study allowed the effect of different degrees of heterogeneity to be studied on cell physiology and metabolism and negated the requirement for gas composition change required for the stirred tank compartment systems. Also, the loop circulation of the airlift reactor resulted in the cells experiencing the different DOT zones at the same time which would be similar to the changes observed in a production scale stirred tank and in the two compartment model systems. However, in a single tank system all the cells experience a set value of DOT at the same time. The stirred tank compartment models require laboratory scale reactors due to the requirement of changing gas composition which to some extent limits the working volume of the system, the sampling frequency and volume removal. It was for this reason that Brandes *et al.* (1993) chose a (60 L) pilot scale airlift reactor as opposed to a small 5 L scale compartment system to allow a greater working volume for off line analysis while studying the effect of a changing environment on the stability of a temperature induced plasmid in *E.coli*. A disadvantage of the pilot scale airlift reactor as a scale down tool was that although the propeller could be used to reduce the DOT heterogeneity, the circulation time also improved and hence, the frequency the cells experienced the cycling DOT was also reduced. The stirred tank compartment systems are more flexible allowing the cycling DOT amplitude and frequency to be altered independently. With the airlift reactor a change in vessel height was required to study the effect of the frequency of cycling DOTs on the cells metabolism, as discussed with the yeast suspension (section 4.3.2). Also, for the airlift reactor configurations in this study and for the tubular loop studies of Katinger (1976), McNeil and Kristiansen (1990) the mean circulation time was used and the circulation time distribution was not modelled. This was completed by Sweere *et al.* (1988b) using the two compartment systems which produced a more representative model of the large scale environment.

4.4.1.7 Summary

The DOT heterogeneity (involving DOTs below 1% air saturation for part of the vessel loop) observed with conventional aeration operation of the airlift reactor produced a two fold reduction of the erythromycin production rate and final titre, when compared to the reduced DOT heterogeneity of the aeration and combined propeller operation involving changing DOTs above 5%. However, this DOT heterogeneity with propeller operation was also detrimental to erythromycin production when compared to the well

mixed DOT of the stirred tank. The improved erythromycin production rate was found to be proportional to the increase of energy dissipation rate within the range used in this study from conventional aeration (600 - 700 Wm^{-3}) to the combined aerated and propeller operated airlift reactor (1576 Wm^{-3}) and through to the stirred tank (7120 Wm^{-3}). Comparison between the different degrees of reactor DOT heterogeneity revealed that the growth (oxygen uptake rate or dry cell weight) of either the mycelial or pelleted broths was not affected by the extreme DOT heterogeneity of conventional aeration. However, the OUR during the stationary phase was reduced by up to 2 fold by the cycling DOT involving limiting values (below 1% air saturation) and this was probably associated with the reduced erythromycin production. The erythromycin productivity from the viscous mycelial broth from the conventionally aeration reactor was considered to be poor when compared to the other reactor configurations and the manipulation of the broth morphology to a pelleted broth (maximum diameter of 135 μm) was detrimental to the reactors productivity performance in relation to erythromycin production.

4.4.2 Rheology and morphology

All *S. erythraea* fermentations in the pilot scale airlift reactor and lab. stirred tank, including pelleted broths, were described in this study as pseudoplastic and the power law model was fitted for the duration of the fermentations. Similar observations were made for *S. erythraea* broths by Warren *et al.* (1995) and Gavrilescu *et al.* (1992) including a number Actinomycetes; *S. griseus, S. aureofaciens* and *S. rimosus.* Also, the model has been used for the majority of a *S. aureofaciens* fermentation (Tuffile and Pinho, 1970), and for *S. leavis* (Allen and Robinson, 1990). The Casson model was used for *S. fradiae* fermentation broths (Ghildyal *et al.* 1987) and the Bingham model for *S. niveus* broths (Steel and Maxon, 1966).

4.4.2.1 Rheology of the *S. erythraea* broths from the annulus gas sparged airlift reactor and lab. scale stirred tank

Fermentations with the airlift reactor using the annulus sparger configuration and the lab. scale stirred tank showed a rapid increase in consistency index (K), apparent viscosity and decrease in flow behaviour (n) during the growth phase (figures 3.54b, 3.56b, 3.77). This was followed by a more gradual change in flow behaviour, consistency and apparent viscosity (μ_a) during the production phase. The consistency index correlated reasonably well with the increase in dry cell weight during the growth phase (figure 4.5a). The relationship could probably be improved if more measurements had been taken during the growth phase. Morphological changes may also be important as an increase in main hyphal length and hyphal growth unit were also observed during the growth phase (figures 3.55 & 3.78). Warren (1994) showed a similar correlation of consistency with dry cell weight during the growth phase of *S. rimosus, Actinomadura roseorufa* and during the whole of the fermentation for the *S. erythraea* broths.

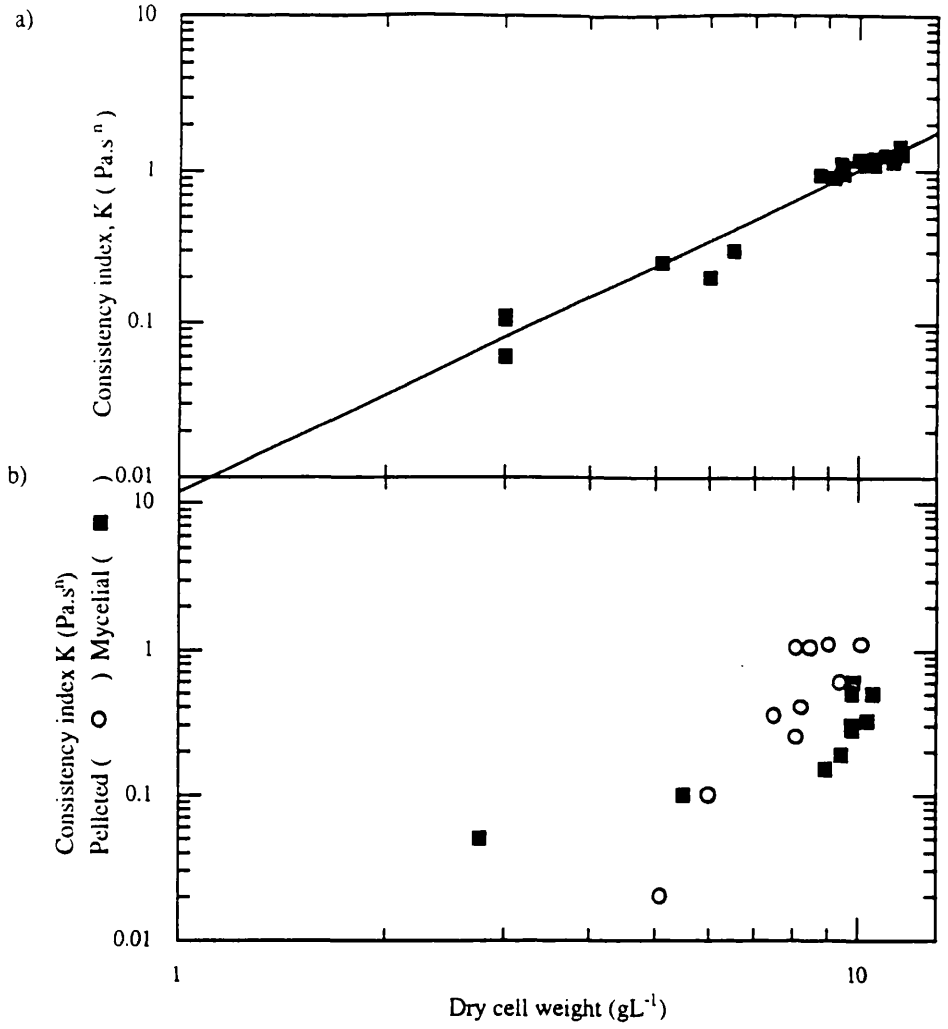

Figure 4.5 The relationship of between dry cell weight and consistency index for *S. erythraea* broths;
a) mycelial broths with the airlift reactor (annulus sparged) and stirred tank
b) mycelial and pelleted broths with the airlift reactor (draft tube sparged)

However, rheological changes did not correlate with a change in morphology as investigated by the image analysis method used in this study, as no significant change in morphology could be related to rheology or engineering environment parameter. Warren *et al.* (1995) observed a rapid decrease in n during the growth phase as in this study, but n then remained between 0.2 to 0.4 for the remainderof the fed batch fermentation. Meanwhile K gradually increased up to maximum values of 7 - 9 Pa.s^n (20 gL^{-1} DCW) between 70 - 100 h into the fermentation. Similar observations were made by Tuffile and Pinho (1970) with *S. aureofaciens* from a 300 L stirred tank fed batch fermentation. Gavrilescu *et al.* (1992) observed similar K values to those of Warren *et al.* (1995) also using production media but with batch *S. erythraea* fermentations in 20 m^3 and 100 m^3 stirred tanks. Consistency (K) and flow behaviour (n) were found to change together and both parameters remained relatively constant during the production phase as observed in this study. This indicated that the gradual increase in K throughout the fermentation

with Warren *et al.* (1995) and Tuffile and Pinho (1970) was due to the fed batch operating conditions whereas, batch fermentation was used by Gavrilescu *et al.* (1992) with the similar rheological changes during the fermentation as observed from the batch fermentations in this study. The larger K values of 7 - 9 $Pa.s^n$ of the industrial fermentations compared to 1.2 - 1.4 $Pa.s^n$ in this study were mainly due to the larger dry cell weight (DCW) of the fed batch fermetnations of 20 gL^{-1} DCW compared to the batch fermentation of 10 gL^{-1} DCW in this study. The differences of morphology may also have contributed to the rheological differences as the mutated production strain of *S. erythraea* used by Warren *et al.* (1995) had a main hyphal length of 10 - 30 μm compared to 30 - 70 μm of the wild type strain used in this study. The industrial strains were also grown on an industrial medium containing insoluble components such as starch and flours. Warren (1994) showed that the media constituents had no significant direct contribution towards the total viscosity of the broth, yet zeta potential measurements and particle precipitation theory suggested that the interparticle forces affected rheology by the influence of pH. This was less important in this study as a soluble medium was used for the batch culture. Similar correlations of biomass to rheological parameters, n and K have been made for non-Newtonian broths by other researchers (Metz *et al.*, 1979, Ghuildyal *et al.*, 1987, Allen and Robinson, 1990) but morphological factors have also shown to be equally important from correlations involving the mycelial aggregate and cell concentration with *A. niger* broths (Fatile 1985). More recently Tucker *et al.* (1993) and Olsvik *et al.* (1993) have directly correlated measured morphological parameters from image analysis and cell concentration to rheological parameters with *P. chrysogenum* and *A. niger* broths. Tucker *et al.* (1993) have shown that *P. chrysogenum* broths of similar age and broth concentration had different rheological properties due to the different measured clump (mycelial entanglements) characteristics.

4.4.2.2 Rheology and morphology of the *S. erythraea* broths in the conventionally aerated reactor with draft tube gas sparging and comparison to the broths from the annulus gas sparged reactor

For the mycelial and pelleted broths in the draft tube sparger, only small changes in K occurred during the growth phase with more rapid changes occurring once maximum dry cell weight (DCW) was obtained. This resulted in a maximum peak value at 39 h (figures 3.50b & 3.52b). Hence, the correlation of K to DCW (figure 4.5b) was less pronounced than with broths from the annulus sparger configuration. This suggested that changes in morphology may have had a greater influence on the rheology of broths from the draft tube sparger reactor than from the broths with annulus gas sparging. The morphological differences between the mycelial broths of the two aerated configurations included a shorter main hyphal length during the growth phase by 5- 10 μm with the broth in the draft tube sparged reactor which may not be that significant (figure 3.64). Changes in branch length and hyphal growth unit did correspond to

changes in K during the production phase with the mycelial draft tube sparged broths. For the annulus sparged reactor no significant change of the two parameters were observed with the mycelial broth during the production phase. Researchers have observed an increase in length of some morphological parameters, including hyphal and branch length due to secondary growth after the growth phase with *P. chrysogenum* and *S. clavuligerus* broths (Packer and Thomas, 1990, Belmar-Beiny and Thomas, 1991). The morphological difference between the two mycelial broths from both sparger configurations would suggest that it was due to the influence from the difference in engineering environments of the two aerated sparger configurations. Both reactor configurations were operated with the same superficial gas velocity, similar gas holdup and k_La values during the fermentation, so the only considerable engineering environment difference between the two aerated configurations was the differences in liquid velocity profiles brought about by the different A_D/A_R ratios. In general liquid circulation rates were faster with the draft tube sparger configuration than with the annulus sparged reactor and the riser liquid velocity with the draft tube sparged reactor was 20% greater than the riser liquid velocity with the annulus sparger. This may have resulted in greater turbulence in the riser of the draft tube gas sparged configuration which effected morphology. Differences of DOT heterogeneity between the aerated configurations may have been another influence on the cell morphology, as the cells in the draft tube sparged reactor would spend less time in the oxygen limited riser than in the annulus sparged reactor due to the greater riser liquid velocity and vice-a-versa for the high DOT in the downcomer. The pelleted broth in the draft tube sparger followed a similar shaped rheological profile as the mycelial broth and the change in pelleted diameter followed the change in K (figure 3.53). This provided further evidence towards the environmental engineering factors of the draft tube sparged reactor which influenced the rheology and morphology of the cells. Further work is required to distinguish between the possible parameters, such as DOT heterogeneity, growth rates, metabolism, hydrodynamics which may have caused the difference in rheological profiles between the broths of the aerated configurations. The complicated factors influencing the rheology of fermentations were described by Olsvik and Kristiansen (1992). The dissolved oxygen concentration, specific growth rate, as well as cell concentrations were found to influence the rheology of *Aspergillus niger* in continuous culture as measured by an on-line rheometer. Also, Olsvik *et al.* (1993) studied clump morphology which made up over 80% of the *A. niger* broth in terms of compactness and roughness, whereas clump area could only be used in this study. The power law consistency index could be correlated with the biomass concentration and the roughness factor describing the hairiness of the clumps for the *A. niger* broths. Constant dissolved oxygen tensions of 7, 12 and 40% saturation did not effect hyphal length, but the roughness factor decreased with increasing DOT indicating a possible effect on hyphal - hyphal interactions within the clump. The proportion of the broths as clumps was also above 80% in this study so, further analysis of clump

morphology in this study may reveal further morphological differences between the reactor configurations which may elucidate the rheological differences between the broths from the two aerated configurations. This was highlighted from the comparison of the rheological and morphological characteristics from the mycelial broths with aeration, aeration and propeller operation and the lab. scale stirred tank. All three broths had similar dry cell weights, yet a maximum K value for propeller operation was 1.3-1.4 Pa.s^n compared to 1-1.1 Pa.s^n for aeration only operation and the main hyphal length for propeller operation was consistently longer than with aeration operation. Whereas, for the stirred tank, the hyphal length was similar to the aeration only operation yet, the maximum K was similar to profiles for aeration and propeller operation at 1.4 Pa.s^n. Therefore, the morphological measurements could not fully explain the differences in rheological parameters between the broths in the different reactor configurations.

4.4.2.3 Rheological and morphological changes after the antibiotic production phase: comparison between the reactor configurations and to literature examples

Warren *et al.* (1995) showed that the decrease in consistency after the growth phase of *S. erythraea* in a stirred tank was associated with a decrease in DCW. In this study the change in DCW after the growth phase was not as significant as the rapid decreases in K which occurred during both pelleted and mycelial broths in all reactor configurations. To some degree the decrease in morphological parameters, main hyphal length, branch length and hyphal growth unit occurred with the change in K. For example, the rapid decrease of K from 39 and 69 h in into both mycelial and pelleted broths in the draft tube sparged reactor occurred with a decrease in branch length and hyphal growth unit with the mycelial broth, (figure 3.51) and a decrease in pelleted diameter with the pelleted broth (figure 3.53). However, no significant change in morphology could account for the gradual decline in K after 60 h. For the mycelial broths in the annulus sparger configurations, K decreased with the three morphological parameters. In the lab. scale stirred tank the hyphal length decreased after the growth phase but this could not be related to the change in rheology (figure 3.78). The earlier onset of the significant decrease in K and viscosity at 60 h with the mechanically agitated systems of annulus propeller operation compared to the decrease at 75 h with aeration only operation implied that mechanical agitation brought about the earlier onset of hyphal fragmentation effects. For aeration and propeller operation the hyphal length decreased after the main growth phase compared to the aeration only operation (both spargers), where hyphal length decreased after 65 h with the annulus sparged reactor. Also, the main hyphal length remained constant after the growth phase with the draft tube sparged reactor. A decrease in hyphal length after the growth phase was also observed with the lab. scale stirred tank which was similar to the decreases observed by Belmar-Beiny and Thomas (1991) where the degree of fragmentation after the growth phase was associated

with increasing stirrer speed in batch fermentations of *S. clavuligerus*. This implied that the aeration only configuration provided a lower shear environment than with the mechanical agitation from propeller and stirred tank. However, this was probably due to the lower energy dissipation rate of the aeration operated airlift reactor (table 4.2). The low shear environment of the aerated airlift reactor (without propeller operation) compared to the stirred tank could only be concluded from a comparison upon equal energy dissipation rate.

4.4.2.4 The comparison of apparent viscosity between the reactor configurations

The different n and K values but also the different operating conditions of the reactor configurations were found to influence the apparent viscosity. For both mycelial and pelleted broths in the draft tube gas sparged reactor, the apparent viscosity followed a similar change to consistency index with peak values of 2.5 & 0.8 Pa.s respectively at 39 h and 40 h into the fermentations. For the mycelial broth with annulus gas sparging the apparent viscosity followed a similar shape with K up to 30 h, but the following peak in apparent viscosity to 1.25 Pa.s, was due to the sensitivity of apparent viscosity to a small change in n & K and to a small increase in liquid circulation time (11.2 to 11.75 s) (figure 3.54). With propeller operation the propeller speed had a large influence on the apparent viscosity brought about by the increased liquid circulation compared to conventional aeration operation. The apparent viscosity remained below 1.0 Pa.s during the fermentation and decreased to 0.7 Pa.s at 40 h into the fermentation due to the decrease in liquid circulation time under constant operating conditions which will be further discussed in section 4.4.3. On the removal of propeller operation, the apparent viscosity returned to a high aeration only value which was above 1.0 Pa.s. In the lab. scale stirred tank, the stirrer speed had a large influence on the apparent viscosity. The apparent viscosity decreased with increases of stirrer speed from 400 to 700 rpm to the extent that the apparent viscosity at 40 h into the fermentation was similar to that observed after the first 10 h (figure 3.77). So an increase of the energy dissipation rate decreased the apparent viscosity of the broth. This was further highlighted from the 10 fold greater energy dissipation rate in the stirred tank reactor than in the conventional aerated reactor resulting in a 10 fold lower apparent viscosity in the stirred tank (table 4.2). It must be considered that this difference in apparent viscosity between the airlift reactor and stirred tank may have been exaggerated by the difference in the calculation of apparent viscosity. For the airlift reactor the apparent viscosity used the shear stress closest to the vessel wall and so the largest apparent viscosity of the vessel was estimated whereas, the apparent viscosity for the stirred tank was an estimated value at the vicinity of the impeller which would be the lowest value in the vessel.

4.4.2.5 Comparison of the apparent viscosity between pelleted and mycelial broths of the airlift reactor configurations

A direct comparison of apparent viscosity with pelleted to mycelial with the draft tube sparger was complicated by the use of the different viscometers, but it was shown from the comparison of the mycelial annulus sparged broth that the maximum apparent viscosity was greater (1.2 Pa.s) compared to the pelleted broth (below 0.8 Pa.s with the draft tube sparged reactor : table 4.3). Examples of reduced broth viscosity from pelleted broths compared to mycelial broths have been demonstrated Metz *et al.* (1979). Similarly Kim *et al.* (1983) observed Newtonian broth rheology with a pelleted broth (1 mm in diameter) of *Absidia corymbifera* up to dry cell weights of 28 gL^{-1} above which non-Newtonian rheology was observed. At a 20 gL^{-1} DCW the mycelial broth had a consistency of 8000 cP and a flow behaviour of 0.4 compared to a K of 5 cP and n of 1.0 respectively for the pelleted broth. For this reason pelleted fermentations have been studied in airlift reactors due to the lower viscosity of the broths which produces greater gas holdup, and oxygen transfer than mycelial broths and these advantages will be further discussed in sections 4.4.4. This resulted in a lower power input requirement for the pelleted broths, and similar productivity of the mycelial broths, as the oxygen transfer problems from high viscosity mycelial broths were avoided (Moller *et al.* 1992, Koenig *et al.*, 1981a, Kim *et al.*, 1983). Airlift reactors have been chosen against stirred tanks as the uniform energy dissipation in the airlift made it easier to produce the required pellet size whereas, the non -uniform energy dissipation in a stirred tank from impeller edge to vessel wall by a factor of 100, made maintenance of the pellet size difficult (Schugerl, 1990). In this study pelleted broths up to 135 μm in diameter were developed by inoculation of the airlift reactor with half the inoculum concentration than used with for mycelial broths. Thus, the low inoculum concentration promoted pellet development which was shown to be one of the important factors for pellet formation as reported by van Suijdam *et al.* (1980) which included shearing forces and polymer additives. Pellet formation from the mycelial entanglements of the seed vessel inoculum only produced a maximum pellet size of 135 μm in diameter and 10% of the broth was mycelia. The pellet size was not sufficiently large enough to produce a large difference in rheology between pelleted and mycelial broths as described by Kim *et al.* (1983) and so, oxygen transfer and DOT heterogeneity were similar to the mycelial broths. To produce larger pellets, pellet development would probably be required from the shake flask stage during the scale up process as used by Moller *et al.* (1992) and Schugerl (1990).

4.4.2.6 Summary

The consistency index from the mycelial broths in the annulus sparged reactor configurations and the lab. scale stirred tank correlated reasonably well with the dry cell weight during the growth phase. This coincided with an increase of hyphal length and growth unit. For mycelial and pelleted broths in the draft tube sparged reactor the

relationship between consistency and dry cell weight was less pronounced. In the production phase of these draft tube air sparged fermentations, the branch length and growth unit changed with the rapid change in consistency index. It was suggested that the morphological and subsequent rheological differences between the broths from the two different gas sparged reactor configurations were related to the different engineering environments of the sparger configurations. In particular, the effect of the difference in cross sectional area ratios on the liquid linear velocity of the individual sections of the reactor. The increase of energy dissipation rate was shown to produce an equivalent decrease in apparent viscosity as demonstrated between the airlift to stirred tank comparison. The earlier onset of hyphal fragmentation was observed from the mechanically agitated reactor configurations which could be related to the reduced consistency and apparent viscosity. The pelleted broth apparent viscosity was reduced compared to the mycelial broth rheology although the pelleted broth remained highly pseudoplastic.

4.4.3 The effect of morphology and rheology on the hydrodynamics of the airlift reactor

The change of gas holdup, liquid circulation rate and mixing time throughout the *S. erythraea* fermentations will be discussed in relation to morphology, rheology and reactor configuration. The hydrodynamic measurements as a function of superficial gas velocity at two intervals during the fermentations will also be discussed and compared to the Newtonian baker's yeast suspension.

4.4.3.1 Gas holdup

In general, once the operating conditions became constant, the gas holdup (overall, riser and downcomer) was found to decrease with increasing apparent viscosity during the pelleted and mycelial *S. erythraea* fermentations in the different airlift reactor aerated configurations (figures 3.50d, 3.52d, 3.54d). Russell (1989) observed similar reductions in gas holdup from the increase in apparent viscosity during a batch *P. chrysogenum* fermentation with the airlift reactor used in this study but using the perforated plate sparger. Moo-Young *et al.* (1987) observed a reduction in gas holdup from increasing non -Newtonian broth viscosity when compared to water, from interval measurements as a function of gas velocity during the fermentation of *Chaetomium cellulolyticum* and *Neurospora sitophila* for SCP production in a 1.3 m^3 split tube airlift reactor. Similar results were obtained during the production of xanthan gum from *Xanthomonas campestris* in a 1.2 m^3 concentric tube airlift reactor (Suh *et al*, 1992). Other examples demonstrated similar measurements of gas holdup reduction with increasing apparent viscosity in a variety of airlift configurations and scales. These were mostly with non-biological pseudoplastic fluids including xanthan gum (Fields *et al.*, 1984, Philips *et al.*, 1990), CMC (Erickson and Deshpande, 1981, Kawase and Moo-

Young, 1986) and cellulose fibre suspension (Chisti and Moo-Young 1988) with gas holdup performance compared against water as a function of gas velocity. The flow visualisation studies from the above examples (especially Chisti, 1989 and Philips *et al.*, 1990) observed the formation of large bubbles 15-20 mm in diameter in the presence of a non-Newtonian fluid (CMC and xanthan gum) as the gas velocity was increased. Homogeneous flow existed for increases in gas velocity upto 0.03-0.05 ms^{-1}, which was followed by the heterogeneous - churn turbulent flow from the formation of large bubbles 10 - 20 mm in diameter at gas velocities above 0.05 ms^{-1}. This was followed by slug flow at higher gas velocities. Amongst the large bubbles in heterogeneous and slug flow there was also a large proportion of small bubbles less than 2 mm in diameter as observed by Erickson and Deshpande (1981) and Kawase Moo-Young (1986). This led to the existence of a bimodal distribution of bubbles in the reactors with the non-Newtonian fluids (Philip *et al.*, 1990, Chisti, 1989). The small bubbles were observed in the downcomer of the *S. erythraea* broths and xanthan gum experiments used in this study. Therefore, the above examples described that the decrease in gas holdup with increasing apparent viscosity of non-Newtonian fluids was due to the enhancement of bubble coalescence in the riser. This lead to the formation of large spherical capped bubbles in the riser. Clift *et al.* (1978) predicted that the rise velocity of spherical cap bubbles showed no velocity dependence on viscosity. Thus, the large fast rising bubbles would have a short residence time in the riser leading to a reduction of riser gas holdup. The downcomer gas holdup also decreased due to the tendency of large bubbles to disengage from the vessel. The small bubbles were generated from large bubbles rupturing in the top section and from the break up of larger bubbles rising up the riser and top section due to increased turbulence (Philip *et al.*, 1990). The small bubbles would have a greater tendency of entrainment into the downcomer.

Therefore, the rapid reduction in gas holdup with increases in apparent viscosities up to 0.8 Pa.s for the annulus sparged reactor (figure 3.54d) and 0.1 Pa.s with the draft tube sparged reactor (figure 3.50d), during the mycelial and pelleted fermentations were probably due to the enhancement of coalescence. This lead to the formation of the bimodal bubble size distribution with the fast rising bubbles causing a reduction in gas holdup as discussed above. Although bubble measurements were not made with the *S. erythraea* broths, further evidence of the change in flow regime and bubble size distribution was shown by the increased turbulence of the liquid surface during the decrease in gas holdup and the observation of the large number of small 1 - 2 mm bubbles at the vessel side sight glasses. Research with xanthan gum and antifoam solutions in this study suggested that the antifoam constituent of the *S. erythraea* broths further enhanced coalescence leading to a greater reduction in gas holdup (figure 3.74a). Similar effects were demonstrated by Suh *et al.* (1992) from an addition of 0.007% volume of antifoam during the growth phase of *Xanthaomonas campestris* in a 0.05 m^3 bubble column for xanthan gum production. Gas holdup with antifoam was found to remain

relatively constant during an increase in apparent viscosity from 0.001 to 0.1 Pa.s with similar low values to that observed at slug flow. This was compared to the 50% greater gas holdup values from broths without antifoam.

After the growth phase of the *S. erythraea* broths a reduction of the rate of decrease of gas holdup with further increases in apparent viscosity was observed. For example, a reduction of the gas holdup dependency on apparent viscosity with further increases of apparent viscosity from 0.8 to 1.2 Pa.s was observed with the mycelial annulus sparged broth (figure 3.54e). A similar reduction of the rate of gas holdup decrease with increasing apparent viscosity above 1 Pa.s was observed with the xanthan / antifoam solutions (figures 3.73 & 3.74a). This reduction of the rate of gas holdup decrease with increasing apparent viscosity could be explained by two possible reasons : the mean bubble diameter did not significantly increase with further increases of apparent viscosity above 0.8 Pa.s, or the mean bubble diameter still increased due to enhanced coalescence with the further increase in viscosity but, the rate of increase of the terminal rise velocity with increasing bubble size may have been reduced. Clift *et al.* (1978) showed there to be a power law relationship between bubble diameters above 6 mm and terminal rise velocity. As the terminal rise velocity is inversely proportional to gas holdup then a change in the rate of increase of the bubble rise velocity with increasing apparent viscosity would effect the rate of gas holdup reduction. The change of flow behaviour (*n*) during the most viscous regions of the aerated fermentations was also similar to the change in gas holdup and this may also demonstrate the importance of broth pseudoplasticity on gas holdup. Kawase and Moo Young (1987) have shown the importance of flow behaviour in a theoretical correlation involving flow behaviour and superficial gas velocity compared to the usual empirical correlations of gas holdup with superficial gas velocity by power law relationships with non-Newtonian broths.

4.4.3.1.2 Influences of the reactor configuration on gas holdup

Comparison between the reactor configurations revealed that the reactor geometry and operating condition influenced the liquid velocity and bubble distributions of the individual sections of the reactor. These parameters were found to influence the relationship between gas holdup and broth rheology. Mycelial broths from both configurations demonstrated a similar decrease in gas holdup during the first 20 hours. However, the rheological changes in the annulus configured reactor were considerably larger (*n* reduced from 0.82 to 0.5) than with the draft tube sparger (0.75 - 0.63). This indicated that the different liquid velocity profiles brought about by the different A_D/A_R of the reactor configurations may influence the relationship of gas holdup and broth rheology. The influence of the engineering environment was further emphasised from the mycelial fermentations with propeller operation. Once the constant propeller operation at 900 rpm was maintained the liquid circulation time decreased due to the pseudoplasticity of the broth. This resulted in a decrease of apparent viscosity although

the gas holdup was further reduced. This indicated the importance of liquid linear velocity profiles and bubble distribution influences on the relationship between gas holdup and apparent viscosity with the non-Newtonian broths.

4.4.3.1.3 Effect of apparent viscosity and morphology on the density difference between the riser and downcomer with conventional aeration

A decrease of the difference between the riser and downcomer gas holdup was also associated with the increasing apparent viscosity during the conventionally aerated fermentations. This indicated that an increase of the proportion of gas from the riser was entrained into the downcomer with increasing apparent viscosity. The large bubbles formed by coalescence would be expected to have a greater tendency to disengage from the vessel. This would suggest that bubble breakup in the riser and top section (as discussed earlier) was occurring where the smaller bubbles would more likely to be entrained. Philip *et al.* (1990) showed that the small bubbles (diameter of 1mm) provided a 20% contribution to the total gas holdup at the gas velocity of 0.12 ms^{-1} with a 1% xanthan gum concentration in a internal loop airlift reactor. Similarly, Carrington *et al.* (1992) concluded that the small bubbles contributed to 25% of the gas holdup during a non-Newtonian (unnamed) fermentation with an apparent viscosity of 420 cP at 36 h to 1350 cP at 83 h into the fermentation. The fermentation was performed in a 20 m^3 airlift reactor with a type of split draft tube resulting from the internal helical heating coils. The entrainment tendency of the small bubbles may also make a large contribution to the downcomer gas holdup as well as the total gas holdup, as the small bubbles may coalescence as they flow towards the bottom of the downcomer. The increase in bubble size would result in an increase of the slip velocity which would ultimately lead to an increase in residence time of the bubbles in the downcomer and a subsequent increase in gas holdup in the downcomer. The formation of large bubbles in the downcomer of a split tube airlift (4.5 m tall) was observed by Chisti (1989) with 0.5 % CMC solutions until the bubbles became so large (20 - 30 mm in diameter) that there flow direction reversed and moved up the vessel against the liquid flow. Similar bubble spherical capped shaped bubbles were seen rising up the outside wall of the downcomer during the most viscous duration (20 - 50 h) of the pelleted and mycelial fermentations with the draft tube sparged configuration. It was speculated that the large bubbles may also rise up the centre of the downcomer as the visualisation of the flow was impossible from the sight glasses. However, Fields *et al.* (1984) observed that the large coalescence bubble flow was predominately against the outside vessel wall with 0.2 to 0.5% xanthan gum solutions in an internal airlift reactor 1.6 m tall. As the liquid velocity of the downcomer velocity profile was strongest in the centre then, the counter flowing bubbles would rise via the route of the weaker liquid velocity against the vessel wall.

The close proximity of the riser and downcomer gas holdup of the non-Newtonian broths as compared to the wider difference observed with the Newtonian

yeast broths (figure 3.65) would indicate that the *S. erythraea* broths had only a small density difference for liquid circulation yet, the circulation times were similar between the two rheologically different broths. This demonstrated the importance of the bubble wake in that liquid velocity was assisted by the carrying of liquid in the bubble wakes (Philip *et al.*, 1990). Ayazi Shamlou *et al.* (1994) demonstrated the importance of bubble wakes to the liquid circulation rates of airlift reactors with a gas holdup and liquid circulation rate model which incorporated a contribution to the primary liquid circulation from the bubble wakes as discussed for the yeast broths (section 4.1.1). The gas holdup and liquid circulation rates from the interval measurements at 29 h (as a function of gas velocity) for the mycelial broth (draft tube sparged) in this study were successfully modelled. A distribution parameter, C_0 (radial distribution of the liquid velocity and gas holdup) of unity and a loss coefficient due to flow reversal at the base of the vessel (K_F) of 30 was used due to the extra frictional resistance associated with liquid circulation of a non-Newtonian broth compared to a C_0 of 0.7 and K_F of 5 for the Newtonian yeast broths. The model was also successful at modelling the gas holdup and liquid circulation rates from other airlift reactors including, Russell *et al.* (1994), Fields and Slater (1983), Philip *et al.* (1990).

4.4.3.1.4 Effect of rheology on gas holdup as a function of superficial gas velocity

The interval measurements enabled the effect of superficial gas velocity on gas holdup to be compared between the Newtonian baker's yeast suspensions and the non-Newtonian *S. erythraea* broths. The pelleted fermentation with a viscosity of some 100 times greater than the viscosity of the yeast broth (table 4.3), resulted in a two fold reduction of the overall gas holdup when compared to the yeast suspension. However, the overall gas holdup from both broths showed a similar relationship to the increase in gas velocity (figure 3.65). This implied that both fluids had a similar flow regime change during the increase of gas velocity. For the yeast suspensions this began with a homogenous flow regime at low superficial gas velocities (below 0.054 ms^{-1}) resulting in a rapid increase in gas holdup. Heterogeneous flow developed at gas velocities above 0.054 ms^{-1}. The formation of larger bubbles reduced the rate of increase of gas holdup due to the counter acting effect of the bubble rise velocity (section 4.1.1). For the pelleted broth gas holdup measurements were not made below the superficial gas velocity 0.06 ms^{-1} to avoid effecting the OUR of the broth. However, it could be speculated that gas velocities increases up to 0.06 ms^{-1} would produce a corresponding rapid increase in gas holdup as observed with the yeast broth and from the xanthan gum solution of equivalent viscosity (0.375% w/v) (figure 3.73). As coalescence increased with viscosity the pelleted broth at 39 h (apparent viscosity of 0.77 Pa.s) probably resulted in an increase of the proportion of large bubbles during the flow regime change and hence, gas holdup was reduced by 28% at the gas velocity of 0.14 ms^{-1} compared to the gas holdup

Table 4.3 Comparison of the hydrodynamic and oxygen transfer characteristics between the airlift reactor configurations and stirred tank with the rheologically different broths of *S. erythraea* and the baker's yeast suspension

Reactor configuration and morphology		Flow behaviour, n (-)	Consistency index, K ($Pa.s^n$)	App. viscosity (Pa.s)	Liquid circulation time (s)	Liquid mixing time (s)	Overall gas holdup (-)	Lower riser k_La (s^{-1})	Lower riser DOT (% air saturation)
Draft tube sparged									
Pelleted	29h	0.66	0.625	0.33	11	34	0.085	0.032	< 1
	39h	0.47	1.1	0.77	11.3	25	0.065	0.02	< 1
Mycelial	29h	0.5	0.525	0.098	11.6	25	0.045	0.018	< 1
	39h	0.35	0.6	0.215	11.2	24	0.042	0.019	< 1
Annulus sparged									
Pelleted	29h	0.5	0.95	0.76	12.5	25	0.072	0.014	< 1
	39h	0.48	1.01	0.9	12.5	23	0.065	0.013	< 1
Mycelial	29h	0.47	1.1	0.91	12.5	24.8	0.062	0.012	< 1
	39h	0.43	1.15	1.1	12.5	21.5	0.057	0.011	< 1
Annulus + propeller									
Mycelial	29h	0.41	1.24	0.99	11	26	0.098	0.026	18
	39h	0.37	1.29	0.67	8.8	24	0.072	0.026	3
Lab.scale stirred tank									
Mycelial	29h	0.39	1.28	0.065	-	-	-	0.049	6
	39h	0.31	1.4	0.055	-	-	-	0.084	40
Draft tube sparger									
Yeast broth $10gL^{-1}$DCW		1	0.012	0.0012	11	33	0.13	0.058	< 1
Annulus sparger									
Yeast broth $10gL^{-1}$DCW		1	0.012	0.0012	12.5	35	0.115	0.06	< 1
Yeast broth $5gL^{-1}$DCW		1	0.012	0.0012	12.5	35	0.114	0.058	37
Annulus sp. + propeller									
Yeast broth $10gL^{-1}$DCW		1	0.012	0.0012	11.9	32	0.142	0.09	10
Yeast broth $5gL^{-1}$DCW		1	0.012	0.0012	11.9	32	0.142	0.09	60

at 29h. For the mycelial broths (draft tube gas sparged) gas holdup increased at a constant rate suggesting that the flow regime remained within a heterogeneous regime during the increase in gas velocity (figure 3.65). Similar effects were observed with the studies with the annulus sparger configuration. The importance of morphology in relation to gas holdup was further emphasised as the pelleted and mycelial broths (annulus gas sparged reactor) had similar rheological behaviour (table 4.3) yet, the gas holdup was greater with the pelleted broth. This effect is not fully understood but the higher gas holdup suggested the existence of lower coalescence rates in the pelleted broth than with the mycelial broths. This reduced interaction between the bubbles within the pelleted broth may have been due to the easier bubble flow between the pellet particles. The propeller was observed to successfully increase the gas holdup above the conventional aeration values during the mycelial fermentations. The increase in gas holdup above aeration only values was found to be similar to the increase observed with propeller operation with the yeast broths (figure 3.66). Hence, the mechanism of the gas holdup increase with propeller operation was probably similar to that proposed for the yeast broths (section 4.3). The propeller reduced the liquid circulation time and bubble diameter resulting in lower apparent viscosities and gas holdup with the mycelial broths.

4.4.3.2 Mixing and liquid circulation

The enhancement of coalescence and subsequent change in flow regime during the non-Newtonian fermentations resulted in an improvement of mixing performance of the vessel in the aerated only fermentations. However, unlike the changes in gas holdup, the largest improvements of mixing time were associated with changes in apparent viscosity during the most viscous region of the fermentations (above 0.8 Pa.s with annulus sparged mycelia broth), where it was assumed that a degree of bimodal bubble distribution existed in the vessel. The improvement of mixing time with the baker's yeast broth was associated with an improvement of circulation time. However, for the *S. erythraea* broths the circulation time remained constant during the fermentation. Hence, the improved mixing with increases of high broth viscosities was due to the greater turbulence from the formation of large bubbles associated with the viscous broths. This would also suggest that the bubble diameter further increased during the high viscosity duration of the fermentation. This provided evidence to suggest that it was the terminal rise velocity that limited the rate of decrease of gas holdup rather than a reduction in the rate of change of the bubble diameter as discussed previously (section 4.4.3.1). Similar improvement of mixing, a decrease of the Bodenstein number (Bo) with increasing concentrations of xanthan gum (1 - 5%), was observed by Fields *et al.* (1984) in a internal loop airlift reactor with a liquid height of 1.6 m. The mixing was associated with an improved dispersion coefficient and turbulence in the top section from the disengagement of bubble slugs. Russell (1989) observed improved mixing times during the increase in apparent viscosity during the fermentation of *P. chrysogenum* but this

was associated with a corresponding increase in liquid velocity. This, indicated that the frequency that the fluid passed the end sections of the vessel, dictated the mixing performance of the vessel, which was also concluded for this study with the yeast broth (section 4.1.2).

The xanthan gum experiments in this study provided evidence to suggest that the antifoam content in the *S. erythraea* broths prevented the broth apparent viscosity from influencing the liquid circulation time of the conventionally aerated vessel. The riser liquid velocity for aerated xanthan solutions was reduced with apparent viscosity increases above 0.4 Pa.s, presumably due to the increase in viscous drag (figure 3.74b). However, for xanthan and combined antifoam solutions, the riser liquid velocity remained relatively constant up to apparent viscosity of 1.2 Pa.s, but then, decreased with further increases in apparent viscosity (figure 3.74b). Nevertheless, the riser liquid velocity remained above the values for the xanthan only solutions. This indicated that the presence of antifoam in the *S. erythraea* fermentations suppressed an increase of frictional resistance with increasing viscosity and hence, prevented a reduction in the liquid circulation rates due to viscous drag around the vessel. It could be construed that the prevention of a reduction of the liquid circulation rates by the antifoam constituent of the media also prevented further increases in apparent viscosity. The xanthan gum studies implied that if higher apparent viscosities (above 1.2 Pa.s) had been obtained during the *S. erythraea* fermentations then, a reduction in riser liquid velocity would have been expected with conventional aeration operation. The improvement of liquid circulation with antifoam addition to the xanthan gum solutions may have been due to an effect on the bubble size distribution and the density difference between the riser and downcomer. However, the gas holdup profiles with increasing gas velocity revealed that the density difference between overall and downcomer gas holdup were similar between the solutions with or without antifoam addition and at all the concentrations studied (figure 3.73). The effects of antifoam on liquid circulation have not been previously reported, but researchers have shown a similar dependence of liquid circulation rates on the apparent viscosity of the fluid but mostly with non-biological solutions. Increased liquid velocities above those obtained with water have been obtained with low viscosity solutions of CMC with concentrations in the range of 0.3 - 1% for internal and external loop reactors (lab and pilot scale) and were concluded to be due to reduced fluid drag, (Wachi *et al.*, 1991, Fields and Slater, 1983). Reductions in liquid circulation rates with higher viscosity fluids (concentrations of xanthan gum above 1%) have been observed when compared to water (Fields *et al.*, 1984, Glennon *et al.*, 1988). Similarly, Russell (1989) showed that the riser liquid velocity increased during the increase in apparent viscosity up to 0.07 Pa.s during a *P. chrysogenum* fermentation however, the riser liquid velocity decreased during another fermentation which involved higher apparent viscosities, although the actual values were not given.

The comparison of the liquid circulation rates between the conventionally operated reactor to the aerated and propeller operated mycelial fermentation (annulus sparged) demonstrated the influence of the operating conditions on the liquid velocity and subsequent apparent viscosity of the broth. When the operating conditions became constant at 24h into the annulus sparged plus propeller operated mycelial fermentation then, the apparent viscosity of 1.0 Pa.s was similar to that observed at the same time into the annulus sparged (without propeller operation) mycelial fermentation. However, from the beginning of constant operating conditions with the propeller operated fermentation, the circulation time decreased from 11 s to 8.75 s over a duration of 20 h. This resulted in a reduction of the apparent viscosity from 1.0 Pa.s to 0.66 Pa.s. Whereas, with conventional aeration (without propeller operation) the circulation time remained constant at 12.5 s with constant operating conditions. This indicated that the faster liquid circulation from propeller operation due to the greater energy dissipation rate from propeller operation (table 4.2), was in some way responsible for providing a more conducive environment for a reduction in circulation time during the constant operating conditions of the fermentation. It was proposed in section 4.3.1 that propeller operation may cause a more streamlined- velocity profile across the riser and downcomer sections of the vessel. Therefore, in conjunction with the results discussed above, this indicated the importance of the liquid velocity profile across the individual sections of the vessel in the relationship between liquid circulation rates and non -Newtonian broth rheology. This also demonstrated the importance of the reactor operating conditions and configurations which have already been shown to influence liquid circulation rates with the Newtonian yeast broths.

4.4.3.2.1 The effect of superficial gas velocity on the circulation and mixing times

The interval measurements at 29 and 39 h into the aerated *S. erythraea* fermentations showed that the circulation times and mixing profiles followed a similar rate of decrease during the increase in gas velocity (figures 3.68 & 3.69). This implied that no change in flow regime occurred during the increase in gas velocity. This provided further evidence of heterogeneous flow and the subsequent presence of a majority of large bubbles in the reactor. Hence, the decrease of the liquid circulation time with increasing gas velocity was limited by the increase in turbulence, which reduced the amount of energy available for liquid circulation, as discussed with the yeast broths (section 4.1.2). The mixing to circulation time ratios for the pelleted and mycelial aeration only fermentations under constant rheological conditions were found to remain constant with increasing gas velocity (figures 3.68 & 3.70), indicating that the frequency that the liquid passed the end sections of the vessel determined the mixing performance of the vessel, as observed with the yeast broth. Similar conclusions were observed by Popovic and Robinson (1993) using a 60 L external loop airlift reactor with CMC solutions with a

apparent viscosity range of 0.04 to 0.6 Pa.s, and by Russell (1989) from a *P. chrysogenum* fermentation in the airlift reactor used in this study. This was different to the effect observed under constant gas velocity conditions during the fermentation, where the change in apparent viscosity influenced mixing time rather than liquid circulation for reasons that have already been discussed. Nevertheless, the ratio of mixing to circulation time for the *S. erythraea* fermentations remained constant at 2.0 for both reactor configurations, with the increase in gas velocity demonstrating the greater mixing performance than the yeast broths with ratio values of 2.5.

4.4.3.2.2 Comparison of the liquid circulation and mixing time profiles between reactor configurations as a function of superficial gas velocity

In general, the liquid circulation times for the mycelial fermentations in the aerated annulus sparger reactor were slower than with the draft tube sparger reactor over the gas velocity range studied, although the rheological characteristics were relatively similar between the two broths (figure 3.68 and table 4.3). This was presumably due to the effect of the different A_D/A_R on the liquid velocity profiles of the two sparger configurations as the liquid circulation times were equivalent to those observed with the yeast broths (figure 3.68). The different degrees of rheological change between the 29 and 39 h intervals (table 4.3) for the mycelial broths in the two sparger configurations (without propeller operation) had no effect on circulation time which further indicated the independence of circulation time from the rheological changes within this study. This was further emphasised by the similar liquid circulation times from the pelleted and mycelial broths of the draft tube sparged reactor, although the apparent viscosity was lower with the pelleted broth. However, the lower apparent viscosity of the pelleted broth did effect the liquid mixing as the mixing times were longer than with the mycelial broths at the same gas velocity (figure 3.70, table 4.3). This was presumably due to the lower coalescence rates of a lower apparent viscosity broth resulting in a smaller proportion of large bubbles, and subsequent reduction in turbulence in the riser and top section compared to a higher viscosity mycelial broth. This provided further evidence that it was the flow regime that influenced the mixing performance of the viscous broth.

The comparison of the mixing time interval measurements between the mycelial aeration only broths revealed that the mixing times were quite similar at 29 h. However, a greater reduction in mixing time occurred between 29 and 39 h with the annulus sparged broth than for the broth in the draft tube sparged reactor (figure 3.70 table 4.3). Yet, a greater change in rheology occurred with the broth in the draft tube sparged reactor and so a greater change in mixing time between 29 and 39 h might have been expected. The results were difficult to explain but probably indicated the influence of different engineering environments of the two sparger configurations leading to different effects on the bubble distribution and flow regimes, as partly discussed with the yeast studies (section 4.1).

The improvement of the aerated vessel circulation time by propeller operation with the mycelial broth, as shown at 29 h, was similar to that observed with the yeast broth (figure 3.68). This indicated that despite the rheological differences between the yeast broth and mycelial broth at 29 h, the propeller was able to improve the circulation rates of the aerated reactor to similar values. However, the liquid circulation rate improvement at 29 h with propeller operation was only similar to the liquid circulation times associated with the draft tube sparged reactor. At 39 h, propeller operation resulted in a large improvement of circulation time compared to the aeration only mycelial broth values and hence, there was a greater improvement of circulation time than observed with propeller operation with the yeast broths. This was presumably due to the improved liquid circulation rates observed under constant operation conditions during the fermentation as discussed previously (4.4.3.2). At 39 h a reduction in the rate of decrease of circulation time with gas velocities above 0.13 ms^{-1} was observed with propeller operation. This was presumably due to the increase in bubble diameter with gas velocity resulting in energy dissipation from bubble turbulence and a reduction in the amount of energy available for liquid circulation.

Although the propeller improved the circulation performance of the annulus sparged vessel the mixing performance was not changed which was a characteristic of the propeller, as discussed with the yeast broths (section 4.3). Essentially the propeller was unaffected by the viscosity of the *S. erythraea* broths and performed equally well as with the yeast broths at improving circulation rates and gas holdup as discussed previously.

4.4.3.3 Summary

During the *S. erythraea* fermentations the gas holdup was found to decrease with increasing apparent viscosity due to the enhanced bubble coalescence and subsequent formation of large bubbles. Thus, the overall gas holdup at 29 h into the mycelial fermentation (annulus gas sparged) with an apparent viscosity of 0.91 Pa.s was reduced by 2 fold when compared to the baker's yeast broth with a apparent viscosity of 1×10^{-3} Pa.s. It was suggested that the heterogeneous flow regime with the presence of the large bubbles (10 - 15 mm) amongst a population of small bubbles (0.5 - 2 mm in diameter), increased the turbulence in the riser and top section resulting in an increase of the mixing performance of the vessel. The liquid circulation time with conventional airlift operation (without propeller operation) remained unaffected by the change in broth viscosity due to the reduction of viscous drag from the presence of antifoam in the media as indicated from the xanthan gum solution studies. Gas holdup was improved by using pelleted broth instead of mycelial broths although, the mixing performance of the reactor was poorer with the lower viscosity pelleted broths. This was suggested to be due to the lower rates of turbulence associated with the lower viscosity broth. The increase in the energy dissipation rate of the vessel with propeller operation, improved gas holdup and liquid circulation of the conventionally aerated vessel and provided an environment which

allowed the liquid circulation to improve under constant operating conditions resulting in a reduction of apparent viscosity. Propeller operation produced similar improvements of the gas holdup and liquid circulation rate performance of the conventionally aerated vessel with the viscous *S. erythraea* broths as observed with the baker's yeast suspensions.

4.4.4 Oxygen transfer and k_La

On attainment of constant operating conditions the k_La values from the three fixed DOT probe positions followed the similar changes of the overall gas holdup and apparent viscosity during the aerated *S. erythraea* fermentations. Of the three probe positions the lower riser k_La values showed the closest relationship with changing gas holdup, especially during the most viscous region of the fermentations from approximately 20 to 60 h. As the lower riser DOT (% air saturation) remained below 1% during the growth and production phase of the conventionally aerated fermentations then, the changes of k_La with changing apparent viscosity could be easily distinguished. It was discussed in section 4.1.3 for the yeast suspensions that the k_La measurements were not positional measurements but described the oxygen transfer history of the liquid prior to reaching the probe position. The riser k_La measurements from the upper and lower probe positions with the annulus sparger configuration and from the mobile probe with the yeast suspensions showed that riser k_La remained relatively constant along the length of the riser. As a result, it was presumed that the lower k_La measurements were indicative of the oxygen transfer in the whole of the riser and all the reactor configurations had a lower riser measurement position which made it suitable for comparative purposes.

In general the reduction of k_La with increasing apparent viscosity was probably due to the reduction in gas holdup from the increased coalescence rates and subsequent formation of large bubbles. Consequently, the decrease in apparent viscosity near the end of the fermentation resulted in an increase in gas holdup and k_La. Comparison between k_La values of the yeast and *S. erythraea* broths with conventional aeration revealed that the development of a majority of large bubbles with poor interfacial area and short residence times in the riser with *S. erythraea* broths resulted in a 3 to 5 fold reduction in k_La compared to the yeast broth at the same biomass concentration (table 4.3). However, the difference between the two rheologically different broths may also have been influenced by the 4 fold greater concentration of the antifoam required for the medium with the *S. erythraea* broths (1 mL L^{-1}) compared to 0.25 mL L^{-1} for the yeast broth. Kawase and Moo-Young (1990) showed experimental results to indicate that the liquid mass transfer coefficient with water decreased by 50% with addition of 10 ppm antifoam C. The characteristic large number of small bubbles in non-Newtonian broths probably did not make a significant contribution to the oxygen transfer as Carrington *et al.* (1992) found that the small bubbles only contributed to less than 15% of overall oxygen transfer in a non-Newtonian broth. Russell (1989) observed a reduction of lower riser k_La from 0.12s^{-1} at 20 h into a *P. chrysogenum* fermentation to 0.06 s^{-1} at 40 h which then,

followed a more gradual decrease to 0.005 s^{-1} at 190 h. The k_La changes followed similar but gradual increases in apparent viscosity from 0.015 Pa.s to 0.07 Pa.s. Russell (1989) also showed that the decrease in lower riser k_La and downcomer gas holdup correlated well with increasing apparent viscosity. Bayer *et al.* (1989) observed a reduction in k_La from 120 h^{-1} to 40 h^{-1} during the growth phase of *Cephalosporium acremonium* in a 60 L working volume external loop reactor for cephalosporin C production which was due to an increase in viscosity, although quantitative rheological details were not given. Similarly, Tuffile and Pinho (1970) observed a decrease in k_La from 300 h^{-1} at 25 h to 160 h^{-1} at 30 h followed by a gradual change to 40 h^{-1} at 100 h in a 300 L stirred tank fermentations of *S. aureofaciens* which followed the similar trend to the decrease in flow behaviour from 0.8 at the start of the fermentation to 0.3 after 40 h. Similar reductions in k_La were observed by Roman and Gavrilescu (1994) during batch erythromycin production at 14 m^3 working volume in a 20 m^3 stirred tank reactor. The k_La reduced from 55 h^{-1} at 20 h to 35 h^{-1} at 90 h and demonstrated that k_La decreased exponentially with increasing apparent viscosity, from 100 h^{-1} at 50 mPa.s to 45 h^{-1} at 300 mPa.s.

The extent of the k_La reduction during the *S. erythraea* fermentations depended not only on the rheology / morphology but also the engineering environment from the different configurations changes and operating conditions (table 4.3). The influence of the reactor configurations and changing rheology of the broths on k_La were partly demonstrated by the comparison of the lower riser k_La during the two mycelial fermentations in the draft tube and annulus sparged configurations. The apparent viscosity increased rapidly during the first 20 h of an annulus sparged fermentation resulting in a rapid reduction in k_La from 0.1 to 0.02 s^{-1} (figure 3.54f). Whereas, the slow change of rheology during the same period of the draft tube sparged fermentation resulted in a higher k_La value of 0.025 s^{-1}. Hence, the lower riser DOT did not reach below 1% until 19 h compared to 12 h with the broth in the annulus sparger. This was not an effect from different growth rates as DCW and OUR profiles were similar between the two profiles. Although the riser k_La values with the annulus gas sparged mycelial broth were lower than with the draft tube sparger broth, the actual gas holdups were higher (table 4.3). This indicated the existence of different flow regimes and bubble distributions between the sparger configurations which effected the oxygen transfer rates between the configurations (table 4.3). Despite the greater k_La values of the draft tube sparged mycelial broth, the erythromycin production was not improved compared to production from the annulus sparger configuration. This was presumably due to the similar DOT heterogeneity present in the vessel during the production phase in both configurations as discussed in section 4.4.1. The influence of the engineering environment and operating conditions were further emphasised from the comparison of k_La values between the mycelial broths of the aerated annulus sparged broth to aeration plus propeller operation. Propeller operation increased gas holdup and increased lower

riser k_La by 2 fold from aeration only operation (table 4.3) which corresponded to the 2 fold greater total energy dissipation rate from the propeller and aeration operation. DOTs were maintained above 10% for most of the fermentation resulting in an increase erythromycin production, as previously discussed in section 4.4.1. Similarly the k_La values from 29 and 39 h during the mycelial broth with the stirred tank fermentation (estimated using the gas balance method) were between 4 and 8 fold greater than with the conventional airlift reactor (annulus sparged) operation (table 4.3). This was due to the estimated 10 fold greater energy dissipation rate resulting in lower broth viscosity than with broths with the airlift reactor configurations.

The influence of *S. erythraea* morphology on rheology and therefore k_La was observed from the comparison of k_La values from the pelleted and mycelial fermentations in the two aerated only configurations. The pelleted broth (draft tube sparger) had a lower apparent viscosity than with the mycelial broth and so the gas holdup and k_La values were 2 fold greater than with the mycelial broth (table 4.3). However, the improved oxygen transfer was not sufficient to prevent the lower riser DOTs from falling below 1%. Thus, the cycling DOTs involving limiting DOT values had a greater detrimental effect on erythromycin production than with mycelial broths (section 4.4.1). The improvement of gas holdup and oxygen transfer by using a lower viscosity pelleted broth rather than a more viscous mycelial broth as shown in this study was also demonstrated by Schugerl (1990), Koenig *et al.* (1981a) and Bayer *et al.* (1989) and was previously discussed in relation to morphology (section 4.4.2) and gas holdup (section 4.4.3). Schugerl (1990) found that the airlift reactor for Penicillin V production was only a viable alternative to stirred tanks on the basis of specific productivity rates (especially with power input) if a pelleted broth 400 μm in diameter was used compared to a mycelial broth in the stirred tank. Similar examples from Schugerl (1990) included tetracycline production *S. aureofaciens,* where the specific productivity from a tower loop airlift reactor was 2 fold greater than with a stirred tank (as described in section 4.4.1.5). Schugerl (1990) claimed that a power input of 4 - 5 kW m^{-3} can be required to reduce the effective viscosity of a pseudoplastic mycelial broth and to prevent dissolved oxygen limitation in a stirred tank fermentation whereas, with a pelleted broth the power input requirement decreases by 4 - 5 fold. Similarly, Koenig *et al.* (1981a) found that the power input required for a mycelial fermentation in a lab. scale stirred tank in order to achieve 'effective' penicillin production was 7 - 10 fold greater than with a 80 L lab. scale bubble column containing 1 mm pellets of *P. chrysogenum.* Specific penicillin production was similar between the two reactors although specific penicillin yield coefficient, penicillin /g O_2 was two fold greater with the pelleted broth in the bubble column than with the stirred tank. Therefore, the comparison of the mycelial fermentations in this study from conventional aeration and aerated / propeller operation to stirred tank confirmed the view of the above literature examples that the use of conventionally aerated airlift reactors for the production of secondary metabolites with

pseudoplastic broths is limited from the enforced oxygen limitation. Further observations by Bhavaraju *et al.* (1978) and Anderson *et al.* (1982) have indicated the possible poor interfacial area at high viscosities in airlift reactors, and Suh *et al.* (1992) indicated that the poor performance of a tower loop reactor was due to high apparent viscosity, which reduced oxygen transfer resulting in stagnant zones during xanthan gum production. However, the oxygen transfer may be greater at production scale as k_La may increase with scale up as observed by Barker and Worgan (1981). Also, the greater hydrostatic pressure would improve the oxygen saturation concentration, as discussed for antibiotic production (section 4.4.1) and in relation to oxygen transfer with the yeast broths (section 4.1.3).

4.4.4.1 Summary

Larger k_La values and hence, greater oxygen transfer occurred in the downcomer than in the riser with conventional airlift operation. This was due to the larger gas residence time of the downcomer when compared to the riser, as discussed in section 4.1.3 for baker's yeast. The formation of large bubbles from the increase of apparent viscosity reduced the gas holdup and the interfacial area for oxygen transfer which decreased the k_La values around the reactor. The magnitude of the reduction of k_La with increasing apparent viscosity depended on broth morphology, reactor configuration and operating conditions. Higher k_La values were achieved when using lower viscosity pelleted broths rather than mycelial broths. An increase of energy dissipation rate reduced the apparent viscosity and its impact on k_La. The increase of oxygen transfer with energy dissipation rate aided the improvement of erythromycin production.

5.0 CONCLUSIONS

Hydrodynamics and oxygen transfer with baker's yeast

1.1) For all airlift reactor configurations an increase of superficial gas velocity improves the gas holdup, oxygen transfer, liquid circulation and mixing performance of the vessel within the range of gas velocities used in this study.

1.2) The dependency of the hydrodynamics and oxygen transfer on the gas velocity reduces as the gas velocity increases, due to the change in bubble flow regime from bubbly to a more turbulent heterogeneous flow.

Comparison of the hydrodynamics and oxygen transfer between sparger configurations

2.1) The hydrodynamic performance (gas holdup, liquid circulation and mixing time) of the aerated airlift reactor is improved by using a draft tube ring sparger rather than an annulus ring sparger as a result of the ratio of the downcomer to riser cross sectional area A_D/A_R.

2.2) The influence of the A_D/A_R in conjunction with the effect of the liquid velocity and C_o parameter (distribution of the liquid velocity and gas holdup across the riser) on the coalescence rates, explain the differences of sectional gas holdups, liquid circulation and mixing times between the two sparger configurations with the baker' s yeast suspension.

2.3) Despite the hydrodynamic advantages of the draft tube sparged reactor the oxygen transfer characteristics are similar for both sparger configurations.

Oxygen transfer characteristics of the airlift reactor

3.1) Greater oxygen transfer occurs in the downcomer rather than in the riser (aerated section) with both baker's yeast and non - Newtonian *S. erythraea* broths for airlift operation.

3.2) The high gas content and large slip velocity, both of which influence the gas residence time, and smaller bubble diameter of the downcomer relative to the riser, aids oxygen transfer in this region of the vessel.

3.3) The change in bubble size distribution between the riser and downcomer dominates the oxygen transfer changes around the reactor rather than the combined effect of gas holdup and liquid circulation, as shown by the modelling of the oxygen transfer.

Liquid mixing and top section characteristics of the airlift reactor

4.1) The mixing performance of an airlift reactor is dominated by the frequency of the passage of the broth through the end sections of the reactor.

4.2) A two zone model describes the liquid circulation through the top section once a certain critical height is achieved. The circulating fluid passes through the lower zone bypassing the upper layer.

4.3) The liquid velocity and degree of gas entrainment shows little dependency on top section size.

4.4) The height of the liquid above the draft tube is important for reactor operation as an optimum liquid height for liquid mixing is reached, above which no further improvement in mixing occurs.

Hydrodynamics and oxygen transfer with *S. erythraea* broths

5.1) The extent of gas holdup reduction with increasing *S. erythraea* apparent viscosity is dependent on the cell morphology, reactor configuration and operating conditions.

5.2) Increasing pseudoplastic broth apparent viscosity enhances bubble coalescence and reduces the interfacial area leading to the reduction of gas holdup and local k_La values.

5.3) The formation of large bubbles enhances turbulence which improves liquid mixing.

5.4) The relationship between liquid velocity and apparent viscosity is influenced by the pseudoplastic rheology of the broth, the medium constituents and the reactor design and operation.

5.5) Liquid velocity is independent of the apparent viscosity of *S. erythraea* broths (up to 1.2 Pa.s) with airlift reactor operation. The enhancement of energy dissipation rate can improve the liquid velocity under constant operating conditions with viscous broths.

Erythromycin production and *S. erythraea* morphology

6.1) Erythromycin production in a aerated pilot scale airlift reactor (without propeller operation) is reduced due to poor oxygen transfer. However, an increase of oxygen transfer (DOC, and k_La) with scale up may reduce the impact of DOT heterogeneity on cell metabolism and lead to improved erythromycin yield at production scale.

6.2) For *S. erythraea* broths with similar apparent viscosities, gas holdup is improved when the morphology of the culture is pelleted rather than mycelial. However, possible oxygen limitation within the pellets can lead to poor erythromycin productivity when compared to mycelial broths.

6.3) The engineering environment influences the relationship of *S. erythraea* broth rheology to the dry cell weight and cell morphology.

6.4) Cell concentration and morphology (hyphal length & hyphal growth unit) influence broth consistency (K) during the growth phase of fermentation broths in the annulus sparged airlift configuration and stirred tank.

6.5) Cell morphology has a larger influence than cell concentration on the rheology of broths with the draft tube sparged reactor. Cell morphology, particularly branch and hyphal length, may be influenced by the hydrodynamic and oxygen transfer differences between the sparger configurations. This may be due to the larger liquid linear velocity of the draft tube sparger compared with the annulus sparged reactor.

6.6) Cell morphology, particularly hyphal and branch length, influence the broth apparent viscosity during the production phases of all fermentations rather than a change in cell concentration irrespective of the reactor configuration.

6.7) The morphology particularly hyphal length after the growth phase is influenced by the energy dissipation rate as hyphal fragmentation occurs earlier in the fermentation with increasing energy dissipation from mechanical agitation.

Vessel characterisation with the marine propeller and annulus air sparger

7.1) Sectional gas holdups, liquid velocity, and local k_La values are improved by the operation of the annulus air sparged reactor with the marine propeller to aid liquid circulation down the downcomer. The combined affect on hydrodynamics and oxygen transfer reduces the DOT heterogeneity.

Reactor heterogeneity

8.1) The airlift reactor can be used to study the impact of reactor heterogeneity on the physiology of fermentation broths and as a means of studying the impact of scale up. Different degrees of heterogeneity can be generated from the two sparger configurations in conjunction with the marine propeller.

8.2) DOT heterogeneity affects the OUR of the baker's yeast broth in batch culture. Increases of the energy dissipation rate reduce the DOT heterogeneity leading to an increase of the oxygen uptake rate of the culture. Once the lowest value of the DOT heterogeneity is up to 10%, further increases in OUR are not observed.

8.3) For liquid circulation times greater than 8 seconds, cell metabolism is affected by the DOT heterogeneity to a greater extent than the average value of DOT experienced in one circulation of the vessel.

8.4) Growth of the *S. erythraea* cells remain unaffected by DOT heterogeneity in this study. The specific erythromycin production rate and final specific production are reduced by DOT heterogeneity. Both production parameters improve by a proportional increase of energy dissipation rate (studied up to 7130 Wm^{-3}) and reduction in DOT heterogeneity.

RECOMMENDATIONS FOR FURTHER WORK

1) Further investigation of the dissolved oxygen heterogeneity of the airlift reactor

Gas residence time measurements for the individual sections of the vessel, using helium pulse techniques, would elucidate the magnitude of the difference between the gas and liquid circulation. This would provide further evidence of the different fluid dynamics between the riser and downcomer which influence the DOT heterogeneity.

2) Dissolved oxygen heterogeneity during *Saccharopolyspora erythraea* fermentations

The development of further probe locations in the vessel, along the downcomer, or a sterilisable mobile DOT probe would enhance the understanding of the change in DOT around the vessel with fermentations operated under sterile conditions.

3) Bubble distribution measurement

Accurate bubble distribution measurements would enhance the understanding of the fluid hydrodynamics and oxygen transfer. Bubble size measurement at four positions in the vessel, (lower & upper riser and downcomer) would enable the effect of viscosity, operating conditions and reactor configurations to be studied on the bubble size distribution.

4) The effect of DOT cycling on erythromycin production and morphology

A greater understanding of the effect of reactor heterogeneity of large scale vessels on erythromycin production would be gained from the determination of C_{CRIT} for erythromycin production and the effect of cycling DOT around and below C_{CRIT}. This would allow an evaluation as to whether the proportionality of energy dissipation to erythromycin production and the hyphal breakup theory applied to *S. erythraea* fermentations above C_{CRIT}.

5) Comparison of stirred tank to airlift reactor for erythromycin production

A direct comparison of stirred tank to airlift reactor as a function of power input (Wm^{-3}) using identical inoculum and sterilisation conditions would be essential in determining possible advantages of using airlift reactors. The comparison must include the study of morphology, productivity, hydrodynamic and oxygen transfer comparisons. Investigation of fed batch fermentations in the airlift reactor operation would also be important due to the poor performance of conventional airlift operation for erythromycin production observed in this study.

6) Method of predicting shear rates in the airlift reactor

A comparison of stirred tank to airlift reactor would be aided by an accurate method of predicting the shear rates in airlift reactors. This would allow accurate comparison of the apparent viscosity between stirred tank and airlift reactor.

6.0 REFERENCES

Abel, C., Hubner, U., Schugerl, K. (1994). Transient behaviour of Baker's yeast during enforced periodical variation of dissolved oxygen concentration. J. Biotechnol. **32**: 45-57.

Adler I., Schugerl. K. 1983. Cultivation of *E.coli* in single and ten stage tower loop reactors. Biotechnol. Bioeng. **25**: 417-436.

Allen, G.D., Robinson, C.W. 1990. Measurement of rheological properties of filamentous fermentation broths. Chem. Eng. Sci. **45**(1): 37-48.

Allen, G.D., Robinson, C.W. 1991. On the calculation of shear rate and apparent viscosity in airlift and bubble column bioreactors. Biotechnol. Bioeng. **38**: 212-216.

Anderson, C., LeGrys, G.A., Solomons, G.L. 1982. Concepts in the design of large scale fermenters for viscous culture broths. The Chem. Engr. Feb:43.

Arathoon, W.R., Birch,J .R. 1986. Large scale cell culture in biotechnology. Science. **232**: 1390-1395.

Arcuri, E.J., Nichols, J.R., Brix, T.S., Santamarina, V.G., Buckland, B.C., Drew, S.W. 1983. Thienamycin production by immobilised cells of *Streptomyces cattleya* in a bubble column. Biotechnol. Bioeng. **25**: 2399-2411.

Ayazi Shamlou, P.A., Pollard, D.J., Ison, A.P., Lilly, M.D. 1994. Gas holdup and liquid circulation rate in concentric-tube airlift bioreactors. Chem. Eng. Sci. **49**(3): 303-312

Ayazi Shamlou P.A., Pollard, D.J., Ison, A.P. 1995. Volumetric mass transfer coefficient in concentric-tube airlift bioreactors. Chem. Eng. Sci. accepted for publication.

Azbel, D. 1981. Two phase flows in chemical engineering. Cambridge University Press.

Bajpai, R.K., Reuss, M. 1982. Coupling of mixing and microbial kinetics for evaluation of the performance of bioreactors. Can. J. Chem. **60**: 384-392.

Banerjee, S., Scott, D.S., Rhodes, E. 1970. Studies of cocurrent gas liquid flow in helically coiled tubes. II. Theory and experiments with and without chemical reaction. Can. J. Eng. **48**: 542-551.

Banks,G.T. 1977. Aeration of Mould and Streptomycete culture fluids. Topics.Enz.Ferm.Biotech. **1**: 72-110.

Barker, T.W., Worgan, J.T. 1981. The application of air-lift fermenters to the cultivation of filamentous fungi. Eur. J. Appl. Microbiol. Biotechnol. **13**: 77-83.

Bartholomew, W.H., Karrow, E.O., Sfat, M.R., Wilhelm, R.H. 1950. Oxygen transfer and agitation in submerged fermentations. Mass transfer of oxygen in submerged fermentations of *Streptomyces griseus*. Ind. Eng. Chem. **42**(9): 1801-1809.

Battino, R. 1981. IUPAC Solubility data series. Pergamon Press.Oxford. **7**: 1.

Bavarian, F., Linn, C-J., Ramesh, T.S., Fan, L-S. 1991. Effect of static liquid height on gas-liquid mass transfer in a draft-tube bubble column and three-phase fluidised bed. Chem. Eng. Comm. **108**: 347-364.

Bayer, T., Zhou, W., Holzhauer, K., Schugerl, K. 1989. Investigations of cephalosporin C production in an airlift tower loop reactor. Appl. Microbiol. Biotechnol. **30**: 26 -23

Bello, R.A. 1981. A characterisation study of airlift contactors for applications to fermentations. PhD thesis. University of Waterloo. Ontario, Canada.

Bello, R.A., Robinson, C.W., Moo-Young, M. 1981. Mass transfer and liquid mixing in external-circulation loop contactors, pp. 547-552. In: Moo-Young, M., Robinson, C.W., and Vezina, C. (eds.), Advances in biotechnology vol. **1**. Pergamon Press, Toronto, Canada.

Bello, R.A., Robinson, C.W., Moo-Young, M. 1984. Liquid circulation and mixing characteristics of airlift contactors. Can. J. Chem. Eng. **62**: 573-577

Bello, R.A., Robinson, C.W., Moo-Young, M. 1985. Gas holdup and overall volumetric oxygen coefficient in airlift contactors. Biotechnol. Bioeng. **27**: 369-381.

Belmar-Beiny, M.T., Thomas, C.R. 1991. Morphology and clavulanic acid production of *Streptomyces clavuligerus* : effect of stirrer speed in batch fermentations. Biotechnol. Bioeng. **37**: 456-462.

Bhavaraju, S.M., Russell, T.W.F., Blanch, H.W. 1978. The design of gas sparged devised for viscous liquid systems. AIChE.J. **24**(3): 454-465.

Bjorkman, U. 1987. Properties and principles of mycelial flow: experiments with a tube rheometer. Biotechnol. Bioeng. **29**: 114-129.

Blakebrough, N., McManamey, W.J., Tart, K.R. 1978a. Heat transfer to fermentation systems in an airlift fermenter. Trans. Inst. Chem. Eng. **56**: 127-135.

Blakebrough, N., McManamey, W.J., Tart, K.R. 1978b. Rheological measurements on *Aspergillus niger* fermentation systems. J. Appl. Chem. Biotechnol. **28**: 453-461.

Blenke, H. 1979. Loop reactors. Adv. Biochem. Eng. **13**: 121-124

Blenke, H. 1985. Biochemical Loop reactors, pp. 465-517. In: Rehm, H.J., Reed, G. (eds.), Biotechnology, vol. **2:** Fundamentals of biochemical engineering. VCH, Weinheim.

Bongenaar, J.J.T.M., Kossen, N.W.F., Metz, B., Mijiboom, F.W. 1973. A method of characterising the rheological properties of viscous fermentation broths. Biotechnol. Bioeng. **15**: 201-206.

Bovonsombut, S., Wilhelm, A.M., Riba, J-P. 1987. Influence of gas distributor design on the oxygen transfer characteristics of an airlift fermenter. J. Chem. Tech. Biotechnol. **40**: 167-176.

Boysan, F., Cliffer, K.R., Leckie, F., Scragg, A.S. 1988. The growth of *Catharanthus roseus* in stirred tank bioreactors, pp. 245-258. In: King, R. (ed.), Proceedings: 2nd Int. conf. bioreactor fluid dynamics. Cambridge. Elsevier Appl. Sci. Pub. London. U.K.

Brandes, L., Wu, X., Maschke, H.E., Jurgens, H., Reinhardt, B., Schugerl, K. 1993. Production of fusion protein SpA::*Eco*RI in batch culture in a 60-L airlift tower loop reactor. Biotechnol. Prog. **9**: 122-127.

Brauer, H. 1979. Power consumption in aerated stirred tank reactor systems. Adv. Biochem. Eng. **13**: 87-117.

Brinberg, S.L. 1959. Antibiotics. Antibiotiki. **4**: 15-20.

Buckland, B.C. 1993. Personal communication.

Buckland, B.C., Lilly, M.D. 1993. Fermentation: an overview, pp. 9-22. In: Stephanopoulos, G (ed.), Bioprocessing vol. 3 of Biotechnology, 2nd. Ed. VCH, Weinheim.

Bukur, D.B., Patel, S.A. 1989. Hydrodynamic studies with foaming and non-Newtonian solutions in bubble columns. Can. J. Chem. Engng. **67**: 741-751.

Bushell, M.E. 1988. Growth, Product formation and Fermentation Technology, pp. 185-217. In: Goodfellow, M., Williams, S.T., Mondarski, M. (ed.), Actinomycetes in biotechnology. Academic Press, London. U.K.

Calvo, E.G. 1989. A fluid dynamic model for airlift loop reactors. Chem. Eng. Sci. **44**: 321-323.

Calvo, E.G., Leton, P. 1991. A fluid model for bubble columns and airlift reactors. Chem.Eng.Sci. **46**(11): 2947-2951.

Carrington, R., Dixon, K., Harrop, A.J. 1992. Oxygen transfer in industrial air agitated fermenters, pp. 183-188. In: Ladisch, M.R., Bose, A. (eds.), Harnessing biotechnology for the 21st century. ACS, Washington, D.C.

Chakravarty, M., Singh, H.D., Baruah, J.N., Iyengar, M.S. 1974. Liquid velocity in a gas-lift column. Indian Chem. Engrs. **16**: 17-22.

Chang, C-M., Lu, W.J., Own, K.S., Hwang, S-J. 1994. Comparison of airlift and stirred tank reactors for immobilised enzyme reactions. Proc. Biochem. **29**: 133-138.

Charles, M. 1978. Technical aspects of the rheological properties of micrbial cultures. Adv. Biochem. Eng. **8**: 1-62.

Chen, N.Y. 1990. The design of airlift fermenters for use in biotechnology. Biotechnol. Genetic Eng. Revs. **8**: 379-396.

Chen, H.C., Wilde, F. 1991. The effect of dissolved oxygen and aeration rate on antibiotic production of *Streptomyces fradiae*. Biotechnol. Bioeng. **37**: 591-595.

Chisti, M.Y., Moo-Young, M. 1987. Airlift reactors characteristics, applications and design considerations. Chem. Eng. Commum. **60**: 195-242.

Chisti, M.Y., Moo-Young, M. 1988. Hydrodynamics and oxygen transfer in pneumatic bioreactor devices. Biotechnol. Bioeng. **31**: 487-494.

Chisti, M.Y., Harlard, B., Moo-Young, B. 1988. Liquid circulation in air-lift reactors. Chem. Eng. Sci. **43**: 451-457.

Chisti, M.Y. 1989. Airlift Bioreactors. Elsevier Applied Science, U.K.

Choi, P.B. 1990. Designing Airlift Loop Fermenters. Chem. Eng. Prog. Dec. : 32-37.

Choi, K.H., Lee, W.K. 1990. Recirculation and flow structure of gas in downcomer section of concentric cylindrical airlift reactor. J.Chem. Tech. Biotechnol.**48**: 81-95.

Clark, N.N., Flemmer, R.L. 1985. Prediction of holdup in two phase bubble upward and downward flow using the Zuber and Findlay drift flux method. A.I.Ch.E. J. **31**: 500-503.

Clark, M., Jones, A.G. 1987. The prediction of liquid circulation in a draft-tube column. Chem. Eng. Sci. **42**: 378-378.

Clift, R., Grace, J.R., Weber, M.E. 1978. Bubbles, Drops and Particles. Academic Press. New York.

Collier, J.G. 1972. Convective boiling and condensation. 2nd Ed. McGraw-Hill Int.New York. ch.**2**. pp: 26-69.

Cooper, C.M., Fernstrom, G.A., Miller, S.A. 1944. Performance of agitated gas-liquid contacters. Ind.Eng.Chem. **36**: 504-509.

Corcoran, J.W., Hahn, F.E. 1975. Mechanisms of action of antimicrobial and antitumour agents, Antibiotics III. Springer - Verlag.

Corum, C.J., Stark, W.M., Wild., G.M., Bird, H.L. 1954. Biochemical changes in a chemically defined medium by submerged cultures of *Streptomyces erythreus*. Appl. Microbiol. **2**: 326.

Darton, R.C., Harrison, D. 1975. Gas and liquid holdup in three phase fluidisation. Chem. Engng. Sci. **30**: 581-586.

Deckwer, W.D. 1985. Bubble column reactors. Biotechnology 2 Rehm,H.J., Reed,G.(eds). ch.**20**:pp.445-464.

Deindorfer, F.H., West, J.M. 1960. Rheological examination of some fermentation broths. J. Microbial. Biochem. Technol. Eng. **2**:165-175.

Dion, W.M., Carilli, A., Sermonti, G., Chain, E.B. 1954. The effect of mechanical agitation on the morphology of Penicillium chrysogenum Thom in stirred fermentors. Rend. 1st. Super. de Sanita. **17**: 187-205.

Divers, M. 1990. Molecular biology of Streptomyces. Conf. report: UCLA Colloquim, Colorado, U.S.A.

Erickson, L.E., Deshpande, V. 1981. Gas-liquid dispersion characteristics in airlift fermenters, pp. 553-558. In: Moo-Young, M., Robinson, C.W., Vezina, C. (eds.), Advances in biotechnology, vol. **1**. Pergamon Press, Toronto, Canada.

Erickson, L.E., Patel., S.A., Glasgow, L.A., Lee, C.H. 1983. Effects of viscosity and small bubble segregation on mass transfer in airlift fermenters. Proc. Biochem. **5**: 16-37.

Escalante, L., Lopez, H., Carmen Mateos, R., Lara, F., Sanchez, S. 1982. Transient repression of erythromycin formation in *Streptomyces erythraeus*. J. Gen. Microbiol. **128**: 2011-2015

Fatile, I.A. 1985. Rheological characteristics of suspensions of *Aspergilus niger*: correlation of rheological parameters with microbial concentration and shape of the mycelial aggregate. Appl. Microbiol. Biotechnol. **21**: 60-64.

Faust, U., Prave, P., Sukatsch, D.A. 1977. Continous biomass production from methanol by *Methylomonas clara*. J. Ferm. Tech. **55**: 609-614

Favre, E., Deront, M., Peringer, P. 1994. Influence of a rotating sieve on pumping and mixing performances of an internal loop reactor. Bioproc. Eng. **11**: 91-95

Feren, C.J., Squires, R.W. 1969. The relationship between the critical oxygen level and antibiotic synthesis of capreomycin and cephalosporin C. Biotechnol. Bioeng. **11**: 583-592.

Fields, P.R., Slater, N.K.H. 1983. Tracer dispersion in a laboratory air-lift reactor. Chem. Eng. Sci. **38**(4): 647-653.

Fields, P.R., Mitchell, F.R.G., Slater, N.K.H. 1984. Studies of mixing in a concentric tube air-lift reactor containing xanthan gum by means of an improved flow follower. Chem. Eng. Commun. **25**: 93-104.

Flores, E.Ma., Sanchez, S. 1985. Nitrogen regulation of erythromycin formation in *Streptomyces erythreus*. FEMS Microbiol. Letts. **26**: 191-194.

Freedman, W., Davidson, J.F. 1969. Holdup and liquid circulation in bubble columns. Trans. Inst. Chem. Engrs. **47**: T251-262.

Frohlich, S., Lotz, M., Korte, T., Lubbert, A., Schugerl, K., Seekamp, M. 1991a. Characterisation of a pilot plant airlift tower loop bioreactor.I: evaluation of the phase properties with model media. Biotechnol. Bioeng. **38**: 43-55.

Frohlich, S., Lotz, M., Korte, T., Lubbert, A., Schugerl, K., Seekamp, M. 1991b. Characterisation of a pilot plant airlift tower loop bioreactor: II. Evaluation of global mixing properties of the gas phase during yeast cultivation. Biotechnol. Bioeng. **37**: 910-917.

Frohlich, S., Lotz, M., Larson, B., Lubbert, A., Schugerl, K., Seekamp, M. 1991c. Characterisation of a pilot plant airlift tower loop reactor: III. Evaluation of local properties of the dispersed gas phase during yeast cultivation and in model media. Biotechnol. Bioeng. **38**: 56-64.

Galindo, E., Nienow, A.W. 1992. Mixing in highly viscous simulated xanthan fermentation broths with the lightin A-315 impeller. Biotechnol. Prog. **8**: 233-239.

Gallo, T., Sandford,D.S. 1979. 86th AIChE. Houston Texas.

Garcia, C. E., Leton, P., Arranz, M.A. 1991. A fluid dynamic model for bubble columns and airlift reactors. Chem. Eng. Sci. **46**: 2951-2954.

Garrod, L.P., Lambert, H.P., O'Grady, F., Waterworth, P.M. 1981. Macrolides and lincosamides, pp. 183-192. In: Antibiotic and Chemotherapy. Churchhill Livingstone. London.

Gavrilescu, M., Roman, R.V., Efimov, V. 1992. Rheological behaviour of some antibiotic biosynthesis liquids. Acta. Biotechnol. **12**(5); 383-396.

Geraats, S.G.M. 1994. Scaling-up of a lipase fermentation process: a practical approach, pp. 41-46. In: Galindo, E., Ramirez, O.T. (eds.), Advances in bioprocess engineering. Kluwer Acad. Dorddrecht.

Ghildyal, N.P., Thakur, M.S., Srikanta, S., Jaleel, S.A., Prapulla, S.G., Prasad, M.S., Devi, P.N., Lonsane, B.K. 1987. Rheological studies on *Streptomyces fradiae* ScF-5 in submerged fermentation. J. Chem. Tech. Biotechnol. **38**: 221-234.

Glennon, B., MacLoughlin, P.F., Malone, D.M. 1988. Mixing and dispersion studies in an air-lift reactor, pp. 415-429. In: King, R. (ed.), Proceedings: Second Int. Conference on Bioreactor Fluid Dynamics, Cambridge. Elsevier Applied Science Publishers, London.

Godpole, S.P., Schumpe, A., Shah, Y.T., Carr, N.L. 1984. Hydrodynamics and mass transfer in non-Newtonian solutions in a bubble column. A.I.Ch.E. J. **30**(2): 213-220.

Gopal, J.S., Sharma, M.M. 1982. Hydrodynamic and mass transfer characteristics of bubble and packed bubble columns with downcomer. Can. J. Chem. Eng. **60**: 353-362.

Govier, G.W., Aziz, K. 1972. The flow of complex mixtures in pipes. Van Nostrand, New York.

Guo, Y., Lou, F., Peng, Z.Y., Yuan, Z.Y., Korus, R.A. 1990. Kinetics of growth and alpha-amylase production of immobilised *Bacillus subtilis* in an airlift bioreactor. Biotechnol. Bioeng. **35**: 99-102.

Guy, C., Carreau, P.J., Paris, J. 1986a. Comments on the paper: 'Liquid circulation and mixing characteristics of airlift contactors. Can. J. Chem. Eng. **64**: 521-523.

Guy, C., Carreau, P.J., Paris, J. 1986b. Mixing characteristics and gas holdup of a bubble column. Can. J. Chem. Eng. **64**: 23-35.

Halard, B., Kawase, Y., Moo-Young, M. 1989. Mass transfer in a pilot plant airlift column with non-Newtonian fluids. Ind. Eng. Chem. Res. **28**(2): 243-245.

Heijnen, J.J., van't Riet, K., 1984. Mass transfer, mixing and, heat transfer phemomena in low viscosity bubble column reactors. Chem. Eng. J. **28**: B21-42.

Henstock, W.H., Hanratty, T.J. 1979. Gas absorption by a liquid layer flowing on the wall of a pipe. A.I.Ch.E. J. **25**: 122-131.

Henzler, H-J. 1980. Begasen hoherviskoser Flussigkeiten. Chem. Ing. Techn. **52**(S): 643-652.

Higashide, E. 1984. The macrolides: properties, biosynthesis and fermentation. pp. 451-510. In: Vandamme, E.J. (ed.), Biotechnology of industrial antibiotics. Marcel Dekker Inc. New York.

Higbie, R. 1935. Rate of absorption of a pure gas into a still liquid during short period of exposure. Trans. A.I.Ch.E. **31**: 365-389.

Hilgendorf, P., Heiser, V., Diekmann, H., Thoma, M. 1987. Constant dissolved oxygen concentrations in cephalosporin C fermentation : applicability of different controllers and effect on fermentation parameters. Appl. Microbiol. Biotechnol. **27**: 247-251.

Hines, D.A., Bailey, M., Ousby, J.C., and Roesler, F.C. 1975. The ICI deep shaft aeration process for effluent treatment. Int. Chem. Eng. Symp. Ser. 41.

Ho, C.S., Erickson, L.E., Fan, L.T. 1977. Modelling and simulation of oxygen transfer in airlift fermenters. Biotechnol. Bioeng. **19**: 1503-1522.

Hobbs, G. 1994. Biochemical and Chemical Engineering Dept., University College London. Personnel communication.

Holt, J.G., 1989. Bergey's manual of systematic bacteriology vol. IV, The Williams and Wilkins Company

Hsu, Y.C., Dudukovic,M.P. 1980. Gas holdup and liquid circulation in gas-lift reactors. Chem. Eng. Sci. **35**: 135-141.

Huang, S.Y., Yeh, M.C., Liou, K.T. 1976. International Fermentation Symposium, Berlin. p.65.

Imai, Y., Suzuki, M., Masamoto, M., Nagayasu, K. 1993. Amylase production by *Aspergillus oryzae* in a new kind of fermentor with a rotary draft tube. J. Ferm. Bioeng. **76**(6): 459-464.

Jones, A.G. 1985. Liquid circulation in a draft tube bubble column. Chem. Eng. Sci. **40**: 449-462.

Joshi, J.B., Sharma, M.M. 1979. A circulation model for bubble columns. Trans. Inst. Chem. Eng. **57**: 244-251.

Joshi, J.B., Pandit, A.B., Sharma, M.M. 1982. Mechanically agitated gas-liquid reactors. Chem. Eng. Sci. **37**(6): 813-844.

Katinger, H.W.D. 1976. Physiological response of *Candida tropicalis* grown on n-paraffin to mixing in a tubular closed loop fermenter. Eur. J. Appl. Microbiol. Biotechnol. **3**: 103-114.

Katinger, H.W.D., Scheirer, W., Kromer, E. 1979. Bubble column reactor for mass propagation of animal cells in suspension culture. Ger. Chem. Eng. **2**: 31-32.

Kawase, Y., Moo-Young, M. 1986a. Influence of non-Newtonian flow behaviour on mass transfer in bubble columns with and without draft tubes. Chem. Eng. Commun. **40**: 67-83.

Kawase, Y., Moo-Young, M. 1986b. Liquid phase mixing in bubble columns with Newtonian and non-Newtonian fluids. Chem. Eng. Sci. **41**: 1969-1977.

Kawase, Y., Moo-Young, M. 1987. Influence of very small bubbles on k_La measurement in viscous microbiological cultures. Biotechnol. Bioeng. **30**: 345-347.

Kawase, Y., Moo-Young, M. 1989. Hydrodynamics in a bubble column bioreactors with fermentation broths having a yield stress. Appl. Microbiol. Biotechnol. **30**: 596-603.

Kawase, Y., Moo-Young, M. 1990. The effect of antifoam agents on mass transfer in bioreactors. Bioproc. Eng. **5**: 169-173.

Kawase, Y., Tsujimura, M., Yamaguchi, T. 1993. Hydrodynamics in airlift bioreactors with non-Newtonian fermentation broths, pp. 69-77. In: Nienow, A.W. (ed.), Third international conference on bioreactor and bioprocess fluid dynamics. MEP Ltd. London.

Keitel, G., Onken, U. 1981. Gas-liquid mass transfer in as stirred loop reactor. Ger. Chem. Eng. **4**: 250-258.

Kemblowski, Z., Kristiansen, B. 1986. Rheometry of fermentation liquids. Biotechnol. Bioeng. **28**: 1474-1483.

Kennard, M., Janekeh, M. 1991. Two- and three-phase mixing in a concentric draft tube gas-lift fermenter. Biotechnol. Bioeng. **38**: 1261-1270.

Keshavarz, T., Eglin, R., Walker, E., Bucke, C., Holt, G., Bull, A.T., Lilly, M.D. 1990. The large-scale immobilisation of *Penicillium chrysogenum*: batch and continuous operation in an air-lift reactor. Biotechnol. Bioeng. **36**: 763-770.

Kim, J.H., Lebeault, J.M., Reuss, M. 1983. Comparative study on rheological properties of mycelial broth in filamentous and pelleted forms. Eur. J. Appl. Microbiol. Biotechnol. **18**: 11-16.

Klein, C. 1994. The effect of the engineering environment on the fermentation of *Saccharopolyspora erythraea*. Research project, ACBE, Dept. Chem. & Biochem. Eng.. University College London.

Kloosterman, J., Lilly, M.D. 1985. An airlift fermenter for transformation of steroids by immobilised cells. Biotech. Letts. **7**(1): 25-30.

Koenig, B., Seewald, C., Schugerl, K. 1981a. Penicillin production in a bubble column air lift loop reactor, pp. 573-579. In: Moo-Young, M., Robinson, C.W., Vezina, C. (eds.), Advances in biotechnology, vol. **1**. Pergamon Press, Toronto, Canada.

Koenig, B., Seewald, C., Schugerl, K. 1981b. Process engineering investigations of penicillin production. Eur. J. Appl. Microbiol. Biotechnol. **12**: 205-211.

Koide, K., Iwamoto, S., Takasaka, Y., Matusura, S., Takasashi, E., Kimura, M., Kubota, H. 1984. Liquid circulation, gas holdup and pressure drop in a bubble column with draught tube. J. Chem. Eng. Jpn. **17**: 611-618.

Koide, K., Kimura, M., Nitta, H., Kawabata, H. 1988. Liquid circulation in a bubble column with a draught tube. J. Chem. Eng. Japan. **21**(4): 393-399.

Kristiansen, B., McNeil, B. 1987. The design of a tubular loop reactor for scale-up and scale down of fermentation processes. Bioreactors and Biotransformations. Eds. Moody, G.W., Baker, P.B. Elsevier Pub. London. pp. 321- 334.

Kubota, H., Hosono, Y., Fujie, K. (1978). Characteristic evaluations of ICI air-lift type deep shaft aerator. J. Chem. Eng. Japan. **11**:(4) 319- 325.

Kuraishi, M., Terao, I., Ohkouchi, H., Matsuda, N. and Nagai, I. 1977. SCP - process development with methanol as substrate. DECHEMA Monograph. 1978. **83**: (1704-1723)111-124.

Kuznetsov, L.E. 1985. Temperature effect on erythromycin biosynthesis. Antibiot. Med. Biotekhnol. **30**(7): 485-489.

Ladwa, H., Cameron, A., Bulmer, M., Pickett, A.M., Merchuk, J.C. 1988. Influence of draft tube clearance on pressure drop and gas holdup in a 250 litre airlift reactor, pp.

395-412. In: King, R. (ed.), Proceedings: 2nd international conference bioreactor fluid dynamics. Elsevier, London.

Larsson, G., Enfors, S.-O. 1988. Studies of insufficient mixing in bioreactors: Effects of limiting oxygen concentrations and short term oxygen starvation on *Pencillium chrysogenum*. Bioproc. Eng. **3**: 123-127.

Lee, C.H., Glasgow, L.A., Erickson, L.E., Patel, S.A. 1987. Liquid circulation in airlift fermenters, pp: 50-59. In: Ho, C.S., Oldshue, J.Y. (eds.), Biotechnology

Lee, J.C., Meyrick, D.L. 1970. Coalescence in non and coalescing solutions. Trans.I.Chem.E. **48**: T37.

Lehrer, I.H. 1968. Gas agitation of liquids. Ind. Engng. Chem. Proc. Des. Dev. **7**: 226-239.

Lilly, M.D. 1983. Problems in process scale-up, pp. 79-89. In: Winstanley, D.J., Nisbet, l.J. (eds.), Bioactive microbial products **2**. Academic Press, London.

Lin, C.H., Fang, B.S., Wu, C.S., Fang, H.Y., Kuo, T.F., Hu, C.Y. 1976. Oxygen transfer and mixing in a tower cycling fermentor. Biotechnol. Bioeng. **28**: 1557-1572.

Lindert, M., Kochbeck, B., Pruss, J., Warnecke, H-J., Hempel, D.C. 1992. Scale-up of airlift -loop bioreactors based on modelling the oxygen mass transfer. Chem. Eng. Sci. **47**(9-11): 2281-2286.

Lippert, J., Adler, I., Meyer, H.D., Lubbert, A., Schugerl, K. 1983. Characterisation of the two-phase systems in airlift tower loop bioreactors during the cultivation of E.coli. Biotechnol. Bioeng. **25**: 437-450.

Lubbert, A., Frochlich, S., Larson, B., Schugerl, K. 1988. Fluid dynamics in airlift loop bioreactors as measured during real cultivation processes, pp. 379-393. In: King, R (ed.), Proceedings: 2nd international conference bioreactor fluid dynamics. Elsevier, London.

Luttmann, R., Munack, A., Thoma, M. 1985. Mathematical modelling parameter identification and adaptive control of single cell protein processes in tower loop bioreactors. Adv. Biochem. Eng. **32**: 95-205.

Makagiansar, H.Y. 1992. Influence of shear on the fermentation of Pencillium chrysogenum. PhD. thesis. University of London, London, U.K.

Makagiansar, H.Y., Ayazi Shamlou, P., Thomas, C.R., Lilly, M.D. 1993. The influence of mechanical forces on the morphology and penicillin production of Penicillin chrysogenum. Bioproc. Eng. **9**: 83-90.

Malfait, J.L., Wilcox, D.J., Mercer, D.G., Barker, L.D. 1981. Cultivation of a filamentous mould in a glass pilot scale airlift fermenter. Biotechnol. Bioeng. **23**: 863-877.

Manfredini, R., Cavallera, V. 1983. Mixing and oxygen transfer in conventional stirred fermentors. Biotechnol. Bioeng. **25**: 3115-3131.

Margaritis, A., Sheppard, J.D. 1981. Mixing time and oxygen transfer characteristics of a double draft tube airlift fermenter. Biotechnol. Bioeng. **23**: 2117-2135.

Markl, H., Bronnenmeier, R. 1985. Mechanical stress and microbial production, pp. 370-392. In: Brauer, H. (ed.), Fundamentals of biochemical engineering, vol. **2**. VCH Verlagsgesell schaft, Germany.

Marquart, R., Blenke, H. 1980. Circulation of moderately to highly viscous Newtonian and non-Newtonian liquids in propeller pumped circulating loop reactors. Int. Chem. Eng. **20**(3): 368 - 378.

Marrucci, G., Nicodemo, L. 1967. Coalescence of gas bubbles in aqueous solutions of inorganic electrolytes. Chem. Eng. Sci. **22**: 1257-1261.

Martin, J.F., McDaniel, L.E. 1975. Kinetics of biosynthesis of polyene macrolide antibiotics in batch cultures: cell maturation time. Biotechnol. Bioeng. **27**: 925-938.

Martin, J.R., Rosenbrook, W. 1967. Studies on the biosynthesis of the erythromycins. II. Isolation and structure of a biosynthetic intermediate, 6-Deoxyerythronolide B. Biochemistry. **6**(2): 435-440.

McGuire, J.M., Bunch, R.L., Anderson, R.C., Boaz, H.E., Flynn, E.H., Powell, H.M., Smith, J.W. 1952. Antibiotics and Chemotherapy. **2**:281.

McNeil, B., Kristiansen, B. 1990. Simulated scale-up of a yeast fermentation using a loop bioreactor. Biotechnol. Letts. **12**(1): 39-44.

Merchuk, J.C., Stein, Y., Mateles. 1980. Distributed parameter model for an airlift fermenter. Biotechnol. Bioeng. **22**: 1189-1211.

Merchuk, J.C., Stein, Y. 1981a. Local gas holdup and liquid velocity in airlift reactors. AIChE J. **27**: 377-388.

Merchuk, J.C., Stein, Y., 1981b. A distribution parameter model for an airlift fermenter. Effects of pressure. Biotechnol. Bioeng. **23**: 1309 - 1324.

Merchuk, J.C. 1986. Gas holdup and liquid velocity in a 2-dimensional airlift reactor. Chem.Eng.Sci. **41**: 11-16.

Merchuk, J.C. 1990. Why use airlift bioreactors ?. TIBTECH. **8**:66-71.

Merchuk, J.C., Yunger, R. 1990. The role of the gas-liquid separator of airlift reactors in the mixing process. Chem. Eng. Sci. **45**(9): 2973-2975.

Merchuk, J.C. 1991. Tower reactor models, pp. 349-382. In: Schugerl, K., Rehm, H-J., Reed, G., Puhler, A., Stadler, P. (ed.), Biotechnology, vol.**4**: Measuring modelling and control. VCH, Weinheim.

Merchuk, J.C., Ladwa, N., Bulmer, M. 1993. Improving the airlift reactor: helical flow promoter, pp. 61-63. In: Nienow, A.W. (ed.), Third international conference bioreactor and bioprocess fluid dynamics. MEP Ltd, London.

Merchuk, J.C., Ladwa, N., Cameron, A., Bulmer, M., Pickett, A. 1994. Concentric-tube airlift reactors: effects of geometrical design on performance. A.I.Ch.E. J. **40**(7): 1105-1117.

Metz, B., Kosen, N.W.F., van Suijdam, J.C. 1979. The rheology of mould suspensions. Adv. Biochem. Eng. **11**: 103-156.

Metzner, A. B., Otto, R.E. 1957. Agitation of non-Newtonian fluids. A.I.Ch.E. J. **3**: 3-10.

Metzner, A. B., Feehs, R.H., Ramos, H.L., Otto, R.E., Tuthill, J.D. 1961. Agitation of viscous Newtonian and non-Newtonian fluids. A.I.Ch.E. J. **7**: 3-9.

Michel, B. J. and Miller, S. A. (1962). Power requirements of gas-liquid agitated system. A.I.Ch.E. J. **8**: 262-266.

Mohan, P., Lilly, M.D., Ison, A.P., Keshavarz-Moore, E., Saad, S.K. 1995. Scale up - Scale down : A review. For submission.

Moller. J., Niehoff, J. Hotop, S., Dors, M., Schugerl, K. 1992. The influence of preculture on the process performance of penicillin V production in a 100-l air-lift tower loop reactor. Appl. Microbiol. Biotechnol. **37**: 157-163.

Moo-Young, M., Blanch, H.W., 1981. Design of biochemical reactors: mass transfer criteria for simple and complex systems. Adv. Biochem. Eng. **19**: 1-16.

Moo-Young, M., Halard, B., Allen, G., Burrell, R., Kawase, Y. 1987. Oxygen transfer to mycelial fermentation broths in an airlift fermentor. Biotechnol. Bioeng. **30**: 746-753.

Moresi, M. 1981. Optimal design of airlift fermenters. Biotechnol. Bioeng. **23**: 2537-2560.

Murakami, Y., Hiroshe, T., Ono, S., Nishijima, T. 1982. Mixing properties in loop reactor. J. Chem. Eng. Jpn. **15**: 121-125.

Nagata, S. 1975. Mixing principles and applications. Kodansha Ltd, Tokyo.

Namdev, P.K., Irwin, N., Thompson, B.G., Gray, M.R. 1993. Effect of oxygen fluctuations on recombinant *Escherichia coli* fermentation. Biotechnol. Bioeng. **41**: 666-670.

Nash, C.H. 1974. Effect of carbon dioxide on synthesis of erythromycin. Antimicrobial Agents and Chemotherapy. **5**(5): 544-545.

Nienow, A.W. 1990. Agitators for mycelial fermentations. TIBTECH. **8**: 224-233.

Nishikawa, M., Kato, H., Hashimoto, K. 1977. Heat transfer in aerated tower filled with non-Newtonian liquid. Ind. Eng. Chem. Proc. Des. Develop. **16**: 133-137.

Olsvik, E., Kristiansen, B. 1992. Influence of oxygen tension, biomass concentration and specific growth rate on the rheological properties of a filamentous fermentation broth. Biotechnol. Bioeng. **40**: 1293-1299.

Olsvik, E., Tucker, K.G., Thomas, C.R., Kristiansen, B. 1993. Correlation of *Aspergillus niger* broth rheological properties with biomass concentration and shape of mycelial aggregates. Biotechnol. Bioeng. **42**: 1046-1052.

Onken, U., Weiland, P. 1981. Liquid velocity as an important design parameter for airlift loop-fermentors, pp. 559-564. In: Moo-Young, M., Robinson, C.W., Vezina, C. (ed.), Advances in biotechnology, vol. **1**. Pergamon Press, Toronto, Canada.

Onken, U., Weiland, P. 1983. Airlift fermenters: construction, behaviour and uses. p.67-95. In : Mizrahi, A., van Wezel, A.L. (eds.). Advances in biotechnological processes vol. **1**. Liss,A.R. Inc. New York.

Onken, U., Kiese, S., Jostmann, Th. (1984). An airlift fermenter for continuous cultures at elevated pressure. Biotech. Letts. **6**(5): 283-288.

Oosterhuis, N.M.G., Kossen, N.W.F. 1984. Dissolved oxygen concentration profiles in a production scale bioreactor. Biotechnol. Bioeng. **26**: 546-550.

Orazem, M.E., Erickson, L.E. 1979. Oxygen transfer rates and efficiencies in one- and two-stage airlift towers. Biotechnol. Bioeng. **21**: 69-88.

Orazem, M.E., Fan, L.T., Erickson, L.E. 1979. Bubble flow in the downflow section of an airlift tower. Biotechnol. Bioeng. **21**: 1579-1606.

Osman, H.G., Abou-Zeid, A.A., El-Gamal, A.A. 1968. Factors influencing the biosythesis of erythromycin by *Streptomyces erythreus*. Zeitschrift f. Allg. Mikrobiologie. **8**(5): 421-428.

Paca, J., Gregr, V. 1976. Design and performance characteristics of a continuous multistage tower fermentor. Biotechnol. Bioeng. **28**: 1075-1090.

Paca, J., Ettler, P., Gregr, V. 1978. Oxygen transfer rate in media used for erythromycin biosynthesis. J. Ferment. Technol. **56**(2): 144-151.

Packer, H.L., Thomas, C.R. 1990. Morphological measurements on filamentous microorganisms by fully automatic analysis. Biotechnol. Bioeng. **35**: 870-881.

Pandit, A.B., Joshi, J.B. 1983. Mixing in mechanically agitated gas-liquid contactors, bubble columns and modified bubble columns. Chem. Eng. Sci. **38**; 1189-1215.

Perry, R.H., Green, D. 1984. Perry's chemical engineer's handbook. 6th ed. McGraw-hill Book Co. New York.

Petrovic, D.L.J., Posarac, D., Dudukovic, A. 1990. Mixing time in gas-liquid-solid draft tube airlift reactors. Chem. Eng. Sci. **45**(9): 2967-2970.

Philip, J., Proctor, J.M., Niranjan, K., Davidson, J.F. 1990. Gas hold-up and liquid circulation in internal loop reactors containing highly viscous Newtonian and non-Newtonian liquids. Chem. Eng. Sci. **45**(3): 651-664.

Pigache, S., Trystram, G., Dhoms, P. 1992. Oxygen transfer modeling and simulations of an industrial continuous airlift fermentor. Biotechnol. Bioeng. **39**: 923-931.

Pons, A., Dussap,C.G., Gros, J.B. 1990. Xanthan batch fermentations: compared performances of a bubble column and a stirred tank fermentor. Bioproc. Eng. **5**: 107-114.

Popovic, M.K., Robinson, C.W. 1989. Mass transfer studies of external-loop airlifts and a bubble column. A.I.Ch.E. J. **35**: 393-405.

Popovic, M.K., Robinson, C.W. 1993. Mixing characteristics of external-loop airlifts: non-Newtonian systems. Chem. Eng. Sci. **48**(8): 1405-1413.

Potucek, F. 1989. Oxygen transfer during batch cultivation in an airlift tower fermenter. Collect. Czech. Chem. Comm. **54**: 3213-3219.

Potvin, J., Peringer, P. 1994. Ammonium regulation in *Saccharopolyspora erythraea*. Part I & II. Biotechnol. Letts. **16**(1): 69-74.

Queener, S.W., Day, L.E. 1986. Antibiotic-producing *Streptomyces* IX. In: The bacteria - A treatise on structure and function. Gunsalus I.C. (ed.). Academic Press. London.

Reitema, K., Ottengraf, S.P.P. 1970. Laminar liquid circulation and bubble street formation in gas - liquid systems. Trans. Instn. Chem. Engrs. **48**: T54-T62.

Reiter, M., Bluml, G., Gaida, T., Zach, F. Unterluggauer, O., Doblhoff-Dier, M., Noe, R., Huss, S., Katinger, H. 1991. Modular integrated fluidised bed bioreactor technology. Bio/technology **9**: 1100- 1102.

Robinson, C.W., Wilke, C.R. 1973. Oxygen absorption in stirred tanks: a correlation for ionic strength effects. Biotechnol. Bioeng. **15**: 755-761.

Roels, J.A., von den Berg, J., Voncken, R.M. 1974. The rheology of mycelial broths. Biotechnol. Bioeng. **16**: 181-208.

Rollins, M.J., Jensen, S.E., Westlake, D.W.S. 1988. Effect of aeration on antibiotic production by *Streptomyces clavuligerus*. J. Ind. Microbiol. **3**: 357-364.

Rollins, M.J., Jensen, S.E., Wolfe, S., Westlake, D.W.S. 1990. Oxygen derepresses desacetoxycephalosporin C synthase and increases the conversion of penicillin N to cephamycin C in *Streptomyces clavuligerus*. Enzyme Microb. Technol. **12**: 40-46.

Rollins, M.J., Jensen, S.E., Westlake, D.W.S. 1991. Effect of dissolved oxygen level on ACV synthetase synthesis and activity during growth of *Streptomyces clavuligerus*. Appl. Microbiol. Biotechnol. **35**: 83-88.

Roman, R.V., Gavrilescu, M. 1994. Oxygen transfer efficiency in the biosynthesis of antibiotics in bioreactors with a modified Rushton turbine agitator. Acta. Biotechnol. **14**(2): 181-192.

Rushton, J.H., Oldshue, J.Y. 1953. Chem. Eng. Sci. **28**: 1031

Russell, A.B. 1989. Hydrodynamics and oxygen transfer in a pilot scale airlift fermenter. PhD Thesis. University of London, London, U.K.

Russell, A.B., Thomas, C.R., Lilly, M.D. 1994. The influence of vessel height and top-section size on the hydrodynamic characteristics of airlift fermentors. Biotechnol. Bioeng. **43**: 69-76.

Russell, A.B., Thomas, C.R., Lilly, M.D. 1995. Oxygen transfer measurements during yeast fermentations in a pilot scale airlift fermenter. Bioprocess Eng. **12**: 71-79.

Rymowicz, W., Kautola, H., Wojtatowicz, M., Linko, Y-Y., Linko, P. 1993. Studies on citric acid production with immobilised *Yarrowia lipolytica* in repeated batch and continuous air-lift bioreactors. Appl. Microbiol. Biotechnol. **39**: 1-4.

Sachs, J.P., Rushton, J. 1954. Discharge flow from turbine type mixing impeller. Chem. Eng. Prog. **50**(12):597.

Schugerl, K., Lucke, J., Oels, U. 1977. Bubble column bioreactors. Adv. Biochem. Eng. **7**:1-84.

Schugerl, K., Lucke, J., Lehmann, J., Wagner, F. 1978. Application of tower bioreactors. Adv. Biochem. Eng. **8**: 63-162.

Schugerl, K. 1990. Comparison of the performances of stirred tank and airlift loop reactors. J. Biotechnol. **13**: 251-256.

Schumpe, A., Deckwer, W-D. 1980. Analysis of chemical methods for determination of interfacial areas in gas-in-liquid dispersions with non-uniform bubble sizes. Chem. Eng. Sci. **35**: 2221-2233.

Schumpe, A., Quicker, G., Deckwer, W.D. 1982. Gas solubility in microbial culture media. Adv. Biochem. Eng. **24**: 1-38.

Schumpe, A., Deckwer, W-D. 1987. Viscous media in tower bioreactors: hydrodynamic characteristics and mass transfer properties. Bioproc. Eng. **2**: 79-94.

Seipenbusch, R., Birckenstaedt, J.W., Blenke, H., Schindler, F. 1976. International Fermentation Symposium, Berlin. p.65.

Shah, Y.T., Deckwer, W.D. 1983. Hydrodynamics of bubble columns, pp: 583-620. In: Cheremisinoff, N.P.(ed.), Handbook of fluids in motion. Ann Arbor. Michigan.

Shah, Y.T., Yang, N., Gharat, S.D., Wisecarver, K. 1991. Circulation in large scale jet bubble columns. **110**: 53-70.

Shi, L.K., Riba, J.P., Angelino, H. 1990. Estimation of effective shear rate for aerated non-Newtonian liquids in airlift bioreactor. Chem. Eng. Comm. **89**: 25-35.

Siegel, M.H., Merchuk, J.C., Schugerl, K. 1986. Air-lift reactor analysis: interrelationships between riser, downcomer, and gas-liquid separator behaviour, including gas recirculation effects. A.I.Ch.E. J. **32**(10): 1585-1596.

Siegel, M.H., Merchuk, J.C. 1988. Mass transfer in a rectangular airlift reactor: effects of geometry and gas recirculation. Biotechnol. Bioeng. **32**: 1128-1137.

Siegel, M.H., Hallaile, M., Merchuk, J.C. 1988. Air-lift reactors: design, operation, and applications, pp.79-124. In: Mizrahi, A. (ed.), Advances in biotechnological processes, vol. **7**. Liss, A.R. Inc, New York, U.S.A.

Siegel, M.H., Merchuk, J.C. 1991. Hydrodynamics in rectangular air-lift reactors: scale-up and the influence of gas-liquid separator design. Can. J. Chem. Eng. **69**: 465-473.

Smith, S.R.L. 1980. Single cell protein. Phil. Trans. Roy. Soc. (London). B:**290**: 341-354

Smith, G.M., Calam, C.T. 1980. Variations in inocula and their influence on the productivity on antibiotic fermentations. Biotechnol. Letts. **2**(6): 261-266.

Smith, J.M. 1985. Dispersion of gases in liquids. In: Mixing of liquids by mechanical agitation. Ulbrecht, J.J., Patterson, G.K.(eds). Gordon and Breach, New York. ch.**5** pp: 139-202.

Smith, B.C., Skidmore, D.R. 1990. Mass transfer phenomena in airlift reactors: effects of solids loading and temperature. Biotechnol. Bioeng. **35**: 483-491.

Smith, J.J., Lilly, M.D., Fox, R.I. 1990. The effect of agitation on the morphology and penicillin production of *Penicillium chrysogenum*. Biotechnol. Bioeng. **35**: 1011-1023.

Sobotka, M., Prokop, A., Dunn, I.J., Einsele, A. 1982. Review of methods for measurement of oxygen transfer in microbial systems. Ann. Rep. Ferm. Proc. **5**(5): 127-210.

Sonnleitner, B., Kappeli, O. 1986. Growth of *Saccharomyces cerevisiae* is controlled by its limited respiratory capacity: formulation and verification of a hypothesis. Bitechnol. Bioeng. **28**: 927-937.

Stanbury, P.F., Whitaker, A. 1984. Principles of Fermentation Technology. Pergamon Press, Oxford.

Stark, W.M., Smith, R.L. 1961. The erythromycin fermentation. Progress in Ind. Microbiol. **3**: 213-230

Stasinopoulos, S.J., Seviour, R.J. 1992. Exopolysaccharide production by *Acremonium persicium* in stirred-tank and air-lift fermentors. Appl. Microbiol. Biotechnol. **36**: 465-468.

Steel, R., Maxon, W.D. 1966. Studies with a multiple-rod mixing impeller. Biotechnol. Bioeng. **8**: 109-115.

Suh, I-S., Schumpe, A., Deckwer, W-D. 1992. Xanthan production in bubble columns an air-lift reactors. Biotechnol. Bioeng. **39**: 85-94.

Sukan, S.S., Vardar-Sukan, F. 1987. Mixing performance of air-lift fermenters against working volume and draft tube dimensions. Bioproc. Eng. **2**: 33-38.

Suphantharika, M. 1992. The influence of dissolved oxygen on the production of difficidin by *Bacillus sp.* PhD thesis. University of London, London.

Suphantharika, M., Ison, A.P., Lilly, M.D., Buckland, B.C. 1994. The influence of dissolved oxygen tension on the synthesis of the antibiotic difficidin by *Bacillus subtilis*. Biotechnol. Bioeng. **44**: 1007-1012.

Sweere, A.P.J., Mesters, J.R., Janse, L., Luyben, K.Ch.A.M., Kossen, N.W.F. (1988a). Experimental simulation of oxygen profiles and their influence on baker's yeast production: I. One-fermenter system. Biotechnol. Bioeng. **31**: 567-578.

Sweere, A.P.J., Janse, L., Luyben, K.Ch.A.M., Kossen, N.W.F. (1988b). Experimental simulation of oxygen profiles and their influence on baker's yeast production: II. Two-fermenter system. Biotechnol. Bioeng. **31**: 579-586.

Taylor, I.J. 1954. The disperision of mass turbulent flow in a pipe. Proc. R. Soc. I. **A223**: 446-468.

Taylor, I.J., Senior, P.J. 1978. Single cell proteins:a new source. Endeavour. **2**: 31-34.

Trager, M., Qazi, G.N., Onken, U., Chopra, C. 1989. Comparison of Airlift and Stirred Reactors for Fermentation with *Aspergillus niger*. J. Ferm. Bioeng. **68**(2): 112-116.

Trager, M., Hollmann, D., Buse, R., Onken, U. 1991. Device for fermentations with oscillations of dissolved oxygen. J. Ferment. Bioeng. **72**: 46-53.

Trager, M., Qazi, G.N., Buse, R., Onken, U. 1992. Comparison of direct glucose oxidation by Gluconobacter oxydans subsp. suboxydans and *Aspergillus niger* in a pilot scale airlift reactor. J. Ferm. Bioeng. **74**(5): 274-281.

Trilli, A., Crossley, M.V., Kontakou, M. 1987. Relation between growth rate and erythromycin production in *Streptomyces erythraeus*. Biotechnol. Letts. **9**(11): 765-770.

Tsuji, K., Goetz, J. 1978. HPLC as a rapid of monitoring erythromycin and tetracycline fermentation processes. J. Antibiotics. **31**(4): 302-308.

Tucker, K.G., Mohan., Thomas, C.R. 1993. The influence of mycelial morphology on the rheology of filamentous fermentation broths, pp. 261-273. In: Nienow, A.W. (ed.), Third international conference bioreactor and bioprocess fluid dynamics. MEP Ltd, London.

Tuffile, C.M., Pinho, F. 1970. Determination of oxygen transfer coefficients in viscous *Streptomycete* fermentations. Biotechnol. Bioeng. **12**: 849-971.

van der Laan, E.T. 1958. Notes on the dispersion-type model for the logitudinal mixing flow . Chem. Eng. Sci. **7**: 187-191.

van'Riet, K., Tramper, J. 1991. Basic bioreactor design. Marcel Dekker. New York.

van Suijdam, J.C., Kossen, N.W.F., Paul, P.G. 1980. An inoculum technique for the production of fungal pellets. Eur. J. Appl. Microbiol. Biotechnol. **10**: 211-221.

van Suijdam, J.C., Metz, B. 1981. Influence of engineering variables upon the morphology of filamentous molds. Biotechnol. Bioeng. **23**: 111-148.

Vardar, F., Lilly, M.D. 1982. Effect of cycling dissolved oxygen concentrations on product formation in penicillin fermentations. Eur. J. Appl. Microbiol. Biotechnol. **14**: 203-211.

Varecka, R.M., Bliem, R.F. 1990. Investigations into pumping characteritics of axial flow impellers in an internal loop reactor for animal cell culture. Chem. Eng. Comm. **96**: 81- 96.

Verlaan, P., Tramper, J., van'Riet, K., Luyben, K. 1986. A hydrodynamic model for an airlift-loop bioreactor with external loop. Chem. Eng. J. **33**: B43-53.

Verlaan, P., van Eijs, A.M.M., Tramper, J., van't Riet, K., Luyben, K. Ch. A.M. 1989. Estimation of axial dispersion in individual sections of an airlift-loop reactor. Chem. Eng. Sci. **44**(50): 1139-1146.

Voigt, J., Schugerl, K. 1979. Adsorption of oxygen in countercurrent multi-stage bubble columns. I. Chem. Eng. Sci. **34**:1221-1229.

Wachi, S., Jones, A.G., Elson, T.P. 1991. Flow dynamics in a draft tube bubble column using various liquids. Chem. Eng. Sci. **46**(2): 657-663.

Wallace, K.K., Payne, G.F., Speedie, M.K. 1992. *Streptomyces* bioprocessing: from secondary metabolites to heterologous proteins, pp 168-180. In: Ladisch, L.R. (ed.), Harnessing biotechnology for the 21st century. ACS, Washington, D.C.

Wang, D.I.C., Fewkes, R.C.J. 1977. Effect of operating and geometric parameters on the behaviour of non-Newtonian, mycelial, antibiotic fermentations. Dev. Ind. Microbiol. **18**: 39-56.

Warnecke, H.J., Pruss, J., Langemann, H. 1985. A mathematical model for loop reactors- I. Residence time distributions, moments and eignenvalues. Chem. Eng. Sci. **6**: 89-93.

Warren, S.J. 1994. The relationship between the morphology and rheology of mycelial fermentations. PhD. thesis. University of London, London.

Warren, S.J., Keshavarz-Moore, E., Ayazi Shamlou, P., Lilly, M.D., Thomas, C.R., Dixon, K. 1995. Rheologies and morphologies of three actinomycetes in submerged culture. Biotechnol. Bioeng. **45**: 80-85

Wase, J. D.A., McManamey, W.J., Raymahasay, S., Vaid, A.K. 1985. Comparisons between cellulase production by *Aspergillus fumigatus* in agitated vessels and in an air-lift fermentor. Biotechnol. Bioeng. **27**: 1166-1172.

Weiland, P. 1984. Influence of draft tube diameter on operation behaviour of airlift loop reactors. Ger. Chem. Eng. **7**: 374-385.

Wilkinson, W.L. 1960. Non-Newtonian fluids, pp. 65-68. Pergaomon Press, London, U.K.

Winkler, M.A. 1990. Problems in fermenter design and operation, pp. 215-350. In: Winkler, M.A (ed.), Chemical engineering problems in biotechnology. Elservier App. Sci. New York.

Wittler, R., Matthes, R., Schugerl, K. 1983. Rheology of *Penicillium chrysogenum* pellet suspensions. Eur. J. Appl. Microbiol. Biotechnol. **18**: 17-23.

Wittler, R., Baumgaertl, H., Lubbers, D.W., Schugerl, K. 1986. Investigations of oxygen transfer into *Penicillium chrysogenum* pellets by microprobe measurements. Biotechnol. Bioeng. **28**: 1024-36.

Wood, L.A., Thompson, P.W. 1986. Applications of the airlift fermenter, pp. 157-172. In: King, R. Proceedings: Int. conference on bioreactor fluid dynamics, Cambridge. BHRA, Cranfield, U.K.

Yamamoto, H., Maurer, K.H., Hutchinson, C.R. 1986. Transformation of *Streptomyces erythraeus*. J. Antibiotics. **39**: 1304-1313.

Yegneswaran, P.K., Gray, M.R., Thompson, B.G. 1991. Experimental simulation of dissolved oxygen fluctuations in large fermentors: Effect on *Streptomyces clavuligerus*. Biotechnol. Bioeng. **38**: 1203-1209.

Zhou, W., Holzhauer - Rieger, K., Bayer, T., Schugerl, K. 1993. Cephalosporin C production by highly productive *Cephalosporium acremonium* strain in an airlift tower reactor with static mixers. J. of Biotechnology. **28**: 165 - 177

Zlokarnik, M. 1978. Sorption characteristics for gas-liquid contacting in mixing vessels. Adv. Biochem. Eng. **8**: 133-151.

Zlokarnik, M. 1985. Tower-shaped reactors for aerobic biological waste water treatment, pp. 537-569. In: Brauer, H (ed.), Biotechnology volume 2 Fundamentals of biochemical engineering. VCH, Weiheim.

Zuber, N., Hench, J. 1962. Steady state and transient void fraction of bubbling systems and their operating limits. General Electric Co. report: 626. Lido, New Jersey, U.S.A.

Zuber, N., Findlay, J.A. 1965. Average volumetric concentration in two-phase flow systems. J. Heat Transfer, (Trans. ASME). **87**: 453-468.

Zwietering, M.H., Verlaan, P., Krolikowski, A.K.M. 1992. Optimal control of the dissolved oxygen concentration in an airlift loop reactor. Computers chem. Engng. **16**(6): 563-572.

7.0 NOMENCLATURE

A	initial amplitude of pH response profile	(mm)
A_B	free area for area for flow between the riser and downcomer	(m^2)
A_D	cross sectional area of the downcomer	(m^2)
A_R	cross sectional area of the riser	(m^2)
a	function of n' for calculation of wall shear stress for non-Newtonian fluid	(-)
a_L	mean gas-liquid interfacial area per unit liquid volume	(m^{-1})
b	function of n' for calculation of wall shear stress for non-Newtonian fluid	(-)
Bo	Bodenstein number	(-)
C	concentration of tracer pulse	($mol.m^{-3}$)
C	shear rate constant	(m^{-1})
C'	antibiotic concentration	(mgL^{-1})
C_θ	equilibrium concentration of tracer pulse after complete mixing	($mol.m^{-3}$)
C^*	saturation concentration of dissolved oxygen	($mol.m^{-3}$)
C^*_o	saturation concentration of dissolved oxygen in water	($mol.m^{-3}$)
C_0	dissolved oxygen concentration in water	($mol.m^{-3}$)
C_o	distribution parameter, dependent on the radial position of the gas holdup and superificial liquid velocity across the column	(-)
C_L	dissolved oxygen concentration	($mol.m^{-3}$)
C_t	dissolved oxygen concentration at time t	($mol.m^{-3}$)
C_{crit}	critical dissolved oxygen tension	(% air saturation)
cj	concentration of dissolved species j	($mol.L^{-1}$)
CTD	circulation time distribution	(s)
d	diameter of the inhibition zone from the plate centre	(m)
D	diffusion coefficient	(-)
D	internal diameter of the column	(m)
D_L	liquid phase axial dispersion coefficient	(-)
DOC	dissolved oxygen concentration	($mol.m^{-3}$)
DOT	dissolved oxygen tension	(% air saturation)
DCW	dry cell weight	(gL^{-1})
D_D	internal diameter of the downcomer (shell diameter)	(m)
D_R	internal diameter of the riser	(m)
D_P	propeller diameter	(m)
d_B	Sauter bubble diameter	(m)
E (t)	residence time distribution, RTD	(s)
E_{EXP}	power input due to gas expansion	(W)
f_D	friction factor based on total flow through downcomer	(-)

f_R	friction factor based on total flow through riser	(-)
g	acceleration due to gravity	(ms^{-2})
H	Henry's law constant for water	($Pa.mol\ fr^{-1}$)
H_D	height of the gas - liquid dispersion from the vessel base	(m)
H_{DT}	height of the top of the draft tube from the vessel base	(m)
H_L	height of the unaerated liquid from vessel base	(m)
h	height of dispersion above the draft tube	(m)
Δh	distance between the pressure probe positions	(m)
I_i	number of ions per molecule	(-)
J	volumetric flux density	(ms^{-1})
k	ratio of liquid-wake volume to bubble volume	(-)
K	consistancy index	($Pa.s^n$)
K'	generalised consistancy index	($Pa.s^n$)
k_s	average shear rate constant	(-)
K_B	frictional loss coefficient for the bottom section	(-)
K_T	frictional loss coefficient for the top section	(-)
K_j	empirical constant to account for the effect of species j on oxygen solubility	($mol.L^{-1}$)
k_L	liquid side mass transfer coefficient	(ms^{-1})
k_La	volumetric mass transfer coefficient	(s^{-1})
L	clearance between the bottom of the draft tube and vessel base	(m)
l	length of the horizontal path in idealised path length of liquid circulation	(m)
Mw	molecular weight of water	($kg.m^{-3}$)
N	impeller speed	(s^{-1})
N_A	specific rate of oxygen transfer to the liquid phase	(moles. m^{-3}· liquid. s^{-1})
N_Q	discharge coefficient	(-)
N_p	impeller number	(-)
N_{2EX}	mean nitrogen mole fraction for exit gas stream	(mol fr)
N_{2IN}	mean nitrogen mole fraction for inlet gas stream	(mol fr)
n	flow behaviour index	(-)
n'	generalised flow behaviour index	(-)
O_{2EX}	mean oxygen mole fraction for exit gas stream	(mol fr)
O_{2IN}	mean oxygen mole fraction for inlet gas stream	(mol fr)
OUR	oxygen uptake rate	($mmol.L^{-1}.h^{-1}$)
P	hydrostatic pressure	(Pa)
P_{ATM}	atmospheric pressure	(Pa)
P_{EX}	pressure at the point of gas exit from vessel	(Pa)
P_H	vessel head pressure	(Pa)
P_{IN}	pressure at the point of gas inlet to the vessel	(Pa)

ΔP	hydrostatic pressure difference in the aerated vessel	(Pa)
ΔP_1	pressure loss in the riser	(Pa)
ΔP_2	pressure loss in the top section	(Pa)
ΔP_3	pressure loss in the downcomer	(Pa)
ΔP_B	pressure loss due to flow reversal at the bottom of the column	(Pa)
ΔP_D	pressure drop driving force for liquid circulation	(Pa)
ΔP_F	pressure drop due to flow around the loop	(Pa)
ΔP_{FD}	pressure loss due to friction in flow through the downcomer	(Pa)
ΔP_{FR}	pressure loss due to friction in flow through the riser	(Pa)
ΔP_i	pressure losses in the riser	(Pa)
ΔP_T	pressure loss due to flow reversal at the top of the column	(Pa)
P x	pressure at position x metres from the vessel base	(Pa)
Pe	Peclet number	(-)
P	power input	(W)
P_g	power input due to aeration for an airlift reactor	(W)
P_g	gassed power input of a stirred tank	(W)
P_{VT}	total energy dissipation rate	(Wm^{-3})
P_{VA}	energy dissipation rate for airlift aeration only operation	(Wm^{-3})
P_{VP}	energy dissipation rate for propeller only operation of airlift reactor	(Wm^{-3})
P_0	impeller number	(-)
q_{ery}	specific erythromycin production rate	($mg.g^{-1}.h^{-1}$)
q_{pen}	specific penicillin production rate	($mg.g^{-1}.h^{-1}$)
Q	pumping capacity: liquid volumetric flow rate	($m^3.s^{-1}$)
Q_{GD}	volumetric flowrate of gas through the downcomer	($m^3.s^{-1}$)
Q_{GEX}	volumetric flowrate of gas leaving the vessel	($m^3.s^{-1}$)
Q_{GR}	volumetric flowrate of gas through the riser	($m^3.s^{-1}$)
Q_{GO}	volumetric flowrate of gas through the sparger	($m^3.s^{-1}$)
Q_L	volumetric flowrate of liquid	($m^3.s^{-1}$)
Q_{LR}	volumetric flowrate of liquid through the riser	($m^3.s^{-1}$)
Q_m	molar gas flowrate	($mol.s^{-1}$)
R	universal gas constant	($mol.kg^{-1}.s^{-1}$)
Re	Reynolds number	(-)
S_i	salting out constant for ion i	($L.mol^{-1}$)
T	absolute temperature	(K)
T	diameter of the column / riser section	(m)
T_{EX}	absolute temperature of exit gas stream	(K)
T_{IN}	absolute temperature of exit gas stream	(K)
t	weight in tonnes	(tonne)
t	exposure time or surface renewal time	(s)

t_c	liquid circulation time	(s)
t_{down}	time for liquid to flow down through downcomer	(s)
t_m	mean mixing time to achieve 90% homogeneity	(s)
t_R	mean gas residence time in the riser	(s)
t_{up}	time for liquid to flow up the riser	(s)
u_r	gas - liquid slip velocity	(ms^{-1})
U_{bl}	mean primary bulk liquid velocity along the column	(ms^{-1})
U_{BT}	terminal rise velocity of an isolated bubble	(ms^{-1})
U^c_o	centre-line primary liquid velocity	(ms^{-1})
U_{GD}	mean linear velocity of gas in the downcomer	(ms^{-1})
U_{GR}	mean linear velocity of gas in the riser	(ms^{-1})
U_{LC}	mean liquid circulation velocity	ms^{-1})
U_{LD}	mean liquid linear velocity in the downcomer	(ms^{-1})
U_{LR}	mean liquid linear velocity in the riser	(ms^{-1})
U_m	mean liquid linear velocity	(ms^{-1})
U_{sg}	superficial gas velocity based on the riser	(ms^{-1})
U_{sl}	superficial liquid velocity in the riser	(ms^{-1})
U_{SD}	mean slip velocity in the downcomer	(ms^{-1})
U_{SR}	mean slip velocity in the riser (mean relative velocity between the liquid and the gas phases in the riser section	(ms^{-1})
V_g	aerated liquid volume	(m^3)
V_L	unaerated liquid volume	(m^3)
x	diameter of the antibiotic reservoir	(m)
x	vertical displacement from the base of the vessel	(m)
x_o	saturation mole fraction of oxygen in water when the partial pressure of oxygen in the gas phase is 101325 Pa	(mol fr)
X_c	circulation path length	(m)
y	time in years	(year)
y_{EX}	mean oxygen mole fraction of exit gas stream	(mol fr)
y_{IN}	mean oxygen mole fraction of inlet gas stream	(mol fr)
y_{O2}	oxygen composition of gas	(mol fr)
z_i	ionic charge on ion i	(-)
Z	ratio of liquid flow area in the riser to that in downcomer	(-)

Greek symbols

α	constant for gas holdup, eq. 1.9	(-)
β	constant for gas holdup, eq. 1.9	(-)
ρ_L	density of the liquid phase	($kg.m^{-3}$)
ρw	density of water	($kg.m^{-3}$)
γ	shear rate	(s^{-1})
γ_a	average shear rate	(s^{-1})

ε	gas holdup	(-)
ε_D	mean downcomer gas holdup	(-)
ε_O	mean overall gas holdup	(-)
ε_R	mean riser gas holdup	(-)
ε_{TS}	mean top section gas holdup	(-)
ε_w	gas holdup of the liquid wake	(-)
ζ	liquid diffusivity	($m^2.s^{-1}$)
μ	viscosity of the liquid phase	(Pa.s)
μ_a	apparent viscosity of the liquid phase	(Pa.s)
η	solubility in fermentation medium compared with that in water at same conditions	(-)
τ	shear stress	(Pa)
τ_w	wall shear stress	(Pa)
ϕ_{FD}^2	two phase frictional multiplier for the downcomer	(-)
ϕ_{FR}^2	two phase frictional multiplier for the riser	(-)
ø	dimensionless time	(-)

Subscripts

D	downcomer
ery	erythromycin
O	overall
pen	penicillin
R	riser
TS	top section

Appendix 1.0. Calculation of superficial gas velocity

In an airlift reactor the superficial gas velocity must be based on the cross section area of the riser where air is sparged into the vessel (Chisti, 1989). The other important consideration is the axial variation in volume flow of gas in a reactor, due to the changes in hydrostatic pressure. Therefore, this study used the equation below adapted from Chisti (1989):

$$U_{sg} = \frac{Q_m R T}{A_R H_L \rho_L g} \ln\left(1 + \frac{\rho_L g H_L}{P_H}\right) \qquad \text{A 1}$$

where

Q_m = molar gas flowrate (mole s^{-1})

P_H = vessel head pressure (Nm^{-2}).

A_R = cross sectional area of riser (m^2)

H_L = unaerated liquid height (m)

Appendix 2.0 Derivation of the equation for overall gas holdup

The overall gas holdup was considered to be an average of the sectional holdups of the riser, downcomer and top section, which was derived by a gas balance:

$$\text{overall gas holdup} = \frac{\text{total volume of gas entrained}}{\text{total volume of dispersion}}$$

$$= \frac{\text{gas in riser + gas in downcomer + gas in top section}}{\text{total volume of dispersion}} \qquad \text{A 2.1}$$

Therefore, this derived to:

$$\varepsilon_{overall} = \frac{H_{DT} A_R \varepsilon_R + H_{DT} A_D \varepsilon_D + (H_D - H_{DT})(A_R + A_D).\ \varepsilon_{TS}}{H_D (A_R + A_D)} \qquad 2.6$$

where

H_{DT} = height of draft tube above the vessel base (m)

H_D = height of gas – liquid dispersion (m)

ε_R = riser gas holdup (–)

ε_D = downcomer gas holdup (–)

ε_{TS} = top section gas holdup (–)

A_R = riser cross sectional area (m^2)

A_D = downcomer cross sectional area (m^2)

For each reactor configuration the overall gas holdup and one sectional gas holdup could be experimentally measured hence, rearrangements of equation 2.6 were used to estimate either the riser or downcomer gas holdup from the measured holdup values. The equation also required an estimation of top section gas holdup which could not be directly measured and, was assumed to be equal to the riser gas holdup in this study. Therefore, the overall and downcomer gas holdup measured with the draft tube sparger reactor configuration were used to estimate the riser gas holdup, ε_R using the equation below:

$$\varepsilon_R = \frac{\varepsilon_{overall} \cdot (A_R + A_D) H_D - H_{DT} A_D \varepsilon_D}{H_{DT} A_R + (A_R + A_D)(H_D - H_{DT})} \qquad \text{A 2.2}$$

Thus, the downcomer gas holdup (ε_D) was estimated from the overall and riser gas holdups measured with the reactor configured with the annulus sparger using the equation below:

$$\varepsilon_D = \frac{\varepsilon_{overall} H_D (A_R + A_D) - H_{DT} A_R \varepsilon_R - (H_D + H_{DT})(A_R + A_D) \varepsilon_{TS}}{H_{DT} A_R} \qquad \text{A 2.3}$$

Appendix 3.0 Calculation of liquid linear velocities

An estimation of the mean circulation path length was obtained from figure 2.6. The vertical displacement of liquid beyond the ends of the draft tube was ignored for simplicity. The total vertical distance travelled:

$$= 2(H_{DT} - L) \qquad \text{A 3.1}$$

where H_{DT} = height of draft tube above the vessel base (m).

L = distance between bottom of draft tube and vessel base of 0.06 m

The total horizontal distance travelled

$$= 2\,l$$

where $l = D/4$ A 3.2

and D = internal diameter of vessel, 0.317 m

The liquid circulation time (t_c) was measured by the tracer response technique (section 2.6.1). However, estimation of the liquid velocities was complicated by the fact that the cross-sectional area for flow was different in each section of the vessel.

Two parameters can be defined.

t_{up} = time for liquid to flow up through the riser (s).

t_{down} = time for liquid to flow down the downcomer (s).

The time for the liquid to traverse the short horizontal segments in the end sections was incorporated into both time parameters. This was achieved by assuming that the liquid velocity in the top and bottom sections was the same as that in the riser and downcomer respectively.

Thus t_{up} and t_{down} was defined as :

$$t_{up} = \frac{\text{riser path length + top section path length}}{\text{liquid linear velocity in riser}}$$

$$t_{down} = \frac{\text{downcomer path length + bottom section path length}}{\text{liquid linear velocity in downcomer}}$$

where

$$t_{up} = \frac{(H_{DT} - L) + l}{U_{LR}} \qquad \text{A 3.3}$$

$$t_{down} = \frac{(H_{DT} - L) + l}{U_{LD}} \qquad \text{A 3.4}$$

The circulation time was the sum of these two times.

$$t_c = t_{up} + t_{down} \qquad \text{A 3.5}$$

The volumetric flow of liquid, Q_L was constant in both the riser and the downcomer and was related to the liquid linear velocity as shown below (Russell, 1989) :

$$Q_L = U_{LR}\,(1-\varepsilon_R)\,A_R = U_{LD}\,(1-\varepsilon_D)\,A_D \qquad \text{A 3.6}$$

therefore,

$$U_{LR} = U_{LD}\,\frac{A_D\,(1-\varepsilon_D)}{A_R\,(1-\varepsilon_R)} \qquad \text{A 3.7}$$

So substituting U_{LD} into equation A 3.4 gave:

$$t_{down} = \frac{H_{DT}-L+l}{U_{LR}} \cdot \frac{A_D\,(1-\varepsilon_D)}{A_R\,(1-\varepsilon_R)} \qquad \text{A 3.8}$$

To solve an equation for U_{LR} the equation A 3.5 was re-written using equations A 3.3 and A 3.8 as :

$$t_c = \frac{H_{DT}-L+l}{U_{LR}} + \frac{H_{DT}-L+l}{U_{LR}} \cdot \frac{A_D\,(1-\varepsilon_D)}{A_R\,(1-\varepsilon_R)} \qquad \text{A 3.9}$$

This equation was then expressed for U_{LR} :

$$U_{LR} = \frac{H_{DT}-L+l}{t_c}\left(1 + \frac{A_D\,(1-\varepsilon_D)}{A_R\,(1-\varepsilon_R)}\right) \qquad \text{A 3.10}$$

The appropriate values for a certain reactor configuration were substituted into equation A 3.10 together with the values of L and l. The cross sectional area of the annulus of the vessel was 0.0419 m^2 compared to 0.035 m^2 for the draft tube. So when the draft tube sparger was used A_R = 0.035 m^2 and A_D = 0.0419m^2 whereas, with the annulus sparger A_R = 0.0419 m^2 and A_D = 0.035 m^2. As an example, equation A 3.10 was solved for U_{LR} with the draft tube sparger as shown below:

$$U_{LR} = \frac{1}{t_c}\left[H_{DT} + 0.023.\frac{(1-\varepsilon_D)}{(1-\varepsilon_R)} + 1.197 .\frac{(1-\varepsilon_D)}{(1-\varepsilon_R)}. H_{DT} + 0.019 \right]$$

$$= \frac{1}{t_c}\left[H_{DT}\left(1 + 1.197 . \frac{(1-\varepsilon_D)}{(1-\varepsilon_R)} \right) + 0.023 .\frac{(1-\varepsilon_D)}{(1-\varepsilon_R)} + 0.019 \right]$$

For this work the difference between riser and downcomer gas holdups was small so, the ratio of $(1-\varepsilon_D)/(1-\varepsilon_R)$ was assumed to be unity.
This reduced the equation to:

$$U_{LR} = \frac{2.2\ H_{DT} + 0.04}{t_c}$$

$$= \frac{2.2\ H_{DT}}{t_c} \qquad \text{A 3.11}$$

At the highest gas velocity (0.136 ms^{-1}), where the difference between riser and downcomer gas holdup was at its greatest the $(1-\varepsilon_D)/(1-\varepsilon_R)$ was 1.045, and the subsequent U_{LR} only deviated by 3% from that calculated with a $(1-\varepsilon_D)/(1-\varepsilon_R)$ of unity using equation A 3.11. An expression for U_{LD} with the draft tube sparger was determined in a similar manner to that shown for U_{LR}:

$$U_{LD} = \frac{1.8\ H_{DT}}{t_c} \qquad \text{A 3.12}$$

For the annulus sparger the values of cross sectional area for the riser and downcomer were reversed and, so the ratio of A_D/A_R was 0.83 compared to 1.197 for the draft tube sparger. This resulted in the equations for liquid velocities with the annulus sparger being:

$$U_{LR} = \frac{1.8\ H_{DT}}{t_c} \qquad U_{LD} = \frac{2.2\ H_{DT}}{t_c} \qquad 2.3$$

Appendix 4.0 The measurement path used by the mobile DOT probe around the airlift reactor

The mobile dissolved oxygen tension probe was used to measure the dissolved oxygen tension (DOT) around the vessel and, the DOT values (% air saturation) were presented as a function of the distance from the sparger. The measurement path of the DOT probe for the annulus gas sparged airlift reactor in the tallest configuration (working volume of 0.25 m^3) is shown in figure A 1. This measurement distance was identical for the draft tube sparged reactor although, the direction of liquid circulation was reversed. The measurement distance began at the sparger (0.06 m from the vessel base) and progressed up the riser and, into the top section by a height of 0.74 m above the draft tube. Although, the top section height increased with gas velocity, the same gassed liquid height was used for comparative purposes, as the DOT between this liquid height and the liquid surface remained constant with all operating conditions. For conventional aeration with both sparger configurations the DOT probe could be passed between the static blades of the propeller, to measure the DOT at the vessel base with the annulus sparged reactor or, at the surface of draft tube sparger. For propeller operation the DOT was not measured closer than 0.38 m above the propeller. So, the measurement distance from the annulus sparger with propeller operation was limited to a total length of 6.61 m.

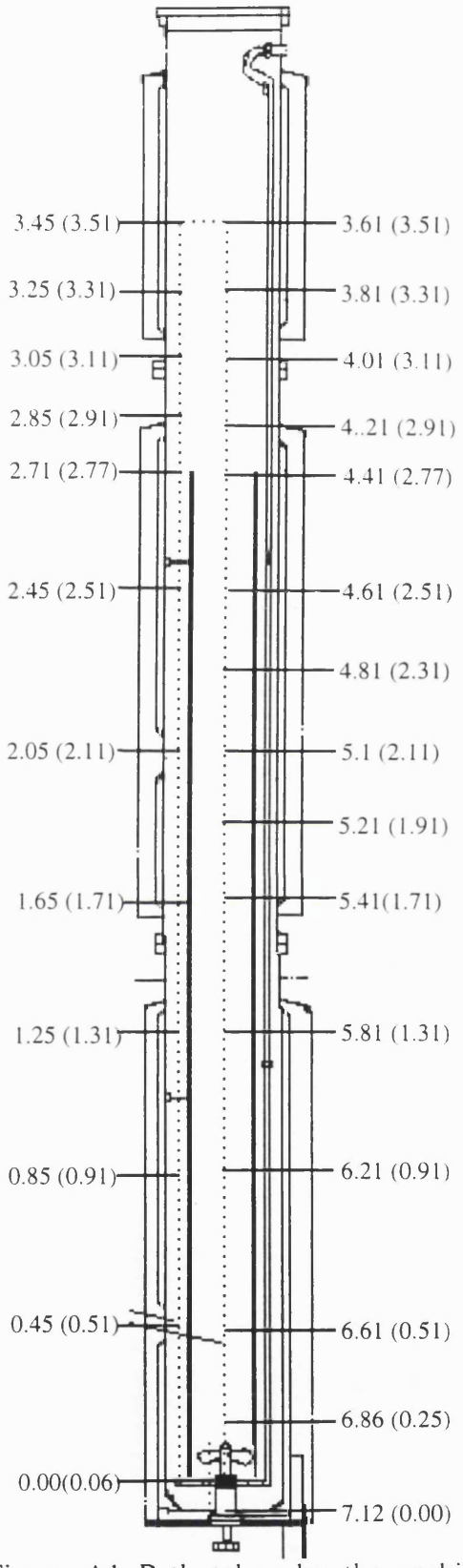

Figure A1 Path taken by the mobile dissolved oxygen tension probe in the airlift reactor (vessel height of 4.11m & H_{DT} of 2.77m) as a function of distance (m) from the annulus sparger. (bracketed values: height above the vessel base (m))

The same measurement path was used for the short draft tube configuration(1. 78 m H_{DT}) (section 3.3.11) although the total measurement distance from the sparger was 4.2 m.

Appendix 5.0 Estimation of oxygen solubility in fermentation media

The method used to calculate the oxygen solubility in the fermentation media was that by Schumpe *et al.* (1982). It was proposed that the contribution of individual components of the fermentation media to the overall solubility was 'log additive' according to:

$$\log_{10}\left(\frac{C_O^*}{C^*}\right) = \sum_j K_j c_j \qquad \text{A 5.1}$$

where

C^* = oxygen solubility in fermentation medium, (mol m^{-3})

C_O^* = solubility of oxygen in water at same temperature and pressure as medium, (mol m^{-3})

c_j = concentration of dissolved species j (mol L^{-1}) for salts ; (gL^{-1}) for organic compounds

K_j = empirical constant accounting for effect of species j on oxygen solubility, (L mol^{-1} salts; Lg^{-1} organics).

The calculation of K_j for salts used the equation below:

$$K_j = \frac{1}{2}\sum_i S_i I_i z_i^2 \qquad \text{A 5.2}$$

where

S_i = 'salting out' constant for ion i, (L mol^{-1})

z_i = ionic charge on ion i

I_i = number of ions per molecule

Schumpe experimentally determined values of S_i for a large number of ions and empirical values were used for the Kj of organic compounds. The method by Schumpe *et al.* (1982) did not predict the effect of cells and antifoam on oxygen solubility. Hence, for this estimation there possible effects have been discounted.

Oxygen solubility in the yeast broth

The medium used (as reported in section 2.3.1):

	gL^{-1}	
Glucose	10	
Yeast extract	10	
Ammonium sulphate	5	(0.0379 mol L^{-1})

Potassium dihydrogen phosphate	2.5 (0.0184 mol L^{-1})
Polypropylene glycol	0.25 mL L^{-1}

Values of K_j for the two salts are as follows:

$(NH_4)_2SO_4$

$$K_j = \frac{1}{2} \sum S_i.I_i \ . z_i^2 \qquad \text{A 5.2}$$

$$= \frac{1}{2} (-0.704 \times 2 \times 1^2 + 0.460 \times 1 \times 2^2)$$

$$= 0.216 \text{ L mol}^{-1}$$

where –0.704 and 0.460 are the values of S_i for NH_4^+ and SO_4^{2-} respectively.

KH_2PO_4

$$K_j = \frac{1}{2} (-0.587 \times 1 \times 1^2 + 0.997 \times 1 \times 1^2)$$

$$= 0.205 \text{ L mol}^{-1}$$

where –0.587 and 0.997 are the values of S_i for K^+ and $H_2PO_4^-$ respectively.

The values of K_j for yeast extract and glucose given by Schumpe *et al.* (1982) are 6.2×10^{-4} Lg^{-1} and 6.58×10^{-4} Lg^{-1} respectively.

Thus:

$$\log_{10}\left(\frac{C_O^*}{C^*}\right) = \sum K_j c_j \qquad \text{A 5.1}$$

$$= (0.0379 \times 0.216) + (0.0184 \times 0.205) + (10 \times 6.58 \times 10^{-4}) + (10 \times 6.2 \times 10^{-4})$$

$$= 0.0247$$

hence,

$$C^* = 0.945.C_O^*$$

and $\eta = 0.945$

where η = factor to account for reduction in oxygen solubility in fermentation medium compared with that in water under the same conditions.

Oxygen solubility of the fermentation medium for *S.erythraea* fermentations

The medium constituents were as follows:

	gL^{-1}	
Bactopeptone	4.0	
Yeast extract	6.0	
Glycine	2.0	
Magnesium sulphate ($MgSO_4.7H_2O$)	0.5	(0.002 mol L^{-1})
Potassium dihydrogen phosphate	0.68	(0.005 mol L^{-1})
Glucose-shake flasks & seed fermentation	10.0	
- Large scale fermentation	30.0	
Polypropylene glycol-large scale	1 mL L^{-1}	

Values of K_j for the salt solutions

KH_2PO_4

$$K_j = \frac{1}{2}\sum_i S_i I_i z_i^2 \qquad \text{A 5.2}$$

$$= \frac{1}{2}(-0.587 \times 1 \times 1^2) + (0.997 \times 1 \times 1^2)$$

$$= 0.205 \text{ L mol}^{-1}$$

where –0.587 and 0.997 were the S_i values for K^+ and $H_2PO_4^{2-}$ respectively

$MgSO_4$

$$K_j = \frac{1}{2}\sum S_i I_i z_i^2 \qquad \text{A 5.2}$$

$$= \frac{1}{2}(-0.297 \times 1 \times 2^2) + (0.46 \times 1 \times 2^2)$$

$$= 0.326 \text{ L mol}^{-1}$$

where –0.297 and 0.46 were the S_i values for Mg^{2+} and SO_4^{2-} respectively

The values of K_j given by Schumpe *et al.* (1982) for the organic constituents were: yeast extract 6.2×10^{-4} Lg^{-1}, peptone 4.3×10^{-4} Lg^{-1}, glucose 6.58×10^{-4} Lg^{-1} and glycine 12.46×10^{-4} Lg^{-1}.

Therefore:

$$\log_{10}\left(\frac{C_O^*}{C^*}\right) = \sum K_j c_j \qquad \text{A 5.1}$$

$$= (6 \times 6.2\times10^{-4}) + (4 \times 4.3\times10^{-4}) + (30 \times 6.58\times10^{-4})$$
$$+ (2.5\times 12.46\times10^{-4}) + (0.005 \times 0.205) + (0.002 \times 0.326)$$
$$= 0.03$$

hence,

$$C^* = 0.933.C_O^*$$

and $\eta = 0.933$

where η = factor to account for reduction in oxygen solubility in fermentation medium compared with that in water under the same conditions.

Appendix 6.0 Sample k_La calculation

The method for estimating the volumetric oxygen mass transfer coefficient (k_La) at positions around the vessel was described in section 2.7. This appendix outlines the procedure for k_La estimation at the lower downcomer position using the airlift reactor with the draft tube sparger and 10 gL^{-1} DCW baker's yeast suspension.

The following conditions and parameters were used:

Draft tube height, H_{DT} = 2.77 m
Ungassed liquid height, H_L = 3.24 m
Total liquid volume, V_L = 0.25 m^3
Density of broth, ρ_L = 1001 kgm^{-3}
Volumetric flowrate of air through the sparger, Q_{GO} = 0.00066 m^3s^{-1}
Temperature of broth, T = 299 K
Head pressure, P_H = 101325 Pa
Dispersion height, H_D = 3.33 m
Downcomer gas holdup, ε_D = 0.014
Riser gas holdup, ε_R = 0.0378
Dissolved oxygen tension, DOT (lower downcomer, % air saturation) = 0.5%
Mean oxygen mole fraction for inlet gas stream, O_{2IN} = 0.2098
Mean oxygen mole fraction for exit gas stream , O_{2EX} = 0.2065
Mean nitrogen mole fraction for inlet gas stream, N_{2IN} = 0.7701
Mean nitrogen mole fraction for exit gas stream, N_{2EX} = 0.79803

Oxygen and nitrogen mole fractions of inlet and exit gases were determined using a mass spectrometer as described in section 2.7.2.

Appendix 6.1 Calculation of dissolved oxygen concentration (C_L)

The DOT probes were calibrated as outlined in section 2.7.3 by immersion in distilled water at a known temperature. The solubility of oxygen in water was correlated with temperature by Battino (1981) using the equation below :

$$\ln x_o = -66.735 + \frac{87.475}{\left(\frac{T}{100}\right)} + 24.453.\ln\left[\frac{T}{100}\right] \qquad \text{A 6.1}$$

where

x_o = saturation mole fraction of oxygen in water when the partial pressure of O_2 in the gas phase is 101325 Pa

T = absolute temperature, (K).

The probe was calibrated at 20.5^{0}C (293.5 K) hence, the mole fraction at this temperature from the equation above gave:

$x_o = 2.48 \times 10^{-5}$ mole fraction

Using this value the Henry's law constant for water (H) at 20.5^0 C was determined as:

$$H = \frac{\text{partial pressure of oxygen in gas phase}}{\text{mole fraction of dissolved oxygen}} \qquad \text{A 6.2}$$

$$= \frac{101325 \text{ Pa}}{2.48 \times 10^{-5} \text{ mole fraction}}$$

$$= 4.09 \times 10^9 \text{ Pa mole fraction}^{-1}$$

The saturation concentration of oxygen in water (C_0^*) was calculated from the equation below:

$$C_O^* = \frac{y_{O2}\ P_{ATM}}{H} \cdot \frac{1000\rho_w}{Mw} \qquad \text{A 6.3}$$

where

y_{O2} = oxygen composition of atmospheric air (mole fraction)

P_{ATM} = atmospheric pressure (Pa)

Mw = molecular weight of water (g mole^{-1})

ρ_L = density of water (kg m^{-3})

$$C_o^* = \frac{0.2098\ .\ 101325}{4.09 \times 10^9} \cdot \frac{998.\ 1000}{18}$$

$$= 0.288 \text{ mol m}^{-3}$$

In this example the dissolved oxygen tension (DOT) was 0.5% (air saturation) in the lower downcomer probe position therefore, the dissolved oxygen concentration was :

$$C_L = \frac{\%\,DOT}{100} \times C_0^* \qquad 2.13$$

where

C_0^* = saturation dissolved oxygen concentration in water, at calibration conditions (mole m^{-3})

DOT = dissolved oxygen tension reading from amplifier (% air saturation)

$$\text{Thus } C_L = \frac{0.5\%}{100} \times 0.288$$

$$= 1.44 \times 10^{-3} \text{ mole } m^{-3}$$

This is the dissolved oxygen concentration at the lower downcomer position as outlined in section 2.7.3.

Appendix 6.2 Calculation of specific oxygen transfer rate, N_A

The overall volumetric rate of oxygen transfer to the liquid phase (N_A) was determined using the equation below as described in section 2.7.1.

$$N_A = \frac{P_{IN}.Q_{GO}}{R\,T\,V_L}(y_{IN} - y_{EX}) \qquad 2.8$$

where

P_{IN} = pressure at bottom of vessel

$$= P_H + \rho_L g H_L \qquad 2.9$$

$$= 101325 + (1001 \times 9.8 \times 3.24)$$

$$= 133108.752 \text{ Pa}$$

The normalised difference in the composition of the inlet and outlet air streams (y_{IN}-y_{EX}) was calculated from the equation below:

$$(y_{IN} - y_{EX}) = O_{2IN} - O_{2EX} \times \frac{N_{2IN}}{N_{2EX}} \qquad 2.12$$

$$= 0.2098 - 0.2065 \times \frac{0.7701}{0.79803}$$

$$= 0.0032 \text{ mole fraction}$$

$$\text{Thus } N_A = \frac{133108.752 \times 0.00066}{8.134 \times 299 \times 0.25} \times 0.0032$$

$$= 4.62 \times 10^{-4} \text{ moles m}^{-3} \text{ s}^{-1}$$

Appendix 6.3 Calculation of saturation concentration of oxygen at probe position $C^*(x)$.

The saturation concentration was determined as described in section 2.7.1 using equation 2.11 shown below :

$$C^*(x) = \frac{y_{O2}(x).\ P(x)}{H} \cdot \frac{1000.\rho_w}{M_w} . \eta \qquad 2.11$$

where

$y_{O2}(x)$ = oxygen composition of gas phase at given position (mole fraction).

$P(x)$ = hydrostatic pressure at given position (Pa)

H = Henry's law constant for water (Pa.mole fraction^{-1})

ρ_w = density of water (kgm^{-3})

M_w = molecular weight of water (g mole^{-1})

η = factor to account for reduced solubility of oxygen in medium compared with that in water

The factor to account for the reduction in oxygen solubility in fermentation medium compared with water at the same conditions (η) was 0.945 for the yeast fermentation broth (appendix 5.0).

The estimation of P(x) for the probe in the lower downcomer uses the equation below:

$$P(x) = P_H + \rho_L\ (1-\varepsilon_{TS})\ gh\ +\ \rho_L\ (1-\varepsilon_D)\ g\ (H_{DT} - x) \qquad A\ 6.4$$

where

h = height of dispersion above the draft tube (m) $= H_D - H_{DT}$

x = height of probe from base of vessel = 0.53m

ε_{TS} = top section gas holdup (–)

The top section gas holdup was assumed to be the equal to the riser gas holdup as discussed in section 2.6.3 and the riser gas holdup was estimated using equation A 2.2. Thus, a value of P(x) was estimated for the lower probe position:

$$P(x) = 101325 + 1001(1-0.0378) \times 9.8 \times (3.33-2.77) + 1001\,(1-0.014) \times (2.77-0.53) \times 9.8$$
$$= 128277.15 \text{ Pa}$$

It was difficult to estimate a value for $y_{O2}(x)$ due to the lack of knowledge of the recirculation of gas through the downcomer. Thus, the gas compositions around the vessel were estimated by assuming that the oxygen composition for the riser probe positions was similar to the inlet gas composition (riser probe: $y_{O2}(x) = O_{2IN}$) and the gas composition in the downcomer was similar to the exit gas composition (downcomer probes: $y_{O2}(x) = O_{2EX}$). The Henry's law constant for water at 299 K required for the calculation of the oxygen saturation concentration was determined using equation A 6.2. Where, the saturation mole fraction of oxygen in water (x_0) at 299 K was 2.26×10^{-5} mole fraction as calculated using equation A 6.1.

Therefore, the saturation concentration at the lower downcomer position was calculated where the temperature was 299 K and the density of water was $\rho_L = 997$ kg m^{-3}:

$$C^* = \frac{0.2065 \times 128277.15}{4.48 \times 10^9} \cdot \frac{1000 \times 997}{18} \cdot 0.945$$
$$= 0.3092 \text{ mol m}^{-3}$$

Appendix 6.4 Estimation of k_La

The value of k_La at a given position can be calculated using the equation below:

$$k_La = \frac{N_A}{C^*(x) - C_L(x)} \qquad 2.10$$

therefore, the lower downcomer k_La =

$$k_La = \frac{4.62 \times 10^{-4}}{0.3092 - 1.44 \times 10^{-3}}$$
$$= 0.0015 \text{ s}^{-1}$$

Appendix 7.0 Sample calculations for the estimation of total energy dissipation rate for the airlift reactor and lab. stirred tank

7.1 Total energy dissipation rate for the airlift reactor

This example shows the calculation of total energy dissipation, P_{VT} (Wm^{-3}) from combined aeration and propeller operation using the annulus ring sparger. The energy dissipation rate from aeration (P_{VA}) was calculated using a well published equation (Chisti, 1989). For the propeller operation, stirred tank derived Reynolds numbers for each propeller speed were used to estimate power numbers resulting in theoretical estimation of energy dissipation rate (P_{VP}).

Summary of operating conditions:

Superficial gas velocity, U_{sg}	=	0.036 ms^{-1}
Propeller speed, N	=	10 rps
Density of yeast broth, ρ_L	=	1000 kgm^{-3}
Viscosity of yeast broth, μ	=	1 x 10^{-3} Pa.s
Cross sectional area of riser, A_R	=	0.0419 m^2
Cross sectional area of downcomer, A_D	=	0.035 m^2
working volume	=	0.25 m^3

Energy dissipation rate for aeration (P_{VA}) using the equation derived by Chisti (1989)

$$P_{VA} = \frac{P_g}{V_L} = \frac{\rho_L \, g \, U_{sg}}{1 + \frac{A_D}{A_R}} \qquad 2.15$$

where

V_L = liquid volume (m^3)

P_g = power input due to aeration (W)

U_{sg} = superficial gas velocity (ms^{-1})

A_R = cross sectional area of the riser (m^2)

A_D = cross sectional area of the downcomer (m^2)

ρ_L = liquid density ($kg.m^{-3}$)

$$= \frac{1000.\ 9.81.\ 0.036}{1 + \frac{0.035}{0.0419}}$$

$$= 192.4 \ Wm^{-3}$$

which is the energy dissipation rate from aeration only without propeller operation (P_{VA}).

Energy dissipation rate for propeller only operation (P_{VP})

Calculation of Reynolds number for the marine propeller rotating at 600 rpm.

$$Re = \frac{\rho N D^2}{\mu} \qquad 2.16$$

$$= \frac{1000.\ 10.\ 0.16^2}{1 \times 10^{-3}}$$

$$= 2.56 \times 10^5$$

Therefore, the power number for a Reynolds number of 2.56×10^5 was 0.225 for a marine propeller in a unaerated stirred tank (Perry and Green, 1984) and energy dissipation rate equaled:

$$P_{VP} = \frac{P}{V_L} = \frac{P_0\ \rho_L\ N^3\ D_p^5}{V_L} \qquad 2.17$$

$$= \frac{0.225.\ 1000.\ 10^3.0.16^5}{0.25}$$

$$= 94.36\ Wm^{-3}$$

Therefore, the total power energy dissipation rate from aeration at the gas velocity of 0.036 ms^{-1} and propeller operation at 600 rpm was :

$$P_{VT} = P_{VA} + P_{VP} \qquad 2.14$$

$$= 192.4 + 94.36$$

$$= 286.76\ Wm^{-3}$$

7.2 Total energy dissipation rate for the lab. scale stirred tank

The stirred tank was used for the fermentation of *Saccharopolyspora erythraea* hence, the following example was for the energy dissipation rate at 29 h into the fermentation (section 3.4.4). The power input was the total power drawn by the three impellers and the bottom impeller was assumed to be under aeration and the other two were considered to be ungassed.

Summary of operating conditions:

gas flow rate, Q		= 5.8 m^3s^{-1}
propeller speed, N		= 11.66 rps
apparent viscosity, μ_a		= 0.065 Pa.s
density, ρ_L		= 1000 kgm^{-3}
working volume, V_L		= 0.025 m^3
Impeller:	number	= 3
	diameter	= 0.1 m
	number of blades	= 6

The Reynolds number (Re) was derived by

$$Re = \frac{\rho N D^2}{\mu_a} \qquad 2.16$$

where

N = rotational speed of the propeller (rps)

D_p= propeller diameter (m)

μ_a = liquid viscosity (Pa.s)

ρ_L= liquid density ($kg.m^{-3}$)

Hence,

$$= \frac{1000.\ 11.66.\ 0.1^2}{0.065}$$

$$= 1794$$

Thus, from the Reynolds number correlation for flat six-bladed turbine a value of the impeller power number was obtained of 4.8. Therefore, the ungassed power of a single impeller at 700 rpm was :

$$P_0 = \rho_L\ N_p\ N^3.D^5 \qquad A\ 7.1$$

$$= 1000.\ 4.8.\ 1166^3.\ 0.1^5$$

$$= 76\ W$$

For the gassed power of the bottom impeller the Michel and Miller (1962) correlation was used:

$$P_g = 0.706\left[\frac{P_0^2\ N\ D^3}{Q^{0.56}}\right]^{0.45} \qquad A\ 7.2$$

$$= 0.706\left[\frac{76^2.11.66.\ 0.1^3}{(5.8 \times 10^{-4})^{0.56}}\right]^{0.45}$$

$$= 30.63\ W$$

Therefore, the total energy dissipation for the three impeller configuration under the summarised operating conditions was:

$$P_{VT} = \frac{P}{V_L} = \frac{P_g + P_0 + P_0}{V_L} \qquad A\ 7.3$$

$$= \frac{30 + 76 + 76}{0.025}$$

$$= 7280\ Wm^{-3}$$

Appendix 8.0 Calculation of apparent viscosity of non-Newtonian broths in the airlift reactor

The apparent viscosity of the *S. erythraea* broths and xanthan gum used in this study with the airlift reactor was calculated from the mean value of the estimated shear stress at the column wall for the riser and downcomer, as described in section 2.9.3.2 and by Russell (1989). The following example was for calculation of the apparent viscosity at 29 h into the *S. erythraea* fermentation of the annulus gas sparged airlift reactor (section 3.4.1.3) although, the same method was used for the aerated and propeller operated reactor.

Summary of experimental conditions:

Flow behaviour, n = 0.475

Consistency index, K = 1.095 Pa.s^n

Liquid linear velocity :

Riser = 0.398 ms^{-1}

Downcomer = 0.488 ms^{-1}

Diameter of the riser (annulus) = 0.106 m

Diameter of the downcomer = 0.211 m

broth density, ρ_L = 1000 kgm^{-3}

N.B. The diameter of the annulus of the vessel was based on the shell diameter.

An estimate of the wall shear stress was obtained from the correlation by Wilkinson (1960) for non-Newtonian broths based on the Blasius equation:

$$\tau_w = \tfrac{1}{2}\rho_L U_m^2 \, a \, (Re')^{-b} \qquad 2.22$$

and the generalised Re' was obtained from:

$$Re' = \frac{D^{n'} U_m^{2-n'} \rho_L}{K' 8^{n'-1}} \qquad 2.23$$

where n' was equivalent to the flow behaviour (n) for power law fluids and, the generalised consistency index was :

$$K' = K\left[\frac{3n+1}{4n}\right]^n \qquad 2.24$$

$$= 1.098\left[\frac{3.\ 0.48 + 1}{4.\ 0.48}\right]^{0.48}$$

$$= 1.23 \text{ Pa.s}^n$$

Therefore, Re' for the riser was obtained from:

$$Re' = \frac{D^{n'} U_m^{2-n'} \rho_L}{K' 8^{n'-1}} \qquad 2.23$$

$$= \frac{0.106^{0.48} .0.398^{2-0.48} .1000}{1.23. \ 8^{0.48-1}}$$

$$= 201$$

and the Re' number for the downcomer was 387 using the same procedure with the diameter of 0.211 m and U_m of 0.488 ms^{-1}. The calculation of the shear stress (equation 2.22) at the column wall required values of a and b which were the functions of the generalised flow behaviour index, n'. These were obtained by fitting non-linear functions to the values shown below and interpolating for the appropriate value of n.

Table A 1 Values of a and b for use in equation 2.22 for various values of generalised n' (Wilkinson, 1960).

n'	a	b
0.2	0.0646	0.349
0.3	0.0685	0.325
0.4	0.0712	0.307
0.6	0.074	0.281
0.8	0.0761	0.263
1.0	0.0779	0.25

Therefore, the shear stress at the wall of the riser was obtained from:

$$\tau_w = \tfrac{1}{2} \rho_L U_m^2 \, a \, (Re')^{-b} \qquad 2.22$$

$$= \tfrac{1}{2} .1000. \ 0.398^2. \ 0.0722(201)^{-02975}$$

$$= 1.18 \text{ Pa}$$

Similarly, the shear stress at the wall of the downcomer was 1.46 Pa using the liquid linear velocity of 0.488 ms^{-1} and Re of 387. Therefore, the average shear at the wall of the vessel (taken as the average from the riser and downcomer) was 1.32 Pa. Hence, the apparent viscosity at 29 h into the *S. erythraea* fermentation with the annulus gas sparged airlift reactor was:

$$\mu_a = \frac{\tau_\omega}{\left(\frac{\tau_\omega}{K}\right)^{\frac{1}{n}}} \qquad 2.25$$

$$= \frac{1.32}{\left(\frac{1.32}{1.095}\right)^{\frac{1}{0.48}}}$$

$$= 0.89 \text{ Pa.s}$$

Appendix 9 Figures

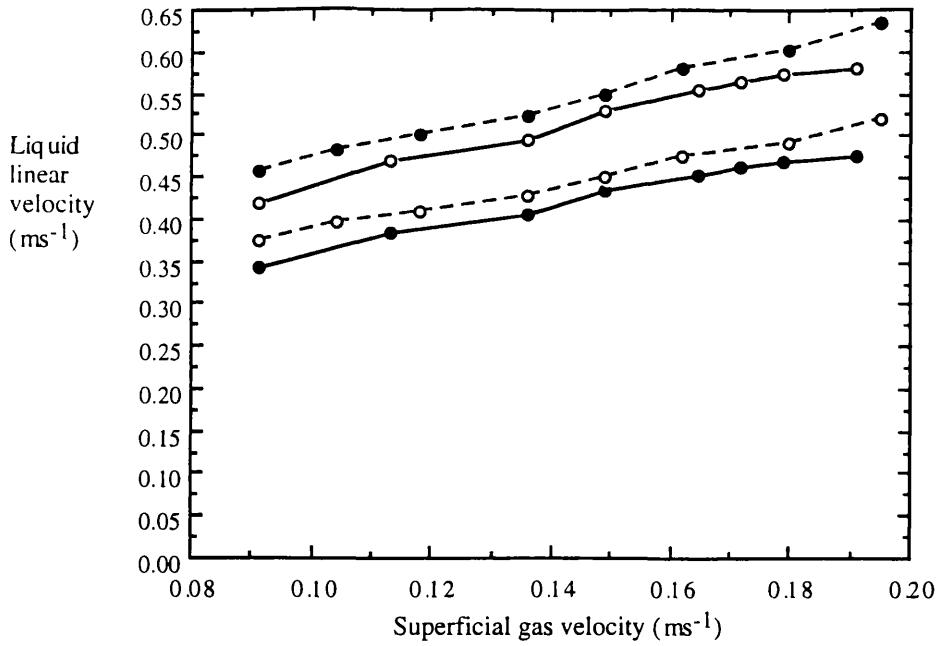

Appendix 9.1 The effect of superficial gas velocity on the riser and downcomer liquid linear velocity, measured at 29 h into the fermentations of *S. erythraea* with air sparging from the draft tube sparger (- - -) and annulus sparger (——). Riser liquid velocity (●), downcomer liquid velocity (o)

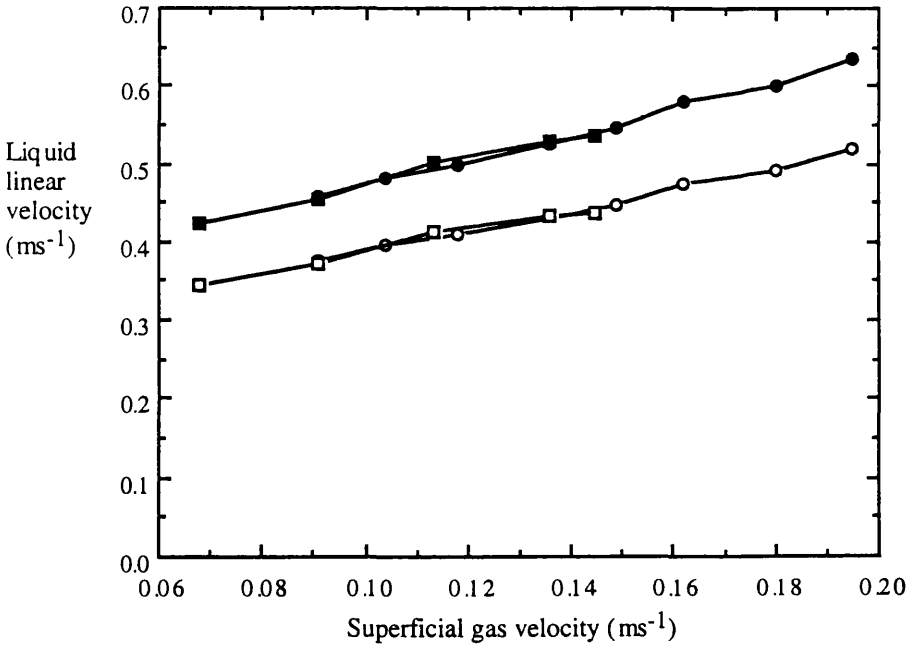

Appendix 9.2 Comparison of the effect of superficial gas velocity on riser (closed symbols) and downcomer (open symbols) liquid linear velocity at 29 h into the pelleted and mycelial fermentations of *S. erythraea* with air sparging from the draft tube sparger. Pelleted (squares symbols) and mycelial (circle symbols).

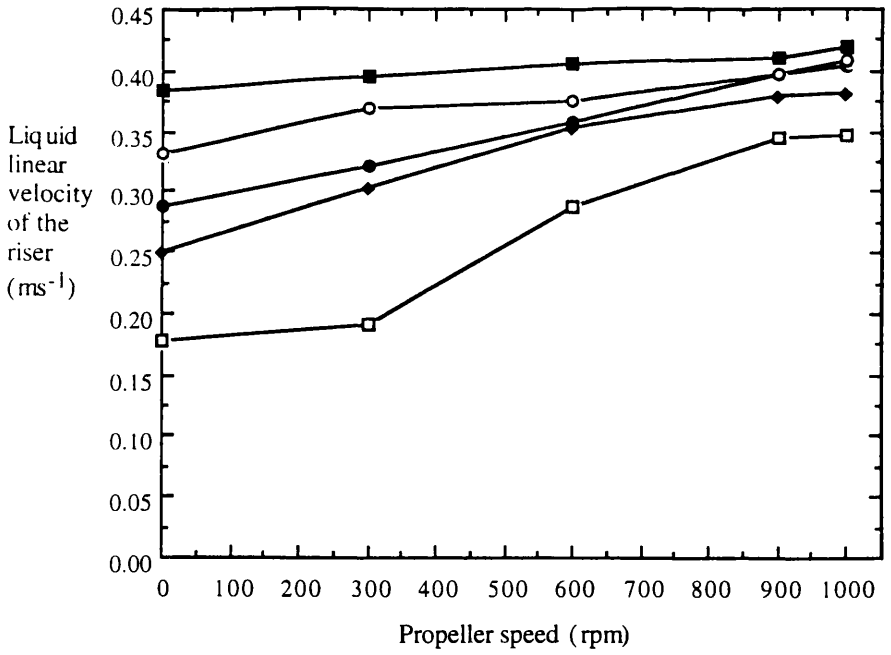

Appendix 9.3 The effect of propeller speed on the riser liquid linear velocity of the annulus gas sparged reactor (H_{DT} of 2.77 m) with baker's yeast suspension at superficial gas velocities (ms^{-1}): 0.036 (□), 0.054 (◆), 0.072 (●), 0.091 (○), 0.136 (■).